

**Universidade de Évora - Escola de Ciências e Tecnologia Universidade
Nova de Lisboa - Faculdade de Ciências e Tecnologias**

Mestrado em Paleontologia

Dissertação

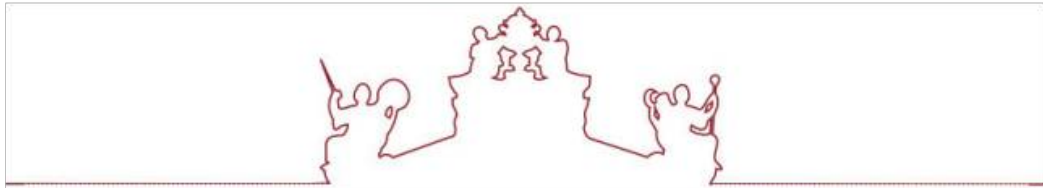
**The theropod dinosaur Ceratosaurus from the Upper
Jurassic of Lourinhã Formation and early theropod from the
Triassic of Grés de Silves, Portugal**

Rui Tiago dos Santos Matos

Orientador(es) | Octávio João Madeira Mateus
Ausenda Cáceres Balbino

Évora 2024





**Universidade de Évora - Escola de Ciências e Tecnologia Universidade
Nova de Lisboa - Faculdade de Ciências e Tecnologias**

Mestrado em Paleontologia

Dissertação

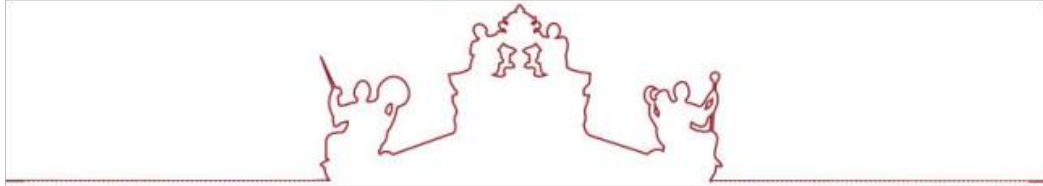
**The theropod dinosaur *Ceratosaurus* from the Upper
Jurassic of Lourinhã Formation and early theropod from the
Triassic of Grés de Silves, Portugal**

Rui Tiago dos Santos Matos

Orientador(es) | Octávio João Madeira Mateus
Ausenda Cáceres Balbino

Évora 2024





A dissertação foi objeto de apreciação e discussão pública pelo seguinte júri nomeado pelo Diretor da Escola de Ciências e Tecnologia:

Presidente | D. Figueiredo (Universidade de Évora)

Vogais | Octávio João Madeira Mateus (Universidade Nova de Lisboa - Faculdade de Ciências e Tecnologias) (Orientador)
Pedro Daniel Mocho Lopes (Universidade de Lisboa) (Arguente)

Évora 2024



Acknowledgments

I would like to thank all my family, specially my mother, my closest friends and all colleagues in the Master's of Paleontology for all the help and support.

I want to thank my Master's thesis tutors: professor Ausenda Balbino for all administrative help, and my main scientific tutor, professor Octávio Mateus, for giving me the opportunity to study this material, for all the precious help, availability and useful guidance through the whole process.

I want to thank Bruno Camilo from Sociedade de Historia Natural de Torres Vedras for providing access to the specimen under SHN(JJS)065 and *Ceratosaurus* teeth, and for helping with the transport to Assenta locality.

I also want to thank Carla Alexandra Tomás and all the staff from the Lourinhã Museum and Dinoparque for providing easy and quick access to all the material under ML352.

I would like to thank Maciej Ruciński for providing the Triassic vertebra to be studied and Dr. Steve Brusatte, who kindly shared some useful pictures for me to compare my material with.

I am also deeply thankful to the city council of Loulé for all the support given to the paleontological research regarding the Algarve Basin.

Overseas, I want to thank Alyson Wilkins, Carrie Levitt-Bussian and the whole team at the Natural History Museum of Utah for sharing useful pictures of *Ceratosaurus dentisulcatus* UMNH 5278 specimen and to Julia McHugh and the team at the Museum of Western Colorado for sharing useful pictures of *Ceratosaurus magnicornis* MWC1 specimen.

This work could never be completed without the help of all people mentioned above.

Thank you.

Abstract

Our knowledge of the vertebrate fauna of Late Triassic Silves Group, Algarve, Portugal is now more complete with the description of a single vertebra ascribed to the oldest dinosaur ever found in the Iberian Peninsula, enriching our understanding of this paleoenvironment where metoposaurids, mastodonsaurids, placodonts, phytosaurs and fishes were also identified. Compared anatomy and phylogenetic analysis, with 12 new characters, place the material within Neotheropoda with close affinity with the Early Jurassic *Sarcosaurus* from England.

-

The Late Jurassic theropod *Ceratosaurus* from the Lourinhã Formation was previously described on two separate occasions, each dealing with a different set of bones from the same individual. With new elements waiting description, this work aims to compile and describe all this material. Phylogenetic specimen-based analysis, with the introduction of 37 new characters, compares this specimen with the North American *Ceratosaurus* and solidifies its position close to this genus.

Keywords: Theropod, Phylogeny, Triassic, Jurassic, Algarve Basin, Lourinhã Formation, *Ceratosaurus*.

**O dinossauro terópode *Ceratosaurus* do
Jurássico Superior da Formação da Lourinhã
e
terópode basal do Triássico de Grés de Silves, Portugal**

Resumo

O nosso conhecimento da fauna de vertebrados do Triássico Superior do Grupo de Silves, Algarve, Portugal, está agora mais completo com a descrição de uma vértebra isolada pertencente ao mais antigo dinossauro encontrado na Península Ibérica, enriquecendo a nossa compreensão deste paleoambiente onde metopossaurídeos, mastodonssaurídeos, placodontes, fitossauros e peixes foram também identificados. Anatomia comparada e análise filogenética, com 12 novos caracteres, coloca este material em Neotheropoda com afinidade próxima a *Sarcosaurus* do Jurássico Inferior de Inglaterra.

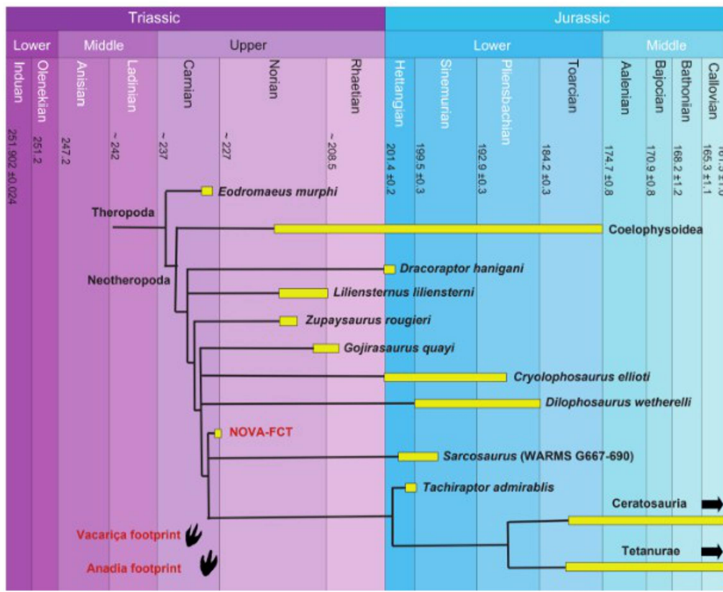
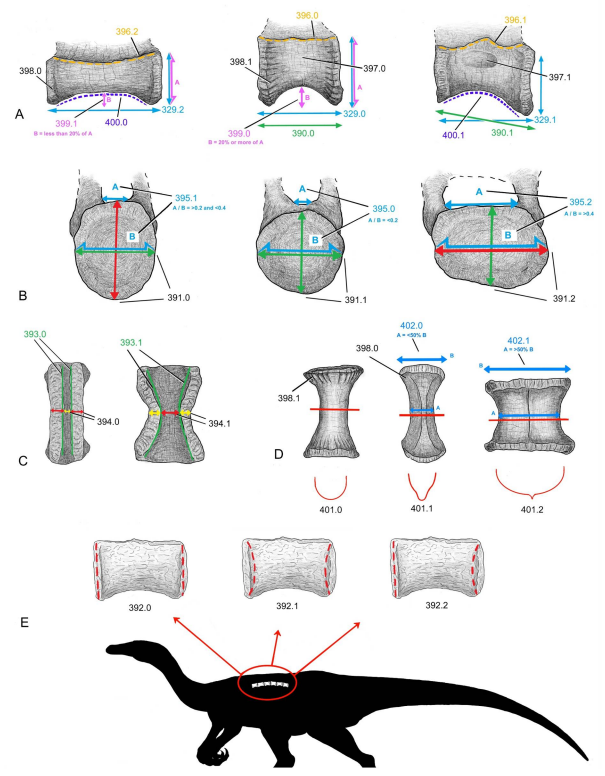
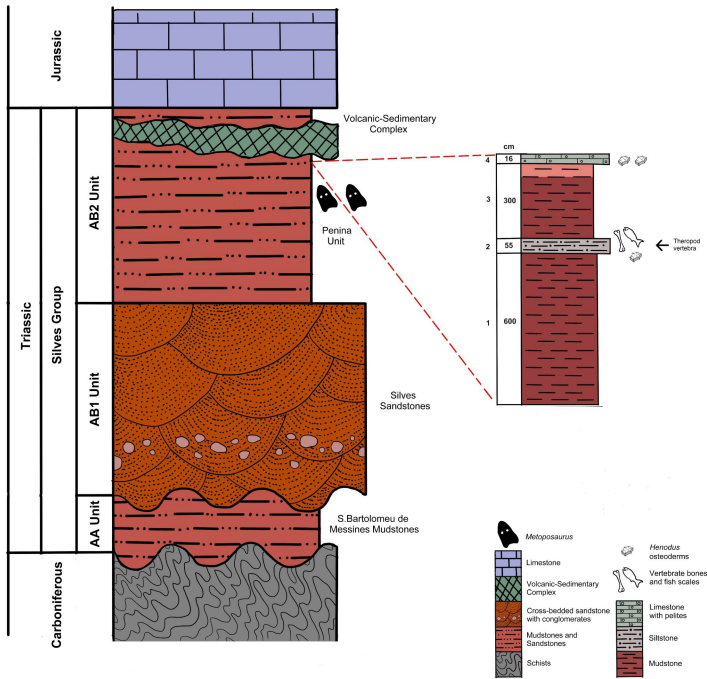
-

O terópode *Ceratosaurus* do Jurássico Superior da Formação da Lourinhã foi previamente descrito em duas ocasiões separadas, cada uma abordando um conjunto diferente de ossos pertencentes ao mesmo indivíduo. Com novos elementos a aguardar descrição, este trabalho procura compilar e descrever todo este material. Análise filogenética com base em espécie, introduzindo 37 novos caracteres, compara este espécime com os *Ceratosaurus* norte americanos e solidifica a sua posição próxima a este género.

Palavras-chave: Terópode, Filogenia, Triássico, Jurássico, Bacia Algarvia, Formação da Lourinhã, *Ceratosaurus*.

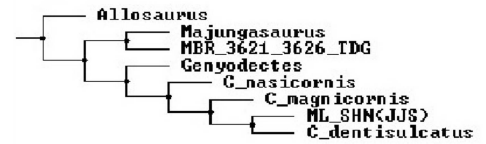
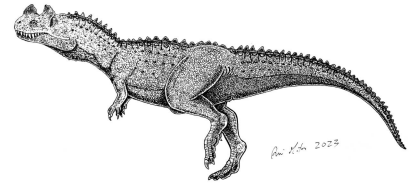
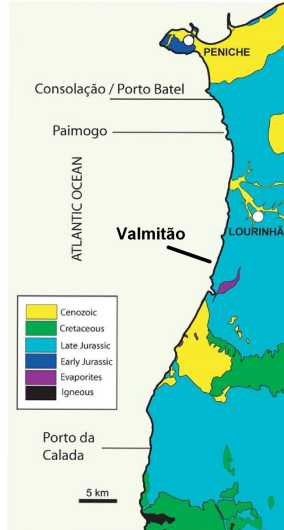
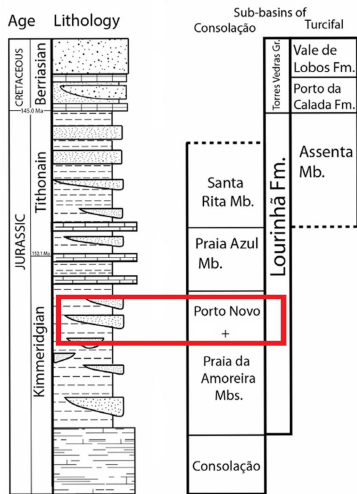
Graphical abstract

Chapter I - Early theropod from the Triassic of Grés de Silves



Graphical abstract

Chapter II - The theropod dinosaur *Ceratosaurus* from the Upper Jurassic of Lourinhã Formation



Institutional Abbreviations

Chapter I: NOVA-FCT-DCT – Universidade NOVA de Lisboa, Faculdade de Ciências e Tecnologia, Departamento de Ciências da Terra, Monte da Caparica, Setúbal, Portugal; **WARMS** - Warwickshire Museum, Warwick, UK; **SMF** - Sauriermuseum Frick, Frick, Switzerland; **UNL** – Universidade NOVA de Lisboa, Lisboa, Portugal.

Chapter II: BYU – Brigham University (Earth Science Museum), Provo, Utah, United States; **DNM** – Dinosaur National Monument, Jensen, Utah, United States; **JJS** – José Joaquim dos Santos (coleção); **MWC** – Museum of Western Colorado, Grand Junction, Colorado, United States; **ML** – Museu da Lourinhã, Lourinhã, Portugal; **SHN** – Sociedade de História Natural (de Torres Vedras), Torres Vedras, Portugal; **UMNH** – Utah Museum of Natural History, University of Utah, Salt Lake City, Utah, United States; **USNM** – United States National Museum (Smithsonian Institution), Washington DC, United States, **VP** – Vertebrate Paleontology.

Contents

Chapter I - Early theropod from the Triassic of Grés de Silves.....	12
Introduction.....	12
Early theropod evolution, findings, history, problematics.....	12
Theropods in Portugal.....	13
Triassic vertebrates and Silves Group paleofauna.....	13
Geologic context.....	15
Algarve Basin.....	15
Silves Group.....	16
Materials and Methods.....	22
Systematic Paleontology.....	22
Locality.....	22
Horizon and Age.....	22
Material Description.....	23
Measurements.....	23
Comparative anatomy.....	25
Comparison with other taxa.....	25
Phytosauria.....	25
Ornithosuchidae.....	26
Shuvosauridae.....	27
Silesauridae.....	28
Basal Sauropodomorpha.....	30
Herrerasauridae.....	33
Basal Theropoda.....	35
Coelophysoidea.....	36
Coelophysidae.....	40
Derived Neotheropoda.....	43
Comparative anatomy (<i>Sarcosaurus</i> and <i>Notatesseraeraptor</i>).....	48
Phylogenetic analysis.....	49
Phylogenetic analysis with Ezcurra et al. 2023 matrix.....	57
Phylogenetic analysis with Zahner and Brinkmann (2019) matrix.....	59
Discussion.....	61
Conclusions.....	62
Chapter II - The theropod dinosaur <i>Ceratosaurus</i> from the Upper Jurassic of Lourinhã Formation.....	63
Introduction.....	63
<i>Ceratosaurus</i> overview.....	63
History of <i>Ceratosaurus</i> study.....	64
<i>Ceratosaurus</i> closest relatives.....	65
Ceratosauria: history of study and major evolution (Abelisauridae and Noasauridae).....	66
Ceratosauria problematics and misconceptions.....	68
<i>Ceratosaurus</i> paleobiology.....	69
Major contributors for the <i>Ceratosaurus</i> study.....	71
<i>Ceratosaurus</i> in Portugal.....	73
Dinosaurs from the Late Jurassic of Portugal.....	74

The Lusitanian Basin and Lourinhã Formation.....	75
<i>Ceratosaurus</i> species – material, main characteristics and diagnosis.....	79
<i>Ceratosaurus nasicornis</i> Marsh, 1884.....	79
<i>Ceratosaurus magnicornis</i> Madsen & Welles, 2000.....	80
<i>Ceratosaurus dentisulcatus</i> Madsen & Welles, 2000.....	81
Materials and Methods.....	82
Systematic Paleontology.....	82
Locality.....	83
Horizon and Age.....	83
Material Description.....	84
Cervical Vertebra.....	84
Sacral Vertebra.....	87
Femora.....	89
Tibiae.....	94
Fibulae.....	99
Osteoderm.....	102
Measurements.....	104
Additional <i>Ceratosaurus</i> material.....	105
Comparative anatomy (comparison with the other <i>Ceratosaurus</i>).....	109
Phylogenetic specimen-based analysis.....	117
New characters.....	125
Discussion.....	143
Comparative anatomy.....	143
Specimen-based analysis.....	144
Ontogeny.....	146
Conclusions.....	147
References cited.....	148
Chapter I - Early theropod from the Triassic of Grés de Silves.....	148
Chapter II - Theropod dinosaur <i>Ceratosaurus</i> from Upper Jurassic of Lourinhã Formation.....	157
Appendix I - Tooth Plates.....	168
Appendix II – Bone illustrations (for compared anatomy).....	191
Appendix III – Matrices and List of Characters.....	202
Character list for the new matrix based on Ezcurra et al. (2023), after Nesbitt et al. (2009).....	202
Matrix for the phylogenetic analysis with Ezcurra et al. 2023 data.....	218
Character list for the new matrix based on Zahner and Brinkmann (2019).....	227
Matrix for the phylogenetic analysis with Zahner and Brinkmann (2019) data.....	251
Character list for <i>Ceratosaurus</i> specimen-based analysis based on Cau (2024).....	255
Matrix for the <i>Ceratosaurus</i> specimen-based analysis (modified after Cau 2024).....	263

Author remarks

The general subject of this dissertation is the description of basal theropod material from Portugal. Since the studied elements came from different taxonomic groups, different locations and from different geologic periods, this work was divided in two chapters: starting with the stratigraphical older “Early theropod from the Triassic of Grés de Silves” and then “Theropod dinosaur *Ceratosaurus* from the Upper Jurassic of Lourinhã Formation”. Figure numbering follows in sequence from Chapter I to Chapter II. Citations section is divided in two, one for each chapter, both at the end of the document.

Portuguese *Ceratosaurus* material is separated in two institutions with two different serial numbers for the same individual: ML352 in the Lourinhã Museum and SHN(JJS)065 for Sociedade de História Natural de Torres Vedras. To simplify and avoid confusion, this specimen as a whole is referred to as ML352/SHN(JJS)065 throughout the document, except when reference to a specific element is made.

All images and illustrations were created or modified by the author, except where source is noted.

Chapter I - Early theropod from the Triassic of Grés de Silves

Introduction

Early theropod evolution, findings, history, problematics

Late Triassic saw the rise of dinosaurs and one of the first groups to diversify and expand over the world were the carnivorous theropods.

Among the first meat-eating dinosaurs were the herrerasaurids, small to medium sized predators that were particularly common in the Southern hemisphere, from which *Herrerasaurus ischigualastensis* is the most notorious member (Novas, 1992). However, the phylogenetic relationships of these animals has been controversial, with some authors placing them within Theropoda (Nesbitt et al., 2009; Sues et al., 2011) but others finding the two groups unrelated (Brinkman & Sues, 1987; Novas, 1992; Ezcurra, 2010; Novas et al., 2010; Baron et al., 2017; Baron & Williams, 2018; Cau, 2018).

The first definitive basal theropods include North American taxa such as *Tawa hallae* (Nesbitt et al., 2009; Ezcurra & Brusatte, 2011; Baron et al., 2017) and South America's *Eodromaeus murphi* (Martinez et al., 2011; Baron et al., 2017). These taxa helped shed some light on early theropod evolution, which for sometime was mainly known through the more advanced coelophysoids such as *Coelophysis bauri* (Cope, 1889) and *Procompsognathus triassicus* (Fraas, 1913).

Coelophysoidea were a branch of more derived theropods which together with Ceratosauria and Tetanurae form the clade Neotheropoda (Bakker, 1986; Sereno, 1998; Rauhut, 2000; Ezcurra & Cuny, 2007; Hendrickx et al., 2015). Coelophysoids, common in Late Triassic and Early Jurassic, marked the first expansion of neotheropods (Carrano & Sampson, 2004; You et al., 2014; Martínez & Apaldetti, 2017) and taxa such as *Coelophysis bauri* are among the most studied and well known Mesozoic dinosaurs with hundreds of individuals of different ages found in a mass grave site from Ghost Ranch New Mexico (Colbert, 1989; Rinehart et al., 2009). In Europe this group is best represented by Germany's Late Triassic taxa such as *Procompsognathus triassicus* (Ezcurra & Novas, 2007; Knoll, 2008) and, according to some studies, by *Liliensternus liliensterni* (Smith et al., 2007; Ezcurra et al., 2020), as well as several other fragmentary taxa (Rauhut & Hungerbühler, 1998). While for some time coelophysoids were regarded as ceratosaurs (Gauthier, 1986), recent studies do not found the two groups closely related (Rauhut, 2000; Carrano & Sampson, 2008).

The first non-coelophysoid neotheropods likely arose by the Late Triassic if taxa such as *Zupaysaurus rougieri*, *Liliensternus liliensterni* or *Gojirasaurus quayi* are within this branch (Smith et al., 2007; Nesbitt et al., 2009; Sues et al., 2011; Marsh et al., 2019; Zahner & Brinkmann, 2019; Ezcurra et al., 2020). This group would eventually give rise to the dominant terrestrial predators of the Jurassic and Cretaceous, namely, the ceratosaurs and tetanurans.

The recently described *Notatesseraeraptor frickensis* from Late Triassic of Switzerland is one of the most complete theropods from Europe and apparently belonged to this branch as well (Zahner & Brinkmann, 2019).

The Early Jurassic was marked by an increased diversification of neotheropods, with one of the largest and most well known being North America's *Dilophosaurus*. Together with some of its relatives, such as South Africa's *Dracovenator* or Asia's *Sinosaurus*, the group would achieve worldwide distribution (Young, 1940; Welles, 1954; Welles, 1970; Marsh & Rowe, 2020; Yates, 2005; Zhang et al., 2023).

In Europe, one of the earliest Jurassic neotheropods is the genus *Sarcosaurus*, a small to medium size predator, dated from the Hettangian-Sinemurian (199-196 Ma), initially regarded as a coelophysoid (Carrano & Sampson, 2004), but more recent analysis placing it as a basal non-coelophysoid neotheropod (Ezcurra et al., 2020). The holotype species, *Sarcosaurus woodi*, was described by Andrews in 1921 based on fragmentary remains: isolated vertebra, pelvic elements and an upper femur (Andrews, 1921). A second species, *Sarcosaurus andrewsi*, was later named based on a tibia (Huene, 1932). In 2020, all these elements, including additional material referred as WARMS G667-690 (isolated dorsal and caudal vertebrae, rib fragments, pelvic fragments and hindlimbs), were lumped together as a single species *Sarcosaurus woodi* (Ezcurra et al., 2020).

More recently, a single vertebral centrum recovered from the Upper Triassic Silves Group in Algarve, Portugal, might give new insights about theropod early evolution.

Theropods in Portugal

Portugal is famous for its rich dinosaurian fauna, specially theropods from the Upper Jurassic (Kimmeridgian/Tithonian) Lusitanian Basin, with taxa from various groups including: the ceratosaur *Ceratosaurus* sp., the megalosauroid *Torvosaurus gurneyi*, the allosauroids *Lourinhanosaurus antunesi*, *Allosaurus europaeus* and *Lusovenator santosi*, the coelurosaur *Aviatyrannis jurassica* and some isolated teeth attributed to several taxa such as cf. *Richardoestesia* sp., cf. *Compsognathus* sp., *Euronychodon portucalensis*, aff. *Paronychodon* sp. and cf. *Archaeopteryx* sp. (Antunes & Sigogneau-Russell, 1991; Mateus, 1998; Zinke, 1998; Pérez-Moreno et al., 1999; Mateus & Antunes, 2000; Antunes & Mateus, 2003; Rauhut, 2000; Mateus et al, 2006; Malafaia et al, 2010; Hendrickx & Mateus, 2014, Malafaia et al, 2015; Malafaia et al, 2017a, 2017b, 2017c; Malafaia et al., 2019; Malafaia et al, 2020; Hendrickx et al., 2022).

Several nests with hundreds of eggs and some embryos are also part of the theropod fossil assemblage of Upper Jurassic Portugal, being most of them attributed to *Lourinhanosaurus* (Mateus et al, 1998; Mateus et al, 2001; Antunes & Mateus, 2003; Hendrickx et al., 2022) and some tentatively attributed to *Torvosaurus* (Araújo et al, 2013; Hendrickx & Mateus, 2014).

The Portuguese Jurassic theropod record is also made of several ichnofossil footprint tracks (Dantas et al., 1994; Antunes & Mateus, 2003; Mateus & Milàn, 2010; Hendrickx & Mateus, 2014; Santos et al., 2024).

The Cretaceous Portuguese theropod fauna is not as rich and diverse as in the Jurassic, yet, the recently described spinosaurid *Iberospinus natarioi* (Mateus & Estraviz-López, 2022) is worth mentioning, along with other fragmentary remains and footprints of undetermined taxa (Antunes & Mateus, 2003).

In comparison with Late Jurassic and Cretaceous, the Triassic and Early-Middle Jurassic dinosaur fauna from Portugal is rather poor.

The oldest, and only, dinosaurian bone material from the Early Jurassic Portugal is the basal thyreophoran *Lusitanosaurus liasicus*, from S.Pedro de Moel, with an estimated age dated to the Sinemurian (Lapparent & Zbyszewski, 1957; Antunes & Mateus, 2003). The Middle Jurassic is represented by ornithopod fragmentary remains and sauropod and theropod footprints (Thulborn, 1973; Santos et al., 1994; Antunes & Mateus, 2003).

Triassic rocks outcrop at the Silves Group of the Algarve Basin, in the southernmost region of Portugal and up until recently no dinosaur remains have been found there. Equivalent Triassic rocks can also be found in Anadia and Mealhada Municipalities, North of Coimbra. Isolated footprints, apparently of theropod origin, were reported from both localities in the 70's but eventually this information went unnoticed up until recently (Courbouleix, 1974; Palain, 1976).

Triassic vertebrates and Silves Group paleofauna

The Triassic was a remarkable period in Earth's history. After the worst recorded mass extinction, at the end of the Permian, had devastated almost all lifeforms due to climate change, nature eventually recovered and expanded in diversity, occupying every niche. Among vertebrates, diapsid reptiles were on the center stage of both dominance and innovation, replacing most of the mammal-like synapsids that dominated in the previous period (Tucker & Benton, 1982; Sahney & Benton, 2008; Benton, 2016; Ezcurra & Butler, 2018).

Triassic reptiles conquered air, land and sea, with all the major Mesozoic clades evolving in this period – aerial pterosaurs, terrestrial dinosaurs and pseudosuchians and aquatic sauropterygians (Ezcurra & Butler, 2018; Romano et al, 2020; Sues, 2024). The first true mammals arose by this time, as well as turtles, crocodiles, lizards and frogs, and some remnants of the Permian faunas could still be found - in the rivers, giant temnospondyl amphibians and in land, the synapsid dicynodonts (Benton, 2016; Romano et al., 2020; Sues, 2024).

The Triassic ended up in another mass extinction where many of the Triassic lineages went extinct - most notably, several pseudosuchian and synapsid groups - paving the way to the dominance of dinosaurs, pterosaurs and marine reptiles for the rest of the Mesozoic (Olsen et al., 1987; Benton, 1991; Benton, 1993). The Silves Group, in the Algarve Basin, has recently been giving some hindsight about the Upper Triassic vertebrate life in Portugal, with new taxa and new species being described such as temnospondyl amphibians like *Metoposaurus algarviensis* (Witzmann & Gassner, 2008; Brusatte et al. 2015), the identification of the first Portuguese phytosaur (Mateus et al., 2014), the sauropterygian placodont *Henodus*, as well as actinopterygian fish remains and the oldest evidence of hybodont sharks in Portuguese strata (Ruciński, 2020).

There are no known theropod bones from the Triassic of Portugal, but there are tracks. These were first reported in 1974 by Serge Courbouleix. He describes the first dinosaur tracks from the Triassic of Portugal. These are from the top of unit A of the Silves Group (Carnian) of Vacariça, in Mealhada municipality. Courbouleix (1974) advances “*In the Vacariça area, to the east of the Água-de-Cruzeiro enclosure wall [...] we found a possible footprint of a large dinosaur in these levels. The three digits are 20, 27 and 21 cm long. Their width is 19, 9 and 10 cm. The middle toe is offset forward in relation to the other two. The total length of the track is around 50 cm, with a maximum width of 40 cm. Unfortunately, this footprint is isolated, and only a trackway could remove the uncertainty of its origin.*”. There are no images, but the description and measurements are consistent with a large theropod track. Two years later, Palain (1976) reports vertebrate footprints in the same layers (Silves Group, top of AB1 unit) of Crasto de Anadia in Anadia Municipality. A photograph is supplied, but the identification is difficult, although consistent with theropod. Fifty years have passed since Courbouleix’s (1974) article, and his information has never been cited in any dinosaur research until now. The nowadays physical existence of these tracks is not known.

The first vertebrate bone remains (attributed to stegocephalians) were reported by Christian Palain in São Bartolomeu de Messines (Palain, 1976, 1977).

Suggested by Miguel Telles Antunes, the Russell couple (Donald and Denise) conducted a three-week paleontological prospection in the Triassic of Algarve, namely São Bartolomeu de Messines, in November 1976. There, they reported (Russell & Russell, 1977) stegocephalians (temnospondyls), without figuring, in the same layers where Christian Palain had also reported bones in his 1975 PhD Thesis, published one year later (Palain, 1976).

Recent visits to São Bartolomeu de Messines never reported temnospondyls but *Henodus* placodonts osteoderms are abundant. These osteoderms can be easily mistaken in the field for portions of temnospondyls skull roofs or shoulder shields.

In this work we complete the picture of the Silves Group vertebrate fauna with a vertebra element found in Loulé, Algarve with what might be the oldest Portuguese dinosaur remains ever found.

Geologic context

Algarve Basin

The Algarve Basin (fig. 1&2), located in the southern-most region of continental Portugal, consists of Meso-Cenozoic units stretching for about 140 km, from Cabo de São-Vicente at West, to Guadiana river in the East; and extending between 3 to 25 km from the South coastline Northwards into the mainland. It lays above Carboniferous igneous, sedimentary and metamorphic material from the Ossa-Morena/South Portuguese Zone. (Terrinha et al., 2006; Pereira et al., 2017; Ruciński, 2020).

The Carboniferous metamorphic sedimentary units and the Meso-Cenozoic sedimentary units are both separated by a 70 Ma hiatus and are both the result of two Wilson cycles: with the former being formed by the tectonic forces that led to the formation of Pangaea and the later resulting from the flattening of the continental landmasses of Africa, America and Eurasia when Pangaea started to fracture. (Terrinha et al., 2006; Ruciński, 2020).

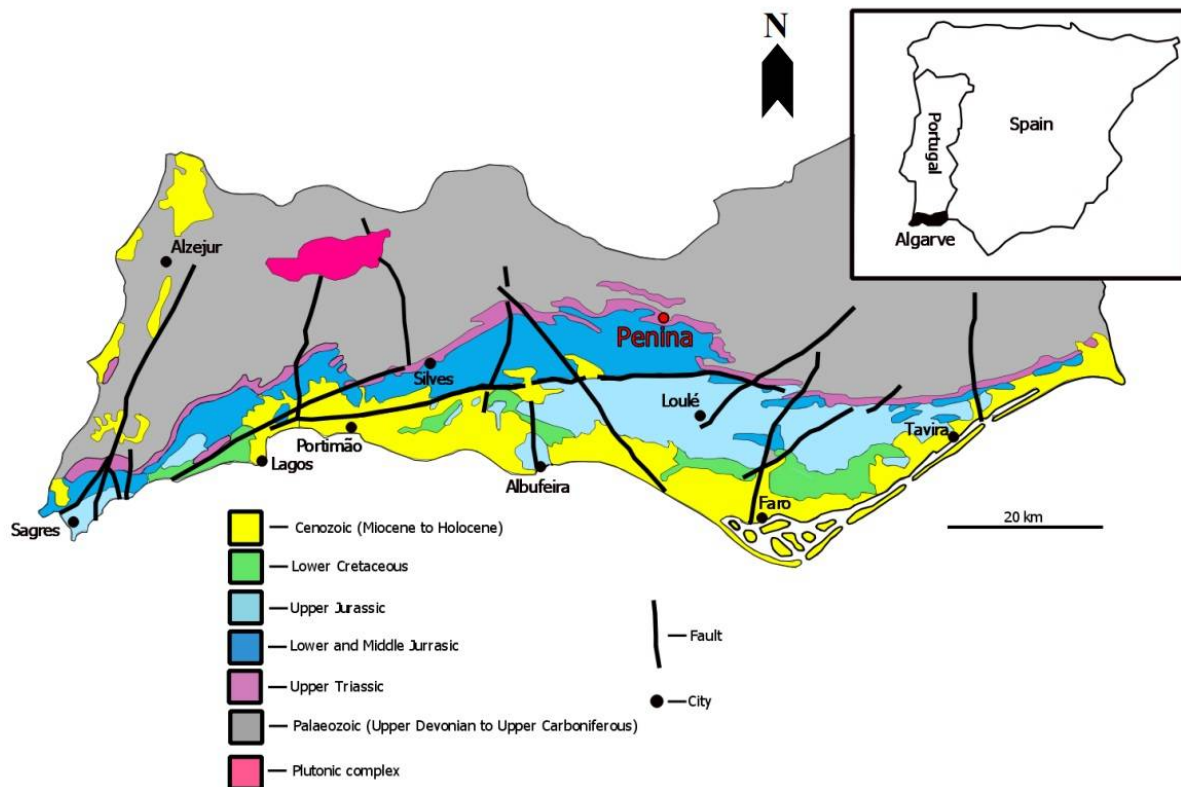


Figure 1. Geology of the Algarve basin. Source: Ruciński (2020).

For the formation of the Mesozoic units contributed both the forces related to the opening of the Central Atlantic and the genesis of oceanic crust related to the development of the Western Tethys Sea. In fact, both events played a key role throughout all the geologic history and evolution of the Algarve Basin due to its particular geographic position right between these seaways (Terrinha et al., 2002; Terrinha et al., 2006).

Sedimentation was uniform from the Early Triassic until the Lower Jurassic (Sinemurian), with the sedimentary environment throughout the Triassic shifting from a continental fluvial setting to a shallow marine one. The Triassic is here represented by the Silves Group, a sequence starting at the base with a layer of sandstone/conglomeratic rock and red pelites with fine intercalations of siltstone and dolomite, and the upper ones by red sandstones (Rocha, 1976; Terrinha et al., 2006; Pereira et al., 2017). The pelites are attributed by some authors to the Lower Triassic based on the presence of tetrapodomorph fragmentary remains in some of these units, whereas the red sandstones are attributed to the Upper Triassic due to the presence of the branchiopod *Euestheria* and vertebrate fossil assemblage (Terrinha et al., 2006; Mateus et al. 2014; Brusatte et al. 2015).

The Late Triassic is marked by the opening of the Atlantic which created a series of volcanic episodes and magma accumulation, commonly referred as Central Atlantic Magmatic Province (CAMP). This event resulted in the deposition of the volcanic siliciclastic complex from the latest Triassic to the earliest Jurassic rocks of the Algarve Basin (Palain, 1976; Manuppella, 1988; Nomade et al., 2007) and might have been the trigger of the Late Triassic mass extinction event (Nomade et al., 2007).

In the Lower Jurassic (Pliensbachian), the basin started to subdivide in two, with the West basin made of outer platform marine sediments and the East basin made of inner platform marine ones. This event lasted until the Callovian-Tithonian uplifting episodes and left a complicated stratigraphy in the limestones and marls that built the Jurassic of this region. In the Cretaceous, the basin is more uniform, and consequently, the stratigraphy is simpler with successions of mostly limestones and marls (Rocha, 1976; Terrinha et al., 2006).

Another 70 Ma hiatus takes place after the Cenomanian, with the Cenozoic being first represented by the Miocene. This hiatus is the result of a massive shift in the tectonic dynamics of the region during the Upper Cretaceous, which resulted in the end of the rift-type stretching of the Algarve Basin. In some areas the hiatus is longer than 70 Ma, with the Miocene overlaying older Mesozoic and Paleozoic units. These Neogene sequences are characterized by older carbonated and siliciclastic layers with several macrofossils, mostly in West Algarve; and younger siliciclastic sandstones with high grain size variability, mostly in the East (Terrinha et al., 2006; Ruciński, 2020).

The geology of the region can be easily understood in the region's general topography, with the older, harder Paleozoic and Mesozoic rocks forming an erosion resistant mountain plateau in the interior and the younger and less resistant Neogene sandstones forming a lower topographic planar landscape towards the coast (Octavio Mateus, pers. communication and pers. observation).

Silves Group

The Silves Group was first named by Choffat (1887), without a formal ranking (formation or other) as was usual at the time, being erected to Group (Grés de Silves Group) by Soares et al. (1985).

Stratigraphy of the Group (fig. 2) has been interpreted in different ways by authors (Palain, 1976; Manuppella, 1988; Terrinha et al., 2006; Pereira et al., 2017; Ruciński, 2020) with the age interval, depending on the author, starting either on the Lower or Upper Triassic and ending on the Lower Jurassic (Ruciński, 2020).

A correlation between the Algarve and Lusitanian basins can also be made at the Silves Group level (fig. 2), with different interpretations and nomenclature been given throughout its research history (Choffat, 1887,1894; Palain, 1976,1979; Soares et al., 1985, 2012; Manuppella, 1988; Rocha et al., 1990).

Starting at the base, an angular unconformity separates the Mesozoic from the folded South Portuguese Zone Paleozoic rocks where Carboniferous turbidites can be found.

The first level of the Silves Group is represented by the oldest Silves Sandstones (level AA in Palain (1976) and São Bartolomeu de Messines Mudstones in Manuppella (1988)) with a 100m thick unit of reddish brown mudstone with siltstones intercalations.

Above it, the sequence transitions to layers of reddish to yellowish fine to coarse grained sandstones intercalated with varied sized clast and matrix supported conglomerates and pelites (level AB1 in Palain (1976) and Upper Silves Sandstones in Manuppella (1988)) 25 to 70m thick and Carnian in age (Palain, 1976; Manuppella, 1988; Pereira et al., 2017; Ruciński, 2020).

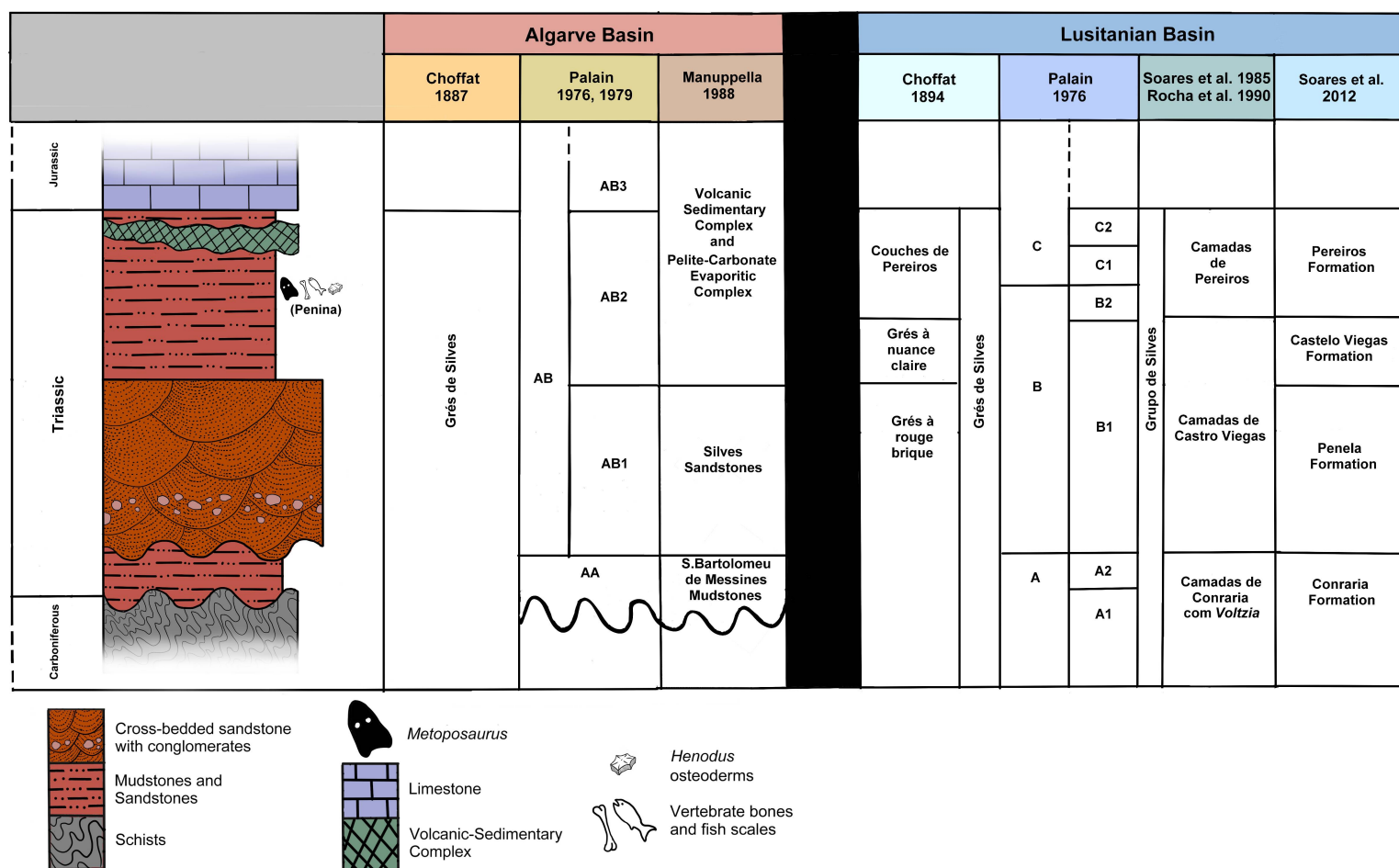


Figure 2. Schematic representation of the general stratigraphy of the Triassic in the Algarve Basin; the nomenclature by Choffat (1887), Palain (1976, 1979) and Manuppella (1988) and comparison with the different interpretations of equivalent sequences in the Lusitanian Basin by Choffat (1894), Palain (1976), Soares et al. (1985, 2012) and Rocha et al., (1990).

The stratigraphic and sedimentary information of the Upper Triassic terrigenous layers show these units were deposited in a continental rift setting with semi-arid climate, suitable for the formation of evaporites. The region was filled with alluvial fans and, between these, river and alluvial plains with temporary meandering rivers completed the sedimentary depositional environment (Palain, 1976; Azerêdo et al., 2003; Pereira et al., 2017). In the uppermost layers, a transition to shallow lagoon and/or marine/coastal influenced environment is apparent (Ruciński, 2020).

The next level, the Pelite-Carbonate-Evaporitic Complex, is defined by Manuppella (1988) as a single unit showing a transition from Triassic pelites intercalated with sandstones, dolostones and evaporites, 2-100m thick, to Lower Jurassic (Hettangian) pelitic dolostone, 5-15m thick. Palain (1976) separated this transition in two different units, AB2 for the Triassic pelites and AB3 for the Jurassic.

The upper part of the sandstone units of the Silves Group (AB2) was for some time considered as transitory from Upper Triassic (Rhaetian) to the Lower Jurassic (Hettangian) (Palain 1979), but this has recently been put into question. A precise isotopic dating is needed because the basalt stratigraphic correlates from North Africa and North America, as well as the vertebrate fossil assemblage and palynological association, suggests a Late Triassic (Late Carnian or Early Norian) age estimate (Blackburn et al. 2013; Mateus et al. 2014; Brusatte et al. 2015; Pereira et al., 2017; Vilas-Boas et al., 2024).

The transition from the Triassic to the Jurassic is characterized by the beginning of the marine transgression, with the stratigraphic and sedimentary sequence revealing a shallow marine/coastal lagoon depositional environment (Azerêdo et al., 2003; Pereira et al., 2017).

The last unit of the Silves Group is the Lower Jurassic (Hettangian-Sinemurian) Volcanic Sedimentary Complex with carbonates, dolomites and volcanic rocks (Palain, 1976; Manuppella, 1988; Pereira et al., 2017; Ruciński, 2020).

In his Master's thesis, Ruciński (2020) worked on three areas of the Silves Group at Penina locality, with the material here reported, NOVA-FCT-DCT-5562, being found near station number three.

This outcrop, located in the Penina Sul (South Penina) area, consists of a near 10 meter thick sequence of mudstones and siltstones (fig. 3) tilted about 25 degrees southward. The lowermost layer, measuring six meters, is mainly made of brownish red mudstones to siltstones, lacking fossil content. The upper next layer (fig. 3) is a 55 centimeter unit of greyish siltstone with high moscovite concentration in certain areas. Small sized fossil content is abundant along this unit, being unevenly distributed horizontally and consisting mainly of small fish scales and other unidentified material. NOVA-FCT-DCT-5562 was found among the debris at the bottom of the outcrop but likely came from this unit.

The uppermost layers consists of a three meter thick brownish red (pinkish near the top) mudstone without fossil remains and, above it, the outcrop ends in a 16 centimeter thick whitish to greenish grey carbonated unit with peloids and some *Henodus* shell fragments.

This whole sedimentary sequence seems to be younger than the *Metoposaurus algarviensis* and phytosaur units based on field view correlations (fig. 3&4).

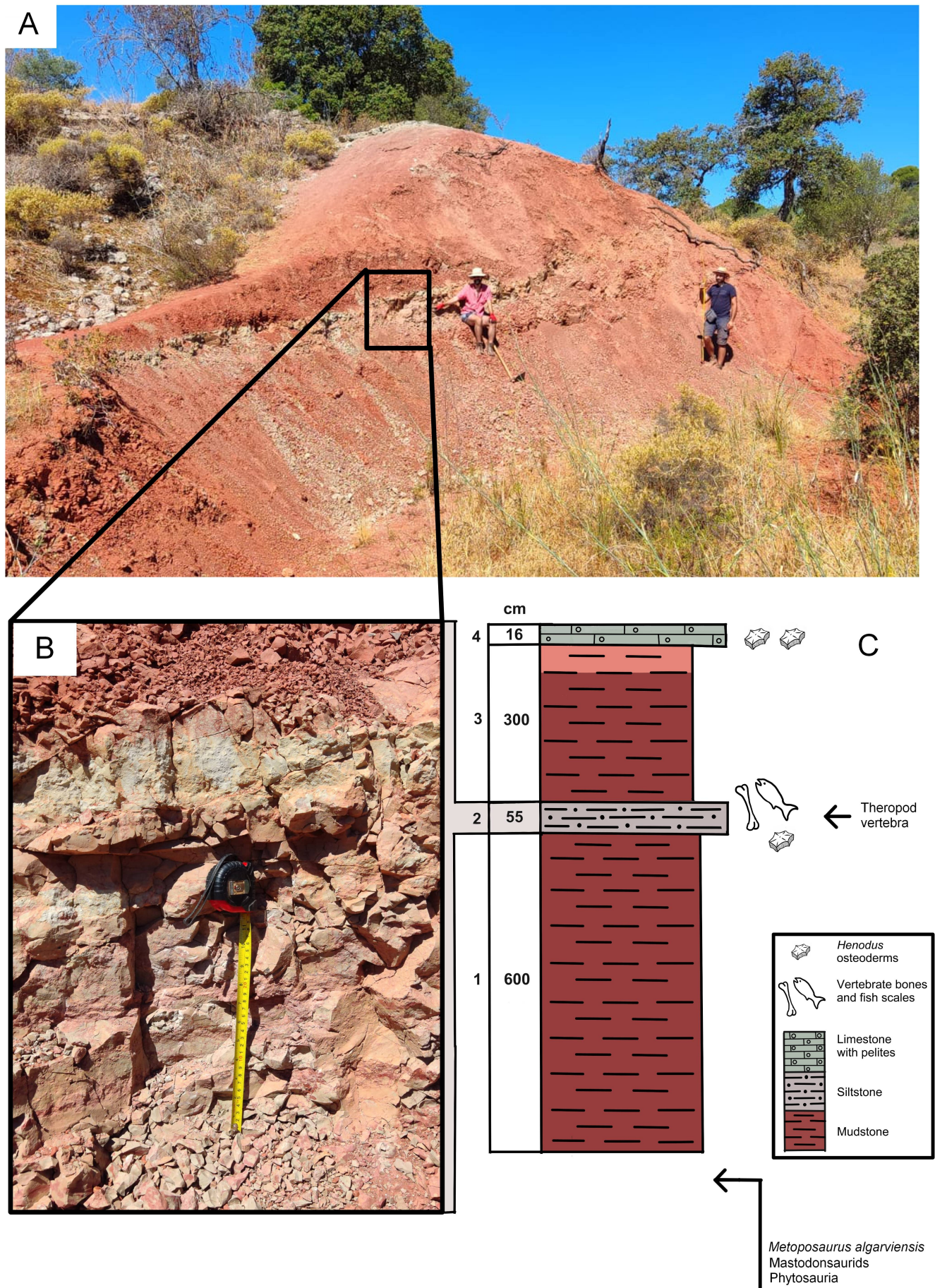


Figure 3. Penina Sul outcrop of the Silves Group, (A) general outcrop view, (B) detail of the fossiliferous layer where NOVA-FCT-DCT-5562 was found, (C) stratigraphy of the Penina Sul outcrop.

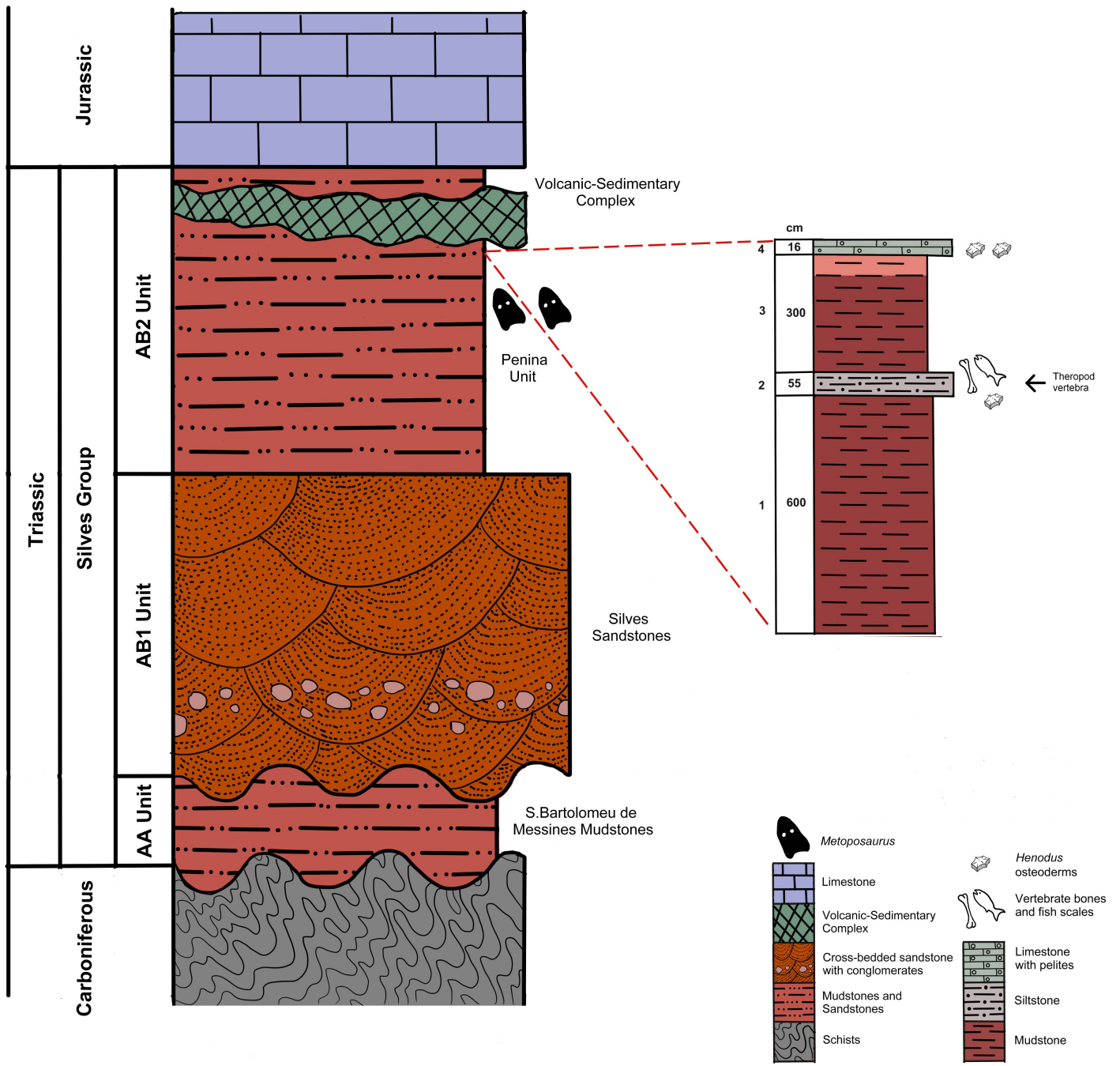


Figure 4. Silves Group stratigraphy. **(Left)** General Stratigraphy of the Silves group, based on Brusatte et al. (2015) and Ruciński (2020), **(Right)** Penina Sul stratigraphy and its position within the Silves Group.

Triassic rocks also outcrop in Anadia and Mealhada localities at Center-North Portugal. These units are lithologically and stratigraphically similar and correlated to those found in Triassic Algarve (fig. 2&5), being considered part of the Silves Group (Palain, 1976, 1979).

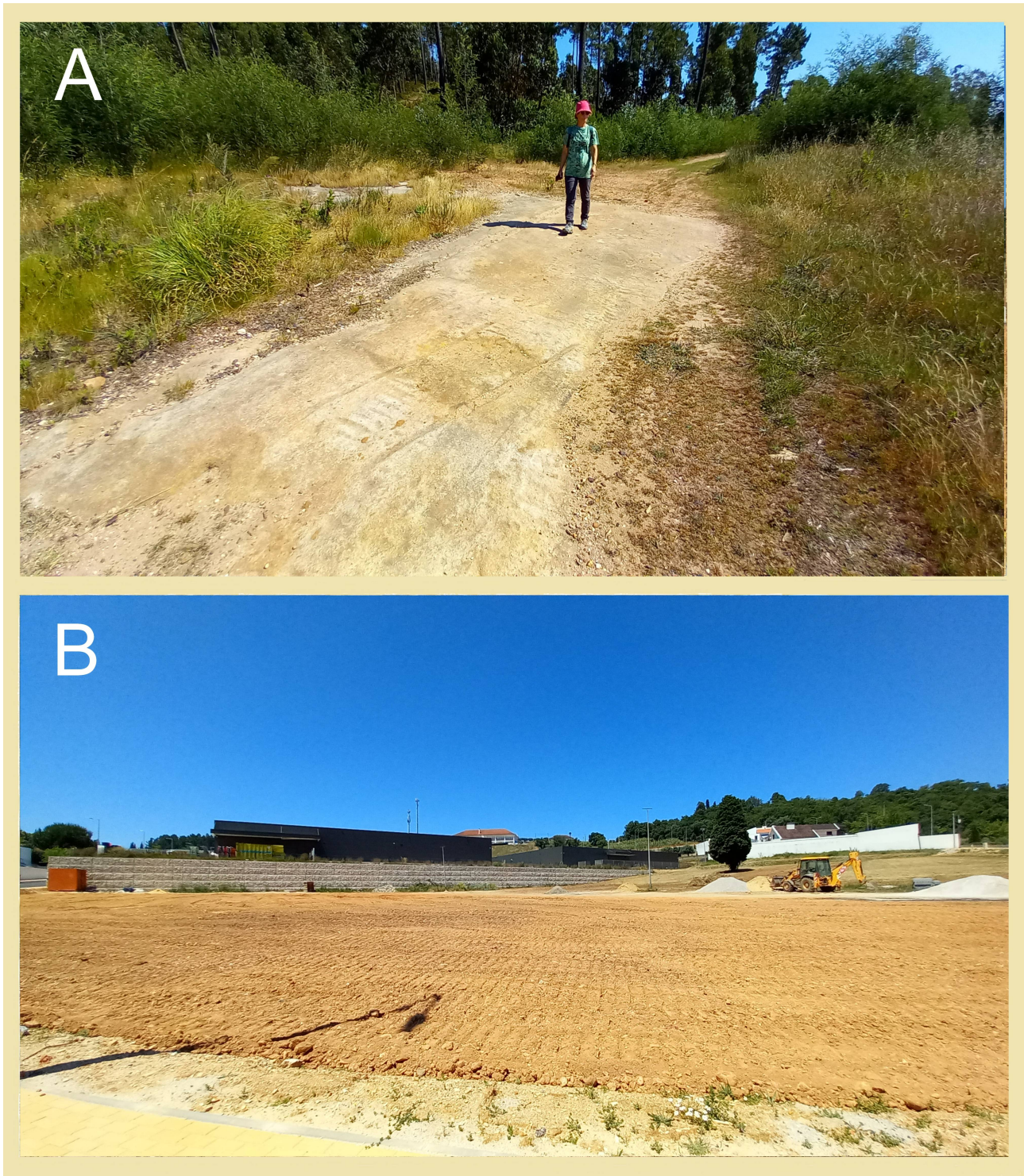


Figure 5. (A) Triassic outcrop at Vacariça, Mealhada; (B) remains of Triassic outcrop at Crasto da Anadia.

Materials and Methods

The focus of this study is a single isolated vertebra centrum, NOVA-FCT-DCT-5562, located at Departamento de Ciências da Terra, Faculdade de Ciências e Tecnologia, Universidade NOVA de Lisboa (DCT FCT UNL).

For the compared anatomy, extensive bibliographic research was made in order to find as most Triassic archosaur dorsal vertebrae images and descriptions as possible.

For the phylogenetic analysis two matrices were used, one from Nesbitt et al. (2009) with the latest update by Ezcurra et al. (2023) and another by Zahner and Brinkmann, (2019). In order to properly analyze our material we needed more dorsal vertebrae related characters, so, 13 new entries were created and both matrices were updated for new characters across all taxa. All characters have the same weight. The phylogenetic analysis was performed in TNT version 1.6 (Goloboff & Morales, 2022) and a traditional search was employed with 1000 added sequences and 100 trees saved per replication via tree bisection reconnection (TBR). Consensus trees were obtained via Majority Rule with a 50% cut-off.

Systematic Paleontology

Archosauria Cope, 1869
Dinosauria Owen, 1942
Theropoda Marsh, 1981
Neotheropoda Bakker, 1986
Neotheropoda gen.et sp. Indet.

Locality: The material was found in Penina Sul, Freguesia (administrative area equivalent to “Parrish”) of Salir, municipality of Loulé, Algarve, Southern Portugal (fig. 1). Approximated coordinates: 37.250°N, -8.108°W.

Horizon and Age: Silves Group, unnamed Formation, AB2 layer of the stratigraphic sequence (fig.2&4) which is dated Upper Triassic, Late Carnian-Early Norian, based on its vertebrate fauna (Mateus et al., 2014; Brusatte et al., 2015; Vilas-Boas et al., 2024).

Material Description

The single vertebra from Penina Sul, Loulé, Algarve only has the centrum preserved (fig. 6). The centrum does not show signs of major damage or deformation. The neurocentral suture is unfused and well defined, with the neural arch attachment points still visible. The layer sediment was covering the suture, evidence that the centrum was deposited and fossilized already without the neural arch attached.

The centrum is 37mm long and the articular surfaces are 26mm tall and 20mm wide (table 1). The length/height ratio is 1.42 and the height/width ratio is 1.3.

The articular facets are amphicoelous with an elliptical shaped outline in both anterior and posterior views. Both facets are about the same size. The concave articulation is funnel shaped and well defined on both ends, being 3mm deep on the anterior facet and 5mm deep on the posterior one.

In dorsal view, the articular facets are wider than the midcentrum. The lateral walls of the neural canal are each one 4 to 5mm thick being formed by the unfused parallel pedicels of the neurocentral suture, creating a rugous texture. The neural canal is about 2mm wide through the whole extent except on both ends where is slightly larger, with the anterior opening still wider than the posterior one. The neural canal becomes more deeply excavated towards the mid centrum.

In lateral view, the articular facets are vertical and taller than the midcentrum, with a flat dorsal surface and a concave ventral ridge. The curvature degree of the ventral ridge is about the same on both anterior and posterior halves. The texture of the lateral surface is smooth and there is no evidence of groves or pleurocoels.

In ventral view, the articular facets are also wider than the midcentrum but the concave curvature of the lateral walls is more pronounced than in dorsal view, with the midcentrum being less than half the width of the articular facets, giving the vertebra an hourglass shaped outline. Along the ventral midline, the antero-posterior ridge forms a smooth and subtle keel.

The vertebra is considered dorsal (mid or posterior) due to the our-shaped general outline and slender, elongated proportions with amphicoelous facet articulations. Other body positions were excluded based on the i) absence of paraphyseal facets typical of cervical vertebrae, ii) absence of lateral pleurocoels as in most anterior presacral vertebrae of neotheropods, iii) absence of rib attachments, fused elements or fused textures and proportions typical of sacral vertebrae, iv) absence of ventroposterior chevron connection facets typical of caudal vertebrae.

Measurements (mm)

	Max Height Centrum	Max Width Centrum	Max Length Centrum	Anterior Articular Facet Depth	Anterior Articular Facet Depth	Width Neural Canal	Width Neural Canal Lateral Walls
Dorsal	26	20	37	3	5	2	4-5

Table 1. Measurements for NOVA-FCT-DCT-5562

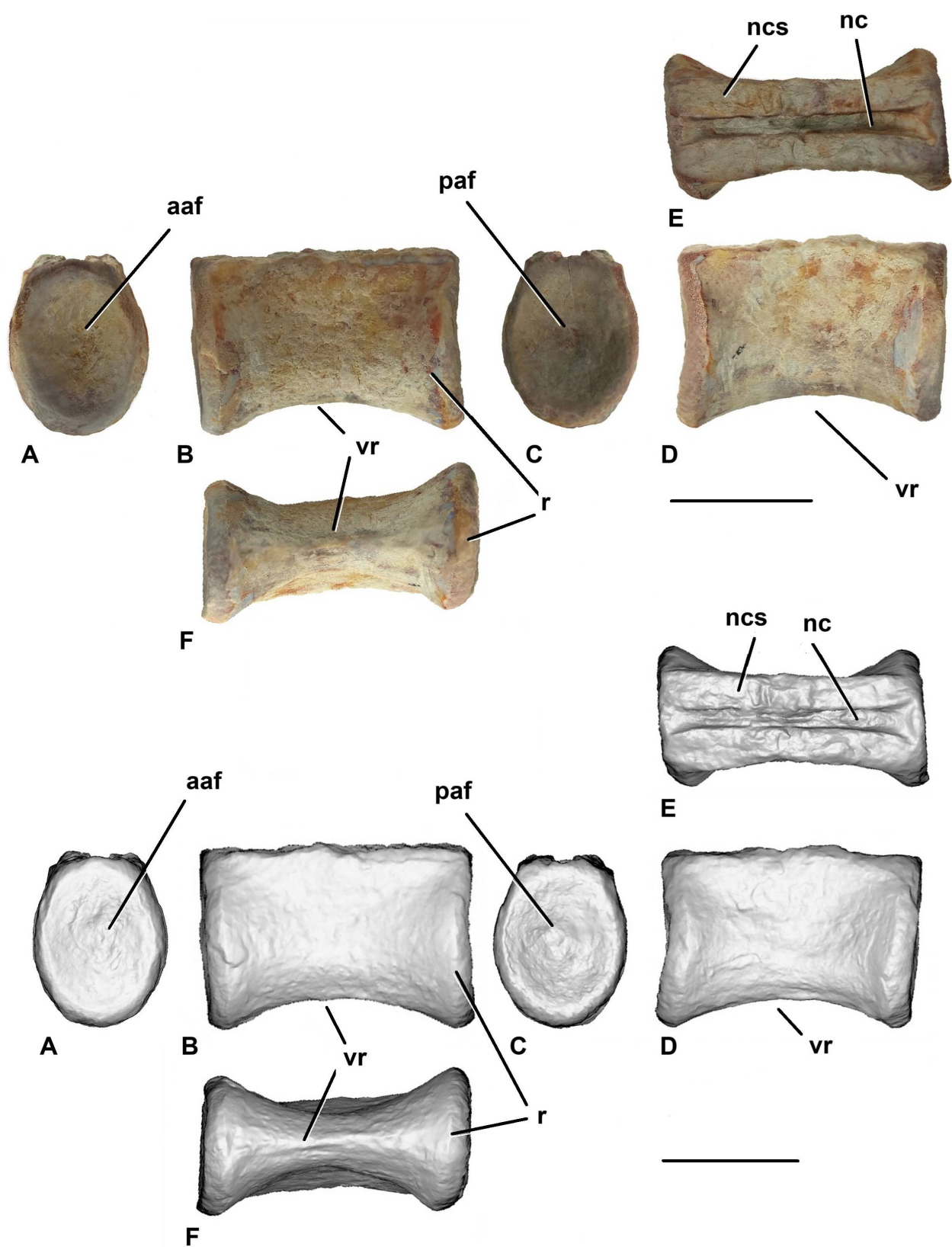


Figure 6. Dorsal vertebra centrum NOVA-FCT-DCT-5562 in anterior (A), left lateral (B), posterior (C), right lateral (D), dorsal (E) and ventral (F) views. Abbreviations: **aaf** – anterior articular facet, **paf** – posterior articular surface; **nc** – neural canal; **ncs** – neurocentral suture, **r**- rim, **vr** – ventral ridge. Scale bars: 20mm.

Comparative anatomy

Comparison with other taxa

In order to identify the closest taxonomic affinities of this material, a comparison was made with some Upper Triassic and Early Jurassic theropods and theropod-like archosaur groups which by their size, morphology, age or location might be considered relevant in the context of this analysis.

Phytosauria

Phytosaurs were, depending on the author, either a group of archosauriform (Nesbitt, 2011) or basal pseudosuchian (Sereno & Arcucci, 1990; Brusatte et al., 2010; Ezcurra, 2016) semi-aquatic reptiles from the Late Triassic that convergently evolved a body plan and lifestyle similar to that of today's crocodiles (Brusatte et al., 2010; Jones & Butler, 2018).

Comparing vertebrae of taxa such as *Myrstriosuchus* Fraas, 1896 (fig. 7) with NOVA-FCT-DCT-5562, the former tends to be anteroposteriorly shorter, the articular facets are less dorsoventrally elongated, the neurocentral suture is more curved and the neural canal at the midcentrum is also wider than its lateral walls.

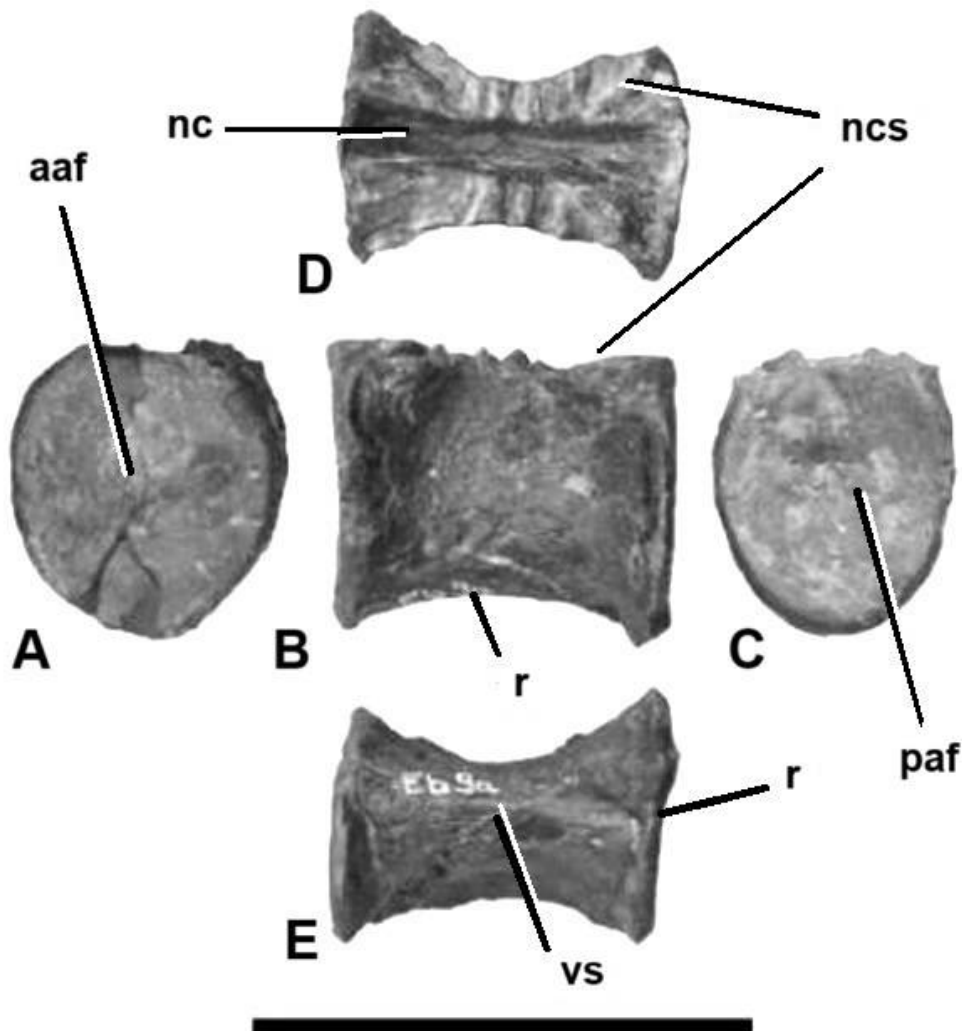


Figure 7. *Myrstriosuchus alleroi* specimen NHMD-916783 dorsal vertebrae in anterior (A), lateral (B), posterior (C), dorsal (D) and ventral (E). Source: López-Rojas et al., 2023. Abbreviations: **aaf** – anterior articular facet, **nc** – neural canal, **ncs** – neurocentral suture, **paf** – posterior articular facet, **r** – rim, **vs** – ventral surface. Scale bar equals 50mm.

Ornithosuchidae

Ornithosuchidae von Huene, 1908, was a clade of small to medium carnivore Pseudosuchians from the Triassic that superficially resembled medium sized theropods (Von Baczko & Ezcurra, 2013; Von Baczko et al., 2019).

Ornithosuchus woodwardi Newton, 1896 from Scotland was described in detail by Walker in 1964. Mid to posterior dorsal centra differ from NOVA-FCT-DCT-5562 in having more shallow concave articular facets with circular outline, the lateral facets are pinched-in just below the neurocentral suture and the ventral surface is keelless.

Von Baczko et al. (2019) described the postcranial anatomy of the Argentinian ornithosuchid *Riojasuchus tenuisiceps* Bonaparte, 1969 including some mid to dorsal centra (fig. 8). These differ from NOVA-FCT-DCT-5562 vertebrae by being as tall as they are long and the ventral keel is absent.

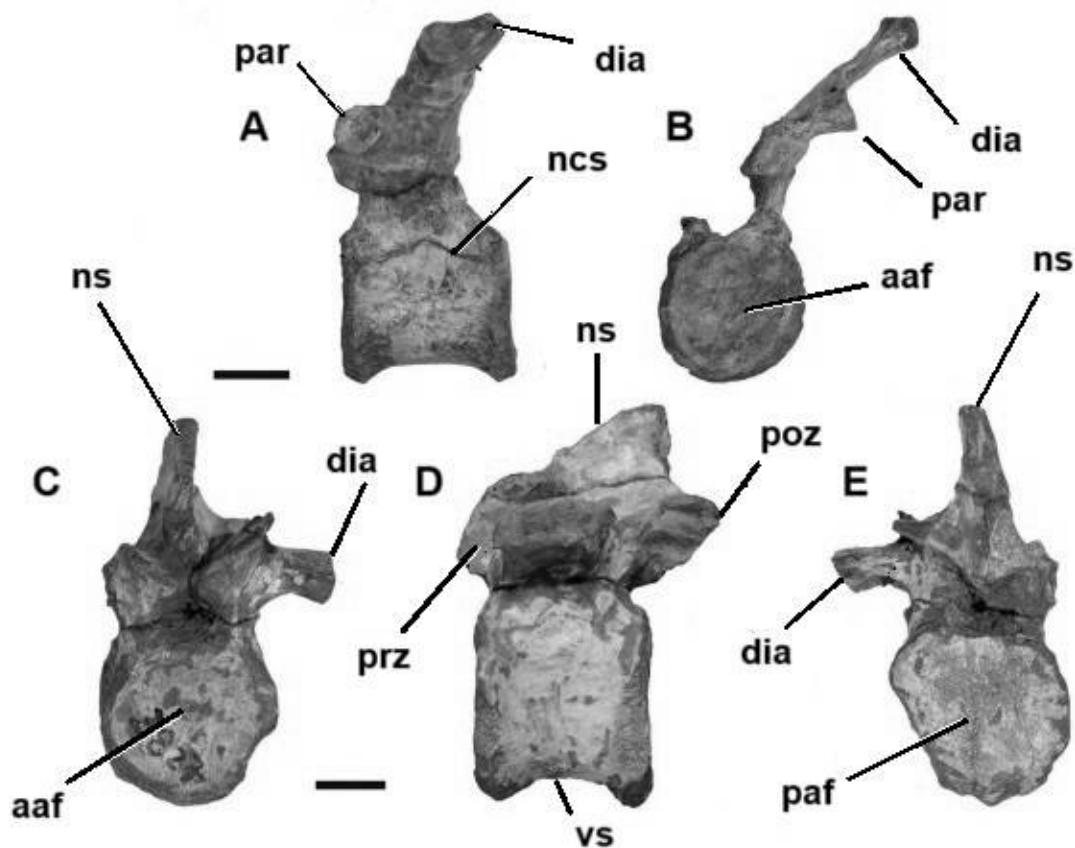


Figure 8. *Riojasuchus tenuisiceps* holotype specimen PVL 3827 posterior dorsal vertebrae in lateral (A) and anterior (B) views and last dorsal in anterior (C), lateral (D) and posterior (E) views. Source: Von Baczko et al., 2019. Abbreviations: **aaf** – anterior articular facet, **dia** – diapophysis, **ncs** – neurocentral suture, **ns** – neural spine, **paf** – posterior articular facet, **par** – parapophysis, **poz** – postzygapophysis, **prz** – prezygapophysis, **vr** – ventral surface. Scale bar equals 10mm.

Shuvosauridae

Shuvosauridae Chatterjee, 1993, were Triassic theropod-like poposauroid pseudosuchians including taxa such as *Shuvosaurus inexpectatus* Chatterjee, 1993, from Texas USA, or *Effigia okeeffeae* Nesbitt and Norell, 2007 (Nesbitt, 2007) from New Mexico USA. They were so similar to theropods that upon the first descriptions were classified as such (Chatterjee, 1993; Rauhut, 1997; Rauhut, 2000). Due to these similarities a comparison with the NOVA-FCT-DCT-5562 seems necessary. Should be noted that Nesbitt (2007) stated that generally *Shuvosaurus* and *Effigia* isolated dorsal vertebrae centra cannot be distinguished from those of Early theropods.

Shuvosaurus and *Effigia* dorsal vertebrae are amphicoelus with pronounced centrum rims like in the NOVA-FCT-DCT-5562 specimen, and the general outline shape is similar too. However, several characteristics such as a radiating pattern of small ridges directed from the edge of the centrum rim towards the center, shallow fossae between the centrum body and the neural canal are not found on the NOVA-FCT-DCT-5562 vertebra.

In *Effigia okeeffeae* (fig. 9), some of the vertebrae articulation facets have an oval shape but these are mediolaterally expanded, whereas in the NOVA-FCT-DCT-5562 specimen the expansion runs dorsoventrally. *Effigia okeeffeae* also has a well defined concave excavation in the ventral surface of the centra, but the curvature is more pronounced and there is no ventral keel. The dorsal vertebrae neural canal of *Effigia okeeffeae* also seems wider.

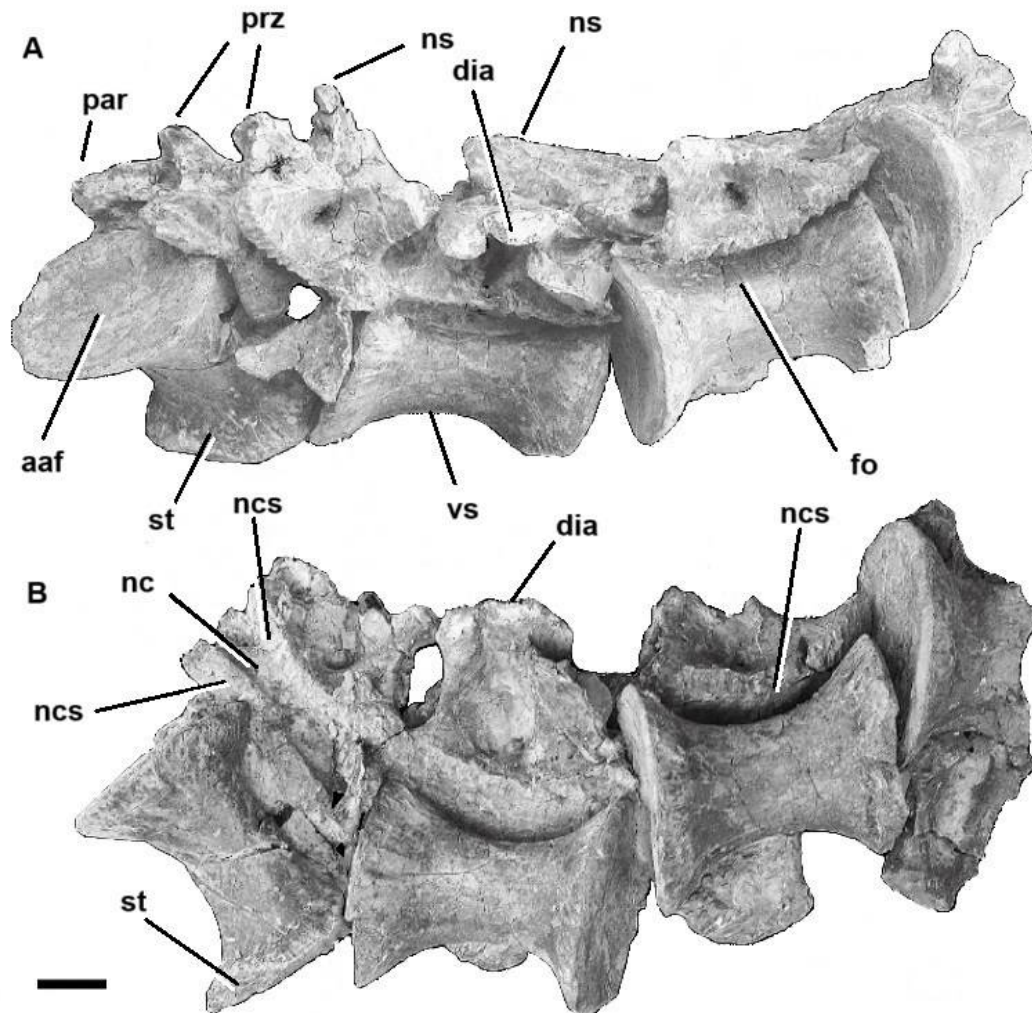


Figure 9. *Effigia okeeffeae* holotype specimen AMNH FR 30587 dorsal vertebrae in lateral (A) and ventral (B) views; Source: modified from Nesbitt, 2007. Abbreviations: **aaf** – anterior articular facet, **dia** – diapophysis, **fo** – fossa, **nc** – neural canal, **ncs** – neurocentral suture, **par** – parapophysis, **prz** – prezygapophysis, **st** – striation, **vs** – ventral surface. Scale bar equals 10mm.

Silesauridae

Silesauridae Langer et al., 2010, such as *Silesaurus opolensis* Dzik, 2003, were small bipedal to quadrupedal herbivorous and carnivorous avemetatarsalians from the Triassic, with most authors classifying them as dinosauriformes, sister group to Dinosauria (Nesbitt et al., 2010; Baron et al., 2017), but with others finding them as basal ornithischians (Müller & Garcia, 2020; Norman et al., 2022). Due to their shady taxonomic placement and relevancy for understanding early dinosaur evolution, a comparison with NOVA-FCT-DCT-5562 seems reasonable.

In 1999, Sullivan and Lucas described the silesaurid *Eucoelophysis baldwini*, from New Mexico USA, which included some fragmentary dorsal vertebrae. The authors pointed out the presence of a large and well defined pleurocoel on both sides between the articular ends; this feature is not found in NOVA-FCT-DCT-5562.

Piechowski and Dzik (2010) described Germany's *Silesaurus opolensis* axial skeleton in detail (fig. 10). Based on the description and images, the articulation of the dorsal centra is circular and slightly concave, whereas in NOVA-FCT-DCT-5562 is elliptical and the concavity more pronounced. The lateral surface of the centra has a shallow elliptical depression with a semicircular prominence along the upper rim; this is not found in NOVA-FCT-DCT-5562, which has a smooth lateral surface.

The dorsal centra of *Silesaurus opolensis* tend to decrease their length in relation to their height posteriorly. The vertebra with the closest length/height ratio to what is seen in NOVA-FCT-DCT-5562 is the 15th dorsal (fig. 10.C & 10.D), but the ventral curvature is slightly more pronounced in *Silesaurus opolensis* (even more in the other vertebra). Also, this curvature in *Silesaurus opolensis* generally is not as symmetrical antero-posteriorly as in NOVA-FCT-DCT-5562, with the closest one in this regard being again the 15th.

In 2020, Ezcurra et al. described a new specimen of the silesaurid *Lewisuchus admixtus* Romer, 1972, from Argentina, with two partial mid to posterior dorsal vertebrae (fig. 11). Compared with NOVA-FCT-DCT-5562, the centrum of *Lewisuchus admixtus* differs in being more robust, with articular facets slightly wider than tall, the neural canal is much wider relative to the overall centrum size and the ventral surface does not have a ventral keel.

Also in 2020, Nesbitt et al. described new material associated to the silesaurid *Asilisaurus kongwe* Nesbitt et al., 2010, from Tanzania, with the referred material including some dorsal vertebrae. The authors describe the articular surfaces as circular to slightly higher than broad, however not as much as we see in NOVA-FCT-DCT-5562. The ventral surface is also much less constricted and without a ventral keel.

To summarize, silesaurids in general do not seem a good match for NOVA-FCT-DCT-5562 vertebra. From the analyzed taxa, *Silesaurus opolensis* was found the most similar but the general shape and structure of most dorsal vertebra is still slightly different from NOVA-FCT-DCT-5562; the 15th shows most similarities but the articular facet is more circular and the ventral curvature slightly more pronounced.

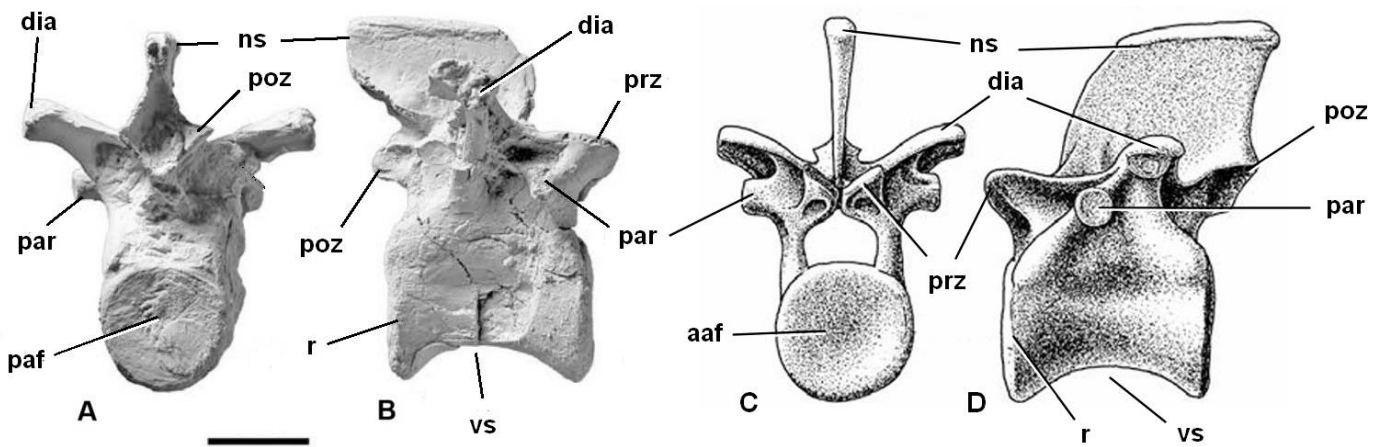


Figure 10. *Silesaurus opolensis* specimen ZPAL AbIII/ 362/11 dorsal 13 in posterior (A) view, ZPAL AbIII/1991 dorsal 14 in right lateral (B) view, ZPAL AbIII/1930 and 361 (based in) dorsal 15 in anterior (C) and left lateral (D) views. Source: Piechowski & Dzik, 2010. Abbreviations: **aaf** – anterior articular facet, **dia** – diapophysis, **ns** – neural spine, **paf** – posterior articular facet, **par** – parapophysis, **poz** – postzygapophysis, **prz** – prezygapophysis, **r** – rim, **vs** – ventral surface. Scale bar equals 10mm.

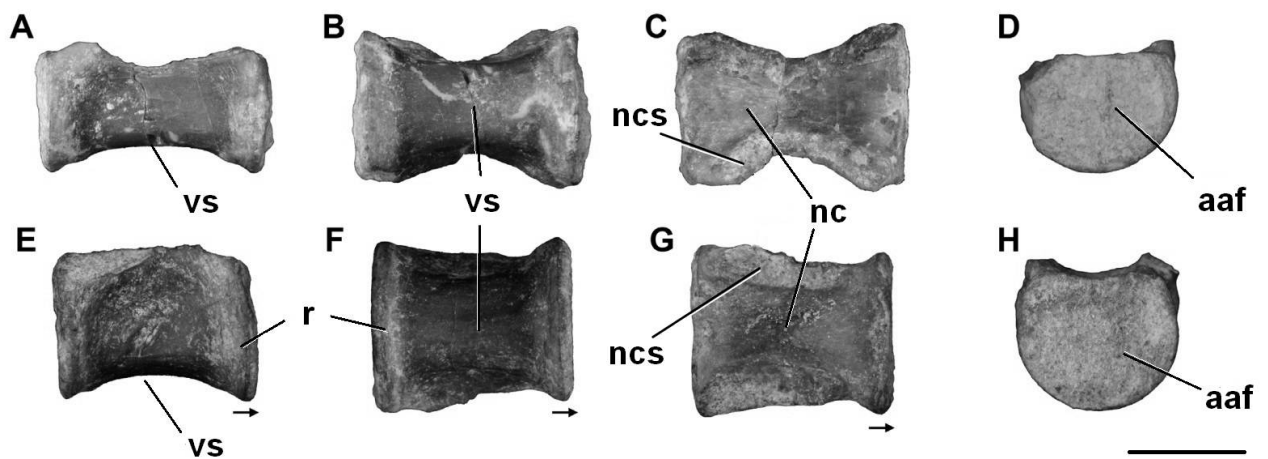


Figure 11. *Lewisuchus admixtus* specimen CRILAR-Pv 552 dorsal centra in lateral (A, E), ventral (B, F), dorsal (C, G), anterior (D, H). Source: Ezcurra et al., 2020. Abbreviations: **aaf** – anterior articular facet, **nc** – neural canal, **ncs** – neurocentral suture, **r** – rim, **vs** – ventral surface. Scale bar equals 5mm. Arrows point anteriorly.

Basal Sauropodomorpha

Sauropodomorpha Huene, 1932 includes the famous giant herbivorous long-necked sauropods, the biggest land animals to ever walk the Earth, however, their early evolution in the Upper Triassic revealed smaller, bipedal, carnivorous and omnivorous forms with body plans similar to those of early theropods (Heeren, 2011; Sander et al., 2011; Baron et al., 2017; Pol et al., 2021). Among the most basal sauropodomorphs are included taxa such as *Thecodontosaurus antiquus* Morris, 1843, *Eoraptor lunensis* Sereno et al., 1993, *Guaibasaurus candelariensis* Bonaparte et al., 1999, *Panphagia protos* Martinez & Alcober, 2009, *Pampadromaeus barberenai* Cabreira et al., 2011 or *Buriolestes schultzi* Cabreira et al., 2016.

Thecodontosaurus antiquus Morris, 1843 (fig. 12), from England, was re-examined in 2000 by Benton et al., including several dorsal vertebrae assigned to this species. They differ from NOVA-FCT-DCT-5562 material by being more robust, by having circular articular surfaces, by possessing a depression or groove along the lateral surface of the centrum and by having the ventral concave curvature more pronounced.

Re-described by Sereno et al. (2013), Argentinian sauropodomorph *Eoraptor lunensis* posterior dorsals (fig. 13) differ from NOVA-FCT-DCT-5562 in having circular articular facets not deeply concave, some neural canals expanding into the upper centra and the ventral curve runs deeper.

Guaibasaurus candelariensis (fig. 14) from Brazil, described by Bonaparte et al. (1999), has a dorsal vertebrae lateral outline shape similar to NOVA-FCT-DCT-5562, however, unlike it, the articular surfaces are described as being platycoelous and the neural canal is much wider and with neurocentral sutures mediolaterally compressed.

Panphagia protos from Argentina was described by Martinez and Alcober in 2009. The dorsal vertebra is described as similar to those of *Eoraptor lunensis*, only less laterally excavated.

Langer et al. (2019) performed a detailed description of *Pampadromaeus barberenai* from Southern Brazil, which included some mid to posterior dorsal vertebrae (fig. 15). The articular surface is circular to lateromedially compressed, ovoid in shape, however the authors point out that this might be the result of preservation factors to some extent. These vertebrae differ from NOVA-FCT-DCT-5562 specimen in being only slightly laterally depressed, in lacking a distinct ventral keel and by having a ventral concave curvature more pronounced.

A particular well preserved specimen of *Buriolestes schultzi* (fig. 16) from Southern Brazil was described by Müller et al. in 2018. The mid to posterior dorsal vertebrae centra differ from NOVA-FCT-DCT-5562 in having articular surfaces circular to slightly wider than tall, the lateral surfaces bear a shallow depression, there is a laminar striation extending from the rims towards the mid lateral and mid ventral surfaces and there is no keel on the ventral surface.

In conclusion, none of the basal sauropodomorph dorsal centra analyzed closely resemble NOVA-FCT-DCT-5562.

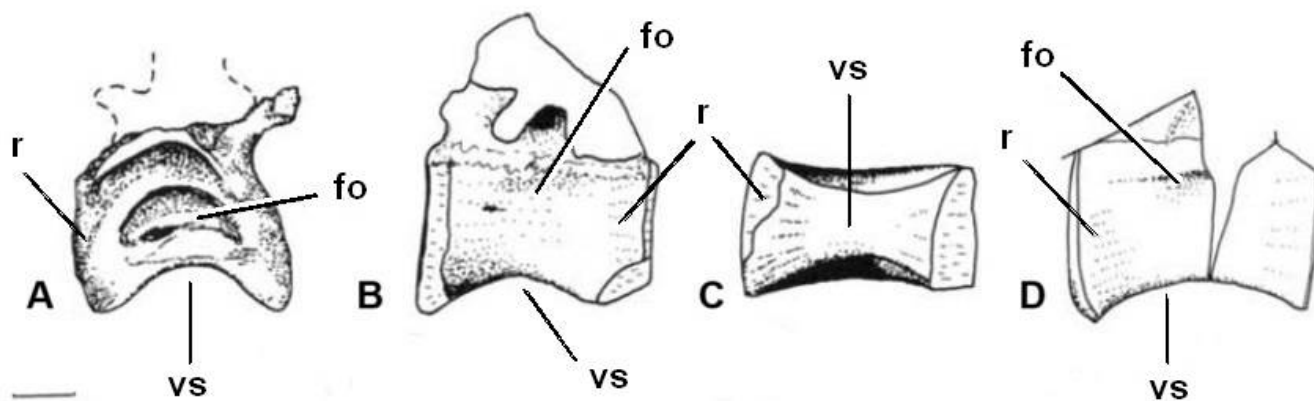


Figure 12. *Thecodontosaurus antiquus* dorsal vertebrae centra. Left lateral (A) view based on specimen YPM 2192; left lateral (B) and ventral (C) views based on specimen BRSMG Cb4182 and left lateral (D) view based on specimen BRSMG Cb4154. Source: Benton et al., 2000. Abbreviations: fo – fossa, r – rim, vs – ventral surface. Scale bar equals 10mm.

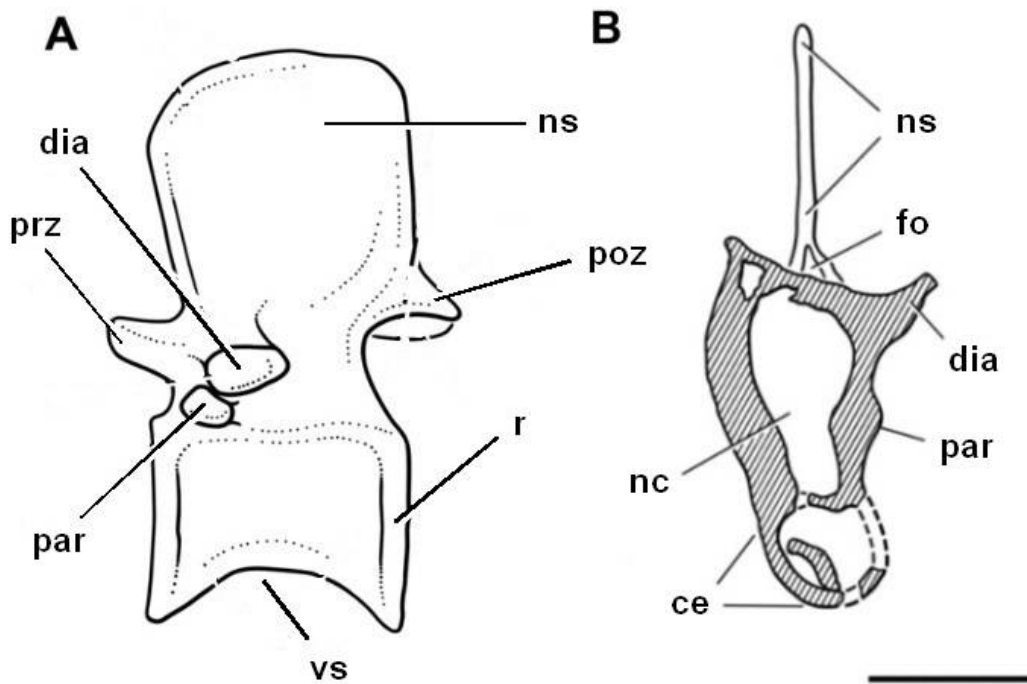


Figure 13. *Eoraptor lunensis* dorsal vertebrae 14 in left lateral (A) and dorsal vertebrae 13 in cross section in anterior view (B), based on holotype specimen PVSJ 512. Source: Sereno, 2013. Abbreviations: **ce** – centrum, **dia** -diapophysis, **fo** – fossa, **nc** – neural canal, **ns** – neural spine, **par** – parapophysis, **poz** – postzygapophysis, **prz** – prezygapophysis, **r** – rim, **vs** – ventral surface. Scale bar equals 10mm.

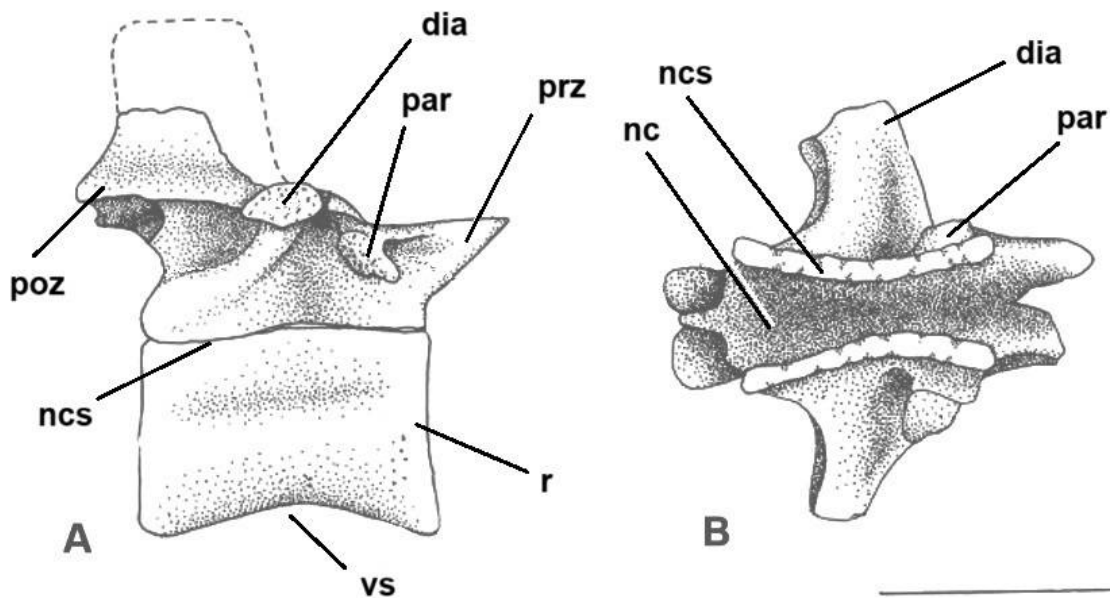


Figure 14. *Guaibasaurus candelariensis* holotype specimen MCN-PV 2355 mid dorsal vertebra in lateral view (A) and neural canal in ventral view (B). Source: Bonaparte et al., 1999. Abbreviations: **dia** - diapophysis, **nc** – neural canal, **ncs** – neurocentral suture, **ns** – neural spine, **par** – parapophysis, **poz** – postzygapophysis, **prz** – prezygapophysis, **r** – rim, **vs** – ventral surface. Scale bar equals 20mm.

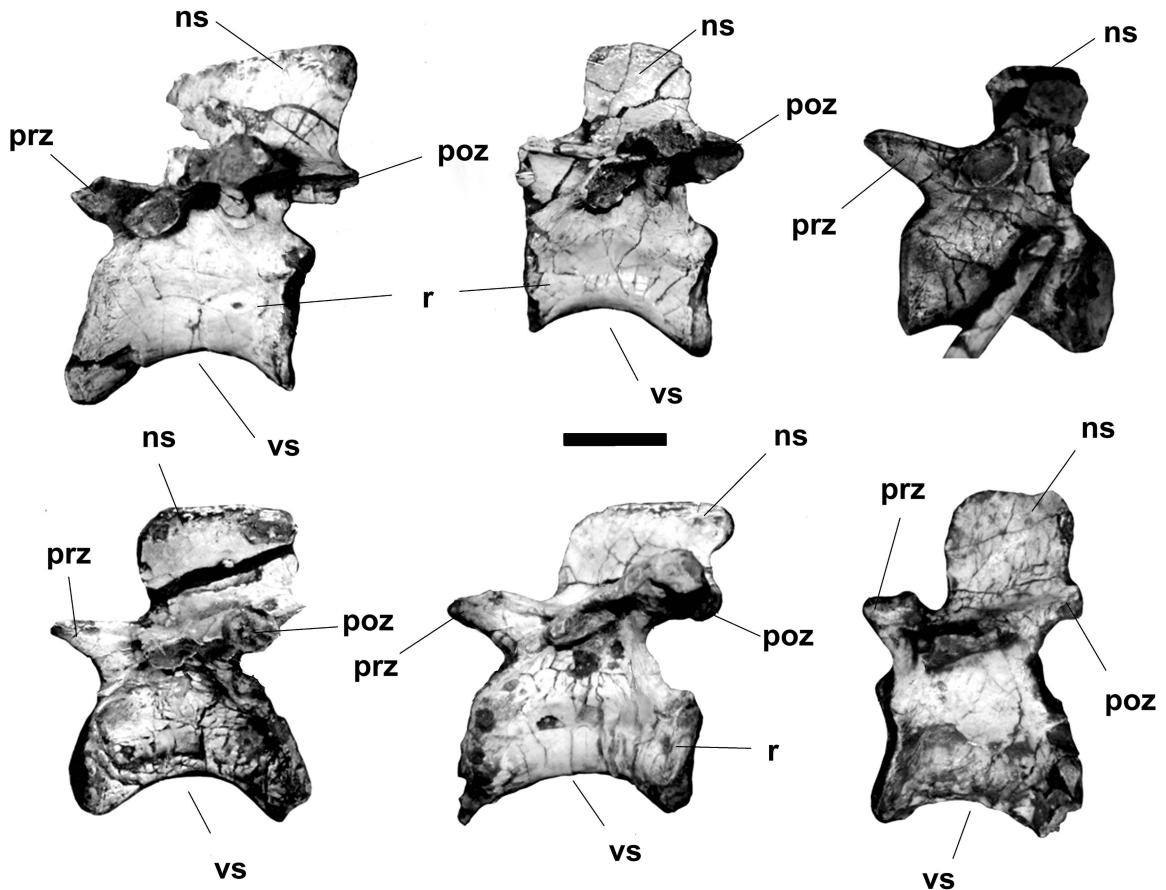


Figure 15. *Pampadromaeus barberenai* holotype specimen ULBRA-PVT016 dorsal vertebrae in lateral view. Source: Langer et al., 2019. Abbreviations: **ns** – neural spine, **par** – parapophysis, **poz** – postzygapophysis, **prz** – prezygapophysis, **r** – rim, **vs** – ventral surface. Scale bar equals 10mm.

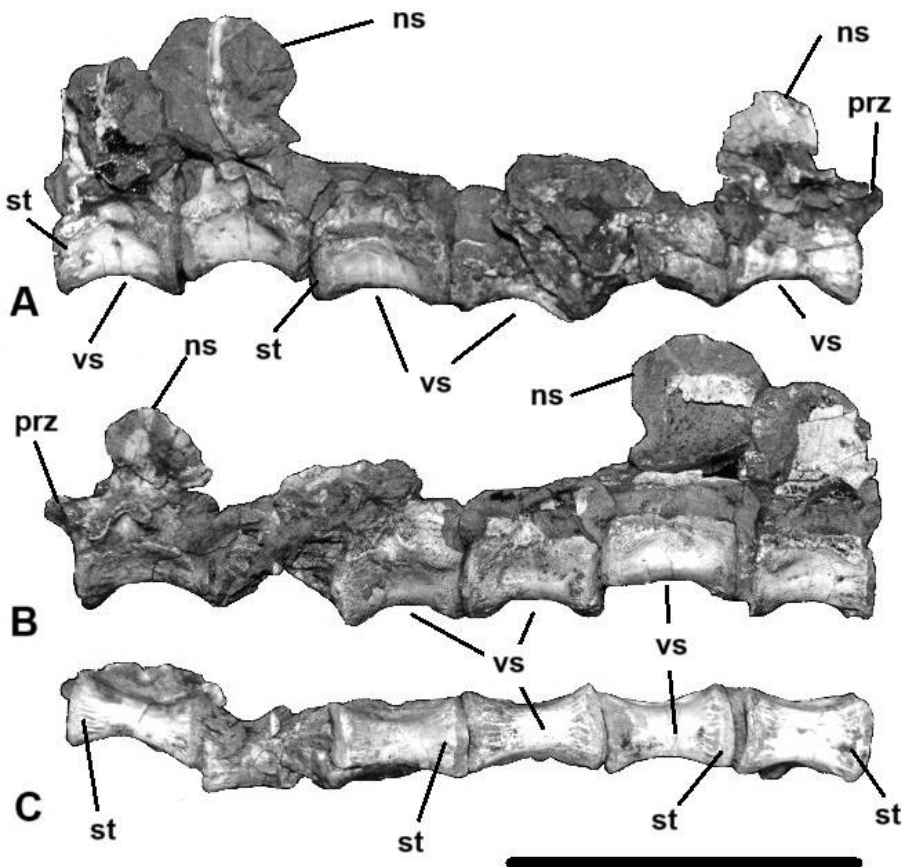


Figure 16. *Buriolestes schultzi* specimen CAPPA/UFSM 0035 dorsal vertebrae in right lateral (A), left lateral (B) and ventral (C) views. Source: Müller et al., 2018. Abbreviations: **ns** – neural spine, **prz** – prezygapophysis, **st** – striation, **vs** – ventral surface. Scale bar equals 50mm.

Herrerasauridae

Herrerasauridae Benedetto, 1973, were a group of small to medium sized bipedal Triassic carnivores (Novas, 1992) with a problematic taxonomic placement, having been classified as basal theropods (Nesbitt et al., 2009; Sues et al., 2011), basal saurischians (Ezcurra, 2010; Novas et al., 2010; Baron et al., 2017), basal dinosaurs outside Saurischia and Ornithischia (Brinkman & Sues, 1987; Novas, 1992) and sometimes even falling arguably outside Dinosauria (Baron & Williams, 2018; Cau, 2018).

The best known members of the group come from South America, including *Herrerasaurus ischigualastensis* Reig, 1963 and *Sanjuansaurus gordilloi* Alcober & Martinez, 2010 from Argentina and *Staurikosaurus pricei* Colbert, 1970 and *Gnathovorax cabreirai* Pacheco et al., 2019 from Brazil.

Herrerasaurus ischigualastensis (fig. 17) postcranium was described in detail by Novas (1994). Dorsal vertebrae centra differ considerably from NOVA-FCT-DCT-5562 in being more robust, deep and anteroposteriorly short, with circular anterior facets, lateral faces bear an elliptical depression and the ventral concavity is more pronounced in lateral view. Based on photographic material shared by Dr. Steve Brusatte it is also noticeable that the neurocentral sutures are curved, compressed mediolaterally and the neural canal much wider than in NOVA-FCT-DCT-5562 centrum. The ventral surface is also keelless.

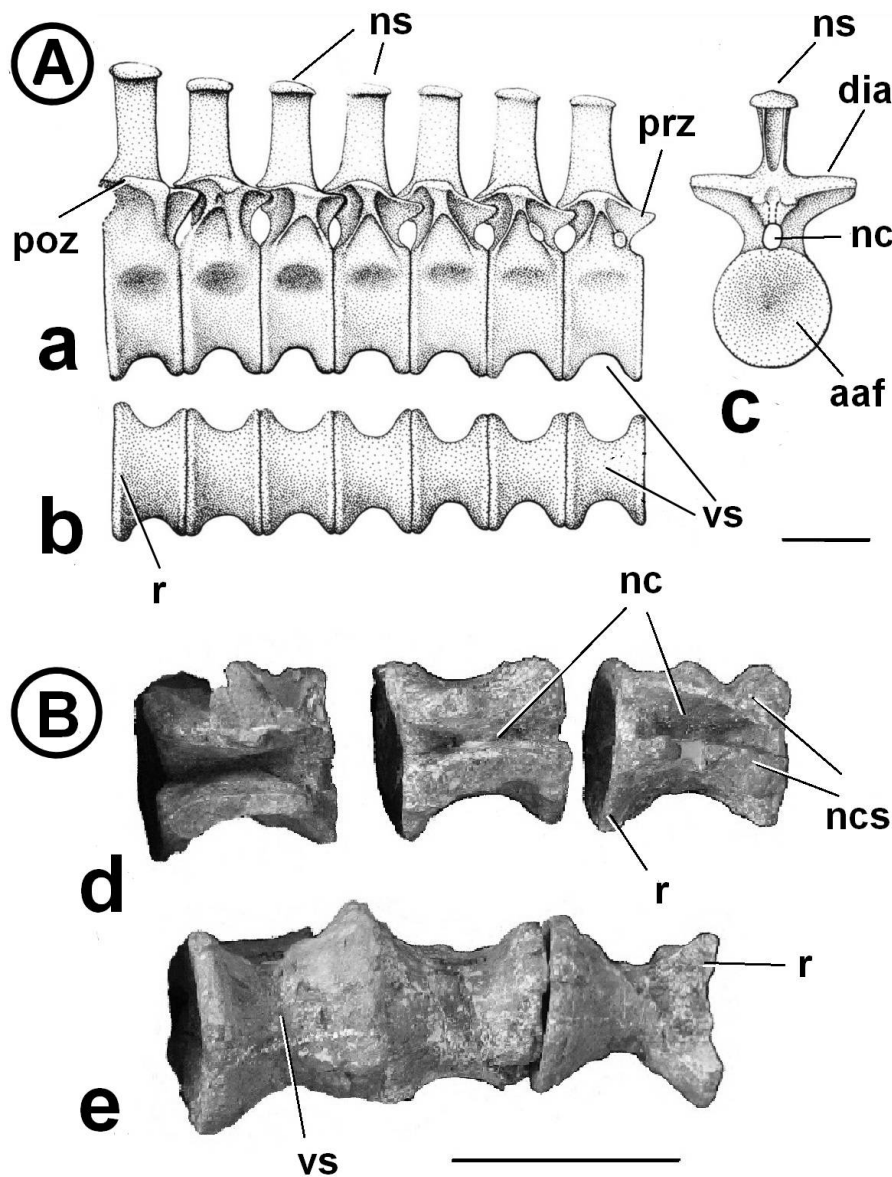


Figure 17. **A)** *Herrerasaurus ischigualastensis* dorsal vertebrae 9 to 15 in lateral **(a)**, ventral **(b)** and anterior **(c)** views, based on holotype specimen PVL 2566. Source: Novas, 1994; **B)** *Herrerasaurus ischigualastensis* dorsal vertebrae in dorsal **(d)** and ventral **(e)** views. Source: photos kindly shared by Steve Brusatte. Abbreviations: **aaf** – anterior articular facet, **dia** – diapophysis, **nc** – neural canal, **ncs** – neurocentral suture, **ns** – neural spine, **poz** – postzygapophysis, **prz** – prezygapophysis, **r** – rim, **vs** – ventral surface. Scale bars equals 50mm.

Colbert et al. (1970) described *Staurikosaurus pricei* from Brazil, including some dorsal vertebrae (fig. 18). These are similar to *Herrerasaurus ischigualastensis* and differ from NOVA-FCT-DCT-5562 in the same way.

Sanjuansaurus gordilloi material from Argentina was described by Alcober and Martinez (2010). They differ from NOVA-FCT-DCT-5562 in being anteroposteriorly short, like in *Herrerasaurus ischigualastensis* and *Staurikosaurus pricei*, and by lacking a ventral keel.

Gnathovorax cabreirai from Brazil, described by Pacheco et al. (2019), is similar to other herrerasaurids regarding the vertebrae morphology.

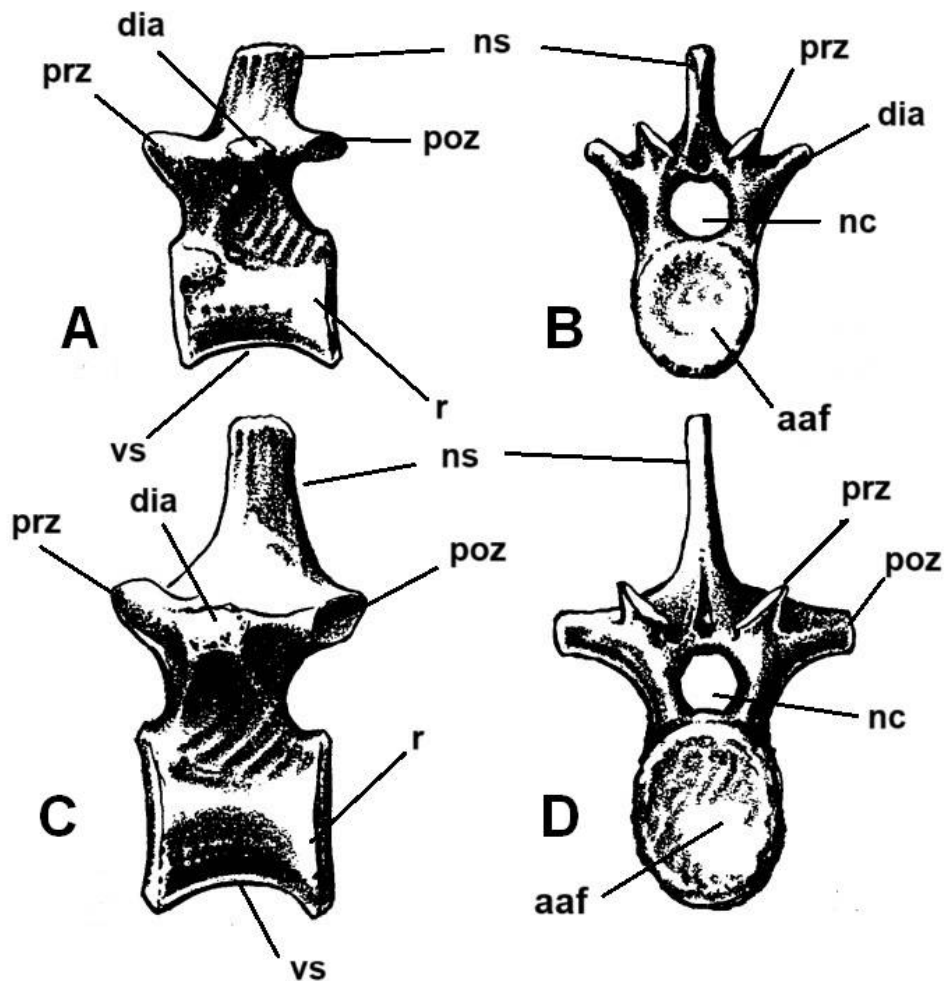


Figure 18. *Staurikosaurus pricei* dorsal vertebra 9 in left lateral (A) and anterior (B) views and dorsal vertebra 22 in left lateral (C) and anterior (D) views, based on holotype specimen MCZ 1669. Source: Colbert et al., 1970. Abbreviations: **aaf** – anterior articular facet, **dia** - diapophysis, **nc** – neural canal, **ns** – neural spine, **poz** – postzygapophysis, **prz** – prezygapophysis, **r** – rim, **vs** – ventral surface. Scale not given.

Basal Theropoda

The clade Neotheropoda Bakker, 1986, includes *Coelophysis* and all more derived theropods (Sereno, 1998; Hendrickx et al., 2015), however, several important non-neotheropod theropods from the Triassic should be considered in the context of this analysis. Species with material suitable for comparison with NOVA-FCT-DCT-5562 include *Chindesaurus bryansmalli* Long & Murry, 1995 from Arizona, USA, *Tawa hallae* Nesbitt et al., 2009 from New Mexico, USA, and *Eodromaeus murphi* Martinez et al., 2011 from Argentina.

Chindesaurus bryansmalli classification has been problematic over the years with some authors finding it as an *Herrerasaurus* relative, either outside Dinosauria (Baron & Williams, 2018) or inside Dinosauria (Baron et al., 2017; Novas et al., 2021) and others finding it closer to *Tawa* and other non-neotheropod theropods (Nesbitt & Ezcurra, 2015; Langer et al., 2017; Marsh et al., 2019). *Chindesaurus bryansmalli* dorsal vertebrae centra (fig. 19) are anteroposteriorly short and dorsoventrally deep, similar to herrerasaurids but different from NOVA-FCT-DCT-5562 specimen. These centra also have wider and circular articular facets, much wider neural canals that expand near the articular edges and pneumatic lateral fossae.

Tawa hallae is usually considered one of the closest taxa to Neotheropoda (Nesbitt et al., 2009; Ezcurra & Brusatte, 2011; Baron et al., 2017), although some studies found it to be closer to the herrerasaurids (Cau, 2018; Novas et al., 2021). Due to the absence of photographic material it was not possible to compare *Tawa hallae* dorsal vertebrae material in the context of this study.

Eodromaeus murphi is usually found as one of the most basal theropods (Martinez et al., 2011; Baron et al., 2017), however some authors found it as a basal Saurischian outside Theropoda (Cabreira et al., 2016; Langer et al., 2017). Comparing with NOVA-FCT-DCT-5562, the neurocentral suture seems to be positioned lower along the centrum, reaching the lateral surface.

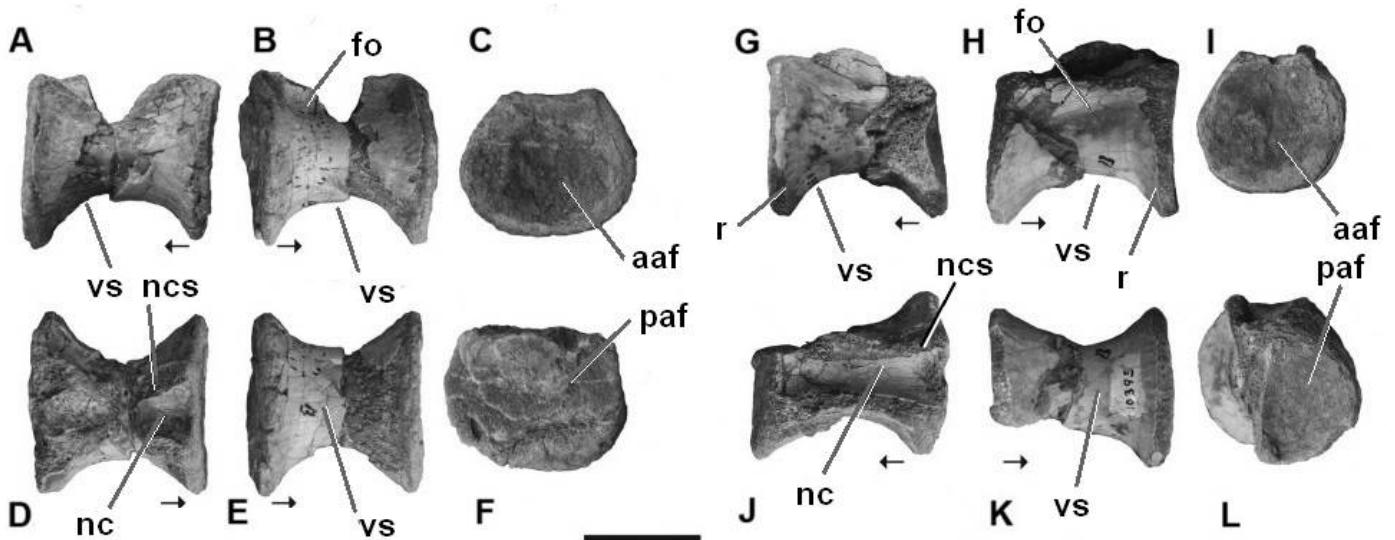


Figure 19. *Chindesaurus bryansmalli* holotype specimen PEFO 10395 dorsal vertebrae in left lateral (A, G), right lateral (B, H), anterior (C, I), dorsal (D, J), ventral (E, K) and posterior (F, L) views. Source: Marsh et al., 2019. Abbreviations: aaf – anterior articular facet, fo – fossa, nc – neural canal, ncs – neurocentral suture, paf – posterior articular facet, r – rim, vs – ventral surface. Scale bar equals 20mm. Arrows point anteriorly.

Coelophysoidea

Coelophysoidea Nopcsa, 1928 is the sister group of all other neotheropods, Ceratosauria and Tetanurae (Rauhut, 2000; Ezcurra & Cuny, 2007), a stem based node including all theropods more close to *Coelophysus bauri* than to *Ceratosaurus nasicornis* (Sereno, 1998). Being common during the Late Triassic and Early Jurassic, this group represents the first major radiation of Neotheropoda (Carrano & Sampson, 2004; You et al., 2014; Martínez & Apaldetti, 2017). Some of the most basal members of the group include *Liliensternus liliensterni* Huene, 1934, *Lophostropheus airelensis* Cuny & Galton, 1993, *Gojirasaurus quayi* Carpenter, 1997 and *Pendraig milnerae* Spiekman et al., 2021.

Liliensternus liliensterni was a medium sized theropod from the Upper Triassic of Germany and although some studies place it as a coelophysoid (Smith et al, 2007; Ezcurra et al., 2020), others found it outside this clade (Nesbitt et al., 2009; Marsh et al, 2019). Based on photographic material shared by Dr. Steve Brusatte (fig. 20), the dorsal vertebrae of this species is larger than NOVA-FCT-DCT-5562 but the general geometrical proportions are similar. Differences were found in the articular surfaces nearly circular and less deeply excavated, in small ridges extending from the rims towards the mid lateral and mid ventral regions, the ventral surface lacks a keel and the curvature is more pronounced towards the mid centrum.

Lophostropheus airelensis (fig. 21), from the Triassic-Jurassic boundary of France, was re-described by Ezcurra and Cuny (2007). This species was for some time classified in the *Halticosaurus* or *Liliensternus* genera (Larsonneur & Lapparent, 1966; Cuny & Galton, 1993) but the authors in their re-description found enough differences to erect a new genus. The general shape of the centrum is similar to *Liliensternus liliensterni*, but the upper lateral surface has a large shallow fossa, absent in NOVA-FCT-DCT-5562.

Gojirasaurus quayi from New Mexico, USA, was described by Carpenter (1997) as a coelophysoid and one of the largest Triassic theropods. Recent analysis however putted doubts in its coelophysoid affiliation (Ezcurra et al., 2020) or even the own validity of the genus (Nesbitt et al., 2007). Among the material described there were a few dorsal vertebrae (fig. 22). These differ from NOVA-FCT-DCT-5562 by having circular articular facets, a shallow and elongated depression on the lateral sides and a series of coarsed ridges on the ventral surface extending from the rim of the centra. The height/length ratio for the 3 centra analyzed varies between 1.32 and 1.42, similar to NOVA-FCT-DCT-5562. In 2007, Nesbitt et al. conducted a re-evaluation of the North American Late Triassic dinosaurs and questioned the assignment of these vertebrae centra to Dinosauria, stating that they were more similar to those of shuvosaurids.

Pendraig milnerae (fig. 23), a small coelophysoid from the Late Triassic of Wales (Spiekman et al., 2021), has anteroposteriorly elongated dorsal centra with a length about 2.6 times the anterior articular surface height. This is akin to more derived coelophysoid genera such as *Coelophysus* and *Procompsognathus* and differs from the NOVA-FCT-DCT-5562 centrum which has a length/height ratio of 1.42. The articular surfaces are broader than tall, the neural canal (based on the neural arch in anterior view) seems wider, the lateral surface has a shallow fossa and the ventral surface is smooth without a keel.

Griffin (2019) described unnamed coelophysoid material from New Mexico, USA, under the reference NMMNH P-4569. Among the material there is an isolated dorsal centrum (fig. 24) and, although fragmented, it is possible to infer that the overall shape and length/height ratio is pretty similar to NOVA-FCT-DCT-5562. However NMMNH P-4569 differs in the circular articular surfaces, in the neural canal morphology which is here more V shaped on the distal ends, in the presence of a lateral fossa and by the presence of small ridges extending from the rims towards the mid lateral and mid ventral regions.

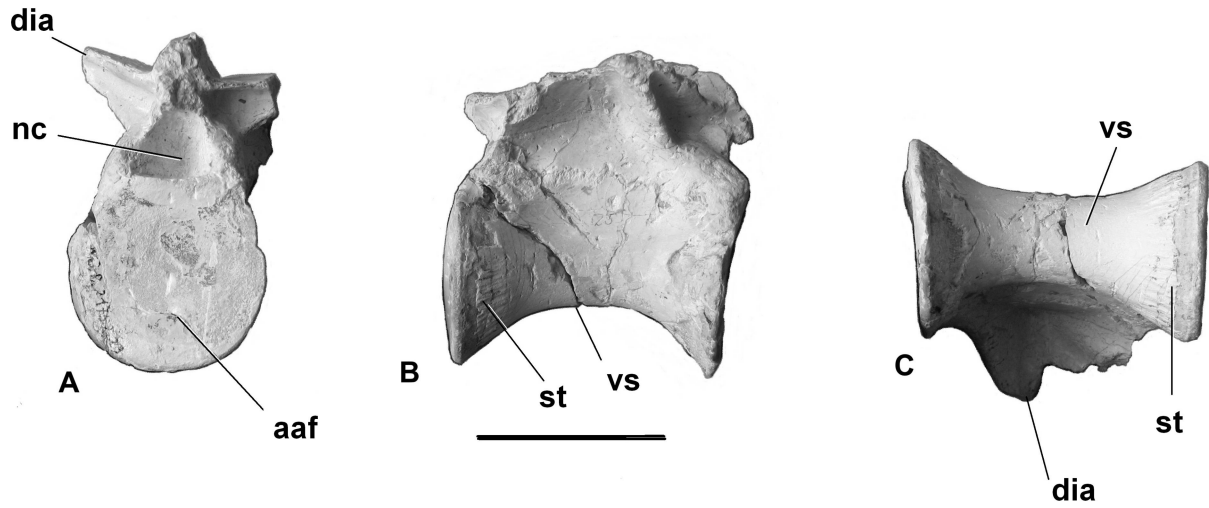


Figure 20. *Liliensternus liliensterni* dorsal vertebrae on anterior (A), lateral (B) and ventral (C) views; edited from photos kindly shared by Steve Brusatte. Abbreviations: **aaf** – articular facet, **dia** – diapophysis, **nc** – neural canal, **st** – striation, **vs** – ventral surface. Scale bar equals to 50mm.

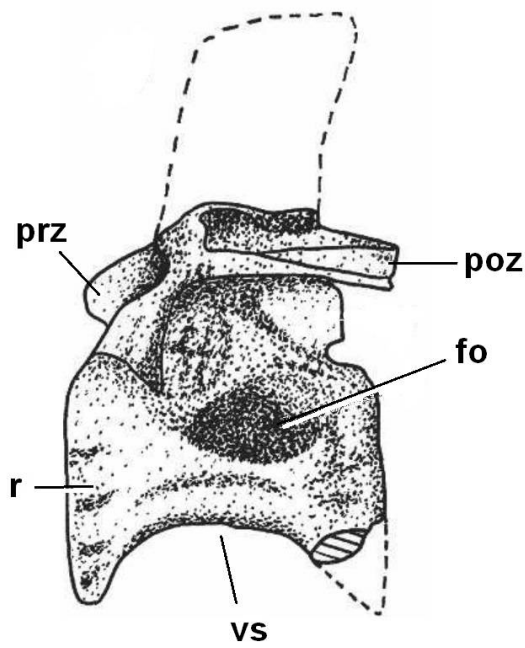


Figure 21. *Lophostropheus airelensis* posterior dorsal vertebrae in lateral view based on holotype specimen. Source: Ezcurra & Cuny, 2007, modified from Cuny & Galton, 1993. Abbreviations: **fo** – fossa, **poz** – postzygapophysis, **prz** – prezygapophysis, **r** – rim, **vs** – ventral surface. Scale not given.

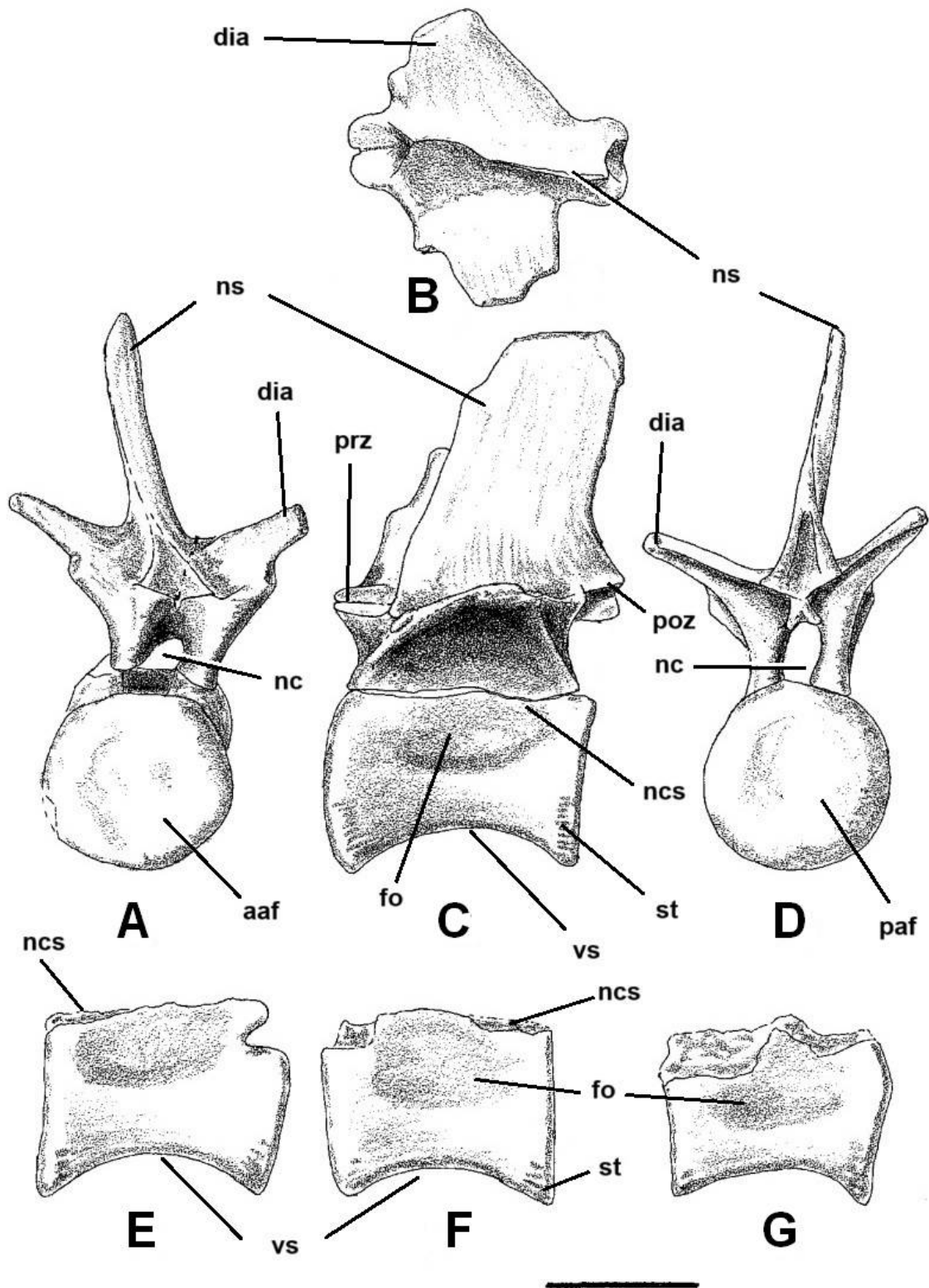


Figure 22. *Gojirasaurus quayi* specimen UCM 47221 mid to posterior dorsal vertebrae in anterior (A), dorsal (B), left lateral (C) and posterior (D) views and dorsal vertebra centra in lateral (E, F, G) views. Source: Carpenter, 1997. Abbreviations: **aaf** – anterior articular facet, **dia** - diapophysis, **fo** – fossa, **nc** – neural canal, **ncs** – neurocentral suture, **ns** – neural spine, **paf** – posterior articular facet, **poz** – postzygapophysis, **prz** – prezygapophysis, **st** – striation, **vs** – ventral surface. Scale bar equals 50mm.

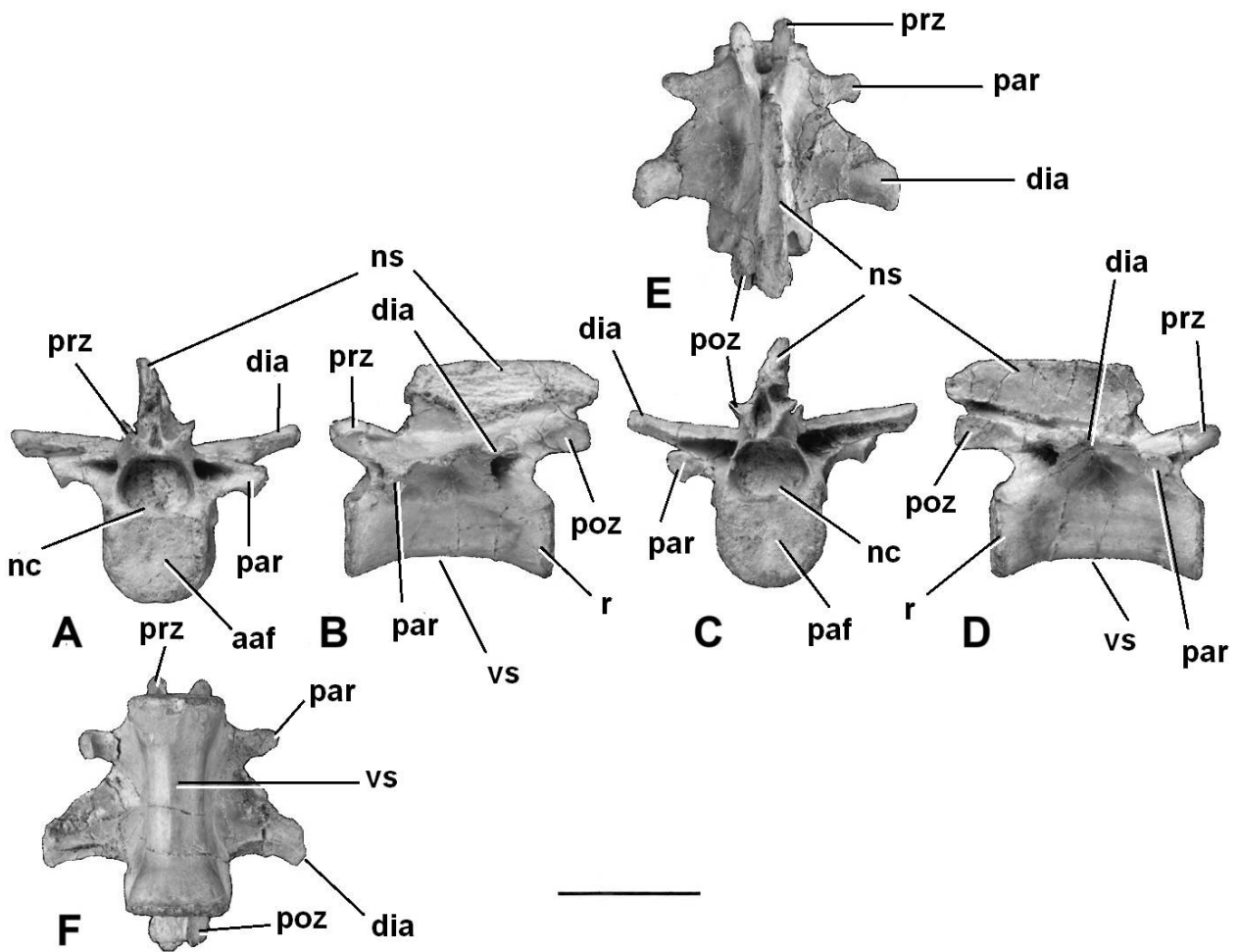


Figure 23. *Pendraig milnerae* specimen NHMUK PV 37596 dorsal vertebrae in anterior (A), left lateral (B), posterior (C), right lateral (D), dorsal (E) and ventral (F) views. Source: Spiekman et al., 2021. Abbreviations: **aaf** – anterior articular facet, **dia** - diapophysis, **nc** – neural canal, **ns** – neural spine, **paf** – posterior articular facet, **par** – parapophysis, **poz** – postzygapophysis, **prz** – prezygapophysis, **vs** – ventral surface. Scale bar equals 10mm.

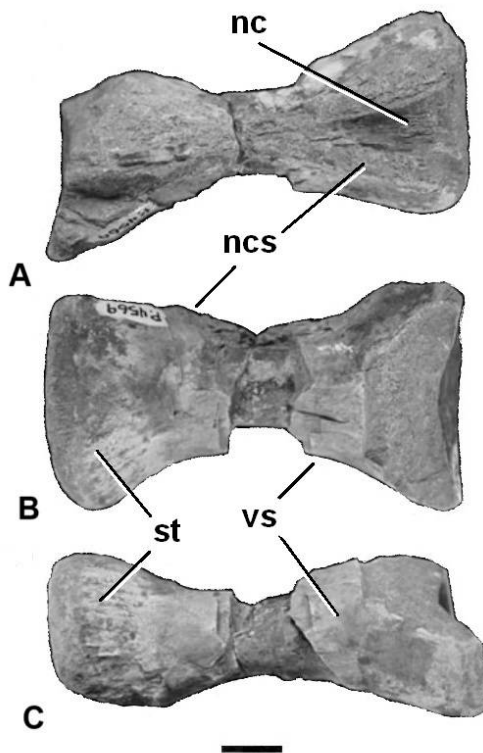


Figure 24. Coelophysoid specimen NMMNH P-4569 dorsal vertebrae in dorsal (A), lateral (B) and ventral (C) views. Source: Griffin, 2019. Abbreviations: **nc** – neural canal, **ncs** – neurocentral suture, **st** – striation, **vs** – ventral surface. Scale bar equals 10mm.

Coelophysidae

Coelophysidae Nopcsa, 1928 is a most inclusive group within Coelophysoidea including the most recent common ancestor of *Coelophysis bauri* (Cope, 1887) Cope, 1889 and *Procompsognathus triassicus* Fraas, 1913 and all its descendants (Serenó, 1998).

Besides *Procompsognathus triassicus* and *Coelophysis bauri*, the clade includes taxa such as *Pterospondylus trielbae* Jaekel, 1913, *Segisaurus halli* Camp, 1936 and *Megapnosaurus rhodesiensis* (Raath, 1969) Ivie et al., 2001.

The genus *Coelophysis* comes from the Late Triassic USA. This animal was first assigned to the genus *Coelurus* by Cope in 1887 but reassigned two years later to its own genus *Coelophysis* (Cope, 1889). Our knowledge of this dinosaur would improve substantially in 1947 when a fossil assemblage with several complete specimens was found in Ghost Ranch New Mexico (Colbert, 1989; Rinehart et al., 2009). *Coelophysis bauri* is the type species for the genus *Coelophysis* with other species been proposed over the years, however only *Coelophysis bauri* remains consensual among researchers.

Megapnosaurus rhodesiensis from the Early Jurassic Southern Africa, was first named *Syntarsus rhodesiensis* by Raath (1969); however this name was later found to have been previously given to a species of beetle, so, in 2001, entomologists Ivie et al. renamed the genus as *Megapnosaurus*. Some authors have also considered *Syntarsus* a junior synonym of *Coelophysis* (Bristowe & Raath, 2004).

“*Megapnosaurus*” (“*Coelophysis*”) *kayentakatae* (Rowe, 1989) Ivie et al., 2001, from Early Jurassic Arizona, USA, was first assigned to the genus *Syntarsus* (Rowe, 1989) and later to *Megapnosaurus* (Ivie et al., 2001). In 2021, Ezcurra et al., running a phylogenetic analysis on basal theropods, found “*Megapnosaurus*” *kayentakatae* not closely related to neither *Coelophysis bauri* or *Megapnosaurus rhodesiensis* but still within Coelophysinae. The validity of the species “*Megapnosaurus*” *kayentakatae* is currently uncertain until a new formal description is made (McDavid & Bugos, 2022).

Both *Coelophysis* and *Megapnosaurus* have very long dorsal vertebrae centra (fig. 25) with *Coelophysis bauri* presenting length/height ratios between 1.98–2.87 and *Megapnosaurus rhodesiensis* around 2.10 (Spiekman et al., 2021). This alone is enough to distinguish from NOVA-FCT-DCT-5562 material, with a 1.42 ratio. Other differences were found in the curved neurocentral sutures and in the asymmetrical anterior and posterior centrum ends, with the posterior facet being taller.

Procompsognathus triassicus was a slender carnivorous dinosaur from Late Triassic Germany (Knoll, 2008). Comparing the available photographic material with NOVA-FCT-DCT-5562, the dorsal vertebrae of *Procompsognathus triassicus* has a higher length/height ratio.

Pterospondylus trielbae was originally described by Jaekel (1913) based on a single vertebra (fig. 26) from the Late Triassic Germany and was reviewed in 1998 by Rauhut and Hungerbühler. The vertebra is long and slender, similar to other coelophysids, and with the articular facets wider than tall. NOVA-FCT-DCT-5562 vertebra has a smaller ratio between length and height and the articular facets are taller than wide. In anterior view, the neural arch is wide, indicative of a wide neural canal, unlike what we see on NOVA-FCT-DCT-5562.

Segisaurus halli comes from the Early Jurassic Arizona, USA (Carrano et al., 2005). The dorsal vertebrae centra (fig. 27), based on Carrano et al. description, is more cylindrical than hourglass shaped, unlike NOVA-FCT-DCT-5562 specimen. Also, the articular facet appears to be wider than tall and the neural canal wider than in NOVA-FCT-DCT-5562.

In the context of this work it was not possible to compare with “*Megapnosaurus*” *kayentakatae*, however since this species is within Coelophysidae we assume it had the typical elongate centra of the clade.

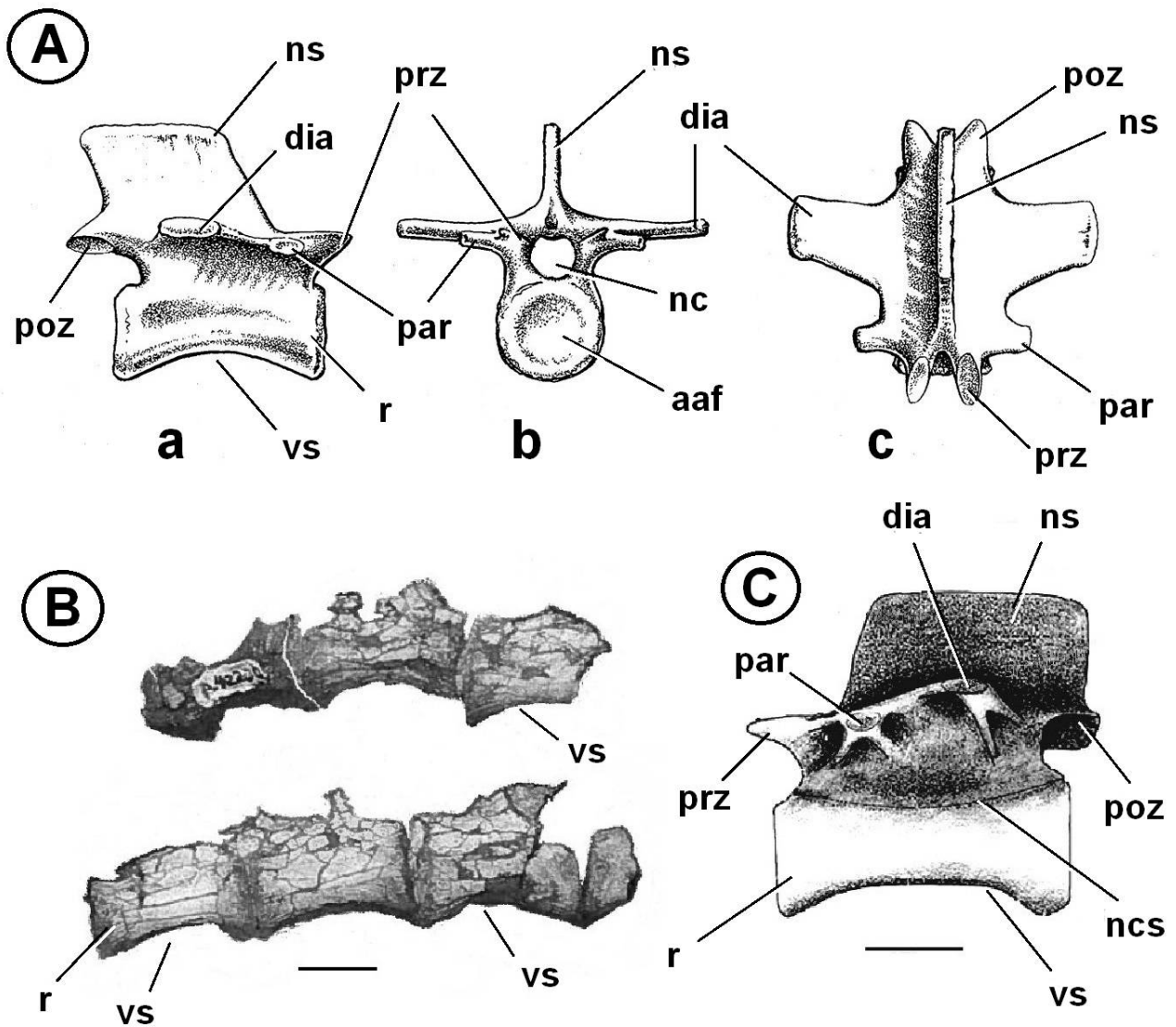


Figure 25. **A)** *Coelophysis bauri* dorsal vertebrae in right lateral (**a**), anterior (**b**) and dorsal (**c**) views based on AMNH 7223 and AMNH 7224 specimens. Source: Colbert, 1989; **B)** *Coelophysis bauri* specimen NMMNH P-42200 fragmented dorsal vertebrae in lateral view. Source: Rinehart et al., 2009 **C)** *Megapnosaurus rhodesiensis* dorsal vertebra 11, based on holotype specimen QG 1. Source: Rauhut, 2000. Abbreviations: **aaf** – anterior articular facet, **dia** - diapophysis, **nc** – neural canal, **ncs** – neurocentral suture, **ns** – neural spine, **par** – parapophysis, **poz** – postzygapophysis, **prz** – prezygapophysis, **r** – rim, **vs** – ventral surface. Scale bars equals 10mm, except for 1. where there is no scale.

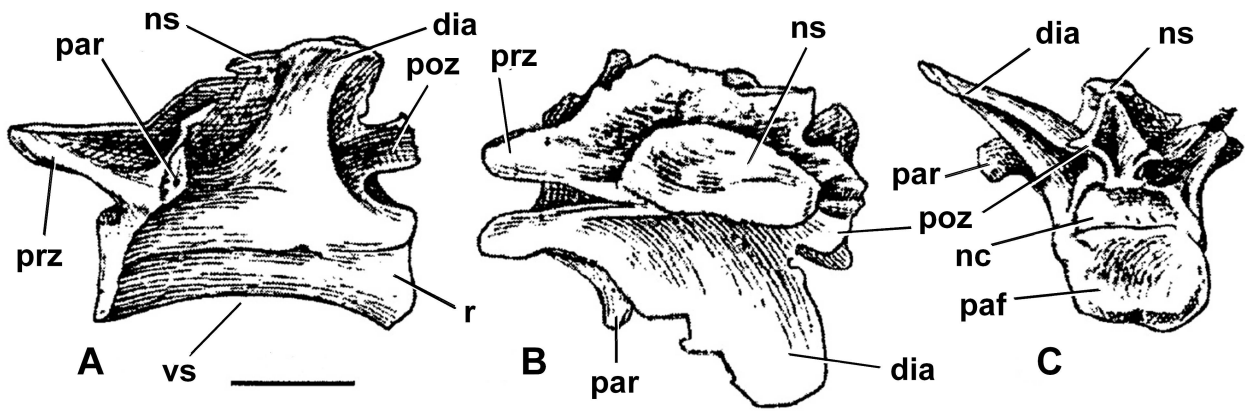


Figure 26. *Pterospondylus trielbae* holotype specimen dorsal vertebra in left lateral (A), dorsal (B) and posterior (C) views. Source: Rauhut & Hungerbühler, 1998, modified from Huene, 1921. Abbreviations: **dia** - diapophysis, **nc** - neural canal, **ns** - neural spine, **paf** - posterior articular surface, **par** - parapophysis, **poz** - postzygapophysis, **prz** - prezygapophysis, **r** - rim, **vs** - ventral surface. Scale bar equals 10mm.

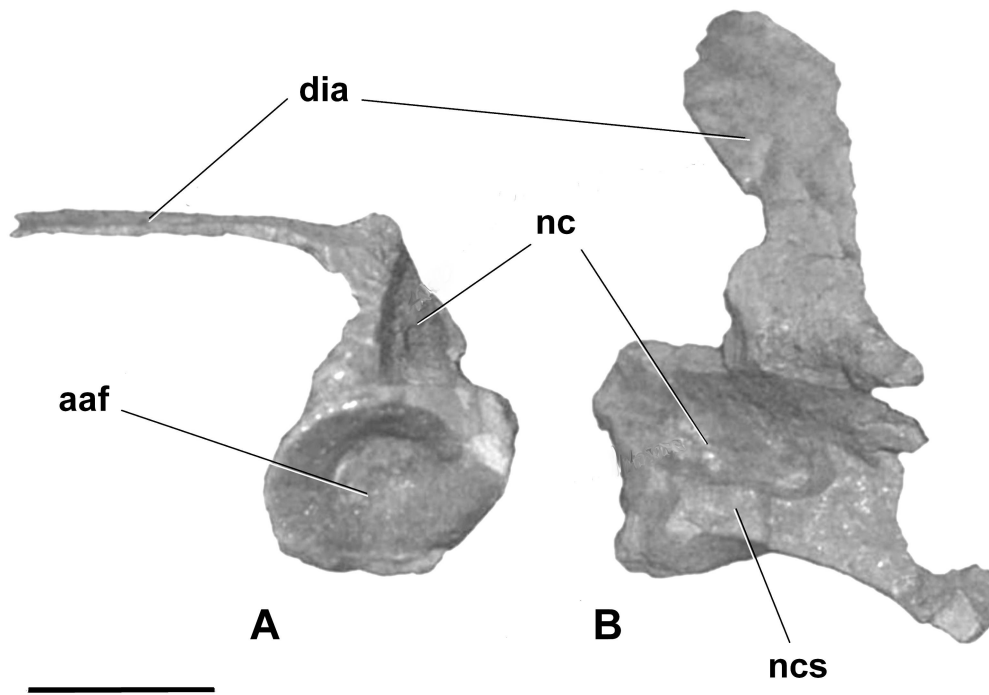


Figure 27. *Segisaurus halli* holotype specimen UCM 32101 dorsal vertebra in anterior (A) and dorsal (B) views. Source: Carrano et al., 2005. Abbreviations: **aaf** - anterior articular facet, **dia** - diapophysis, **nc** - neural canal, **ncs** - neurocentral suture. Scale bar equals 10mm.

Derived Neotheropoda

More derived theropods replaced coelophysoids during the Latest Triassic/Early Jurassic; for the context of this dissertation we will focus on some relevant taxa within Neotheropoda but outside *Averostra* Paul, 2002 (Ceratosauria + Tetanurae). Such taxa include *Sarcosaurus woodi* Andrews, 1921 *Dilophosaurus wetherilli* (Welles, 1954), *Cryolophosaurus ellioti* Hammer & Hickerson, 1994, *Zupaysaurus rougieri* Arcucci & Coria, 2003 and *Notatesseraeraptor frickensis* Zahner & Brinkmann, 2019.

Some of these taxa were previously considered related to coelophysoids and/or ceratosaurs (Welles & Long, 1974; Paul, 1988; Holtz, 1994; Tykoski & Rowe, 2004; Ezcurra & Novas, 2007; Carrano et al., 2012; Hugi, 2008) but the most recent phylogenetic analysis contradicts this idea; instead, the data shows an evolutionary grade among stem-*averostrans* such as *Zupaysaurus*, *Cryolophosaurus* and *Dilophosaurus* (Marsh et al., 2019; Marsh & Rowe, 2020; Ezcurra et al., 2020).

Dilophosaurus wetherilli (Welles, 1954) from the Early Jurassic USA, is one of the better known early theropods, with several specimens known. This genus was re-described in detail in 2020 by Marsh and Rowe. The mid to posterior dorsal vertebrae centra (fig. 28) differ from NOVA-FCT-DCT-5562 in being amphiplatyan (or only slightly amphicoelus), the neural canal is relatively wide and deep, there is a laminar striation extending from the rim towards the mid lateral and mid ventral surfaces of the centra and the anteroposteriorly oriented ventral concavity is much more deep in lateral view.

Zupaysaurus rougieri comes from the Late Triassic Argentina and, although a remarkable specimen, there are no posterior dorsal vertebrae preserved. Some anterior dorsal vertebrae were recovered but their state of preservation is poor and no in-depth description was made, except for the fact that they are constricted at mid-length and amphiplatyan (Arcucci & Coria, 2003).

Cryolophosaurus ellioti was a medium sized theropod that lived in the Early Jurassic Antarctica. A complete description of the specimen was made by Smith et al. in 2007. Similar to *Dilophosaurus wetherilli*, the posterior dorsal centra (fig. 29) differ from NOVA-FCT-DCT-5562 in being amphiplatyan, by having lateral striations projecting from the rims and in the deeper anteroposteriorly oriented ventral concavity.

Sarcosaurus was a theropod genus from the Early Jurassic (Late Hettangian – Early Sinemurian) England, described based on a few remains by Andrews (1921) who named the type species as *Sarcosaurus woodi* Andrews, 1921. Over the years more fragmentary specimens were described, including a new species, *Sarcosaurus andrewsi* Huene, 1932 (Huene, 1932). Carrano & Sampson (2004) found the material similar to *Liliensternus liliensterni* and *Dilophosaurus wetherilli* but with enough differences to be considered distinct from them; it was classified as a coelophysoid. The authors described the vertebrae (fig. 30) as being weakly concave on the anterior facet and having a small neural canal, features similar to NOVA-FCT-DCT-5562.

Additional *Sarcosaurus* material was also described in 2020 by Ezcurra et al. who lumped all the known individuals to the type species *Sarcosaurus woodi* and found it as one of the closest sister-taxa to *Averostra*. The description included material ascribed to the specimen WARMS G667-690, which includes a mid/posterior dorsal centrum, WARMS G678 (fig. 31), with strong visual resemblance to NOVA-FCT-DCT-5562. Although the right side of the centrum is damaged, the general shape can be inferred. The articular surfaces are of similar shape and relative dimensions to NOVA-FCT-DCT-5562 (WARMS G678 height/width ratio: 1.26 for anterior, 1.20 for posterior; NOVA-FCT-DCT-5562 with 1.3 on both ends), and the anteroposteriorly oriented ventral concavity has the same degree of curvature. The neurocentral suture is in the same position as NOVA-FCT-DCT-5562 and the neural canal has the same width. In ventral view, the hourglass shape is also similar. The main differences are in the ventral ridge which is not as sharp as NOVA-FCT-DCT-5562, and in the higher length/height ratio (which is around 1.7, versus 1.42 in NOVA-FCT-DCT-5562), however this ratio can vary along the dorsal series (table 2). Overall, despite these subtle differences, *Sarcosaurus* WARMS G678 general shape is the most similar to all of those who were compared with NOVA-FCT-DCT-5562.

Notatesseraeraptor frickensis Zahner & Brinkmann, 2019 is a Late Triassic theropod from Switzerland, originally classified as a coelophysoid (Hugi, 2008) but more recent analysis found it as non-*Averostran* basal Neotheropod (Zahner & Brinkmann, 2019). Postcranial material includes some dorsal vertebrae (fig. 32) similar to NOVA-FCT-DCT-5562 material, mostly in the lateral and anterior outline shape. However some differences are found in the apparent absence of a ventral keel and in the wider and "V" shaped floor of the neural canal.

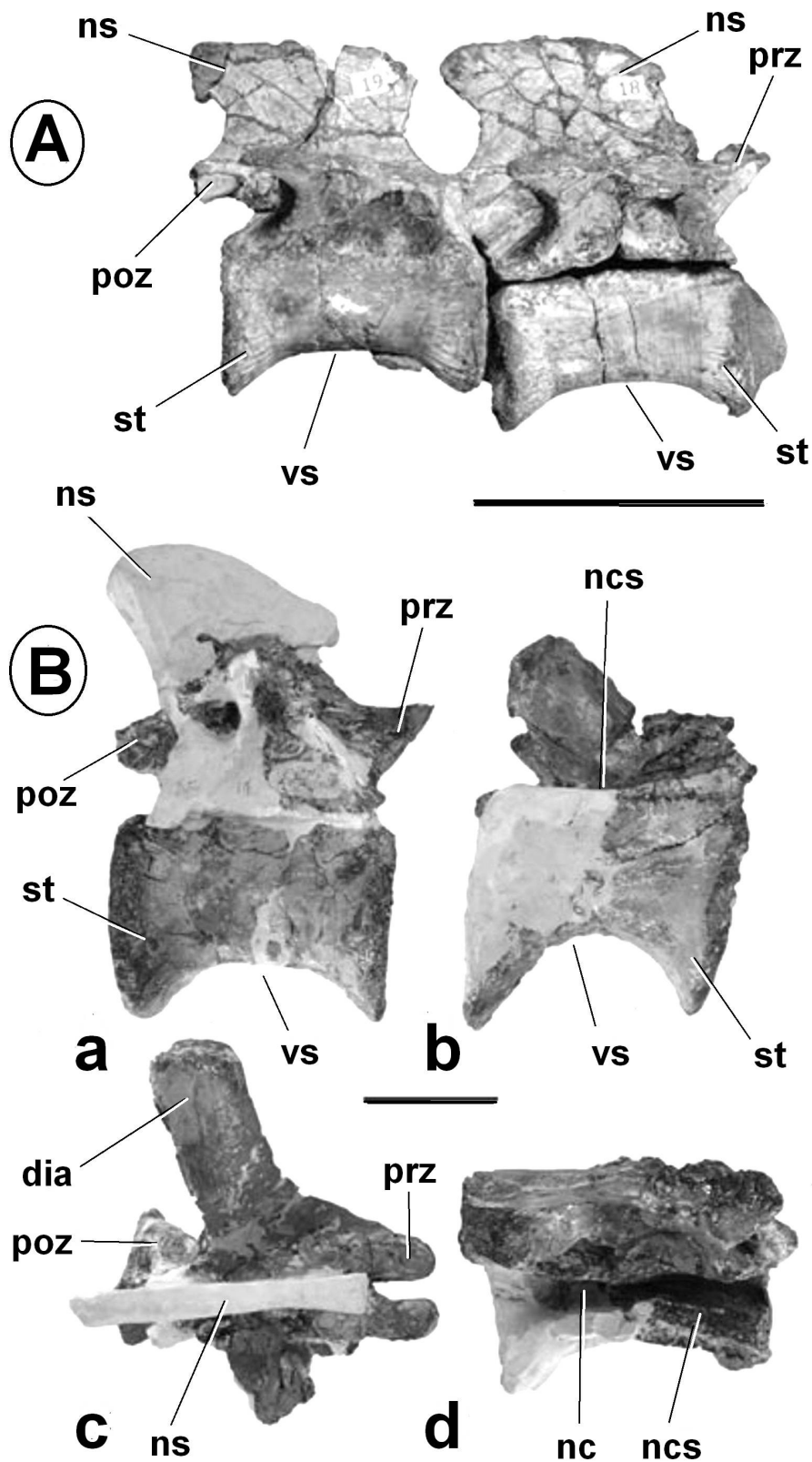


Figure 28. A. *Dilophosaurus wetherilli* specimen TMM 47006-1 dorsal vertebrae 18 and 19 in right lateral view; B. *Dilophosaurus wetherilli* holotype specimen UCMP 37302 dorsal vertebra 19 in right lateral (a) and dorsal (b) views and dorsal vertebra 23 in right lateral (c) and dorsal (d) views. Source: Marsh & Rowe, 2020. Abbreviations: **dia** - diapophysis, **nc** - neural canal, **ncs** - neurocentral suture, **ns** - neural spine, **poz** - postzygapophysis, **prz** - prezygapophysis, **st** - striation, **vs** - ventral surface. Scale bars equal 50mm.

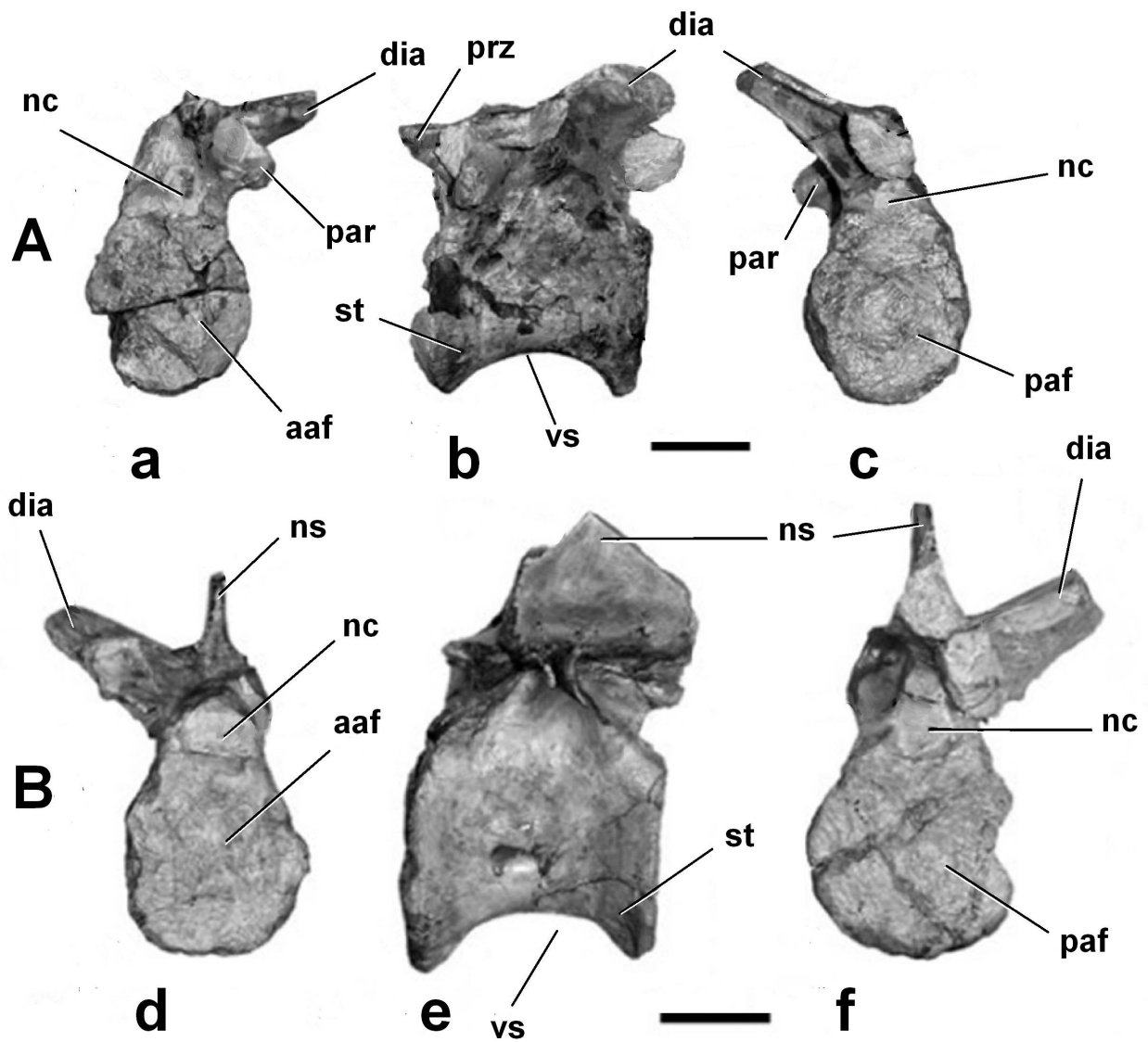


Figure 29. *Cryolophosaurus ellioti* holotype specimen FMNH PR1821 mid to posterior dorsal vertebrae: **1)** mid-posterior dorsal seven in anterior (**A**), left lateral (**B**) and posterior (**C**) views; **2)** posterior dorsal 14 in anterior (**D**), left lateral (**E**) and posterior (**F**) views. Source: Smith et al., 2007. Abbreviations: **aaf** – anterior articular facet, **dia** - diapophysis, **nc** – neural canal, **ns** – neural spine, **paf** – posterior articular facet, **par** – parapophysis, **prz** – prezygapophysis, **st** – striation, **vs** – ventral surface. Scale bars equals 50mm.

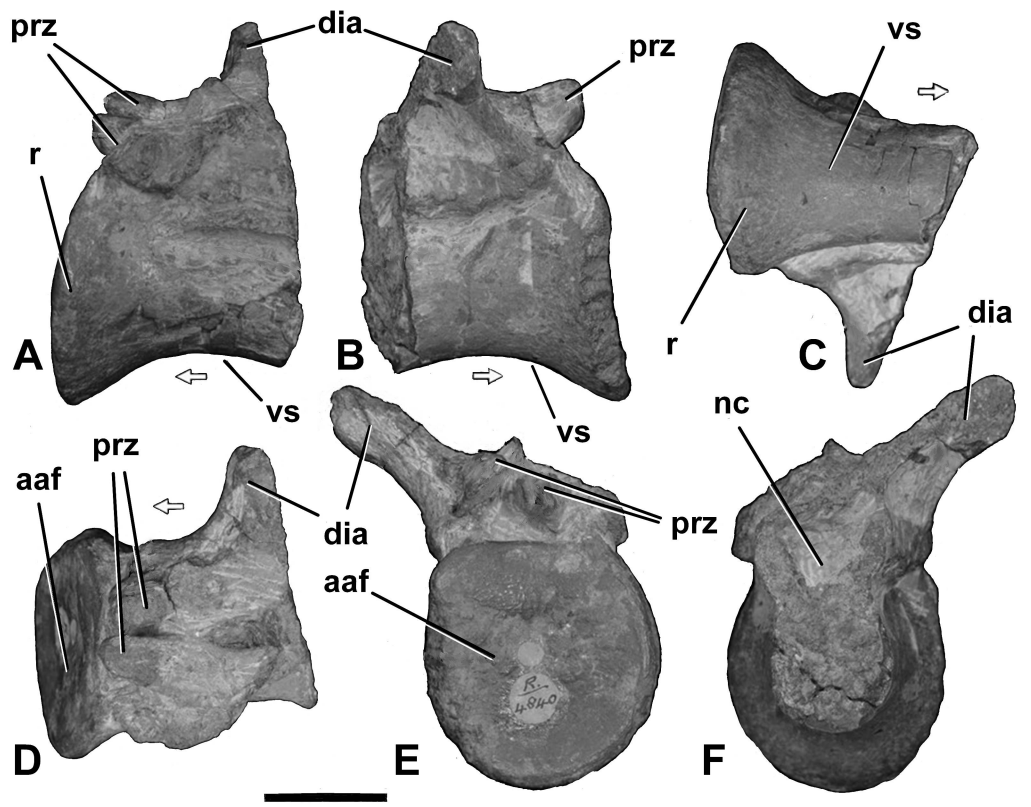


Figure 30. *Sarcosaurus woodi* holotype specimen NHMUK PV R4840 dorsal vertebra in left lateral (A), right lateral (B), ventral (C), dorsal (D), anterior (E) and posterior (F) views. Source: Ezcurra et al., 2020. Abbreviations: aaf – anterior articular facet, dia - diapophysis, nc – neural canal, prz – prezygapophysis, r – rim, vs – ventral surface. Scale bar equals 20mm. Arrows point anteriorly.

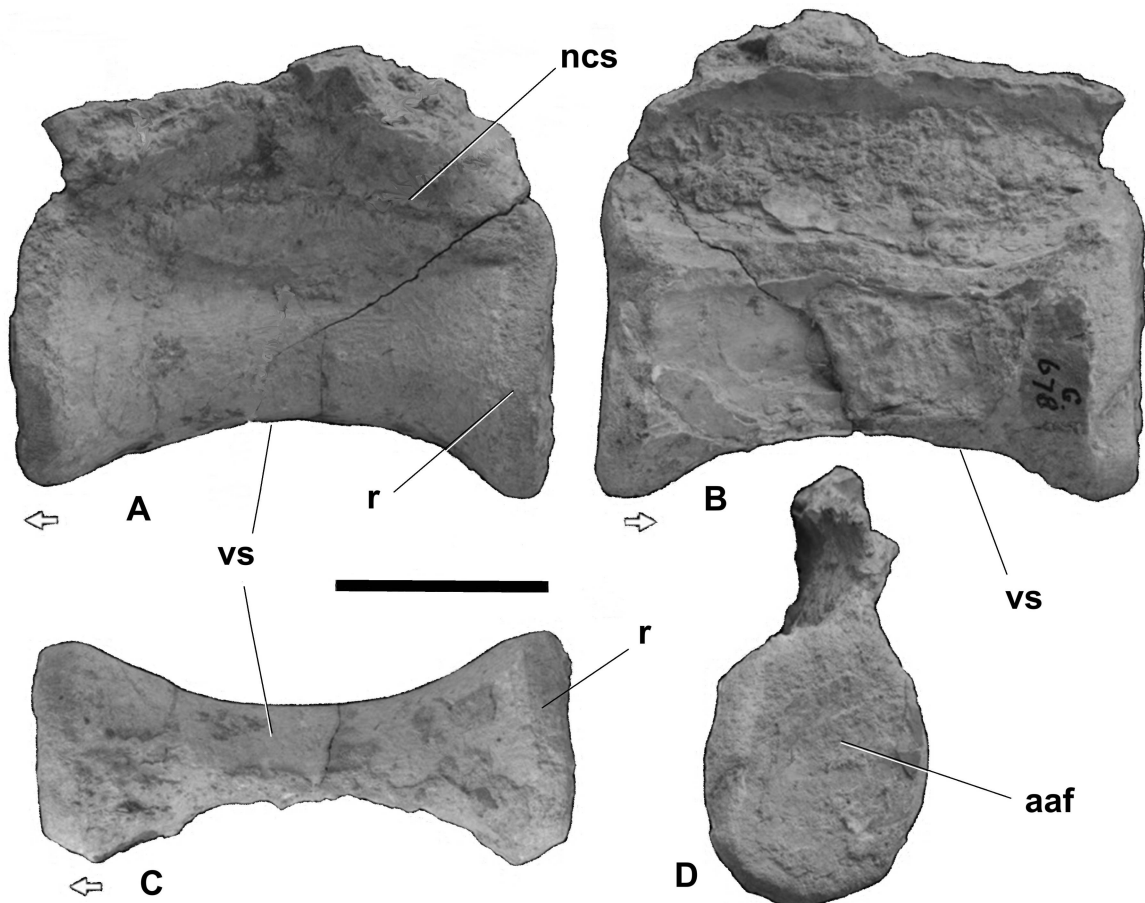


Figure 31. *Sarcosaurus woodi* specimen WARMS G678 mid/posterior dorsal vertebra in left lateral (A), right lateral (B), ventral (C) and anterior (D) views. Source: Ezcurra et al., 2020. Abbreviations: aaf – anterior articular facet, ncs – neurocentral suture, r- rim, vs – ventral surface. Scale bar equals 20mm. Arrows point anteriorly.

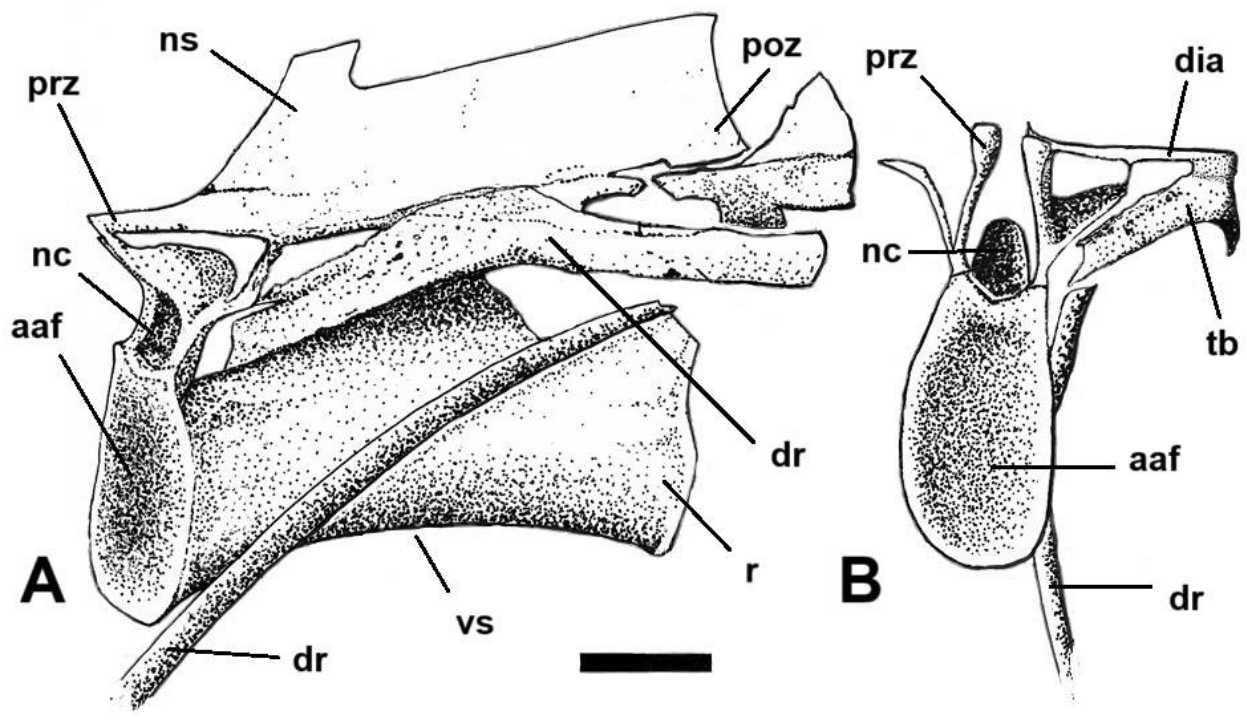


Figure 32. *Notatesseraeraptor frickensis* holotype specimen SMF 06-1 dorsal vertebra 10 in left lateral (A) and anterior (B) views. Source: Hugi, 2008. Abbreviations: **aaf** – anterior articular facet, **dia** – diapophysis, **dr** – dorsal rib, **nc** – neural canal, **ns** – neural spine, **poz** – postzygapophysis, **prz** – prezygapophysis, **r** – rim, **tb** – tuberculum, **vs** – ventral surface. Scale bar equals 10mm.

Taxa	Ratio	Source
Herrerasauridae (<i>Staurikosaurus</i>)	0.77 - 1.11	Galton, 1977
<i>Ceratosaurus</i>	0.83 – 1.03	Madsen (unpublished illustrations)
<i>Coelophysis</i>	0.53 – 0.55	AMNH 7224
<i>Dilophosaurus</i>	0.68 – 0.86	Welles, 1984
<i>Gojirasaurus</i>	0.72 – 0.76	Carpenter, 1997
<i>Syntarsus</i>	0.38 – 0.59	Raath, 1973
<i>Sinraptor</i>	0.93 – 1.02	Currie & Zhao, 1993
Abelisauridae (<i>Carnotaurus</i>)	0.85 – 1.07	Bonaparte et al., 1990
Ornithomimidae (<i>Gallimimus</i>)	0.58 – 0.74	Osmólska, Roniewicz & Barsbold, 1972

Table 2. Variability of height/length ratio of dorsal centra on different theropods. Source: Carpenter, 1997.

Comparative anatomy (*Sarcosaurus* and *Notatesseraeraptor*)

Based on this comparison, two taxa ended up notably important due to both anatomical similarities and associated paleogeographical relevancy: Switzerland's Late Triassic *Notatesseraeraptor frickensis* Zahner & Brinkmann, 2019 (specimen SMF 06-1 and SMF 09-2) and England's Early Jurassic *Sarcosaurus woodi* Andrews, 1921, particularly the WARMS G667-690 specimen with the dorsal vertebra reference WARMS G678.

The dorsal vertebrae of *Notatesseraeraptor frickensis* (fig. 32) is similar to NOVA-FCT-DCT-5562, mostly in the centrum proportions and lateral and anterior outline shape. However some differences are found in the apparent absence of a ventral keel and in the wider and "V" shaped floor of the neural canal. The majority of the compared vertebrae were still encased in the matrix which made it difficult to properly compare (Hugi, 2008).

The material attributed to the *Sarcosaurus* with the reference WARMS G678 (fig. 31) is a mid/posterior dorsal centrum with strong visual resemblance to NOVA-FCT-DCT-5562. Out of all the taxa compared, *Sarcosaurus woodi* vertebra WARMS G678 resembles our material the most in general shape. Some proportions, namely the length/height ratio differ, however it is still within the accepted variability seen along the dorsal series of theropods.

Phylogenetic analysis

A phylogenetic analysis was made using the matrix from Ezcurra et al. (2023) for basal theropods. This matrix is adapted from Nesbitt et al. (2009) and includes 63 taxa, comprising mostly Triassic archosaurs, with the archosauromorph *Erythrosuchus africanus* as the outgroup. Several iterations were added to the original Nesbitt et al. (2009) matrix, with the latest version from Ezcurra et al. (2023) including 389 characters. Since the dorsal vertebrae centra characters in the matrix were neither numerous or detailed enough to properly classify NOVA-FCT-DCT-5562, 13 new characters were created and coded for all taxa.

The characters used to define vertebrae centrum, 329) from Nesbitt et al. (2009) + new set of characters 390)-402), are described below. A schematic diagram of each character is present after each description (figs. 33-46), and a general overview of all the characters is presented at the end (fig. 47).

329) Posterior dorsal vertebrae, length: strongly shortened, centrum length less than 1.33 times the height of the anterior articular surface (0); relatively short, centrum length equal or more than 1.33 times the height of the anterior articular surface (1); significantly elongated, centrum length more than two times the height of the anterior articular surface (2).

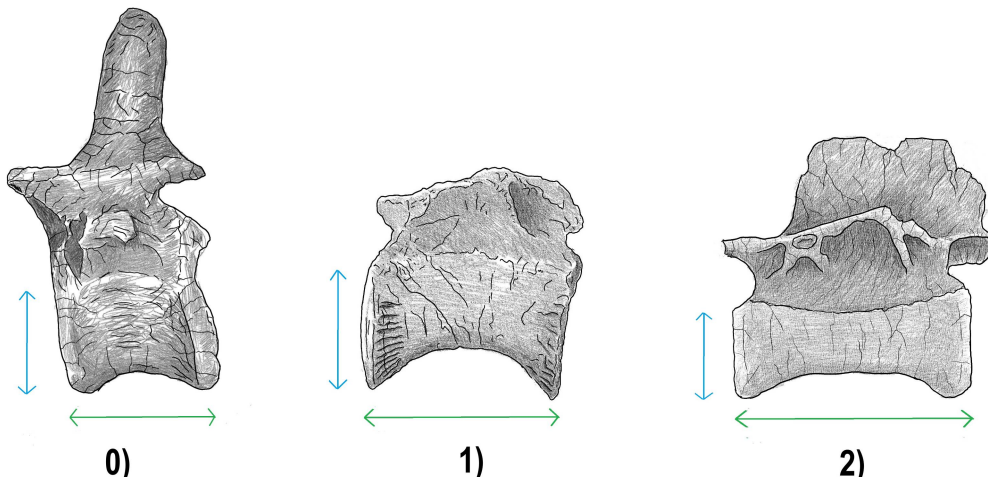


Figure 33. Graphic representation of the character states for character 329). Numbers refer to the character respective state. Images are not to scale.

390) Mid dorsal vertebral centrum, ventral limit of articular facet relative position*: anterior and posterior at the same level, or close (0); anterior facet elevated in comparison to the posterior (1).

*Character 286) on Zahner and Brinkmann (2019) matrix.

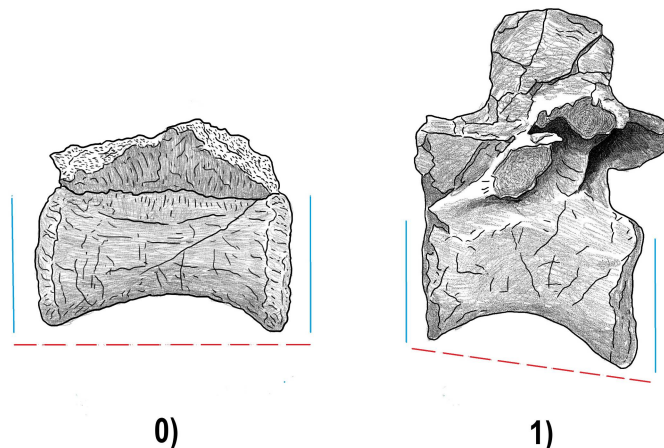


Figure 34. Graphic representation of the character states for character 390). Numbers refer to the character respective state. Images are not to scale.

391) Mid dorsal vertebral central articular facets outline*: taller than wide (0); sub-circular (as tall as wide) (1); wider than tall (2).

*Character 287) on Zahner and Brinkmann,(2019) matrix.

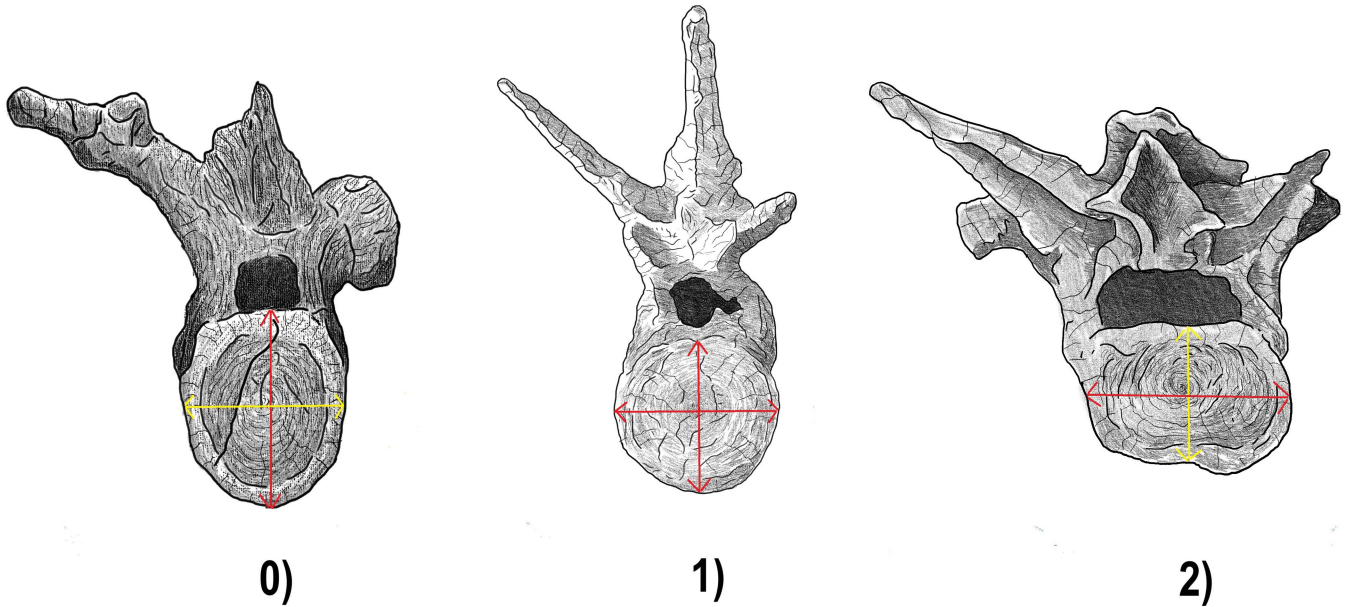


Figure 35. Graphic representation of the character states for character **391)**. Numbers refer to the character respective state. Images are not to scale.

392) Dorsal vertebrae articular facet type*: amphiplatyan (both nearly planar) (0); amphicoelus (both concave) (1); opisthocelous (planar anteriorly, concave posteriorly) (2).

*Character 288) on Zahner and Brinkmann,(2019) matrix.

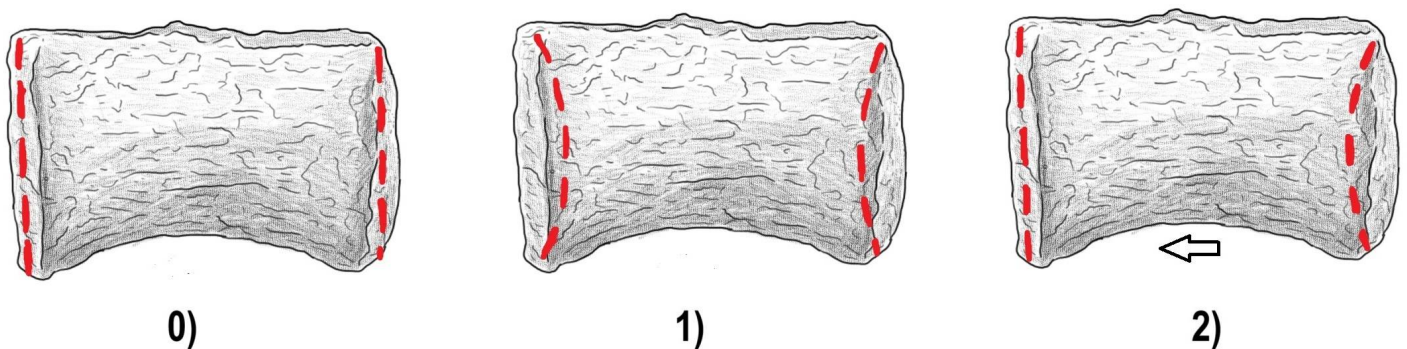


Figure 36. Graphic representation of the character states for character **392)**. Numbers refer to the character respective state. Arrow points anteriorly. Images are not to scale.

393) Dorsal vertebrae neural canal walls shape*: straight and subparallel (width nearly constant along the canal) (0); curved (hourglass curvature of the pedicels, width narrower at the mid centrum) (1).

*Character 289) on Zahner and Brinkmann,(2019) matrix.

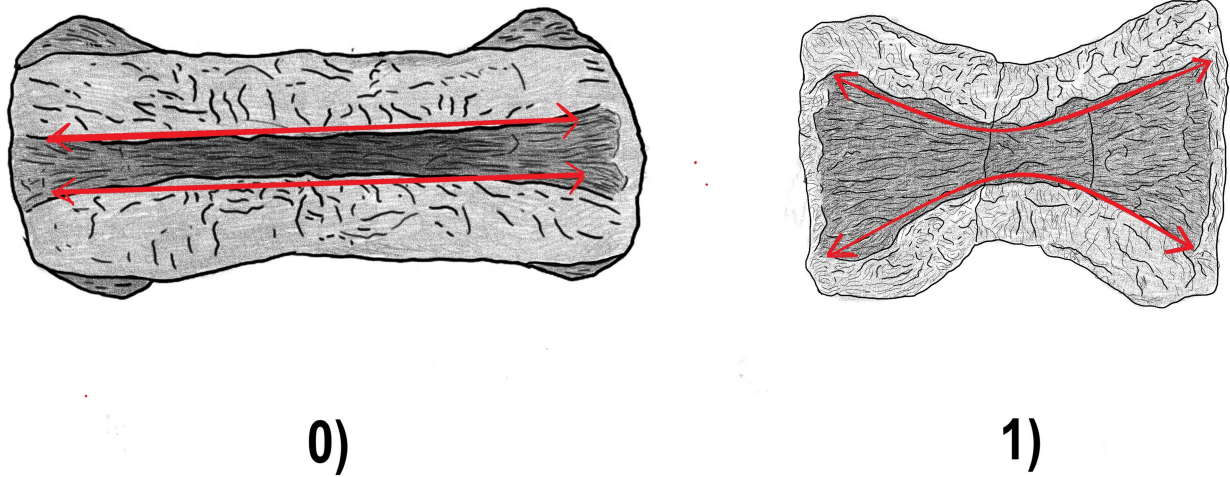


Figure 37. Graphic representation of the character states for character **393)**. Numbers refer to the character respective state. Images are not to scale.

394) Dorsal vertebra, midcentrum floor of neural canal width relative to the base of the pedicels width (best seen in unfused vertebrae in dorsal view)*: narrower (0); wider (1).

*Character 290) on Zahner and Brinkmann (2019) matrix.

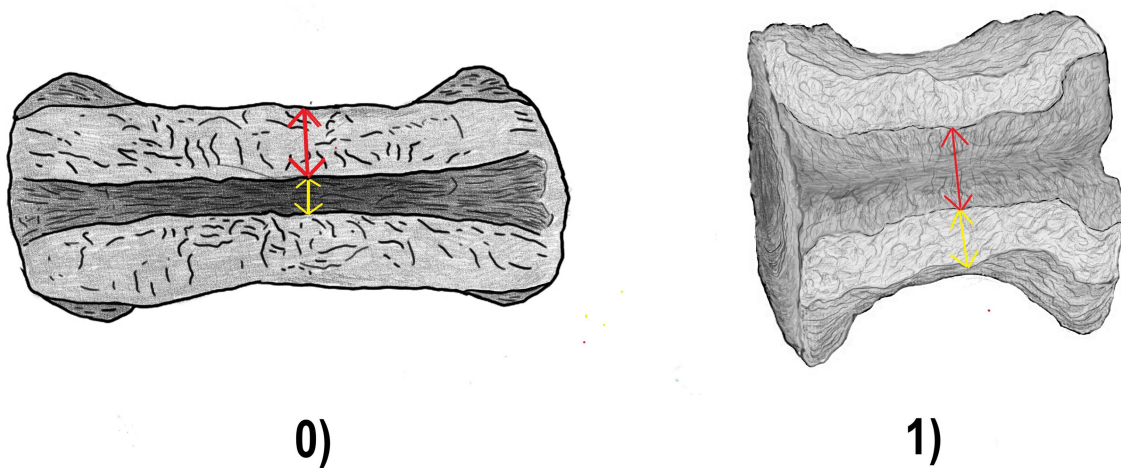


Figure 38. Graphic representation of the character states for character **394)**. Numbers refer to the character respective state. Images are not to scale.

395) Dorsal vertebra: floor of neural canal / centrum maximum width*: narrow: less than 0.2 (0); between 0.2 and 0.4 (1); wide neural canal: more than 0.4 (2).

*Character 291) on Zahner and Brinkmann (2019) matrix.

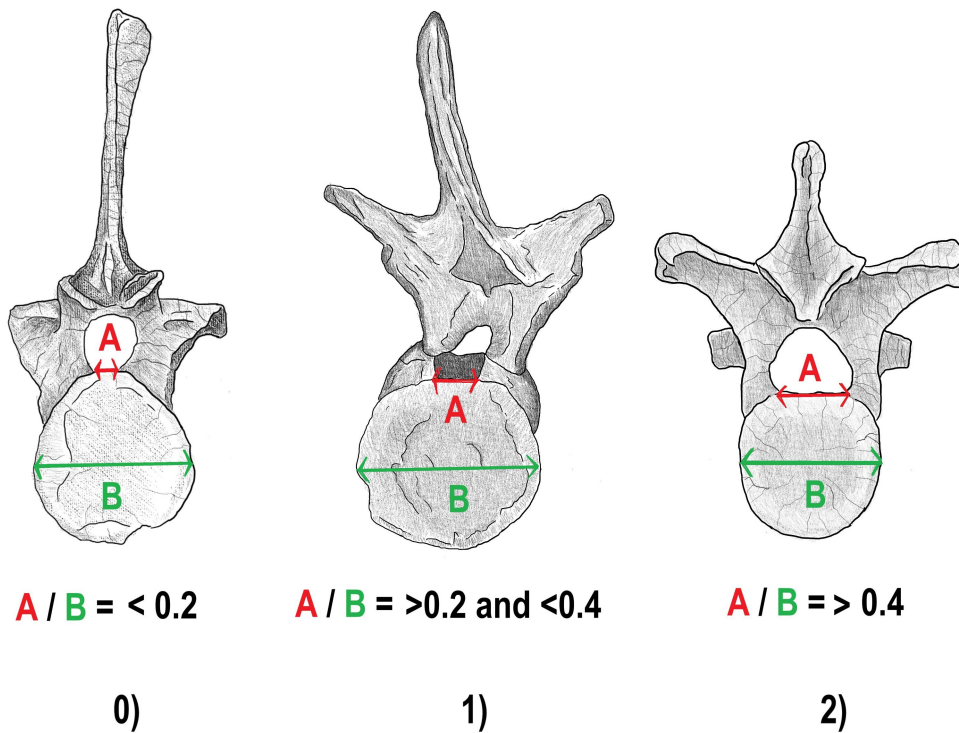


Figure 39. Graphic representation of the character states for character **395)**. Numbers refer to the character respective state. Images are not to scale.

396) Dorsal vertebra: neurocentral suture orientation (this refers to the main line trend not to the serrated suture)*: straight and horizontal (anterior, mid and posterior section leveled) (0); sinusoidal (normally, the anterior portion is lower) (1); bowed (higher toward the ends) (2).

*Character 292) on Zahner and Brinkmann (2019) matrix.

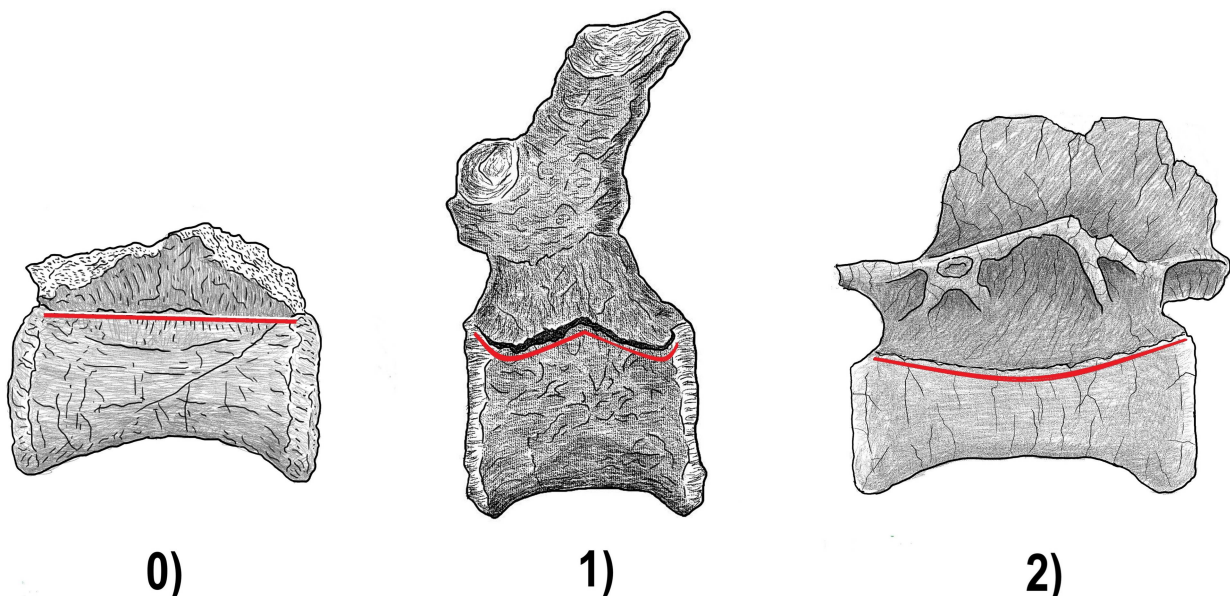


Figure 40. Graphic representation of the character states for character **396)**. Numbers refer to the character respective state. Images are not to scale.

397) Mid to posterior dorsal vertebral centrum: lateral walls: continuous or gently concave, without a clear excavated fossa (0); excavated, forming a fossa (shallow lateral depression) (1).

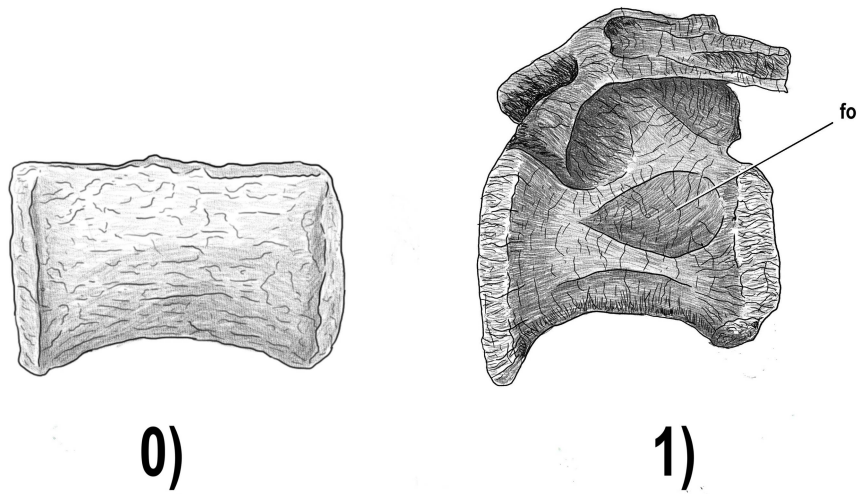


Figure 41. Graphic representation of the character states for character 397). Numbers refer to the character respective state. fo – fossa/depression. Images are not to scale.

398) Mid to posterior dorsal vertebral centrum: surface near the rim*: smooth (0); lateral and ventral longitudinal striations (1).

*Character 293) on Zahner and Brinkmann (2019) matrix.

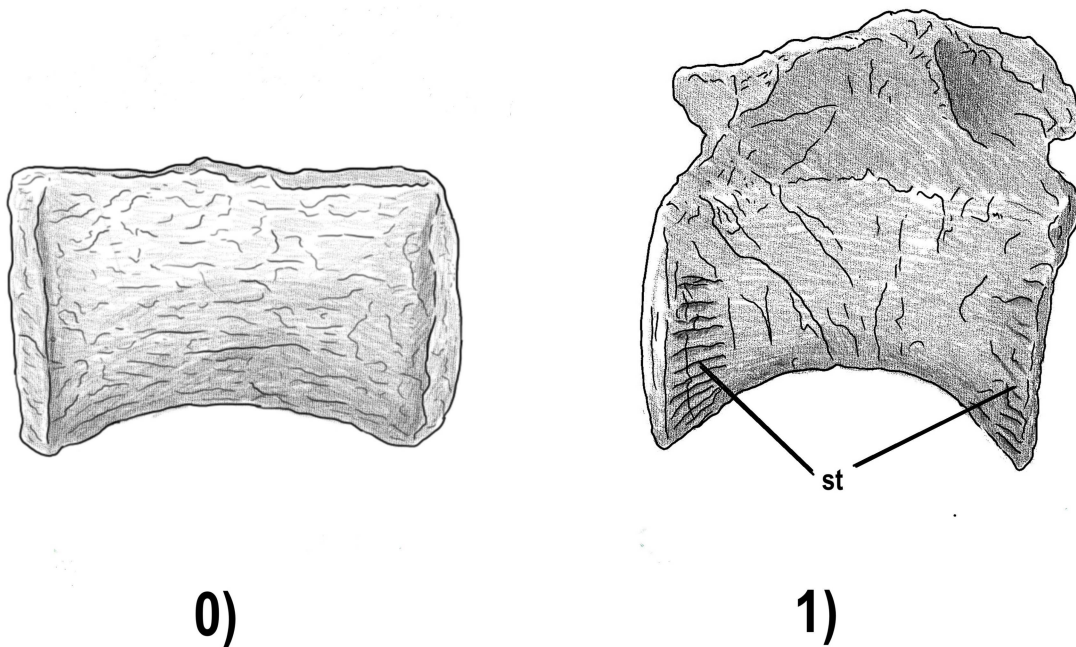


Figure 42. Graphic representation of the character states for character 398). Numbers refer to the character respective state. Images are not to scale.

399) Mid to posterior dorsal vertebral centrum: ventral ridge excavation curvature in the midcentrum*: deep, 20% or more of the anterior facet height (curves strongly towards the mid centrum) (0); shallow, less than 20% of the anterior facet height (the curve is more subtle) (1).

*Character 294) on Zahner and Brinkmann (2019) matrix.

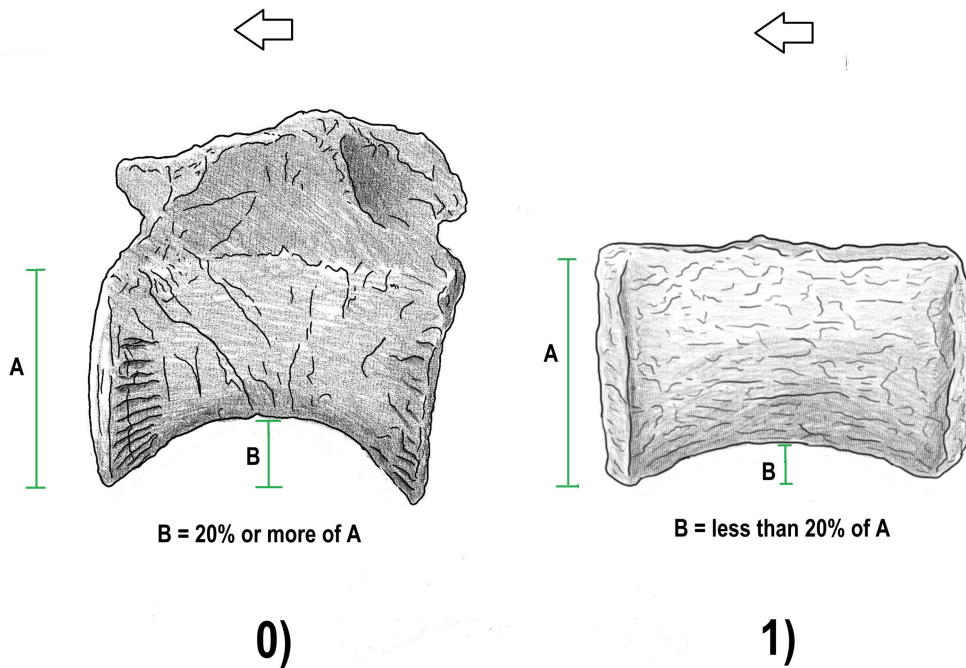


Figure 43. Graphic representation of the character states for character **399)**. Numbers refer to the character respective state. Arrows point anteriorly. Images are not to scale.

400) Mid to posterior dorsal vertebral centrum: ventral surface curve symmetry in lateral view*: symmetric (anterior and posterior halves of the curve are sub-equal) (0); asymmetrical (ventral curve clearly more pronounced anterior or posteriorly) (1).

*Character 295) on Zahner and Brinkmann (2019) matrix.

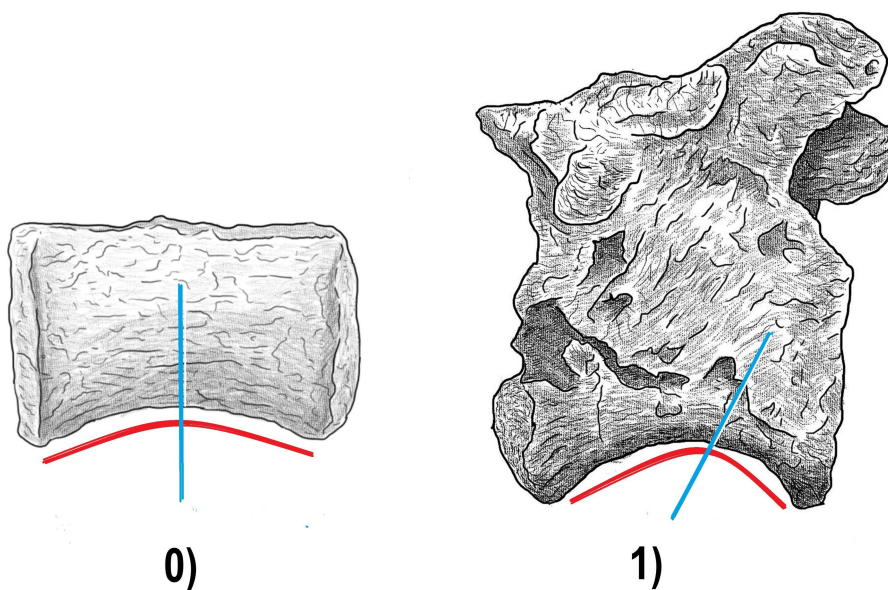


Figure 44. Graphic representation of the character states for character **400)**. Numbers refer to the character respective state. Images are not to scale.

401) Mid to posterior dorsal vertebral centrum: ventral surface keel condition*: cylindrical (U-shaped), without obvious longitudinal keel (0); cylindrical (V-shaped) forming a subtle keel in the continuation of the centrum shape (1); noticeably present lamina-like keel (2).

*Character 296) on Zahner and Brinkmann (2019) matrix

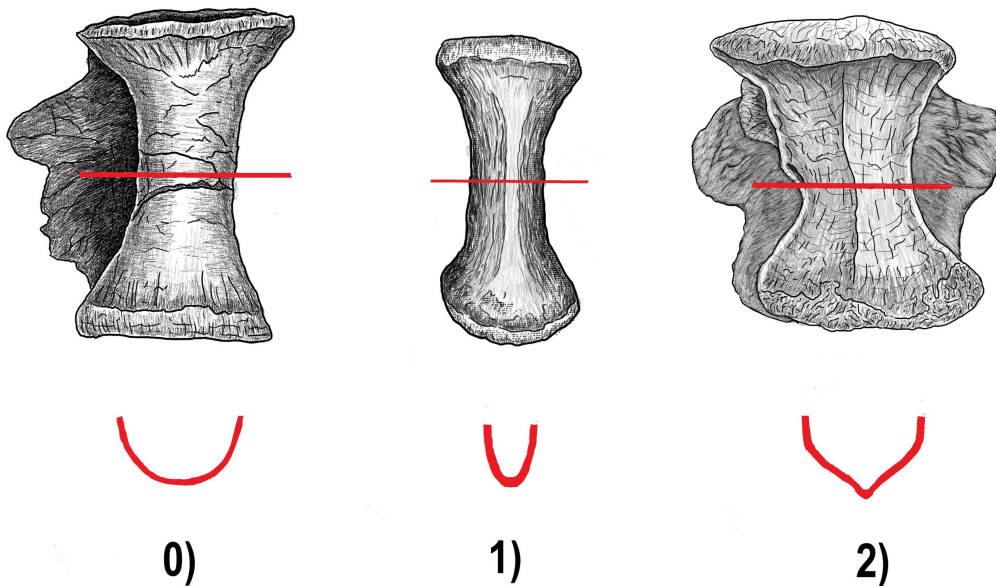


Figure 45. Graphic representation of the character states for character 401). Numbers refer to the character respective state. Images are not to scale.

402) Mid to posterior dorsal vertebral centrum lateral excavation*: strongly laterally constricted at the mid-centrum (hourglass shaped in ventral view), mid centrum width <50% of posterior facet width (0); poorly laterally constricted at mid centrum (more cylindrical and less hourglass shaped in ventral view), mid centrum width >50% of posterior facet width (1).

*Character 297) on Zahner and Brinkmann (2019) matrix.

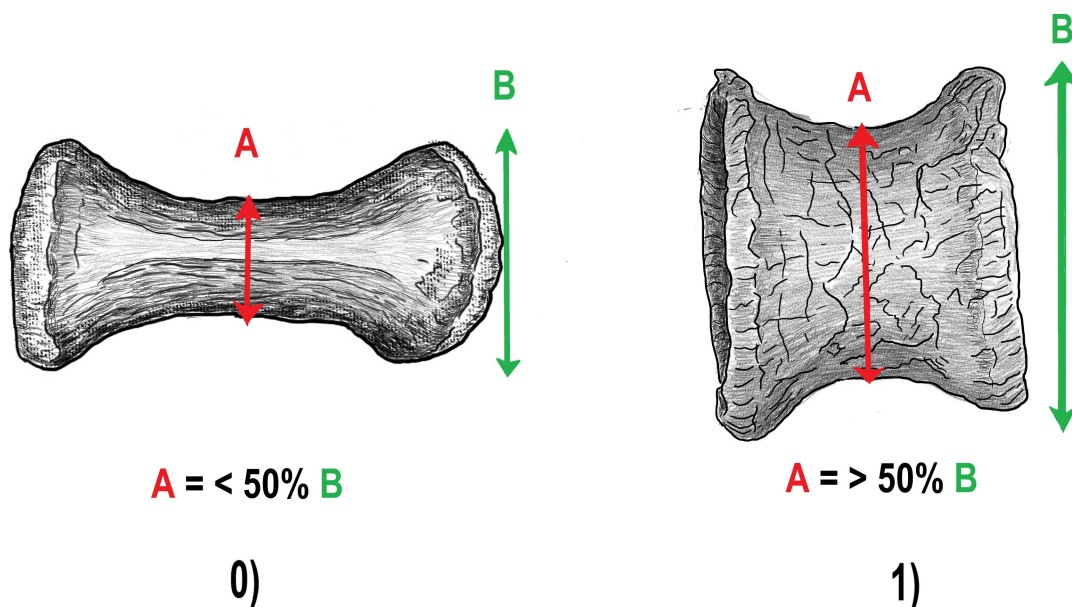


Figure 46. Graphic representation of the character states for character 402). Numbers refer to the character respective state. Images are not to scale.

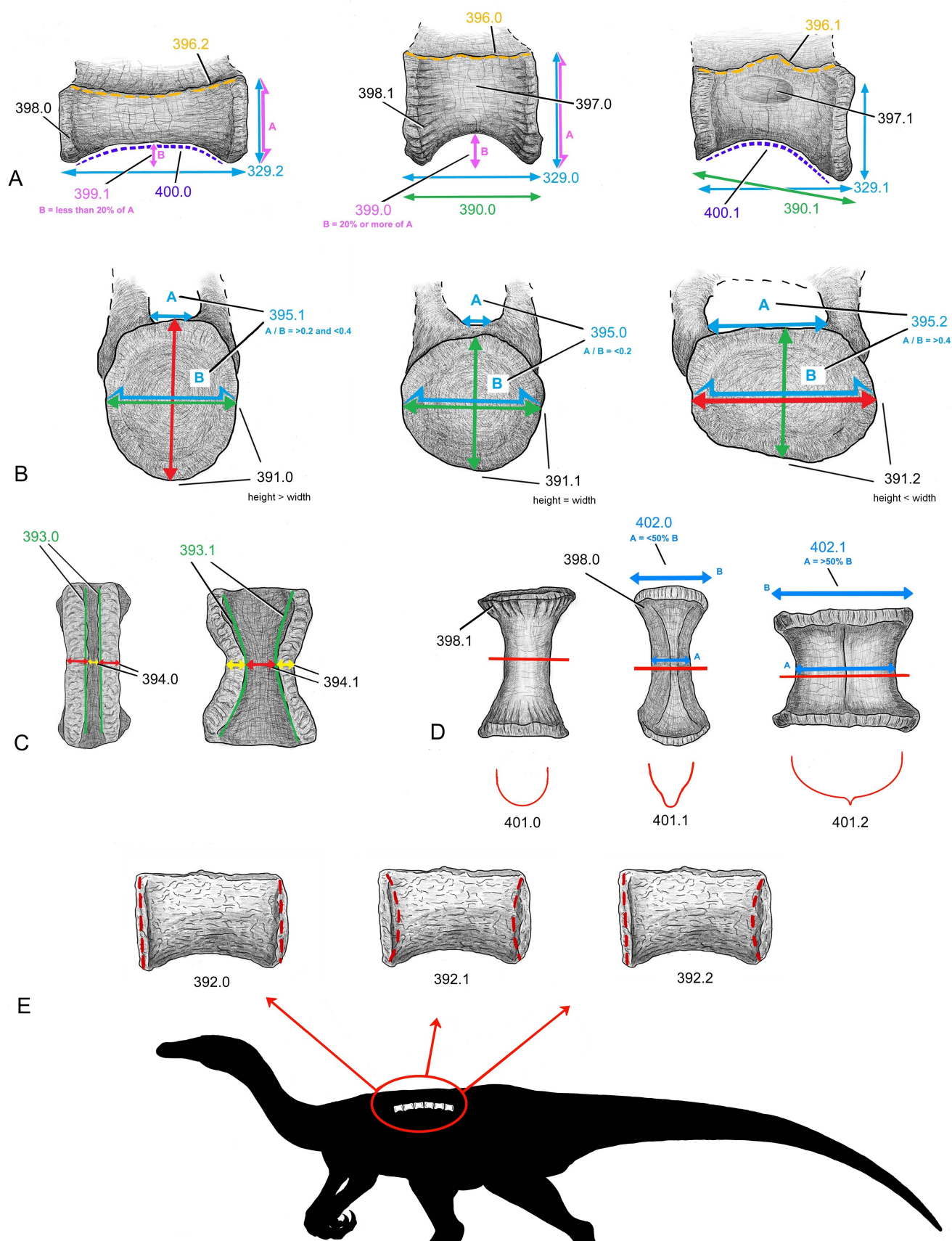


Figure 47. General graphic representation of the set of character states used to define the dorsal vertebrae centra in left lateral (A & E), anterior (B), dorsal (C) and ventral (D) views. Numbers refer to the character and respective state (ex. 400.1 refers to character “400” with state condition “1”). Images are not to scale.

The initial draft of this new data set included two additional characters; one for the level of similarity between the anterior and posterior articular facets and the other for the shape of neural canal floor. After the first analysis, these two characters revealed zero or close to zero variation being their presence redundant and not significant in the results, so they were removed.

Phylogenetic analysis with Ezcurra et al. 2023 matrix

The original matrix includes 2 characters regarding dorsal centra length/height ratio, 328) for the anterior and mid-dorsals and 329) for the posterior dorsals. NOVA-FCT-DCT-5562 vertebra is here interpreted as mid to posterior and, due to the significant differences between anterior and posterior dorsals morphology, this vertebra was coded in character 329).

Only one change was made to the original matrix, with character 328) for *Revueltosaurus callenderi* being updated to state 0).

Due to unavailability of *Ceratosaurus nasicornis* material for analysis, the coding for characters 391), 393), 394), 395), 396), 397), 398), 399) and 401) was based on elements assigned to *Ceratosaurus dentisulcatus* and *Ceratosaurus magnicornis* because the validity of these two species is still contested (Rauhut, 2000; Carrano & Sampson, 2008) and no differences to the type species regarding these characters are mentioned in their original description by Madsen and Welles (2000).

For *Dracoraptor hanigani*, the coding was based on some scattered vertebrae among the main material which were interpreted by Martill et al. (2016) as putative dorsals.

Due to the apparent similarity of NOVA-FCT-DCT-5562 with *Sarcosaurus*, instead using just *Sarcosaurus woodi* as in the original matrix, we chose to transpose all *Sarcosaurus* entries available in the Ezcurra et al. (2020) revision of the genus (*Sarcosaurus woodi*, *Sarcosaurus andrewsi*, WARMS G677-690 and all combined) to the new matrix.

The isolated tibia of the Ezcurra et al. (2023) study, NMS.G.1994.10.1, was removed.

After several tests in TNT, the best result (131 trees with a best score of 1491 steps) was achieved after removing all *Sarcosaurus* entries except the WARMS G677-690 specimen.

The results (fig. 48) do not differ considerably from the Ezcurra et al. (2020) and Ezcurra et al. (2023) studies. The 50% cut-off majority rule analysis placed NOVA-FCT-DCT-5562 within Neotheropoda, closely related to *Sarcosaurus*, *Tachiraptor* and *Averostra* with 64% consensus rate.

Dracoraptor, *Liliensternus*, *Zupaysaurus*, *Cryolophosaurus*, *Gojirasaurus* and *Dilophosaurus* still occupy a more basal position within Neotheropoda but *Cryolophosaurus*, *Gojirasaurus* and *Dilophosaurus* appear now in polytomy. *Tachiraptor* is shown more derived than *Sarcosaurus* and just outside *Averostra*. Coelophysoidea again appears as a monophyletic clade at the base of Neotheropoda.

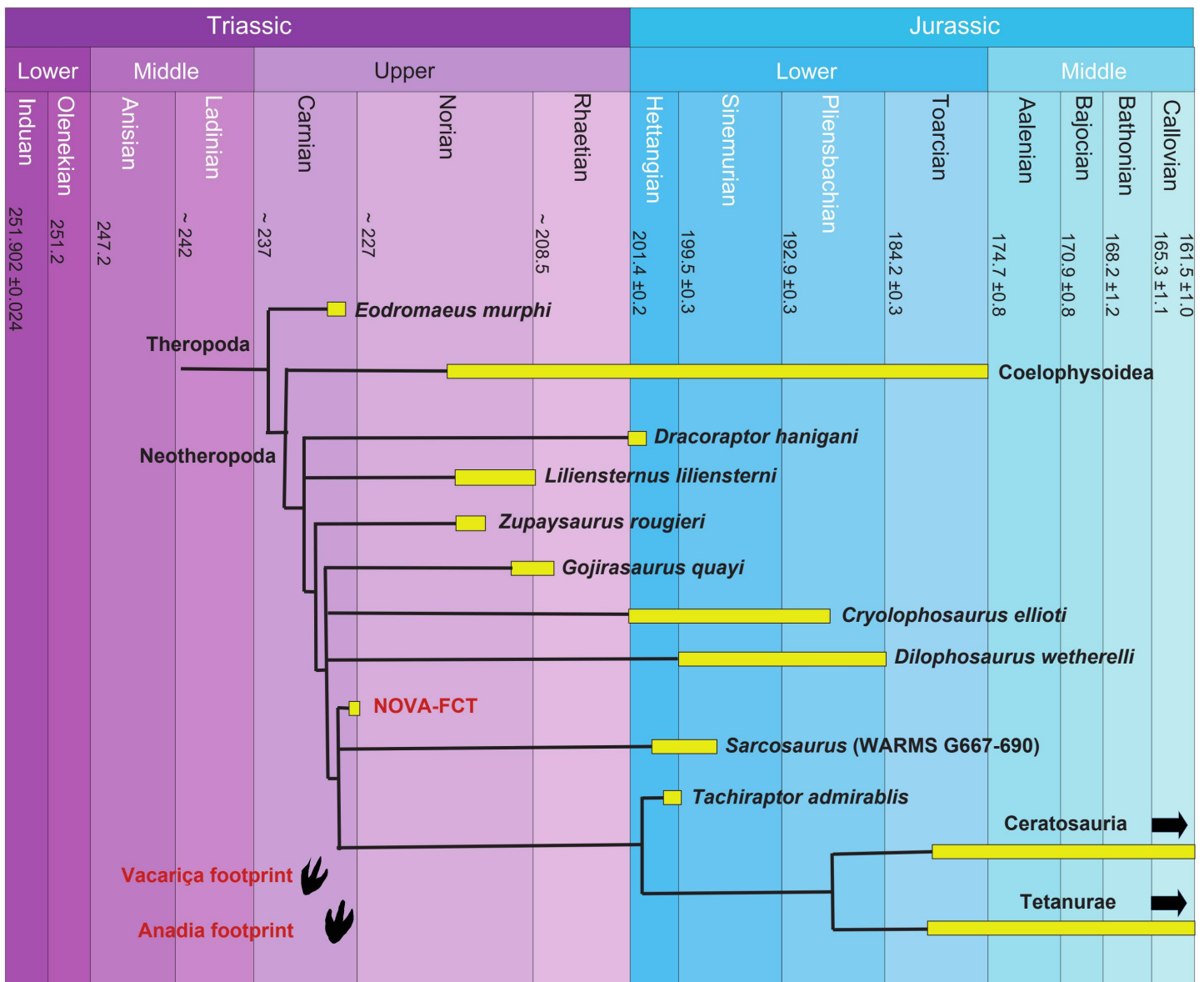


Figure 48. Phylogenetic results based on a TNT strict consensus analysis for NOVA-FCT-DCT-5562 vertebra within the updated matrix from Ezcurra et al. (2023) adapted from Nesbitt et al. (2009).

Phylogenetic analysis with Zahner and Brinkmann (2019) matrix

With the available digital material, some characters of *Notatesseraeraptor frickensis* were impossible to code in the Ezcurra et al. (2023) matrix. Instead, both NOVA-FCT-DCT-5562 and all the material referred to *Sarcosaurus* from Ezcurra et al. (2020) were added to the *Notatesseraeraptor frickensis* matrix from Zahner and Brinkmann (2019).

This matrix has fewer characters (285) and fewer taxa (23) than the one from Ezcurra et al. (2023), includes only dinosaurs (with *Eoraptor lunensis* as the outgroup) and has a main focus on basal theropods.

The same new characters created for the Ezcurra et al. (2023) matrix were added to the Zahner and Brinkmann (2019) matrix and re-numbered accordingly (table 3).

Character description	Character number for Ezcurra et al. (2023)	Character number for Zahner & Brinkmann (2019)
Mid dorsal vertebral centrum: ventral limit of articular facet relative position	390	286
Mid dorsal vertebral central articular facets outline	391	287
Dorsal vertebrae articular facet type	392	288
Dorsal vertebrae neural canal walls shape	393	289
Dorsal vertebra, midcentrum floor of neural canal width relative to the base of the pedicels width	394	290
Dorsal vertebra: floor of neural canal / centrum maximum width	395	291
Dorsal vertebra: neurocentral suture orientation	396	292
Mid to posterior dorsal vertebral centrum: lateral walls	397	Considered the same as 185
Mid to posterior dorsal vertebral centrum: surface near the rim	398	293
Mid to posterior dorsal vertebral centrum: ventral ridge excavation curvature in the midcentrum	399	294
Mid to posterior dorsal vertebral centrum: ventral surface curve symmetry in lateral view	400	295
Mid to posterior dorsal vertebral centrum: ventral surface keel condition	401	296
Mid to posterior dorsal vertebral centrum lateral excavation	402	297

Table 3. New characters to define dorsal vertebrae centra for the Ezcurra et al (2023) matrix and their equivalent character number in the Zahner & Brinkmann (2019) matrix.

Character 397, for the presence of a fossa along the lateral surface of the centrum, was already described by Zahner and Brinkmann (2019) in their matrix in character 185, albeit having 3 character states (distinguishing anterior from posterior dorsals) instead of two. In this context, new character 397 became redundant and was excluded. Some entries for 397 in Ezcurra et al. (2023) differ from what Zahner and Brinkmann (2019) coded for the same taxa in 185, however the matrices was not changed because of the subjectivity in this character interpretation.

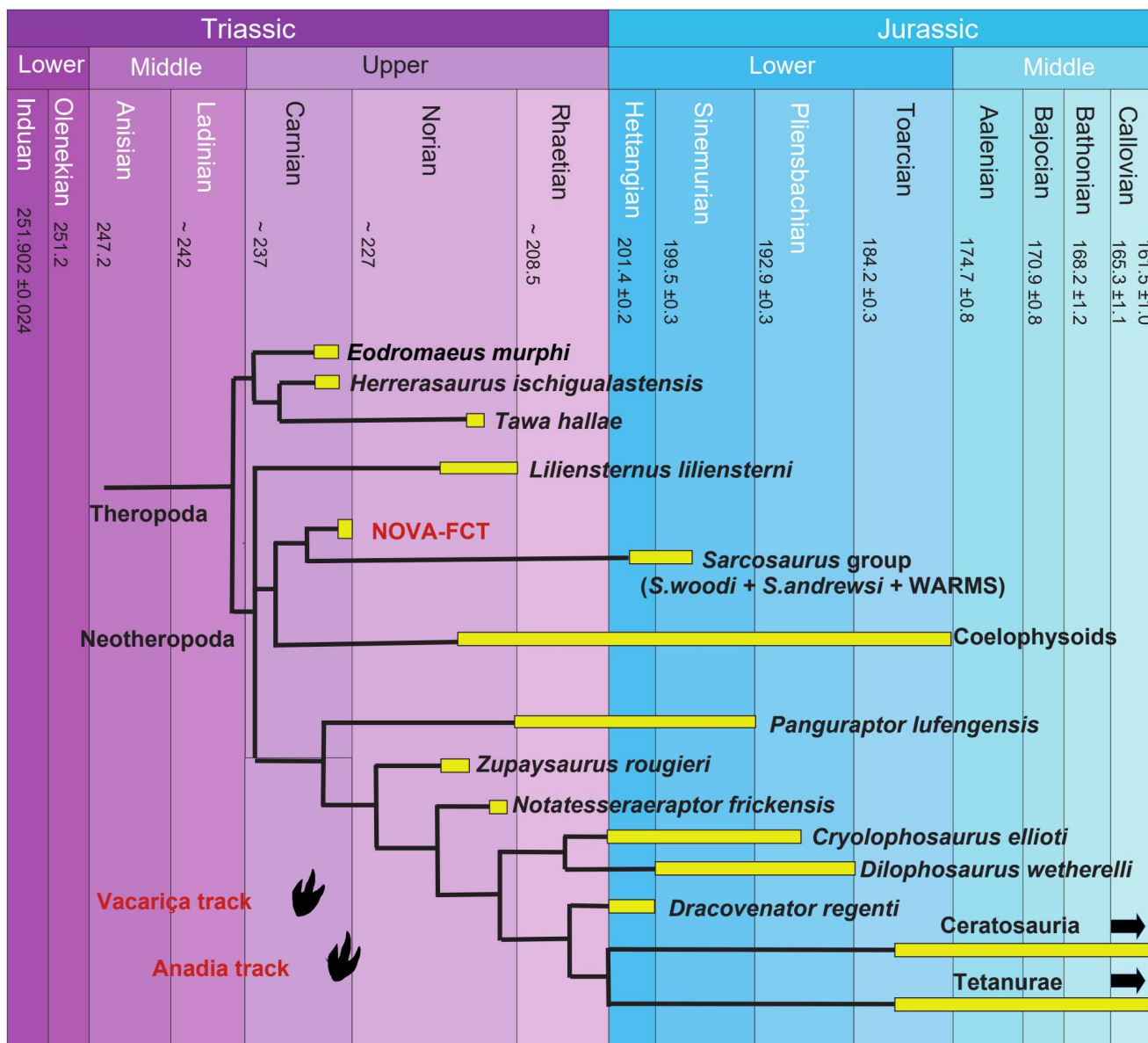


Figure 49. Phylogenetic results based on a TNT strict consensus analysis for NOVA-FCT-DCT-5562 within the updated matrix from Zahner & Brinkmann (2019).

Several tests were conducted in TNT regarding the “*Sarcosaurus* group”: in this matrix, having either only WARMS G677-690 specimen or only all *Sarcosaurus* material combined would result in large politomies in a 50% cut-off majority rule scenario. The most consistent tree (with 746 steps and 58 trees generated) was obtained with all the entries from the “*Sarcosaurus* group” present.

The final result (fig. 49) shows *Notatesseraeraptor frickensis* phylogenetic position unchanged with the new characters, placed as a basal neotheropod with a 58% consensus rate.

NOVA-FCT-DCT-5562 is found closely associated to the “*Sarcosaurus* group”, however the whole group appear in a 51% consensus polytomy closer to coelophysoids and unrelated to *Notatesseraeraptor frickensis* and other stem averostrans.

Discussion

The results of both phylogenetic analyses (based on matrices from Ezcurra et al. (2023) and Zahner and Brinkmann (2019)), show an affinity between NOVA-FCT-DCT-5562 and *Sarcosaurus* and both also place them within Neotheropoda, but varying significantly in where they fall within this group. Should be noted that *Sarcosaurus* has previously been regarded as a coelophysoid by Carrano and Sampson (2004) and this result is retained when the dataset of Zahner and Brinkmann (2019) is used. Alternatively, *Sarcosaurus* is found as a clade more close to *Averostra* when is based in the matrix of Ezcurra et al. (2023). However, when comparing both matrices, Ezcurra et al. (2023) has a higher count of characters (402 vs. 297) and its final consensus percentages are also higher; so, we chose to follow these results with *Sarcosaurus* still considered a non-coelophysoid neotheropod and, by association, the same for NOVA-FCT-DCT-5562. Nevertheless, due to the fragmentary nature of these specimens, these results should be taken with caution.

Regarding *Notatesseraeraptor frickensis*, despite the chronological, relative geographical proximity and apparent visual similarities, this taxon was not recovered in close relationship to NOVA-FCT-DCT-5562. However, since most of the characters defining all *Sarcosaurus* specimens are related to hindlimb bones and these are missing for *Notatesseraeraptor*; the analysis between all these taxa ended up being rather poor, being based mainly on few vertebrae and pelvic characters. Should also be noted that the coding for *Notatesseraeraptor frickensis* regarding the new characters was not complete, essentially lacking character states for the neural canal attributes. Hence, conclusions regarding the phylogeny between *Notatesseraeraptor* and *Sarcosaurus* are still uncertain.

The Carnian vertebra NOVA-FCT-DCT-5562 from Portugal is, at least, 26 Ma older than the Late Hettangian *Sarcosaurus* from UK, thus very unlikely to be the same species or even the same genus. The specimen is fragmentary and the phylogenetic results are not solid, but assuming that the phylogenetic position is correct, this occurrence represents a potential new species to be supported with further hypothetical findings. The close relationship between these two taxa also pushed back the lineage leading to *Sarcosaurus* from the latest Late Triassic (Ezcurra et al., 2020) to the earliest Late Triassic. In fact, if NOVA-FCT-DCT-5562 is indeed a neotheropod and the estimated age for the Triassic Silves Group correct, this is the oldest known member of this clade, and the origin of the group is about 10 Ma older than previously thought.

NOVA-FCT-DCT-5562 is one of the few examples of Triassic non-coelophysoid stem-averostran neotheropods along with taxa such as South America's *Zupaysaurus*, North America's *Gojirasaurus* and Europe's *Notatesseraeraptor* and, depending on the phylogeny, *Liliensternus* (Smith et al., 2007; Nesbitt et al., 2009; Sues et al., 2011; Marsh et al., 2019; Zahner & Brinkmann, 2019; Ezcurra et al., 2020). This new find from Loulé, Algarve, reinforces the notion that neotheropods were already prevalent during the Late Triassic, well distributed worldwide and well documented in Europe.

Brief note on the dinosaur footprints from the Triassic of Portugal

Courbouleix (1974) made a very detailed description of the footprint he found in Vacariça, Mealhada which enables us to clearly identify it as coming from a theropod dinosaur. This track's remarkable size represents a very large theropod, one of the biggest from the Triassic. The locality referred by Courbouleix still exists today and, as of May 2024, a large slab found at this place (fig. 5.A) is the most likely location of the track - which could not be found, probably having been lost to erosion.

In Crasto da Anadia, where Palain (1976) reported the other track, the best location found is now an urban area (fig. 5.B) without Triassic outcrops, with the tracks probably being lost forever. The exact morphology of the tracks is not clear by the photographs taken by Palain and therefore should be assigned as Tetrapoda indet.

Conclusions

A new dorsal vertebral centrum from the Late Triassic (Carnian) is reported from Penina Sul, Salir, Loulé, Algarve, Portugal. This is the first Triassic dinosaur bone from the Iberian Peninsula and the oldest dinosaur ever found in that region.

Comparisons with other theropods allowed to identify 12 new phylogenetic characters for dorsal centrum alone.

Phylogenetic analysis places this specimen as the oldest known member of Neotheropoda and the southernmost Triassic European member of this clade. Moreover, the phylogenetic analysis nested the Portuguese specimen with Early Jurassic *Sarcosaurus* from England, particularly the WARMS G667-690 specimen. This represents a theropod species, likely yet to be described, but too fragmentary and lacking autapomorphies to be erected or attributed to any known species.

Chapter II - The theropod dinosaur *Ceratosaurus* from the Upper Jurassic of Lourinhã Formation

Introduction

***Ceratosaurus* overview**

Ceratosaurus (fig. 50) was a genus of theropod dinosaur from the Late Jurassic (Kimmeridgian/Tithonian) of North America and Europe (Marsh, 1884; Gilmore, 1920; Madsen & Welles, 2000; Mateus et al., 2006). The name, meaning in Greek “*keratos*” for “horn” and “*sauros*” for “lizard”, references the three horns on the head - two over the eyes and one over the nose. The name of the type species, *Ceratosaurus nasicornis*, reinforces this assumption, meaning “nose horn” in Latin (Marsh, 1884; Gilmore, 1920). Two other species have been described by Madsen and Welles (2000), *Ceratosaurus dentisulcatus* (referencing the grooves on the teeth) and *Ceratosaurus magnicornis* (referencing the bigger horns of the specimen), however this classification is not widely accepted (Rauhut, 2000; Carrano & Sampson, 2008).

It was a medium to large sized carnivore, reaching 6 – 7 m in length and 600kg in weight (Marsh, 1884; Marsh, 1893). Besides the horned head ornamentation other distinctive characteristics include proportional large teeth, small arms with four fingered hands and a row of osteoderms along the back.

This theropod is one of the most emblematic dinosaurs coming from the USA’s Morrison Formation, also famous by *Allosaurus*, *Torvosaurus*, *Apatosaurus*, *Diplodocus*, *Camarasaurus*, *Brachiosaurus* and *Stegosaurus*, which lived along side it (Cope, 1877; Marsh, 1877a, 1877b; Marsh, 1878; Marsh, 1884; Riggs, 1903; Gilmore, 1920; Galton & Jensen, 1979).

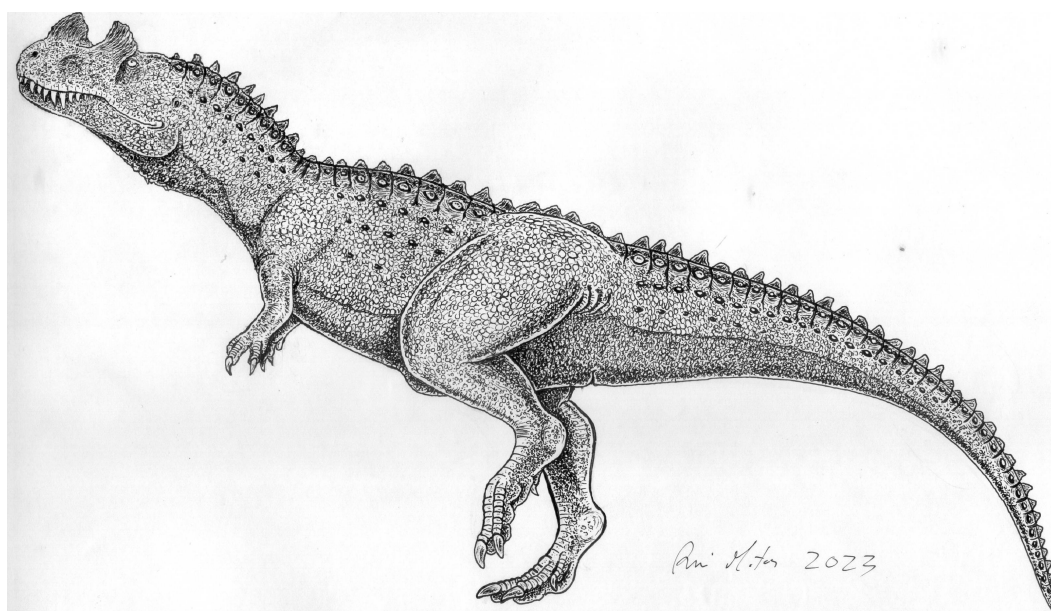
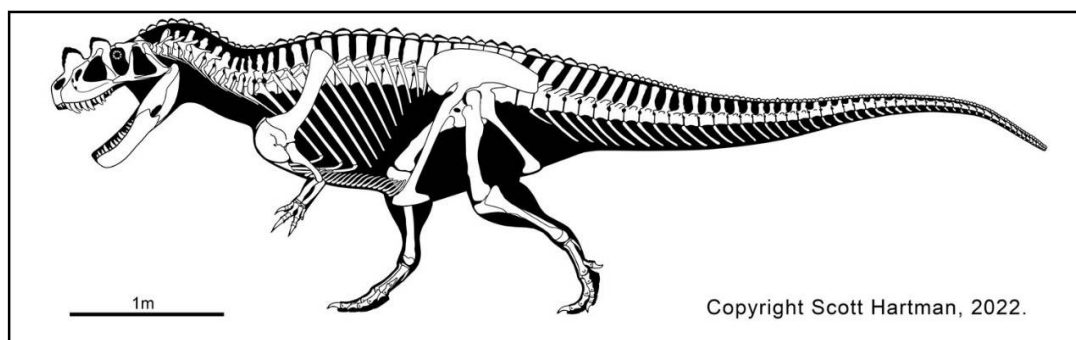


Figure 50. – above, *Ceratosaurus dentisulcatus* skeleton (source: Scott Hartman, 2022); below – life restoration.

History of *Ceratosaurus* study

Ceratosaurus was first described by Othniel Charles Marsh in 1884 based on an almost complete skeleton found in Colorado's Morrison Formation Rocks dated from the Upper Jurassic - Kimmeridgian/Tithonian (Marsh, 1884; Gilmore, 1920; Madsen & Welles, 2000). Marsh named the type species *Ceratosaurus nasicornis* and, based on distinct anatomical characteristics of the animal, set it apart from the other major theropod taxa known at the time, such as *Megalosaurus*, *Allosaurus* or coelurosaurs then creating the new family Ceratosauria (Marsh, 1884; Carrano & Sampson, 2008).

Marsh (1884) cited the following characteristics to define Ceratosauria: (i) horn on the skull, (ii) opisthocoelic cervical vertebrae and the rest amphicoelic, (iii) slender pubis, (iv) co-ossified bones of the pelvis, (v) ascending astragalar process, (vi) row of osteoderms. Most of these characters were defined in a time when few dinosaur genera were known and eventually most of them were later identified in other theropod groups, thus becoming invalid to define Ceratosauridae, however, the horns and osteoderms are still characteristic of *Ceratosaurus* and some closer taxa (Carrano & Sampson, 2008).

In 1920, Gilmore made a detailed re-description of the holotype of *Ceratosaurus nasicornis* and, at the time of writing, is still the most complete overview of this species.

Except for some inconclusive fragmentary remains, reported by Stovall in 1938, the holotype described by Marsh in 1884 was for more than seventy years the only relevant *Ceratosaurus* material known in North America. Only in the second half of the 20th century more important finds came to light, when two new specimens were uncovered. The first one, UMNH VP 5278, was dug up by paleontologist James Madsen in Utah's Cleveland Lloyd Dinosaur Quarry in the 1960's with a partial skull and disarticulated skeleton, representing the largest *Ceratosaurus* officially described. The second one, MCW1 was recovered in Fruita Paleontological Area, Colorado, in 1976, a nearly complete individual with a disarticulated skull (Madsen & Welles, 2000).

These two new specimens were described in detail in 2000 by Madsen and Welles which found enough differences between both of them and *Ceratosaurus nasicornis*, erecting two new species, *Ceratosaurus magnicornis* for the Colorado specimen and *Ceratosaurus dentisulcatus* for the Utah one. Although the majority of arguments to define the new species were size related, the authors also cited morphological differences to support their claim. The validity of the two new species was not consensual among researchers, with some authors citing that the size differences stated can be related to allometric ontogenetic variations of the same species, thus considering only valid the type species, *Ceratosaurus nasicornis* (Rauhut, 2000; Carrano & Sampson, 2008).

Found in Agate Basin Quarry, Emery County, east-central Utah in 1992, BYU-VP-12893 is the largest *Ceratosaurus* yet found. The specimen includes cranial elements, incomplete dorsal vertebrae, parts of pubis and ischium, however the material is still yet to be described (Madsen & Welles, 2000; Carrano & Sampson, 2008).

A juvenile specimen, 30% smaller than the *Ceratosaurus nasicornis* holotype, was reported in 1999 by Britt et al. from Bone Cabin Quarry West with a complete skull and some postcranial material.

More relevant fragmentary North American remains include:

- DNM972 from Dinosaur National Monument, Utah, a right premaxilla found in 1964 identified as *Ceratosaurus* sp. (White, 1964; Madsen & Welles, 2000).

- BYUVP 13024 from Dry Mesa Quarry, Colorado, a complete left scapulocoracoid (Britt, 1991; Madsen & Welles, 2000).

- From Nail Quarry, Como Bluff, Wyoming, a large coossified scapulocoracoid (Madsen & Welles, 2000).

Ceratosaurus was for the first time confidently identified outside North America in the year 2000 after some hindlimb elements coming from the Late Jurassic (Kimmeridgian/Tithonian) Lourinhã Formation, Portugal, as well as from several isolated teeth collected in various sites along the Portuguese Lusitanian Basin (Mateus & Antunes, 2000; Mateus et al., 2006; Malafaia et al., 2015, 2017a).

The genus *Ceratosaurus* has been tentatively assigned to other countries and continents but without strong evidence. In Europe, besides Portugal, there was a report from Switzerland based on a single tooth from Upper Jurassic (Kimmeridgian) beds of Malm, Savoy, Bern Jura, bearing the characteristic lateral grooves found in the mesial teeth of *Ceratosaurus* (Madsen & Welles, 2000). This tooth was assigned first to *Megalosaurus meriani* by Greppin (1870), then to *Labrosaurus meriani* by Janensch (1920) and as *nomen dubium* by Molnar et al., (1990). Madsen and Welles (2000) found the grooved teeth similar to *Ceratosaurus* but stated that teeth alone are not diagnostic enough and thus left it just as *Ceratosaurus* sp.. In the same year, Chure (2000) considered that this material has *Ceratosaurus* affinities.

The Late Jurassic (Kimmeridgian/Tithonian) Tendaguru beds in Tanzania were prospected by Germany and England in a series of expeditions in the early 20th century, which revealed an ancient fauna similar to the contemporary Morrison and Lourinhã Formations (Schuchert, 1918; Schudack, 1999; Cifelli, 2003; Mateus, 2006). In 1920, Janensch described some theropod material from Tendaguru, assigning a set of vertebrae to *Ceratosaurus* sp. and some loose teeth with labial ridges to (?)*Labrosaurus stechowi*. Five years later, Janensch (1925) assigned a partial left quadrate, three partial caudal vertebrae and a partial left fibula to a new *Ceratosaurus* species, *Ceratosaurus roechlingi*. Madsen and Welles (2000), reviewed the material confirming the genus *Ceratosaurus* in Tanzania but not finding the material diagnostic enough to reach species level. However not all authors agree with this assumption, rather classifying it as a basal ceratosaur (Carrano & Sampson, 2008) or a composite of different genera with some elements (caudal vertebrae) with probable ceratosaur affinities (Rauhut, 2011). The teeth of (?)*Labrosaurus stechowi* have been considered either (?)*Ceratosaurus stechowi* (Rauhut, 2011), or from a close *Ceratosaurus* relative (Soto et al., 2020). Also in 1920, Janensch assigned some large theropod teeth from Tendaguru to *Megalosaurus*(?) *ingens* which were sub-sequentially reclassified as *Ceratosaurus ingens* (Paul, 1988; Rowe & Gauthier, 1990); however posterior studies found carcharodontosaurian affinities instead (Rauhut, 1995, 2011).

Some isolated teeth from the Tacuarembó Formation (Kimmeridgian - Hautevirian) in Uruguay have been interpreted as either ceratosaurid or *Ceratosaurus* sp. itself, due to the presence of diagnostic characters found in mesial teeth of this genus such as labial grooves or apical mesial carina (Soto & Perea, 2008; Soto et al., 2020).

***Ceratosaurus* closest relatives**

The evolution of Ceratosauria (fig. 51) was for many decades poorly known but improved significantly in the last 30 years with the description of several new species and more in-depth phylogenetic analyses.

Recent studies place Lower Cretaceous (Aptian) Argentinian theropod *Genyodectes serus* as the closest known relative of *Ceratosaurus* (Rauhut, 2004). This taxon, first described by Woodward (1901), was the first non-avian theropod described in South America; it is known from fragmentary material, notably the tip of the snout (both premaxilla, both partial maxilla, both dentaries, fragments of supradentaries and fragmentary left splenial) with teeth (Woodward, 1901; Rauhut, 2004). The taxonomic placement of this genus was inconclusive for many decades due to the fragmentary remains, been regarded as either a megalosaurid (Huene, 1929), a tyrannosaurid (Huene, 1932), a *incertae sedis* theropod (Molnar, 1990), a possible abelisaurid (Paul, 1988; Bonaparte, 1996), and only more recently a *Ceratosaurus* close relative (Rauhut, 2004). Although the number of premaxillary teeth (four) differs from *Ceratosaurus* (three), their general shape and relative size, as well as their *en-echelon* arrangement in the premaxilla, is a characteristic shared only with *Ceratosaurus* (Rauhut, 2004).

Besides *Genyodectes*, the closest *Ceratosaurus* taxa are much older and they all give important insights about the origins of the group. The first of these taxa being described was *Berberosaurus liassicus* from the Early Jurassic (Toarcian) of Morocco (Allain et al., 2007). The material was initially interpreted as an abelisauroid by the describing authors (Allain et al., 2007) but subsequent studies found it in a more basal position within Ceratosauria (Carrano & Sampson, 2008; Dal Sasso et al., 2018).

In 2012, Pol and Rauhut described a new theropod from the Early Jurassic (Toarcian) of Argentina with abelisauroid affinities, making it the oldest known of its kind, being properly named *Eoabelisaurus mefi*. However other authors disputed this placement and, although still considering it a ceratosaur, they place it in a more basal position within the group just outside *Ceratosaurus/Genyodectes* (Wang et al., 2017; Delcourt, 2018).

The third, and oldest, of these basal ceratosaurs, *Saltriovenator zanellai*, was described in 2018 by Dal Sasso et al. and comes from the Early Jurassic (Sinemurian) of Italy. Although initially identified as a tetanuran (Dal Sasso, 2001), most recent analysis of the fragmentary material place it within Ceratosauria as sister taxa to *Berberosaurus*, making it the oldest known member of the group. *Saltriovenator* possesses ceratosaurian and tetanuran traits, showing the early stage close relationship between both groups (Dal Sasso et al., 2018).

Ceratosauria: history of study and major evolution (Abelisauridae and Noosauridae)

In the 1920's a new theropod was unveiled as part of the previously mentioned Tendaguru expeditions. *Elaphrosaurus bambergi* was a medium sized ceratosaurian from the Late Jurassic (Kimmeridgian/Tithonian) Tanzania; originally described by Janensch (1920), based on postcranial material, as a coelurosaurian (Janensch, 1920, 1925) and, in subsequent analyses, as an ornithomimosaur (Nopcsa, 1928; Galton, 1982). The association of *Elaphrosaurus* to Ceratosauria was first proposed by Paul (1988) as a coelophysoid (when this group was still linked to ceratosaurians), but later studies found this genus firmly within Ceratosauria (Rauhut, 2000; Tykoski & Rowe, 2004; Carrano & Sampson, 2008) with the most recent studies placing it as an Elaphrosaurinae within Noosauridae, Abelisauroidea (Rauhut & Carrano, 2016).

The 1980's were particularly relevant for the development of our understanding of Ceratosauria when, in 1985, *Abelisaurus comahuensis* and *Carnotaurus sastrei* from the Late Cretaceous (Campanian/Maastrichtian) Argentina were described as part of the newly erect clade Abelisauridae (Bonaparte, 1985, Bonaparte & Novas, 1985; Bonaparte et al., 1990).

Abelisaurids were medium to large sized predators with short and deep skulls, often times with horns or rugose textures and ridiculously short forelimbs (Carrano & Sampson, 2008; Delcourt, 2018). In their 1990 publication, Bonaparte et al., also found the clade Noosauridae closely related to Abelisauridae and Ceratosauridae, and created Ceratosauroidea to include all these clades.

Noosauridae was based on the small sized theropod *Noasaurus leali* from Late Cretaceous (Maastrichtian) Argentina which was previously described in 1980 but originally interpreted as a coelurosaur (Bonaparte & Powell, 1980; Bonaparte et al., 1990).

In the following years several new species were described for both Abelisauridae and Noosauridae.

Majungasaurus crenatissimus, from Late Cretaceous (Maastrichtian) Madagascar, is among the best studied abelisaurids, being known from fragmentary material since the 19th century, it was found within Abelisauridae in 1998 after more complete remains were found (Depéret, 1896; Lavocat, 1955; Sampson et al., 1996; Sampson et al., 1998; Krause et al., 2007). Besides South America and Madagascar, the Abelisauridae was also present in Late Cretaceous India, mainland Africa and possibly Europe (Loeuff & Buffetaut, 1991; Wilson et al., 2003; Novas et al., 2004; Sereno et al., 2004; Carrano & Sampson, 2008; Sereno & Brusatte, 2008).

Noosauridae represented a different but equally interesting path of ceratosaur evolution. Jurassic forms were represented by the sub-clade Elaphrosaurinae which include the previously mentioned *Elaphrosaurus bambergi* from the Kimmeridgian/Tithonian of Tanzania and *Limusaurus inextricabilis* from the Oxfordian of China (Xu et al., 2009a; Rauhut & Carrano, 2016). *Limusaurus* is notable for the fact that is known from several individuals at different growth stages, which enabled to reconstruct its ontogenetic development – upon reaching adult stage it would loose the dentition and formed a beak, likely changing the diet from omnivore to herbivore, being the first time ontogenetic edentulism is identified in Gnathostomata fossil record (Wang et al., 2007). Cretaceous noosaurids are more common in the fossil record, being particularly abundant in South America with peculiar forms such as the toothless herbivore *Berthasaura leopoldinae* and the “one-toed runner” *Vespersaurus paranaensis* (Langer et al., 2019; de Souza et al., 2021). The group was also present in Cretaceous Madagascar, mainland Africa, Europe and India (Sereno et al., 2006; Carrano & Sampson, 2008; Wilson et al., 2003; Rauhut & Carrano, 2016; Ibrahim et al., 2020; Mohabey et al., 2023).

Abelisauroida fossil record shows a dominance of ceratosaurians in Gondwana lands in the Late Cretaceous, varying in form and size and occupying several ecological niches, being also worth-noting how carnivorous abelisaurids have replaced giant carcharodontosaurians as the top predators in this region by mid-Cretaceous (Novas et al., 2005; Delcourt, 2018; Delcourt & Grillo, 2018; de Souza et al., 2021).

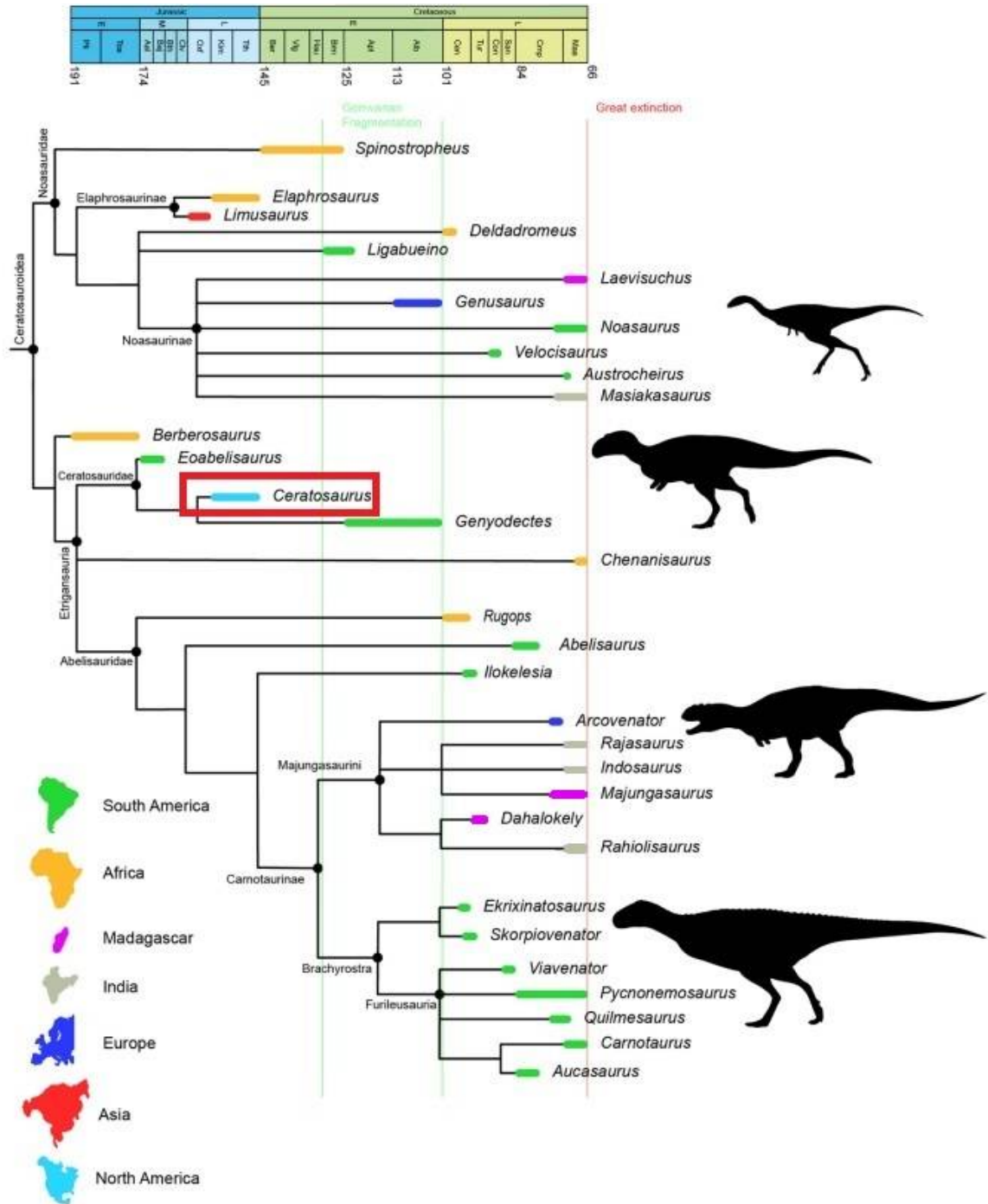


Figure 51. Phylogeny, distribution and evolution of Ceratosauria through the Mesozoic Source: Delcourt, 2018.

Ceratosauria problematics and misconceptions

Due to the lack of good specimens, the origins and relationships of Ceratosauria within Theropoda was poorly understood for quite sometime. Marsh (1884) cleverly noted how *Ceratosaurus* was particularly different from other known theropods in structures such as horns and osteoderms, thus creating Ceratosauridae; later even stating that the ornithomimosaurs were probably the closest known forms to *Ceratosaurus* (Marsh, 1893). Marsh's vision was not widely accepted, with some authors questioning the validity of Ceratosauria and favoring the placement of *Ceratosaurus* within Megalosauridae (Lydekker, 1888) and others not even accepting the genus *Ceratosaurus* itself, calling it *Megalosaurus* instead (Cope, 1892).

Years later, Gilmore (1920) accepted Ceratosauria and noted how certain anatomical details, such as the four fingered hands or the presacral vertebrae more akin to Triassic forms, were pretty primitive for a Jurassic theropod. However, the above mentioned lack of good specimens persisted throughout most of the 20th century, with the term Ceratosauria being somewhat forgotten and *Ceratosaurus* viewed as just an oddity among theropods and with uncertain relationships (Carrano & Sampson, 2008).

The first major development in trying to fit Ceratosauria within the theropod family tree came in 1986 when Gauthier split Theropoda in two major branches, Tetanurae with 'carnosaurs' (allosauroids and megalosauroids) and coelurosaurs, and Ceratosauria with ceratosaurs and the Late Triassic/Early Jurassic coelophysoids. In 1989, Rowe gave the stem based definition of these clades with Tetanurae containing all theropods more closely related to birds whereas Ceratosauria contained all theropods more closely related to *Ceratosaurus nasicornis*.

Subsequent phylogenetic analyses supported the monophyly of Ceratosauria and two main groups were established: the more primitive Coelophysoidea and the more derived Neoceratosauria (Novas, 1991, 1992; Holtz, 1994; Sereno, 1999; Tykoski & Rowe, 2004; Allain et al., 2007). The clade was supported by synapomorphies such as cervical vertebrae with two pairs of pleurocoels, dorsal vertebrae transverse processes strongly pointed posteriorly and triangular-shaped in dorsal view, sacral ribs and ilia fused together, distal end of the femur with tibio-fibular crest clearly separated from the fibular condyle and astragalocalcaneum fused in mature individuals (Tykoski & Rowe, 2004).

New specimens provided new information and morphological data, with most analyses since the turn of the millennium starting to challenge the notion of a monophyletic Ceratosauria that includes coelophysoids. Instead, neoceratosaurs such as *Ceratosaurus* and abelisaurids were being found closer to Tetanurae and further from Coelophysoidea (Carrano & Sampson, 1999, 2000; Rauhut, 2000).

Rauhut's work (2000) was particularly important in this regard, since it made an in-depth review of basal theropods and their relationships. It was found that most of the synapomorphic characters in support of a monophyletic Ceratosauria plus Coelophysoidea were invalid or questionable under the new datasets made up from new or more complete material. On the other hand, the proximity of Ceratosauria to Tetanurae is validated by nine synapomorphies described by Rauhut (2000) as: (i) ascending process of maxilla and anterior end of maxillary body are offset from each other, (ii) paroccipital process ventral margin of medial basis placed mid-height or below the occipital condyle, (iii) mandibular retroarticular process is broad and the attachment for depressor mandibulae muscle develops as a posterior transverse groove, (iv) pleurocoels in the axis, (v) wing-shaped broad lesser trochanter, (vi) anterior region of distal femur with a broad, shallow and well-developed groove bounded medially by an expanded lamella, (vii) round distal end of femur, (viii) tibia distal articular facet with a broad triangular shaped outline and (ix) calcaneum with a facet for contact with the tibia. Subsequent studies agreed with this phylogenetic relationship and ceratosaurs have been consistently found closer to Tetanurae (Carrano & Sampson, 2008; Pol & Rauhut, 2012; Dal Sasso et al., 2018; de Souza et al., 2021).

Ceratosaurian anatomy also created some problems in the proper identification of some particular theropod taxa. In 1926, a Middle Jurassic (Bathonian) theropod from England was described by von Huene. The skull apparently had a broken horn on top of the snout, which led the author to later place it as a possible relative of *Ceratosaurus*, properly naming it *Proceratosaurus bradleyi* (Huene, 1926, 1932). Later studies however have shown that this taxon was instead a more derived theropod than *Ceratosaurus*, being now considered a coelurosaurian tyrannosauroid within the clade Proceratosauridae (Rauhut et al., 2010).

Another possible misidentification was recently brought up regarding theropod remains described from the Early Cretaceous (Barremian) of Spain in 2014. Named *Camarillasaurus cirugedae*, the describing authors initially regarded it as a ceratosaur (Sánchez-Hernández & Benton, 2014) but subsequently analyses found it as a spinosaur (Rauhut et al., 2019; Barker et al., 2021; Santos-Cubedo et al., 2023; Isasmendi et al., 2024). Although the original assignment of *Camarillasaurus* to Ceratosauria was not just based on teeth, the describing authors point out some ceratosaurian synapomorphic attributes to the tooth of *Camarillasaurus* (Sánchez-Hernández & Benton, 2014). This is relevant since some authors (Fowler, 2007; Malafaia et al., 2017a; Soto et al., 2020) have stated the fact that the teeth of some ceratosaurs and baryonychine spinosaurids have some similarities, which might lead to diagnostic errors. Although this is now regarded as just convergence (Soto et al., 2020), at some point these similarities even led some authors to suggest a ceratosaurian ancestry for the baryonychines (Fowler, 2007).

Overall, the teeth of Ceratosauridae can be difficult to distinguish from both Megalosauroida and Allosauroida due to their general shape, crown size, thickness and denticle ratio (Hendrickx et al., 2014), but it is the mesial teeth of some ceratosaurs like *Ceratosaurus* and *Masiakasaurus* that convergently evolved most similarities with baryonychines (Malafaia et al., 2017a). Both groups have vertical striations on their teeth, but in *Ceratosaurus* these are present only in the lingual side of mesial teeth whereas in spinosaurs these striations are present also in the labial side. Baryonychine teeth also have higher number of flukes, mesial carina extending to the root and higher number of denticles on both carinae (Malafaia et al., 2017a).

Some of these differences helped to distinguish some of the previously mentioned Tendaguru teeth attributed to (?)*Labrosaurus stechowi* / (?)*Ceratosaurus stechowi* and assign them to a new putative spinosaurid, *Ostrafrikasaurus crassiserratus* (Janensch, 1920, 1925; Rauhut, 2011; Buffetaut, 2008; Buffetaut, 2012; Soto et al., 2020).

***Ceratosaurus* paleobiology**

Ceratosaurus was a medium sized carnivore that shared his ecosystem with several other theropods (Dodson et al., 1980; Bakker, 1996; Henderson, 1998; Antunes & Mateus, 2003; Mateus, 2006; Mateus et al., 2006; Farlow et al., 2023; Lei et al., 2023), and different studies have been made, particularly on the Morrison Formation paleofauna, trying to reconstruct this environment and how so many medium to big size predators were able to share the same habitat (Dodson et al., 1980; Henderson, 1998; Whitlock et al., 2018; Farlow et al., 2023; Lei et al., 2023).

Stratigraphic and paleontological data from the Morrison Formation has led to different views regarding its paleoenvironment, with some authors interpreting the presence of large herbivores and lush flora typical of humid environments as evidence of rich and wet floodplains (Tidwell, 1990; Ash & Tidwell, 1998), others, based on the abundance of low to mid-height brushy vegetation and relative scarcity of fishes, turtles and crocodiles hypothesize a semi-arid, savanna-like environment, strongly marked by seasonal water availability which only periodically would create lagoons and river floodplains (Stokes, 1944; Dodson et al., 1980; Engelmann et al., 2004; Parrish et al., 2004; Rees et al., 2004). Some researchers see a mixture of both scenarios, either with dry open plains and wet forests across the region (Hotton & Baghai-Riding, 2010; Gee, 2011; Whitlock, 2011; Whitlock et al., 2018) or even a cyclical change of these conditions in space and time throughout the 10 million year time span recorded in the Morrison Formation (Tschopp et al., 2020; Lei et al., 2023).

Considering that the Morrison Formation was indeed a dry seasonal environment with sparse forests, the large sauropod herbivores were forced to migrate regularly in search of vegetation and the large theropod fauna could have evolved these massive sizes as a way to be able to follow and tackle these large prey items (Dodson et al., 1980; Henderson, 1998; Rees et al., 2004; Whitlock et al., 2018).

If no taphonomic bias is conditioning the fossil samples, this large sized dinosaur predatory fauna is abundant relative to the large sized herbivore fauna in the Morrison Formation when compared to today's macro mammal faunal assemblages (Farlow et al., 2023), however, when compared with the other theropods, *Ceratosaurus* is quite rare, with an average of 1 *Ceratosaurus* per 7.5 *Allosaurus* (Dodson et al., 1980; Henderson, 1998; Foster & Chure, 2006; Yun, 2019).

Studies show that Morrison's theropods tackled smaller/juvenile sauropods, large-sized sauropod carcasses and small to medium-sized ornithopods and other animals (Farlow et al., 2023; Lei et al., 2023). The skull and teeth morphologies of different Morrison theropods was compared, suggesting niche partitioning between these predators, with the relatively large teeth of *Ceratosaurus* hinting a different diet or a preference for certain parts of carcasses different from taxa such as *Allosaurus* (Henderson, 1998). At least some niche partitioning is apparent, with *Ceratosaurus* being more common in areas where the *Allosaurus* morphotype present has cranial features different to those of *Ceratosaurus*, and less common where *Allosaurus* skull morphotype is similar to *Ceratosaurus*, suggesting some kind of segregation (Henderson, 1998).

Regarding its behavior and habitat, the anterior caudal vertebrae of *Ceratosaurus* bear long chevrons and tall, vertical neural spines which resulted in a high and thin tail; Marsh (1884) interpreted this feature as an adaptation for swimming and, in 2004, Bakker and Bir came to the same conclusions adding that this genus is commonly found near paleo-water systems and possessed a high flexible tail and torso akin to crocodylians.

These assumptions were questioned by Yun (2019) stating that the evidence is not strong enough to support semi-aquatic adaptations for this genus, being the features mentioned not unusual among terrestrial theropods. Yun also pointed out that the tail of crocodiles has taller neural spines medially and distally and these are sub-circular in cross-section, which is not the case for *Ceratosaurus*; also, its caudal vertebrae were amphicoelous and had hyposphene-hypantrum articulations which would in fact have made the tail more rigid and less flexible (Delcourt, 2018; Yun, 2019). However, Yun does not discard the possibility of *Ceratosaurus* being partially piscivorous based on the crocodile/baryonychine-like conical fluked teeth and in the torsion resistant fused nasals, but other skull features are typical of common theropods, so it's possible that *Ceratosaurus* was more of a generalist in its dietary habits (Yun, 2019). Henderson (1998) also addressed the fact that the deeper *Ceratosaurus* skull was an adaptation to house large muscles and deliver the strong bite forces required to overcome the mechanical resistance faced by the long teeth when penetrating flesh.

When interpreting *Ceratosaurus* unique cranial ornamentation, Marsh (1884) in his original description, described it as "a tool used for both attack and defense". Subsequent authors gave less dramatic explanations, interpreting these structures as either sexual display features (Rowe & Gauthier, 1990) or as means of inter-specific recognition among the several Morrison's theropod species (Henderson, 1998).

Sanders and Smith (2005) studied the braincase of *Ceratosaurus magnicornis* holotype, MWC1, and found it similar to most other theropods, with characteristics similar to those of crocodiles and birds. The shape and size of the semicircular canals are typical of bipedal animals with horizontally oriented head and neck. The olfactory bulb size reveals a good sense of smell, although not as keen as *Tyrannosaurus*. The well developed olfactory region was also mentioned by Marsh (1884) and Gilmore (1920) regarding the *Ceratosaurus nasicornis* holotype, from which they also noted the also well developed optic lobes and pituitary body.

Major contributors for the *Ceratosaurus* study

Othniel Charles Marsh (1831-1899)

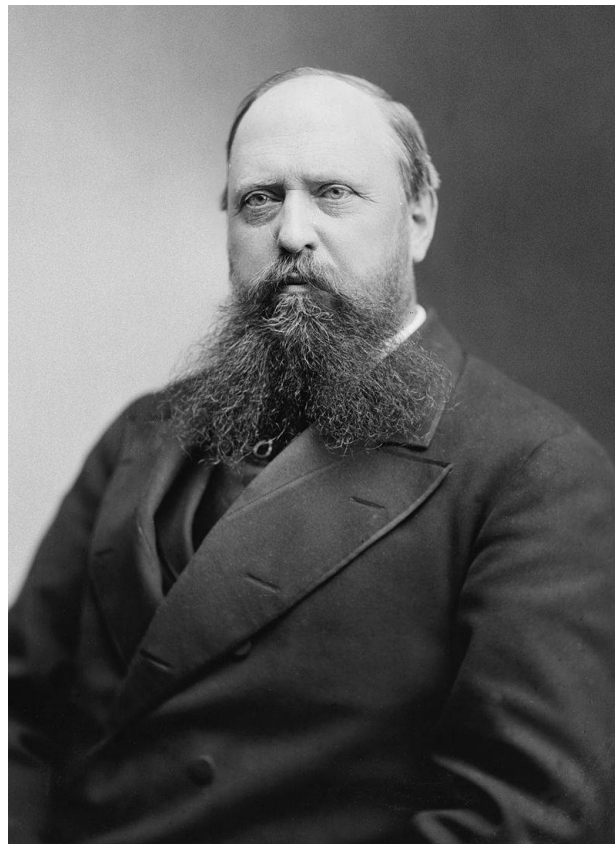


Figure 52. Othniel Charles Marsh. Source: Wikipedia.org.

Othniel Charles Marsh (fig. 52) is one of the most famous names in the history of American paleontology. With the financial support from his uncle, George Peabody, Marsh was able to complete his studies, first in Geology in Yale, and later in Paleontology in Germany. He eventually became professor of Paleontology in Yale and president of the American National Academy of Sciences.

Along with his uncle, Marsh was also responsible for the creation of the Peabody Museum of Natural History and George Peabody's fortune would fill the museum with thousands of fossils (so much that some were still being cataloged during the 1990's) and would pay Marsh's field campaigns in Wyoming and Colorado (Parker & Parker, 1997).

Marsh is most widely known for the long and bitter rivalry with fellow American Paleontologist Edward Drinker Cope where, through the mid 1870's to the 1880's, the two would compete in order to see who would name and describe more fossil species for Science. With both describing dozens of new specimens, most notably dinosaurs, their contend would improve significantly our knowledge of these animals during the 19th century (Plate, 1964; Bakker, 1986; Jaffe, 2000; Johnson, 2012).

Marsh was also an advocate for the, then new, theory of Evolution and his findings and scientific work was acknowledged by Darwin himself for its support of his theory (Plate, 1964; McCarren, 1993, Parker & Parker, 1997). During his life, Marsh published several scientific papers describing new species and findings: he proved horses originated and evolved in North America, described the first American pterosaur and named some of the most iconic dinosaur such as *Stegosaurus*, *Camptosaurus*, *Triceratops*, *Diplodocus*, *Apatosaurus*, *Allosaurus*, *Hesperornis* and, with bigger relevancy regarding the subject of this writing, *Ceratosaurus* (Marsh, 1872, 1877a, 1877b 1878, 1884, 1885, 1889; MacFadden, 1992; Witton, 2010).

James Henry Madsen Jr. (1932-2009)

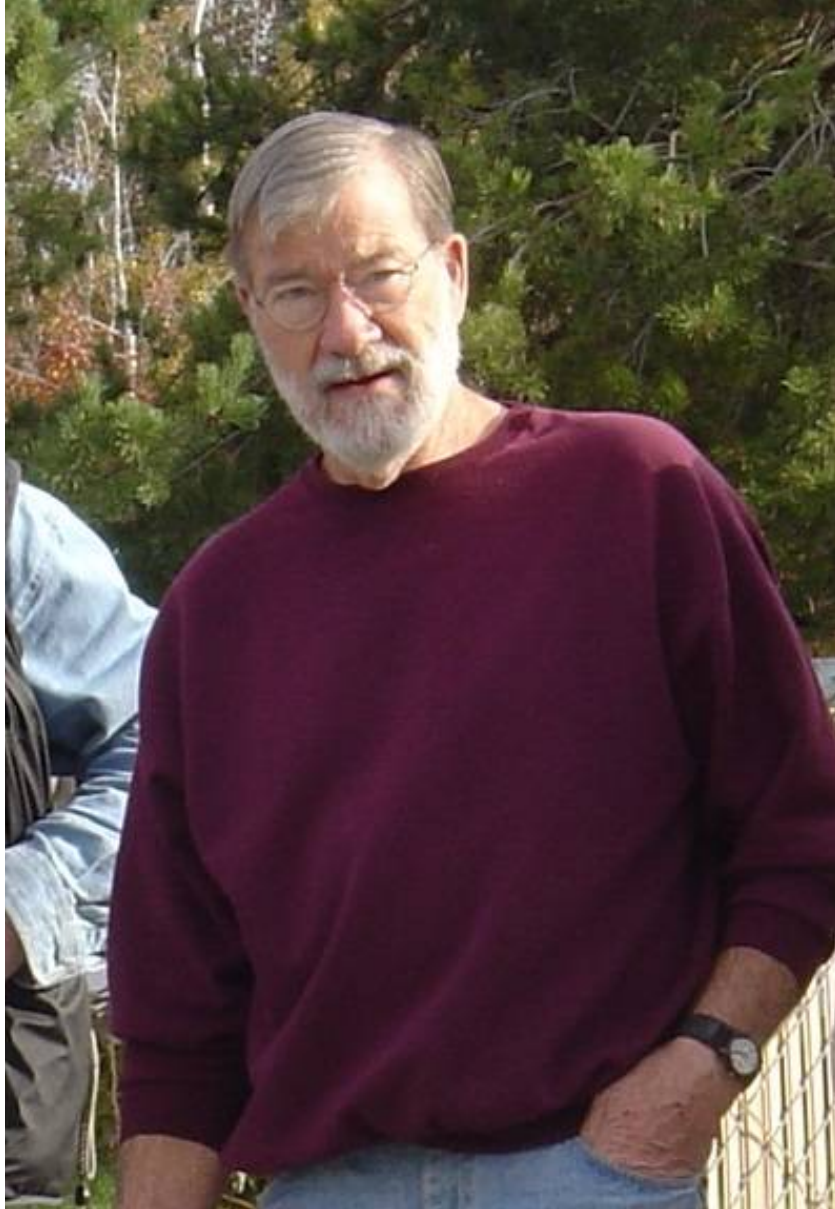


Figure 53. James H. Madsen. Source: photo shared by Octávio Mateus.

Born in Murray, state of Utah, geologist and paleontologist “Jim” Madsen (fig. 53) was one of the main experts in United States Jurassic theropods. After graduating in the University of Utah, in 1959, Madsen started working in the famous Cleveland-Lloyd Dinosaur Quarry, whose rich content in dinosaur material, would provide thousands of fossils, at least 30 complete skeletons and even dinosaur eggs. It was here that Madsen worked for the entirety of his career, specializing in theropods such as *Allosaurus* (particularly abundant in this quarry) and *Ceratosaurus*.

The work he developed was recognized in 2020, when a new *Allosaurus* species, *Allosaurus jimmadseni*, was named in his honor.

His major publications on theropod osteology – 1976 “*Allosaurus fragilis*: a revised osteology” and 2000 “*Ceratosaurus* (Dinossauria, Theropoda): a revised osteology” (together with Samuel P. Welles) are landmark publications for our understanding of these genera, the latter being particularly important in the context of this dissertation. (Madsen, 1976, Madsen & Welles, 2000; Chure & Loe, 2020).

***Ceratosaurus* in Portugal**

In the year 2000, Mateus and Antunes reported for the first time the presence of the genus *Ceratosaurus* in the Late Jurassic (Kimmeridgian/Tithonian) Lourinhã Formation, Portugal, based on a right femur and left tibia (catalog number ML352, fig. 54), without assigning it to any particular species. This was the first occurrence of the genus outside North America based on solid diagnostic material.

In 2006, Mateus et al. made an overview of the large theropod fauna of the Lourinhã Formation and described this material in more detail, finding similarities with *Ceratosaurus dentisulcatus* in the position of the epiphyseal expansions and in the posterior popliteal bridge of the femur, but still classifying it as *Ceratosaurus* sp.. Some teeth attributed to this genus were also reported by the authors in the same paper.



Figure 54. Excavation of *Ceratosaurus* ML352 at Valmitão beach, Lourinhã. Source: photos shared by Octávio Mateus.

In 2015, Malafaia et al. also reviewed the material but added to their description a left femur, a right tibia and a fibula shaft (catalog number SHN(JJS)065) found in the same place as the previous material and likely being all part of the same individual. In their analysis they did not find the material diagnostic enough to assign it to a species level, leaving it as *Ceratosaurus* sp. with affinity to *Ceratosaurus nasicornis*. Analyzing the diversity of theropod teeth from the Lusitanian Basin, Malafaia et al., (2017a) also reported several teeth which were confidently attributed to *Ceratosaurus*, reinforcing the fact that this genus was also present in Europe.

New material eventually came up from the same dig site where the hindlimb bones were found and these elements will be described in this document, along with the previous material.

Dinosaurs from the Late Jurassic of Portugal

The dinosaurian fauna described from the Late Jurassic of Portugal is highly diverse and bears much similarity with the contemporaneous North American Morrison Formation, both being Late Kimmeridgian in age, about 152 Ma (Antunes & Mateus, 2003; Mateus et al., 2006; Mateus et al., 2017).

The genera *Ceratosaurus*, *Torvosaurus*, *Allosaurus*, *Supersaurus* and *Stegosaurus* were described for both continents, and some European speciation has successfully been inferred among some of these taxa with *Torvosaurus gurneyi*, *Allosaurus europaeus* and *Supersaurus lourinhanensis* (Mateus et al., 2017).

In general, all the major dinosaur groups representative of the Late Jurassic have been identified in Portugal. The theropod genera includes the ceratosaurian *Ceratosaurus*, the megalosaurian *Torvosaurus*, the allosauroids *Lourinhanosaurus*, *Allosaurus* and *Lusovenator*, the coelurosaur *Aviatyrannis*, and possibly some abelisaurids, compsognathids and basal maniraptorans. The sauropods are represented by the turiasaur *Zby*, the diplodocids *Supersaurus/Dinheirosaurus* and the macronarians *Lourinhasaurus*, *Oceanotitan* and *Lusotitan*. Ornithischians include the stegosaurs *Miragaia/Dacentrurus* and *Stegosaurus*, the ankylosaur *Dracopelta* and the ornithopods *Draconyx*, *Eousdryosaurus*, *Hesperonyx* and *Phyllodon* (Thulborn, 1973; Galton, 1980; Mateus & Antunes, 2001; Antunes & Mateus, 2003; Mateus et al., 2006; Escaso et al., 2007; Mateus et al., 2009; Mannion et al., 2012; Escaso et al., 2014; Hendrickx & Mateus, 2014; Mateus et al., 2014; Mocho et al., 2014; Mocho et al., 2019; Malafaia et al., 2020; Rotatori et al., 2024; Sánchez-Fenollosa et al., 2024).

The Lusitanian Basin and Lourinhã Formation

The Lusitanian Basin is a sedimentary basin related to the first stages of the North Atlantic rift opening, extending from Aveiro to Cabo Espichel, and comprising ages from the Late Triassic to the Cenomanian (Mateus et al., 2017). The Late Jurassic (Late Oxfordian - Early Kimmeridgian) marked the major rifting event, which created a complex system of faults and salt diapirs in the region that shaped the landscape and gave rise to the main sub-basins we identify today: Bombarral-Alcobaça, Arruda, Consolação and Turcifal (Alves et al., 2003; Mateus et al., 2017).

The Late Jurassic rifting event created a paleogeographic scenario that has been difficult to interpret, and through the years different proposals have been made to define this section of the Lusitanian Basin stratigraphy (fig. 55), however, there is still no consensus among the authors, with several interpretations and nomenclature being given (Choffat, 1901; França et al., 1961; Hill, 1988, 1989; Reis et al., 1996; Leinfelder & Wilson, 1998; Manuppella et al., 1999; Alves et al., 2003; Taylor et al., 2013; Mateus et al., 2017).

An analysis of these different interpretations of the complex stratigraphy of the Lusitanian Basin (and of the Lourinhã Formation in particular) is out of the scope of this work. In order to simplify this issue, the interpretation and nomenclature given by Mateus et al. (2017) will be the main reference for this study due to its recent publication date and in-depth comparison with previous studies. The interpretation given by Mateus et al. (2017) is in itself based mostly on the works by Hill (1988, 1989).

Within the Lusitanian basin, the Lourinhã and Alcobaça Formations are the richest in vertebrate remains in Europe, showing remarkable faunal resemblance with the contemporaneous North American Morrison Formation, albeit within a more coastal setting and with some typical European taxa in the mix. In general, these two formations represent a major regressive event in this region that took place during the Late Jurassic, with the older Alcobaça Formation being, for the most part, a carbonated sequence deposited in a shallow marine to deltaic/estuarine environment and the younger Lourinhã Formation being formed mostly in a continental setting (Mateus et al., 2017).

The Lourinhã Formation (fig. 55) spans from the Late Kimmeridgian to the Late Tithonian and includes, from the oldest to most recent, the Porto Novo/Praia da Amoreira Members, the Praia Azul Member, and the contemporaneous Santa Rita and Assenta Members. All these units belong to the Consolação sub-basin, except Assenta which is part of Turcifal. The Kimmeridgian-Tithonian boundary is defined by a particular transgressive event, which is well expressed in a carbonated sequence located in the Praia Azul Member (Hill, 1988, 1989; Mateus et al., 2017).

The Late Jurassic age of the formation has been consensual among the authors and the precise Late Kimmeridgian - Late Tithonian estimate has been supported by regional stratigraphic and paleontological correlations, magnetostratigraphy and isotope dating (Choffat, 1901; França et al., 1961; Hill, 1988, 1989; Manuppella et al., 1999; Mateus, 2006; Mateus et al., 2017).

The continental setting of the Lourinhã Formation is well expressed at North of Santa Cruz, where it is fully terrestrial, whereas South of Santa Cruz some shallow marine transitions can still be found. The lithologies found across these units are predominantly made of sandstones and mudstones formed in lowland deltas and meandering river channels, with the occasional transitions resulting in brackish estuarine and shallow marine settings (Hill, 1988, 1989; Mateus et al., 2017). Caliche-rich paleosols are common across the formation and they can tell us that the environment was semi-arid, with annual mean temperatures ranging from 16° to 19°C and less than 500mm of precipitation (Myers, 2011; Mateus et al., 2017).

A semi-arid setting is also supported by different studies on floral composition, such as the presence of plant groups adapted to such conditions such as bennettitales and conifers, tree trunk growth ring patterns and palynological data (Batten & MacLennan, 1984; Mohr, 1989; Pais, 1998, Martinius & Gowland, 2011; Mateus et al., 2017).

Estimations of carbon dioxide pressure values indicate higher values than those on the Morrison Formation, suggesting instead more humid conditions, higher trophic productivity and biological diversity on the Lourinhã Formation.

A relatively humid setting is also supported by sedimentological, stratigraphical and paleontological data, such as the evidence of alluvial systems in the form of delta and meandering rivers, brackish water transgressive episodes or by the presence of abundant lignite and wood remains (Leinfelder et al., 2004; Myers, 2011; Myers et al., 2012a; Mateus et al., 2017). Oxygen isotopic data and paleosols distribution pattern also indicate warm, humid and rainy seasonal conditions, an average annual temperature of 31°C and 1100mm per year rainfall (Myers et al., 2012a). All this data leads to different paleoclimatic interpretations for the Late Jurassic Lourinhã Formation, from humid to semi-arid conditions, which can be interpreted as a whole as evidence of a monsoonal type climate strongly marked by seasons, with dry summers and humid winters (Martinius & Gowland, 2011; Mateus et al., 2017).

The environmental characteristics of the Lourinhã Formation, dominated by coastal lagoons, deltaic and meandering fluvial settings with muddy shores and riverbanks, in association with the monsoonal climatic extremes such as heavy rainfall and floods, would create the perfect conditions to trap and/or bury the nearby fauna. Decay would then be prevented and preservation improved by the low acidic carbonate-rich and impermeable sediments. The association of all these factors explain the unique paleontological richness of this region (Mateus et al., 2017).

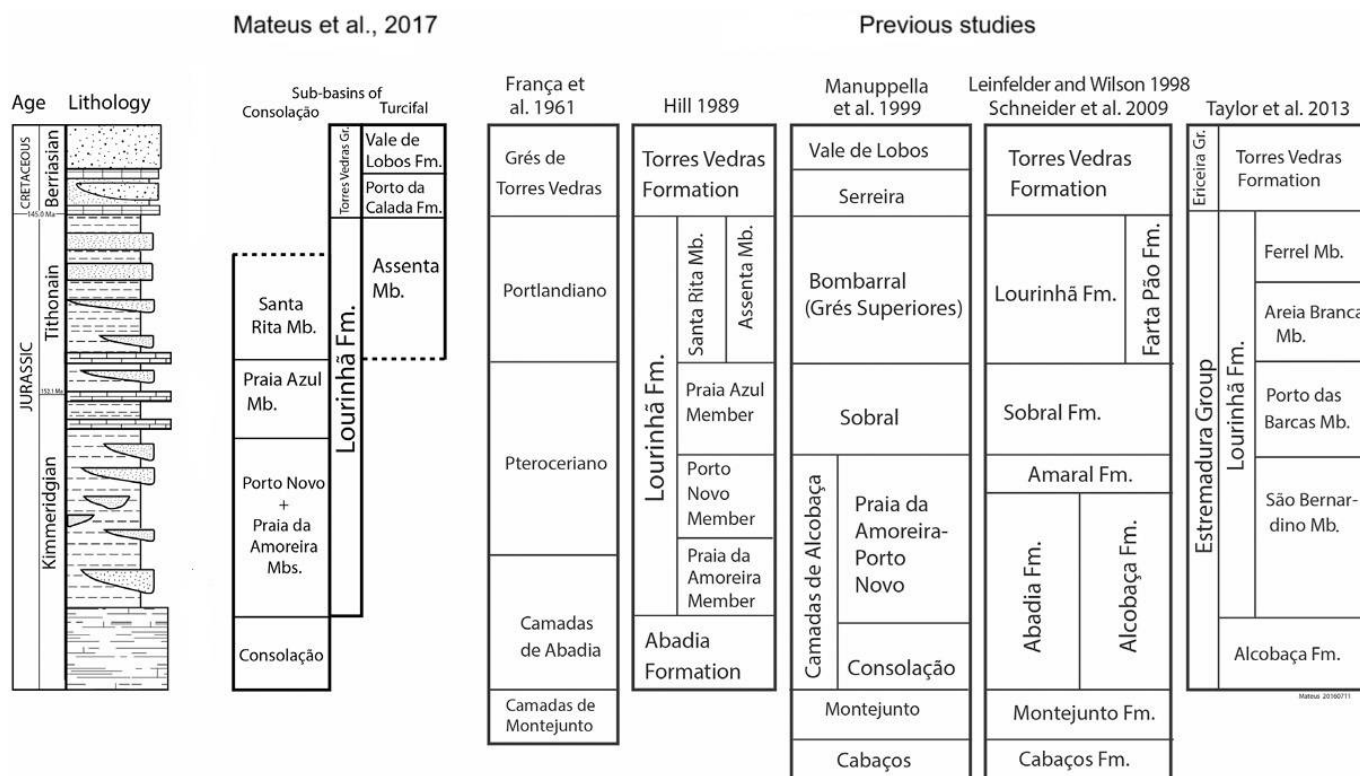


Figure 55. Different interpretations and nomenclature for the Upper Jurassic Lusitanian Basin stratigraphy through the years (adapted and modified from Mateus et al., 2017).

Lourinhã Formation vertebrate fossil assemblage has been useful for understanding the paleogeography and paleobiogeography of North Atlantic Late Jurassic landmasses. The co-occurrence of large sized terrestrial fauna on both Morrison Formation and Lourinhã Formation at around the same time, namely dinosaurs correlated at the genus level on both continents, implies some sort of connection between these regions. By the Late Jurassic, the Atlantic was still in its first opening stages (which had started by the Early Jurassic - Hettangian) and both North America and Europe were closer to each other; Iberia landmass however is reconstructed as an island at this time, being separated from both continents. Land connection with North America mainland was nevertheless still possible, since there was a chain of small islands west of Iberia that theoretically could create temporary land bridges in shallow regions during short term eustatic variations of the sea level (Ziegler, 1988; Shudack & Shudack, 1989; Sibuet et al., 2012; Mateus et al., 2017).

A major regressive event took place by the Callovian-Oxfordian (163 Ma) which would have still enabled the presence of shared fauna on both landmasses by the Kimmeridgian, taking into account the 7.7 Ma geologic average lifespan of most dinosaur genera (Dodson, 1990; Leinfelder & Wilson, 1998; Mateus et al., 2017). Considering dinosaurian distribution across Europe and North America, the faunal interchange across both continents occurred in a bidirectional migration flow, with European megalosauroids reaching America and diplodocoids and allosauroids coming to Europe. The subsequent sea level rise and isolation of Iberia would explain the apparent speciation differences seen in dinosaurian genera on both Formations by the Kimmeridgian/Tithonian. It's also worth noting that, while the majority of Iberian large fauna is similar to that found on North America, smaller forms such as pterosaurs, turtles or fishes bear more resemblance to European and Asian forms (Mateus, 2006; Mateus et al., 2017).

-

Making a general overview, following Mateus et al. (2017), each of the Lourinhã Formation units, oldest to newest, can be summarized as:

Consolação: This is the unit underlying the Lourinhã Formation. Early to early-Late Kimmeridgian in age, based on Sr isotope dating (Schneider et al., 2009), this is a 200m thick layer, with the lower half mostly made of marls and limestones and the upper half rich in cross-bedded carbonate cemented sandstones and thin bioturbated marls and mudstones. The mudstones predominate on the upper 30m with caliche, sandstone concretions and plant remains being common. Invertebrate fossils are common in the lower marine levels with corals, bivalves and gastropods. This unit represents a regressive event from a marine to brackish setting, and finally to a freshwater one (Werner, 1986; Mateus et al., 2017).

Praia da Amoreira / Porto Novo Members: The oldest units of the Lourinhã Formation, these two are usually grouped together (Manuppella et al., 1999, Mateus et al., 2017), with Praia da Amoreira being the oldest, underlying Porto Novo. The lower limit, where it contacts Consolação, appears to be an erosive surface with conglomerates, the result of the fluvial system insertion (França et al., 1961; Hill, 1989; Manuppella et al., 1999). The thickness of these units can change considerably, from less than 100m to about 400m. In Praia da Amoreira Member, bioturbated kaolitic mudstones, with thick sandstone lenses and caliche, predominate; and clasts of plutonic igneous rocks, mostly granite and pink feldspar, are abundant in the lower layers, being the result of the erosion of the Berlengas horst found nearby. Thus, the paleoenvironment here was predominantly fluvial dominated, with the river system coming from northwest, where the Berlengas are found, being either meandering in form (Taylor et al., 2013) or a channel drifting alluvial fan system (Hill, 1989). In Porto Novo Member, the thick caliche rich mudstones are filled by even larger isolated sandstone lenses, which are the result of the distal paleo river channels that meandered the region, albeit laterally gradually shifting to deltaic settings with transgressive tidal influences. The abundant caliche deposition across both units suggest a semi-arid environment. Plant remains (mostly conifer wood) and vertebrate fossil material (mammals, dinosaurs, crocodyliforms, turtles and fish) are commonly found here. These units are estimated being late Kimmeridgian in age (Mateus et al., 2017).

Praia Azul Member: This unit is mostly made of marls and caliche-rich mudstones, with a few sandstone lenses with signs of bioturbation, cross-bedding and ripple marks. Three brackish carbonated layers also characterize this unit, with both the oldest and most recent defining the stratigraphic limits, which can vary in thickness between 80 and 130m. In some areas (south of Santa Cruz) the sandstones predominate and conglomerates can also be found forming cross-bedded layers shifting between clays, silts and sands (Manuppella et al., 1999). The paleoenvironment is interpreted as being set in meandering river systems along the coast, with the interface creating deltas, brackish water lagoons and sandy beaches (Werner, 1986; Taylor et al., 2013; Mateus et al., 2017). The brackish lagoons were the result of short and brief marine transgressions, which created the ideal conditions for the benthic invertebrate macrofauna flourish, leaving behind the now shell-rich units (Werner, 1986). Towards the upper part of the Praia Azul Member there is a regressive tendency hinted by the more prevalent fluvial deposits found. Biostratigraphic and isotope dating point to a Late Kimmeridgian to Early Tithonian Age, with the boundary pinned after the second carbonated layer. This unit is rich in vertebrate fossils, mostly dinosaurs, crocodyliforms, marine reptiles, amphibians and fish, as well as invertebrates, mostly mollusk bivalves (Mateus et al., 2017).

Assenta Member: With an estimated 300m thickness, the uppermost Lourinhã Formation unit is, for the most part, a caliche-rich mudstone deposit with some sandstone cross-beds and occasional bivalve-filled carbonated sequences, with the top limestones and marls of these carbonated levels bearing a distinct nodular shaped bioturbation from *Thalassinoides* ichnotaxa. Plant material can also be found throughout this unit, mostly wood and tree trunks, which often exhibit pyritization (Ramalho, 1971; Hill, 1988; Mateus et al., 2017). The overall stratigraphy suggests a general regression across these layers, particularly evident in the faunal transitions along the carbonated levels from marine to brackish. The paleoenvironment was for the most part a fluvial system of deltas and meandering rivers, with some brief transgressive episodes creating confined shallow lagoons favorable to carbonate precipitation (Ramalho, 1981; Hill, 1988; Mateus et al., 2017).

Microfossil data and magnetostratigraphy point to a Tithonian to Early Berriasian (Cretaceous) age for this unit, with the Jurassic – Cretaceous boundary being somewhere right before the top limit. This upper limit of the Assenta Member (also the upper limit for the Lourinhã Formation) is identified by a transition from the mudstones to the micritic/dolomitic filled sandstones that form the lowermost levels of the overlying Porto da Calada Formation (Rey, 1993; Mateus et al., 2017).

Porto da Calada Formation: This unit is mostly made up of sandstone material, with some conglomerates, mudstones and limestones. The sandstone has a cross-bedded pattern, with the conglomerates often being found at the base of the paleo-river channels and the mudstones along the low energy paleo-river banks. The lower unit levels were formed along the meandering rivers across the alluvial floodplains, whereas the upper ones were formed in tidal transitioned areas and shallow marine platforms based on the limestones and laminated sandstones (Rey, 1972, 1993; Mateus et al., 2017). Palynology data also revealed a conifer based flora in the region at this time (Batten & MacLennan, 1984).

The 43m thick Porto da Calada Formation is Berriasian in age, based on its microfossil assemblage, invertebrate taxa and magnetostratigraphy data (Rey, 1972; Ramalho, 1971, 1981; Mateus et al., 2017).

***Ceratosaurus* species – material, main characteristics and diagnosis**

***Ceratosaurus nasicornis* Marsh, 1884** – *C. nasicornis* (fig. 56) is the type species for the genus *Ceratosaurus*. The genotype (USNM 4735) was collected by M. P. Felch between 1883 and 1884 in Garden Park, Fremont County, Colorado belonging to the Upper Jurassic Morrison Formation (Gilmore, 1920). The specimen was named and described by Marsh in 1884 and additional descriptions were later made, first by Hay in 1908 and then by Gilmore in 1920, which is still to this day the most complete description of the holotype (Marsh, 1884; Hay, 1908; Gilmore, 1920). The specimen is known from a complete skull and partial semi-articulated skeleton, with Marsh (1884) estimating this individual to be about 6 meters long. The complete elements were listed by Gilmore (1920) as follows:

- Complete skull and lower jaws;
- Axial skeleton: atlas, axis, seven cervical vertebrae, 12 dorsal vertebrae fragments, sacrum (complete with five vertebrae), 50 caudal vertebrae, cervical ribs fragments, thoracic rib (last one), 20 chevrons;
- Appendicular skeleton: left scapula, left ulna, left radius, four metacarpals and three phalanges from the left manus, three metacarpals and a phalanx from the right manus, both ilia, pubes (two partial pieces, distal parts missing), ischia (two partial pieces, distal parts missing), both femora, right tibia, right fibula, right astragalus, right calcaneum, left tarsal, three left metatarsals, terminal left phalanx from digit IV;
- Osteoderms.

Considering that, at the time of Gilmore's description, only a few theropod genera were known, he cleverly noticed the more primitive features of this genus, namely the shape of the quadrate, presacral vertebrae and pubis and the higher number of digits. He found these features more similar to older theropods, referring to *Ceratosaurus* as the "most conservative theropod above the Triassic" (Gilmore, 1920).

The skull, for many years the most complete one of a theropod dinosaur (Hay, 1908), is laterally crushed and distorted, which led to an early misconception by Marsh who gave it a wider and robust appearance, whereas in real life the head should have been more narrow (Gilmore, 1920). The presence of the horn was, at the time of description, an unusual feature among theropods, being interpreted by Marsh as a defensive/offensive structure and by Gilmore as a sexual display feature (Marsh, 1893; Gilmore, 1920).

The cervical vertebrae, strongly opisthocoelic, with a deep concave posterior surface and flat anterior surface was also noted by Marsh by being unusual from what was known at the time for reptiles (Marsh, 1884; Gilmore, 1920; Madsen & Welles, 2000).

In his description, Gilmore points out for the fact that, due to the fragmentary nature of the dorsal vertebrae, it's total number was unknown, so the animal was originally reconstructed based on the same number of elements known for *Antrodemus* (= *Allosaurus*). However, the author shows how this made the dorsal region of the animal too long putting it unbalanced (Gilmore, 1920).

This particular specimen was also of great importance at the time of its first description because the co-ossified pelvic girdle enabled paleontologists to finally understood the correct position of these bones in theropod dinosaurs (Marsh, 1884).

The osteoderms, running along the dorsal line of the animal, over the neural spines of the vertebrae, were also seen as a new feature among theropods and Marsh interpreted them as ossified cartilage (Marsh, 1884).

Rauhut (2000) recognized only one species of *Ceratosaurus*, considering the differentiation of the other two species just by size subjective. Carrano and Sampson (2008), agreeing with this, also alerted for the fact that the *C. nasicornis* individual is overly fused and pathological, so the comparison with other specimens in order to define new species should take this in consideration. Therefore, these authors, for the time being, only accepted one *Ceratosaurus* species and defined the following diagnostic characters for the genus: (i) fused nasals with mediolaterally narrow and rounded horn, (ii) medial oval groove on nasals posterior to the horn, (iii) pubis with a large round notch below the obturator foramen, (iv) a row of small osteoderms running along the dorsal midline.

Garden Park section where this individual was found is dated Tithonian and, at 150.33 ± 0.26 Ma, this makes it older than *C. magnicornis* and *C. dentisulcatus* by 3-4 million years (Mateus et al, 2006).

C. nasicornis genotype (USNM 4735) is currently housed at the Smithsonian National Museum of Natural History, in Washington DC.

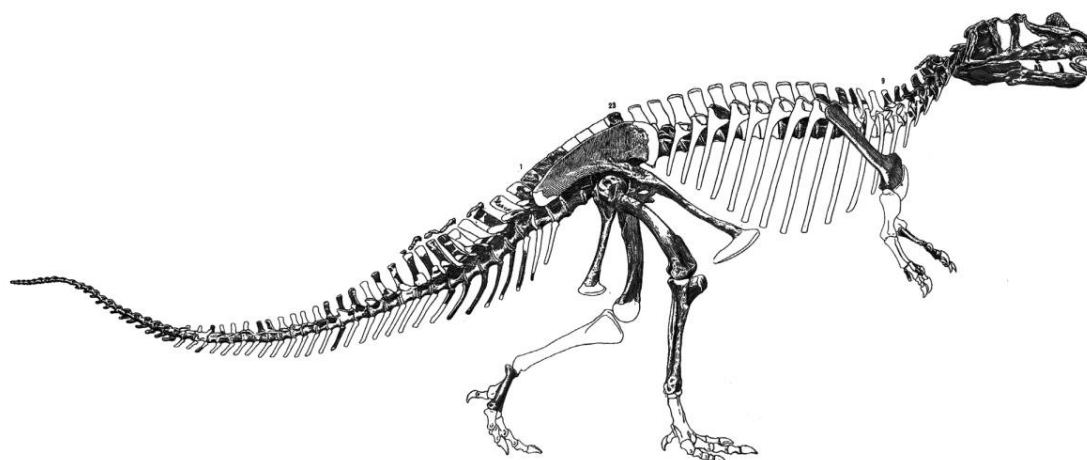


Figure 56. *Ceratosaurus nasicornis* holotype USNM 4735 with known elements in black. Source: Yun 2019, adapted and modified from Gilmore, 1920.

***Ceratosaurus magnicornis* Madsen & Welles, 2000** – *C. magnicornis* (referencing the larger nasal horn) was described in detail by Madsen and Welles (2000) based on a partial articulated skeleton (MWC1) from the Fruita Paleontological Area, Colorado. The specimen was found in layers of the lower part of the Brushy Basin Member, the youngest member of the Morrison Formation, dated Tithonian, Upper Jurassic, 146.7-147.3 Ma (Madsen & Welles, 2000; Mateus et al, 2006). This individual is the most complete of the two new species named by the Madsen and Welles. It is smaller than *C. dentisulcatus* and, according to the authors, not fully grown due to the open sutures found in the skull. The skeleton is almost complete, being the most relevant missing elements the mandible, the distal arms and the gastralia (Madsen & Welles, 2000). The complete elements listed by the authors are:

- Almost complete skull (except for the lower jaw), although some bones are badly crushed, incomplete or missing in one of the sides;
- Axial skeleton: cervical vertebrae (5th, 6th, 7th, 8th, 9th, 10th and 11th, with 10th and 11th being referred by the authors as “pectoral” vertebrae), dorsal vertebrae (2nd, 3rd, 5th, 6th, 7th, 8th and a more posterior one), caudal vertebrae (one anterior, one median and four posterior), cervical rib, median chevron;
- Appendicular skeleton: left humerus, manus ungual, both femora, both tibiae, right astragalus, right calcaneum, metatarsals (II left, II right, III left and one undetermined), pes (six elements);
- Five osteoderms.

Madsen and Welles distinguish it from *C. nasicornis* essentially by being more massive and robust in most skeletal elements, however other significant differences listed are: straighter border of premaxilla, more vertical anterior edge and more convex lower edge of the maxilla, deep maxillary vacuity in the nasal process of the maxilla, upper edge of maxilla, below the antorbital fenestra, dipping less posteriorly, anterior edge of maxilla lower at the front of the antorbital fenestra, quadrate pillar more concave posteriorly; the table of the sixth cervical slants up more steeply posteriorly and the postzygapophyseal centrodiapophyseal fossa is much shorter; straighter femur shaft; tibia tuberosity less developed; dorsal facet of the astragalus completely fills the astragalal facet, astragalocalcaneal suture running dorsolaterally.

Ceratosaurus magnicornis holotype, MWC1, is currently curated at the Museum of Western Colorado.

***Ceratosaurus dentisulcatus* Madsen & Welles, 2000** – *C. dentisulcatus* (referencing the medial grooves on the anterior teeth of the premaxilla and dentary) is the second *Ceratosaurus* species named by Madsen and Welles in 2000. The holotype, UMNH VP 5278, consists of a disarticulated specimen (more incomplete than *C. magnicornis*), coming from the Cleveland Lloyd Dinosaur Quarry, Emery, Utah. Like *C. magnicornis*, it was found in layers belonging to the Brushy Basin Member, of the Upper Jurassic Morrison Formation, dated Tithonian, 146.7-147.3 Ma (Madsen and Welles, 2000; Mateus et al, 2006).

It is the largest *Ceratosaurus* described to date. Madsen and Welles (2000) listed the following material:

- Partial skull and dentary: both premaxilla, left maxilla, right quadrate/quadratojugal, right jugal, right pterygoid, both dentary, left supradentary, right angular, both splenials;
- Axial skeleton: atlantal intercentrum, atlas/odontoid/axial intercentrum/axis (fused), cervicals (3rd, 4th, 5th, 6th, 7th, 8th and 9th), pectorals (1st, 2nd? and 3rd), dorsals (5th, 7th, 8th and 9th), 23 caudals (eight anterior, two median and 12 distal), two cervical ribs, three dorsal ribs, 12 chevrons (two anterior, three median and seven distal);
- Appendicular skeleton: right scapulocoracoid, left humerus, phalanx (manus ?), right manus Metacarpal II, left femur, both tibiae, left astragalus, left calcaneum, both fibulae, left metatarsal IV, tarsal IV, phalanx;
- four osteoderms.

Besides its larger size, Madsen and Welles (2000) distinguish *C. dentisulcatus* from *C. nasicornis* based on the following characteristics: subnarial border of premaxilla more arched and more horizontal, lower nasal process; alveolar border of maxilla more concave, posterior edge of nasal process rising more steeply, maxilla with three openings of large size at front of maxillary recess and at the base of the nasal process, maxilla more upturned, maxilla and dentary with less teeth (12 versus 15; 11 versus 15, respectively); more prominent odontoid, axis centrum shorter, with less curved downwards ventral edge, spine anteroposteriorly shorter, anterior edge dipping anteriorly 70 degrees (vs 20), table edge more steeper and straighter, no prezygapophysis and epipophysis extending behind the neural spine; third cervical vertebra centrum: shorter, posteriorly vertical, neural spine shorter and near vertical; astragalar overhang of the tibia much less inclined; astragalus front with weak horizontal groove and with the dorsal process ossified; fibula in lateral view has a vertical upper end, is broader, the tibial flange dips posteriorly with the upper edge/lower edge projecting anteriorly and the distal end is convex and round.

Besides its larger size, Madsen and Welles distinguish *C. dentisulcatus* from *C. magnicornis* based on the following characteristics: premaxilla with rounder snout and nasal processes with sharper back curve, which makes the anterior part of the skull lower, lower margin of the naris convex behind anterior concavity; steeper nasal process on the maxilla with straight posterior border making the antorbital fenestra more open anteriorly, three more openings into the maxilla (located at the front of the recess and at the base of nasal process), lateral facet of the maxilla higher above the first three teeth, lower half of the anterior border of the maxilla with pronounced posterior dip, more convex alveolar border, most anterior teeth of the maxilla are more curved and the posterior more vertical; fifth cervical vertebra: shorter centrum, diapophysis higher above the parapophysis in the transverse process, shorter table, epipophysis and neural spine; humerus head less laterally inclined and deltoid tuberosity thinner.

The diastema located in the fifth alveolus of the maxilla was interpreted by the authors as pathological instead of taxonomic.

Madsen and Welles (2000) report *C. dentisulcatus* from 150 feet below the top of the Brushy Basin, making it the youngest of the three *Ceratosaurus* described.

C. dentisulcatus holotype, UMNH 5278, is currently curated at the Utah Museum of Natural History, University of Utah, Salt Lake City, Utah.

Materials and Methods

The material described in this work includes all the Portuguese *Ceratosaurus* elements associated to this specimen up until now: one cervical vertebra, both femora, tibiae and fibulae, and one osteoderm. A fifth sacral centrum of dubious origin found near these elements is also described. Most of the material is housed under Museu da Lourinhã with the number ML352, except for the left femur, right tibia and part of the shaft of the right fibula which are under Sociedade de História Natural de Torres Vedras with the number SHN(JJS)065. All material was collected in the same quarry and is considered from the same individual.

An extensive photographic record of the material was made. Two set of photos were taken, the standard scaled photos from the six main angles (anterior, posterior, lateral, medial, dorsal and ventral views) and a detailed set of photos around the fossil for photogrammetry. 3D images were created using KIRI Engine software and Windows 3D Visualizer.

The bones were measured with standard metric tape and the anatomical nomenclature for the description was based on previous studies for this genus.

The *Ceratosaurus* teeth described are part of the Sociedade de História Natural de Torres Vedras fossil collection with serial numbers under both SHN and SHN(JJS). These elements were measured and photographed.

For the phylogenetic specimen-based analysis it was used the Cau (2024) matrix for theropod phylogeny. Only certain taxa deemed useful for the analysis were used. The matrix went through a filtering procedure to select and use only the characters where variability was found among the taxa in study. To better compare our material with the *Ceratosaurus* species from North America, 37 new anatomical entries were created. All characters have the same weight. The phylogenetic analysis was performed in TNT version 1.6 (Goloboff & Morales, 2022) and a traditional search was employed with 10 random seeds, 100 added sequences and 100 trees saved per replication via tree bisection reconnection (TBR).

Systematic Paleontology

Dinosauria Owen, 1842
Saurischia Seeley, 1888
Theropoda Marsh, 1881
Neotheropoda Bakker, 1986
Averostra Paul, 2002
Ceratosauria Marsh, 1884
Ceratosauridae Marsh, 1884
Ceratosaurus Marsh, 1884

Locality: The material comes from Rodela do Valmitão beach, located in Lourinhã, Portugal (fig. 57A).

Horizon and Age: Porto Novo/Praia da Amoreira Members of the Lourinhã Formation (fig. 57A), being Late Kimmeridgian (Late Jurassic) in age. These units lay between the older Consolação member and the younger Praia Azul member (fig. 57B).

The unit where the material was found (fig. 57C) is mainly made up of cross-bedded sandstones being rich in caliche and pink-orange silicate feldspar, the result of the erosion of the Berlengas Horst nearby (Hill, 1988; Manuppella et al., 1999; Mateus et al., 2017). The upper levels are especially rich in silicified or coalified wood and reptile bones. The sandstones frequently appear in lenticular form isolated in large volume mudstones.

This unit has been interpreted as a meandering river channel that evolved to a deltaic tidal influenced system, with the paleopalynological analysis also supporting a terrestrial setting (Mateus et al., 2017).

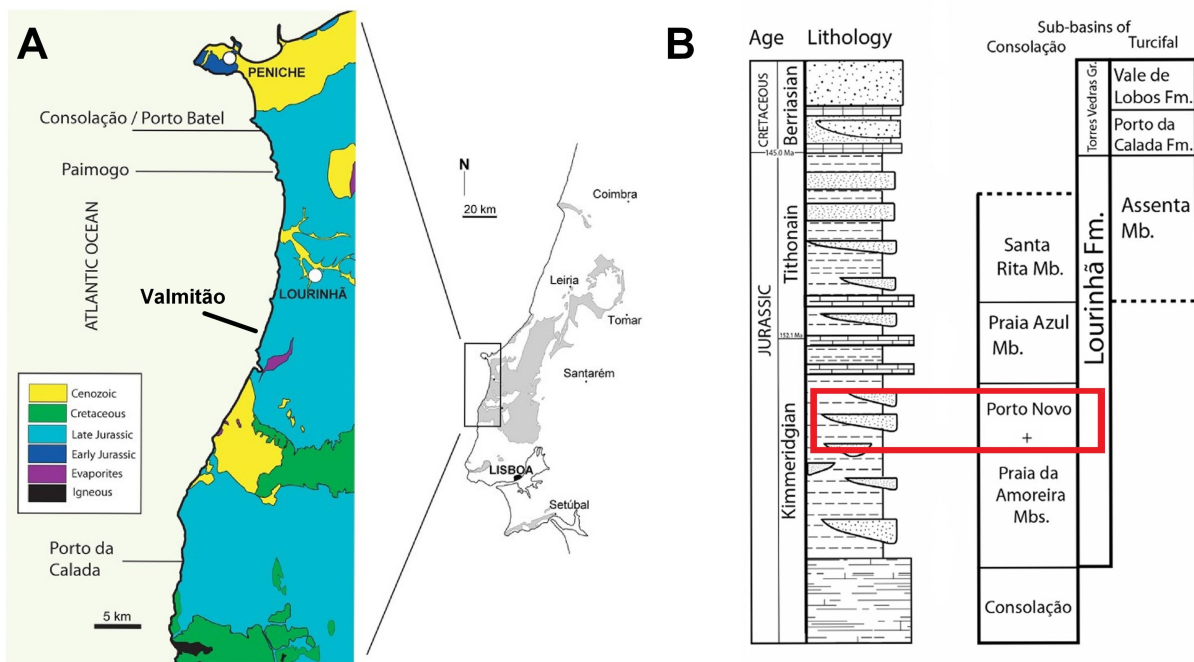


Figure 57. (A) General map of the geology in the West Coast of Portugal with the location of the Valmitão beach (left) and the Jurassic outcrops in grey (right), adapted and modified from Mateus et al., 2017; (B) stratigraphic column of the Lourinhã Formation showing the position of the Porto Novo Member where *Ceratosaurus* was found, adapted and modified from Mateus et al., 2017; (C) outcrop at Valmitão where ML352/SHN(JJS)065 was found.

Material Description

Cervical Vertebra

One cervical vertebra centrum and the base of the neural arch was recovered (fig. 58 & 59). The vertebra is deformed and broken with the anterior half missing, hampering easy comparison and anatomical positioning. However, comparison with the material described and illustrated by Gilmore (1920; plate 20) and Madsen and Welles (2000; plate 6, 14 and 15) might enable a close identification. The dorsoventral position of the parapophysis (which tend to migrate from a ventral position on the anterior cervicals to a more dorsal position on the posterior ones), the vertical height of the anterior and posterior facets and the anteroposterior length of the centrum, all point out to a posterior position in the neck - probably the fifth or sixth cervical.

The anteroposterior axis of the centrum appears to be laterally inclined, probably as a result of anterolateral – posterolateral compression. In anterior view, the outline is heavily damaged.

The most anterior facet of the vertebra centrum is missing showing the internal pneumatization in great detail. At least three large pneumatic cavities can be observed, these chambers subsequently subdivide into smaller ones, creating a complex pattern. A small cavity, lateral to the neural canal, can be probably attributed to the centroprezygapophyseal fossa (prechonos in Madsen & Welles (2000)) based on comparisons with *Ceratosaurus* material described and illustrated by Gilmore (1920) and Madsen and Welles (2000) and based on the nomenclature terms defined by Wilson et al., (2011). The base of the neural arch is intact but the zygapophyses or neural spine are missing. Laterally to the neural canal, two bulges, one from each side, form the base of the diapophysis and below these, expanding laterally and reaching the ventral region, there are two suture marks, one on each side, probably the attachment point of the parapophysis to the centrum.

These features are better visualized on left lateral view; what appears to be the remains of the diapophysis appear here as two bulges, the one seen in anterior view is located more anterodorsally and has an elongated shape that runs vertically until it meets the other bulge located more posteriorly and bearing a more spherical shape. Below this bulge, a small pleurocoel is present. This structure is common in cervical vertebrae centra of ceratosaurs and coelophysoids, where usually both a pair of anterior and posterior pleurocoels is found, however this might change in certain taxa (Tykoski & Rowe, 2004). Since the anterior facet of the vertebra is missing, we can assume that this is the posterior pleurocoel. Above the bulge there is a flat dorsoposterolateral surface, probably what remains of the postzygapophyseal centrodiaepophyseal fossa (posterior chonos in Madsen & Welles (2000)).

The right lateral side of the vertebra is anteroposteriorly shorter than the left one as a result of the compression. In this view, the diapophysis appears as a single structure running anterodorsally to posteroventrally until the center of the lateral surface. The pleurocoel is much less noticeable here. As a result, there is some left/right asymmetry that seems to be more anatomical rather than due to the effect of compression. In this view, the remains of the postzygapophyseal centrodiaepophyseal fossa are less noticeable.

The ventral facet of the centrum has a longitudinal mid-line ridge. On both lateral sides, the ventral ridge of the vertebra still maintains its concave curvature and the anterior and posterior facets of the centrum are vertically longer than the middle.

Posteriorly, the centrum is better preserved. The outline is subcircular and the centrum is deeply concave (opisthocelous). The neural canal is small, just slight taller than wide.

In dorsal and ventral views, the level of damage to the vertebra is more noticeable, especially in ventral view where the leaning of the ventral ridge reflects the leaning of the anteroposterior axis of the centrum as the result of compression.

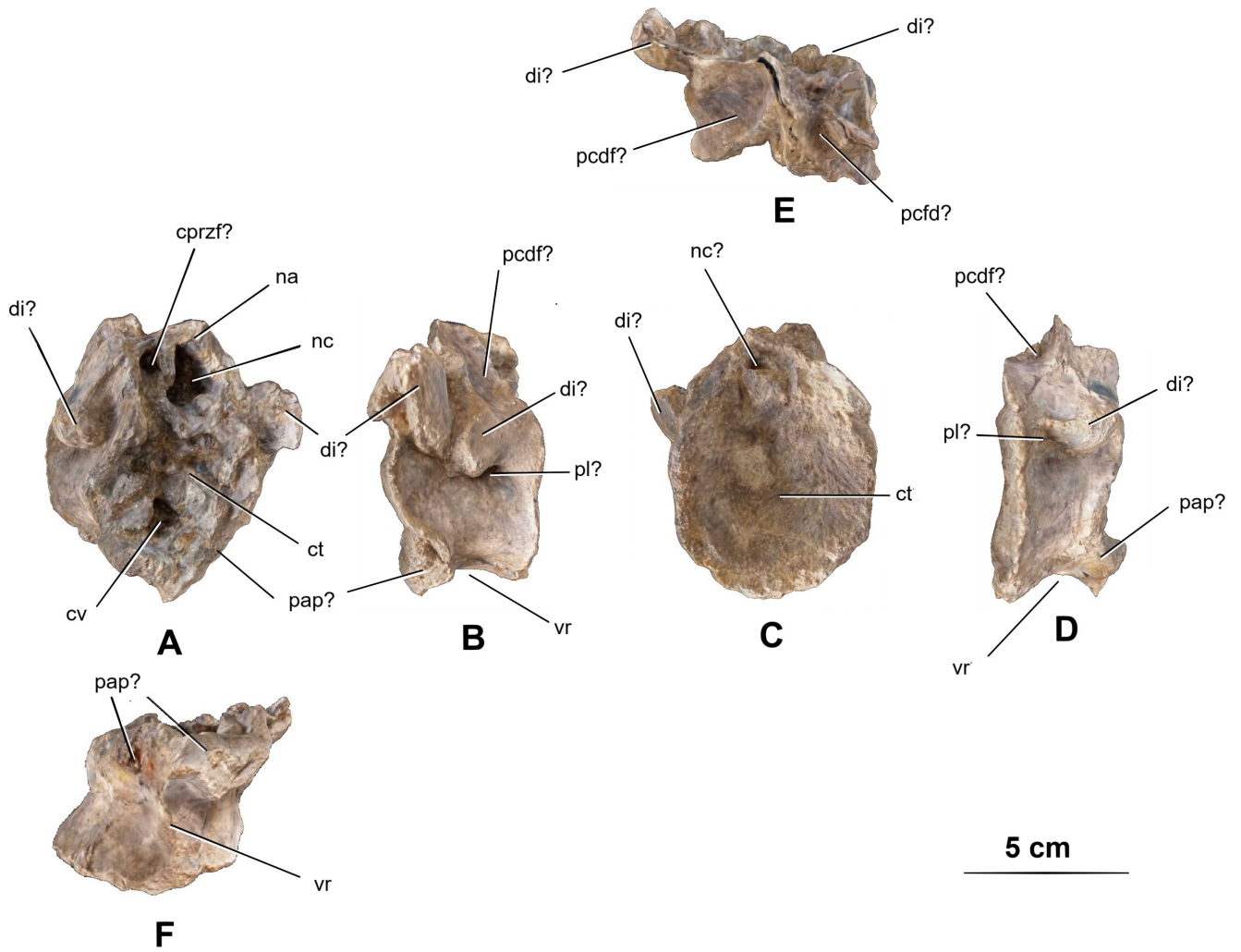


Figure 58. *Ceratosaurus* sp. ML352 cervical vertebra (images based on the 3D scan) in anterior (A), left lateral (B), posterior (C), right lateral (D), dorsal (E) and ventral (F) views. **cprzf** - centroprezygapophyseal fossa, **ct** – centrum, **cv** – cavity, **di** – diapophysis, **na** – neural arch, **nc** - neural canal, **pap** – parapophysis, **pcdf** – postzygapophyseal centrodiapophyseal fossa, **pl** – pleurocoel, **vr** – ventral ridge.

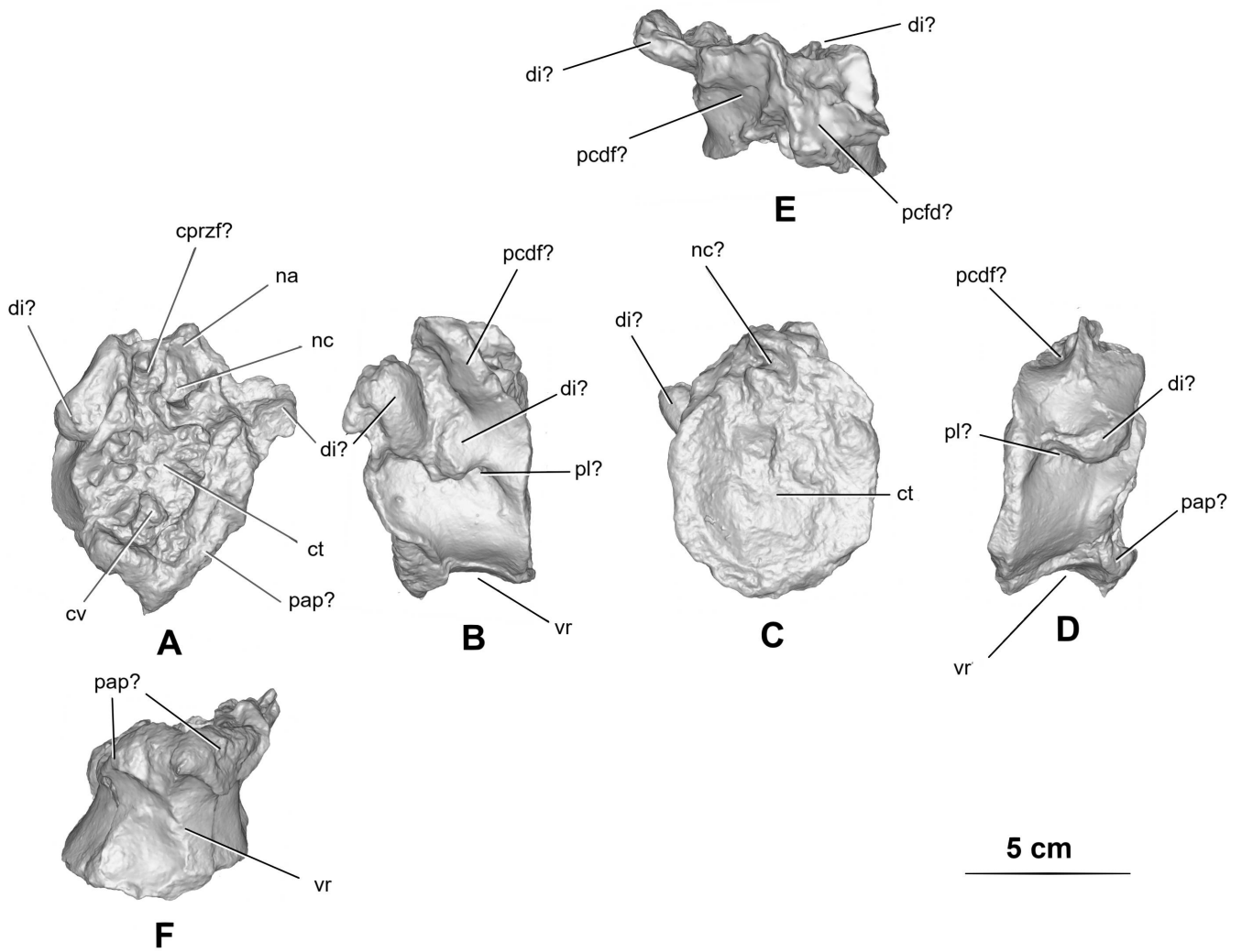


Figure 59. *Ceratosaurus* sp. ML352 cervical vertebra (3D scan in digital greyscale) in anterior (**A**), left lateral (**B**), posterior (**C**), right lateral (**D**), dorsal (**E**) and ventral (**F**) views. **cprzf** - centroprezygapophyseal fossa, **ct** - centrum, **cv** - cavity, **di** - diapophysis, **na** - neural arch, **nc** - neural canal, **pap** - parapophysis, **pcdf** - postzygapophyseal centrodiapophyseal fossa, **pl** - pleurocoel, **vr** - ventral ridge.

Sacral Vertebra

This material corresponds to a well-preserved vertebra centrum (fig. 60 & 61) with the neural arch above the neurocentral suture missing. The vertebra is considered sacral (likely the last, the fifth) due to the fusion attachment of the anterior facet and the regular posterior one, the expanded ends of the neural canal, the broad width, the unfused neurocentral line and lack of chevron facets.

The centrum is opisthocoelous, flat anteriorly and slight concave posteriorly. The outline in anterior view is cordiform (heart-shaped), ventrally is rounded and dorsally there is a concave depression on top for the neural canal. The pedicels (roots of the neural arches) create two dorsolateral projections, giving the dorsal region a U-shaped outline. The anterior facet of the centrum is flat and bears a rugous pattern usually observed in fusion attachments to the adjacent sacral centra.

The posterior facet has a reniform (kidney-shaped) outline where the dorsal U-shaped outline is much less prominent. The dorsal facet of the centrum is slightly concave.

Dorsally, the base of the neural canal is visible as well as both neurocentral sutures for the contact with the neural arches. These ridges develop anteroposteriorly along with the base of the neural canal but are laterally compressed in the middle region along with the rest of the vertebral centrum.

In ventral view, the anterior facet is laterally wider than the posterior one. There is an anteroposterior ridge along the ventral region. This is a single continuous ridge without the groove characteristic of the caudal vertebrae of some ceratosaurs and coelophysoids (Madsen & Welles, 2000; Tykoski & Rowe, 2004).

This element differs considerably from the *Ceratosauros* sacral vertebra illustrated by Gilmore (1920), certainly coming from a different taxa. A detailed analysis is made in the comparative anatomy section.

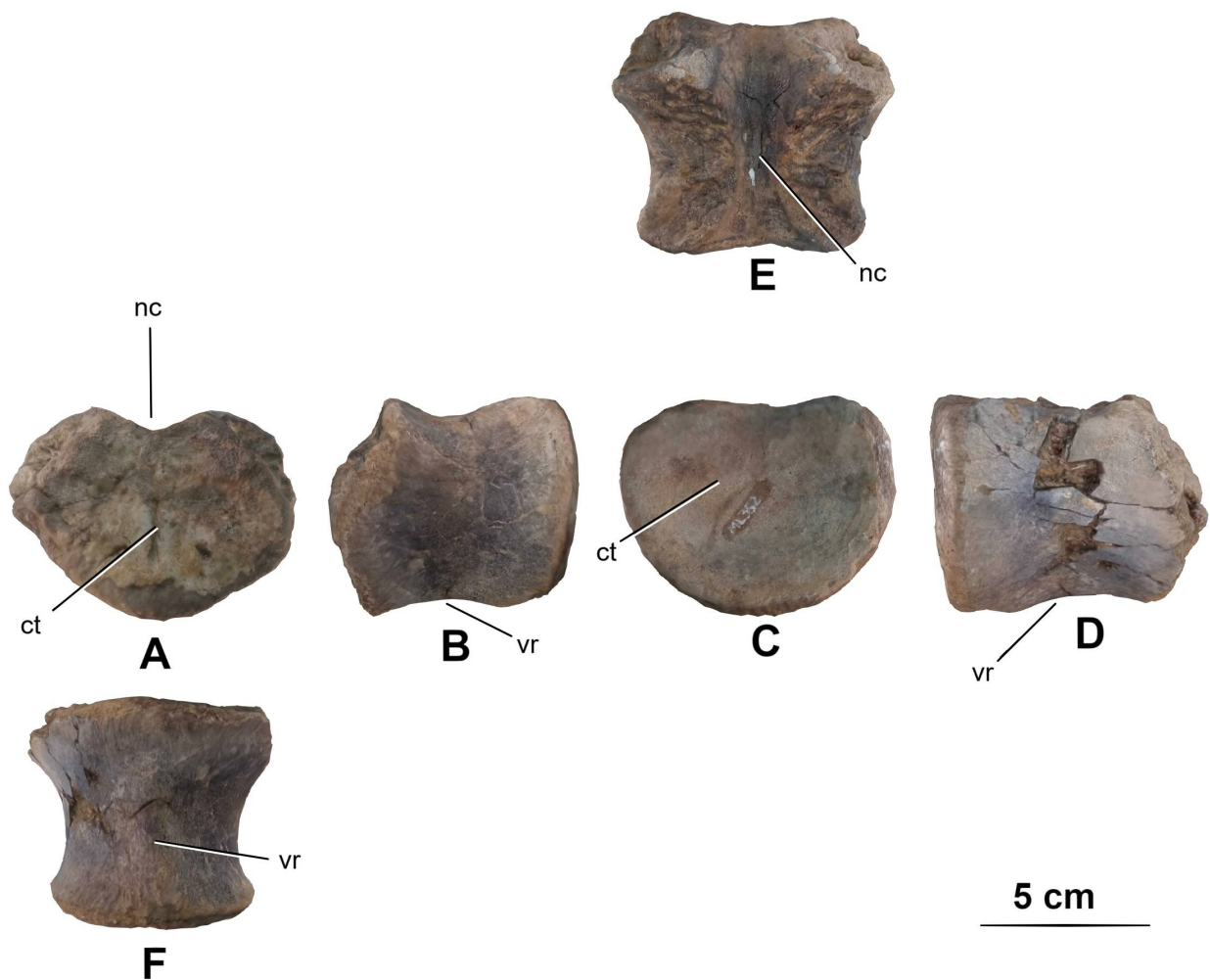


Figure 60. *Ceratosauros* (?) sp. ML352 fifth sacral vertebra centrum (images based on the 3D scan) in anterior (A), left lateral (B), posterior (C), right lateral (D), dorsal (E) and ventral (F) views. **ct** – centrum, **cv** – cavity, **nc** - neural canal, **vr** – ventral ridge.

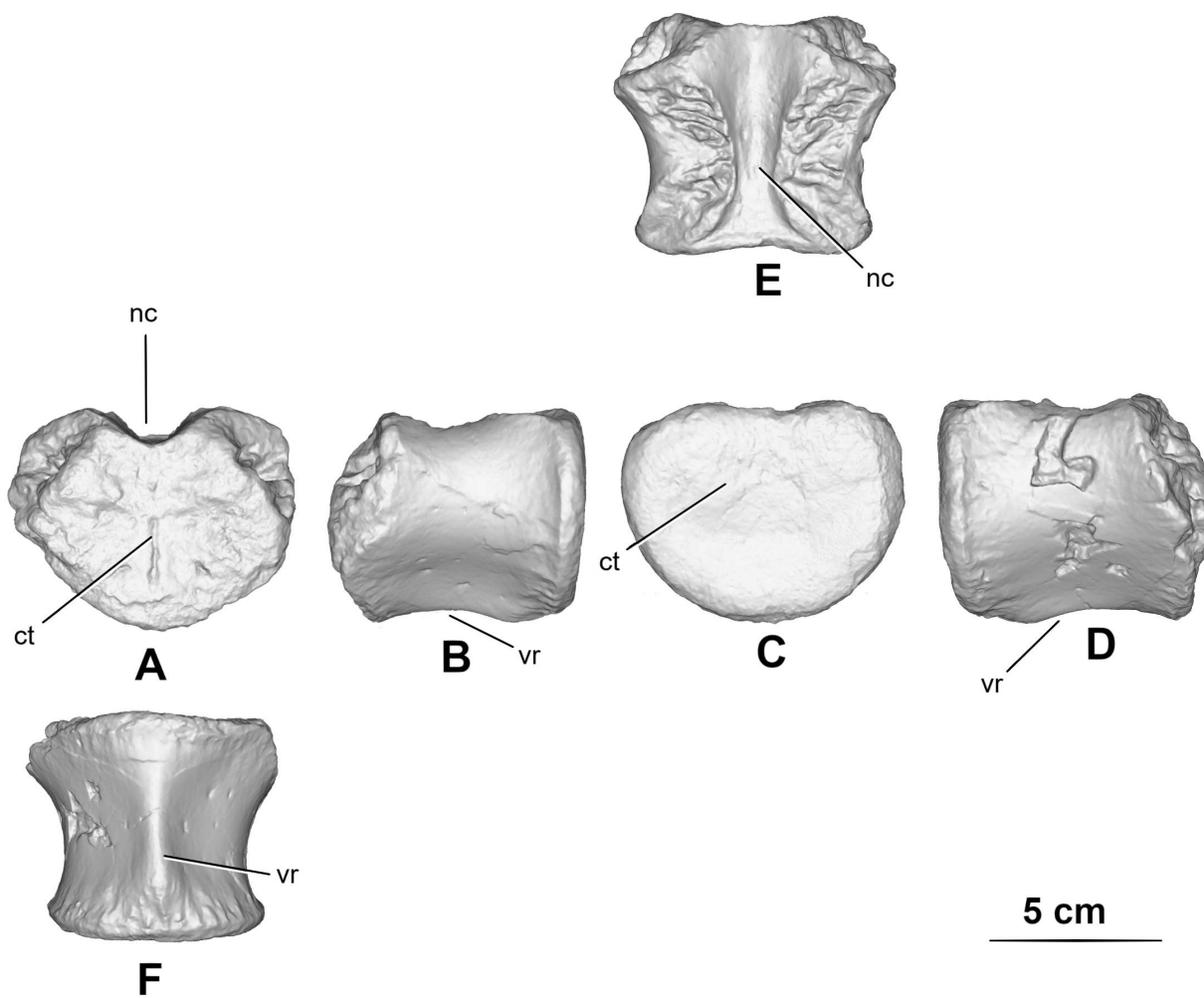


Figure 61. *Ceratosaurus* (?) sp. ML352 fifth sacral vertebra centrum (3D scan in digital greyscale) in anterior (A), left lateral (B), posterior (C), right lateral (D), dorsal (E) and ventral (F) views. **ct** – centrum, **cv** – cavity, **nc** - neural canal, **vr** – ventral ridge.

Femora

Both femora (fig. 62-65) were recovered and formally described in other publications (Mateus & Antunes, 2000; Mateus et al., 2006; Malafaia et al., 2015). Both are mostly complete, being similar in shape and size.

The femur is long and robust, the shaft is subcircular in cross section, straight in anterior and posterior views and slightly curved anteriorly in lateral and medial views.

In proximal view the femur head projects about 45° anteromedially and is anterolaterally-posteromedially compressed into an oval shape, being wider medially.

In anterior and posterior views, the head is tilted slightly medially, has a well defined proximal curvature and ends in a small but prominent notch or hook that points ventrolaterally. The anterior trochanter develops just below the level of the head, extending proximodistally in the same plane of the femur shaft. In SHN(JJS)065 appears in anterior and lateral views as a 9cm long bulbous ridge strongly projected anteriorly and in ML352 has a sharper edge and projects more anteromedially.

In lateral view, the trochanteric shelf extends anterodorsally from the distal end of the anterior trochanter, crossing completely the lateral surface of the femur until it reaches the posterior surface. The ridge of the trochanteric shelf is slender and has a subtriangular shape that projects laterally.

Posteriorly, the strong curvature of the lateral head is particularly evident, defining the well developed greater trochanter. A deep groove develops semi-vertically along the medial head just before the notch. The fourth trochanter projects posteriorly and the ridge extends proximodorsally along the most medial facet of the dorsal shaft, from the proximal end to the middle. In medial view, the ridge of the fourth trochanter has a smooth curvature, being more pronounced proximally than distally.

In the anterior facet of the distal femur the condylar region is proximally and medially outlined by a well-developed sharp and pronounced endocondylar ridge (medial epicondyle) that extends proximolaterally-mediodistally and then curves along the anteromedial side of the endocondyle; this structure outlines a flat surface in this region of the femur. The endocondylar ridge is well preserved in SHN(JJS)065 but in ML352 the anteromedial side of the ridge is mostly missing. This ridge gives the most distal part of the femur an almost square-shaped form in anterior view. Both condyles are robust and well developed. They are separated in anterior view by a small concavity in the distal-most surface of the femur and have an overall rounded shape in lateral and medial views. In dorsal view the ectocondyle is lateromedially wider than the endocondyle, bearing a robust tuberos process (the *crista tibiofibularis*). This ellipse-shaped process is proximodistally to slightly proximolaterally-mediodistally elongated relative to the femur shaft (being more evident on the left femur SHN(JJS)065) and develops a deep sulcus along its lateral side. Along the posterior distal part of the shaft there is smooth popliteal surface that becomes deeper distally creating a fossa between the condyles and ending in a prominent, horizontal and straight popliteal ridge (= intercondylar bridge) connecting both condyles. In distal view, the ectocondyle has a circular shape and the endocondyle is mediolaterally compressed, resulting in a general outline in this view that is rounded laterally, flat medially, slightly concave anteriorly and deeply concave posteriorly in the area separating both condyles. In ML352 this area is partially eroded and some of these features ended up with a slightly different shape.

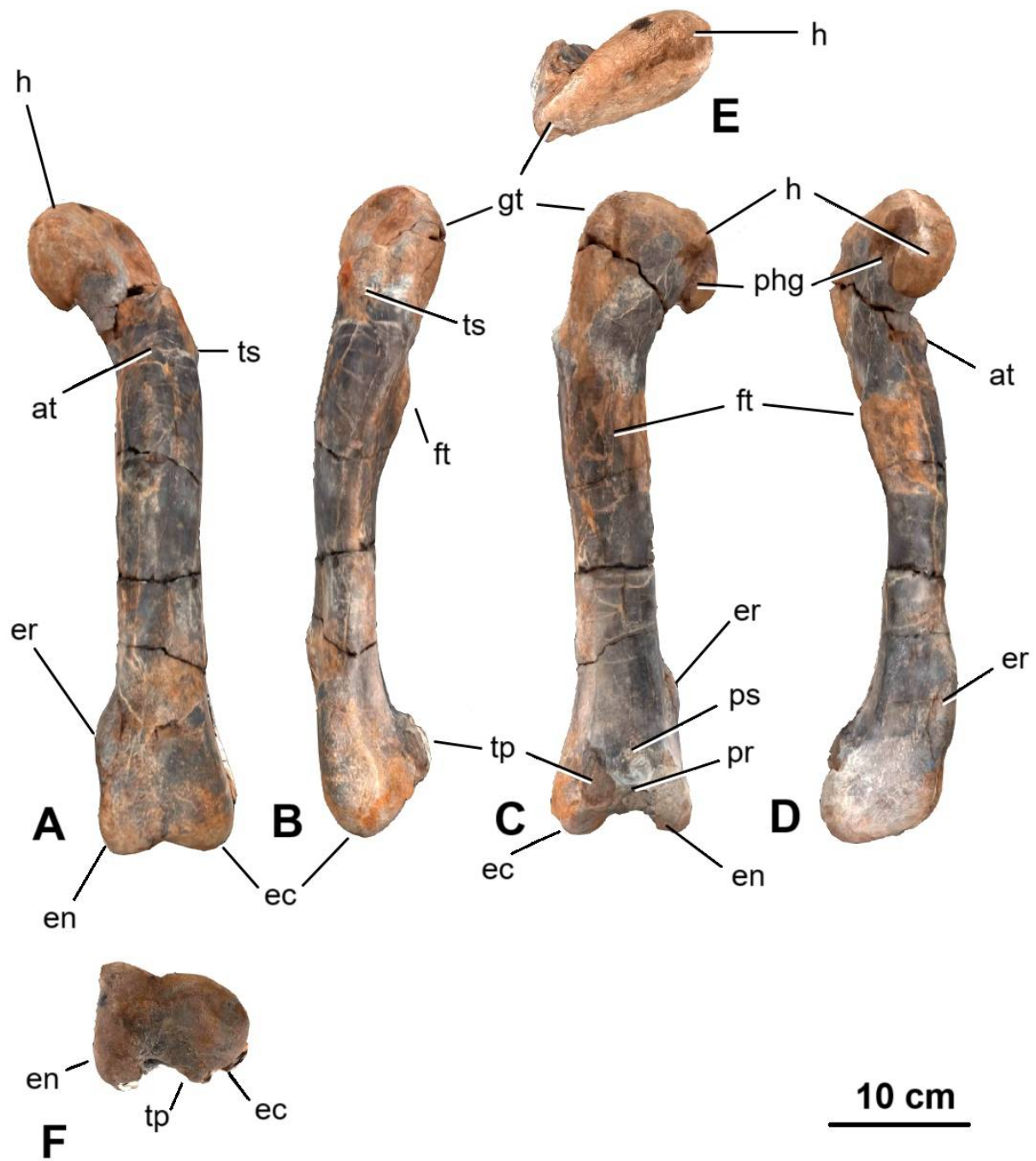


Figure 62. *Ceratosaurus* sp. left femur SHN(JJS)065 (images based on the 3D scan) in anterior (A), lateral (B), posterior (C), medial (D), proximal (E) and distal (F) views. **at** – anterior trochanter, **ec** – ectocondyle, **en** – endocondyle, **er** – endocondylar ridge, **ft** – fourth trochanter, **gt** – greater trochanter, **h** – head, **phg** – posterior head groove, **pr** – popliteal ridge, **ps** – popliteal surface, **tp** – tuberosity process (*crista tibiofibularis*), **ts** – trochanteric shelf.

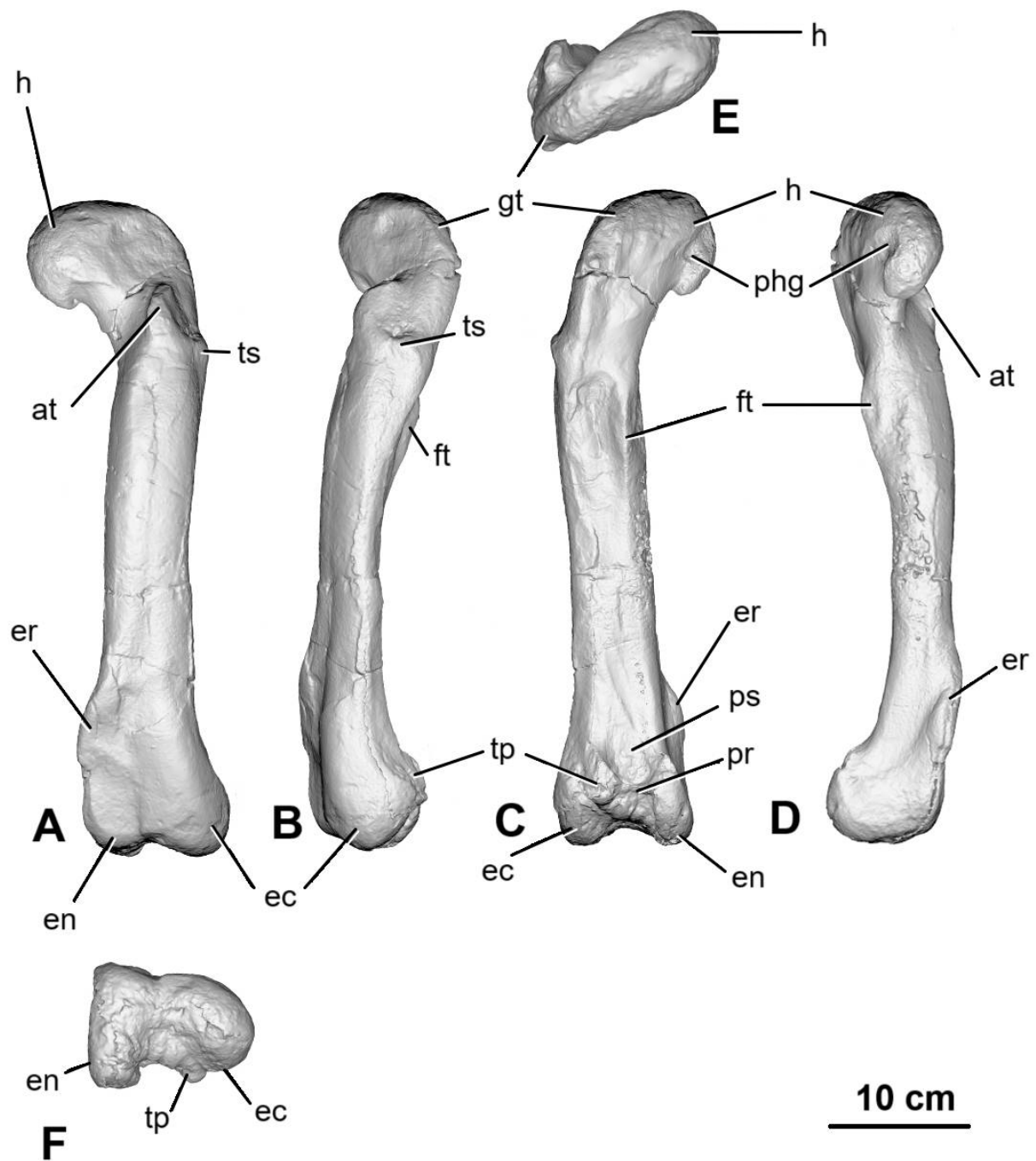


Figure 63. *Ceratosaurus* sp. left femur SHN(JJS)065 (3D scan in digital greyscale) in anterior (A), lateral (B), posterior (C), medial (D), proximal (E) and distal (F) views. **at** – anterior trochanter, **ec** – ectocondyle, **en** – endocondyle, **er** – endocondylar ridge, **ft** – fourth trochanter, **gt** – greater trochanter, **h** – head, **phg** – posterior head groove, **pr** – popliteal ridge, **ps** – popliteal surface, **tp** – tuberous process (*crista tibiofibularis*), **ts** – trochanteric shelf.

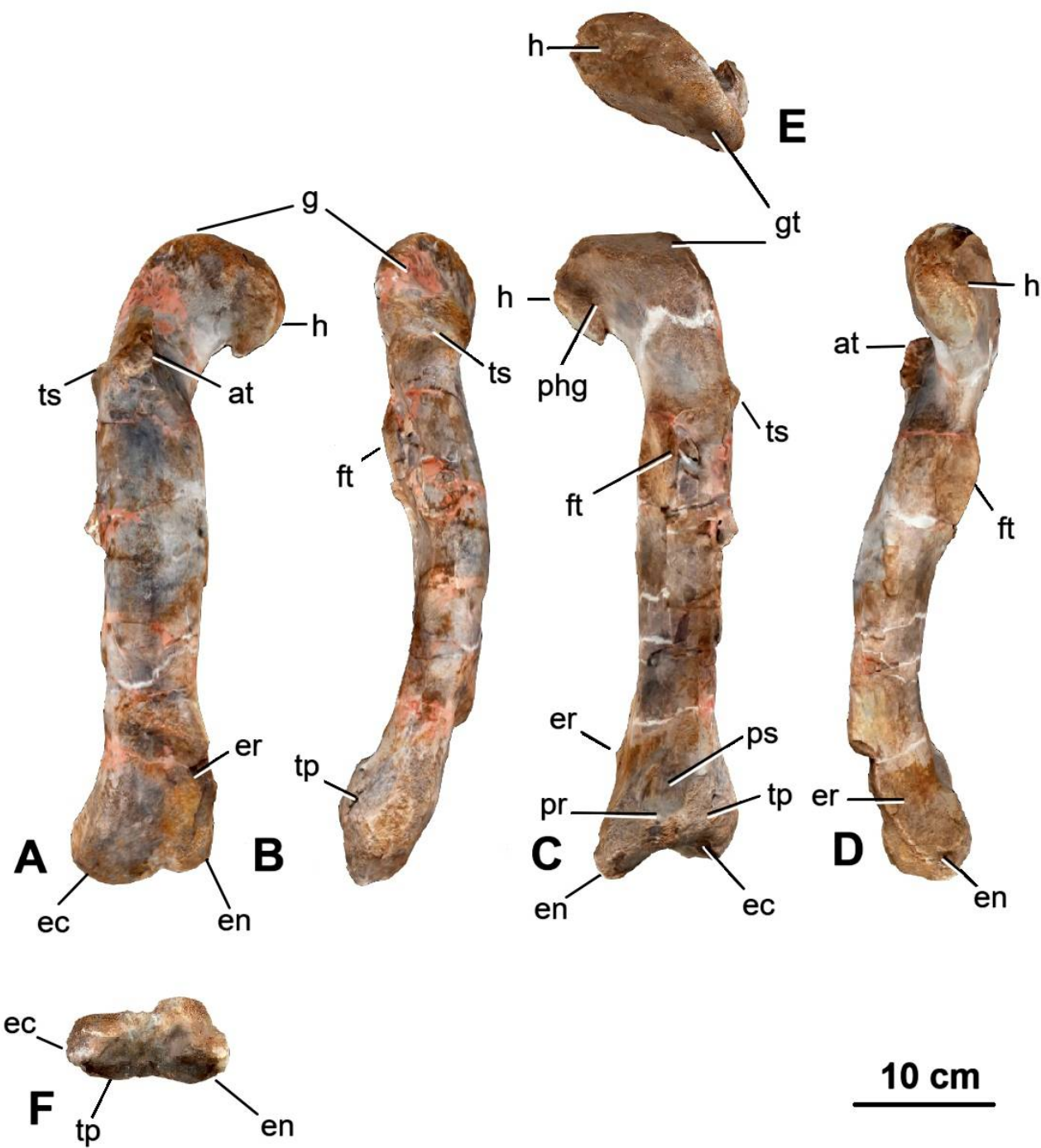


Figure 64. *Ceratosaurus* sp. right femur ML352 (images based on the 3D scan) in anterior (A), lateral (B), posterior (C), medial (D), proximal (E) and distal (F) views. **at** – anterior trochanter, **ec** – ectocondyle, **en** – endocondyle, **er** – endocondylar ridge, **ft** – fourth trochanter, **gt** – greater trochanter, **h** – head, **phg** – posterior head groove, **pr** – popliteal ridge, **ps** – popliteal surface, **tp** – tuberos process (*crista tibiofibularis*), **ts** – trochanteric shelf.

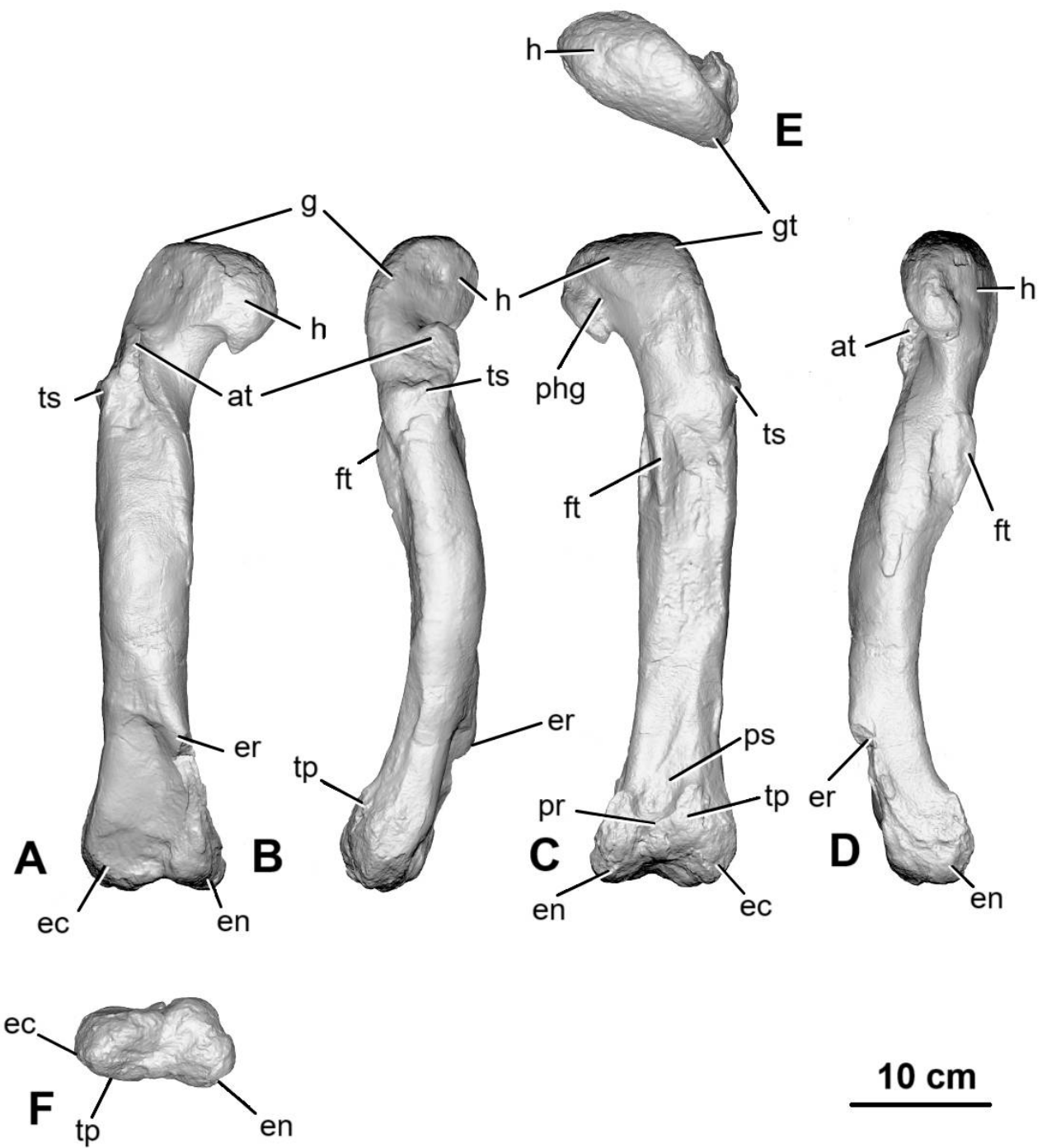


Figure 65. *Ceratosaurus* sp. right femur ML352 (3D scan in digital greyscale) in anterior (A), lateral (B), posterior (C), medial (D), proximal (E) and distal (F) views. **at** – anterior trochanter, **ec** – ectocondyle, **en** – endocondyle, **er** – endocondylar ridge, **ft** – fourth trochanter, **gt** – greater trochanter, **h** – head, **phg** – posterior head groove, **pr** – popliteal ridge, **ps** – popliteal surface, **tp** – tuberous process (*crista tibiofibularis*), **ts** – trochanteric shelf.

Tibiae

Both tibiae (fig. 66-69) were also recovered and described by Mateus and Antunes (2000), Mateus et al. (2006) and Malafaia et al. (2015). They are both fairly complete and well preserved.

The tibiae are robust, straight in anterior and posterior views, but slightly arched posteriorly in lateral and medial views.

In proximal view, the tibia head is anteroposteriorly elongated, concave in the lateral facet and flat in the medial. The proximal articular surface is slightly concave where the contact with the femur is made. The well-developed cnemial crest curves and projects anterolaterally, being anteroposteriorly as long as the articular condyles. In ML352 the cnemial crest is complete but in SHN(JJS)065 the tip is missing. In anterior and lateral views, the expansion of the cnemial crest is clearly more upturned, projecting anteroproximolaterally and above the proximal condyles. The crest is robust, well developed and with a smooth curved outline. Distally, it develops semi-vertically and eventually merges with the proximal-most anteromedial edge of the shaft. In lateral view the cnemial crest bears a deep and wide fossa extending all along the lower facet of the crest.

Posteriorly, in proximal view, the lateral and medial condyles develop with an almost rounded shape, both being less developed than the cnemial crest. These condyles are more evident in ML352 than in SHN(JJS)065. The lateral condyle (or ectocondyle) projects posterolaterally and is more pronounced than the medial one, that projects dorsomedially. The lateral condyle posterolateral projection is more evident in lateral view where a deep groove below it can be seen.

Between the cnemial crest and the lateral condyle, a vertical fibular crest extends along the lateral side of the shaft but being more prominent proximally. This crest is more evident due to its position between the cnemial crest fossa and the above-mentioned groove below the lateral condyle. The fibular crest bifurcates in two ridges towards the cnemial crest and the lateral condyle. The ridge connecting to the cnemial crest is twice as long as the other and projects proximoanteriorly, extending along the uppermost lateral facet of the cnemial crest and above the fossa. The smaller ridge runs along the same plane as the main fibular ridge, connecting proximally to the lateral side of the lateral condyle, almost reaching the articular surface of the tibia. Proximally, in posterior and anterior views, the fibular crest ridge makes a slightly round and elongated curve. Below it, and along the same axis, the ridge develops continually along the rest of the lateral shaft. The fibular ridge gives the shaft an oval shape in cross section.

The medial condyle, in posterior and medial views, is a bulbous protuberance that distally develops a ridge with smooth curvature which becomes part of the posteromedial facet of the shaft.

The distal end of the tibia expands mediolaterally into a medial and lateral *malleolus*. The lateral *malleolus* is broader and more distally expanded than the medial one and both have a round outline. Anteriorly, between the *malleoli*, a semi-triangular shaped depression serves as contact for the astragalus. This depression is deeper on the medial *malleolus* side ridge (astragalus overhang), being inclined about 25°. In ML352 the astragalus overhang is particularly noticeable and prominent. In SHN(JJS)065 a vertical ridge runs between the *malleoli* on the posterior facet of the distal tibia. This feature is also evident in distal view, creating a sharp convex posterior facet, whereas anteriorly the facet for the insertion of the astragalus is concave. In distal view is also noticeable the more expanded lateral *malleolus* relative to the medial one.

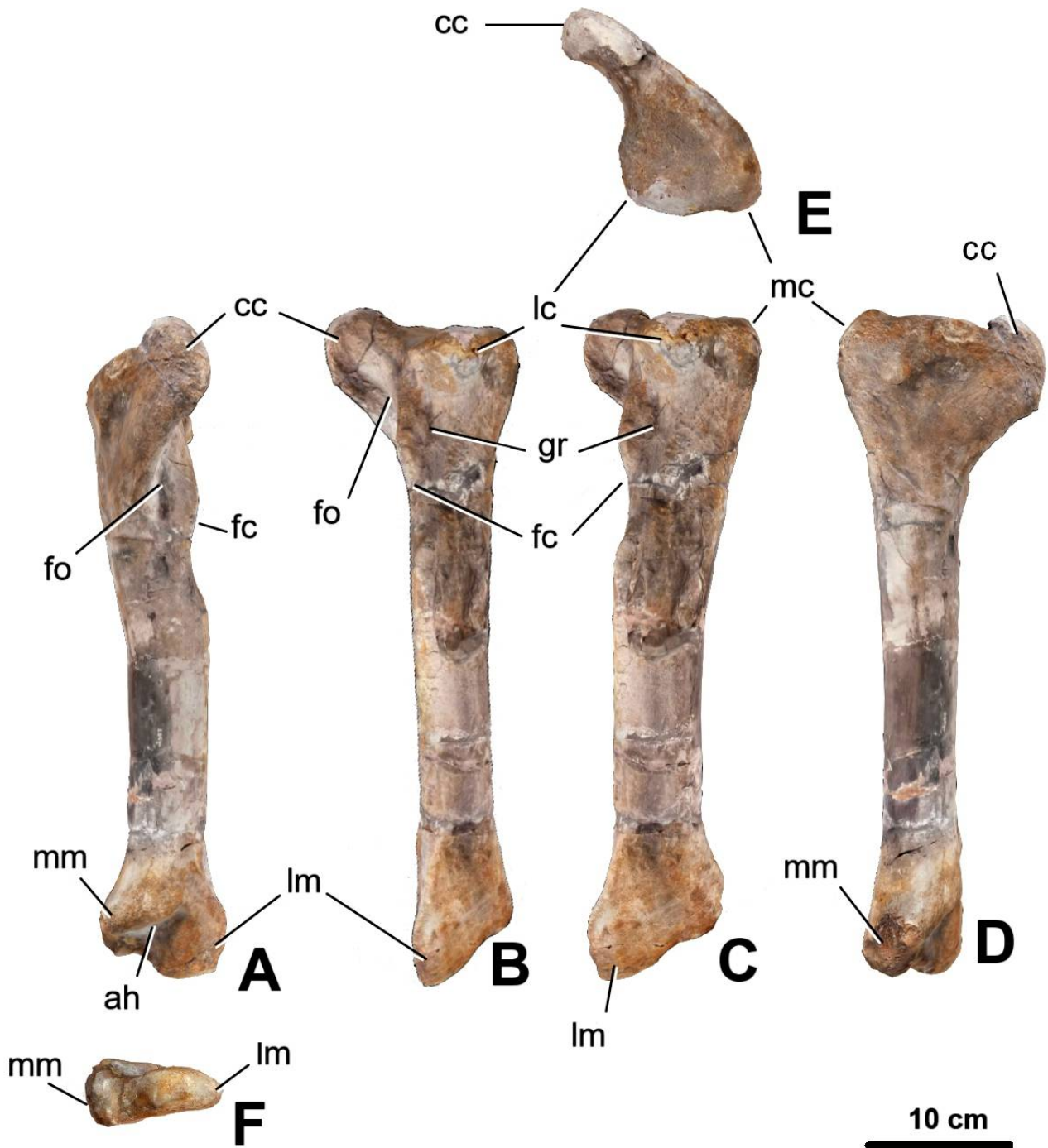


Figure 66. *Ceratosaurus* sp. left tibia ML352 (images based on the 3D scan) in anterior (A), lateral (B), posterior (C), medial (D), proximal (E) and distal (F) views. **ah** – astragalar overhang, **cc** – cnemial crest, **fc** – fibular crest, **fo** – fossa, **gr** – groove, **lc** – lateral condyle, **lm** – lateral malleolus, **mc** – medial condyle, **mm** – medial malleolus.

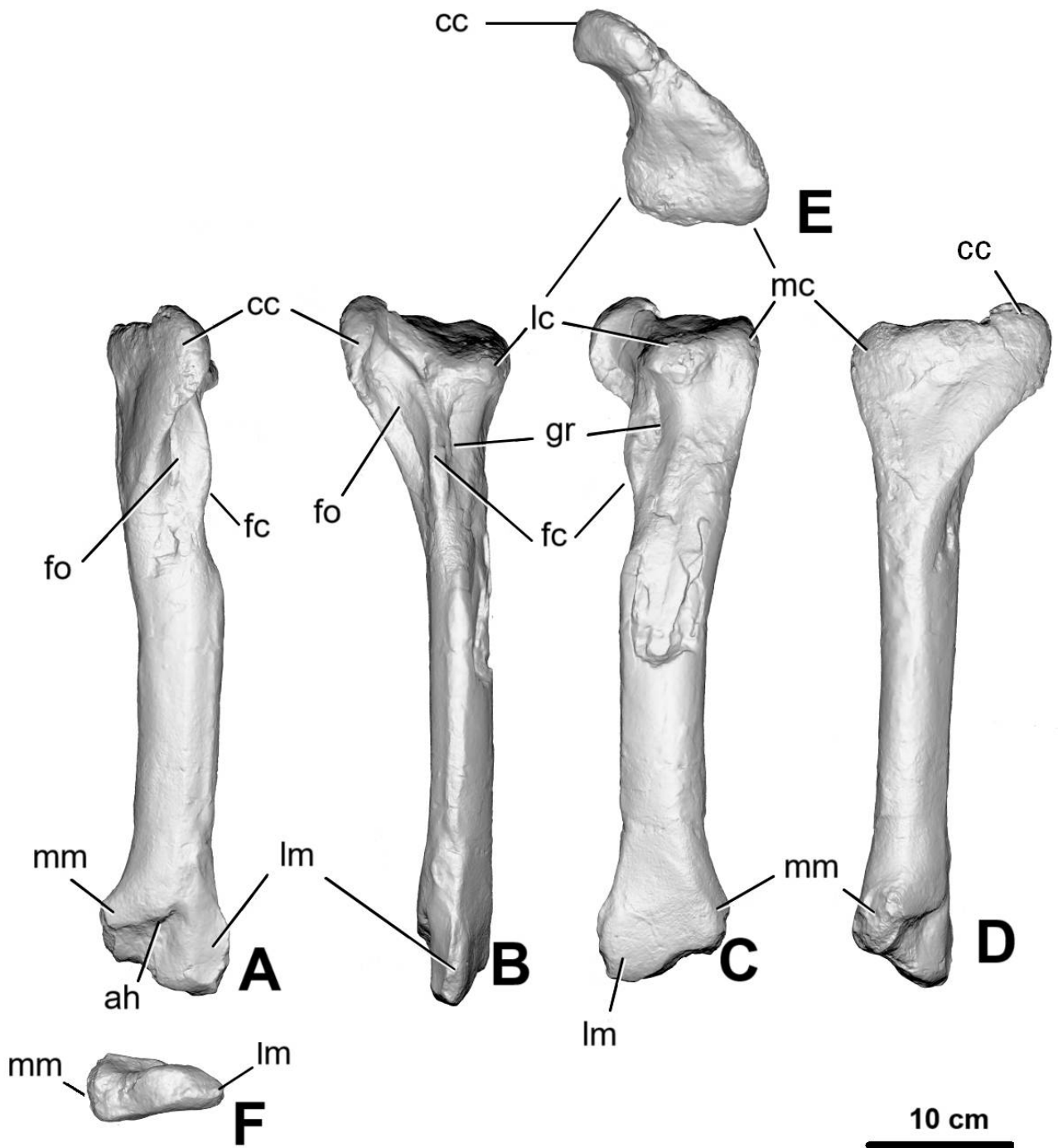


Figure 67. *Ceratosaurus* sp. left tibia ML352 (3D scan in digital greyscale) in anterior (A), lateral (B), posterior (C), medial (D), proximal (E) and distal (F) views. **ah** – astragalar overhang, **cc** – cnemial crest, **fc** – fibular crest, **fo** – fossa, **gr** – groove, **lc** – lateral condyle, **lm** – lateral *malleolus*, **mc** – medial condyle, **mm** – medial *malleolus*.

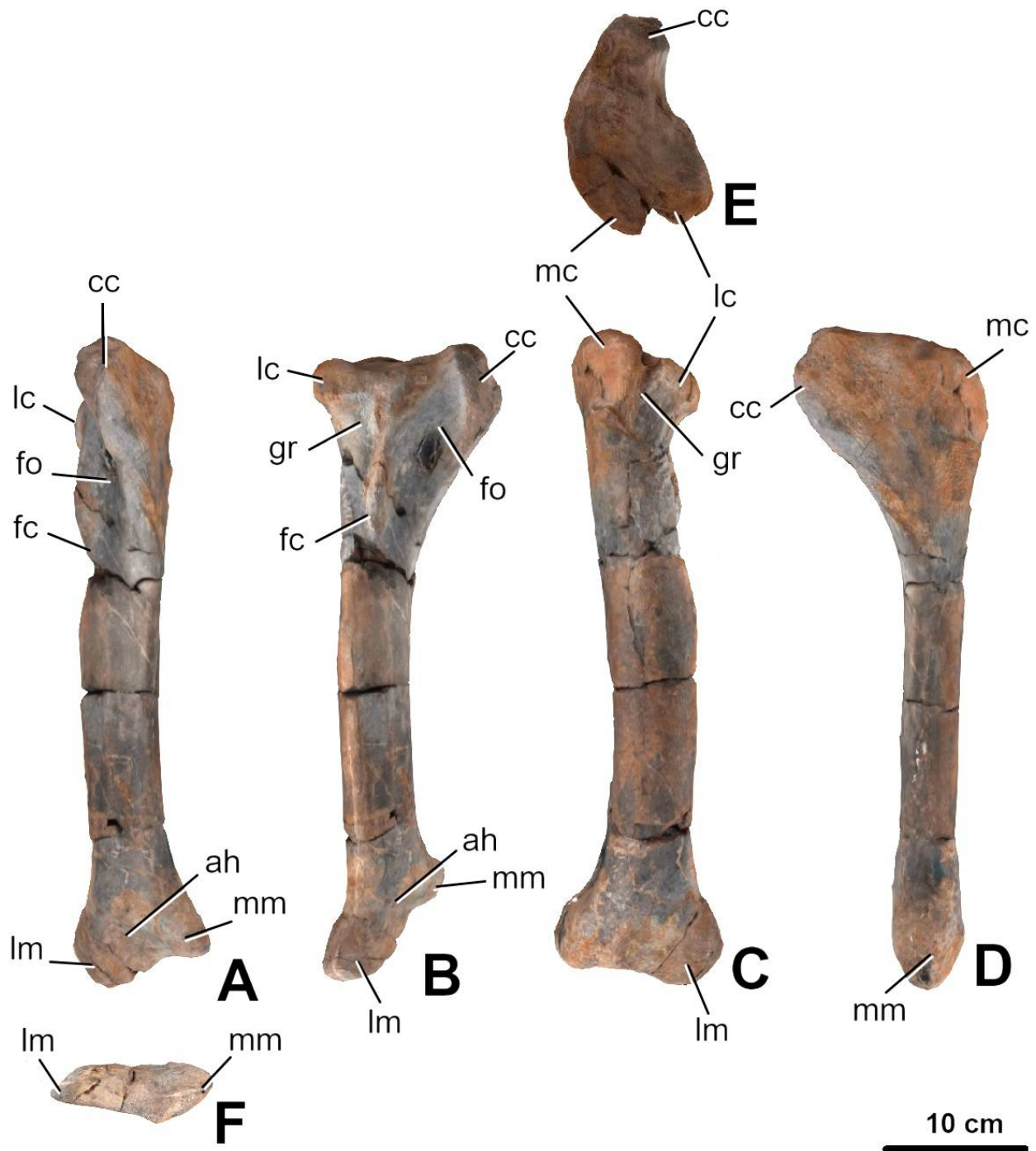


Figure 68. *Ceratosaurus* sp. right tibia SHN(JJS)065 (images based on the 3D scan) in anterior (**A**), lateral (**B**), posterior (**C**), medial (**D**), proximal (**E**) and distal (**F**) views. **ah** – astragalar overhang, **cc** – cnemial crest, **fc** – fibular crest, **fo** – fossa, **gr** – groove, **lc** – lateral condyle, **lm** – lateral *malleolus*, **mc** – medial condyle, **mm** – medial *malleolus*.

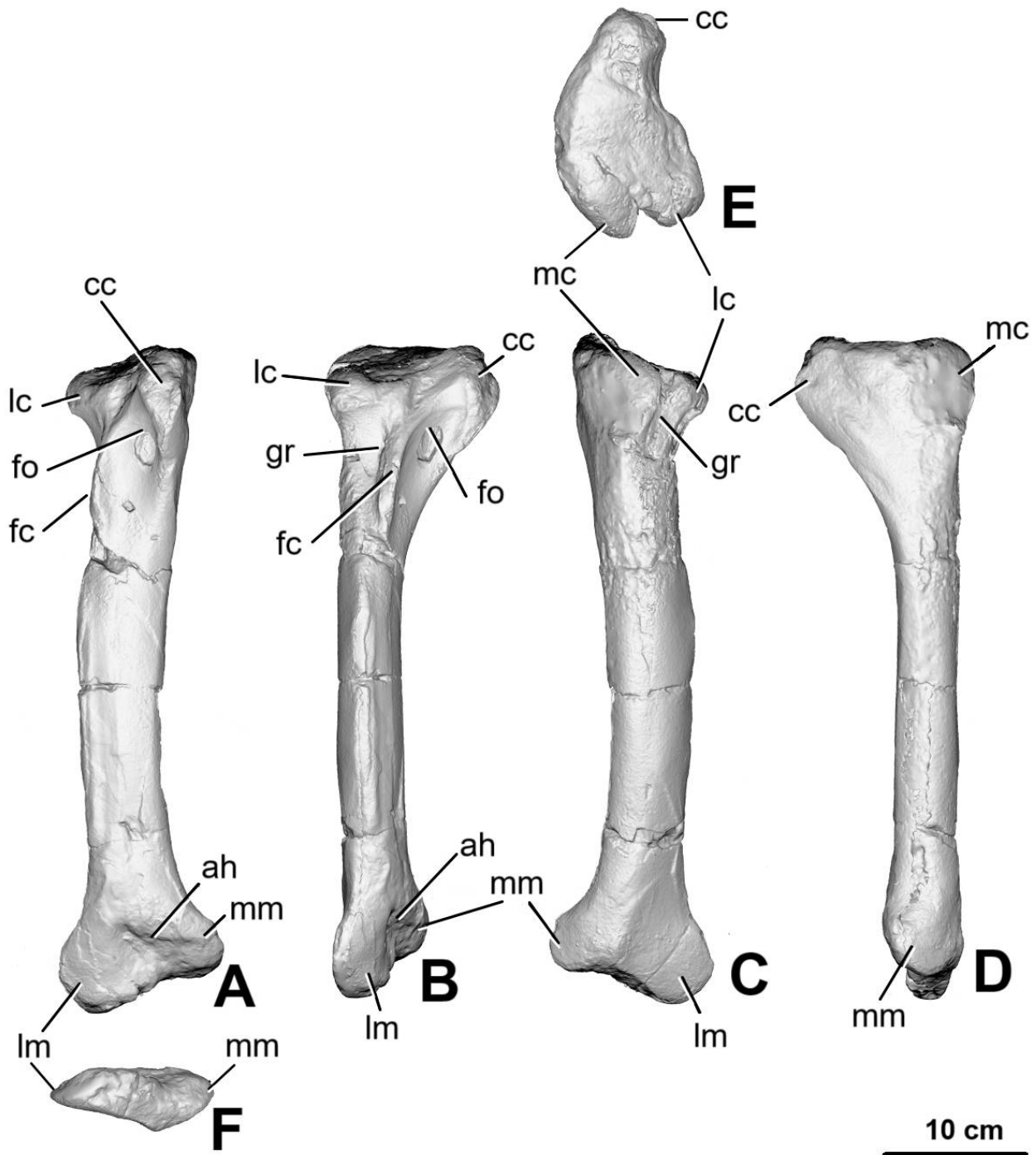


Figure 69. *Ceratosaurus* sp. right tibia SHN(JJS)065 (3D scan in digital greyscale) in anterior (A), lateral (B), posterior (C), medial (D), proximal (E) and distal (F) views. **ah** – astragalar overhang, **cc** – cnemial crest, **fc** – fibular crest, **fo** – fossa, **gr** – groove, **lc** – lateral condyle, **lm** – lateral malleolus, **mc** – medial condyle, **mm** – medial malleolus.

Fibulae

There is a previous description of a fibula shaft from Malafaia et al. (2015) assigned to SHN(JJS)065, however new fragments from both fibulae came up which have been assigned to ML352 (fig. 70 & 71). ML352 is a partial proximal left fibula (only missing the distal end) and a fragment of the head of the right one. SHN(JJS)065 is a right shaft which, by the size and section, is most likely the diaphyseal element from ML352 partial right fibula.

Most of the proximal body of both fibulae (around 2/3) is preserved, only being missing parts of the posterior head and the distal third end on both.

In proximal view, the fibula is elongated anteroposteriorly, being more wide anteriorly than posteriorly, laterally convex and medially concave.

Both fibulae are fairly straight in anterior and posterior views.

The proximal articular surface of the fibula is slightly concave in lateral and medial views. The anterior expansion of the head projects anterodorsally, having a round curvature. The posterior expansion seems more developed, but this structure is missing in both elements (less in SHN(JJS)065), however a dorsoposterior expansion is apparent. This well developed posterior expansion of the head results in a more inclined posterior margin, in comparison with the less prominent anterior expansion which results in more a vertical margin, developing almost in the same axis as the shaft.

In medial view, there is a deep fossa along the proximal posterior margin extending proximoposteriorly to proximodistally along the main shaft, until about the same level where the tibial flange ends in the anterior margin, giving the fossa a lenticular shape with round edges. The anterior margin of the fossa is more deeply excavated than the posterior one, which ends in a thin ridge running along the posterior facet of the fossa.

On the anterior facet of the shaft, the tibial flange is noticeable, especially in the left fibula, as a smooth but long vertical ridge along the margin.

In cross section the shaft has a rounded elongated outline, being more laterally curved and more medially flat.

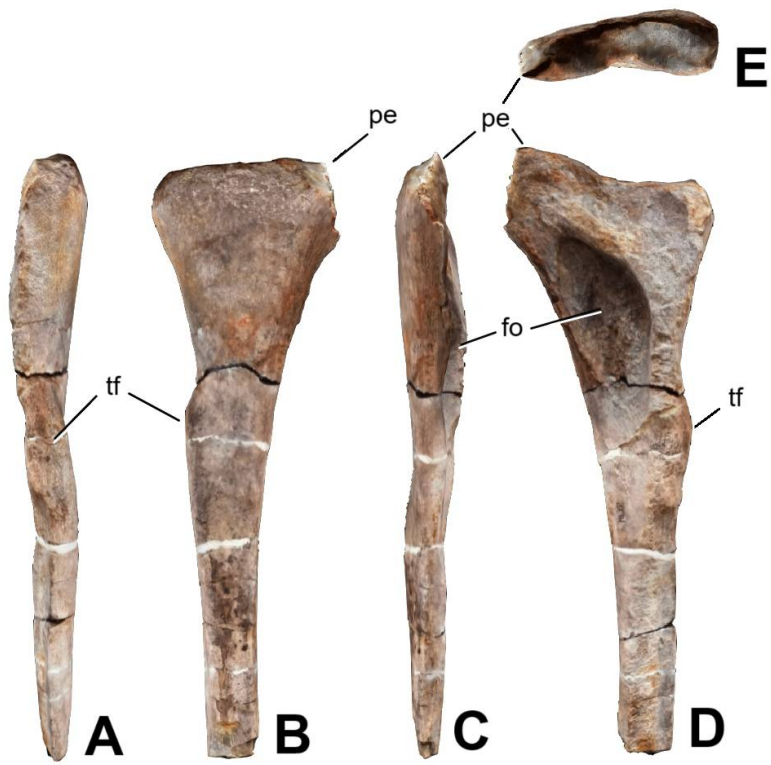


Figure 70. Fibulae from *Ceratosaurus* sp. (images based on the 3D scan), above: upper part of left fibula (ML352), below: upper part of right fibula in two fragments, upper fragment (ML352) and lower fragment (SHN(JJS)065) in anterior (A), lateral (B), posterior (C), medial (D) and proximal (E) views. **fo** – fossa, **pe** – posterior expansion, **tf** – tibular flange.

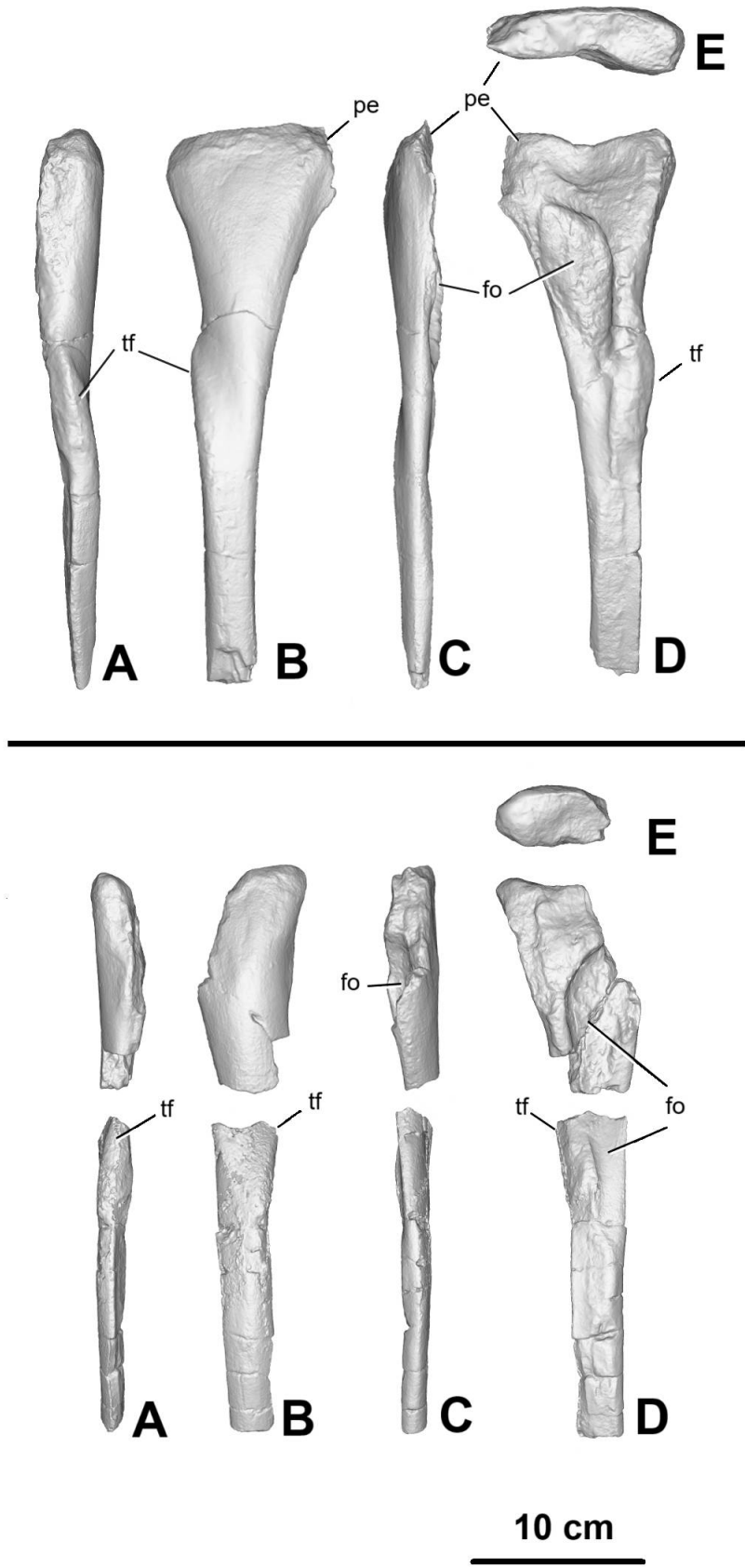


Figure 71. Fibulae from *Ceratosaurus* sp. (3D scan in digital greyscale), above: upper part of left fibula (ML352), below: upper part of right fibula in two fragments, upper fragment (ML352) and lower fragment (SHN(JJS)065) in anterior (A), lateral (B), posterior (C), medial (D) and proximal (E) views. **fo** – fossa, **pe** – posterior expansion, **tf** – tibular flange.

Osteoderm

A dermal ossicle (osteoderm) was also recovered (fig. 72 & 73) and is here described by the first time. This specimen is comparable to the same element described by Madsen and Welles (2000; fig 8.D), however the authors do not pin point the anatomical position of these structures. The material has an elongated shape, being about 10 cm in length and 3,5 cm wide, however appears to be broken at one of the tips. In cross section has a subtriangular shape. The surface has the characteristic intricate dorsal rugosity seen in general osteoderms, being smoother ventrally.

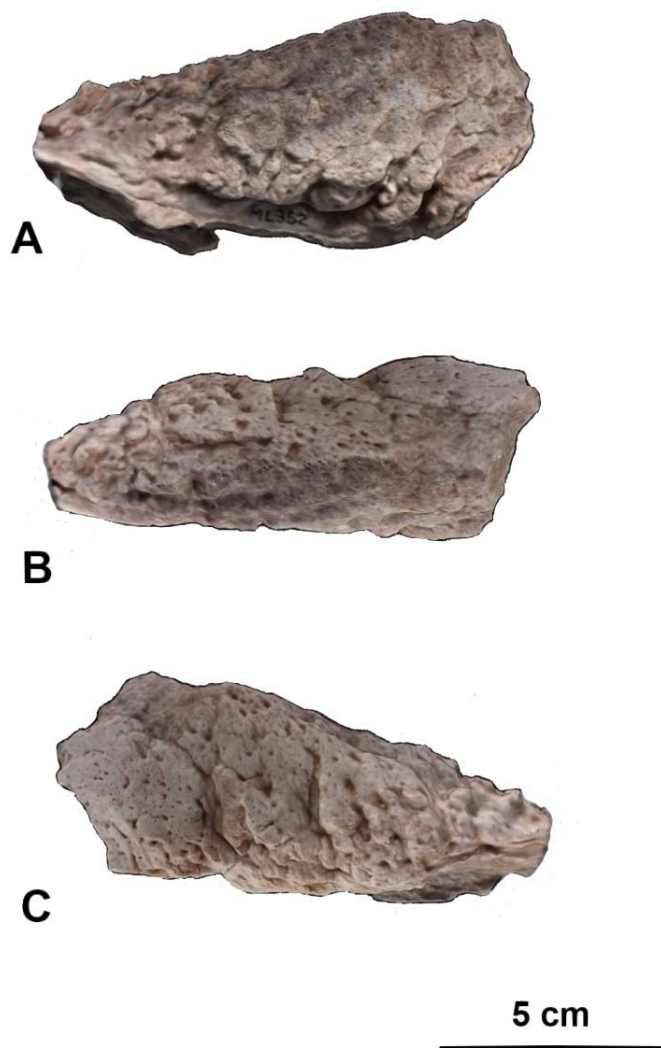


Figure 72. *Ceratosaurus* sp. ML352 osteoderm (images based on the 3D scan), in lateral (**A**, **C**) and dorsal (**B**) views.

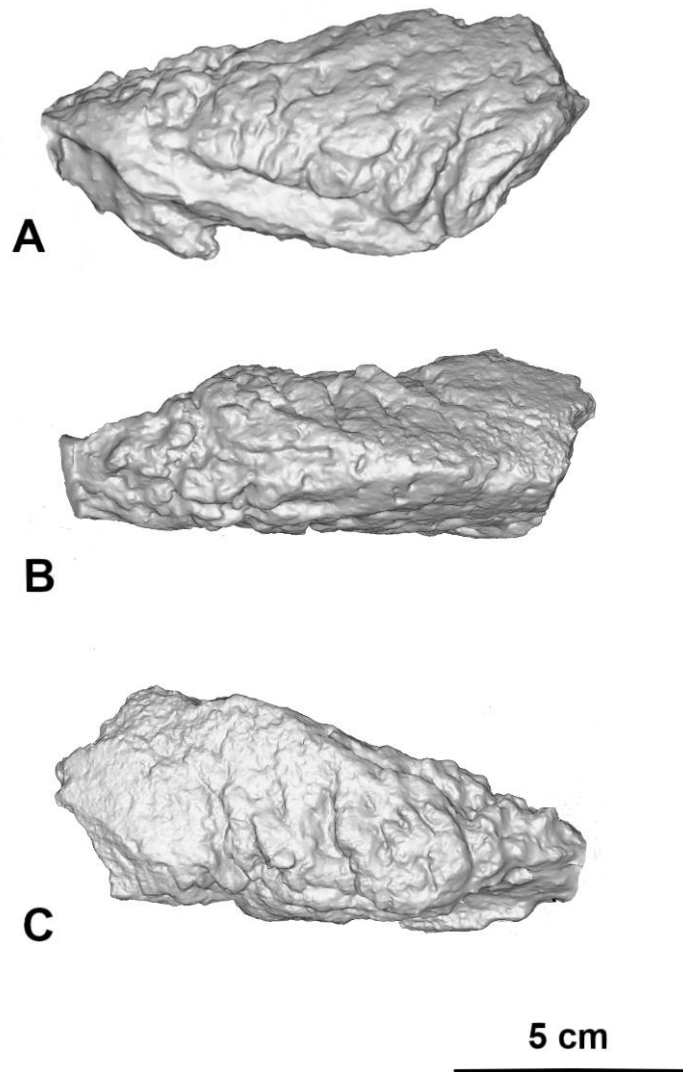


Figure 73. *Ceratosaurus* sp. ML352 osteoderm (3D scan in digital greyscale), in lateral (**A**, **C**) and dorsal (**B**) views.

Measurements

Measurements for the elements of ML352/SHN(JJS)065 are given below (tables 4 – 7).

	Max Height Centrum	Max Width Centrum	Max Length Centrum	Max Width Diapophysis	Max Height Overall	Max Width Neural Arch	Width Center Body
Cervical	70	65	40	8	91	-	-
Sacral	55	78	68	-	55	88	63

Table 4. Vertebrae - tabled measurements in millimeters of cervical and sacral vertebra from ML352.

	Max Length	Middle Shaft Perimeter	Shaft Max Diameter	Head to Great Trochanter (max prox width)	Max Head Width	Ecto to Endo condyle (max distal width)	Ecto Condyle Lateral Width	Endo Condyle Lateral Width
Left Femur	648	233	81	158	59	133	98	106
Right Femur	645	270	90	145	65	142	94	89

Table 5. Femora - tabled measurements in millimeters of left femur SHN(JJS)065 and right femur ML352.

	Max Length	Middle Shaft Perimeter	Shaft Max Diameter	Max length proximal view	Max width proximal view	Lateral to Medial malleolus (max distal width)	Lateral malleolus lateral Width	Medial malleolus lateral Width
Left Tibia	580	195	70	163	78	105	32	58
Right Tibia	560	205	73	145	80	144	28	58

Table 6. Tibiae - tabled measurements in millimeters of left tibia ML352 and right tibia SHN(JJS)065.

	Max Length	Middle Shaft Perimeter	Shaft Max Diameter	Max length proximal view	Max width proximal view
Left Fibula	325	95	37	100	39
Right Fibula	340.2 (200.2 + 140)	-	33	-	-

Table 7. Fibulae - tabled measurements in millimeters of left fibula ML352 and right fibula ML352 + SHN(JJS)065 (the distal 1/3 of both fibulae is not preserved).

Additional *Ceratosaurus* material

To date, besides the Valmitão specimen, other material attributed to *Ceratosaurus* in Portugal includes several isolated teeth collected on various locations along the coastal outcrops of the Lusitanian Basin, most of them coming from the Praia da Amoreira / Porto Novo Member, dated from the Upper Kimmeridgian (Malafaia et al., 2017a).

SHN's collection houses many of these findings, with some teeth confidently assigned to *Ceratosaurus* – mostly conical mesial teeth bearing the diagnostic lingual grooves characteristic of this genus (Morphotype 1 described by Malafaia et al., (2017a)). Other teeth are tentatively attributed to *Ceratosaurus* but with less certainty, mostly laterally compressed, blade-like teeth with less diagnostic features (Morphotype 2 described by Malafaia et al., (2017a)). Should be noted that *Ceratosaurus* teeth are known for typically being conical mesially and highly compressed mediolaterally distally (Madsen & Welles, 2000; Rauhut, 2011; Malafaia et al., 2017a; Lei et al., 2023).

The detailed study of teeth morphology and its diagnostic characteristics have been proved useful in the identification of Late Jurassic theropod taxa (Malafaia et al., 2017a) (fig. 74).

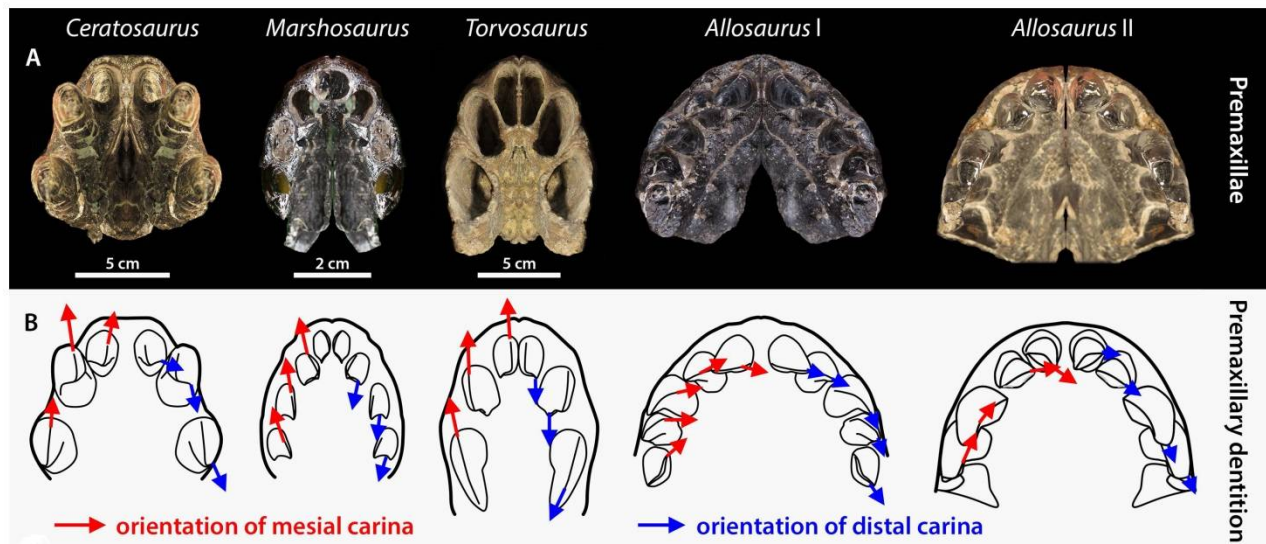


Figure 74. Schematic representation of premaxilla of several Late Jurassic theropod taxa from the Morrison formation and the differences in carina orientation among them. Source: Lei et al., (2023)

The reference numbers of the SHN teeth are listed below (check plates in Appendix I for images) as well as a brief overall description of each batch. The descriptions follows the theropod teeth nomenclature defined by Hendrickx et al. (2015).

Teeth confidently attributed to *Ceratosaurus*:

SHN(JJS)205 – *Ceratosaurus* sp. mesial tooth from Praia da Corva Norte, Torres Vedras (Praia Amoreira – Porto Novo Member).

SHN(JJS)236 - *Ceratosaurus* sp. mesial tooth from Porto Dinheiro, Lourinhã (Praia Amoreira – Porto Novo Member).

SHN(JJS)254 - *Ceratosaurus* sp. mesial tooth from Praia da Corva, Torres Vedras (Praia Amoreira – Porto Novo Member).

SHN(JJS)370 - *Ceratosaurus* sp. teeth fragments from Valmitão/Peralta, Lourinhã (Praia Amoreira – Porto Novo Member).

SHN(JJS)457 - *Ceratosaurus* sp. mesial tooth from Porto Dinheiro Norte, Lourinhã (Praia Amoreira – Porto Novo Member).

SHN(JJS)461 - *Ceratosaurus* sp. mesial tooth from Porto Dinheiro Norte, Lourinhã (Praia Amoreira – Porto Novo Member).

SHN(JJS)462 - *Ceratosaurus* sp. mesial tooth from Praia da Vermelha Norte, Peniche (Praia Amoreira – Porto Novo Member).

Although collected in different places, these seven teeth are all attributed to the Praia da Amoreira – Porto Novo Member.

Being represented by the crowns, these are mostly complete, except for the missing apical ends or the slightly damaged cervix borders on some of them. Small details such as the carina, flukes or undulations are well preserved.

These teeth are medium to moderately large in size. The crown height, when complete, ranges between 26 and 36mm (average: 31.6mm), the cervix length ranges between 14 and 19mm (average: 16.3mm) and the maximum cervix width ranges between 9 and 13mm (average: 11.2mm).

The teeth are long and semi-conical, with wide basal halves both labiolingually and mesialdistally, resulting in a semicircular outline shape in basal view. In lateral view, the mesial border is moderately convex, being more basally straight and more apically curved. The distal border is straight to moderately concave, slightly varying in each tooth. The crown apex points slightly distally and is positioned distally relative to the cervix plane. The labial facet is slightly convex in distal/mesial view, whereas the lingual facet is nearly flat.

All these teeth bear vertical flukes or striations on their lingual facets with the pattern of these striations varying considerably on each tooth. Some of them have higher count of flukes (SHN(JJS)462 with 9) than others (SHN(JJS)254 with 3), some flukes are wide (SHN(JJS)457), others thin (SHN(JJS)205) and some teeth have both (SHN(JJS)462). Some flukes occupy the whole mesial-distal length of the lingual surface (as in SHN(JJS)457 or SHN(JJS)462) whereas others are only present along its more central surface (as in SHN(JJS)254 or SHN(JJS)205). When the whole crown is preserved, the flukes occupy 2/3 to 3/4 of the apical-basal length of the tooth starting from the crown apex but not reaching the cervix.

These flukes are found in other theropod groups, but its exclusive presence on the lingual side of mesial teeth is only found in *Ceratosaurus* among Late Jurassic theropods from the Morrison Formation and Lusitanian Basin and thus often considered diagnostic of this genus under these conditions (Madsen & Welles, 2000; Rauhut, 2004; Hendrickx et al., 2014; Malafaia et al., 2017a).

In most teeth, the carina is only present in the distal margin (SHN(JJS)205 and SHN(JJS)254 possess carina on both sides) apparently running all along from the crown apex to the cervix. In distal view, the carina follows the distal margin edge, being either straight or labially convex, depending on each tooth shape (except in SHN(JJS)236 where the carina runs more labiodistally). In general, there are 2 to 3 denticles per millimeter on the distal carina, with each denticle having rounded margins. The interdenticular spaces can be either narrow (ex. SHN(JJS)236) or wider (ex. SHN(JJS)461).

Due to its geological age and morphology (the presence and position of the flukes), these seven teeth have been confidently attributed as mesial (premaxillary) teeth of the genus *Ceratosaurus*.

Teeth tentatively attributed to *Ceratosaurus*:

SHN212 – Possible *Ceratosaurus* lateral tooth from Baleal, Peniche, Abadia (?Praia Amoreira – Porto Novo Member).

SHN218 - Possible *Ceratosaurus* lateral tooth from Praia da Vermelha, Peniche (Praia Amoreira – Porto Novo Member).

SHN(JJS)243 - Possible Ceratosauria fragmentary tooth from Praia de Pedrogãos (Praia Amoreira – Porto Novo Member).

SHN(JJS)263 - Possible *Ceratosaurus* lateral tooth from Praia da Corva, Torres Vedras (Praia Amoreira – Porto Novo Member).

SHN(JJS)269 - Possible *Ceratosaurus* lateral tooth from Peralta, (?)Sobral (?Praia Azul Member).

SHN(JJS)295 - Possible *Ceratosaurus* tooth from Valmitão Sul, Lourinhã (Praia Amoreira – Porto Novo Member).

SHN(JJS)305a - Possible *Ceratosaurus* lateral tooth from Cambelas, Freixial.

SHN(JJS)307 - Possible *Ceratosaurus* tooth from Peralta Centro, (?)Sobral (?Praia Azul Member).

SHN321a - Possible *Ceratosaurus* lateral tooth from Porto Novo, Torres Vedras (Praia Amoreira – Porto Novo Member).

SHN321b - Possible *Ceratosaurus* lateral tooth from Porto Novo, Torres Vedras (Praia Amoreira – Porto Novo Member).

SHN321c - Possible *Ceratosaurus* lateral tooth from Porto Novo, Torres Vedras (Praia Amoreira – Porto Novo Member).

SHN(JJS)359c - Possible *Ceratosaurus* tooth from Porto Novo, Torres Vedras (Praia Amoreira – Porto Novo Member).

SHN(JJS)377 - Possible *Ceratosaurus* tooth from São Bernardino (Praia Amoreira – Porto Novo Member).

SHN(JJS)425 - Possible Ceratosauria tooth fragment from Valmitão, Lourinhã (Praia Amoreira – Porto Novo Member).

SHN(JJS)458 - Possible *Ceratosaurus* tooth from Santa Rita, Torres Vedras (?Praia Amoreira – Porto Novo Member).

SHN459 - Possible *Ceratosaurus* lateral tooth from Santa Rita, Torres Vedras (?Praia Amoreira – Porto Novo Member).

These 16 teeth were collected in several different locations, mostly in rocks attributed to the Praia da Amoreira - Porto Novo Member, however a few of them are assigned to Freixial and Sobral Formations.

The teeth are, for the most part, preserved with the complete crowns, except for a few where the apical end is missing and others where the mesial and distal borders are shattered. The state of preservation is good in most of them, with the small features such as carina and striations clearly visible.

These teeth vary in size from small to large. The crown height, when complete, ranges between 27.5 and 76mm (average: 48.1mm), the cervix length ranges between 8 and 27mm (average: 19.8mm) and the maximum cervical width ranges between 4 and 13mm (average: 8.4mm).

The long crowns and strong labiolingual compression in some of the larger specimens (ex. SHN(JJS)263 or SHN(JJS)305a) give these teeth a blade like shape (zyphodont condition), a feature that strongly distinguishes them from the other batch. However, some are less constricted and more sub-circular in basal view (ex. SHN(JJS)243 or SHN(JJS)425) and others are somewhat intermediate between both conditions (ex. SHN(JJS)295 or SHN459).

The labial and lingual facets are similar in shape for the most part, being nearly straight to slightly convex in mesial/distal views. Some teeth, such as SHN(JJS)295, SHN321b or SHN(JJS)458, bear thin striations along the crown height on both facets. Subtle transverse undulations can be found in several of these teeth, most notably in SHN212, SHN(JJS)269, SHN(JJS)305a and SHN321b. Marginal undulations are present on the lingual side of SHN(JJS)269 and on the labial side of SHN(JJS)243 and SHN321a.

In labial/lingual view the mesial border has a noticeable convex curvature and the distal border is straight to slightly concave. The crown apex is subtly pointing distally, being positioned distally relative to the cervix plane.

Carina is present on both borders on most of the teeth, distally from the cervix to the apex and mesially more apically, however, in some larger zyphodont specimens carina also reaches the cervix (ex. SHN(JJS)263). In general, there are 2 to 3 denticles per millimeter with rounded margins. The interdenticular diaphysis extend transversely relative to the crown and vary in size from small (0.2-0.3mm) to large (0.8-1.2mm) depending on the specimen.

The general zyphodont shape of most of these teeth point to a more distal position in the maxilla/dentary. Rauhut (2004) and Hendrickx et al. (2014), refer to the flat/slightly concave area adjacent to both distal and mesial carina, present in taxa such as *Ceratosaurus*, *Genyodectes* or *Majungasaurus*, as a ceratosaurian synapomorphy. Malafaia et al. (2017a), noted the absent of this feature in these specimens, however the authors found their general shape similar to *Ceratosaurus*, particularly in the strongly labiolingual flatness of the crowns, the carina in the mesial border touching the cervix, the mesial carina running sigmoidally apposed to the central distal one and in the numerous and densely distributed transverse undulations, which led to their putative classification as *Ceratosaurus*.

Comparative anatomy (comparison with the other *Ceratosaurus*)

The new elements described in this dissertation might give some more insights of the phylogenetic position of this individual. In order to understand its similarity with the other *Ceratosaurus*, each ML352/SHN(JJS)065 element should be compared with their equivalent in other specimens.

The **cervical vertebrae** is known for every putative *Ceratosaurus* species from North America. Madsen and Welles (2000) found differences in the fifth cervical of *C. magnicornis* and *C. dentisulcatus*, namely, *C. dentisulcatus* has shorter centrum, the diapophysis is higher above the parapophysis in the transverse process and has shorter table, epipophysis and neural spine.

Regarding *C. nasicornis* the authors found differences with *C. magnicornis* in the sixth cervical: the *C. magnicornis* vertebra table slants up more steeply posteriorly and the postzygapophyseal centrodiapophyseal fossa is much shorter. Since the cervical of the Portuguese specimen is either the fifth or sixth, a comparison might be possible, however the material is too incomplete and damaged to take certain conclusions. Although the anterior facet of ML352 is the one in worst condition, it is worth mentioning that the structure seen in anterior view, lateral to the neural canal centroprezygapophyseal fossa, is, in relative size and shape, similar to what we can see in the fifth cervical vertebrae of *C. magnicornis*, but to what extent this might be conditioned by the distortion it is difficult to say.

Overall, the elements in ML352 more suitable for comparison are the relative positions of the diapophysis and parapophysis, the pleurocoel, the posterior facet and the posterior ventral ridge. The posterior facet of the centrum does not change considerably along the neck vertebrae and neither between each putative *Ceratosaurus* species, and although a similarity is noticeable between ML352 neural canal shape and size and the same element of the sixth cervical of *C. dentisulcatus*, the distortion and damage of ML352 might be conditioning the analysis. In ventral view, the shape of the ventral ridge and the position of the pleurocoel is comparable to the seventh and eight cervical vertebrae of *C. magnicornis*. The vertebrae in *Ceratosaurus* becomes anteroposteriorly shorter as we go posteriorly in the neck. In ML352 the anterior facet is partially destroyed and the anterior ventral projection, specially evident in left lateral view, can either be the result of deformation or what remains of the parapophysis. If the latter is true, the anteroposterior length and general shape of the centrum in lateral view, resembles that of eight cervical vertebrae of *C. magnicornis*. The size and position of the pleurocoel, and the shape of the laminae above it, is similar to what we can see on the seventh cervical vertebrae of *C. dentisulcatus*, however the posterior ventral ridge is less ventrally expanded on ML352.

The **sacral vertebra** currently under ML352 was first associated to the other *Ceratosaurus* elements due to being found pretty close to them, probably no more than 20 meters apart. The comparison with sacral elements from *C. nasicornis* holotype (the only one with these elements formally described) revealed itself a difficult task because there was no ideal media available for a proper analysis. The best we had to work with were the drawings of the sacral region of the holotype in ventral view from Gilmore (1920) and Tykoski's (2005) dissertation, which in itself is also based on Gilmore (1920). Just based on this material is clearly noticeable that ML352 does not resemble any of the sacral elements from USNM 4735, which are all anteroposteriorly longer and more laterally compressed (fig. 75).

With ML352 being clearly sacral (see description), these differences alone distinguishes it from *Ceratosaurus*. Due to its robustness and general shape, this vertebra was compared with other taxa contemporary to *Ceratosaurus*, namely, ornithopods, thyreophorans and sauropods, however no successful equivalent was found.

The proper classification of the sacral vertebra under ML 352 still needs further research; for the time being, and under the scope of this dissertation, we can just conclude that it does not belong to *Ceratosaurus*.

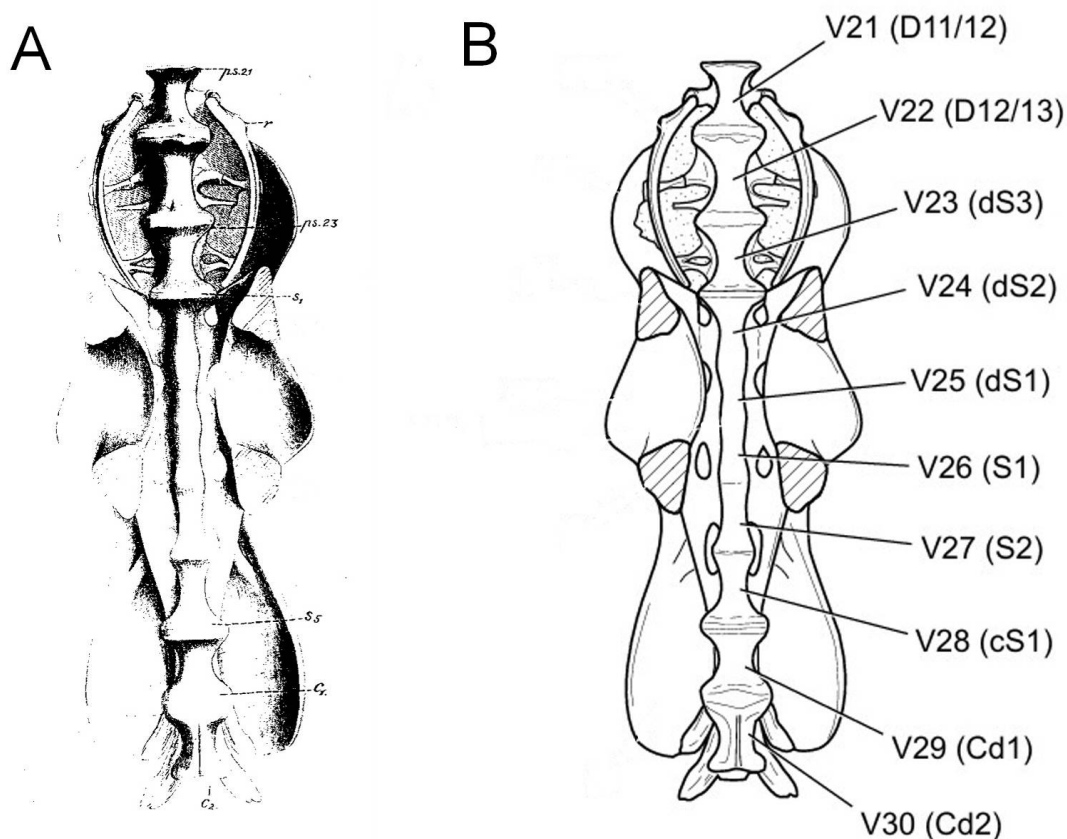


Figure 75. Schematic representation of the sacral region of *Ceratosaurus nasicornis* holotype USNM 4735 in ventral view. (A) source: Gilmore (1920), (B) source: Tykoski (2005).

The **femur** is known for all three putative North American species. Madsen and Welles (2000) found the femur shaft of *C. magnicornis* straighter than the one of *C. nasicornis*, however, besides the differences in size, this was the only character pointed by the authors. Gilmore (1920) alerted for the fact that the femur of *C. nasicornis* is smashed and deformed, which might lead to incorrect interpretation of its characters; so, any comparison made with this element in this text should take this in consideration.

Comparing with the Portuguese specimen (fig. 76), the femoral head of ML352/SHN(JJS)065 is more massive and rounder than *C. nasicornis*, specially on the proximal surface, being more similar to *C. dentisulcatus*. ML352/SHN(JJS)065 also has a more developed end of the femoral head with a more prominent downturned hook-like expansion. These features cannot be compared with *C. magnicornis* because this part of the right femur head is missing (there are no pictures of left femur). The trochanteric shelf in *C. magnicornis* seems more developed and proximolaterally expanded than in any other femora we compared with. The distal end of ML352/SHN(JJS)065 is more massive and more square shaped, with a endocondylar ridge more developed medially, similar to *C. dentisulcatus*. *C. nasicornis* and *C. magnicornis* appear to have the endocondylar ridge with the edge running more anteriorly than medially, however this might be due to deformation especially in *C. nasicornis*.

In dorsal view, ML352/SHN(JJS)065 femora head is more anteriorly expanded than in other specimens.

In lateral view, the curvature of ML352/SHN(JJS)065 resembles more *C. nasicornis* and *C. magnicornis*; *C. dentisulcatus* is much more straight.

In posterior view ML352/SHN(JJS)065 has a distinct and pronounced popliteal ridge between both condyles, similar to *C. dentisulcatus*; this structure appears to be less developed or absent in the other two taxa. The popliteal surface seems to be deeper and extend more proximally in *C. nasicornis* and *C. magnicornis*, however this feature is difficult to confirm in the photographic material. The tuberos process (*crista tibiofibularis*) is more developed in *C. dentisulcatus* and less in *C. nasicornis*, however the shape is similar across all North American individuals, being proximolaterally-mediodistally expanded with rounded edges. This structure in ML352/SHN(JJS)065 is smaller, expands more vertically and the proximal end is more pointier. In *C. nasicornis* the posterior head of medial condyle is proximolaterally-mediodistally elongated, in other species is round.

In medial view, the fourth trochanter is similar in shape and size in *C. nasicornis*, *C. magnicornis* and ML352/SHN(JJS)065; in *C. dentisulcatus* this structure seems bigger, sharper and more posteriorly and distally expanded.

Next page: **Figure 76.** Comparative illustration of left femora from ML352/SHN(JJS)065, *C. nasicornis*, *C. magnicornis* and *C. dentisulcatus* in anterior, posterior, lateral and medial views. Some views are the reversed right femur to better highlight certain elements or to represent elements missing in the left femur. Scale bars equals 10cm.

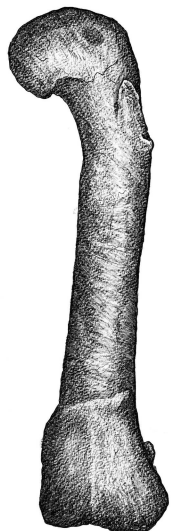
ML352

C.dentisulcatus

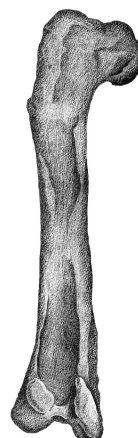
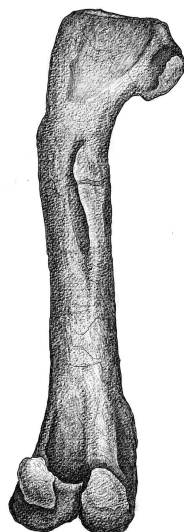
C.magnicornis

C.nasicornis

Anterior



Posterior



Lateral



Medial



The **tibia** is known for all the putative North American species. Madsen and Welles (2000) comparing *C. nasicornis* with *C. magnicornis* found the cnemial crest of the former more developed. Comparing *C. nasicornis* with *C. dentisulcatus*, the astragalar overhang of the tibia in *C. dentisulcatus* is much less inclined. Regarding *C. magnicornis* and *C. dentisulcatus*, besides the size difference, the authors do not list any other characters.

Comparing these with the Portuguese elements (fig. 77), in anterior view, the cnemial crest of ML352/SHN(JJS)065 expands anterolaterally like in *C. nasicornis* and *C. magnicornis*, whereas *C. dentisulcatus* has the cnemial crest strongly developed laterally. This is also noticeable in dorsal view, where the cnemial crest of *C. dentisulcatus* is more strongly curved. *C. nasicornis* and ML352/SHN(JJS)065 have an upturned end of cnemial crest in medial/lateral view, *C. dentisulcatus* seems less upturned and more horizontal. In ML352/SHN(JJS)065 the fibular crest bifurcates towards the tibia head and one branch merges with the lateral side of the cnemial crest. In *C. dentisulcatus* the fibular crest does not bifurcate and runs more dorsally along the cnemial crest, leaving space for a bigger fossa along its the lateral side. In *C. nasicornis* this structure seems similar to ML352/SHN(JJS)065, but in *C. magnicornis* the images are not clear enough to confirm. Malafaia et al (2015) also pointed out that ML352/SHN(JJS)065 does not have a nutrient foramina at the distal end of fibular crest, unlike *C. dentisulcatus*. Madsen and Welles (2000) described a short inclination of the astragalar overhang for *C. dentisulcatus*, whereas *C. nasicornis* and *C. magnicornis* are more similar in shape, with a higher inclination of at least 45°. ML352/SHN(JJS)065 has this condition more similar to *C. dentisulcatus*. Detailed comparison regarding the most distal edge of the tibia and the *malleoli* shape cannot be made in detail for the anterior view because all North American material analyzed has both the calcaneum and the astragalus connected to the distal tibia covering these structures, whereas in ML352/SHN(JJS)065 these elements are missing.

In posterior view, *C. dentisulcatus* has the most expanded medial condyle, ML352/SHN(JJS)065 is similar to *C. nasicornis* and *C. magnicornis* in this regard. Also, ML352/SHN(JJS)065 lateral *malleolus* is more distolaterally expanded than in other taxa.

Next page: **Figure 77.** Comparative illustration of left tibiae from ML352/SHN(JJS)065, *C. nasicornis*, *C. magnicornis* and *C. dentisulcatus* in anterior, posterior, lateral and medial views. Some views are the reversed right tibia to better highlight certain elements or to represent elements missing in the left tibia. Scale bars equals 10cm.

Anterior



Posterior



Lateral



Medial



The **fibula** of North American *Ceratosaurus* is known for *C. nasicornis* and *C. dentisulcatus*. Madsen and Welles (2000), found the fibula of *C. dentisulcatus* broader and with a vertical proximal end in lateral view, the tibial flange dips posteriorly, the upper edge/lower edge projects anteriorly and the distal end is convex and round. In *C. nasicornis* the fibula is narrower and inclined 70° posteriorly in lateral view, the tibial flange dips anteriorly and the distal end is truncated.

Comparing with the Portuguese specimen (fig. 78), in anterior view, ML352/SHN(JJS)065 has the tibial flange more strongly curved medially, creating a smooth “S” shaped curvature, and an offset between the axis of the head and the shaft (this is seen in both ML352/SHN(JJS)065 fibulae); this is not the case with *C. nasicornis* and *C. dentisulcatus*, where the fibula is much more straight.

In lateral view, as stated by Madsen and Welles (2000), the fibula head of *C. nasicornis* is tilted posteriorly, but in both ML352/SHN(JJS)065 and *C. dentisulcatus* the head is straight. The tibial flange of ML352/SHN(JJS)065 is clearly less anteriorly expanded than in both other taxa.

Both *C. nasicornis* and *C. dentisulcatus* have a subtle concave curvature in the lateral facet of the fibula head (more evident in *C. nasicornis*), in ML352/SHN(JJS)065 this facet is flat. Also, in ML352/SHN(JJS)065 the fibula head anterior expansion in lateral view is round and smooth whereas in the others is sharp.

The available material does not enable a clear comparison with *C. nasicornis* in medial view, however a comparison can be made with *C. dentisulcatus*. The medial fossa in ML352/SHN(JJS)065 seems deeper, wider and less proximodistally extended and the posterior ridge of the shaft is completely straight whereas in *C. dentisulcatus* there is a slight convex curve in the proximal shaft. This curvature seems to occur in *C. nasicornis* however it is less noticeable than in *C. dentisulcatus*. In medial view, the tibial flange is also noticeably less developed than in both *C. nasicornis* and *C. dentisulcatus*.

The **osteoderms** are known for all putative North American species, several for each one of them. ML352 is ellipsoid in shape with a longitudinal dorsal keel (sagittate type) being similar in proportions to equivalent elements from the other species, only slightly larger.

Next page: **Figure 78.** Comparative illustration of left fibula from ML352/SHN(JJS)065, *C. nasicornis*, *C. magnicornis* and *C. dentisulcatus* in anterior, posterior, lateral and medial views. Some views are the reversed right fibula to better highlight certain elements or to represent elements missing in the left fibula. Scale bars equals 10cm.

Anterior



Posterior



Lateral



Medial



Phylogenetic specimen-based analysis

In order to clarify the position of ML352/SHN(JJS)065 within Ceratosauria, a phylogenetic specimen-based analysis was made. This analysis also attempted to clarify the relationships between the three North American *Ceratosaurus* species in order to give a more solid consensus about the validity of these species. This is the most in-depth phylogenetic study ever performed specifically for the genus *Ceratosaurus*.

The recent matrix from Cau (2024) was chosen to perform this task due to its level of detail (1944 characters) and up-to-date status.

From the 502 taxa used in the matrix, *Allosaurus* was selected as outgroup for being one of the better known representatives of Tetanurae, the sister group of Ceratosauria (Gilmore, 1920; Madsen, 1976; Carrano et al., 2012; Cau, 2024). For the comparative analysis, *Genyodectes* was chosen for being regarded as one of the closest known genus to *Ceratosaurus* (Rauhut, 2004; Delcourt, 2018). *Majungasaurus* was added for its more derived abelisaurid ceratosaur condition and for having very complete and detailed osteological descriptions (Carrano, 2007; O'Connor, 2007; Sampson & Witmer, 2007; Smith, 2007; Burch & Carrano, 2012). The putative Tendaguru abelisaurid(?) ceratosaur MB R 3621-3626 (Rauhut, 2011) was also added to clarify its placement within Ceratosauria.

After selecting the taxa to compare to *Ceratosaurus*, the 3888 characters (1944 characters duplicated for ontogenetic purposes from Cau (2024)) had to be filtered in order to remove those that had no variation within these five taxa. Excel formulae were applied to leave in the matrix just the characters where variability was found (characters with both 0's and 1's across the five taxa) which ended in 502 characters. The last 15 characters were among the duplicated for the ontogenetic analysis of Cau (2024), since they were out of the context of this study they were removed, leaving 487 characters.

A total of 37 new characters were added to the matrix. These were created based on the anatomical differences found within the three *Ceratosaurus* species cited by Madsen and Welles (2000) and based on additional differences we found among North American *Ceratosaurus* and also in ML352/SHN(JJS)065. Not all differences cited by Madsen and Welles (2000) were made into new characters: size-related differences were ignored, others were discarded for being too subtle or not relevant enough and some were already described as characters in the original matrix.

Since we needed to analyze the differences among the different *Ceratosaurus* species, the genus entry in the matrix was split in four – *C. nasicornis*, *C. magnicornis*, *C. dentisulcatus* and ML352/SHN(JJS)065. The original *Ceratosaurus* coding from Cau (2024) was used for control and help in the coding process, but the data did not ended up in the final analysis. For the different North American *Ceratosaurus* species the coding was based only on their respective holotypes, specimens not formally described were not considered.

The coding for taxa other than ML352/SHN(JJS)065 was accomplished using variable sources, from descriptive articles and figures, to photographic material shared by several sources for the context of this study (detailed in the acknowledgments section).

Some of the previous character coding was changed either due to incorrect coding, mistaken inverted polarity or due to more updated research enabling a more precise interpretation of anatomical features. In some instances these changes did not affect the variability of the characters; others however did, making the character redundant. These cases where there was no variability beyond the outgroup (just 0's, 1's or “?”) ended up removed.

Changes made to the character state of the original matrix which did not affect the variability of the characters:

55): Lacrimal, orbital margin, suborbital process: absent (0); present (1). (Currie and Carpenter 2000).
Allosaurus changed from (1) to (0).

68): Lacrimal, laterodorsal recess, position: exposed laterally (0); in an anteriorly facing recess (1). (Cau 2024).
C. nasicornis and *C. magnicornis* changed from (?) to (0).

80): Parietals: unfused (0); fused (1). (Cau 2024).
C. magnicornis changed from (0) to (1).

142): Pterygoid, accessory fenestra with the palatine: absent (0); present (1). (Gauthier 1986; Rauhut 2000).
C. nasicornis changed from (?) to (0).

196): Cervical ribs, articulation to vertebrae in adults: loose (0); firmly attached/fused (1). (Holtz 2000).
C. nasicornis changed from (1) to (0).

205): Axis, neural spine, dorsal surface, shape: mediolaterally narrow (0); mediolaterally expanded (1). (Currie and Carpenter 2000; Holtz 2000; Brusatte et al. 2010).
C. dentisulcatus changed from (0) to (1).

429): Femur, shape in lateral/medial view: straight or slightly sigmoidal (0); strongly bowed, posteriorly concave along the entire length (1). (Cau 2024).
C. dentisulcatus changed from (0) to (1).

467): Fibula, relationships with the astragalar-tibial complex in adult: unfused or loosely appressed (0); tightly appressed or fused (1). (Cau 2024).
C. nasicornis changed from (0) to (1) and *Majungasaurus* changed from (1) to (0).

468): Astragalus, ascending process, mediolateral diameter of the base: no more than (0); more than (1) 1/2 of mediolateral diameter of the astragalar body. (Cau 2024, modified from Rauhut 2000).
Allosaurus changed from (0) to (1).

491): Mt IV, proximal end, medial margin, shape: flat to convex (0); concave (1).
Majungasaurus changed from (0) to (1). (Cau 2024).

493): Mt IV, proximal end in anterior/posterior view, lateral projection clearly distinct from shaft margin: present (0); absent (1). (Cau 2024, modified from Senter 2010).
Majungasaurus changed from (1) to (0), it is more similar to *Allosaurus* than to *Ceratosaurus*.

580): Tibiotarsus, complete fusion in adult: absent, proximal tarsals and tibia unfused, sutures clearly visible (0); present, astragalocalcaneum fused to the tibia (1). (Cau 2024).
Majungasaurus changed from (1) to (0). Tendaguru ceratosaur MBR_3621_3626_TDG changed from (?) to (0).

700): Axis, neural spine, anterior tip, position: anteriorly to (0); at the same level or posterior to (1) the prezygapophyses. (Tykoski 2005).
C. dentisulcatus changed from (0) to (1).

765): Femur, posterodistal (popliteal) fossa in adults, infrapopliteal ridge between medial (=tibial) distal condyle and tibiofibular crest: absent (0); present (1). (Tykoski 2005).
C. magnicornis changed from (1) to (0).

880): Quadratojugal and quadrate: unfused (0); fused (1). (Cau 2024).
C. magnicornis and *Majungasaurus* changed from (1) to (0).

923): Astragalus, ascending process, angle between the proximomedial corner and the transverse axis of the astragalus: no more than (0); more than (1) 45°. (Cau 2024).
C. nasicornis and *C. magnicornis* changed from (0) to (1). Tendaguru ceratosaur MBR_3621_3626_TDG changed from (?) to (0). ML352/SHN(JJS)065 coded based on the shape of the astragalar overhang.

960): Nasal, premaxillary process, anterodorsal end, notch: absent (0); present (1). (Brusatte et al. 2010).
Majungasaurus changed from (?) to (1).

965): Femur, tibiofibular crest (ectococondylar tuber), shape and orientation in posterior view: narrow, longitudinal (0), broad, oblique (1). (Carrano and Sampson 2008).
Majungasaurus and Tendaguru ceratosaur MBR_3621_3626 changed from (1) to (0).

972): Lacrimal, antorbital fossa, exposition: exposed laterally (0), covered by dermal ossifications (1). (Carrano and Sampson 2008).
C. nasicornis and *C. magnicornis* changed from (1) to (0). It resembles more *Allosaurus*.

974): Occipital condyle, dorsal groove, size: wide (0); narrow (1). (Carrano and Sampson 2008).
The original coding had the polarity inverted. *C. nasicornis* and *C. magnicornis* changed from (0) to (1).
Allosaurus changed from (0) to (1) and *Majungasaurus* changed from (1) to (0).

976): Dentary, lateral groove, position: at mid-height or dorsally (0), in ventral half (1). (Carrano and Sampson 2008).
C. nasicornis and *C. dentisulcatus* changed from (0) to (1), it resembles more *Majungasaurus*.

1036): Fibula, proximomedial end, fossa/groove, posterior margin: closed by a lip (0); open (1). (Cau 2024, modified from Carrano and Sampson 2008).
C. nasicornis and *Majungasaurus* changed from (1) to (0).

1114): Tibia, lateral cnemial crest, orientation: mainly anteriorly directed (0); mainly laterally directed (1). (Xu et al. 2009b).
Allosaurus changed from (0) to (1).

1124): Odontoid, foramen/depression on anterolateral surface: absent (0); present (1). (Brusatte et al. 2008).
C. nasicornis and *C. dentisulcatus* changed from (1) to (0). *Majungasaurus* changed from (?) to (1).

1132): Femur, anterior cleft between anterior and greater trochanters, elongation: short, less than half (0); elongate, more than half (1) dorsoventral depth of femur head. (Cau 2024).
Majungasaurus changed from (1) to (?), the femoral head is missing.

1154): Occipital condyle, distinct neck: absent (0); present (1). (Cau 2024).
Allosaurus changed from (1) to (0). *Majungasaurus* changed from (0) to (1). *Majungasaurus* condylar neck is longer and slender than those of *Allosaurus* and *Ceratosaurus*.

1179): Femur, distal end, morphology: central depression connected to *crista tibiofibularis* by a narrow groove (0); anteroposteriorly oriented shallow trough separating medial and lateral convexities (1). (Benson et al. 2010).
Tendaguru ceratosaur MBR_3621_3626 changed from unknown (?) to (1).

1210): Premaxilla and maxilla, lateral surface, neurovascular foramina, position: well distant to the occlusal margin (0); very close to the occlusal margin (1). (Cau 2024 modified from Sereno and Brusatte 2008).
Allosaurus changed from (0) to (1).

1266): Supraoccipital nuchal wedge and parietal alae, position of dorsal extremity: slightly (0); considerably (1) above frontoparietal skull table. (Wilson et al. 2003).
Allosaurus changed from (?) to (0), it resembles *Ceratosaurus*.

1441): Quadrate, shaft, proximal half, inclination relative to rest of shaft: straight (0); posteriorly curved (1). (Ezcurra and Novas 2007).

C. magnicornis and *C. dentisulcatus* changed from (0) to (1).

1540): Basioccipital, basal tubera, dorsoventral depth: subequal or less (0); more (1) than occipital condyle midline depth. (Cau 2024, modified from Brusatte et al. 2010).

C. nasicornis and *C. magnicornis* changed from (?) to (0).

1682): Maxillary/dentary teeth, mesial carina, denticle at 2/3 of the carina, proportions: longer apicobasally than mesiodistally (0); mesiodistally as wide or wider than apicobasally long (1). (Cau 2024, modified from Hendrickx and Mateus 2014a).

Ceratosaurus changed from (1) to inconclusive (-), this character was not possible to determine among the different *Ceratosaurus* species.

1685): Tibia, lateral surface, fibular crest, proximal end, shape: single crest (0); forked crest delimiting a proximal fossa (1). (Cau 2024).

C. magnicornis and *C. dentisulcatus* changed from (1) to (0); this feature is much more evident in ML352/SHN(JJS)065.

1732): Mc I, proximal width: less (0); subequal or more (1) than bone mid-line proximodistal diameter.

Allosaurus changed from (1) to (0). (Cau 2024).

1734): Maxilla, articular facet for premaxilla, inclination in dorsal view: mostly anteriorly (0); beveled anteromedially (1). (Cau 2024).

C. magnicornis and *C. dentisulcatus* changed from (?) to (0).

1736): Maxilla, palatal shelf, dorsoventral thickness: shallow shelf (0); thick torus maxillaris confluent with anteromedial process (1). (Cau 2024).

C. magnicornis and *C. dentisulcatus* changed from (?) to (0).

1941): Tibia, medial condyle, posterior margin, shape in proximal view: posteriorly rounded, symmetrical (0); posteriorly conical, asymmetrical (rounded medially, more angular laterally) (1). (Cau 2024).

C. dentisulcatus changed from (?) to (0).

The following character states were also changed from the original matrix but the change affected the variability of the state character among the different species (all just 0's, 1's or "?") making their presence redundant, so they ended up removed:

54): Frontal-lacrimal contact: absent (0); present (1). (Cau 2024, modified from Gauthier 1986; Rauhut 2000).

Ceratosaurus changed from (0) to inconclusive (-). The information regarding this character is absent or contradictory and the character itself difficult to evaluate.

193): Angular, anterior prong, contact with the dentary-splenial cavity: absent (0); present (1). (Holtz 2000).

Ceratosaurus changed from (1) to inconclusive (-), it was not possible to distinguish among the different *Ceratosaurus* species.

198): Axis, neural spine in lateral view: low and antero-posteriorly expanded (0); mediolaterally compressed and dorso-ventrally elongate (1). (Currie and Carpenter 2000).

C. dentisulcatus changed from (0) to (1). Character was eventually modified into a new character (250) and eliminated.

225): Dorsal vertebrae, anterior centra, ventral processes anterior to the keel (hypapophysis): poorly developed (0); strongly developed (1). (Cau 2024, modified from Rauhut 2000; O'Connor 2009).

All *Ceratosaurus* changed from (1) to (0).

253): Scapula, dorsal and ventral margins in lateral/costal view: markedly diverge posteriorly (0); not diverging posteriorly (1). (Cau 2024).
The original coding had the polarity inverted – *Allosaurus* changed from (1) to (0) and *Majungasaurus* changed from (0) to (1).

264): Coracoid, lateral tubercle: absent (0); present (1). (Cau 2024, modified from Holtz 2000).
C. dentisulcatus changed from (0) to (1).

282): Humerus, distal condyles, shape: broadly convex or hemispherical (0); proximodistally depressed, flattened (1). (Cau 2024, modified from Wilson et al. 2003).
C. magnicornis and *C. dentisulcatus* changed from (0) to (1)

291): Radius in adult, proximodistal length: more than (0); less than (1) 3/5 of the proximodistal length of the humerus. (Cau 2024).
Ceratosaurus changed from (1) to (?) because the two elements are unknown from the same individual.

350): Sacral neural spines: unfused (0); fused into a lamina (1). (Holtz 2000).
C. nasicornis changed from (0) to (1).

358): Caudal vertebrae, anterior neural arches, ventral rib laminae: absent (0); present (1). (Cau 2024).
C. dentisulcatus changed from (0) to (1).

365): Caudal vertebrae, anterior centra, shape of the ventral surface: flattened or slightly convex medio-laterally (0); strongly constricted medio-laterally or keeled (1). (Cau 2024, modified from Rauhut 2000).
C. nasicornis and *C. dentisulcatus* changed from (1) to (0). This was coded based just on the latero-medial constriction because *Ceratosaurus* was doubled keeled. *Allosaurus* changed from (0) to (1).

374): Caudal vertebrae, proximal and median ribs, inclination in anterior/posterior view: laterally directed or slightly dorso-laterally directed (0); strongly dorso-laterally directed (1). (Canale et al. 2008).
Ceratosaurus changed from (1) to (0).

382): Ilium, lateral vertical crest dorsal to the acetabulum: absent (0); present (1). (Rauhut 2000).
Allosaurus changed from (1) to (0), based on Rauhut, 2000.

449): Tibia, fibular condyle, posteriormost extent in proximal view: anteriorly to (0); at the same level of (1); the posterior margin of the medial condyle. (Cau 2024).
C. dentisulcatus changed from (?) to (0). *Majungasaurus* changed from (1) to (0).

463): Astragalus, posteromedial process (and corresponding fossa on the posterodistal margin of the tibia): absent (0); present (1). (Cau 2024).
Majungasaurus changed from (0) to (1).

466): Tibia, proximal end, posterior cleft between the proximal condyles, development: indistinct (0); deep (1). (Rauhut 2000).
Ceratosaurus changed from (1) to (0) because the cleft between condyles is not as deep as in *Allosaurus*.
Majungasaurus changed from (1) to (0).

530): Astragalus, ascending process, fibular articular facet: absent (0); present (1). (Cau 2024)
Ceratosaurus changed from (0) to (1) and *Majungasaurus* changed from (0) to (1).

559): Scapula in adult, acromion, inclination of the posterior margin relative to shaft: steeply inclined dorsally (0); gently sloping (1). (Cau 2024).
Majungasaurus changed from (0) to (1), it is more similar to *Ceratosaurus* than to *Allosaurus*.

560): Mt IV, cross section at mid-shaft, shape: deeper than wide, transversely compressed (0); as wide as deep or wider, uncompressed (1). (Cau 2024, modified from Senter 2010).
Ceratosaurus changed from (0) to inconclusive (-), it was not possible to distinguish among the different *Ceratosaurus* species.

561): Tibia, laterodistal end, distalmost extent: proximally to or at the same level of the distal extent of the medioidistal end (0); distally to the distal extent of the medioidistal end (1). (Cau 2024).
Ceratosaurus changed from (0) to (1). Although this change led to the removal of the character from the matrix, it was eventually modified to create the new character 269.

565): Maxilla, antorbital diverticulum connecting the external naris and the antorbital fossa: absent (0); present (1). (Cau 2024).
Allosaurus changed from (1) to (0).

606): Ilium, posterior margin, posteroventral process (and brevis shelf) projected posteriorly beyond level of mid-height of posterior margin: absent (0); present (1). (Cau 2024, modified from Makovichy et al. 2005).
Ceratosaurus changed from (1) to (?). The distal end of the ilium is missing.

626): Caudal vertebrae, anterior and middle neural arches, prezygocostal lamina: absent (0); present (1). (Cau 2024).
Ceratosaurus changed from (?) to (1). *Allosaurus* changed from (1) to (0). *Majungasaurus* changed from (0) to (1).

627): Ischium, obturator foramen, ossification of the ventral border: complete, connecting the pubic peduncle of the ischium with the obturator lamina (0); open notch (1). (Cau 2024).
Majungasaurus changed from (0) to unknown (?).

663): Ischio-pubic medioventral shelves, development: broad and widely contacting medially (pelvic foramen reduced) (0); reduced (wide pelvic fenestra) (1). (Cau 2024, modified from Sereno 1999).
Allosaurus changed from (1) to (0).

668): Presacral vertebrae, anterior surface, peduncular fossae placed laterally to the neural canal: absent (0); present (1). (Cau 2024).
Ceratosaurus changed from (0) to (1).

685): Tibia, proximal surface, anteroposterior diameter: more (0); less (1) than 9/5 of the mediolateral diameter of the same surface. (Cau 2024).
Allosaurus changed from (0) to (1). *Majungasaurus* changed from (1) to (0).

705): Astragalus, ascending process, anterolateral margin, groove converging with astragalar base: absent (0); present (1). (Ezcurra and Novas 2007).
Ceratosaurus changed from (0) to inconclusive (-), it was not possible to evaluate the different *Ceratosaurus* species.

714): Dorsal vertebrae, ossified connective tissue bridging the transverse processes: absent (0); present (1). (O'Connor 2009).
Ceratosaurus changed from (1) to inconclusive (-), it was not possible to evaluate the different *Ceratosaurus* species.

815): Ilium, postacetabular process, brevis shelf (lateroventral crest), development: diminishes anteriorly (0); developed anteriorly (1). (Langer and Benton 2006).
Ceratosaurus changed from (1) to inconclusive (-). *Majungasaurus* changed from unknown (?) to inconclusive (-).

905): Postacetabular process, posterior margin, posterodorsal process projected posteriorly beyond level of mid-height of posterior margin: absent (0); present (1). (Cau 2024).
C. nasicornis changed from (1) to (?). the posterior end of the ilium is missing.

953): Squamosal, ventral (= precotyloid) process, length relative to the posterior (= postcotyloid) process in lateral view: longer (0); subequal (1). (Brusatte and Sereno 2008).
C. nasicornis changed from (?) to (0).

982): Pubis, foot, dorsal surface, mid-line shape: convex (0); concave (1). (Carrano and Sampson 2008).
Ceratosaurus and *Majungasaurus* changed from (1) to (?). The distal pubis is missing.

986): Lacrimal, medial recess: absent (0); present (1). (Brusatte et al. 2010).
Majungasaurus changed from (?) to (1).

1003): Humerus, proximal end, posterior surface, capital incisure between head and internal (medial) tuberosity: absent (0); present (1). (Cau 2024).
The original coding had the polarity inverted. *C. dentisulcatus* and *Majungasaurus* changed from (0) to (1) and *Allosaurus* changed from (1) to (0).

1025): Humerus, head, long axis in proximal view: collinear with the plane of the proximal expansion of the humerus (0); oriented slightly obliquely (1). (Cau 2024).
Majungasaurus changed from (?) to (0).

1053): Frontal-postorbital facet, anterior depth: less (0); more (1) than 2/5 facet length. (Cau 2024).
Ceratosaurus changed from (0) to inconclusive (-), it was not possible to evaluate for the different *Ceratosaurus* species.

1055): Ilium, preacetabular process, anteroventral corner with distinct ventral projection (antiliac process): absent, anteroventral margin rounded (0); present, anteroventral margin acuminate (1). (Cau 2024).
Ceratosaurus changed from (0) to unknown (?), the anterior part of the ilium is missing. *Majungasaurus* changed from (1) to (0).

1065): Pedal unguals, ventral fossa: absent (0); present (1). (Cau 2024).
C. nasicornis changed from (0) to inconclusive (-).

1069): Pedal unguals, collateral groove, confluence with the ventral surface: absent (0); present (1). (Cau 2024).
C. nasicornis changed from unknown (?) to inconclusive (-).

1080): Skull, supratemporal fenestra, proportions: longer than wide or as long as wide (0); wider than long (1). (Cau 2024, modified from Canale et al. 2008).
C. nasicornis and *C. magnicornis* changed from (1) to inconclusive (-).

1092): Maxilla, preantorbital process, lateral subcutaneous surface, proportion: taller than long (0); longer than tall (1). (Cau 2024).
Ceratosaurus changed from (1) to (0).

1135): Ischium, distal expansion, anteroposterior diameter: less (0); more (1) than twice minimum ischial shaft anteroposterior diameter. (Cau 2024).
Allosaurus changed from (0) to (1). *Majungasaurus* and *C. nasicornis* changed from (1) to (?), both have the distal ischia missing.

1171): Fibula, proximal end, anterior and posterior margins: subequal in transverse width (0); transverse width of proximal fibula narrows posteriorly (1). (Zanno 2010).
Allosaurus changed from (0) to (1). *C. nasicornis* and *C. dentisulcatus* changed from (?) to (1).

1207): Cervical vertebrae, anterior and middle parapophyses, relationship with the diapophyses articular facet: well separated (0); closely placed (1). (Cau 2024).
Majungasaurus changed from (?) to (1).

1209): Ischium, symphysis, proximodistal extent: limited to the distal end (0); proximally expanded as an apron (1). (Cau 2024).
Majungasaurus changed from (0) to (?).

1268): Dentary, medial articular prong for surangular (separate from dorsal prong that is exposed laterally): absent (0); present (1). (Wilson et al. 2003).
Ceratosaurus changed from (0) to inconclusive (-), it was not possible to distinguish among the *Ceratosaurus* species.

1273): Cervical vertebrae, middle (C4-6) neural spines, orientation: vertical (0); dorsoposteriorly inclined (1). (Wilson et al. 2003).
Allosaurus changed from (1) to (0).

1323): Frontal, internal pneumatic sinus: absent (0); present (1). (Cau 2024).
Ceratosaurus changed from (1) to inconclusive (-), it was not possible to distinguish among the *Ceratosaurus* species.

1327): Frontal in adult, participation to dorsal orbital margin: extensive (0); extremely reduced or obliterated (1). (Cau 2024).
C. nasicornis and *C. magnicornis* changed from (0) to (1).

1440): Pubis, foot, maximum longitudinal axis, angle formed with the distal half of pubis in lateral view: more (0); less (1) than 75°. (Cau 2024).
Ceratosaurus changed from (0) to unknown (?), the pubic foot is missing.

1584): Pubis, distal foot, posterior process, anteroposterior length: less than (0); more than (1) 1/5 of the length of the pubis. (Cau 2024, modified from Holtz 2000).
C. nasicornis changed from (0) to (?), the distal pubis is missing.

1631): Fibula, shaft distal to M. iliofibularis insertion, medial surface, shape: flat to convex (0); concave due to presence of groove (1). (Loewen et al. 2013).
Majungasaurus changed from (?) to (0).

1670): Teeth, enamel microstructure, boundary between first and second enamel types from the enamel-dentine junction: parallel to enamel-dentine junction (0); jagged, varies in distance from enamel-dentine (1). (Hwang 2007; Hendrickx and Mateus 2014a).
Ceratosaurus changed from (0) to inconclusive (-), it was not possible to compare between the *Ceratosaurus* species.

1683): Maxillary/dentary teeth, distal carina, denticle at 1/2 of the carina, proportions: as long or longer apicobasally than mesiodistally (0); mesiodistally wider than apicobasally long (1). (Cau 2024, modified from Hendrickx and Mateus 2014a).
Ceratosaurus changed from (1) to inconclusive (-), this character was not possible to determine among the different *Ceratosaurus* species.

1760): Ischium, pubic peduncle, ventrodistal margin in lateral view, “neck” between pubic facet and obturator region producing a notch and a “hooked” peduncle: absent (0); present (1). (Cau 2024).
Majungasaurus changed from (0) to (?), the ischium is unknown. *C. nasicornis* changed from (?) to (0).

1793): Axis, centrum, shape in ventral view: mediolaterally constricted posterior to the intercentral suture (0); lateral margins subparallel (1). (Wang et al., 2017).
C. nasicornis and *C. dentisulcatus* changed from (?) to (1).

1824): Sacral series in taxa with more than four sacral vertebrae, ventral surface, shape in lateral view: straight (0); curved (ventrally concave) (1). (Cau 2024, modified from Carrano and Sampson 2008).
Allosaurus changed from (0) to (1).

1858): Fronto-nasal suture, shape in dorsal view: simple curve (0); complex, interdigitating (1). (Agnolin et al., 2022).

Majungasaurus changed from (1) to (0).

1902): Tibia, cnemial crest, lateral fossa, anteroposterior extent: less (0); more (1) than 70% of crest anteroposterior extent. (Cau 2024, modified from Tortosa et al., 2013).

Ceratosaurus changed from (0) to (1).

1919): Supraoccipital, posterior surface adjacent to exit of mid-cerebral vein, curved groove leading towards the posttemporal fenestra: absent (0); present (1). (Cau 2024, modified from Schade et al., 2023).

Ceratosaurus changed from (0) to inconclusive (-), it was not possible to evaluate among the different *Ceratosaurus* species.

1922): Parasphenoid, rostrum, dorsal process anterior to the pituitary fossa: absent (0); present (1). (Schade et al., 2023).

Majungasaurus changed from (?) to (0).

Before adding the new characters, a search was made among the original ones to assure that they were not repeated. When the new character was already described it was discarded. Some were adapted in the form of the new character to better fit the differences we were describing.

Characters 429) and 1114) had no variability in the original matrix, being among those that were first filtered, however, when defining new characters, they described two of the differences we identified, so they were also added to the matrix.

The 37 new characters added to the matrix (fig. 79-89) are described below (already identified by their number in the final version of the matrix).

New characters

233) External naris dorsoventral expansion: deep, i.e., ascending nasal process of premaxilla well diverging from the lower border of naris (0); narrow or slit-like, i.e., ascending nasal process of premaxilla nearly parallel to the lower border of naris (1). Fig. 79.

* In *C. dentisulcatus* the nasal ascending process of the premaxilla is much lower making the naris opening much more narrow than in other *Ceratosaurus* species (Madsen & Welles, 2000).

234) External naris lower margin: convex or flat (0); concave (1). Fig. 79.

* In *C. dentisulcatus* the lower margin of the naris is flat or subtly convex when compared with the other *Ceratosaurus* species (Madsen & Welles, 2000).

235) Maxilla, ventral half of the anterior border contacting the premaxilla: posterior dip (anteroventral corner recesses posteriorly), giving a convexity outline (0); anterior dip (anteroventral corner more anterior), usually in a straight line (1). Fig. 79.

* In *C. magnicornis* the lower half of the anterior border of the maxilla, where it contacts the premaxilla, dips anteriorly, whereas in other *Ceratosaurus* species dips posteriorly (Madsen & Welles, 2000). This is particularly evident in the left maxilla of *C. magnicornis* holotype, MWC1.

236) Maxilla, ventral border (best seen in lateral view): straight or slightly bowed (0); clearly convex (1). Fig. 79.

* In *C. nasicornis* the ventral border of the maxilla is less convex than in the other *Ceratosaurus* species (Madsen & Welles, 2000).

237) Maxilla lateral surface, ventral margin of antorbital fossa: well defined, forming a step (0), subtle or absent (1). Fig. 79.

* In *C. nasicornis* the step of the ventral margin of antorbital fossa is more subtle than in the other *Ceratosaurus* species.

238) Maxilla, number of teeth: 14 or more (0); 13 (1); 12-0 (2).

* The number of teeth in the maxilla of *Ceratosaurus* differs among the different species with 15 in *C. nasicornis*, 13 in *C. magnicornis* and 12 in *C. dentisulcatus* (Madsen & Welles, 2000). In *Allosaurus* this feature is quite variable with number of teeth varying between 14 and 17 (Madsen, 1976), this must be taken into account when considering this feature.

239) Lacrimal, ventral process, lateral surface just below the anterior crest (at the rim of the antorbital fossa): flat (0); with a well defined vacuity (lower lacrimal recess) (1). Fig. 79.

* *C. magnicornis* differs from *C. nasicornis* by having a more deeply excavated and well defined lower lacrimal recess.

240) Dentary, number of teeth: at least 14 (0); less than 13 (1).

* Similar to the maxilla, the number of teeth in the dentary of *Ceratosaurus* differs for each species with 15 in *C. nasicornis* and 11 or 12 in *C. dentisulcatus* (Madsen & Welles, 2000). *C. magnicornis* dentary is unknown. In *Allosaurus* it varies between 14 and 17 teeth (Madsen, 1976), this fact must be with taken into account when using this character.

241) Dentary anterior half in lateral/medial view: straight (0); upturned (bowed upwards, ventral convexity and dorsal concavity) (1). Fig. 79.

* The dentary of *C. dentisulcatus* is bowed upwards, differing from the more straight condition observed in *C. nasicornis*.

This character has some overlap with characters 1328 (dentary, dorsal surface, shape in lateral/medial view: flat to convex (0); anteriorly concave (1). Cau 2024) and 1334 (mandible, ventral margin, shape in lateral view: straight to moderately convex ventrally (0); markedly convex ventrally, with a distinct bend at the dentary-angular contact (1). Senter 2011) from Cau (2024).

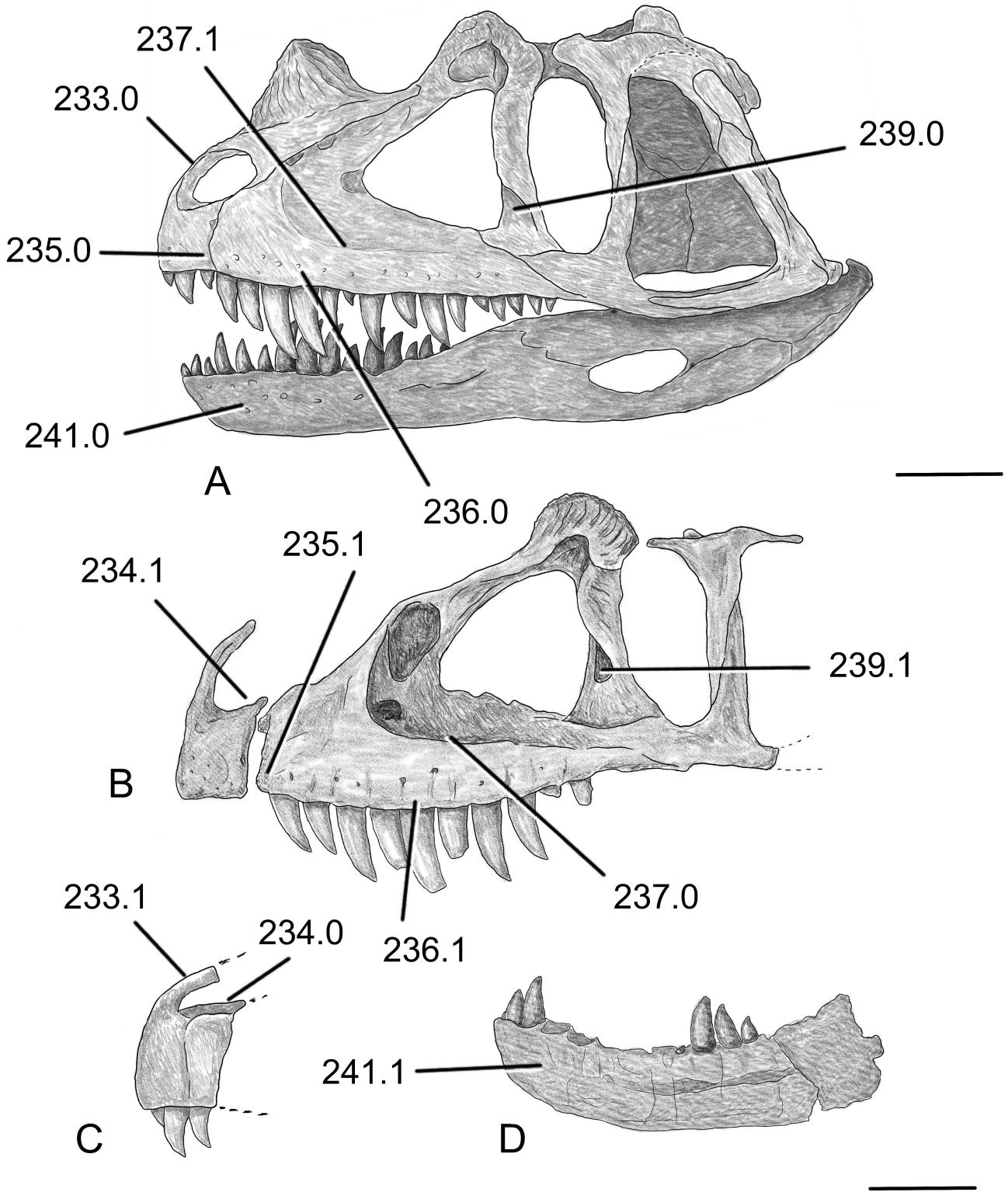


Figure 79. Schematic representation of the new set of characters defined for the skull and dentary of *Ceratosaurus*. **A.** left skull and dentary of *Ceratosaurus nasicornis* holotype USNM 4735, adapted and modified from Gilmore (1920); **B.** left skull elements of *Ceratosaurus magnicornis* holotype MCW1, adapted and modified from Madsen and Welles (2000); **C.** left premaxilla of *Ceratosaurus dentisulcatus* holotype UMNH VP 5278, adapted and modified from Madsen and Welles (2000); **D.** left dentary of *Ceratosaurus dentisulcatus* holotype UMNH VP 5278, adapted and modified from Madsen and Welles (2000). All elements in lateral view. Scale bar equals 10cm.

- 242)** Axis, odontoid process length: poorly developed (less than 20% of the axial centrum length) (0); very prominent (25% or more of the axial centrum length) (1). Fig. 80.
 * The odontoid of *C. dentisulcatus* is more prominent and anteriorly developed than in *C. nasicornis* (Madsen & Welles, 2000). The percentage given expresses the difference between these two species by the ratio between the odontoid length versus the axial centrum length.
- 243)** Axis, odontoid process outline in anterior view: moon shaped or reniform (0); subcircular (1). Fig. 80.
 * The shape of the odontoid differs in anterior view. In *C. nasicornis* is subcircular whereas in *C. dentisulcatus* the dorsal surface is flattened to slightly concave giving it a moon-shaped form.
- 244)** Axis centrum length (elongation coefficient: length/posterior height): longer (coefficient 1.5 or more) (0); shorter (coefficient 1.2 or less) (1). Fig. 80.
 * The ratio between length and height of the axis centrum differs between *C. nasicornis* and *C. dentisulcatus* with the former being longer (Madsen & Welles, 2000). The coefficient values defined express the difference observed using the centrum length and the posterior facet height.
 This character is related to character 1158 (axis, centrum, anteroposterior length: elongate, longer than 1.2 times the height of the posterior articular face (0); short, less than 1.1 times the height of the anterior articular face (1); Benson et al., 2010) from Cau (2024).
- 245)** Axis prezygapophysis: present (0); absent (1). Fig. 80.
 * The axis of *C. dentisulcatus* differs from *C. nasicornis* in the absence of prezygapophysis (Madsen & Welles, 2000).
- 246)** Axis posterior notch above the epiphysis: present, epiphysis well separated from neural spine (0); absent, epiphysis confluent with neural spine (1). Fig. 80.
 * The axis epiphysis of *C. dentisulcatus* is well differentiated and developed, extending behind the neural spine, whereas in *C. nasicornis* is less defined, being merged with the spinopostzygapophyseal lamina (Madsen & Welles, 2000).
- 247)** Axis centrum ventroposterior corner: leveled with ventroanterior corner (0); well below the ventroanterior corner (1). Fig. 80.
 * The axis of *C. dentisulcatus* differs by having both centrum ventral corners leveled while in *C. nasicornis* the ventroposterior corner is lower.
- 248)** Axis, ventral surface between centrum and intercentrum: well defined transversal ridge (0); continuous (1). Fig. 80.
 * The axis centrum and intercentrum are ventrally separated by a well defined transversal ridge in *C. dentisulcatus*. In *C. nasicornis* this separation is less defined.
- 249)** Axial neural spine: taller than long, (anterior edge slightly inclined posteriorly, anterior and posterior edges steeper) (0); longer than tall, (anterior edge very inclined posteriorly) (1). Fig. 80.
 * The axis neural spine is clearly distinct in *C. nasicornis* and *C. dentisulcatus*. In *C. nasicornis* is longer than tall and posteriorly inclined, in *C. dentisulcatus* is taller than long and more vertical (Madsen & Welles, 2000).
 This character was modified from character 198 (axis, neural spine in lateral view: low and antero-posteriorly expanded (0); mediolaterally compressed and dorso-ventrally elongate (1); Currie and Carpenter, 2000) from Cau (2024).
- 250)** Axial spinopostzygapophyseal lamina, edge curvature (in axial view): convex (confluent with neural spine tip) (0); concave (well defined neural spine tip) (1). Fig. 80.
 * In *C. dentisulcatus* the spinopostzygapophyseal lamina of the axis merges with the tip of the neural spine and has a convex shape in anterior view. In *C. nasicornis* this lamina is more concave forming a more well defined neural spine tip.
 This character was modified from character 1270 (axis, spinopostzygapophyseal lamina, form: straight or gently concave (0); deeply notched (1); Wilson et al., 2003) from Cau (2024). Character 1270 became redundant and was removed.

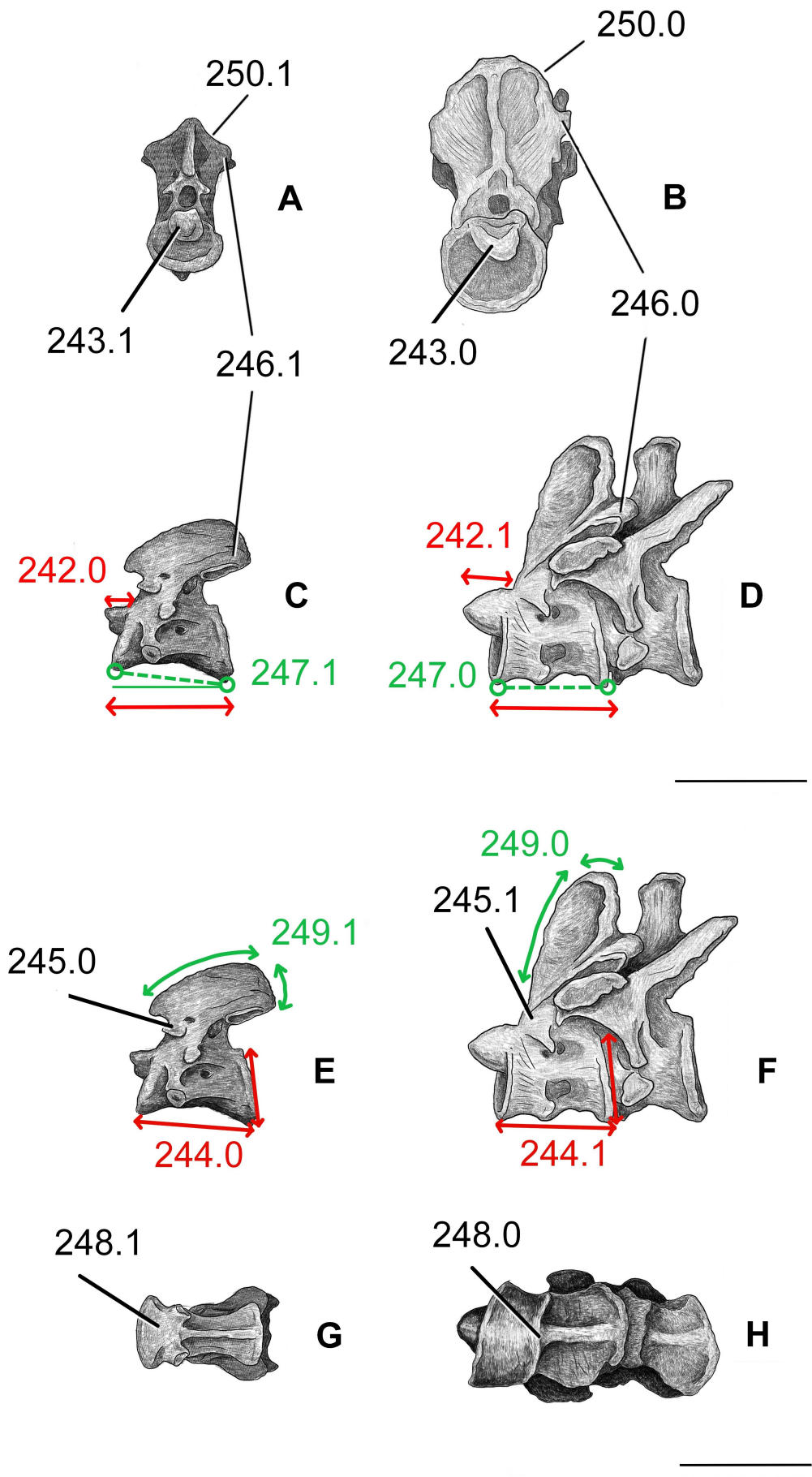


Figure 80. Schematic representation of the new set of characters defined for the axis of *Ceratosaurus*. **A, C, E and G**, axis of *Ceratosaurus nasicornis* holotype USNM 4735, adapted and modified from Gilmore (1920); **B, D, F and H**, axis of *Ceratosaurus dentisulcatus* holotype UMNH VP 5278 (with attached third cervical), **B, D and F** adapted and modified from Madsen and Welles (2000); in anterior (**A, C**), left lateral (**C-F**) and ventral (**G, H**) views. Scale bar equals 10cm.

251) Cervical vertebrae, third to fifth epiphyses: present (0); absent or very reduced (1). Fig. 81.

* In *C. nasicornis* the epiphysis in the anterior cervicals are much less developed than in other *Ceratosaurus* species.

This character was partially transformed from character 208 (postaxial cervical vertebrae epiphyses: absent (0); present (1); Rauhut, 2000) from Cau (2024).

252) Third cervical vertebra neural spine: nearly vertical and straight (0); inclined posteriorly, and curved (1). Fig. 81.

* The third cervical neural spine of *C. dentisulcatus* is more straight and vertical when compared with the more posteriorly curved one of *C. nasicornis* (Madsen & Welles, 2000).

253) Third cervical vertebra posterior central articular facet: nearly vertical (0); very inclined (1). Fig. 81.

* The posterior articular facet of the third cervical vertebra centrum is more vertical in *C. dentisulcatus* than *C. nasicornis* (Madsen & Welles, 2000).

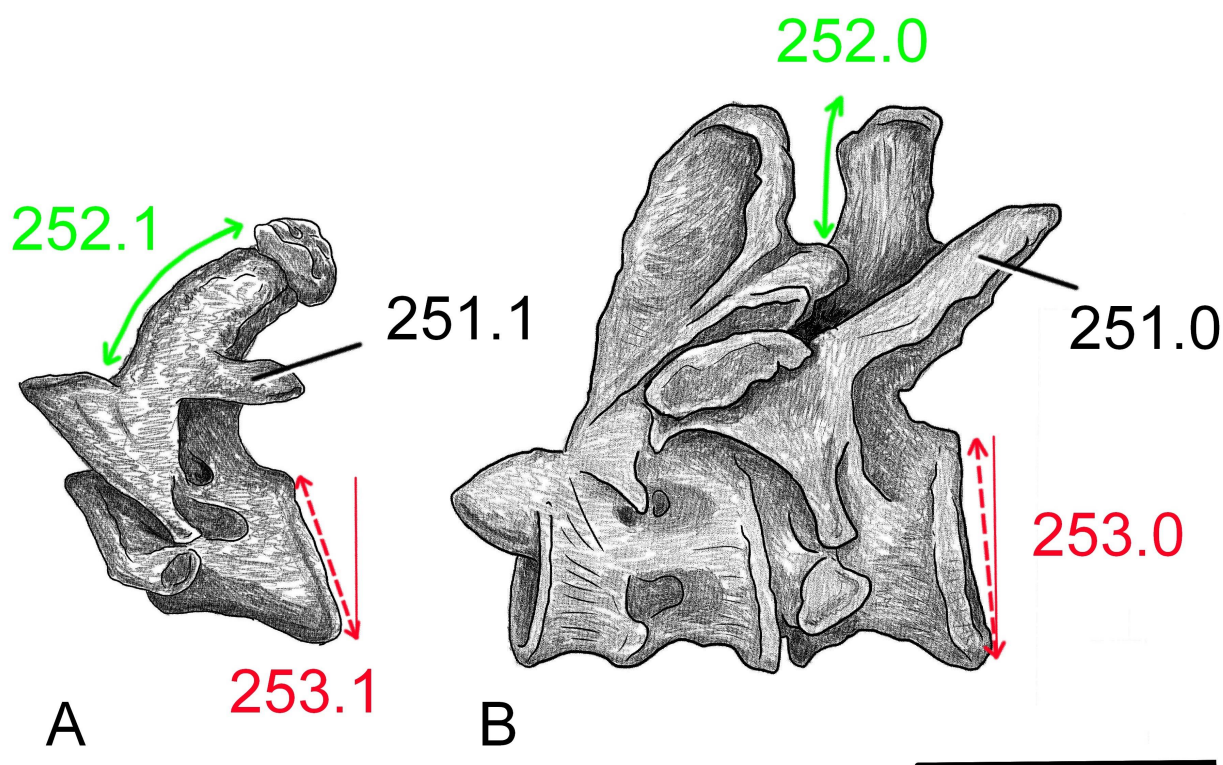


Figure 81. Schematic representation of the new set of characters defined for the anterior cervical vertebrae of *Ceratosaurus*. **A.** third cervical vertebrae of *Ceratosaurus nasicornis* holotype USNM 4735, adapted and modified from Gilmore (1920); **B.** third cervical vertebrae of *Ceratosaurus dentisulcatus* holotype UMNH VP 5278 (with axis attached), adapted and modified from Madsen and Welles (2000). Both elements in left lateral view. Scale bar equals 10cm.

254) Humerus distal end mediolateral expansion: very expanded (3 times or more the minimum mediolateral shaft diameter (0); moderately expanded (less than 3 times the minimum mediolateral shaft diameter) (1). Fig. 82.

* The mediolateral expansion of the distal humerus is wider relative to the humeral mediolateral diameter in *C. magnicornis* than *C. dentisulcatus*. Should be noted that in *C. magnicornis* the distal humerus is incomplete, the measurements and coding was based on the reconstruction by Madsen and Welles (2000).

This character was modified from character 283 (humerus, distal epiphysis, mediolateral width: less than (0); more than (1); 3/2 of mid-shaft humeral width) from Cau (2024). This new character was made in order to differentiate the more mediolaterally wider distal humeri because 283) only distinguishes *Majungasaurus* from other taxa whereas 254) reinforces that *C. magnicornis* is wider than *C. dentisulcatus*.

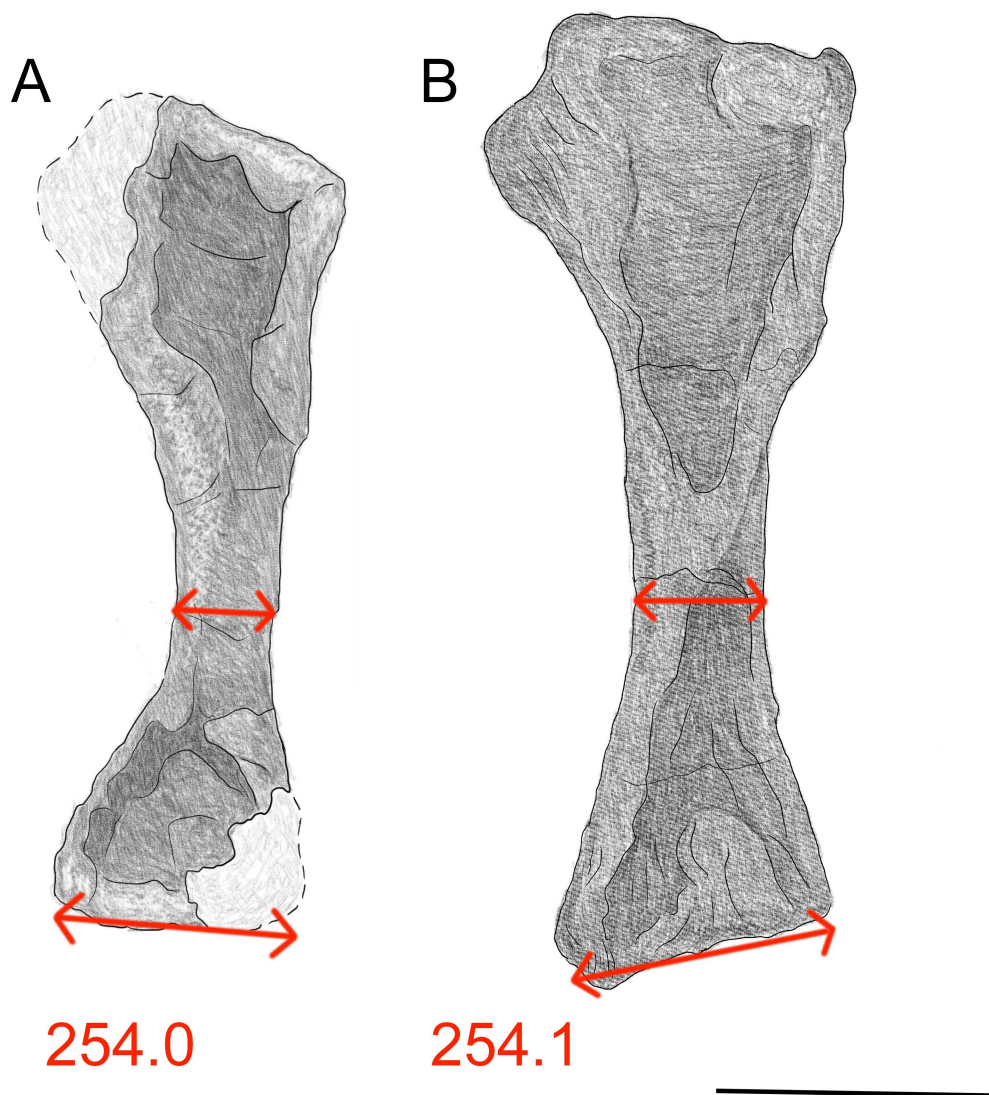


Figure 82. Schematic representation of the new character defined for the humerus of *Ceratosaurus*. **A.** left humerus of *Ceratosaurus magnicornis* holotype MCW1; **B.** left humerus of *Ceratosaurus dentisulcatus* holotype UMNH VP 5278. Adapted and modified from Madsen and Welles (2000). Both elements in anterior view. Scale bar equals 10cm.

255) Femur, head, ventromedial end in anterior/posterior view: round / not distally expanded (0); developed with a prominent ventral spur (giving a hook outline to the femur proximal end) (1). Fig. 83.
 * In *C. dentisulcatus* and ML352/SHN(JJS)065 the ventromedial femoral head develops a spur-like projection, which is absent in *C. nasicornis*. In *C. magnicornis* it was not possible to evaluate this character.

256) Femur trochanteric shelf: absent or poorly developed (0); moderately developed (as a low ridge) (1); extremely developed, forming an incipient lamina (2). Fig. 83.
 * The trochanteric shelf of *C. magnicornis* is much more developed, forming a projecting lamina, whereas in other *Ceratosaurus* and ML352/SHN(JJS)065 is more moderately developed. This character was modified from character 435 (femur, trochanteric shelf, development: poorly developed anterolateral crest (0); prominent, shelf-like (1), modified from Tykoski, 2005) from Cau (2024). Character 435 became redundant and was removed.

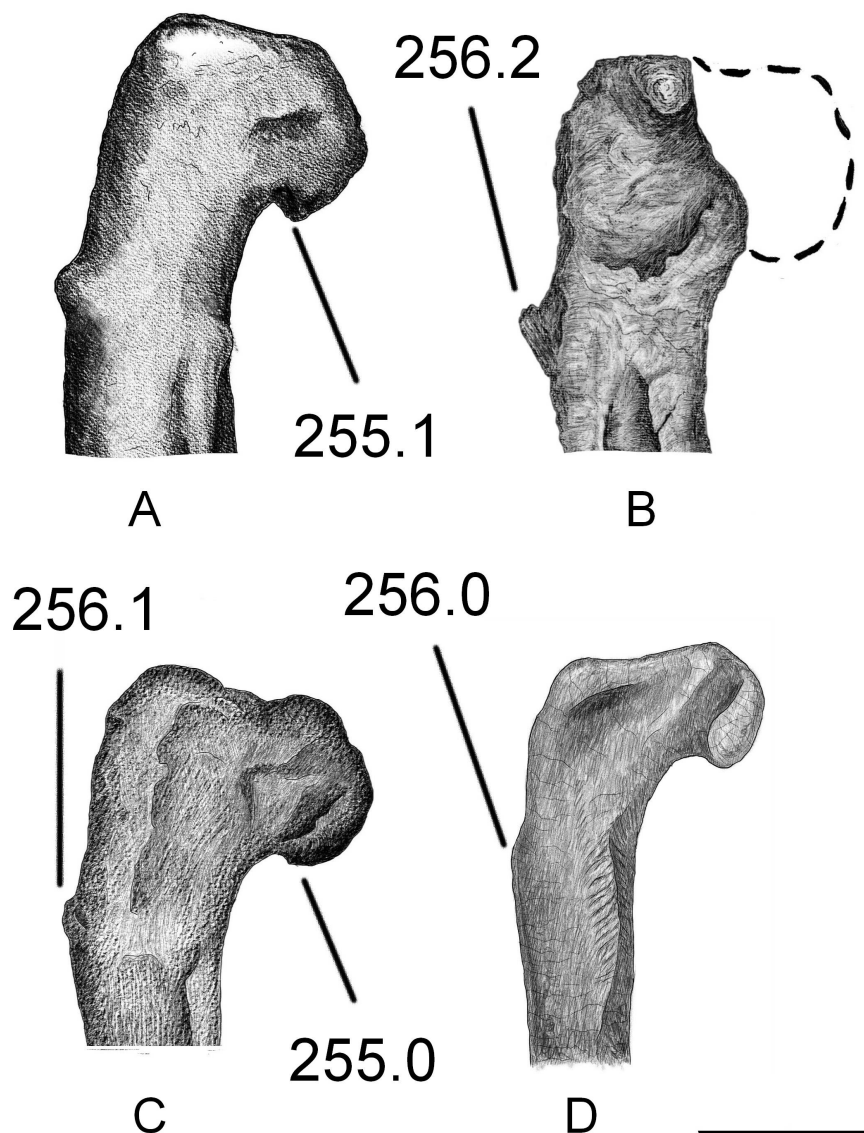


Figure 83. Schematic representation of the new set of characters defined for the femur of *Ceratosaurus*. **A.** proximal left femur of ML352/SHN(JJS)065; **B.** proximal right femur of *Ceratosaurus magnicornis* holotype MCW1 reversed for left view representation; **C.** proximal right femur of *Ceratosaurus nasicornis* holotype USNM 4735, adapted and modified from Gilmore (1920), reversed for left view representation; **D.** proximal left femur of *Allosaurus fragilis* (illustrated to showcase the absence of a trochanteric shelf), adapted and modified from Madsen (1976). All elements in posterior view. Scale bar equals 10cm.

257) Femur, proximal edge of endocondylar ridge: nearly vertical, confluent to the femur shaft (0); curves abruptly laterally, forming a nearly horizontal ridge in the anterior facet (1). Fig. 84.

* In *C. nasicornis* and *C. magnicornis* the proximal development of the endocondylar ridge is more subtle and vertical, in *C. dentisulcatus* and ML352/SHN(JJS)065 forms a well define ridge that curves and crosses along the anterior distal femur.

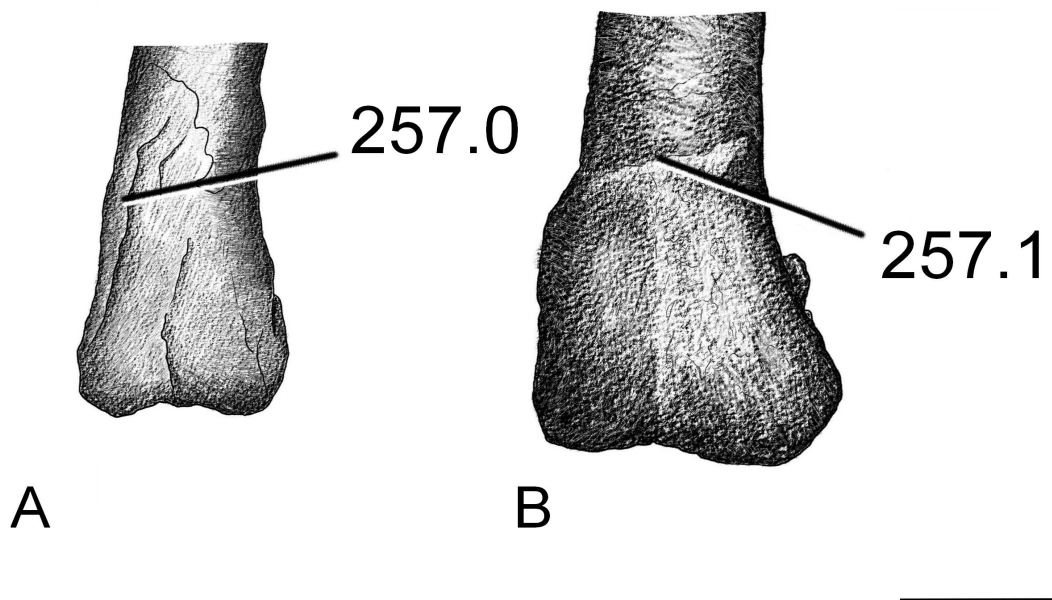


Figure 84. Schematic representation of the new set of characters defined for the femur of *Ceratosaurus*. **A.** distal right femur of *Ceratosaurus nasicornis* holotype USNM 4735, adapted and modified from Gilmore (1920), reversed for left view representation; **B.** distal left femur of *Ceratosaurus dentisulcatus* holotype UMNH VP 5278. Both elements in anterior view. Scale bar equals 10cm.

258) Femur, posterior facet (distal third) in the popliteal surface: concave, homogeneous (0); oblique, shallow ridge, extending from lateroproximal to mediolateral (1). Fig. 85.

* *C. magnicornis* and ML352/SHN(JJS)065 both have a lateroproximal-mediolaterally developed ridge along the posterior distal femur. This is not found in *C. dentisulcatus*. In *C. nasicornis* it was not possible to clearly evaluate.

259) Femur, posterior head of endocondyle: round or subvertically elongated (0); oblique (dorsolaterally to ventromedially elongated) (1). Fig. 85.

* The posterior endocondyle of *C. nasicornis* is more oblique and elongate than the more subvertical ones of *C. magnicornis* and ML352/SHN(JJS)065. In *C. dentisulcatus* this structure is partially broken so its shape could not be properly verified.

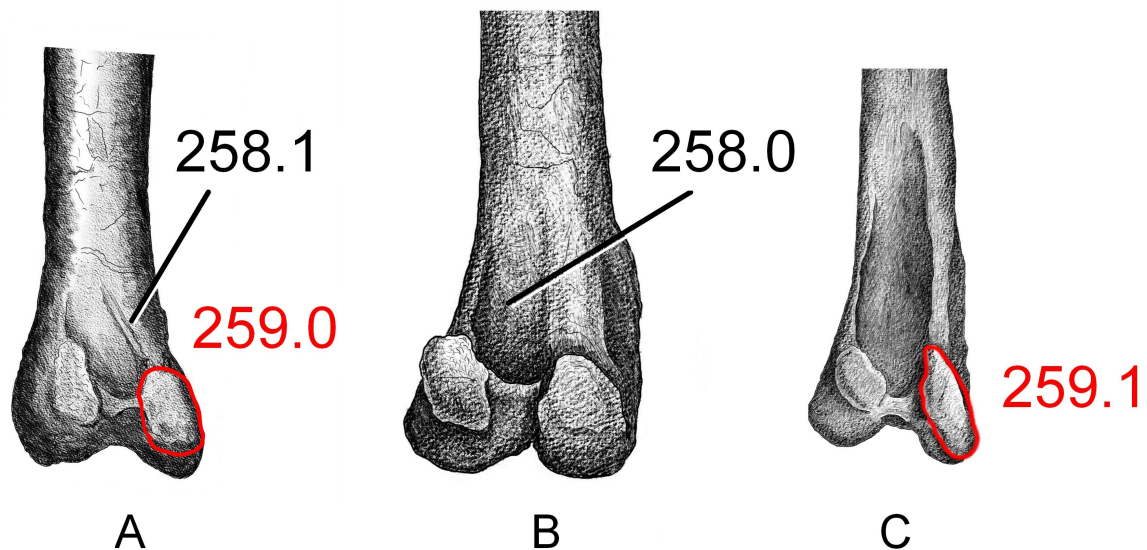


Figure 85. Schematic representation of the new set of characters defined for the femur of *Ceratosaurus*. **A.** distal left femur of ML352/SHN(JJS)065; **B.** distal left femur of *Ceratosaurus dentisulcatus* holotype UMNH VP 5278; **C.** distal right femur of *Ceratosaurus nasicornis* holotype USNM 4735, adapted and modified from Gilmore (1920), reversed for left view representation. All elements in posterior view. Scale bar equals 10cm.

260) Tibia, length relative to femur: less than 85% femur length (0); 85% or more the femur length (1).

* *C. nasicornis* has a tibia/femur length ratio of 0.90 and ML352/SHN(JJS)065 of 0.90 on the left femur and 0.87 on the right one. The other species ratios are lower, 0.83 for *C. magnicornis* and 0.78 for *C. dentisulcatus*. A boundary of 0.85 was established in the character state definition to express this difference. This character was modified after character 1774 (tibia-femur ratio: less (0); more (1) than 3/2) from Cau (2024) to better adapt to the taxa of this study.

261) Tibia, cnemial crest development: moderate, about 1/4 (<27%) or less of the tibia total length (0); very expanded, about 1/3 (>32%) or more of the tibia total length (1). Fig. 86.

* Although a well developed cnemial crest is characteristic for Ceratosauria (Tykoski & Rowe, 2004; Carrano & Sampson, 2008) in *C. magnicornis* and ML352/SHN(JJS)065 it is less expanded than in *C. nasicornis* and *C. dentisulcatus* (Madsen & Welles, 2000). A ratio between the cnemial crest anteroposterior length and the total length of the tibia was defined to express this difference.

262) Tibia, nutrient foramina at the distal end of fibular crest: present (0); absent (1). Fig. 86.

* A nutrient foramina is present in the distal end of the fibula crest of *C. dentisulcatus*, this feature is not found in ML352/SHN(JJS)065 (Malafaia et al., 2015). In the other *Ceratosaurus* species it was not possible to clearly analyze this character.

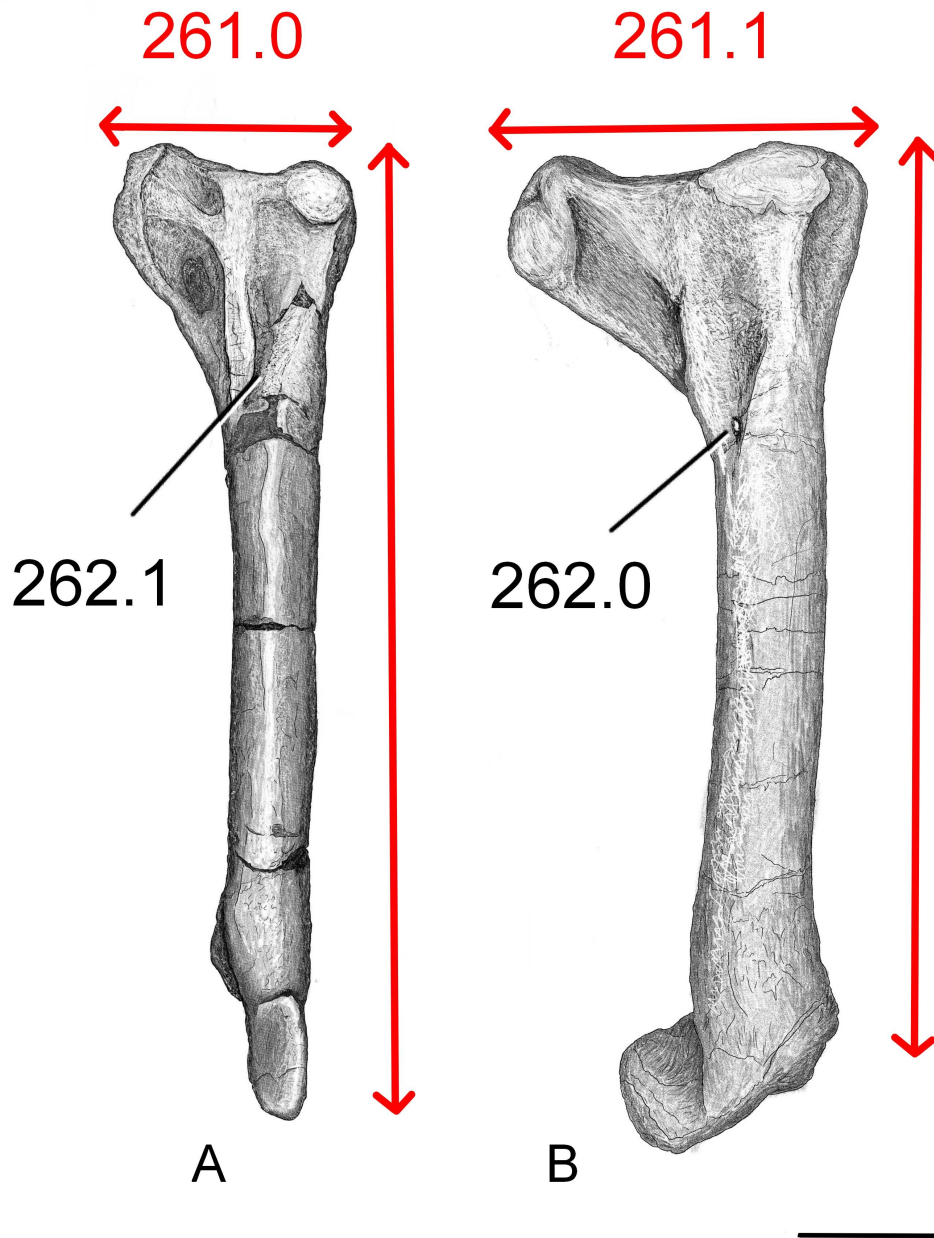


Figure 86. Schematic representation of the new set of characters defined for the tibia of *Ceratosaurus*. **A.** right tibia of ML352/SHN(JJS)065, reversed for left view representation; **B.** right tibia of *Ceratosaurus dentisulcatus* holotype UMNH VP 5278, reversed for left view representation. Both elements in lateral view. Scale bar equals 10cm.

263) Tibia, *malleoli* distal position, lateral *malleolus* distal-most point relative to the medial *malleolus*: at the same level or just slightly more distal (malleolar proximodistal distance less than 4% the full tibial length) (0); lateral *malleolus* clearly more distal than medial one (malleolar proximodistal distance more than 4% the full tibial length) (1). Fig. 87.

* In ML352/SHN(JJS)065 the lateral *malleolus* extends farther distally relative to the medial one than in the three *Ceratosaurus* species. A ratio was defined for the vertical distance between the distal-most points of both *malleoli* and the total length of the tibia to express this condition. ML352/SHN(JJS)065 has a ratio of 4.6%, higher than the other *Ceratosaurus* (*C. nasicornis* 2.2, *C. magnicornis* 3.6, *C. dentisulcatus* 2.4), *Allosaurus* (3.1) and MB R 3621-3626 (3.8). *Majungasaurus* was not possible to code due to incomplete material.

This character was modified from character 561 (tibia, laterodistal end, distal-most extent: proximally to or at the same level of the distal extent of the mediiodistal end (0); distally to the distal extent of the mediiodistal end (1)) from Cau (2024) in order to precisely quantify the vertical distance between both *malleoli*. Character 561 became redundant and was removed.

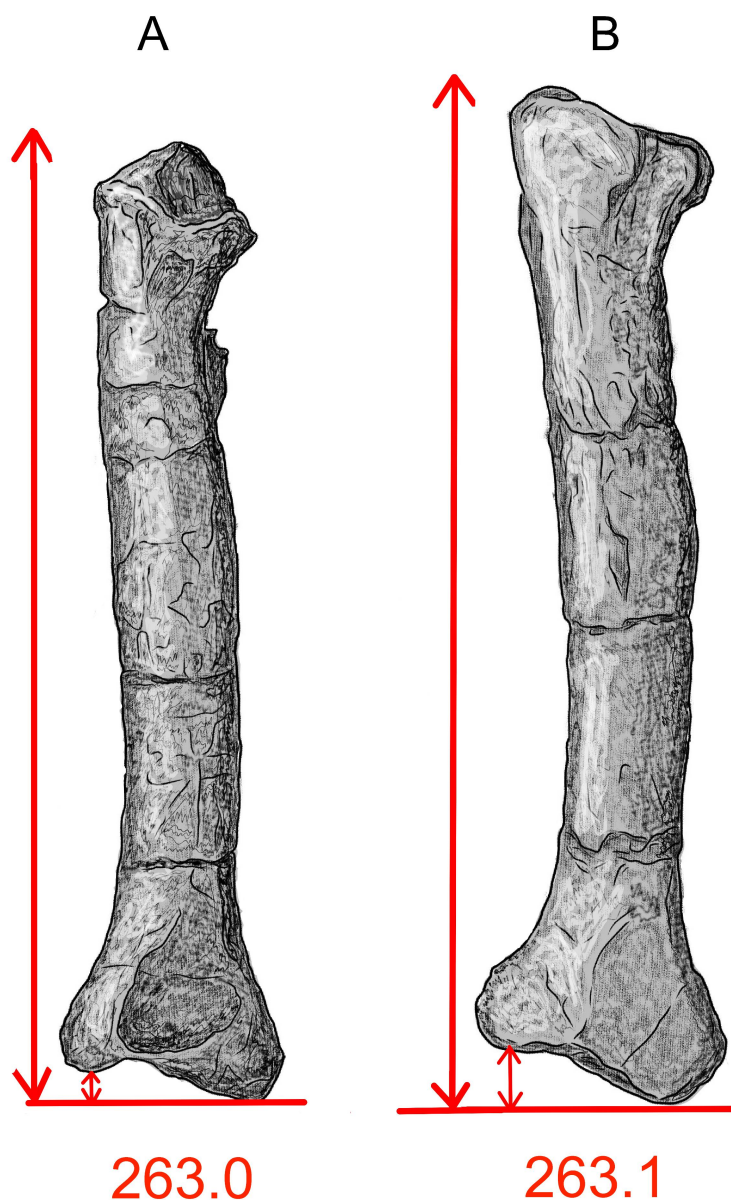


Figure 87. Schematic representation of the new set of characters defined for the tibia of *Ceratosaurus*. **A.** right tibia of *Ceratosaurus magnicornis* holotype MCW1, adapted and modified from Madsen and Welles (2000); **B.** right tibia of ML352/SHN(JJS)065. Both elements in posterior view. Scale bar equals 10cm.

264) Fibula head, lateral facet in lateral view: flat or convex(0); concave (1). Fig. 88.

* The lateral facet of the fibula head of *C. nasicornis* is slightly concave whereas in *C. dentisulcatus* and ML352/SHN(JJS)065 is flat/convex.

265) Fibula, proximal end (above the tibial flange), position relative to the shaft in lateral view: straight (0); tilted / bended posteriorly (1). Fig. 88.

* The proximal fibula of *C. nasicornis* is bended posteriorly in lateral view whereas in *C. dentisulcatus* and ML352/SHN(JJS)065 is vertical and in line with the shaft (Madsen & Welles, 2000).

266) Fibula, shaft in anterior view: straight (0); slightly curved (“S” shaped) (1). Fig. 88.

* In anterior, view the fibular shaft and the tibular flange of ML352/SHN(JJS)065 fibula are slightly curved creating a vertical offset between the head and the shaft. This is not the case with *C. nasicornis* and *C. dentisulcatus* which are completely straight.

267) Fibula, medial fossa: wide, shallow, less proximoposteriorly extended (not reaching the posterior expansion if the head) (0); narrow, deep, proximoposteriorly excavated (invading the posterior expansion if the head) (1). Fig. 88.

* Compared with *C. dentisulcatus*, the medial fibular fossa of ML352/SHN(JJS)065 is anteroposteriorly wider, less deeply excavated and less proximoposteriorly expanded. This feature could not be properly evaluated for *C. nasicornis*.

268) Fibula, distal end: convex and round edges (0); concave, with sharper angles (1). Fig. 88.

* In *C. dentisulcatus*, the distal margin of the fibula is round, in *C. nasicornis* is concave and angled (Madsen & Welles, 2000). This structure is missing in ML352/SHN(JJS)065.

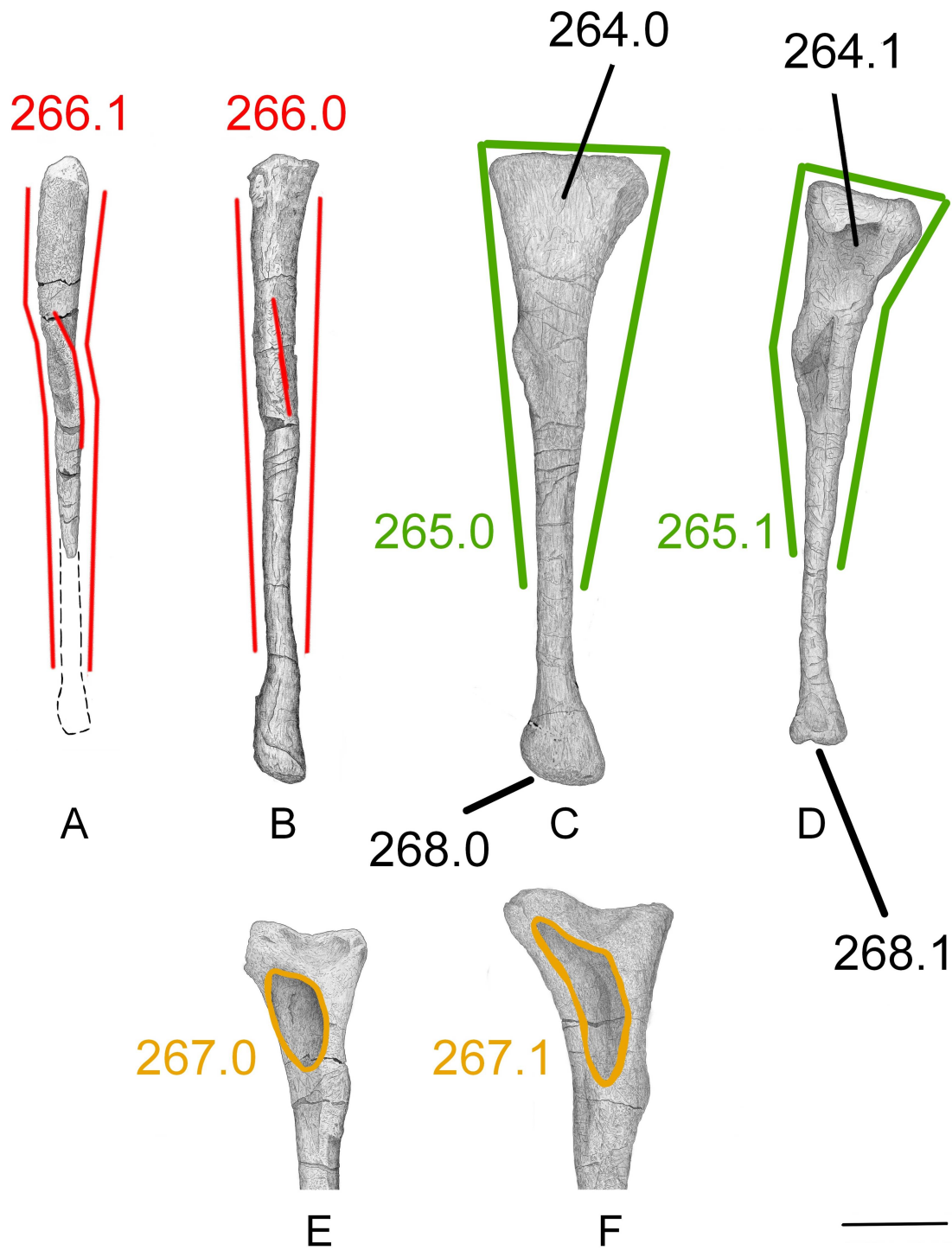


Figure 88. Schematic representation of the new set of characters defined for the fibula of *Ceratosaurus*. **A** and **E**, left fibula ML352/SHN(JJS)065; **B**, **C** and **F**, right fibula of *Ceratosaurus dentisulcatus* holotype UMNH VP 5278, **B** adapted and modified from Madsen and Welles (2000), all reversed for left side illustration; **D**, right fibula of *Ceratosaurus nasicornis* holotype USNM 4735, reversed for left side illustration; in anterior (**A**, **B**), lateral (**C**, **D**) and medial (**E**, **F**) views. Scale bar equals 10cm.

269) Astragalus, position of the proximal-most tip of ascending process relative to the distal tibial expansion: in the lateral half of the distal tibial expansion, above the astragalocalcaneal suture (0); centrally positioned relative to the distal tibial expansion, medial to the astragalocalcaneal suture (1). Fig. 89.

* *C. magnicornis* has the proximal end of the ascending process of the astragalus centrally positioned in relation to the distal expansion of the tibia, in *C. nasicornis*, *C. dentisulcatus* and ML352/SHN(JJS)065 it is positioned more laterally. The astragalocalcaneum is missing for ML352/SHN(JJS)065, its form was inferred based on the shape of the astragalar socket of the tibia.

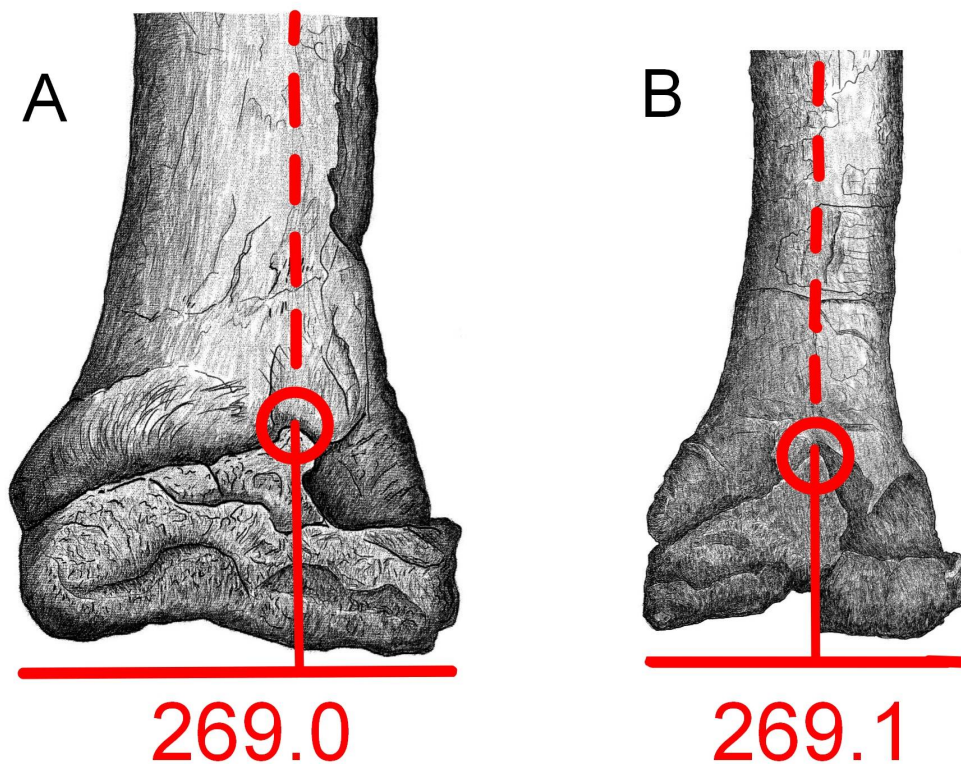


Figure 89. Schematic representation of the new character defined for the astragalus of *Ceratosaurus*. **A.** left tibia and astragalocalcaneum of *Ceratosaurus dentisulcatus* holotype UMNH VP 5278; **B.** right tibia and astragalocalcaneum of *Ceratosaurus magnicornis* holotype MCW1 reversed for left view representation. Both elements in anterior view. Scale bar equals 10cm.

After coding and all the changes and corrections applied to the matrix, some characters ended up with no variability beyond the outgroup. They were eliminated via a second filtering procedure.

The final matrix was made-up of eight taxa (*Allosaurus*, *Genyodectes*, Tendaguru MB R 3621-3626, *Majungasaurus*, *C. nasicornis*, *C. magnicornis*, *C. dentisulcatus* and ML352/SHN(JJS)065) and 269 anatomical characters (232 filtered from the original matrix plus 37 newly defined for this study).

Among the *Ceratosaurus* species alone, including ML352/SHN(JJS)065, were identified 53 anatomical differences, 16 in the original set of characters plus the 37 new ones.

The characters from the original matrix were re-numbered from 1-232.

Together with the 37 new characters defined above, the other 16 differences within the genus *Ceratosaurus* found in the original matrix are:

- **Character 20** (character 80 in the original matrix) parietals: unfused (0); fused (1). (Cau 2024).
*Madsen and Welles (2000) state that in *C. magnicornis* these sutures are fused. In *C. nasicornis* these appear unfused.
- **Character 43** (character 196 in the original matrix) cervical ribs, articulation to vertebrae in adults: loose (0); firmly attached/fused (1). (Holtz 2000).
*Marsh (1884) states that in *C. nasicornis* the cervical ribs are unfused to the centra. In *C. magnicornis* these elements are fused (Madsen & Welles, 2000).
- **Character 45** (character 205 in the original matrix) axis, neural spine, dorsal surface, shape: mediolaterally narrow (0); mediolaterally expanded (1). (Currie and Carpenter 2000; Holtz 2000; Brusatte et al. 2010).
**C. dentisulcatus* differs from *C. nasicornis* by having the axis neural spine dorsal surface more mediolaterally expanded.
- **Character 70** (character 429 in the original matrix) femur, shape in lateral/medial view: straight or slightly sigmoidal (0); strongly bowed, posteriorly concave along the entire length (1). (Cau 2024).
* *C. dentisulcatus* femur is straight in lateral view, whereas in other *Ceratosaurus* and ML352/SHN(JJS)065 it is curved.
- **Character 75** (character 467 in the original matrix) fibula, relationships with the astragalar-tibial complex in adult: unfused or loosely appressed (0); tightly appressed or fused (1). (Cau 2024).
*Fibula in *C. nasicornis* is tightly appressed to the tibia and astragalocalcaneum distally (Gilmore, 1920), this is not observed in other *Ceratosaurus* and ML352/SHN(JJS)065.
- **Character 88** (character 580 in the original matrix) tibiotarsus, complete fusion in adult: absent, proximal tarsals and tibia unfused, sutures clearly visible (0); present, astragalocalcaneum fused to the tibia (1). (Cau 2024).
*In ML352/SHN(JJS)065 these elements are unfused; in the holotypes of the three *Ceratosaurus* species they are fused (Malafaia et al., 2015).
- **Character 95** (character 700 in the original matrix) axis, neural spine, anterior tip, position: anteriorly to (0); at the same level or posterior to (1) the prezygapophyses. (Tykoski 2005).
*In *C. dentisulcatus* the anterior tip of the axis neural spine is positioned posteriorly to the prezygapophyses, whereas in *C. nasicornis* is more anteriorly positioned.
- **Character 102** (character 765 in the original matrix) femur, posterodistal (popliteal) fossa in adults, infrapopliteal ridge between medial distal condyle and tibiofibular crest: absent (0); present (1). (Tykoski 2005).
*In *C. magnicornis*, contrary to what is observed in other *Ceratosaurus* and ML352/SHN(JJS)065, the infrapopliteal ridge is poorly developed.
- **Character 114** (character 880 in the original matrix) quadratojugal and quadrate: unfused (0); fused (1). (Cau 2024).
*Contrary to other *Ceratosaurus*, the quadrate-quadratojugal complex is unfused in *C. magnicornis* (Madsen & Welles, 2000).
- **Character 120** (character 923 in the original matrix) astragalus, ascending process, angle between the proximomedial corner and the transverse axis of the astragalus: no more than (0); more than (1) 45°. (Cau 2024).
*In *C. nasicornis* and *C. magnicornis* this angle is lower than 45°, in *C. dentisulcatus* the angle value is higher. Based on the shape of the astragalar socket of the tibia, the condition in ML352/SHN(JJS)065 is similar to *C. dentisulcatus*.

- **Character 130** (character 965 in the original matrix) femur, tibiofibular crest, shape and orientation in posterior view: narrow, longitudinal (0), broad, oblique (1). (Carrano and Sampson 2008).
*ML352/SHN(JJS)065 differs from other *Ceratosaurus* in having a more narrow and elongated tibiofibular crest.

- **Character 144** (character 1036 in the original matrix) fibula, proximomedial end, fossa/groove, posterior margin: closed by a lip (0); open (1). (Cau 2024, modified from Carrano and Sampson 2008).
*In *C. nasicornis* and ML352/SHN(JJS)065 the posterior border of the medial fibular fossa is bordered by a thin wall; this structure is much less developed in *C. dentisulcatus*, leaving the posterior border of the fossa more open.

- **Character 151** (character 1114 in the original matrix) tibia, lateral cnemial crest, orientation: mainly anteriorly directed (0); mainly laterally directed (1). (Xu et al. 2009b).
*The cnemial crest of ML352/SHN(JJS)065 is more laterally directed than in *C. dentisulcatus* (it was not possible to compare with the other species).

- **Character 186** (character 1441 in the original matrix) quadrate, shaft, proximal half, inclination relative to rest of shaft: straight (0); posteriorly curved (1). (Ezcurra and Novas 2007).
*Quadrate shaft is straight in *C. nasicornis* but more posteriorly concave in both *C. magnicornis* and *C. dentisulcatus*.

- **Character 206** (character 1638 in the original matrix) tibia, fibular crest, orientation: straight, proximodistal (0); curved anteroproximally (1). (Cau 2024, modified from Tortosa et al. 2013).
*Contrary to what is observed in *C. magnicornis* and *C. dentisulcatus*, in ML352/SHN(JJS)065 the fibular crest of the tibia is anteroproximally curved as a result of its proximal bifurcation. It was not possible to clearly evaluate this condition for *C. nasicornis*.

- **Character 210** (character 1685 in the original matrix) tibia, lateral surface, fibular crest, proximal end, shape: single crest (0); forked crest delimiting a proximal fossa (1). (Cau 2024).
*The forked condition of the fibular crest is much more well expressed in ML352/SHN(JJS)065 than in *C. magnicornis* and *C. dentisulcatus*. It was not possible to clearly evaluate this condition for *C. nasicornis*.

The matrix was read in TNT via “Traditional search” with 10 random seeds, 100 added sequences and 100 trees saved by replication. This resulted in six trees (fig. 90) with a TBR best score of 297.

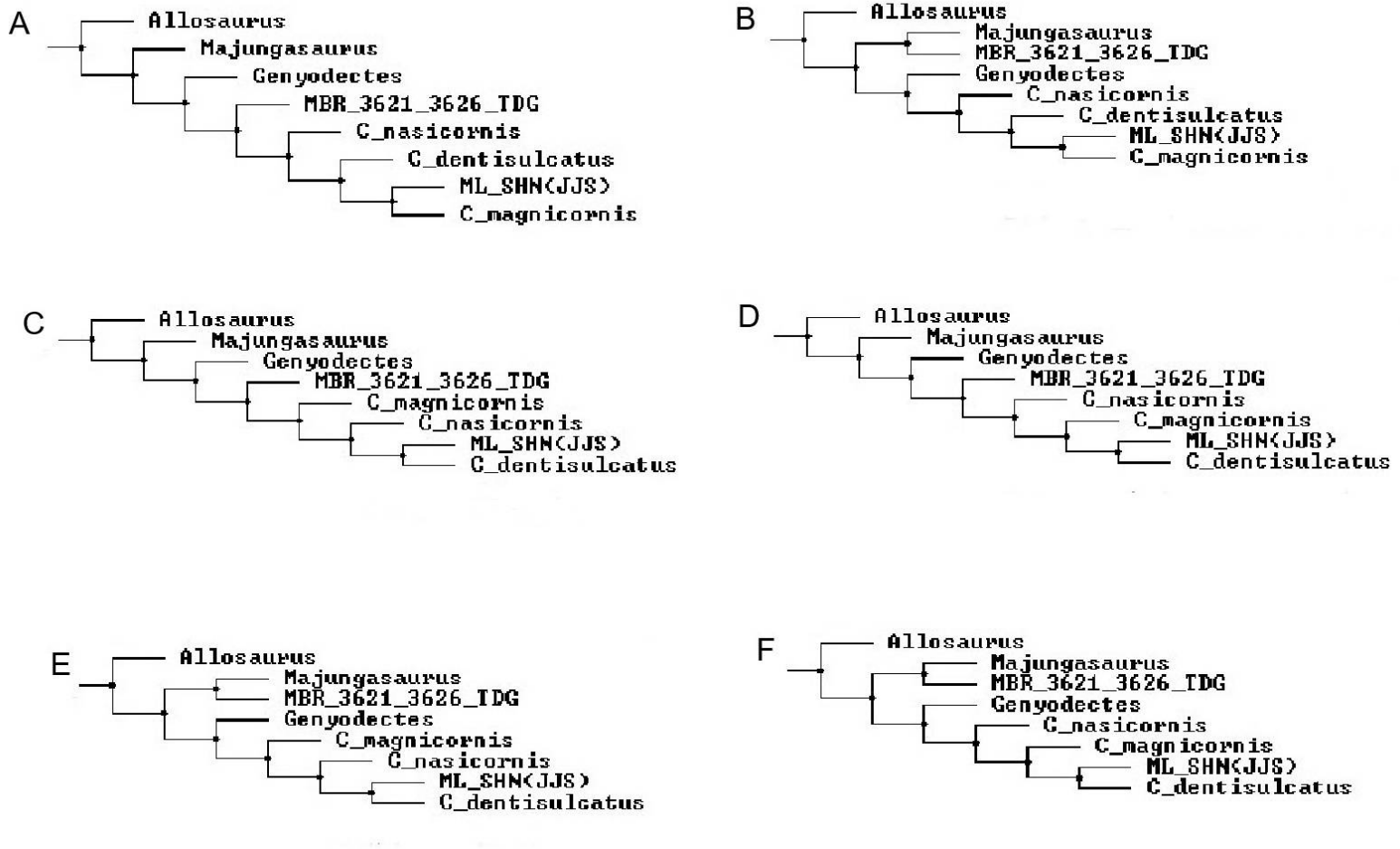


Figure 90. The final six phylogenetic trees for the *Ceratosaurus* specimen-based analysis done with TNT.

Discussion

Comparative anatomy

Based just on the visual comparative analysis with other *Ceratosaurus*, ML352/SHN(JJS)065 can be considered part of Ceratosauria based on the following synapomorphies:

- Presence of well developed pleurocoels in the cervical vertebrae centra (Tykoski & Rowe, 2004);
- Anteromedial projection of 45° of the femur head (Mateus et al., 2006; Malafaia et al., 2015 after Carrano et al., 2002);
- Head of the femur directed ventrally (Malafaia et al., 2015 after Carrano et al., 2002);
- Presence of a trochanteric shelf on the femur (Mateus et al., 2006);
- Shallow/absent extensor groove (for stretching the leg) and flat surface on the anterior facet of the distal femur (Tykoski & Rowe, 2004; Malafaia et al., 2015 after Benson, 2009);
- Deep sulcus along the lateral side of *crista tibiofibularis*, on the posterior distal end of the femur (Mateus et al., 2006; Malafaia et al., 2015 after Carrano et al., 2002);
- Cnemial crest of the tibia well-developed, anteroposteriorly as long or longer than the articular condyles, strongly hook-shaped laterally, expanded above the proximal condyles and ventrally projected (Tykoski & Rowe, 2004; Malafaia et al., 2015 after Carrano & Sampson, 2008);
- Medial condyle of the tibia distally extended, developing a ridge that becomes part of the head's posterior surface (Malafaia et al., 2015 after Benson, 2009);
- Presence of a dorsoventral deep sulcus in the medial facet of the fibula (Tykoski & Rowe, 2004; Carrano & Sampson, 2008).

Still just based on the visual comparative analysis, ML352/SHN(JJS)065 shares the following synapomorphies with the genus *Ceratosaurus*:

- Dimorphism in the proximal femur trochanters (Malafaia et al., 2015 after Carrano & Sampson, 2008);
- Anterior trochanter not blade shaped (Mateus et al., 2006);
- Endocondylar ridge develops as a sharp ridge with striations along the medial edge (Malafaia et al., 2015 after Carrano & Sampson, 2008);
- Presence of popliteal ridge connecting both epicondyles on dorsal femur (Malafaia et al., 2015 after Benson, 2009);
- *Crista tibiofibularis* broad and obliquely expanded relative to femur shaft (Malafaia et al., 2015 after Carrano & Sampson, 2008);
- Lack of the lateral longitudinal groove at the distal end of the tibia (Mateus et al., 2006).
- Presence of small median dorsal osteoderms (Carrano & Sampson, 2008)

The new material here described also reinforces the assumption that both SHN(JJS)065 and ML352 material comes from the same individual. Malafaia et al., (2015) justified this by referring the similar shape and size of the bones, the proximity within the place of discover and the lack of duplicate bones from the same side of the body. The new fibulae material gives further proof: the shaft under SHN(JJS)065 seems the continuation of the new right fibula under ML352. Also, a new fibula piece came up and this one, being a mirror image of the other, is obviously from the left leg.

Specimen-based analysis

Across all six final trees (fig. 90), the specimen-based analysis is consensual with the placement of *Ceratosaurus* as the closest taxa to ML352/SHN(JJS)065. Variation occurs in which taxa is the closest one, with *C. dentisulcatus* being the closest in four trees and *C. magnicornis* in two. Considering the three North American species as valid, *C. nasicornis* seems less related to ML352/SHN(JJS)065 and *C. dentisulcatus* the closest.

Five mapped autapomorphies for ML352/SHN(JJS)065 are common across the six trees, distinguishing it from other *Ceratosaurus*:

88) character 580 in the original matrix, unfused tibiotarsus in adult; **130)** character 965 in the original matrix, narrow and longitudinal tibiofibular crest of the femur, **206)** character 1638 in the original matrix, anteroproximally curved fibular crest of the tibia, **210)** character 1685 in the original matrix, forked fibular crest of the tibia, and new character **263)** way distally expanded lateral *malleolus* of the tibia.

In trees C, D, E and F, where ML352/SHN(JJS)065 is sister-taxa to *C. dentisulcatus*, two additional autapomorphies were identified:

New character **262)** absence of nutrient foramina at the distal end of fibular crest of the tibia and new character **266)** curved and “S” shaped shaft of the fibula in anterior view.

The new character **260)** tibia/femur ratio more than 85%, is identified as a autapomorphy in trees A, B, D and F. In trees C and D one last autapomorphy is identified: **151)** character 1114 in the original matrix, mainly laterally directed cnemial crest of the tibia.

The total number of autapomorphies for ML352/SHN(JJS)065 across all six trees is nine (table 8), with tree D being the only one were all nine autapomorphies appear together.

	Trees					
	A	B	C	D	E	F
Autapomorphies	88	88	88	88	88	88
	130	130	130	130	130	130
	-	-	151	151	-	-
	206	206	206	206	206	206
	210	210	210	210	210	210
	260	260	-	260	-	260
	-	-	262	262	262	262
	263	263	263	263	263	263
	-	-	266	266	266	266

Table 8. Autapomorphies of ML352/SHN(JJS)065 identified for each of the six trees.

Should be noted that the only instances where ML352/SHN(JJS)065 confidently differs from the other three *Ceratosaurus* is in autapomorphic characters 88), 130) and 263); for the other five autapomorphies the coding for all taxa was not possible (either a specific bone was not preserved or the character in question could not be properly evaluated).

The specimen-based analysis corroborates previous comparative anatomy studies that found ML352/SHN(JJS)065 in close association to *Ceratosaurus* (Mateus & Antunes, 2000; Mateus et al., 2006; Malafaia et al., 2015),

In 2006, Mateus et al. found the Portuguese specimen more similar to *C. dentisulcatus* than to the other proposed species based on the position of the epiphyseal expansions and in the posterior intercondylar bridge of the femur. They also found similarities to the same species in some teeth collected in other localities of the Lourinhã Formation. However, the authors just noted the resemblance and didn't assign it to any concrete species, leaving it as *Ceratosaurus* sp. Malafaia et al., (2015) classified ML352/SHN(JJS)065 as *Ceratosaurus* aff. *Ceratosaurus nasicornis* (although considering *C. nasicornis* the only valid species).

The phylogenetic analysis place the Portuguese material closer to *C. dentisulcatus* than to *C. nasicornis*, but the results are not strong enough to confidently assign it in any known species, being this aggravated by fact that there is still no consensus regarding the validity of the American ones. For now we can only say that ML352/SHN(JJS)065 certainly belongs to the genus *Ceratosaurus* or, at least, to a very close, still unidentified, relative. Many genera of other typical Morrison dinosaur fauna ended up specializing in new forms in the Iberian Peninsula, it would not be surprising if that also occurred with *Ceratosaurus*, but the eventual naming of a new species still needs to be further discussed within the scientific community.

Regarding the North American species, the relationships between them are quite variable among the resulted trees and a solid consensus cannot be taken based in these results alone. Even if ML352/SHN(JJS)065 or the more fragmentary taxa (*Genyodectes* and MB R 3621-3626) are inactive, the result is still the same and inconclusive.

The validity of the *Ceratosaurus* species, *C. dentisulcatus* and *C. magnicornis*, proposed by Madsen and Welles (2000) has been questioned by other authors (Rauhut, 2000; Carrano & Sampson, 2008) stating that the main arguments for assigning these two new species are subjective and size-related and that the differences found should probably reflect individual and/or ontogenetic variation.

The work of Madsen and Welles (2000) and the phylogenetic specimen-based analysis here conducted revealed several non-sized related anatomical differences between the different North American *Ceratosaurus* holotypes. Although the results regarding the interrelationships between these taxa are inconclusive, these several differences should not be disregarded and the validity of these *Ceratosaurus* species is within the realm of possibility. It should be noted that there have been instances where generic and specific variation was accepted based just on few hindlimb characters, such as the distinction within Lagerpetidae taxa *Lagerpeton* and *Dromomeron* (Irmis et al., 2007; Nesbitt et al., 2009).

If the American *Ceratosaurus* material really represents three different species (instead of ontogenetic variation), and all the individuals are all fully grown, then we can see an increase in size from the smaller and oldest *C. nasicornis* to the largest and more recent *C. dentisulcatus*. This scenario is difficult to corroborate with just a few specimens, however this trend is common in Archosauria and has been previously observed in instances with few sampled specimens (O'Gorman & Hone, 2012; Martínez et al., 2016).

Nonetheless, the analysis here presented laid the foundations for future work regarding the relationships within *Ceratosaurus*, with the possibility of this matrix being updated with more info and perhaps include some of the still undescribed specimens.

Regarding the other taxa, *Genyodectes* is the sister taxa to *Ceratosaurus* and ML352/SHN(JJS)065 in half of the trees, whereas Tendaguru MB R 3621-3626 is in the other half. Although this solidifies their position within Ceratosauria, it should be noted that these taxa are too fragmented and these results should be interpreted with caution. *Genyodectes* has previously been found in close association with *Ceratosaurus*, forming the clade Ceratosauridae (Rauhut, 2004; Delcourt, 2018) but MB R 3621-3626 has been interpreted as a more derived form, closer to abelisaurids (Rauhut, 2011). Nonetheless, MB R 3621-3626 is found in close association with *Majungasaurus* in half of the trees in this analysis which hints to its close relationship with Abelisauoidea.

All trees retrieve *Majungasaurus* as not closely related to *Ceratosaurus*, expressing the more derived condition of Abelisauridae relative to Ceratosauridae.

Ontogeny

Regarding the ontogeny of ML352/SHN(JJS)065, some features of the fossil point out to a mature individual, namely, the cervical vertebra with the neurocentral suture totally fused and obliterated.

Brochu (1996) described the ontogenetic development of these sutures in living crocodylians, where most of the caudal vertebrae fuse even before hatching and the cervical vertebrae are the last to fuse in later ontogenetic stages. The author points out that this fact might be useful to infer maturity in fossil taxa akin to crocodiles but also leaves the warning that among other living reptiles (turtles and squamates) the neurocentral suture fuses the other way around, anteriorly to posteriorly, so conclusions must be taken with care.

Heinrich et al., (2021) took this approach on rhynchosaurs (Archosauromorpha) in the clade Hyperodapedontinae and found out that the neurocentral suture development in this group is also anterior to posterior, inverse to crocodylians. The authors even show that some sutures did not close at all, even in latter stages of life, being the cervicals the only ones that fully closed in this group. This contrasts with early diverging rhynchosaurs where all suture lines close during ontogeny. So, the authors concluded that using neurocentral suture lines to infer ontogeny must be taken with care because the patterns might change for different animal clades.

The vertebrae fusion pattern is a process still misunderstood for dinosaurs. Within Ceratosauria for example, O'Connor (2007) points out that in *Majungasaurus crenatissimus* the fusion pattern of postcervical vertebrae is quite variable and non-linear. One possible immature individual, for example, has the cervical series totally coossified, but the postcervicals are variably fused: with anterior-most dorsals semi-fused and posterior ones unfused, sacrals with both conditions and caudals (only the first five) gradually fusing posteriorly. Sometimes the pattern is even asymmetrical, with the same vertebra having both states. Despite this, O'Connor (2007) considers the general ossification trend in *Majungasaurus* as anteriorly to posteriorly, and more similar to non-archosaur reptiles than to crocodiles. Based on this, and considering the phylogenetic proximity between *Majungasaurus* and *Ceratosaurus*, ML352/SHN(JJS)065 although having a fused cervical could still be an immature individual. Nonetheless, since the vertebrae fusion pattern can vary considerably among Sauropsida, and most in-depth studies were only made for crocodylians, more research is required before could be confidently applied to dinosaurs (Breedon III & Rowe, 2020).

The pattern of ossification in *Ceratosaurus* can be variable in other regions of the body too and even between individuals. Gilmore (1920) stated that the fusion in the pelvic region and metatarsals in *C. nasicornis* suggests a mature individual, however the same individual lacks fusion in the carpals and cervical ribs (*C. magnicornis* and *C. dentisulcatus* ribs are fused).

If we consider all the *Ceratosaurus* individuals as the same species, the body size must also be taken into account. Mateus et al. (2006) used the femur to estimate a weight of 560kg for ML352/SHN(JJS)065, finding it within the values expected for the other *Ceratosaurus*. Malafaia et al., (2015) compared the femur length of the Portuguese specimen with the main North American ones, and, with 650mm, is the second largest, being only surpassed by *C. dentisulcatus* with 759mm. However, even being the second largest, is closer in size to the smaller ones, with *C. nasicornis* at 620mm and *C. magnicornis* at 630mm. If all these individuals really represent different ontogenetic stages of the same species, the Portuguese specimen might have been not fully grown when it died.

These size differences however do not reflect a pattern in the ossification: ML352/SHN(JJS)065 is the second largest when compared with the North American *Ceratosaurus* holotypes but is the only one where the astragalocalcaneum fusion to the tibia does not occur.

Some mention must also be made to the osteoderm, whose size and ossification level might also give ontogenetic clues. This osteoderm, more than 100 mm in length, is bigger than the ones described by Gilmore (1920) for *C. nasicornis* (the longest being 70mm) and, based by the pictures, bigger than the ones reported by Madsen and Welles (2000, fig. 8) for *C. dentisulcatus*. The rugosity of this osteoderm is also much more intricate than the ones compared from North America. However, the shape, size and extent of the complete bony armor set on the living animal is still not fully understood due to either incompleteness or disarticulation of the remains (Gilmore, 1920; Madsen & Welles, 2000).

In general, ontogeny is difficult to address in extinct archosaurs, with factors such as individual variation, sexual dimorphism or even taphonomic distortion being able to condition our interpretations (Nesbitt et al., 2009), so, any conclusions regarding the data presented here should take this into consideration.

Conclusions

The presence of the theropod genus *Ceratosaurus* in Portugal is reinforced with additional diagnostic material here reported for the first time (cervical vertebra, fibulae and an osteoderm) and by a phylogenetic specimen-based analysis.

Although the complete material is associated to different institutions, some of the new elements still support the fact that all bones belong to the same individual.

The animal is within the size range of the smaller North American specimens, however the ontogenetic stage is difficult to determine at this point.

The most in-depth phylogenetic study on the *Ceratosaurus*, with 37 new anatomical characters, gave some light on the interrelationships between this genus and its closer relatives and created the basis for future works regarding these taxa.

References cited

Chapter I - Early theropod from the Triassic of Grés de Silves

- Alcober, O. A., & Martinez, R. N. (2010). A new herrerasaurid (Dinosauria, Saurischia) from the Upper Triassic Ischigualasto formation of northwestern Argentina. *ZooKeys*, 19, 55-81.
- Andrews, C. W. (1921). On some remains of a theropodous dinosaur from the Lower Lias of Barrow-on-Soar. *Annals and Magazine of Natural History* 8: 570-576.
- Antunes, M. T., & Mateus, O. (2003). Dinosaurs of Portugal. *Comptes Rendus Palevol*, 2(1), 77-95.
- Antunes, M. T., & Sigogneau-Russell, D. (1991). Nouvelles données sur les Dinosaures du Crétacé supérieur du Portugal. *Comptes rendus de l'Académie des sciences. Série 2, Mécanique, Physique, Chimie, Sciences de l'univers, Sciences de la Terre*, 313(1), 113-119.
- Araújo, R., Castanhinha, R., Martins, R. M., Mateus, O., Hendrickx, C., Beckmann, F., Schell, N., & Alves, L. C. (2013). Filling the gaps of dinosaur eggshell phylogeny: Late Jurassic Theropod clutch with embryos from Portugal. *Scientific Reports*, 3(1), 1924.
- Arcucci, A. B., & Coria, R. A. (2003). A new Triassic carnivorous dinosaur from Argentina. *Ameghiniana*, 40(2), 217-228.
- Azerêdo, A. C., Duarte, L. V., Henriques, M. H., & Manuppella, G. (2003). Da dinâmica continental no Triásico aos mares do Jurássico Inferior e Médio. *Cadernos de Geologia de Portugal, Instituto Geológico e Mineiro*: 43pp.
- Bakker, R. T. (1986). *The dinosaur heresies*. 481 p. Avon: Bath Press.
- Baron, M. G., Norman, D. B., & Barrett, P. M. (2017). A new hypothesis of dinosaur relationships and early dinosaur evolution. *Nature*, 543(7646), 501-506.
- Baron, M. G., & Williams, M. E. (2018). A re-evaluation of the enigmatic dinosauriform *Caseosaurus crosbyensis* from the Late Triassic of Texas, USA and its implications for early dinosaur evolution. *Acta Palaeontologica Polonica*, 63(1).
- Benton, M. J. (1991). What really happened in the Late Triassic?. *Historical Biology*, 5(2-4), 263-278.
- Benton, M. J. (1993). Late Triassic extinctions and the origin of the dinosaurs. *Science*, 260(5109), 769-770.
- Benton, M. J. (2016). The Triassic. *Current Biology*, 26(23), R1214-R1218.
- Benton, M. J., Juul, L., Storrs, G. W., & Galton, P. M. (2000). Anatomy and systematics of the prosauropod dinosaur *Thecodontosaurus antiquus* from the Upper Triassic of southwest England. *Journal of Vertebrate Paleontology*, 20(1), 77-108.
- Blackburn, T. J., Olsen, P. E., Bowring, S. A., McLean, N. M., Kent, D. V., Puffer, J., McHone, G., Rasbury, E. T., & Et-Touhami, M. (2013). Zircon U-Pb geochronology links the end-Triassic extinction with the Central Atlantic Magmatic Province. *Science*, 340(6135), 941-945.
- Bonaparte Jose, F., Jorge, F., & Maria, R. A. (1999). A new early Late Triassic saurischian dinosaur from Rio Grande do Sul state, Brazil. *National Science Museum Monographs*, 15, 89-109.
- Brinkman, D. B., & Sues, H. D. (1987). A staurikosaurid dinosaur from the Upper Triassic Ischigualasto Formation of Argentina and the relationships of the Staurikosauridae. *Palaeontology*, 30(3), 493-503.
- Bristowe, A., & Raath, M. A. (2004). A juvenile coelophysoid skull from the Early Jurassic of Zimbabwe, and the synonymy of *Coelophysis* and *Syntarsus*. *Palaeontologia africana*, 40(40), 31-41.
- Brusatte, S. L., Benton, M. J., Desojo, J. B., & Langer, M. C. (2010). The higher-level phylogeny of Archosauria (Tetrapoda: Diapsida). *Journal of Systematic Palaeontology*, 8(1), 3-47.

- Brusatte, S. L., Butler, R. J., Mateus, O., & Steyer, J. S. (2015). A new species of *Metoposaurus* from the Late Triassic of Portugal and comments on the systematics and biogeography of metoposaurid temnospondyls. *Journal of Vertebrate Paleontology*, 35(3), e912988.
- Cabreira, S. F., Kellner, A. W. A., Dias-da-Silva, S., da Silva, L. R., Bronzati, M., de Almeida Marsola, J. C., Müller, R. T., de Souza Bittencourt, J., Batista, B. J. A., Raugust, T., Carrilho, R., Brodt, A., & Langer, M. C. (2016). A unique Late Triassic dinosauromorph assemblage reveals dinosaur ancestral anatomy and diet. *Current Biology*, 26(22), 3090-3095.
- Carpenter, K. (1997). A giant coelophysoid (Ceratosauria) theropod from the Upper Triassic of New Mexico, USA. *Neues Jahrbuch für Geologie und Paläontologie, Abhandlungen*, 205: 189-208.
- Carrano, M. T., Benson, R. B., & Sampson, S. D. (2012). The phylogeny of tetanurae (Dinosauria: Theropoda). *Journal of Systematic Palaeontology*, 10(2), 211-300.
- Carrano, M. T., Hutchinson, J. R., & Sampson, S. D. (2005). New information on *Segisaurus halli*, a small theropod dinosaur from the Early Jurassic of Arizona. *Journal of Vertebrate Paleontology*, 25(4), 835-849.
- Carrano, M. T., & Sampson, S. D. (2004). A review of coelophysoids (Dinosauria: Theropoda) from the Lower Jurassic of Europe, with comments on the late history of the Coelophysoidea. *Neues Jahrbuch für Geologie und Paläontologie, Monatshefte* 9: 537-558.
- Carrano, M. T., & Sampson, S. D. (2008). The phylogeny of Ceratosauria (Dinosauria: Theropoda). *Journal of Systematic Palaeontology*, 6(2), 183-236.
- Cau, A. (2018). The assembly of the avian body plan: a 160-million-year long process. *Bollettino della Società Paleontologica Italiana*, 57(1), 2
- Chatterjee, S. (1993). An Unusual Theropod Dinosaur from the Triassic of Texas. *Research and Exploration*, 9, 274-274.
- Choffat, P. (1887). Recherches sur les terrains secondaires au Sud du Sado. *Comissão dos Trabalhos Geológicos de Portugal 1*: 222-312.
- Choffat, P. (1894). Notice stratigraphique sur les gisements de végétaux fossiles dans le Mésozoïque du Portugal. *Memórias dos Serviços Geológicos de Portugal*, 229-282.
- Colbert, E. H., Price, L. I., & White, T. E. (1970). A saurischian dinosaur from the Triassic of Brazil. *American Museum novitates*; no. 2405.
- Colbert, E. (1989). "The Triassic Dinosaur *Coelophysis*". *Museum of Northern Arizona Bulletin*. 57: 160.
- Cope, E. D. (1887). The dinosaurian genus *Coelurus*. *American Naturalist*, 21(5), 367-369.
- Cope, E. D. (1889). On a new genus of Triassic Dinosauria. *American Naturalist*, 23(271), 626.
- Courbouleix, S. (1974). Étude géologique des régions de Anadia et de Mealhada. I – Le socle, le Primaire et le Trias. *Comunicações dos Serviços Geológicos de Portugal, Lisboa*, 58, 5–37.
- Cuny, G., & Galton, P. M. (1993). Revision of the Airel theropod dinosaur from the Triassic-Jurassic boundary (Normandy, France). *Neues Jahrbuch für Geologie und Paläontologie. Abhandlungen*, 187(3), 261-288.
- Dantas, P., Santos, V. F., Lockley, M. G., & Meyer, C. A. (1994). Footprint evidence for limping dinosaurs from the Upper Jurassic of Portugal. *Gaia*, 10, 43-48.
- Ezcurra, M. D. (2010). A new early dinosaur (Saurischia: Sauropodomorpha) from the Late Triassic of Argentina: a reassessment of dinosaur origin and phylogeny. *Journal of Systematic Palaeontology*, 8(3), 371-425.
- Ezcurra, M. D. (2016). The phylogenetic relationships of basal archosauromorphs, with an emphasis on the systematics of proterosuchian archosauriforms. *PeerJ*, 4, e1778.

- Ezcurra, M. D., & Brusatte, S. L. (2011). Taxonomic and phylogenetic reassessment of the early neotheropod dinosaur *Camposaurus arizonensis* from the Late Triassic of North America. *Palaeontology*, 54(4), 763-772.
- Ezcurra, M. D., & Butler, R. J. (2018). The rise of the ruling reptiles and ecosystem recovery from the Permo-Triassic mass extinction. *Proceedings of the Royal Society B*, 285(1880), 20180361.
- Ezcurra, M. D., Butler, R. J., Maidment, S. C., Sansom, I. J., Meade, L. E., & Radley, J. D. (2020). A revision of the early neotheropod genus *Sarcosaurus* from the Early Jurassic (Hettangian–Sinemurian) of central England. *Zoological Journal of the Linnean Society*, 191(1), 113-149.
- Ezcurra, M. D., & Cuny, G. (2007). The coelophysoid *Lophostropheus airelensis*, gen. nov.: a review of the systematics of “*Liliensternus*” *airelensis* from the Triassic–Jurassic outcrops of Normandy (France). *Journal of Vertebrate Paleontology*, 27(1), 73-86.
- Ezcurra, M. D., Marke, D., Walsh, S. A., & Brusatte, S. L. (2023). A revision of the ‘coelophysoid-grade’ theropod specimen from the Lower Jurassic of the Isle of Skye (Scotland). *Scottish Journal of Geology*, 59(1-2), sjg2023-012.
- Ezcurra, M. D., & Novas, F. E. (2007). Phylogenetic relationships of the Triassic theropod *Zupaysaurus rougieri* from NW Argentina. *Historical Biology*, 19(1), 35-72.
- Ezcurra, M. D., Nesbitt, S. J., Fiorelli, L. E., & Desojo, J. B. (2020). New specimen sheds light on the anatomy and taxonomy of the early Late Triassic dinosauriforms from the Chañares Formation, NW Argentina. *The Anatomical Record*, 303(5), 1393-1438.
- Fraas, E. (1913). Die neuesten Dinosaurierfunde in der schwäbischen Trias. *Naturwissenschaften*, 1(45), 1097-1100.
- Gauthier, J. (1986). Saurischian monophyly and the origin of birds. *Memoirs of the California Academy of sciences*, 8, 1-55.
- Goloboff, P., & Morales, M. (2022). TNT version 1.6, with a graphical interface for MacOs and Linux, including new routines in parallel (forthcoming).
- Griffin, C. T. (2019). Large neotheropods from the Upper Triassic of North America and the early evolution of large theropod body sizes. *Journal of Paleontology*, 93(5), 1010-1030.
- Heeren, F. (2011). Rise of the titans: the sauropods were the biggest creatures ever to walk the planet. But the keys to their success emerged in their tiny ancestors. *Nature*, 475(7355), 159-162.
- Hendrickx, C., Bell, P. R., Pittman, M., Milner, A. R., Cuesta, E., O'Connor, J., Loewen, M., Currie, P. J., Mateus, O., Kaye, T. G., & Delcourt, R. (2022). Morphology and distribution of scales, dermal ossifications, and other non-feather integumentary structures in non-avian theropod dinosaurs. *Biological Reviews*, 97(3), 960-1004.
- Hendrickx, C., Hartman, S. A., & Mateus, O. (2015). An overview of non-avian theropod discoveries and classification. *PalArch's Journal of Vertebrate Palaeontology*, 12(1).
- Hendrickx, C., & Mateus, O. (2014). *Torvosaurus gurneyi* n. sp., the largest terrestrial predator from Europe, and a proposed terminology of the maxilla anatomy in nonavian theropods. *PLoS one*, 9(3), e88905.
- Holtz, T. R. (1994). The phylogenetic position of the Tyrannosauridae: implications for theropod systematics. *Journal of Paleontology*, 68(5), 1100-1117.
- Huene, F. V. (1932). Die fossil Reptil-Ordnung Saurischia, ihre Entwicklung und Geschichte. *Monographien zur Geologie und Palaeontologie (Serie 1)*, 4: 1-361.
- Hugi, J. C. (2008). *The Axial and Posterior Appendicular Morphology of the First Theropod Skeleton (Saurischia, Dinosauria) of Switzerland (Late Triassic; Frick, Canton Aargau)*. 161pp. Master's Thesis, Paleontological Institute and Museum of the University of Zurich.
- Ivie, M. A., Slipinski, S. A., & Wegrzynowicz, P. (2001). Generic homonyms in the Colydiinae (Coleoptera: Zopheridae). *Insecta Mundi*, 184.

- Jaekel, O. (1913). Über die Wirbeltierfunde in der oberen Trias von Halberstadt. *Paläontologische Zeitschrift*, 1(1), 155-215.
- Jones, A. S., & Butler, R. J. (2018). A new phylogenetic analysis of Phytosauria (Archosauria: Pseudosuchia) with the application of continuous and geometric morphometric character coding. *PeerJ*, 6, e5901.
- Knoll, F. (2008). On the *Procompsognathus* postcranium (Late Triassic, Germany). *Geobios*, 41(6), 779-786.
- Langer, M. C., Ezcurra, M. D., Rauhut, O. W., Benton, M. J., Knoll, F., McPhee, B. W., Novas, F. E., Pol, D. & Brusatte, S. L. (2017). Untangling the dinosaur family tree. *Nature*, 551(7678), E1-E3.
- Langer, M. C., McPhee, B. W., Marsola, J. C. D. A., Roberto-da-Silva, L., & Cabreira, S. F. (2019). Anatomy of the dinosaur *Pampadromaeus barberenai* (Saurischia—Sauropodomorpha) from the Late Triassic Santa Maria Formation of southern Brazil. *PloS one*, 14(2), e0212543.
- Lapparent, A. F., & Zbyszewski, G. (1957). Les dinosauriens du Portugal. *Mémoires des Services Géologiques du Portugal, Nouvelle Série 2*: 1–63.
- Larsonneur, C., & Lapparent, A. F. D. (1966). Un dinosaurien carnivore, *Halticosaurus*, dans le Réthien d'Airel (Manche). *Bulletin Société Linnéenne de Normandie*, 10, 108-116.
- Madsen, J. H., & Welles, S. P. (2000). *Ceratosaurus* (Dinosauria, Theropoda): a revised osteology. *Utah Geological Survey, Miscellaneous Publications 00-2*: 1-80.
- Malafaia, E., Escaso, F., Mocho, P., Serrano-Martínez, A., Torices, A., Cachão, M., & Ortega, F. (2017a). Analysis of diversity, stratigraphic and geographical distribution of isolated theropod teeth from the Upper Jurassic of the Lusitanian Basin, Portugal. *Journal of Iberian Geology*, 43, 257-291.
- Malafaia, E., Mocho, P., Escaso, F., Dantas, P., & Ortega, F. (2019). Carcharodontosaurian remains (Dinosauria, Theropoda) from the Upper Jurassic of Portugal. *Journal of Paleontology*, 93(1), 157-172.
- Malafaia, E., Mocho, P., Escaso, F., & Ortega, F. (2017b). A juvenile allosauroid theropod (Dinosauria, Saurischia) from the Upper Jurassic of Portugal. *Historical Biology*, 29(5), 654-676.
- Malafaia, E., Mocho, P., Escaso, F., & Ortega, F. (2017c). New data on the anatomy of *Torvosaurus* and other remains of megalosauroid (Dinosauria, Theropoda) from the Upper Jurassic of Portugal. *Journal of Iberian Geology*, 43, 33-59.
- Malafaia, E., Mocho, P., Escaso, F., & Ortega, F. (2020). A new carcharodontosaurian theropod from the Lusitanian Basin: evidence of allosauroid sympatry in the European Late Jurassic. *Journal of Vertebrate Paleontology*, 40(1), e1768106.
- Malafaia, E., Ortega, F., Escaso, F., Dantas, P., Pimentel, N., Gasulla, J. M., Ribeiro, B., Barriga, F., & Sanz, J. L. (2010). Vertebrate fauna at the *Allosaurus* fossil-site of Andrés (Upper Jurassic), Pombal, Portugal. *Journal of Iberian Geology*, 36(2), 193-204.
- Malafaia, E., Ortega, F., Escaso, F., & Silva, B. (2015). New evidence of *Ceratosaurus* (Dinosauria: Theropoda) from the Late Jurassic of the Lusitanian Basin, Portugal. *Historical Biology*, 27(7), 938-946.
- Manuppella, G. (1988). Litoestratigrafia e tectonica da bacia algarvia Lithostratigraphie et tectonique dans le bassin sédimentaire de l'Algarve. *Geonovas*, (10), 67-71.
- Marsh, A. D., Parker, W. G., Langer, M. C., & Nesbitt, S. J. (2019). Redescription of the holotype specimen of *Chindesaurus bryansmalli* Long and Murry, 1995 (Dinosauria, Theropoda), from Petrified Forest National Park, Arizona. *Journal of Vertebrate Paleontology*, 39(3), e1645682.
- Marsh, A. D., & Rowe, T. B. (2020). A comprehensive anatomical and phylogenetic evaluation of *Dilophosaurus wetherilli* (Dinosauria, Theropoda) with descriptions of new specimens from the Kayenta Formation of northern Arizona. *Journal of Paleontology*, 94(S78), 1-103.
- Martill, D. M., Vidovic, S. U., Howells, C., & Nudds, J. R. (2016). The oldest Jurassic dinosaur: a basal neotheropod from the Hettangian of Great Britain. *PLoS One*, 11(1), e0145713.

- Martinez, R. N., & Alcober, O. A. (2009). A basal sauropodomorph (Dinosauria: Saurischia) from the Ischigualasto Formation (Triassic, Carnian) and the early evolution of Sauropodomorpha. *PLoS One*, 4(2), e4397.
- Martínez, R. N., & Apaldetti, C. (2017). A Late Norian—Rhaetian Coelophysid Neotheropod (Dinosauria, Saurischia) from the Quebrada Del Barro Formation, Northwestern Argentina. *Ameghiniana*, 54(5), 488-505.
- Martinez, R. N., Sereno, P. C., Alcober, O. A., Colombi, C. E., Renne, P. R., Montañez, I. P., & Currie, B. S. (2011). A basal dinosaur from the dawn of the dinosaur era in southwestern Pangaea. *Science*, 331(6014), 206-210.
- Mateus, I., Mateus, H., Antunes, M. T., Mateus, O., Taquet, P., Ribeiro, V., & Manuppella, G. (1998). Upper Jurassic theropod dinosaur embryos from Lourinhã (Portugal). *Memórias da Academia das Ciências de Lisboa* 37: 101-109.
- Mateus, O. (1998). *Lourinhanosaurus antunesi*, a new upper Jurassic allosauroid (Dinosauria: Theropoda) from Lourinhã, Portugal. *Memórias da Academia de Ciências de Lisboa*, 37(1998), 111-124.
- Mateus, O., & Antunes, M. T. (2000). *Ceratosaurus* sp.(Dinosauria: Theropoda) in the Late Jurassic of Portugal. In *31st International Geological Congress*. Rio de Janeiro, Brazil.
- Mateus, O., Antunes, M. T., & Taquet, P. (2001). Dinosaur ontogeny: the case of *Lourinhanosaurus* (Late Jurassic Portugal). *Journal of Vertebrate Paleontology*, 21(3), 78A.
- Mateus, O., Butler, R. J., Brusatte, S. L., Whiteside, J. H., & Steyer, J. S. (2014). The first phytosaur (Diapsida, Archosauriformes) from the Late Triassic of the Iberian Peninsula. *Journal of Vertebrate Paleontology*, 34(4), 970-975.
- Mateus, O., & Estraviz-López, D. (2022). A new theropod dinosaur from the early cretaceous (Barremian) of Cabo Espichel, Portugal: Implications for spinosaurid evolution. *PLoS One*, 17(2), e0262614.
- Mateus, O., & Milàn, J. (2010). A diverse Upper Jurassic dinosaur ichnofauna from central-west Portugal. *Lethaia*, 43(2), 245-257.
- Mateus, O., Walen, A., & Antunes, M. T. (2006). The large theropod fauna of the Lourinhã Formation (Portugal) and its similarity to that of the Morrison Formation with a description of a new species of *Allosaurus*. *New Mexico Museum of Natural History and Science, Bulletin* 36: 123–129.
- McDavid, S. N., & Bugos, J. E. (2022). Taxonomic notes on *Megapnosaurus* and 'Syntarsus' (Theropoda: Coelophysidae). *The Mosasaur*, 12, 1–5.
- Müller, R. T., Langer, M. C., Bronzati, M., Pacheco, C. P., Cabreira, S. F., & Dias-Da-Silva, S. (2018). Early evolution of sauropodomorphs: anatomy and phylogenetic relationships of a remarkably well-preserved dinosaur from the Upper Triassic of southern Brazil. *Zoological Journal of the Linnean Society*, 184(4), 1187-1248.
- Müller, R. T., & Garcia, M. S. (2020). A paraphyletic 'Silesauridae' as an alternative hypothesis for the initial radiation of ornithischian dinosaurs. *Biology Letters*, 16(8), 20200417.
- Nesbitt, S. (2007). The anatomy of *Effigia okeeffeae* (Archosauria, Suchia), theropod-like convergence, and the distribution of related taxa. *Bulletin of the American Museum of Natural history*, 302, 1-84.
- Nesbitt, S. (2011). "The Early Evolution of Archosaurs: Relationships and the Origin of Major Clades," *Bulletin of the American Museum of Natural History*, 352, 1-292.
- Nesbitt, S. J., & Ezcurra, M. D. (2015). The early fossil record of dinosaurs in North America: a new neotheropod from the base of the Upper Triassic Dockum Group of Texas. *Acta Palaeontologica Polonica*, 60(3), 513-526.
- Nesbitt, S. J., Irmis, R. B., & Parker, W. G. (2007). A critical re-evaluation of the Late Triassic dinosaur taxa of North America. *Journal of Systematic Palaeontology*, 5(2), 209-243.
- Nesbitt, S. J., Langer, M. C., & Ezcurra, M. D. (2020). The anatomy of *Asilisaurus kongwe*, a dinosauriform from the Lifu Member of the Manda Beds (Middle Triassic) of Africa. *The Anatomical Record*, 303(4), 813-873.

- Nesbitt, S. J., Sidor, C. A., Irmis, R. B., Angielczyk, K. D., Smith, R. M., & Tsuji, L. A. (2010). Ecologically distinct dinosaurian sister group shows early diversification of Ornithodira. *Nature*, *464*(7285), 95-98.
- Nesbitt, S. J., Smith, N. D., Irmis, R. B., Turner, A. H., Downs, A., & Norell, M. A. (2009). A complete skeleton of a Late Triassic saurischian and the early evolution of dinosaurs. *Science*, *326*(5959), 1530-1533.
- Nomade, S., Knight, K. B., Beutel, E., Renne, P. R., Verati, C., Féraud, G., Marzoli, A., Youbi, N., & Bertrand, H. (2007). Chronology of the Central Atlantic Magmatic Province: implications for the Central Atlantic rifting processes and the Triassic–Jurassic biotic crisis. *Palaeogeography, Palaeoclimatology, Palaeoecology*, *244*(1-4), 326-344.
- Norman, D. B., Baron, M. G., Garcia, M. S., & Müller, R. T. (2022). Taxonomic, palaeobiological and evolutionary implications of a phylogenetic hypothesis for Ornithischia (Archosauria: Dinosauria). *Zoological Journal of the Linnean Society*, *196*(4), 1273-1309
- Novas, F. E. (1992). Phylogenetic relationships of the basal dinosaurs, the Herrerasauridae. *Palaeontology*, *35*(1), 51-62.
- Novas, F. E. (1994). New information on the systematics and postcranial skeleton of *Herrerasaurus ischigualastensis* (Theropoda: Herrerasauridae) from the Ischigualasto Formation (Upper Triassic) of Argentina. *Journal of Vertebrate Paleontology*, *13*(4), 400-423.
- Novas, F. E., Ezcurra, M. D., Chatterjee, S., & Kutty, T. S. (2010). New dinosaur species from the Upper Triassic Upper Maleri and Lower Dharmaram formations of central India. *Earth and Environmental Science Transactions of the Royal Society of Edinburgh*, *101*(3-4), 333-349.
- Novas, F. E., Agnolin, F. L., Ezcurra, M. D., Müller, R. T., Martinelli, A. G., & Langer, M. C. (2021). Review of the fossil record of early dinosaurs from South America, and its phylogenetic implications. *Journal of South American Earth Sciences*, *110*, 103341.
- Olsen, P. E., Shubin, N. H., & Anders, M. H. (1987). New Early Jurassic tetrapod assemblages constrain Triassic–Jurassic tetrapod extinction event. *Science*, *237*(4818), 1025-1029.
- Pacheco, C., Müller, R. T., Langer, M., Pretto, F. A., Kerber, L., & da Silva, S. D. (2019). *Gnathovorax cabreirai*: a new early dinosaur and the origin and initial radiation of predatory dinosaurs. *PeerJ*, *7*, e7963.
- Palain, C. (1976). Une série détritique terrigène les " Grès de Silves": Trias et Lias inférieur du Portugal. *Memórias dos Serviços Geológicos de Portugal, Nova Série*, *25*: 377pp.
- Palain, C. (1977). Age et paléogéographie de la base du Mésozoïque (Série des " Grès de Silves») de l'Algarve-Portugal méridional. *Cuadernos de geología ibérica*, *4*: 259-268.
- Palain, C. (1979). Connaissances stratigraphiques sur la base du Mésozoïque portugais. *Ciências da Terra/Earth Sciences Journal*, *5*.
- Paul, G. S. (1988). *Predatory dinosaurs of the world*. Simon & Schuster, New York
- Paul, G. S. (2002). *Dinosaurs of the air: the evolution and loss of flight in dinosaurs and birds*. Johns Hopkins University Press, Baltimore.
- Pereira, M. F., Ribeiro, C., Gama, C., Drost, K., Chichorro, M., Vilallonga, F., Hoffmann, M., & Linnemann, U. (2017). Provenance of upper Triassic sandstone, southwest Iberia (Alentejo and Algarve basins): tracing variability in the sources. *International Journal of Earth Sciences*, *106*, 43-57.
- Pérez-Moreno, B. P., Chure, D. J., Pires, C., Marques da Silva, C., Dos Santos, V., Dantas, P., Póvoas, L., Cachão, M., Sanz, J. L., & Galopim de Carvalho, A. M. (1999). On the presence of *Allosaurus fragilis* (Theropoda: Carnosauria) in the Upper Jurassic of Portugal: first evidence of an intercontinental dinosaur species. *Journal of the Geological Society*, *156*(3), 449-452.
- Piechowski, R., & Dzik, J. (2010). The axial skeleton of *Silesaurus opolensis*. *Journal of Vertebrate Paleontology*, *30*(4), 1127-1141.

- Pol, D., Otero, A., Apaldetti, C., & Martínez, R. N. (2021). Triassic sauropodomorph dinosaurs from South America: The origin and diversification of dinosaur dominated herbivorous faunas. *Journal of South American Earth Sciences*, 107, 103145.
- Raath, M. A. (1969). *A new coelurosaurian dinosaur from the Forest Sandstone of Rhodesia*. National Museums of Rhodesia.
- Rauhut, O. W. (1997). On the cranial anatomy of *Shuvosaurus inexpectatus* (Dinosauria; Theropoda). *Terra Nostra*, 7, 1-4.
- Rauhut, O. W. M. (2000). *The Interrelationships and Evolution of Basal Theropods (Dinosauria, Saurischia)*. 583 pp. PhD thesis, University of Bristol.
- Rauhut, O. W. (2003). A tyrannosauroid dinosaur from the Upper Jurassic of Portugal. *Palaeontology*, 46(5), 903-910.
- Rauhut, O. W., & Hungerbühler, A. (1998). A review of European Triassic theropods. *GAIA: revista de geociências*, 15, 75-88.
- Rinehart, L. F., Lucas, S. G., Heckert, A. B., Spielmann, J. A., & Celeskey, M. D. (2009). *The Paleobiology of Coelophysis bauri (Cope) from the Upper Triassic (Apachean) Whitaker quarry, New Mexico, with detailed analysis of a single quarry block: Bulletin 45 (Vol. 45)*. New Mexico Museum of Natural History and Science.
- Rocha, R. B., (1976). Estudo estratigráfico e paleontológico do Jurássico do Algarve ocidental. *Ciências Terra (UNL)* 2: 1-178.
- Rocha, R. B., Marques, J., & Soares, A. F. (1990). Les unités lithostratigraphiques du Bassin Lusitanien au Nord de l'accident de Nazaré (Trias-Aalénien). *Cahiers Univ. Cath. Lyon, ser. Scy. Lyon*, 4, 121-126.
- Romano, M., Bernardi, M., Petti, F. M., Rubidge, B., Hancox, J., & Benton, M. J. (2020). Early Triassic terrestrial tetrapod fauna: a review. *Earth-Science Reviews*, 210, 103331.
- Rowe, T. (1989). A new species of the theropod dinosaur *Syntarsus* from the Early Jurassic Kayenta Formation of Arizona. *Journal of Vertebrate Paleontology*, 9(2), 125-136.
- Ruciński, M. R. (2020). *Novel Placodont Material and Palaeoenvironment Analysis of Triassic Deposits of Rocha da Pena (Algarve, Southern Portugal)*. 104 pp. Msc Dissertation, NOVA School of Science and Technology, Lisboa,.
- Russel, D., & Russel, D. (1977). Premiers résultats d'une prospection paléontologique dans le Trias de l'Algarve (Portugal). *Ciências da Terra/Earth Sciences Journal (UNL Lisboa)* 3: 167-178.
- Sahney, S., & Benton, M. J. (2008). Recovery from the most profound mass extinction of all time. *Proceedings of the Royal Society B: Biological Sciences*, 275(1636), 759-765.
- Sander, P. M., Christian, A., Clauss, M., Fechner, R., Gee, C. T., Griebeler, E. M., Gunga, H. C., Hummel, J., Mallison, H., Perry, S. F., Preuschoft, H., Rauhut, O. W. M., Remes, K., Tütken, T., Wings, O. & Witzel, U. (2011). Biology of the sauropod dinosaurs: the evolution of gigantism. *Biological Reviews*, 86(1), 117-155.
- Santos, V. F., Berrocal-Casero, M., Callapez, P. M., Cunha, P. P., Dinis, P. A., Malafaia, E., Juanas, S. O., Pimentel, R. J., & Pinto, J. S. (2024). First theropod footprint identified in the middle Kimmeridgian of Buarcos (West Central Portugal): scientific and educational implications. *Historical Biology*, 1-11.
- Santos, V. F., Lockley, M. G., Meyer, C. A., Carvalho, J., Galopim de Carvalho A. M., & Moratalla, J. J. (1994). A new sauropod tracksite from the Middle Jurassic of Portugal. *GAIA: revista de geociências*, (10), 5-14.
- Sereno, P. C. (1998). A rationale for phylogenetic definitions, with application to the higher-level taxonomy of Dinosauria [41-83]. *Neues Jahrbuch für Geologie und Paläontologie-Abhandlungen*, 41-83.
- Sereno, P. C., & Arcucci, A. B. (1990). The monophyly of crurotarsal archosaurs and the origin of bird and crocodile ankle joints. *Neues Jahrbuch für Geologie und Paläontologie, Abhandlungen*, 180(1), 21-52.
- Sereno, P. C., Martínez, R. N., & Alcober, O. A. (2012). Osteology of *Eoraptor lunensis* (Dinosauria, sauropodomorpha). *Journal of Vertebrate Paleontology*, 32(sup1), 83-179.

- Soares, A.F., Marques, J.F., & Rocha, R.B. (1985). Contribuição para o conhecimento geológico de Coimbra. *Memórias e notícias*, 100, 41-71.
- Soares, A. F., Kullberg, J. C., Marques, J. F., da Rocha, R. B., & Callapez, P. M. (2012). Tectono-sedimentary model for the evolution of the Silves Group (Triassic, Lusitanian basin, Portugal). *Bulletin de la Société géologique de France*, 183(3), 203-216.
- Smith, N. D., Makovicky, P. J., Hammer, W. R., & Currie, P. J. (2007). Osteology of *Cryolophosaurus ellioti* (Dinosauria: Theropoda) from the Early Jurassic of Antarctica and implications for early theropod evolution. *Zoological Journal of the Linnean Society*, 151(2), 377-421.
- Spiekman, S. N., Ezcurra, M. D., Butler, R. J., Fraser, N. C., & Maidment, S. C. (2021). *Pendraig milnerae*, a new small-sized coelophysoid theropod from the Late Triassic of Wales. *Royal Society Open Science*, 8 (10), 210915.
- Sues, H. D. (2024). The Triassic: A pivotal period in tetrapod evolution. *The Anatomical Record*.
- Sues, H. D., Nesbitt, S. J., Berman, D. S., & Henrici, A. C. (2011). A late-surviving basal theropod dinosaur from the latest Triassic of North America. *Proceedings of the Royal Society B: Biological Sciences*, 278(1723), 3459-3464.
- Sullivan, R. M., & Lucas, S. G. (1999). *Eucoelophysis baldwini* a new theropod dinosaur from the Upper Triassic of New Mexico, and the status of the original types of *Coelophysis*. *Journal of Vertebrate Paleontology*, 19(1), 81-90.
- Terrinha, P., Ribeiro, C., Kullberg, J. C., Lopes, C., Rocha, R., & Ribeiro, A. (2002). Compressive episodes and faunal isolation during rifting, Southwest Iberia. *The Journal of Geology*, 110(1), 101-113.
- Terrinha, P., Rocha, R.B., Rey, J., Cachão, M., Moura, D., Roque, C., Martins, L., Valadares, V., Cabral, J., Azevedo, M.R., Barbero, L., Clavijo, E., Dias, R.P., Matias, H., Madeira, J., Silva, C.M., Munhá, J., Rebelo, L., Ribeiro, C., Vicente, J., Noiva, J., Youbi, N., & Bensalah, M. K. (2006). A Bacia do Algarve: Estratigrafia, paleogeografia e tectónica. *Geologia de Portugal no contexto da Ibéria*, 1-138.
- Thulborn, R. A. (1973). Teeth of ornithischian dinosaurs from the Upper Jurassic of Portugal". *Memórias dos Serviços Geológicos de Portugal*. 22: 89–134.
- Tucker, M. E., & Benton, M. J. (1982). Triassic environments, climates and reptile evolution. *Palaeogeography, Palaeoclimatology, Palaeoecology*, 40(4), 361-379
- Tykoski, Ronald S.; Rowe, Timothy (2004). "Ceratosauria". In Weishampel, David B.; Dodson, Peter; Osmólska Halszka (eds.). *The Dinosauria* (2nd ed.). Berkeley: University of California Press. pp. 47–70.
- Vilas-Boas, M., Pereira, Z., Cirilli, S., & Fernandes, P. (2024). New Insights on the Upper Triassic Silves Group in Algarve Basin, Portugal: Palynological, paleophytogeography and paleoclimatology advances. *Geobios*, 86: 49-64.
- Von Baczko, M. B., & Ezcurra, M. D. (2013). Ornithosuchidae: a group of Triassic archosaurs with a unique ankle joint. *Geological Society, London, Special Publications*, 379(1), 187-202.
- Von Baczko, M. B., Desojo, J. B., & Ponce, D. (2019). Postcranial anatomy and osteoderm histology of *Riojasuchus tenuisiceps* and a phylogenetic update on Ornithosuchidae (Archosauria, Pseudosuchia). *Journal of Vertebrate Paleontology*, 39(5), e1693396.
- Walker, A. D. (1964). Triassic reptiles from the Elgin area: *Ornithosuchus* and the origin of carnosaurs. *Philosophical Transactions of the Royal Society of London. Series B, Biological Sciences*, 248(744), 53-134.
- Welles, S. P. (1954). New Jurassic dinosaur from the Kayenta formation of Arizona. *Geological Society of America Bulletin*, 65(6), 591-598.
- Welles, S. P. (1970). *Dilophosaurus* (Reptilia, Saurischia), a new name for a dinosaur. *Journal of Paleontology*, 44(5), 989.

- Welles, S. P., & Long, R.A. (1974). The tarsus of theropod dinosaurs. *Annale van die Suid-Afrikaanse Museum*, 64:191–218.
- Witzmann, F., & Gassner, T. (2008). Metoposaurid and mastodontosaurid stereospondyls from the Triassic–Jurassic boundary of Portugal. *Alcheringa*, 32(1), 37-51.
- Yates, A. M. (2005). A new theropod dinosaur from the Early Jurassic of South Africa and its implications for the early evolution of theropods. *Palaeontologia africana*, 41, 105-122.
- You, H. L., Azuma, Y., Wang, T., Wang, Y. M., & Dong, Z. M. (2014). The first well-preserved coelophysoid theropod dinosaur from Asia. *Zootaxa*, 3873(3), 233-249.
- Young, C.C. (1940). Preliminary notes on the Lufeng vertebrate fossils. *Bulletin of the Geological Society of China*, 20(3-4), 235-240.
- Zahner, M., & Brinkmann, W. (2019). A Triassic averostran-line theropod from Switzerland and the early evolution of dinosaurs. *Nature Ecology & Evolution*, 3(8), 1146-1152.
- Zhang, Z. C., Wang, T., & You, H. L. (2023). A New Specimen of *Sinosaurus triassicus* (Dinosauria: Theropoda) from the Early Jurassic of Lufeng, Yunnan, China. *Historical Biology*, 1-15.
- Zinke, J. (1998). Small theropod teeth from the Upper Jurassic coal mine of Guimarota (Portugal). *Paläontologische Zeitschrift*, 72(1-2), 179-189.

Chapter II - Theropod dinosaur *Ceratosaurus* from Upper Jurassic of Lourinhã Formation

- Allain, R., Tykoski, R., Aquesbi, N., Jalil, N. E., Monbaron, M., Russell, D., & Taquet, P. (2007). An abelisauroid (Dinosauria: Theropoda) from the Early Jurassic of the High Atlas Mountains, Morocco, and the radiation of ceratosaurus. *Journal of Vertebrate Paleontology*, 27(3), 610-624.
- Alves, T. M., Manuppella, G., Gawthorpe, R. L., Hunt, D. W., & Monteiro, J. H. (2003). The depositional evolution of diapir and fault-bounded rift basins: examples from the Lusitanian Basin of West Iberia. *Sedimentary Geology*, 162(3-4), 273-303.
- Antunes, M. T., & Mateus, O. (2003). Dinosaurs of Portugal. *Comptes Rendus Palevol*, 2(1), 77-95.
- Ash, S. R., & Tidwell, W. D. (1998). Plant megafossils from the Brushy Basin Member of the Morrison Formation near Montezuma creek Trading Post, southeastern Utah. *Modern Geology*, 22, 321.
- Bakker, R. T. (1986). *The dinosaur heresies*. 481 p. Avon: Bath Press.
- Bakker, R. T. (1996). The real Jurassic park: dinosaurs and habitats at Como Bluff, Wyoming. *The Continental Jurassic. Museum of Northern Arizona Bulletin*, 60, 35-49.
- Bakker, R. T., & Bir, G. (2004). Dinosaur crime scene investigations: theropod behavior at Como Bluff, Wyoming, and the evolution of birdness. *Feathered dragons: studies on the transition from dinosaurs to birds*, 14, 301-342. Indiana University Press.
- Barker, C. T., Hone, D. W., Naish, D., Cau, A., Lockwood, J. A., Foster, B., Clarkin, C. E., Schneider, P., & Gostling, N. J. (2021). New spinosaurids from the Wessex Formation (Early Cretaceous, UK) and the European origins of Spinosauridae. *Scientific Reports*, 11(1), 19340.
- Batten, D. J. & MacLennan, A. M. (1984) - The paleoenvironmental significance of the conifer family Cheirolepidiaceae in the Cretaceous of Portugal. In W. Reif & F. Westphal (Eds.), *Symposium on Mesozoic Terrestrial Ecosystems, Short Papers 3*, pp. 7-12. Tubingen, Germany: Attempto Verlag, Tubigen University Press.
- Benson, R. B. (2009). A description of *Megalosaurus bucklandii* (Dinosauria: Theropoda) from the Bathonian of the UK and the relationships of Middle Jurassic theropods. *Zoological Journal of the Linnean Society*, 158(4), 882-935.
- Benson, R. B., Carrano, M. T., & Brusatte, S. L. (2010). A new clade of archaic large-bodied predatory dinosaurs (Theropoda: Allosauroidea) that survived to the latest Mesozoic. *Naturwissenschaften*, 97, 71-78.
- Bonaparte, J. F. (1985). A horned Cretaceous carnosaur from Patagonia. *National Geographic Research*. 1 (1), 149–151.
- Bonaparte, J. F. (1996). Cretaceous tetrapods of Argentina. *Münchner Geowissenschaftliche Abhandlungen*, 30(7), 73-130.
- Bonaparte, J., & Novas, F. E. (1985). *Abelisaurus comahuensis*, n. sp., Carnosauria from the Late Cretaceous of Patagonia. *Ameghiniana*, 21(2-4), 259-265.
- Bonaparte, J. F., Novas, F. E., & Coria, R. A. (1990). *Carnotaurus sastrei* Bonaparte, the horned, lightly built carnosaur from the Middle Cretaceous of Patagonia, *Contributions in Science Natural History Museum of Los Angeles County*, 416, 1-41.
- Bonaparte, J. F., & Powell, J. E. (1980). A continental assemblage of tetrapods from the Upper Cretaceous beds of El Brete, northwestern Argentina (Sauropoda-Coelurosauria-Carnosauria-Aves). *Mémoires de la Société Géologique de France, Nouvelle Série*. 139: 19-28.
- Breedon III, B. T., & Rowe, T. B. (2020). New specimens of *Scutellosaurus lawleri* Colbert, 1981, from the Lower Jurassic Kayenta Formation in Arizona elucidate the early evolution of thyreophoran dinosaurs. *Journal of Vertebrate Paleontology*, 40(4), e1791894.
- Britt, B. B. (1991). Theropods of Dry Mesa Quarry (Morrison Formation, late Jurassic), Colorado, with emphasis on the osteology of *Torvosaurus tanneri*. *Brigham Young University Geology Studies*, 37, 1-72.

- Britt, B. B., Miles, C. A., Cloward, K. C., & Madsen, J. H. (1999). A juvenile *Ceratosaurus* (Theropoda, Dinosauria) from Bone Cabin Quarry West (Upper Jurassic, Morrison Formation), Wyoming. *Journal of Vertebrate Paleontology*, 19(3).
- Brusatte, S. L., Norell, M. A., Carr, T. D., Erickson, G. M., Hutchinson, J. R., Balanoff, A. M., Bever, G. S., Choiniere, J. N., Makovicky, P. J., & Xu, X. (2010). Tyrannosaur paleobiology: new research on ancient exemplar organisms. *Science*, 329(5998), 1481-1485.
- Buffetaut, É. (2008). Spinosaurid teeth from the Late Jurassic of Tendaguru, Tanzania, with remarks on the evolutionary and biogeographical history of the Spinosauridae. *Travaux et Documents des Laboratoires de Géologie de Lyon*, 164(1), 26-28.
- Buffetaut, É. (2012). An early spinosaurid dinosaur from the Late Jurassic of Tendaguru (Tanzania) and the evolution of the spinosaurid dentition. *Oryctos*, 10, 1-8.
- Brochu, C. A. (1996). Closure of neurocentral sutures during crocodylian ontogeny: implications for maturity assessment in fossil archosaurs. *Journal of Vertebrate Paleontology*, 16(1), 49-62.
- Burch, S. H., & Carrano, M. T. (2012). An articulated pectoral girdle and forelimb of the abelisaurid theropod *Majungasaurus crenatissimus* from the Late Cretaceous of Madagascar. *Journal of Vertebrate Paleontology*, 32(1), 1-16.
- Carrano, M. T. (2007). The appendicular skeleton of *Majungasaurus crenatissimus* (Theropoda: Abelisauridae) from the Late Cretaceous of Madagascar. *Journal of Vertebrate Paleontology*, 27(S2), 163-179.
- Carrano, M. T., Benson, R. B., & Sampson, S. D. (2012). The phylogeny of tetanurae (Dinosauria: Theropoda). *Journal of Systematic Palaeontology*, 10(2), 211-300.
- Carrano, M. T., & Sampson, S. D. (1999). Evidence for a paraphyletic 'Ceratosauria' and its implications for theropod dinosaur evolution. *Journal of Vertebrate Paleontology*, 19(3)
- Carrano, M. T., & Sampson, S. D. (2008). The phylogeny of Ceratosauria (Dinosauria: Theropoda). *Journal of Systematic Palaeontology*, 6(2), 183-236.
- Carrano, M. T., Sampson, S. D., & Forster, C. A. (2002). The osteology of *Masiakasaurus knopfleri*, a small abelisauroid (Dinosauria: Theropoda) from the Late Cretaceous of Madagascar. *Journal of Vertebrate Paleontology*, 22(3), 510-534.
- Cau, A. (2024). A Unified Framework for Predatory Dinosaur Macroevolution. *Bollettino della Società Paleontologica Italiana*, 63(1), 2.
- Choffat, P. (1901). Notice préliminaire sur la limite entre le Jurassique et le Crétacique en Portugal. *Bulletin de la Société Belge de Géologie Paléontologie. Hydrologie XV*, 111-140.
- Chure, D. J. (2000). *A new species of Allosaurus from the Morrison Formation of Dinosaur National Monument (UT-CO) and a revision of the theropod family Allosauridae*. 964pp. Ph.D. dissertation, Columbia University.
- Chure, D. J., & Loewen, M. A. (2020). Cranial anatomy of *Allosaurus jimmadseni*, a new species from the lower part of the Morrison Formation (Upper Jurassic) of Western North America. *PeerJ*, 8, e7803.
- Cifelli, R. L. (2003). A graveyard of titans (review of: Gerhard Maier. 2003. African Dinosaurs Unearthed: The Tendaguru Expeditions. Indiana University Press, Bloomington and Indianapolis, USA). *Acta Palaeontologica Polonica*, 48(4), 608-608.
- Cope, E. D. (1877). On a gigantic saurian from the Dakota epoch of Colorado. *Paleontological Bulletin*, v. 25, p. 5-10.
- Cope, E. D. (1892). On the skull of the dinosaurian *Laelaps incrassatus* Cope. *Proceedings of the American Philosophical Society*, Vol. 30, 240-245.
- Currie, P. J., & Carpenter, K. (2000). A new specimen of *Acrocanthosaurus atokensis* (Theropoda, Dinosauria) from the lower Cretaceous Antlers formation (lower Cretaceous, Aptian) of Oklahoma, USA. *Geodiversitas*, 22(2), 207.
- Dal Sasso, C. (2001). *Dinosauri italiani* (2 ed.). pp. 45–66. Venezia: Marsilio Editori.

- Dal Sasso, C., Maganuco, S., & Cau, A. (2018). The oldest ceratosaurian (Dinosauria: Theropoda), from the Lower Jurassic of Italy, sheds light on the evolution of the three-fingered hand of birds. *PeerJ*, 6, e5976.
- Delcourt, R. (2018). Ceratosaur palaeobiology: new insights on evolution and ecology of the southern rulers. *Scientific reports*, 8(1), 1-12.
- Delcourt, R., & Grillo, O. N. (2018). Reassessment of a fragmentary maxilla attributed to Carcharodontosauridae from Presidente Prudente Formation, Brazil. *Cretaceous Research*, 84, 515-524.
- Depéret, C. (1896). Note sur les dinosauriens sauropodes et théropodes du Crétacé supérieur de Madagascar. *Bulletin de la Société Géologique de France*, 21, 176-194.
- Dodson, P., Behrensmeyer, A. K., Bakker, R. T., & McIntosh, J. S. (1980). Taphonomy and paleoecology of the dinosaur beds of the Jurassic Morrison Formation. *Paleobiology*, 6(2), 208-232.
- Engelmann, G. F., Chure, D. J., & Fiorillo, A. R. (2004). The implications of a dry climate for the paleoecology of the fauna of the Upper Jurassic Morrison Formation. *Sedimentary Geology*, 167(3-4), 297-308.
- Escaso, F., Ortega, F., Dantas, P., Malafaia, E., Pimentel, N.L., Pereda-Suberbiola, X., Sanz, J.L., Kullberg, J.C., Kullberg, M.C., & Barriga, F. (2007). New evidence of shared dinosaur across Upper Jurassic proto-North Atlantic: *Stegosaurus* from Portugal. *Naturwissenschaften*, 94, 367-374.
- Escaso, F., Ortega, F., Dantas, P., Malafaia, E., Silva, B., Gasulla, J. M., Mocho, P., Narváez, I., & Sanz, J. L. (2014). A new dryosaurid ornithopod (Dinosauria, Ornithischia) from the Late Jurassic of Portugal. *Journal of Vertebrate Paleontology*, 34(5), 1102-1112.
- Ezcurra, M. D., & Novas, F. E. (2007). Phylogenetic relationships of the Triassic theropod *Zupaysaurus rougieri* from NW Argentina. *Historical Biology*, 19(1), 35-72.
- Farlow, J. O., Coroian, D., Currie, P. J., Foster, J. R., Mallon, J. C., & Therrien, F. (2023). "Dragons" on the landscape: Modeling the abundance of large carnivorous dinosaurs of the Upper Jurassic Morrison Formation (USA) and the Upper Cretaceous Dinosaur Park Formation (Canada). *The Anatomical Record*, 306(7), 1669-1696.
- Foster, J. R., & Chure, D. J. (2006). Hindlimb allometry in the Late Jurassic theropod dinosaur *Allosaurus*, with comments on its abundance and distribution. *New Mexico Museum of Natural History and Science Bulletin*, 36, 119-122.
- Fowler, D. (2007, September). Recently rediscovered baryonychine teeth (Dinosauria: Theropoda): New morphologic data, range extension & similarity to *Ceratosaurus*. In *Journal of Vertebrate Paleontology*, 27, (suppl. To 3.), 76A.
- Fraas, E. (1908). Ostafrikanische dinosaurier. *Palaeontographica* 55, 105-144.
- França, J. C., Zbyszewski, G., & Almeida, F. M. (1961). Carta geológica de Portugal na escala de 1/50000: Notícia explicativa da folha 30-A, Lourinhã. *Serviços Geológicos de Portugal*, 27p.
- Galton, P. M. (1982). *Elaphrosaurus*, an ornithomimid dinosaur from the Upper Jurassic of North America and Africa. *Paläontologische Zeitschrift*, 56(3), 265-275.
- Galton, P. M. (1980). Partial skeleton of *Dracopelta zbyszewskii* n. gen. and n. sp., an ankylosaurian dinosaur from the Upper Jurassic of Portugal. *Géobios*, 13(3), 451-457.
- Galton, P. M., & Jensen, J. A. (1979). A new large theropod dinosaur from the Upper Jurassic of Colorado. *Brigham Young University Geology Studies*, 26(2), 1-12.
- Gauthier, J. (1986). Saurischian monophyly and the origin of birds. *Memoirs of the California Academy of sciences*, 8, 1-55.
- Gee, C. T. (2011). Dietary options for the sauropod dinosaurs from an integrated botanical and paleobotanical perspective. In *Biology of the sauropod dinosaurs: Understanding the life of giants* (N. Klein, K. Remes, C. Gee, and P. Sander, eds.). 34-56p. Indiana University Press, Bloomington.

- Gilmore, C. W. (1920). *Osteology of the carnivorous Dinosauria in the United State National museum: with special reference to the genera Antrodemus (Allosaurus) and Ceratosaurus* (No. 110). 159p. US Government printing office.
- Goloboff, P., & Morales, M. (2022). TNT version 1.6, with a graphical interface for MacOs and Linux, including new routines in parallel (forthcoming).
- Greppin, J. B. (1870). Description géologique du Jura bernois et de quelques districts adjacents. *Beitraege Geologie Karte Schweiz*, (Vol. 8). 357p., 8 pl.
- Hay, O. P. (1908). On certain genera and species of carnivorous dinosaurs, with special reference to *Ceratosaurus nasicornis* Marsh. *Proceedings of the United States National Museum*, 35, 351-366.
- Heinrich, C., Paes Neto, V. D., Lacerda, M. B., Martinelli, A. G., Fiedler, M. S., & Schultz, C. L. (2021). The ontogenetic pattern of neurocentral suture closure in the axial skeleton of Hyperodapedontinae (Archosauromorpha, Rhynchosauria) and its evolutionary implications. *Palaeontology*, 64(3), 409-427.
- Henderson, D. M. (1998). Skull and tooth morphology as indicators of niche partitioning in sympatric Morrison Formation theropods. *Gaia*, 15, 219-226.
- Hendrickx, C., Mateus, O., & Araújo, R. (2014). The dentition of megalosaurid theropods. *Acta Palaeontologica Polonica*, 60(3), 627-642.
- Hendrickx, C., Mateus, O., & Araújo, R. (2015). A proposed terminology of theropod teeth (Dinosauria, Saurischia). *Journal of Vertebrate Paleontology*, 35(5), e982797.
- Hill, G. (1988). *The sedimentology and lithostratigraphy of the Upper Jurassic Lourinhã Formation, Lusitanian Basin, Portugal*. 292p. PhD thesis. Milton Keynes, Open University (United Kingdom).
- Hill, G. (1989). Distal alluvial fan sediments from the Upper Jurassic of Portugal: controls on their cyclicity and channel formation. *Journal of the Geological Society*, 146(3), 539-555.
- Holtz, T. R. (1994). The phylogenetic position of the Tyrannosauridae: implications for theropod systematics. *Journal of Paleontology*, 68(5), 1100-1117.
- Holtz, T. R. (1998). A new phylogeny of the carnivorous dinosaurs. *Gaia: revista de geociências*, 15, 5-61.
- Hotton, C. L., & Baghai-Riding, N. L. (2010). Palynological evidence for conifer dominance within a heterogeneous landscape in the Late Jurassic Morrison Formation, USA. In *Plants in Mesozoic time: morphological innovations, phylogeny, ecosystems*, (ed. C. T. Gee). Bloomington, Indiana University Press, 295-328.
- Huene, F. v. (1923). Carnivorous saurischia in Europe since the Triassic. *Bulletin of the Geological Society of America*, 34(3), 449-458.
- Huene, F. v. (1929). Los saurisqueos y ornitisqueos del Cretaceo Argentino. In *Anales del Museo de la Plata* (Vol. 3, No. 2).
- Huene, F. v. (1932). Die fossile Reptil-Ordnung Saurischia: ihre Entwicklung und Geschichte. *Monographien zur Geologie und Palaeontologie (Serie 1)*, 4, 1-361.
- Ibrahim, N., Sereno, P. C., Varricchio, D. J., Martill, D. M., Dutheil, D. B., Unwin, D. M., Baidder, L., Larsson H. C. E., Zouhri, S., & Kaoukaya, A. (2020). Geology and Paleontology of the Upper Cretaceous Kem Kem group of Eastern Morocco. *ZooKeys*, 928, 1-216.
- Irmis, R. B., Nesbitt, S. J., Padian, K., Smith, N. D., Turner, A. H., Woody, D., & Downs, A. (2007). A Late Triassic dinosauriform assemblage from New Mexico and the rise of dinosaurs. *Science*, 317(5836), 358-361.
- Isasmendi, E., Cuesta, E., Díaz-Martínez, I., Company, J., Sáez-Benito, P., Viera, L. I., Torices, A., & Pereda-Suberbiola, X. (2024). Increasing the theropod record of Europe: a new basal spinosaurid from the Enciso Group of the Cameros Basin (La Rioja, Spain). Evolutionary implications and palaeobiodiversity. *Zoological Journal of the Linnean Society*, zlad193.

- Jaffe, M.S. (2000). *The gilded dinosaur: the fossil war between ED Cope and OC Marsh and the rise of American science*. New York: Crown.
- Janensch, W. (1920). Über *Elaphrosaurus bambergi* und die megalosaurier aus den Tendaguru-Schichten Deutsch-Ostafrikas. *Sitzungsberichte der Gesellschaft Naturforschender Freunde zu Berlin*, (8), 226-235.
- Janensch, W. (1925). Die Coelurosaurier und Theropoden der Tendaguruschichten Deutsch-Ostafrikas. *Palaeontographica-Supplementbände*, 1-100.
- Johnson, R. L. (2012). *Battle of the Dinosaur Bones: Othniel Charles Marsh vs Edward Drinker Cope*. Twenty-First Century Books.
- Krause, D. W., Sampson, S. D., Carrano, M. T., & O'Connor, P. M. (2007). Overview of the history of discovery, taxonomy, phylogeny, and biogeography of *Majungasaurus crenatissimus* (Theropoda: Abelisauridae) from the Late Cretaceous of Madagascar. *Journal of Vertebrate Paleontology*, 27(S2), 1-20.
- Langer, M. C., Martins, N. D. O., Manzig, P. C., Ferreira, G. D. S., Marsola, J. C. D. A., Fortes, E., Lima, R., Sant'ana, L. C. F., Vidal, L. S., Lorençato, R. H. S., & Ezcurra, M. D. (2019). A new desert-dwelling dinosaur (Theropoda, Noasaurinae) from the Cretaceous of south Brazil. *Scientific reports*, 9(1), 9379.
- Lavocat, R. (1955). Sur une portion de mandibule de Théropode provenant du Crétacé supérieur de Madagascar. *Bulletin du Muséum National d'Histoire Naturelle*, 27, 256-259.
- Lei, R., Tschopp, E., Hendrickx, C., Wedel, M. J., Norell, M., & Hone, D. W. (2023). Bite and tooth marks on sauropod dinosaurs from the Morrison Formation. *PeerJ*, 11, e16327.
- Leinfelder, R. R., & Wilson, R. C. L. (1998). Third-Order Sequences in a Upper Jurassic Rift-Related Second Order Sequence, Central Lusitanian Basin, Portugal. In: *Mesozoic and Cenozoic Sequence Stratigraphy of European Basins*. (Eds. de Graciansky, P. C., Hardenbol, J., Jacquin T. & Vail P. R.) SEPM Special Publication, 60, 507-525.
- Leinfelder, R. R., Nose, M., Schmid, D. U. & Werner, W. (2004). Reefs and Carbonate Platforms in a mixed carbonate-siliciclastic setting. Examples from the Upper Jurassic (Kimmeridgian to Tithonian) of West-Central Portugal. In: *Carboniferous and Jurassic Carbonate Platforms of Iberia*. (Eds. Duarte, L. V. & Henriques, M. H.), 23rd IAS Meet., Coimbra, Field Trip Guidebook Vol. 1, 95-123.
- Loeuff, J. L., & Buffetaut, E. (1991). *Tarascosaurus salluvicus* nov. gen., nov. sp., theropod dinosaur from the Upper Cretaceous of southern France. *Geobios*, 24, 585-594.
- Lydekker, R. (1888). *Catalogue of the Fossil Reptilia and Amphibia in the British Museum (Natural History)*, Cromwell Road, S.W., Part 1. Containing the Orders Ornithosauria, Crocodilia, Dinosauria, Squamata, Rhynchocephalia, and Proterosauria. British Museum of Natural History, London, 309 p.
- MacFadden, B. J. (1992). *Fossil Horses: Systematics, Paleobiology, and Evolution of the Family Equidae*. New York: Cambridge University Press.
- Madsen, J. H. (1976): *Allosaurus fragilis: a revised osteology*. Utah Geological and Mineral Survey, 109: 163p.
- Madsen, J. H., & Welles, S. P. (2000). *Ceratosaurus* (Dinosauria, Theropoda): a revised osteology. *Utah Geological Survey, Miscellaneous Publications 00-2*: 1 -80.
- Malafaia, E., Escaso, F., Mocho, P., Serrano-Martínez, A., Torices, A., Cachão, M., & Ortega, F. (2017a). Analysis of diversity, stratigraphic and geographical distribution of isolated theropod teeth from the Upper Jurassic of the Lusitanian Basin, Portugal. *Journal of Iberian Geology*, 43, 257-291.
- Malafaia, E., Mocho, P., Escaso, F., & Ortega, F. (2020). A new carcharodontosaurian theropod from the Lusitanian Basin: evidence of allosauroid sympatry in the European Late Jurassic. *Journal of Vertebrate Paleontology*, 40(1), e1768106.
- Malafaia, E., Ortega, F., Escaso, F., & Silva, B. (2015). New evidence of *Ceratosaurus* (Dinosauria: Theropoda) from the Late Jurassic of the Lusitanian Basin, Portugal. *Historical Biology*, 27(7), 938-946.

- Mannion, P. D., Upchurch, P., Mateus, O., Barnes, R. N., & Jones, M. E. (2012). New information on the anatomy and systematic position of *Dinheirosaurus lourinhanensis* (Sauropoda: Diplodocoidea) from the Late Jurassic of Portugal, with a review of European diplodocoids. *Journal of Systematic Palaeontology*, 10(3), 521-551.
- Manuppella G., Antunes M. T., Pais J., Ramalho M. M. & Rey J. (1999). Carta Geológica de Portugal à escala 1:50 000. Notícia Explicativa da Folha 30-A, Lourinhã. *Instituto Geológico e Mineiro, Lisboa*, 83 p.
- Marsh, O. C. (1872). Preliminary description of *Hesperornis regalis*, with notice of four other new species of Cretaceous birds. *American Journal of Science*, 3(17), 360-365.
- Marsh, O. C. (1877a). A new order of extinct Reptilia (Stegosauria) from the Jurassic of the Rocky Mountains. *American Journal of Science*, 3(84), 513-514.
- Marsh, O. C. (1877b). Notice of New Dinosaurian Reptiles from the Jurassic formation. *American Journal of Science and Arts (1820-1879)*, 14(84), 514.
- Marsh, O. C. 1878. Principal characters of American Jurassic dinosaurs, Part I. *American Journal of Science (series 3)*, 16, 411-416.
- Marsh, O. C. (1884). II.—The Principal Characters of American Jurassic Dinosaurs belonging to the Order Theropoda 1. *Geological Magazine*, 1(6), 252-262.
- Marsh, O. C. (1885). Names of extinct reptiles. *American Journal of Science*, 29(3), 169.
- Marsh, O. C. (1889). Notice of gigantic horned Dinosauria from the Cretaceous. *American Journal of Science*, 3(224), 173-176.
- Marsh, O. C. (1893). II Restorations of *Anchisaurus*, *Ceratosaurus*, and *Claosaurus*. *Geological Magazine*, 10(4), 150-157.
- Martínez, R. N., Apaldetti, C., Correa, G. A., & Abelín, D. (2016). A Norian lagerpetid dinosauriform from the Quebrada del Barro Formation, northwestern Argentina. *Ameghiniana*, 53(1), 1-13.
- Martinius, A. W. & Gowland, S. (2011). Tide influenced fluvial bedforms and tidal bore deposits (Late Jurassic Lourinhã Formation, Lusitanian Basin, Western Portugal). *Sedimentology* 58(1), 285-324.
- Mateus, O. (2006). Late Jurassic dinosaurs from the Morrison Formation (USA), the Lourinhã and Alcobaça formations (Portugal), and the Tendaguru Beds (Tanzania): a comparison. *New Mexico Museum of Natural History and Science Bulletin*, 36, 223-231.
- Mateus, O., & Antunes, M. T. (2000). *Ceratosaurus* sp. (Dinosauria: Theropoda) in the Late Jurassic of Portugal. In *31st International Geological Congress*. Rio de Janeiro, Brazil.
- Mateus, O., & Antunes, M. T. (2001). *Draconyx loureiroi*, a new camptosauridae (Dinosauria, Ornithopoda) from the Late Jurassic of Lourinhã, Portugal. In *Annales de Paléontologie, Vol. 87, No. 1*, 61-73. Elsevier Masson.
- Mateus, O., Dinis, J., & Cunha, P. P. (2017). The Lourinhã Formation: the Upper Jurassic to lower most Cretaceous of the Lusitanian Basin, Portugal - landscapes where dinosaurs walked. *Ciências da Terra/Earth Sciences Journal*, 19(1), 75-97.
- Mateus, O., Maidment, S. C., & Christiansen, N. A. (2009). A new long-necked 'sauropod-mimic' stegosaur and the evolution of the plated dinosaurs. *Proceedings of the Royal Society B: Biological Sciences*, 276(1663), 1815-1821.
- Mateus, O., Mannion, P. D., & Upchurch, P. (2014). *Zby atlanticus*, a new turiasaurian sauropod (Dinosauria, Eusauropoda) from the Late Jurassic of Portugal. *Journal of Vertebrate Paleontology*, 34(3), 618-634.
- Mateus, O., Walen, A., & Antunes, M. T. (2006). The large theropod fauna of the Lourinhã Formation (Portugal) and its similarity to that of the Morrison Formation with a description of a new species of *Allosaurus*. *New Mexico Museum of Natural History and Science Bulletin*, 36, 123-129.
- McCarren, M. J. (1993). *The scientific contributions of Othniel Charles Marsh: birds, bones, and brontotheres*. p55. Peabody Museum of Natural History, Yale University, New Haven, Connecticut.

- Mohabey, D. M., Samant, B., Vélez-Rosado, K. I., & Wilson Mantilla, J. A. (2023). A review of small-bodied theropod dinosaurs from the Upper Cretaceous of India, with description of new cranial remains of a noosaurid (Theropoda: Abelisauria). *Journal of Vertebrate Paleontology*, e2288088.
- Mohr, B. A. R. (1989). New palynological information on the age and environment of Late Jurassic and Early Cretaceous vertebrate localities of the Iberian Peninsula (eastern Spain and Portugal). *Berliner Geowiss. Abhandl. A*, 106, 291–301.
- Mocho, P., Royo-Torres, R., & Ortega, F. (2014). Phylogenetic reassessment of *Lourinhasaurus alenquerensis*, a basal Macronaria (Sauropoda) from the Upper Jurassic of Portugal. *Zoological Journal of the Linnean Society*, 170(4), 875-916.
- Mocho, P., Royo-Torres, R., & Ortega, F. (2019). A new macronarian sauropod from the Upper Jurassic of Portugal. *Journal of Vertebrate Paleontology*, 39(1), e1578782.
- Molnar, R. E. (1990). "Problematic Theropoda: Carnosaurs". In *The Dinosauria*. (Weishampel, D. B., Dodson P., Osmólska, H., eds). pp. 306-317. Berkeley, University of California Press.
- Molnar, R. E., Kurzanov, J. M., & Zhiming, D. (1990). "Carnosauria". In *The Dinosauria*. (Weishampel, D. B., Dodson P., Osmólska, H., eds). pp. 169-209. Berkeley, University of California Press.
- Myers, T. S. (2011). *Late Jurassic paleoclimate of Europe and Africa*. 218 p. PhD Dissertation. ProQuest, UMI Dissertation Publish. Ann Arbor, MI.
- Myers, T. S., Tabor N. J., Jacobs L. L. & Mateus O. (2012a). Estimating soil pCO₂ using paleosol carbonates: implications for the relationship between primary productivity and faunal richness in ancient terrestrial ecosystems. *Paleobiology* 38(4), 585-604.
- Myers T. S., Tabor N. J., Jacobs L. L. & Mateus O. (2012b). Palaeoclimate of the Late Jurassic of Portugal: Comparison with the Western United States. *Sedimentology* 59(6), 1695–1717.
- Nesbitt, S. J., Irmis, R. B., Parker, W. G., Smith, N. D., Turner, A. H., & Rowe, T. (2009). Hindlimb osteology and distribution of basal dinosauriforms from the Late Triassic of North America. *Journal of Vertebrate Paleontology*, 29(2), 498-516.
- Nopcsa, F. V. (1928). The genera of reptiles. *Palaeobiologica*, 1(1), 163-188.
- Novas, F. E. (1991). Relaciones filogenéticas de los dinosaurios teropodos ceratosaurios. *Ameghiniana*, 28(3-4), 410.
- Novas, F. E. (1992). La evolución de los dinosaurios carnívoros. In *Los dinosaurios y su entorno biótico: II Curso de Paleontología, 10 a 12 de julio de 1990*. *Actas* (pp. 125-163). Instituto Juan de Valdés.
- Novas, F., Agnolin, F., & Bandyopadhyay, S. (2004). Cretaceous theropods from India: a review of specimens described by Huene and Matley (1933). *Revista del Museo Argentino de Ciencias Naturales nueva serie*, 6(1), 67-103.
- Novas, F. E., de Valais, S., Vickers-Rich, P., & Rich, T. (2005). A large Cretaceous theropod from Patagonia, Argentina, and the evolution of carcharodontosaurids. *Naturwissenschaften*, 92, 226-230.
- O'Connor, P. M. (2007). The postcranial axial skeleton of *Majungasaurus crenatissimus* (Theropoda: Abelisauridae) from the Late Cretaceous of Madagascar. *Journal of Vertebrate Paleontology*, 27(S2), 127-163.
- O’Gorman, E. J., & Hone, D. W. (2012). Body size distribution of the dinosaurs. *PLoS One*, 7(12), e51925.
- Pais, J. (1998). Jurassic plant macroremains from Portugal. *Memórias da Academia das Ciências Lisboa*, 37, 25-47.
- Parker, F., & Parker, B. J. (1997). Educational Philanthropist George Peabody (1795-1869) and First US Paleontology Professor Othniel Charles Marsh (1831-99) at Yale University. U.S., Tennessee.
- Paul, G. S. (1988). *Predatory dinosaurs of the world; a New York academy of sciences book*. 464 pp. Simon and Schuster, New York.
- Parrish, J. T., Peterson, F., & Turner, C. E. (2004). Jurassic “savannah” - plant taphonomy and climate of the Morrison Formation (Upper Jurassic, Western USA). *Sedimentary Geology*, 167(3-4), 137-162.

- Plate, R. (1964). *The Dinosaur Hunters: Othniel C. Marsh and Edward D. Cope*. David McKay Company, Inc., New York.
- Pol, D., & Rauhut, O. W. (2012). A Middle Jurassic abelisaurid from Patagonia and the early diversification of theropod dinosaurs. *Proceedings of the Royal Society B: Biological Sciences*, 279(1741), 3170-3175.
- Ramalho, M. M. (1971). Contribution à l'étude micropaléontologique et stratigraphique du Jurassique Supérieur et Crétacé Inférieur des environs de Lisbonne (Portugal). *Memórias dos Serviços Geológicos Portugal, NS, 19*, 212 p.
- Ramalho, M. M. (1981). Note préliminaire sur les microfaciès du Jurassique supérieur portugais. *Comunicações dos Serviços Geológicos de Portugal, 67*, 41–45.
- Rauhut, O. W. M. (1995). Zur systematischen Stellung der afrikanischen Theropoden *Carcharodontosaurus* Stromer 1931 und *Bahariasaurus* Stromer 1934. *Berliner Geowissenschaften Abhandlungen E, 16*, 357-375.
- Rauhut, O. W. M. (2000). *The Interrelationships and Evolution of Basal Theropods (Dinosauria, Saurischia)*. 583 pp. PhD thesis, University of Bristol.
- Rauhut, O. W. M. (2004). Provenance and anatomy of *Genyodectes serus*, a large-toothed ceratosaur (Dinosauria: Theropoda) from Patagonia. *Journal of Vertebrate Paleontology*, 24(4), 894-902.
- Rauhut, O. W. M. (2011). Theropod dinosaurs from the Late Jurassic of Tendaguru (Tanzania). *Special Papers in Palaeontology*, 86, 195-239.
- Rauhut, O. W. M., Canudo, J. I., & Castanera, D. (2019). A reappraisal of the Early Cretaceous theropod dinosaur *Camarillasaurus* from Spain. In *European Association of Vertebrate Paleontologists (EAVP)(Ed), Program and Abstracts XVII Conference of the EAVP* (p. 96).
- Rauhut, O. W., & Carrano, M. T. (2016). The theropod dinosaur *Elaphrosaurus bambergi*, from the Late Jurassic of Tendaguru, Tanzania. *Zoological Journal of the Linnean Society*, 178(3), 546-610.
- Rauhut, O. W., Milner, A. C., & Moore-Fay, S. (2010). Cranial osteology and phylogenetic position of the theropod dinosaur *Proceratosaurus bradleyi* (Woodward, 1910) from the Middle Jurassic of England. *Zoological Journal of the Linnean Society*, 158(1), 155-195.
- Rees, P. M., Noto, C. R., Parrish, J. M., & Parrish, J. T. (2004). Late Jurassic climates, vegetation, and dinosaur distributions. *The Journal of Geology*, 112(6), 643-653.
- Reis, R. P., Dinis, J. L., Cunha, P. P., & Trincão, P. R. (1996). Upper Jurassic sedimentary infill and tectonics of the Lusitanian Basin (Western Portugal). In *Retrospective Collection, Vol. 19*, pp. 377-386. Trans Tech Publications.
- Rey, J. (1972). Recherches géologiques sur le Crétacé inférieur de l'Estremadura (Portugal). *Memórias dos Serviços Geológicos de Portugal, NS 21*, 477 p.
- Rey, J. (1993). Les unités lithostratigraphiques du Grube de Torres Vedras (Estremadura, Portugal). *Comunicações do Instituto Geológico e Mineiro, 79*, 75-85.
- Riggs, E. S. (1903). *Brachiosaurus altithorax*, the largest known Dinosaur. *American Journal of Science (1880-1910)*, 15(88), 299.
- Rotatori, F. M., Ferrari, L., Sequero, C., Camilo, B., Mateus, O., & Moreno-Azanza, M. (2023). An unexpected early-diverging iguanodontian dinosaur (Ornithischia, Ornithopoda) from the Upper Jurassic of Portugal. *Journal of Vertebrate Paleontology*, e2310066.
- Rowe, T. (1989). A new species of the theropod dinosaur *Syntarsus* from the Early Jurassic Kayenta Formation of Arizona. *Journal of Vertebrate Paleontology*, 9(2), 125-136.
- Rowe, T., & Gauthier, J. A. (1990). "Ceratosauria". In *The Dinosauria* (Weishampel, D. B., Dodson, P. and Osmólska, H., eds), pp. 151-168. University of California Press, Berkeley.

- Sampson, S. D., Krause, D. W., Dodson, P., & Forster, C. A. (1996). The premaxilla of *Majungasaurus* (Dinosauria: Theropoda), with implications for Gondwanan paleobiogeography. *Journal of Vertebrate Paleontology*, 16(4), 601-605.
- Sampson, S. D., & Witmer, L. M. (2007). Craniofacial anatomy of *Majungasaurus crenatissimus* (Theropoda: Abelisauridae) from the late Cretaceous of Madagascar. *Journal of Vertebrate Paleontology*, 27(S2), 32-104.
- Sampson, S. D., Witmer, L. M., Forster, C. A., Krause, D. W., O'Connor, P. M., Dodson, P., & Ravoavy, F. (1998). Predatory dinosaur remains from Madagascar: implications for the Cretaceous biogeography of Gondwana. *Science*, 280(5366), 1048-1051.
- Sánchez-Fenollosa, S., Escaso, F., & Cobos, A. (2024). A new specimen of *Dacentrurus armatus* Owen, 1875 (Ornithischia: Thyreophora) from the Upper Jurassic of Spain and its taxonomic relevance in the European stegosaurian diversity. *Zoological Journal of the Linnean Society*, zlae074.
- Sánchez-Hernández, B., & Benton, M. J. (2012). Filling the ceratosaur gap: A new ceratosaurian theropod from the Early Cretaceous of Spain. *Acta Palaeontologica Polonica*, 59(3), 581-600.
- Sanders, R. K., & Smith, D. K. (2005). The endocranium of the theropod dinosaur *Ceratosaurus* studied with computed tomography. *Acta Palaeontologica Polonica*, 50(3), 601.
- Santos-Cubedo, A., de Santisteban, C., Poza, B., & Meseguer, S. (2023). A new spinosaurid dinosaur species from the Early Cretaceous of Cincorres (Spain). *Scientific Reports*, 13(1), 6471.
- Schneider, S., Fürsich, F. T., & Werner, W. (2009). Sr-isotope stratigraphy of the Upper Jurassic of central Portugal (Lusitanian Basin) based on oyster shells. *International Journal of Earth Sciences*, 98, 1949-1970.
- Schudack, M. E. (1999). Some charophytes from the middle dinosaur member of the Tendaguru formation (Upper Jurassic of Tanzania). *Fossil Record*, 2(1), 201-205.
- Schudack M. & Schudack U. (1989). Late Kimmeridgian to Berriasian paleogeography of the northwestern Iberian Ranges (Spain). *Berliner Geowissen. Abhandl. A 106*, 445-457.
- Schuchert, C. (1918). Age of the American Morrison and east African Tendaguru formations. *Bulletin of the Geological Society of America*, 29(1), 245-280.
- Senter, P. (2011). Using creation science to demonstrate evolution 2: morphological continuity within Dinosauria. *Journal of Evolutionary Biology*, 24(10), 2197-2216.
- Sereno, P. C. (1999). The evolution of dinosaurs. *Science*, 284(5423), 2137-2147.
- Sereno, P. C., & Brusatte, S. L. (2008). Basal abelisaurid and carcharodontosaurid theropods from the Lower Cretaceous Elrhaz Formation of Niger. *Acta Palaeontologica Polonica*, 53(1), 15-46.
- Sereno, P. C., Dutheil, D. B., Iarochene, M., Larsson, H. C., Lyon, G. H., Magwene, P. M., Sidor, C. A., Varricchio, D. J., & Wilson, J. A. (1996). Predatory dinosaurs from the Sahara and Late Cretaceous faunal differentiation. *Science*, 272(5264), 986-991.
- Sereno, P. C., Wilson, J. A., & Conrad, J. L. (2004). New dinosaurs link southern landmasses in the Mid-Cretaceous. *Proceedings of the Royal Society of London. Series B: Biological Sciences*, 271(1546), 1325-1330.
- Sibuet J. C., Rouzo S. & Srivastava S. (2012). Plate tectonic reconstructions and paleogeographic maps of the central and North Atlantic oceans. *Canadian Journal of Earth Sciences* 49(12), 1395-1415.
- Smith, J. B. (2007). Dental morphology and variation in *Majungasaurus crenatissimus* (Theropoda: Abelisauridae) from the Late Cretaceous of Madagascar. *Journal of Vertebrate Paleontology*, 27(S2), 103-126.
- Soto, M., & Perea, D. (2008). A ceratosaurid (Dinosauria, Theropoda) from the Late Jurassic–Early Cretaceous of Uruguay. *Journal of Vertebrate Paleontology*, 28(2), 439-444.
- Soto, M., Toriño, P., & Perea, D. (2020). *Ceratosaurus* (Theropoda, Ceratosauria) teeth from the Tacuarembó Formation (Late Jurassic, Uruguay). *Journal of South American Earth Sciences*, 103, 102781.

- de Souza, G. A., Soares, M. B., Weinschütz, L. C., Wilner, E., Lopes, R. T., de Araújo, O. M. O., & Kellner, A. W. A. (2021). The first edentulous ceratosaur from South America. *Scientific Reports*, *11*(1), 22281.
- Stokes, W. L. (1944). Morrison Formation and related deposits in and adjacent to the Colorado Plateau. *Bulletin of the Geological Society of America*, *55*(8), 951-992.
- Stovall, J. W. (1938). The Morrison of Oklahoma and its dinosaurs. *The Journal of Geology*, *46*(4), 583-600.
- Taylor, A. M., Gowland, S., Leary, S., Keogh, K. J., & Martinius, A. W. (2013). Stratigraphical correlation of the Late Jurassic Lourinhã Formation in the Consolação Sub-basin (Lusitanian Basin), Portugal. *Geological Journal*, *49*(2), 143-162.
- Thulborn, R. A. (1973). Teeth of ornithischian dinosaurs from the Upper Jurassic of Portugal with description of a hypsilophodontid (*Phyllodon henkeli* gen. et sp. nov.) from the Guimarota Lignite. *Memórias dos Serviços Geológicos de Portugal*, *22*, 89-134.
- Tidwell, W. D. (1990). Preliminary report on the megafossil flora of the Upper Jurassic Morrison Formation. *Hunteria*, *2*(8), 1-11.
- Tortosa, T., Buffetaut, E., Vialle, N., Dutour, Y., Turini, E., & Cheylan, G. (2014). A new abelisaurid dinosaur from the Late Cretaceous of southern France: Palaeobiogeographical implications. In *Annales de Paléontologie*, *100* (1), 63-86. Elsevier Masson.
- Tschopp, E., Barta, D. E., Brinkmann, W., Foster, J. R., Holwerda, F. M., Maidment, S. C., Poropat, S. F., Scheyer, T. M., Sellés, A. G., Vila, B., & Zahner, M. (2020). How to live with dinosaurs: Ecosystems across the Mesozoic. In *Nature through Time: Virtual field trips through the Nature of the past* (pp. 209-229). Cham: Springer International Publishing.
- Tykoski, R. S. (2005). *Anatomy, ontogeny, and phylogeny of coelophysoid theropods*, 553pp. PhD thesis, The University of Texas at Austin.
- Tykoski, R. S., Rowe, T. (2004). "Ceratosauria". In *The Dinosauria* (Weishampel, D. B., Dodson P., Osmólska, H., eds.), 2nd ed., pp. 47–70. Berkeley, University of California Press.
- Wang, S., Stiegler, J., Amiot, R., Wang, X., Du, G. H., Clark, J. M., & Xu, X. (2017). Extreme ontogenetic changes in a ceratosaurian theropod. *Current Biology*, *27*(1), 144-148.
- Werner, W. (1986). Palökologische und biofazielle analyse des Kimmeridge (Oberjura) von Consolacao, Mittelportugal. *Zitteliana*, *13*, 1-109.
- White, T. E. (1964). "The Dinosaur Quarry". In *Sabatka*, (E. F., ed.), p. 21-28. Guidebook to the Geology and Mineral Resources of the Uinta Basin: Intermountain Association of Petroleum Geologists, thirteenth Annual Field Conference.
- Whitlock, J. A. (2011). Inferences of diplodocoid (Sauropoda: Dinosauria) feeding behavior from snout shape and microwear analyses. *PLoS One*, *6*(4), e18304.
- Whitlock, J., Trujillo, K., & Hanik, G. (2018). Assemblage-level structure in Morrison Formation dinosaurs, western interior, USA. *Geology of the Intermountain West*, *5*, 9-22.
- Wilson, J. A., D'Emic, M. D., Ikejiri, T., Moacdieh, E. M., & Whitlock, J. A. (2011). A nomenclature for vertebral fossae in sauropods and other saurischian dinosaurs. *PLoS One*, *6*(2), e17114.
- Wilson, J. A., Sereno, P. C., Srivastava, S., Bhatt, D. K., Khosla, A., & Shani, A. (2003). A new abelisaurid (Dinosauria, Theropoda) from the Lameta formation (Cretaceous, Maastrichtian) of India. *Contributions from the Museum of Paleontology University of Michigan*. *31* (1): 1–42.
- Witton, M. P. (2010). *Pteranodon* and beyond: the history of giant pterosaurs from 1870 onwards. *Geological Society, London, Special Publications*, *343*(1), 313-323.
- Woodward, A. S. (1901). On some extinct reptiles from Patagonia, of the genera *Miolania*, *Dinilysia*, and *Genyodectes*. In *Proceedings of the Zoological Society of London*, Vol. 70, No. 2, pp. 169-184. Oxford, UK, Blackwell Publishing Ltd.

- Xu, X., Clark, J. M., Mo, J., Choiniere, J., Forster, C. A., Erickson, G. M., Hone, D. W. E., Sullivan, C., Eberth, D. A., Nesbitt, S., Zhao, Q., Hernandez, R., Jia, C. K., Han, F. L., & Guo, Y. (2009a). A Jurassic ceratosaur from China helps clarify avian digital homologies. *Nature*, *459*(7249), 940-944.
- Xu, X., Zhao, Q., Norell, M., Sullivan, C., Hone, D., Erickson, G., Wang, X., Han, F., & Guo, Y. (2009b). A new feathered maniraptoran dinosaur fossil that fills a morphological gap in avian origin. *Chinese Science Bulletin*, *54*(3), 430-435.
- Yun, C. (2019). Comments on the ecology of Jurassic theropod dinosaur *Ceratosaurus* (Dinosauria: Theropoda) with critical reevaluation for supposed semiaquatic lifestyle. *Volumina Jurassica*, *17*(1).
- Ziegler, P. A. (1988). Evolution of the Arctic-North Atlantic and the Western Tethys. *AAPG Memoir* *43*, 198p.

Appendix I - Tooth Plates

Ceratosaurus teeth and unconfirmed *Ceratosaurus* teeth from various locations across the Lusitanian basin in (a) labial, (b) mesial, (c) lingual, (d) distal and (e) basal views. Scale bar equals 10mm.

SHN(JJS)205

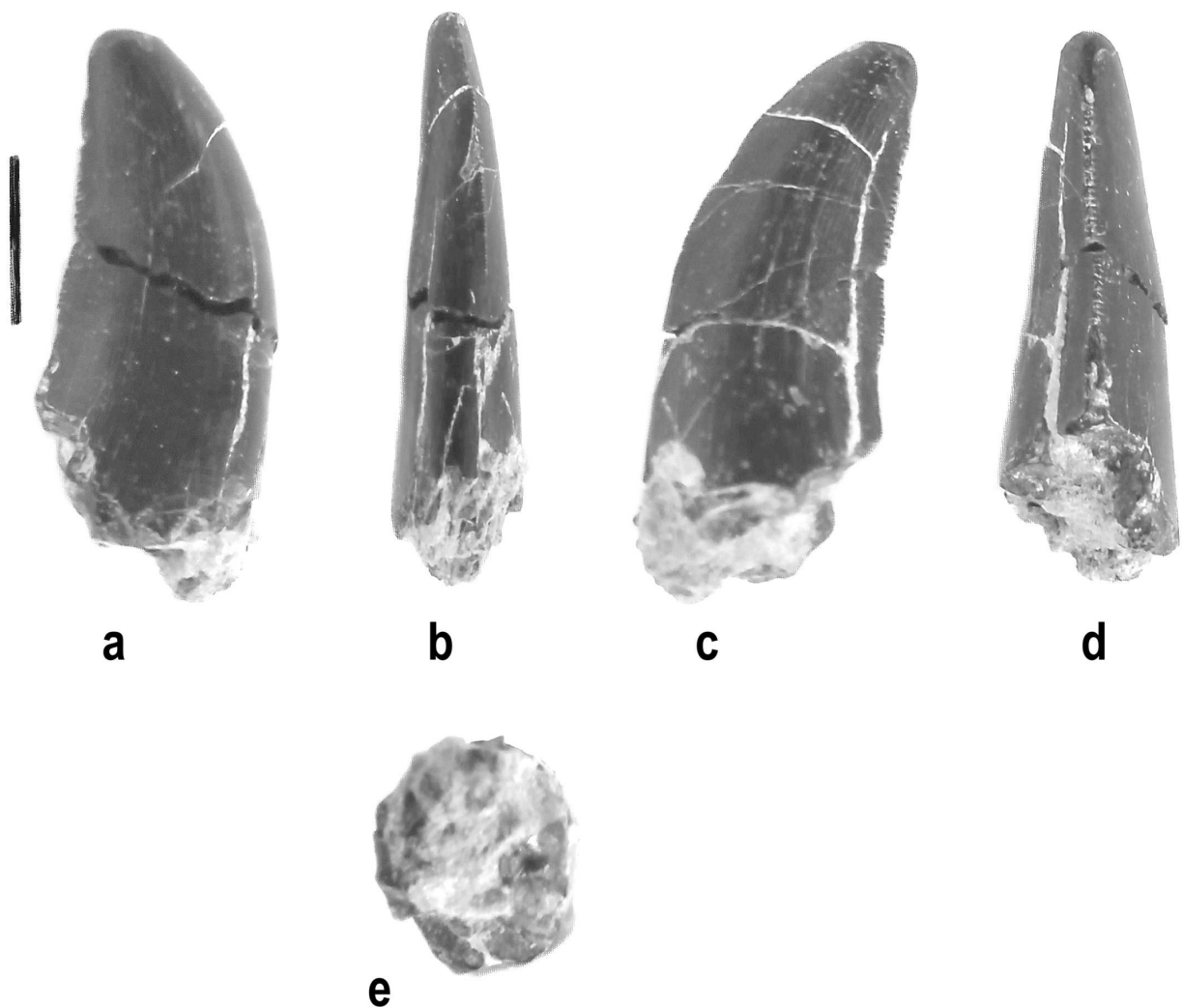


Plate 1. SHN(JJS)205 – *Ceratosaurus* sp. mesial tooth from Praia da Corva Norte, Torres Vedras (Praia Amoreira – Porto Novo Member).

SHN(JJS)236



Plate 2. SHN(JJS)236 - *Ceratosaurus* sp. mesial tooth from Porto Dinheiro, Lourinhã (Praia Amoreira – Porto Novo Member).

SHN(JJS)254

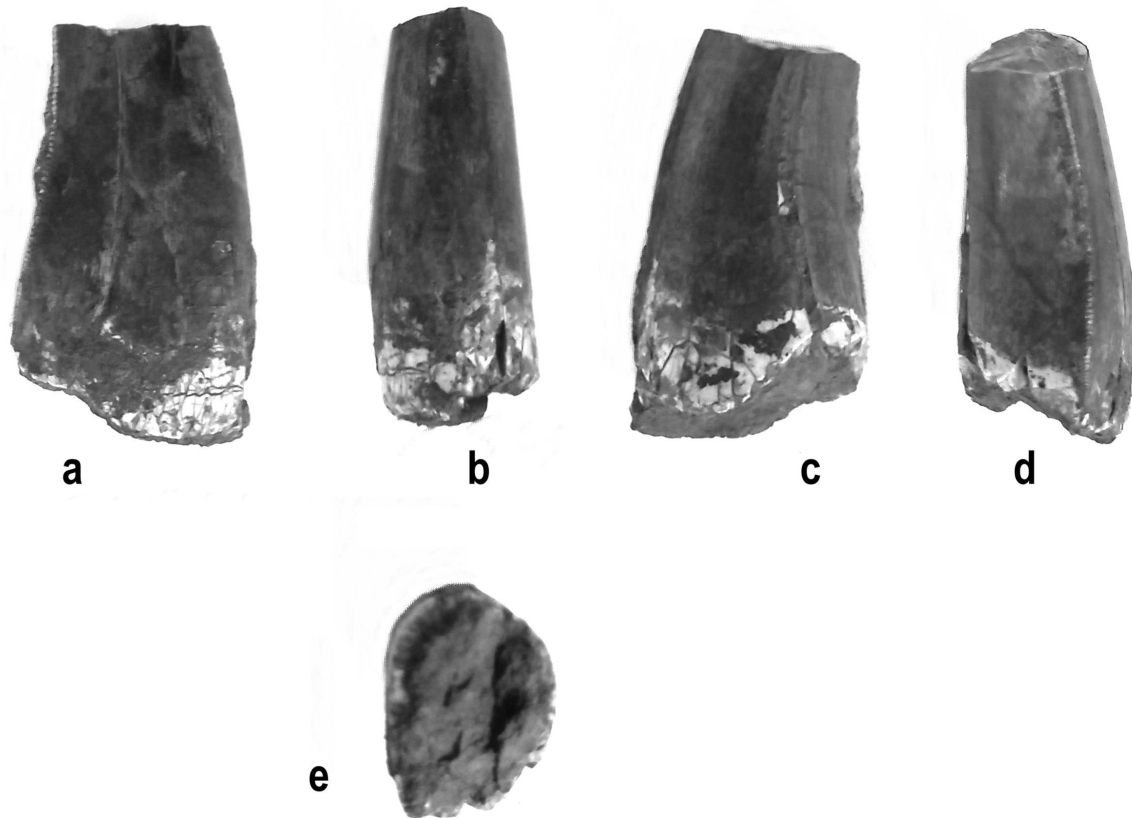


Plate 3. SHN(JJS)254 - *Ceratosaurus* sp. mesial tooth from Praia da Corva, Torres Vedras (Praia Amoreira – Porto Novo Member).

SHN(JJS)370

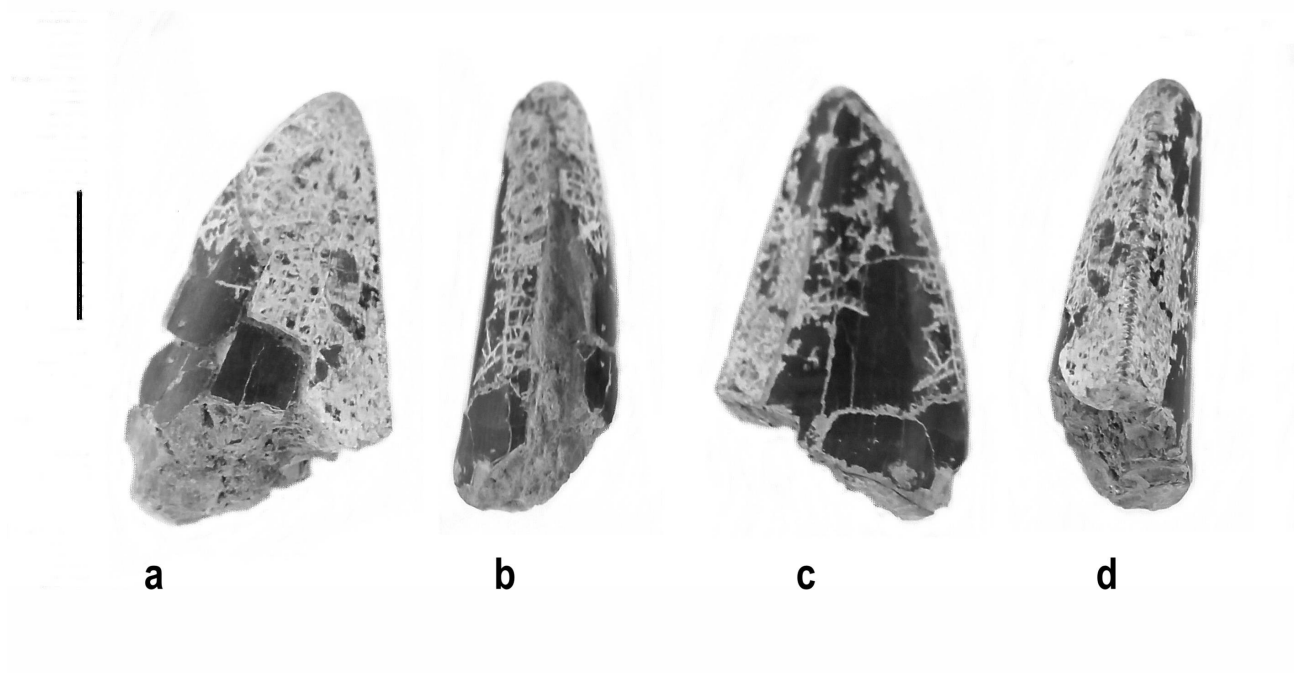


Plate 4. SHN(JJS)370 - *Ceratosaurus* sp. teeth fragments from Valmitão/Peralta, Lourinhã (Praia Amoreira – Porto Novo Member).

SHN(JJS)457

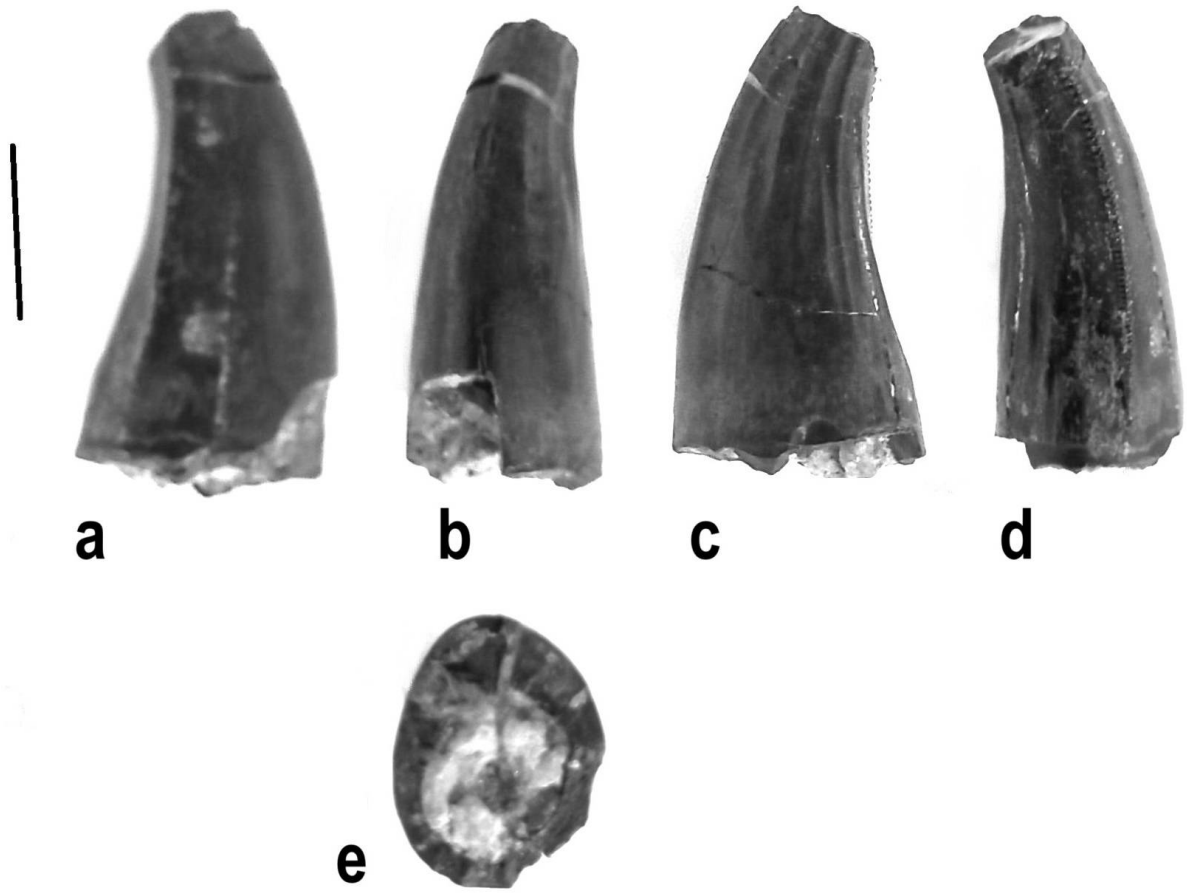


Plate 5. SHN(JJS)457 - *Ceratosaurus* sp. mesial tooth from Porto Dinheiro Norte, Lourinhã (Praia Amoreira – Porto Novo Member).

SHN(JJS)461

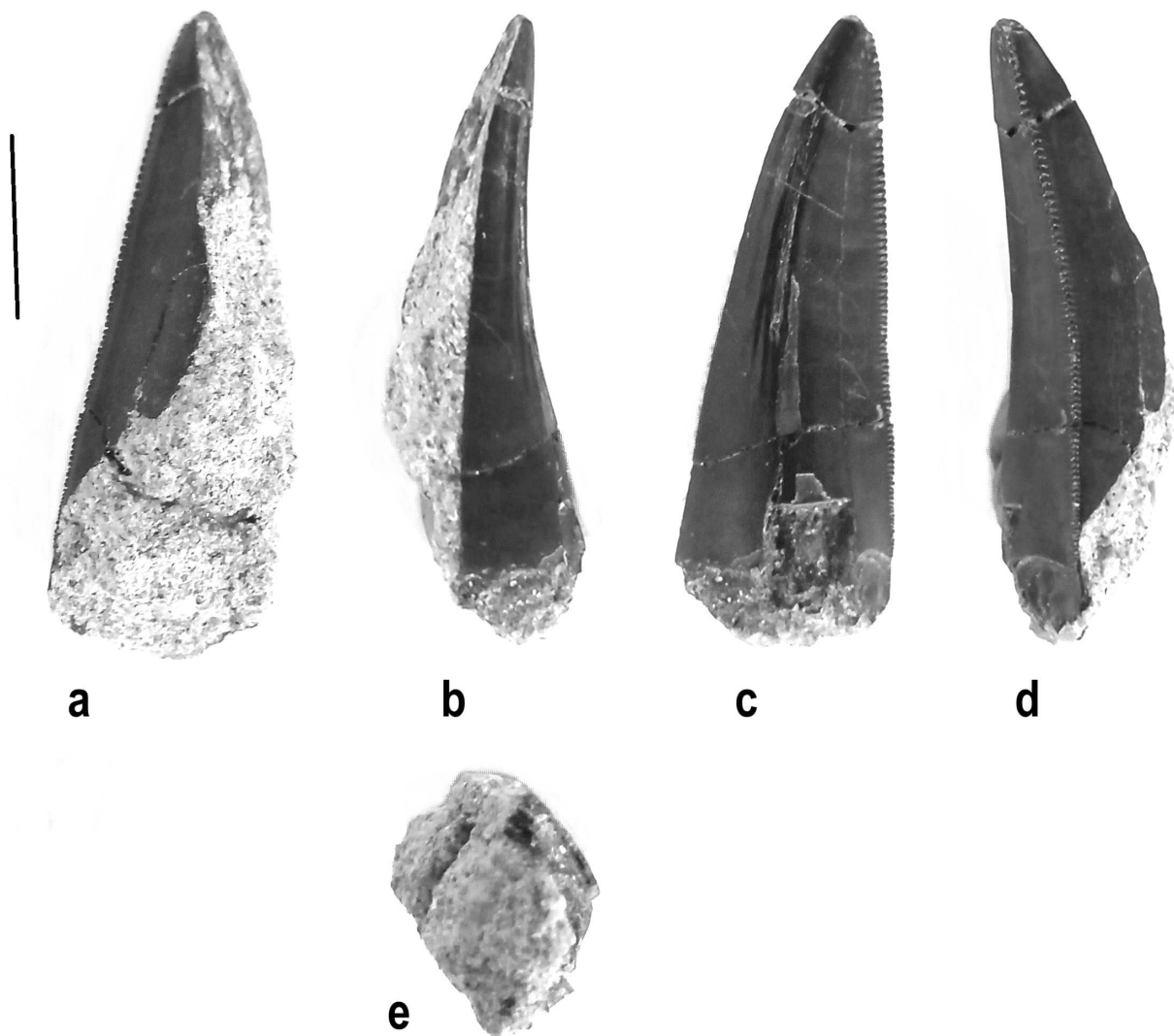


Plate 6. SHN(JJS)461 - *Ceratosaurus* sp. mesial tooth from Porto Dinheiro Norte, Lourinhã (Praia Amoreira – Porto Novo Member).

SHN(JJS)462

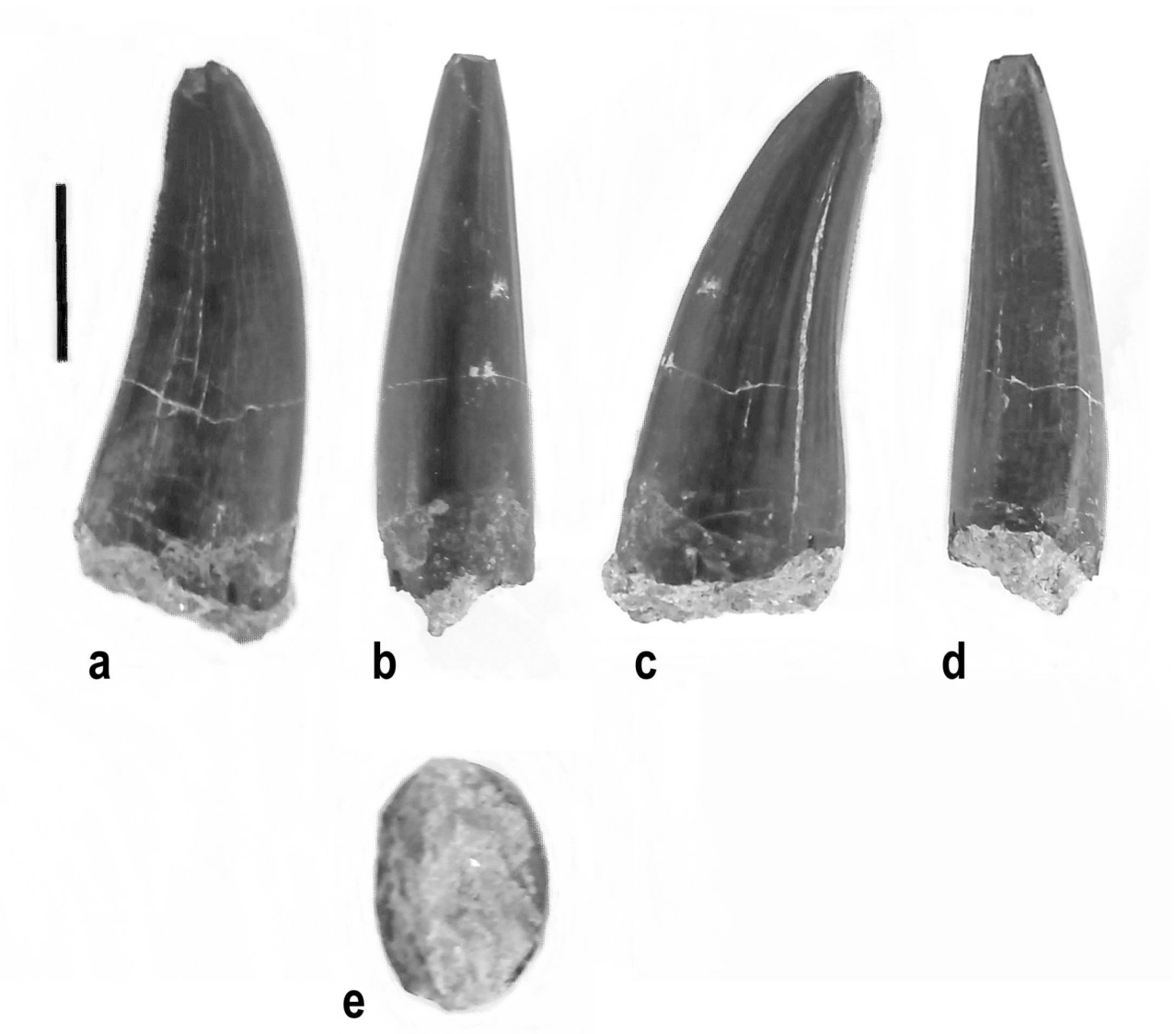


Plate 7. SHN(JJS)462 - *Ceratosaurus* sp. mesial tooth from Praia da Vermelha Norte, Peniche (Praia Amoreira – Porto Novo Member).

SHN212

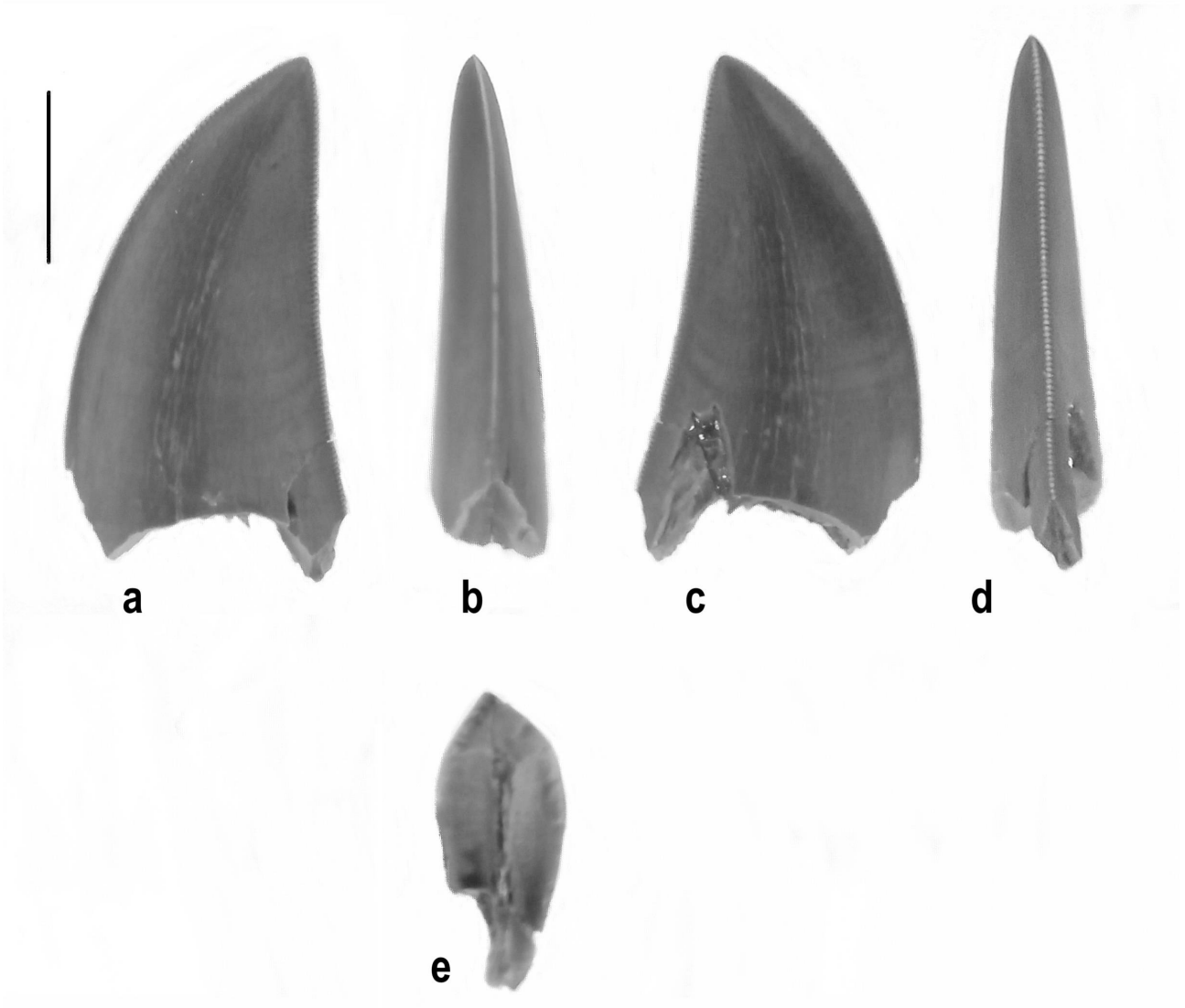
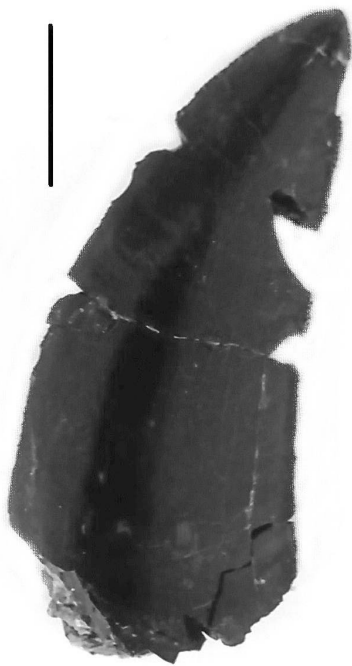
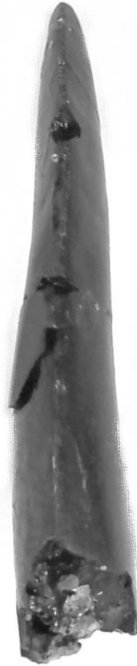


Plate 8. SHN212 – Possible *Ceratosaurus* lateral tooth from Baleal, Peniche, Abadia (?Praia Amoreira – Porto Novo Member)..

SHN218



a



b



c



d



e

Plate 9. SHN218 - Possible *Ceratosaurus* lateral tooth from Praia da Vermelha, Peniche (Praia Amoreira – Porto Novo Member).

SHN(JJS)243

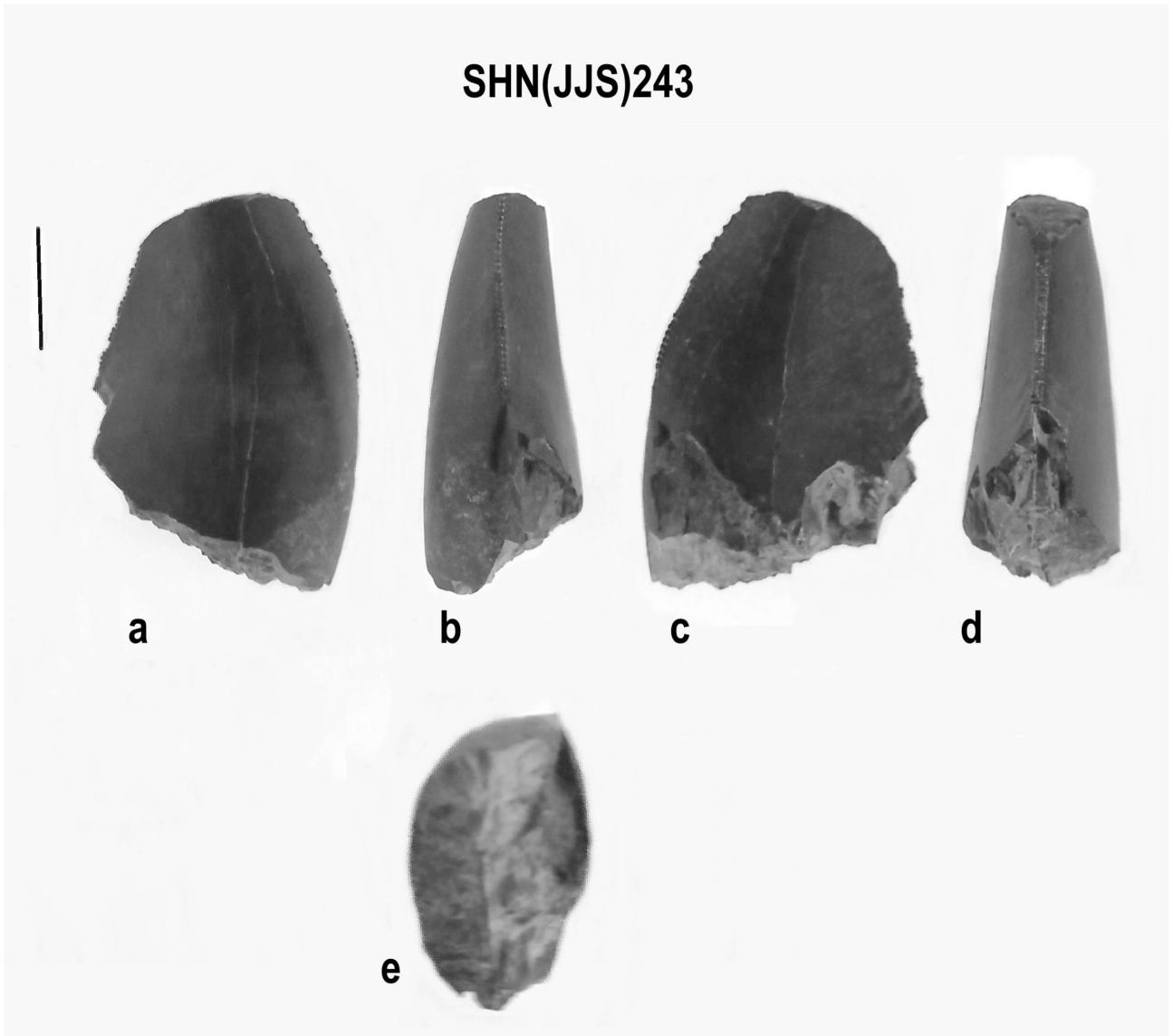


Plate 10. SHN(JJS)243 - Possible Ceratosauria fragmentary tooth from Praia de Pedrogãos (Praia Amoreira – Porto Novo Member).

SHN(JJS)263

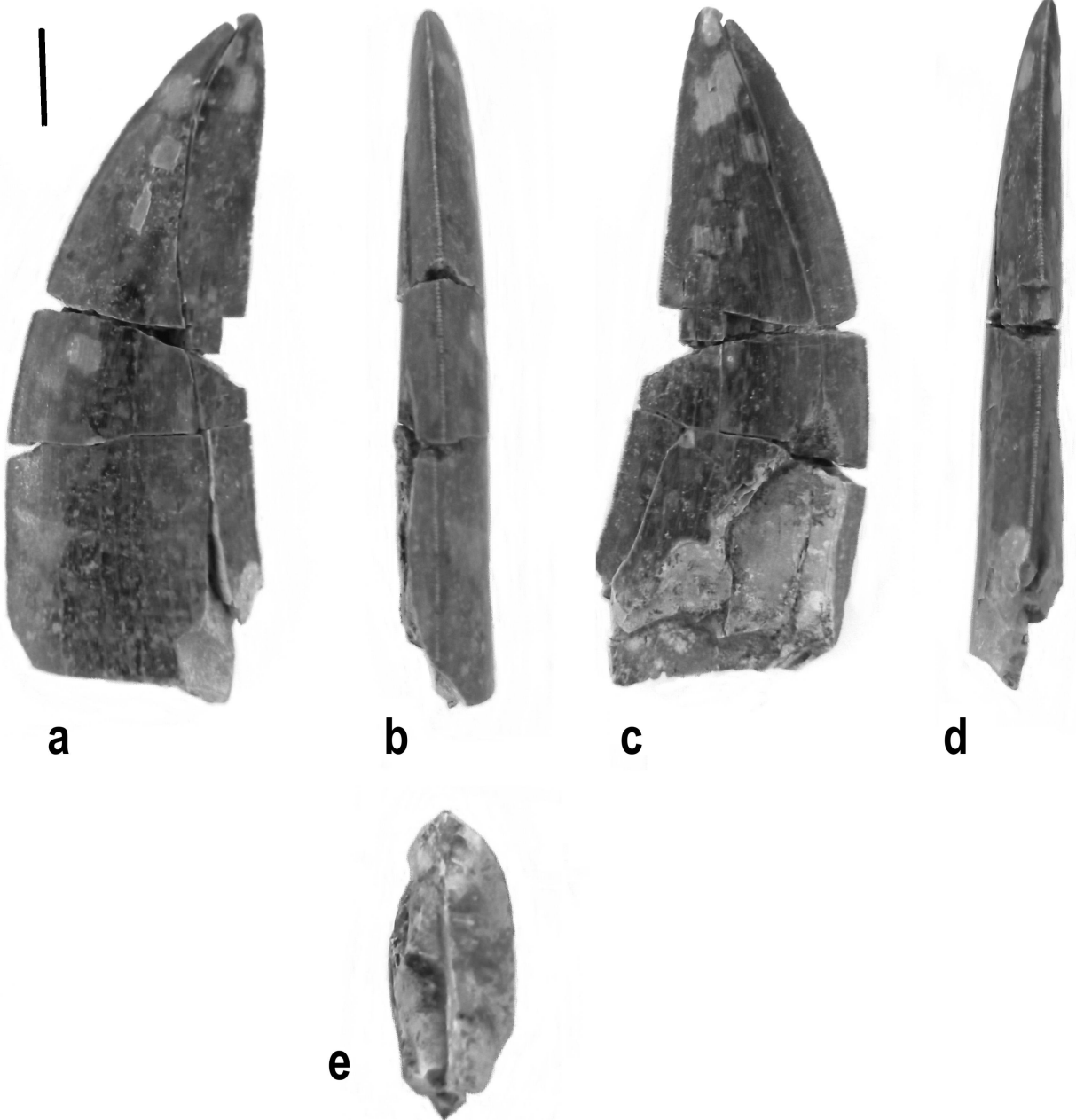


Plate 11. SHN(JJS)263 - Possible *Ceratosaurus* lateral tooth from Praia da Corva, Torres Vedras (Praia Amoreira – Porto Novo Member).

SHN(JJS)269

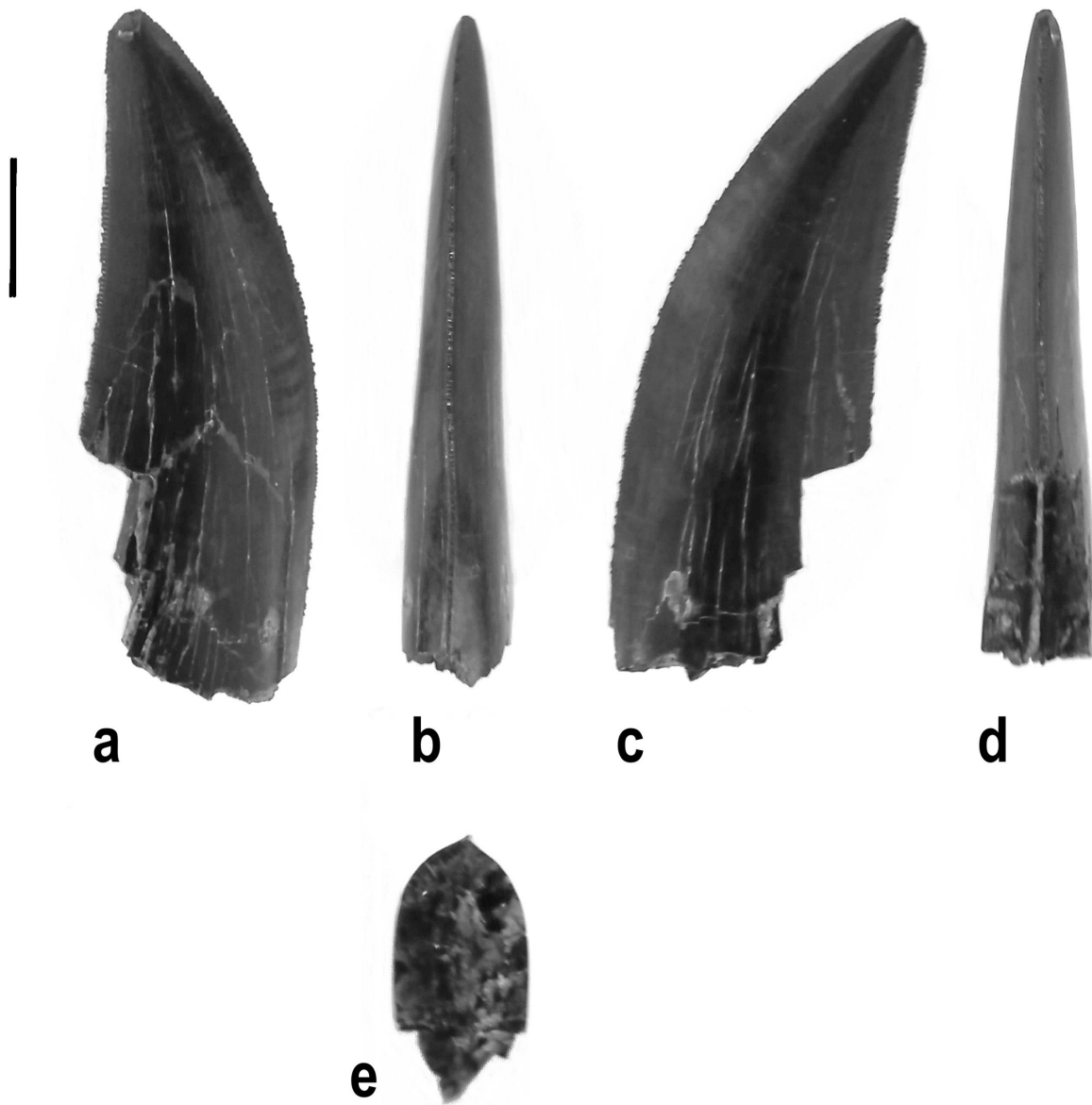


Plate 12. SHN(JJS)269 - Possible *Ceratosaurus* lateral tooth from Peralta, (?)Sobral (?Praia Azul Member).

SHN(JJS)295

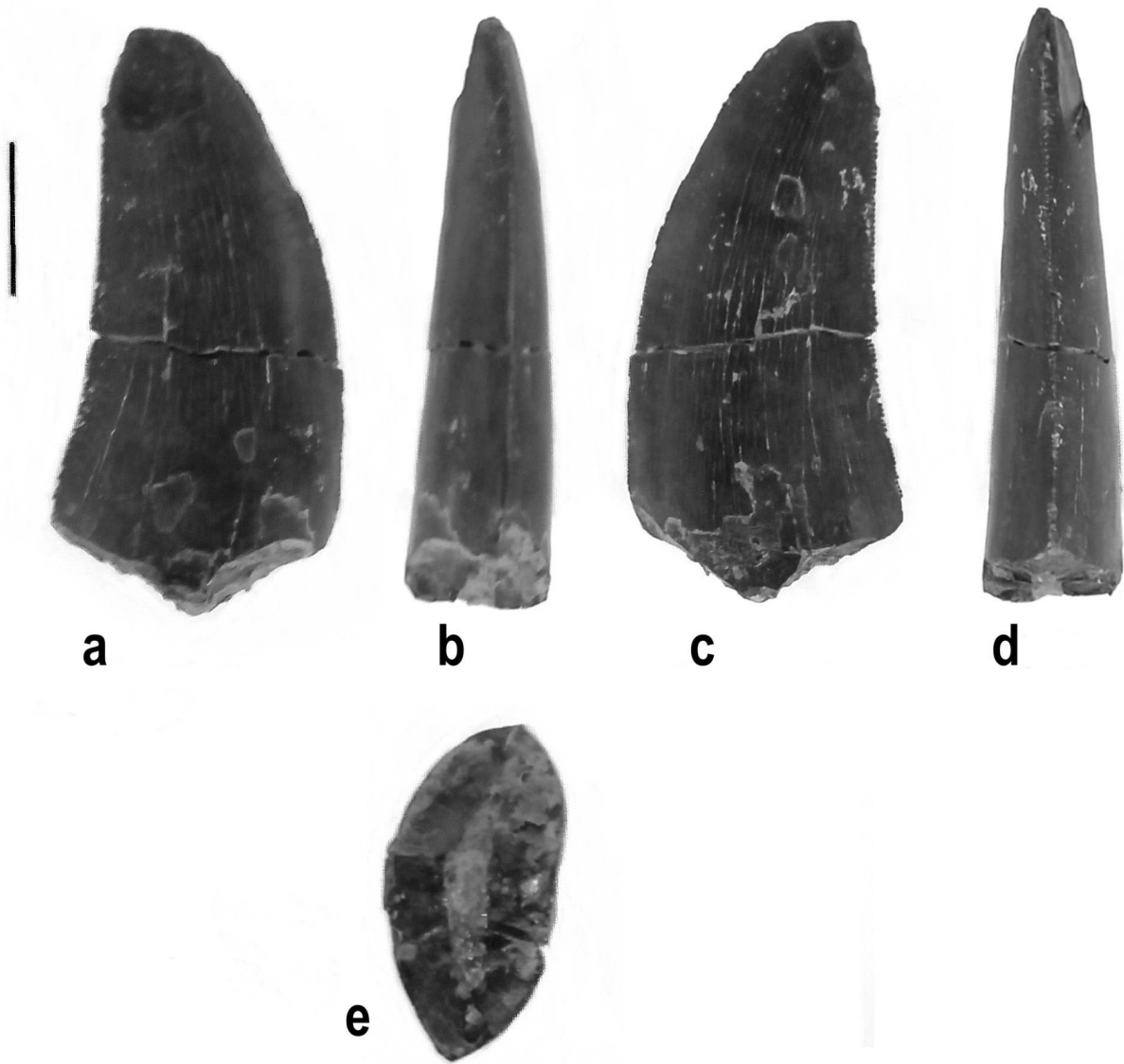


Plate 13. SHN(JJS)295 - Possible *Ceratosaurus* tooth from Valmitão Sul, Lourinhã (Praia Amoreira – Porto Novo Member).

SHN(JJS)305a

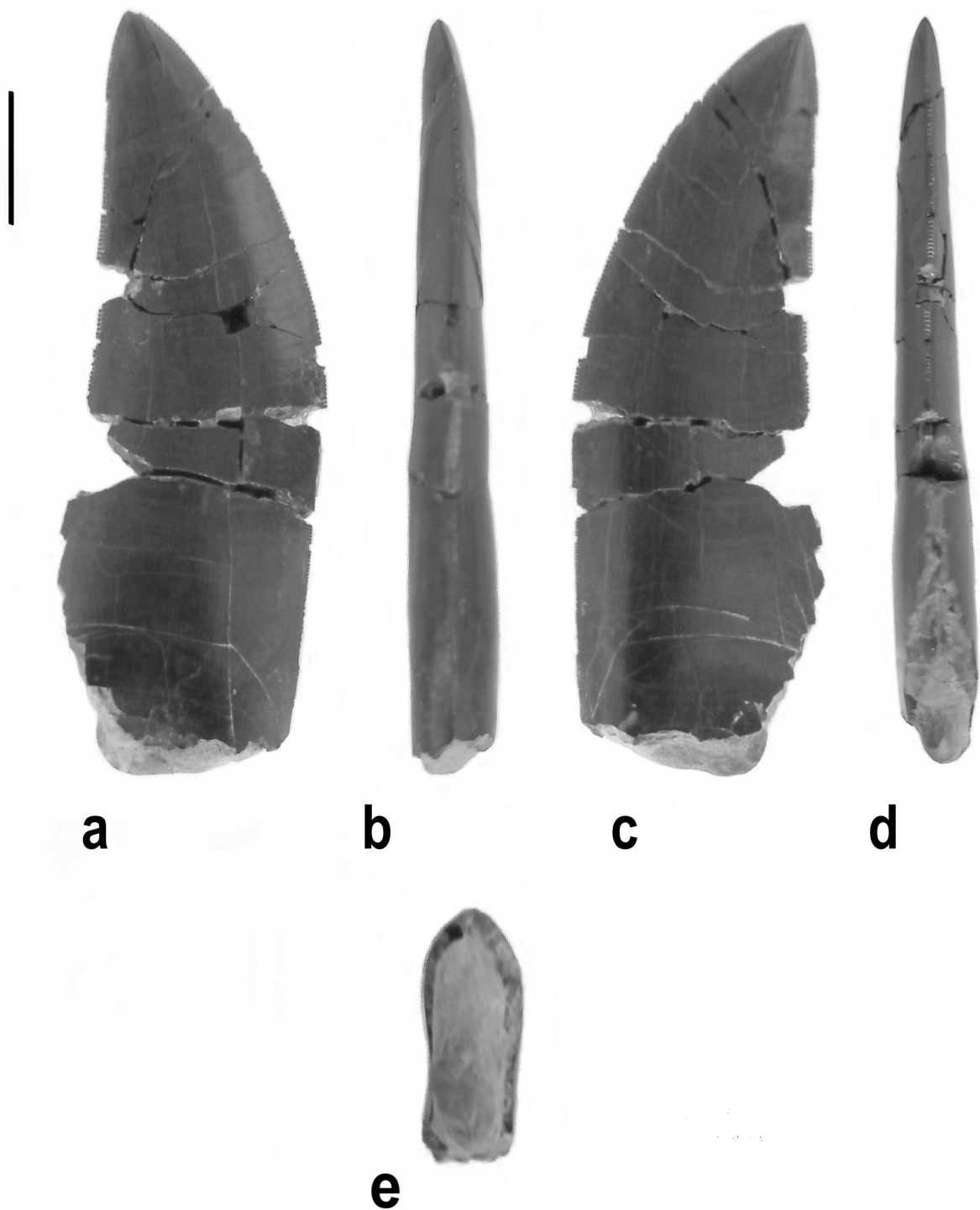


Plate 14. SHN(JJS)305a - Possible *Ceratosaurus* lateral tooth from Cambelas, Freixial.

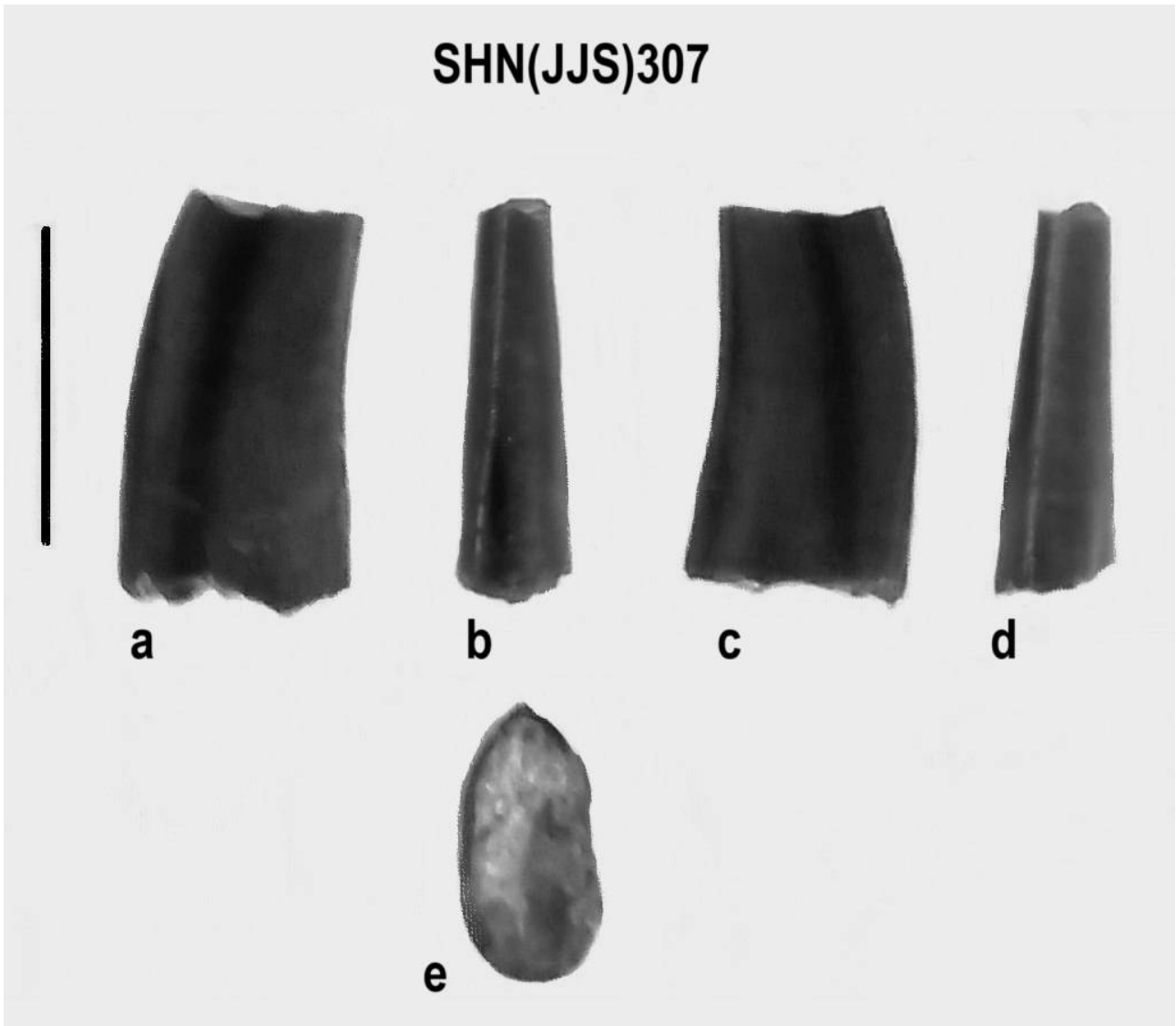


Plate 15. SHN(JJS)307 - Possible *Ceratosaurus* tooth from Peralta Centro, (?)Sobral (?Praia Azul Member).

SHN321a

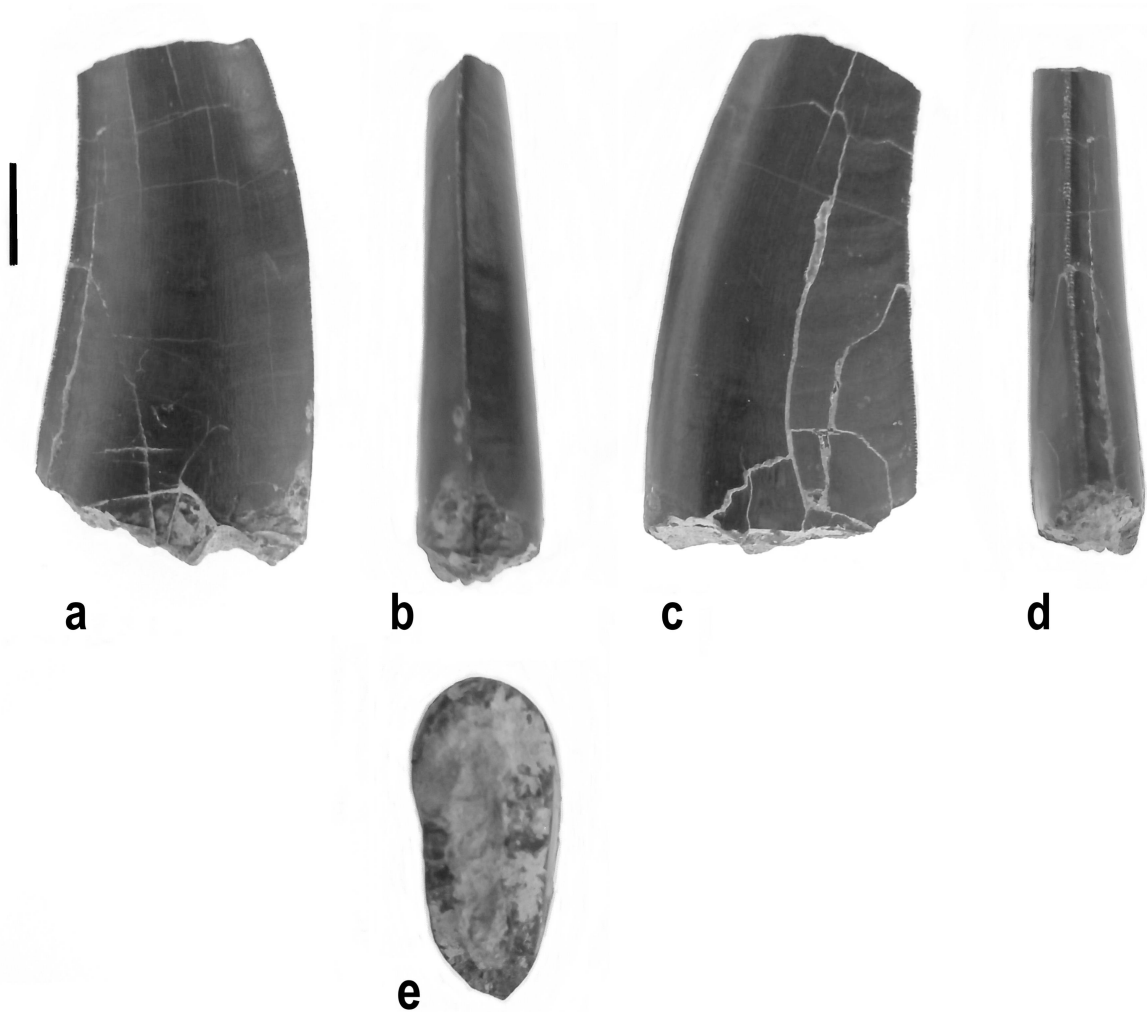


Plate 16. SHN321a - Possible *Ceratosaurus* lateral tooth from Porto Novo, Torres Vedras (Praia Amoreira – Porto Novo Member).

SHN321b

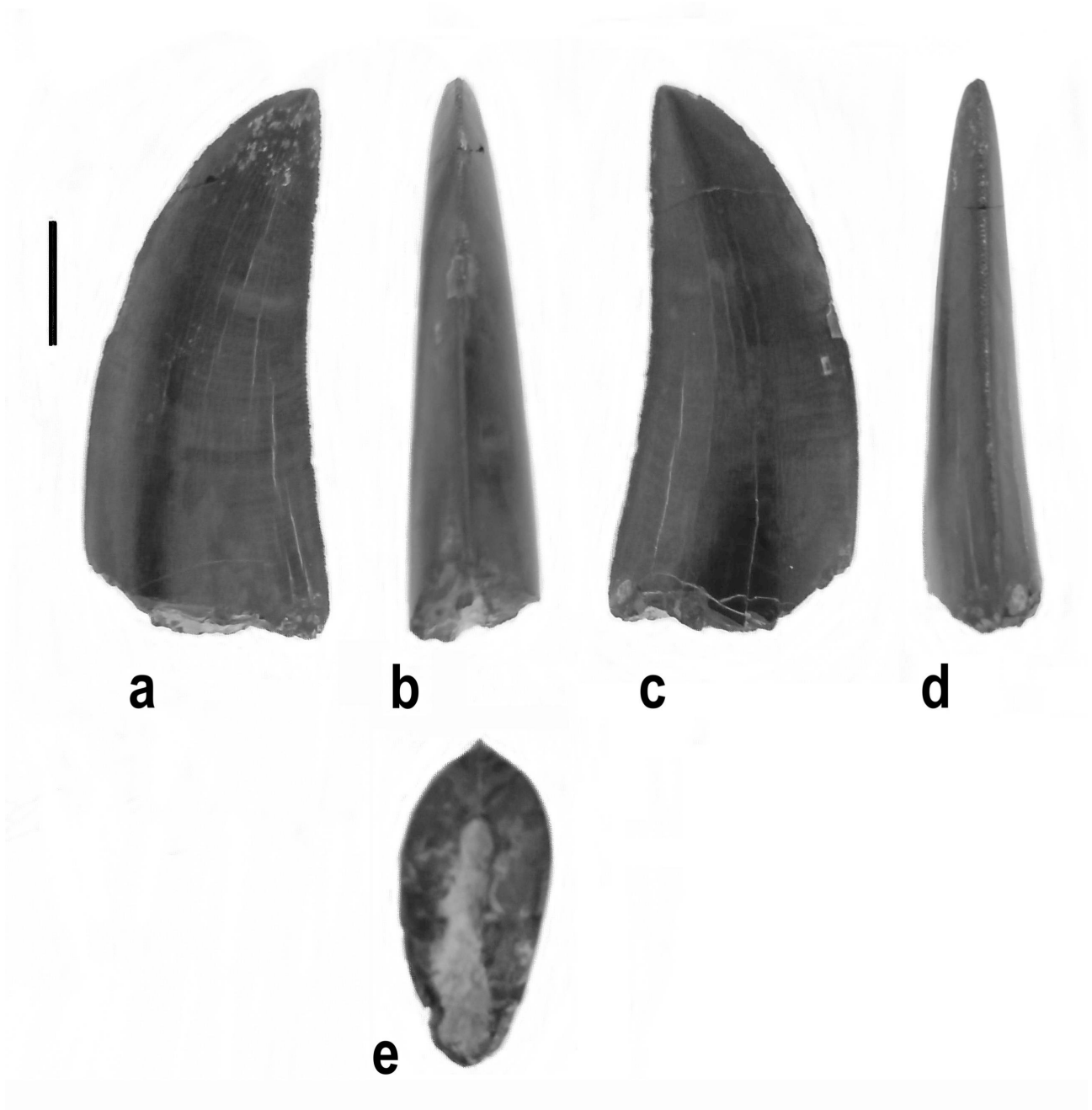


Plate 17. SHN321b - Possible *Ceratosaurus* lateral tooth from Porto Novo, Torres Vedras (Praia Amoreira – Porto Novo Member).

SHN321c



a



b



c



d



e

Plate 18. SHN321c - Possible *Ceratosaurus* lateral tooth from Porto Novo, Torres Vedras (Praia Amoreira – Porto Novo Member).

SHN(JJS)359c

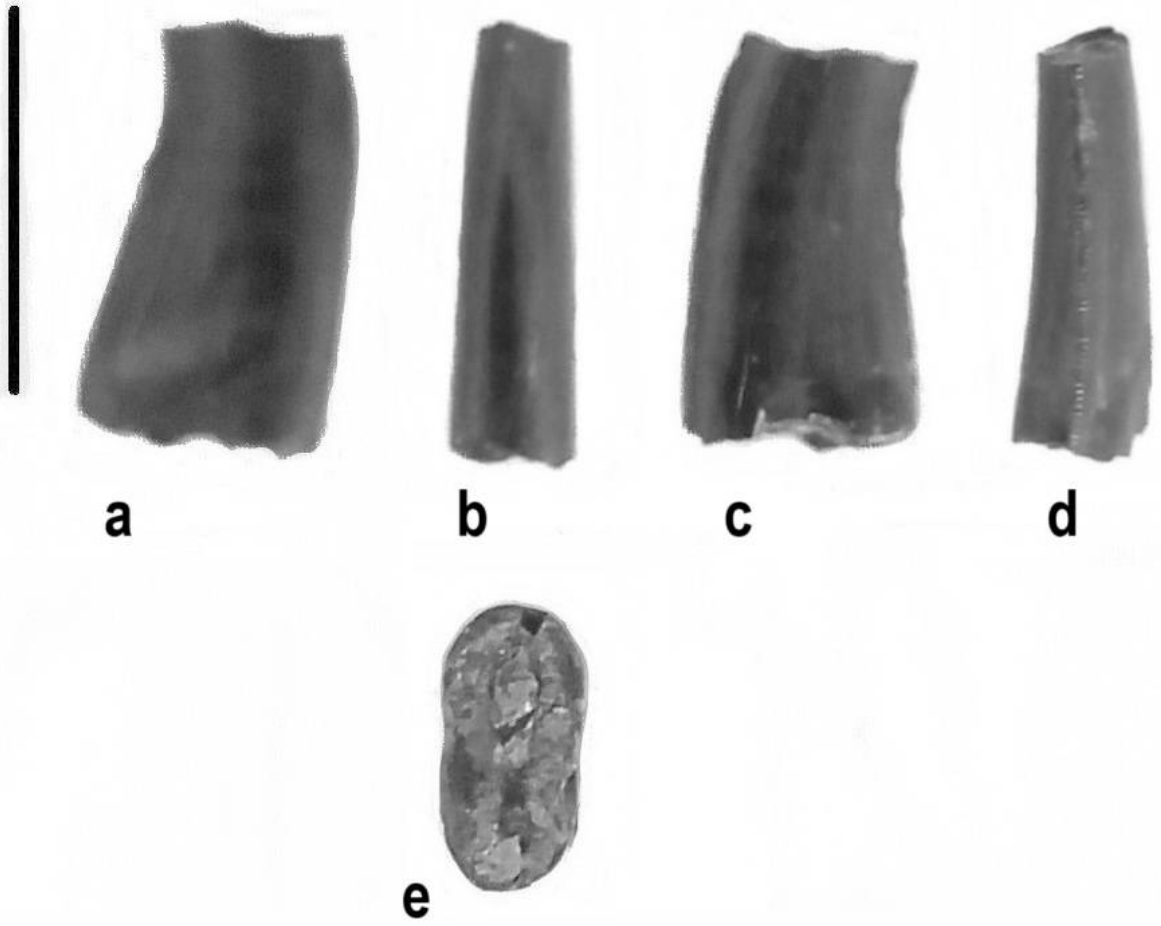


Plate 19. SHN(JJS)359c - Possible *Ceratosaurus* tooth from Porto Novo, Torres Vedras (Praia Amoreira – Porto Novo Member).

SHN(JJS)377

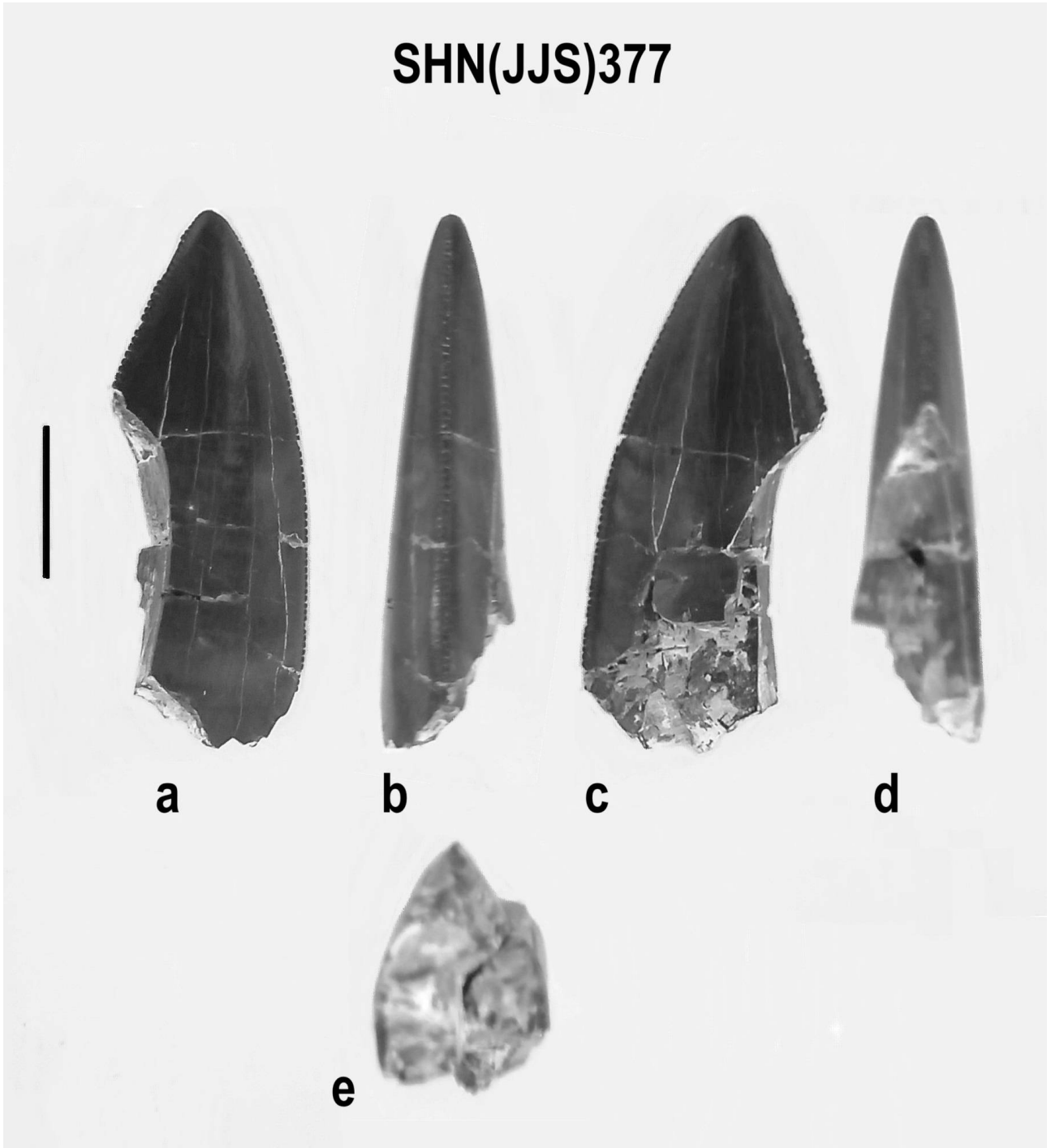


Plate 20. SHN(JJS)377 - Possible *Ceratosaurus* tooth from São Bernardino (Praia Amoreira – Porto Novo Member).

SHN(JJS)425

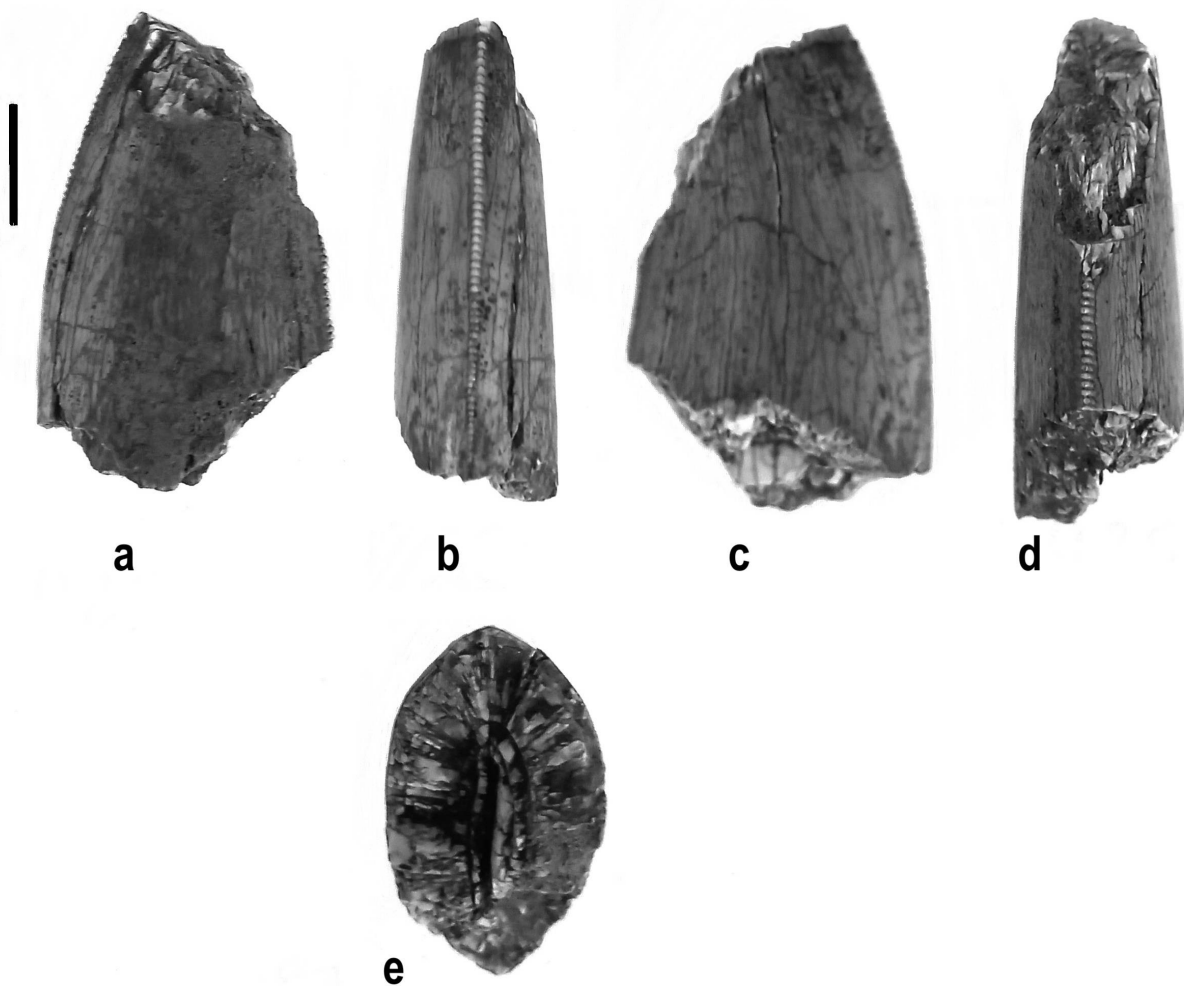


Plate 21. SHN(JJS)425 - Possible Ceratosauria tooth fragment from Valmitão, Lourinhã (Praia Amoreira – Porto Novo Member).

SHN(JJS)458

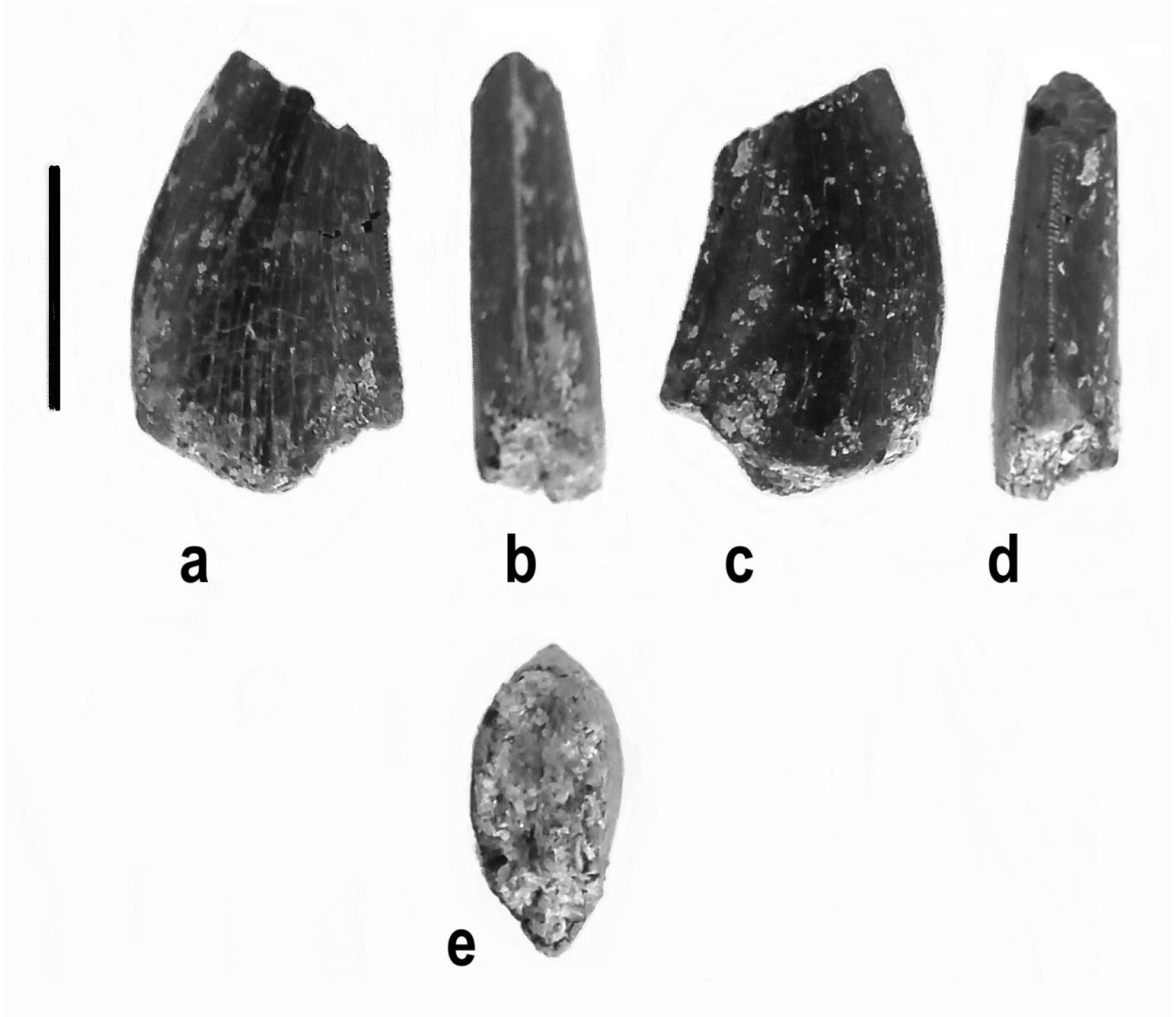


Plate 22. SHN(JJS)458 - Possible *Ceratosaurus* tooth from Santa Rita, Torres Vedras (?Praia Amoreira – Porto Novo Member).

SHN459

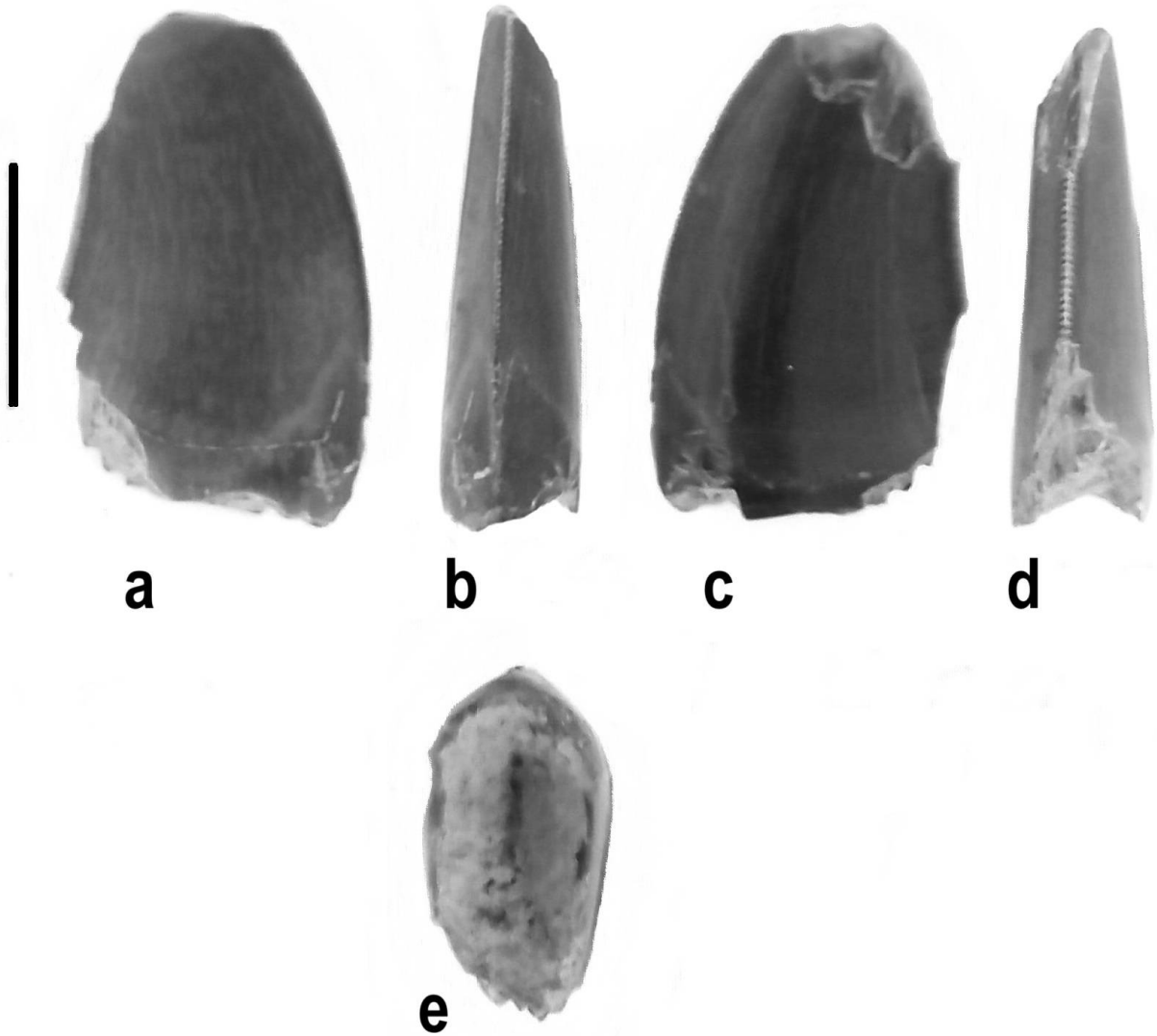


Plate 23. SHN459 - Possible *Ceratosaurus* lateral tooth from Santa Rita, Torres Vedras (?Praia Amoreira – Porto Novo Member).

Appendix II – Bone illustrations (for compared anatomy)

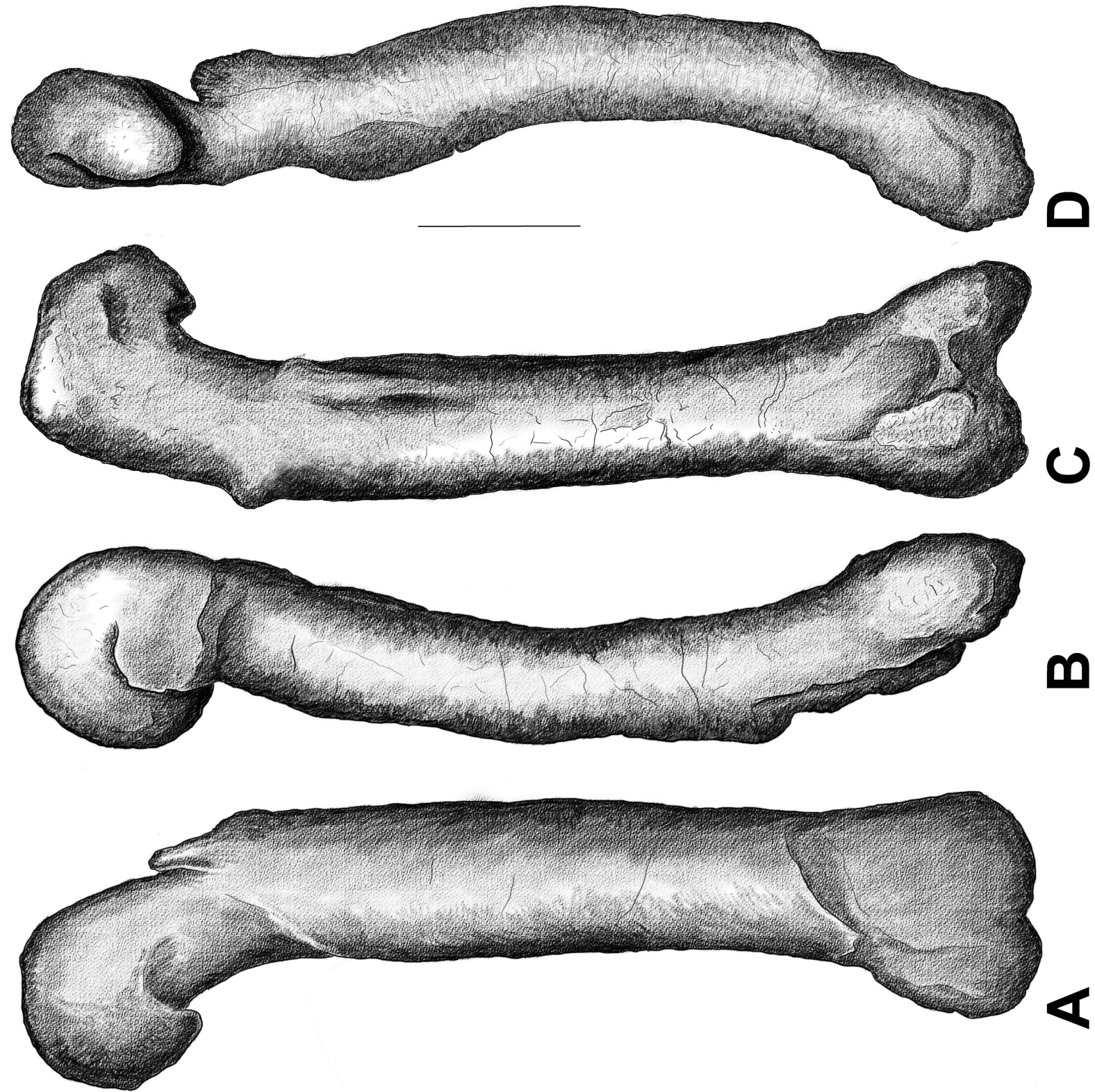


Plate 24. ML352/SHN(JJS)065 right femur (reversed for left side illustration) in anterior (A), lateral (B), posterior (C) and medial (D) view. Scale bar equals 10cm.

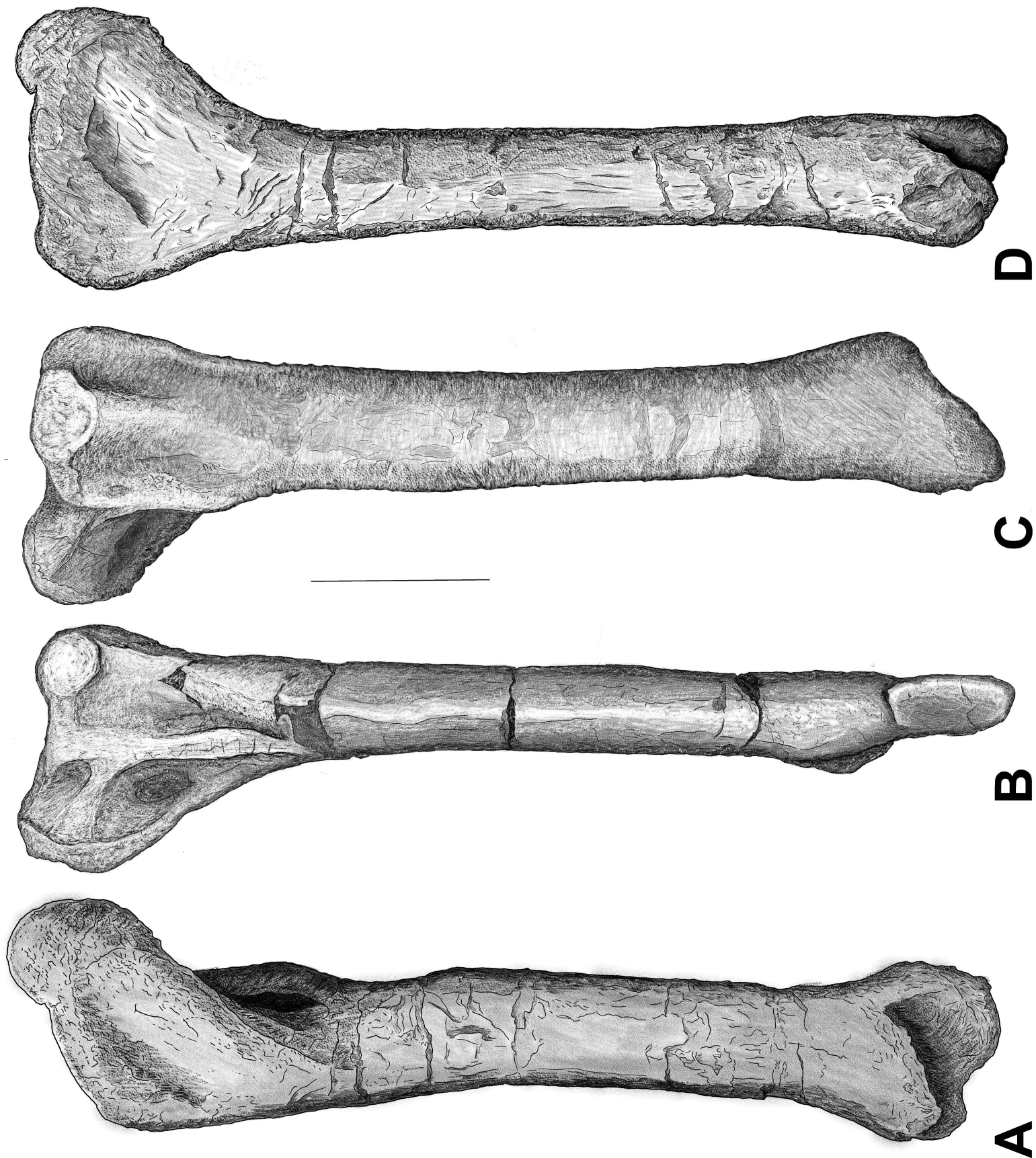


Plate 25. ML352/SHN(JJS)065 left tibia (except **B**, which is the right tibia reversed for left side illustration) in anterior (**A**), lateral (**B**), posterior (**C**) and medial (**D**) view. Scale bar equals 10cm.

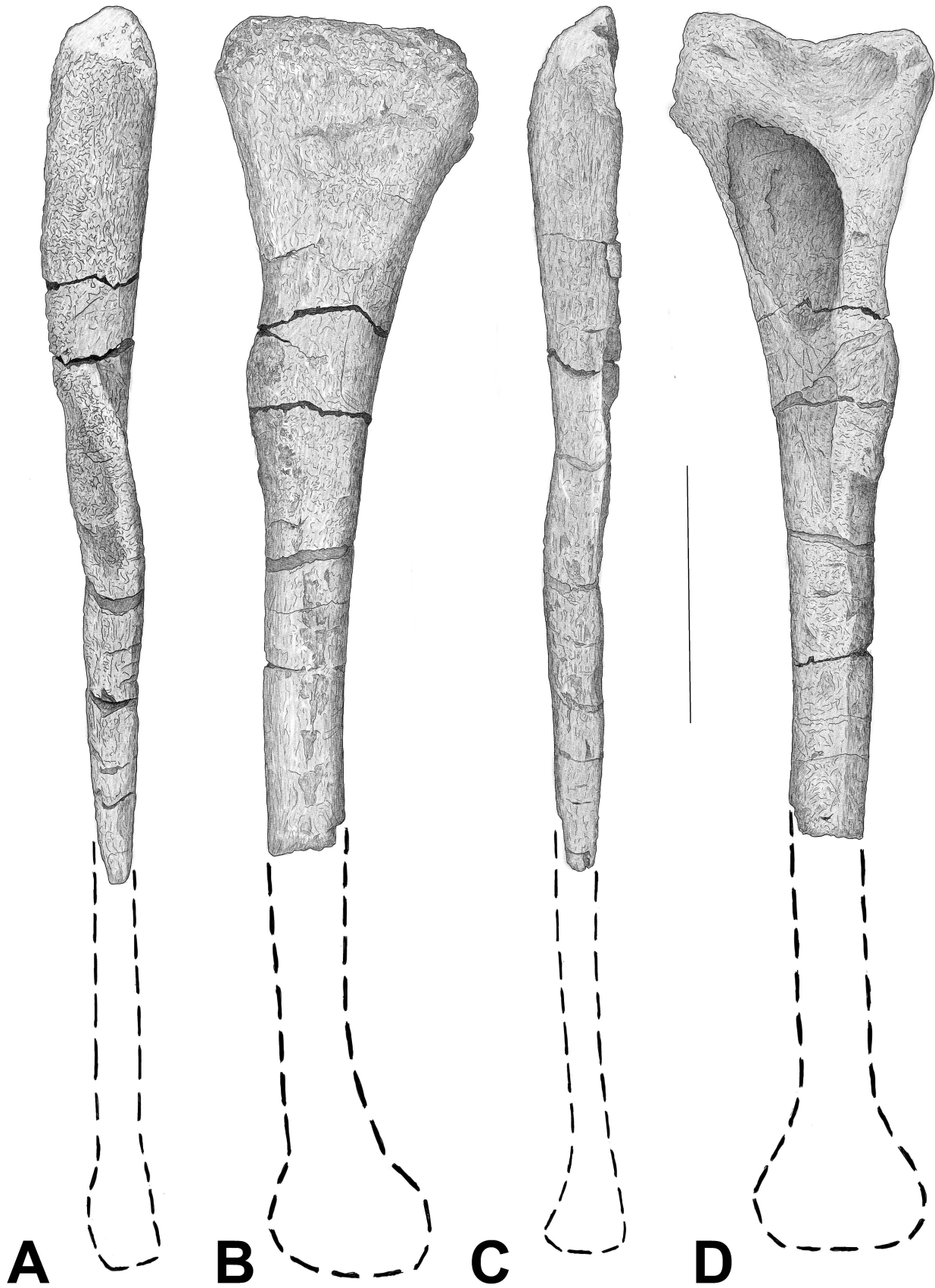


Plate 26. ML352/SHN(JJS)065 left fibula in anterior (A), lateral (B), posterior (C) and medial (D) view. Scale bar equals 10cm.

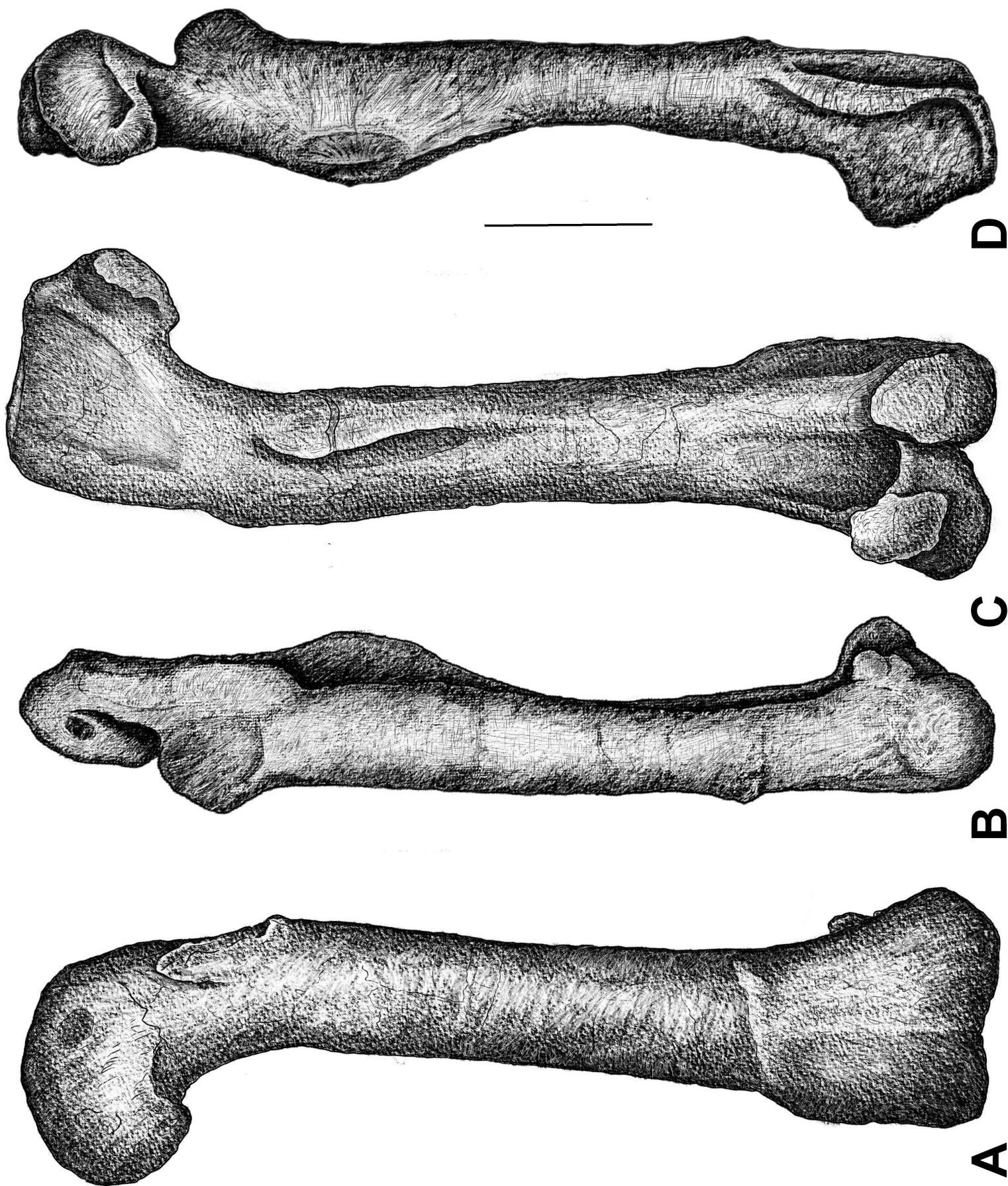


Plate 27. *C. dentisulcatus* left femur in anterior (A), lateral (B), posterior (C) and medial (D) view. Based on Madsen and Welles (2000) and photographic material. Scale bar equals 10cm.

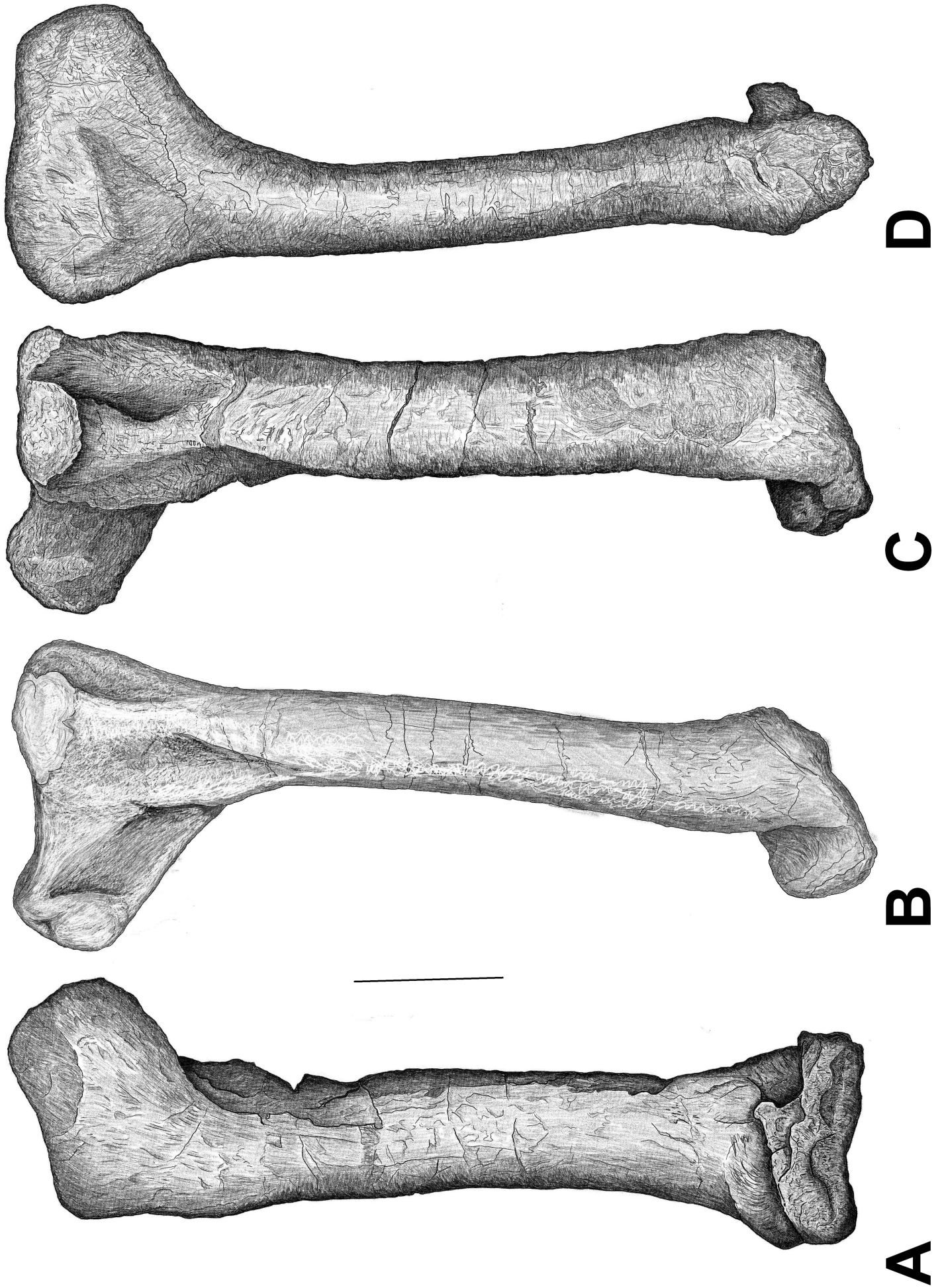


Plate 28. *C. dentisulcatus* left tibia (except **B**, which is the right tibia reversed for left side illustration) in anterior (**A**), lateral (**B**), posterior (**C**) and medial (**D**) view. Based on Madsen and Welles (2000) and photographic material. Scale bar equals 10cm.

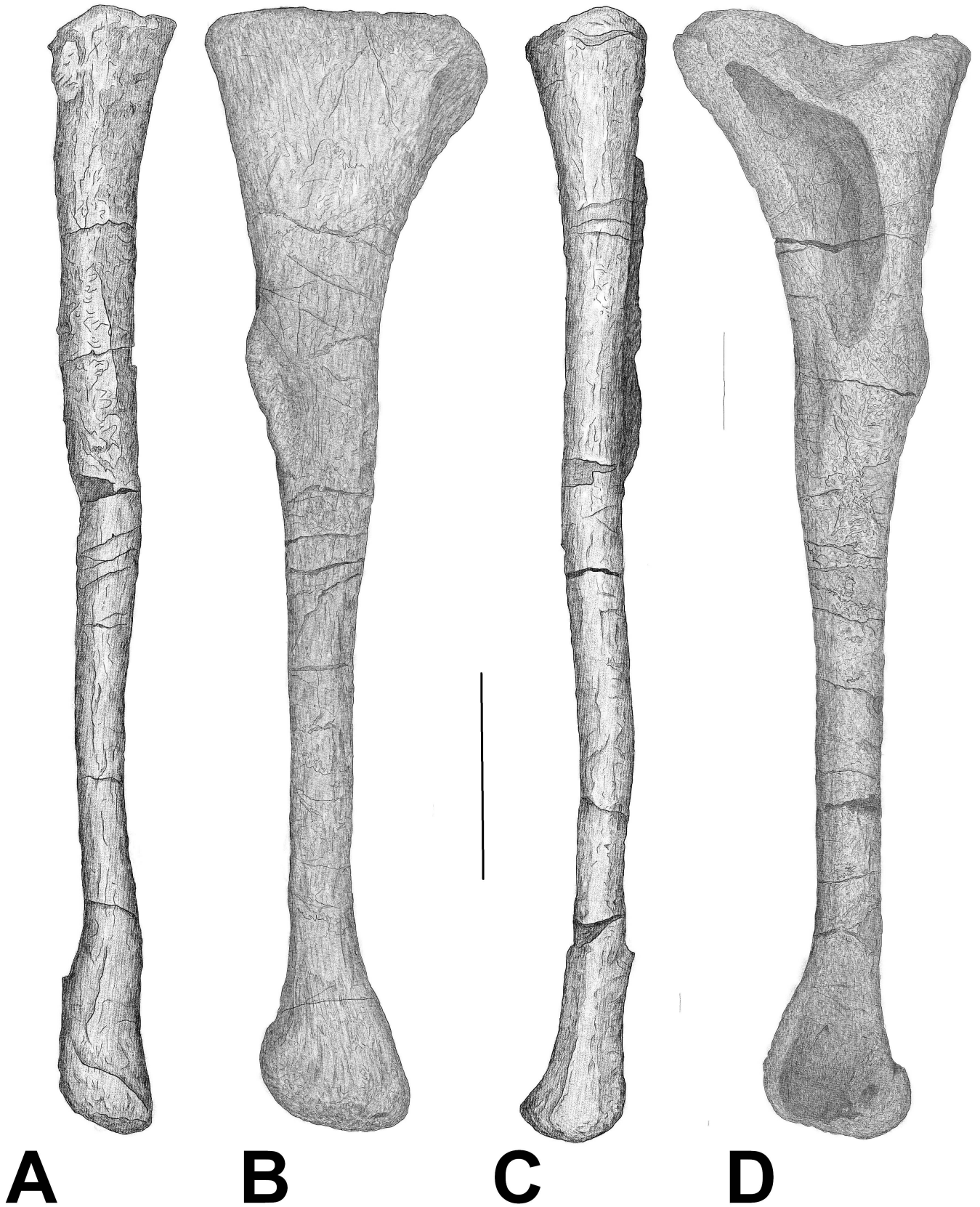


Plate 29. *C. dentisulcatus* left fibula (except **B** and **D** which are the right tibia reversed for left side illustration) in anterior (**A**), lateral (**B**), posterior (**C**) and medial (**D**) view. Based on Madsen and Welles (2000) and photographic material. Scale bar equals 10cm.

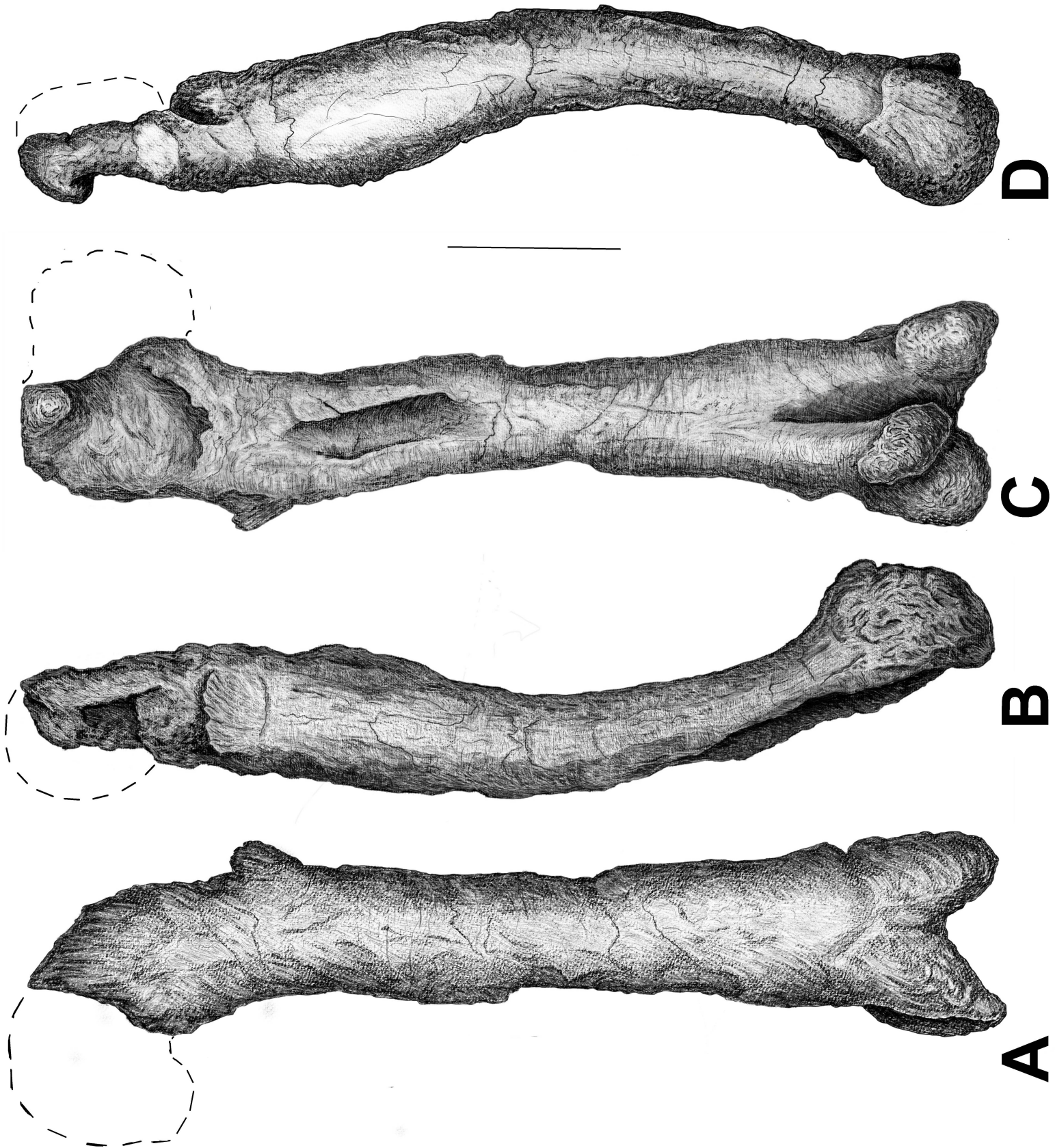


Plate 30. *C. magnicornis* right femur (reversed for left side illustration) in anterior (A), lateral (B), posterior (C) and medial (D) view. Based on photographic material. Scale bar equals 10cm.



Plate 31. *C. magnicornis* right tibia (reversed for left side illustration) in anterior (A), lateral (B), posterior (C) and medial (D) view. Based on Madsen and Welles (2000) and photographic material. Scale bar equals 10cm.

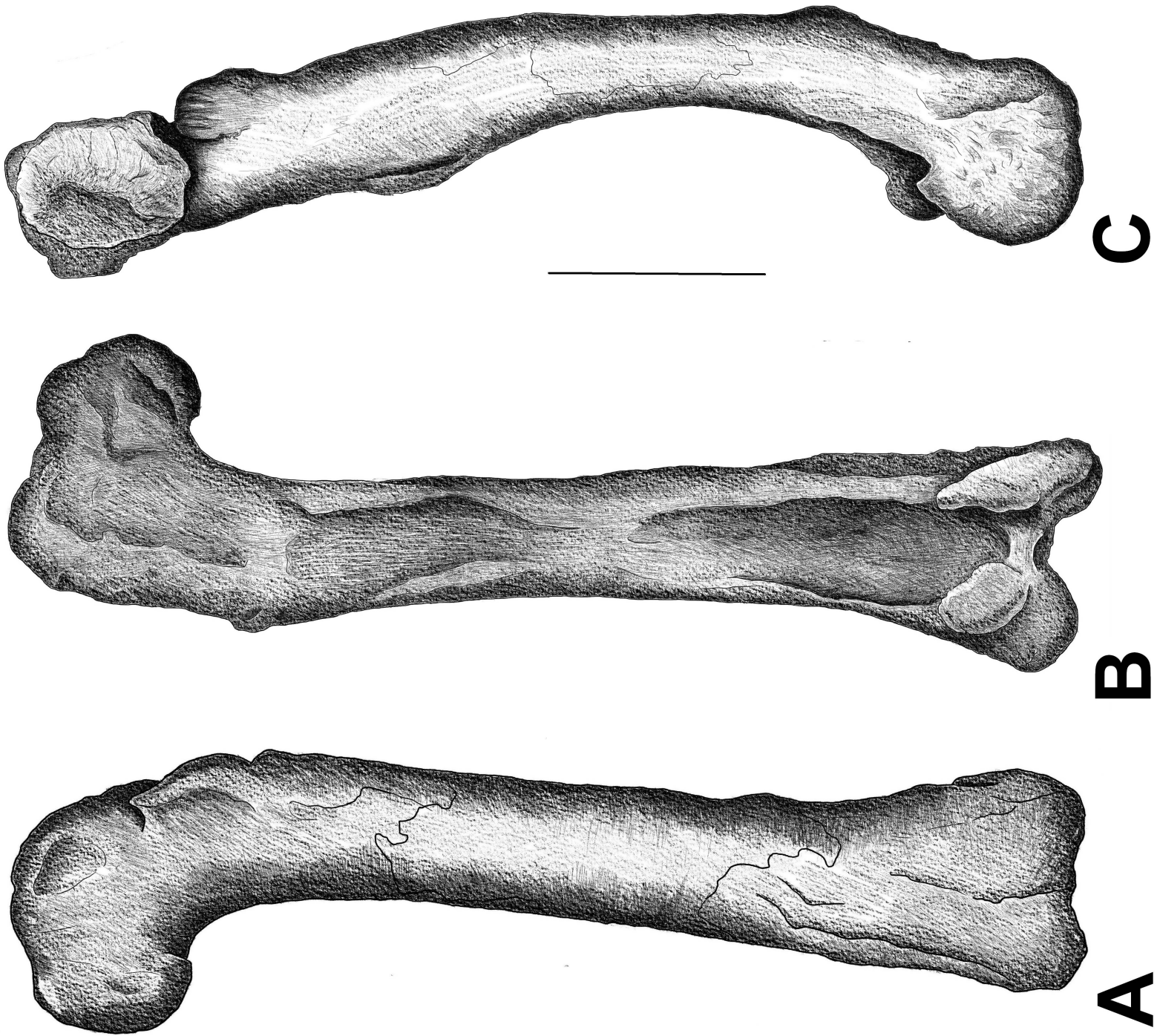


Plate 32. *C. nasicornis* right femur (reversed for left side illustration) in anterior (A), posterior (B), and medial (C) view. Based on Gilmore (1920) and photographic material. Scale bar equals 10cm.

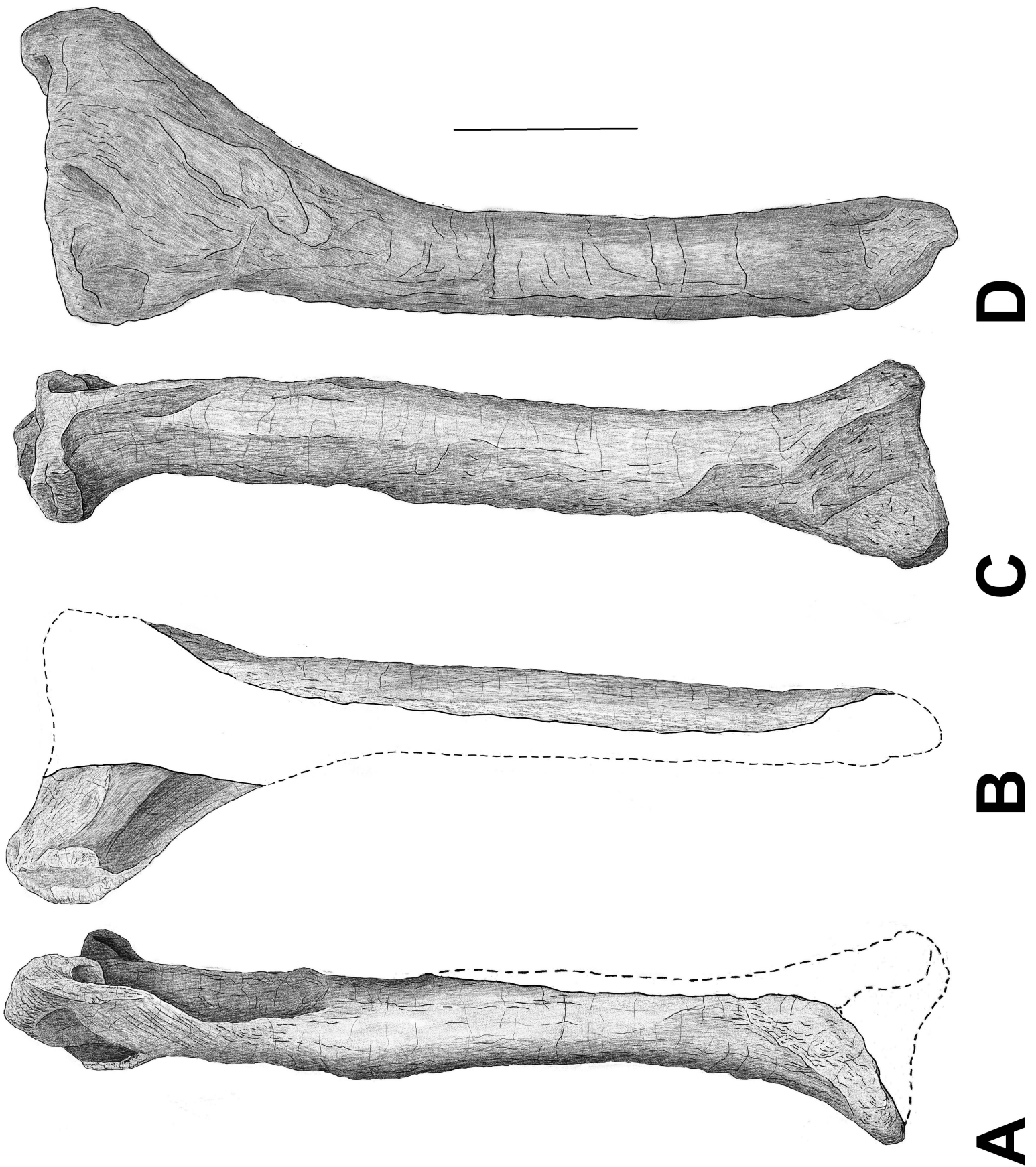


Plate 33. *C. nasicornis* right tibia (reversed for left side illustration) in anterior (A), lateral (B), posterior (C) and medial (D) view. Based on Gilmore (1920) and photographic material. Scale bar equals 10cm.



Plate 34. *C. nasicornis* right fibula (reversed for left side illustration) in anterior (A), lateral (B), posterior (C) view. Based on Gilmore (1920) and photographic material. Scale bar equals 10cm.

Appendix III – Matrices and List of Characters

Character list for the new matrix based on Ezcurra et al. (2023), after Nesbitt et al. (2009).

Characters 1–389 follows Ezcurra et al. (2023), which is the latest iteration of this phylogenetic data matrix. Characters 390–402 have been added here.

Characters:

- 1) Premaxilla, height: length ratio below external naris: 0.5-1.25 (0); <0.5 (1); >1.25 (2). Smith et al. 2007: 5; Irmis 2008: 9; Nesbitt et al. 2009:1
- 2) Premaxilla, anterodorsal process (=nasal process), length: less than the anteroposterior length of the premaxilla (0); greater than the anteroposterior length of the premaxilla (1). Nesbitt and Norell 2006; Nesbitt 2009: 1; Nesbitt et al. 2009:2
- 3) Premaxilla, angle of the anterodorsal process (=nasal process) relative to the alveolar margin: more than 75 degrees (0); less than 70 degrees (1). Smith et al. 2007: 6; Irmis 2008: 10; Nesbitt et al. 2009:3
- 4) Premaxilla, posterodorsal process (=maxillary process, = subnarial process), length: less than or about the same as the anteroposterior length of the premaxilla (0); greater than the anteroposterior length of the premaxilla (1). Nesbitt 2009: 2; Nesbitt et al. 2009:4
- 5) Premaxilla, posterodorsal process (=maxillary process, = subnarial process): wide, plate-like (0); thin (1). Parrish 1993; Clark et al. 2000; Olsen et al. 2000; Benton and Walker 2002; Sues et al. 2003; Clark et al. 2004; Nesbitt 2009: 3; Nesbitt et al. 2009:5
- 6) Premaxilla, posterodorsal process (=maxillary process, = subnarial process): extends posteriorly to the external naris (0); restricted to the ventral border of the external naris (1). Smith et al. 2007: 7; Irmis 2008: 13; Nesbitt et al. 2009:6
- 7) Premaxilla, ventral process at the posterior end of the premaxillary body: absent (0); present (1). Langer and Benton 2006; Nesbitt 2009: 5; Nesbitt et al. 2009:7
- 8) Premaxilla-nasal suture, on the internarial bar: V-shaped (0); W-shaped (1). Smith et al. 2007: 16; Irmis 2008: 17; Nesbitt et al. 2009:8
- 9) Premaxillary teeth, number: ≤ 2 (0), 3(1); 4 (2); 5 (3); ≥ 6 (4). Nesbitt and Norell 2006; Nesbitt 2009: 6; Nesbitt et al. 2009:9
- 10) Premaxillary teeth, serrations: present (0); absent (1). Heckert et al. 1996; Parker 2007; Nesbitt 2009: 7; Nesbitt et al. 2009:10
- 11) Premaxilla, teeth: present along entire length of the premaxilla (0); absent in the anterior portion of the premaxilla (1). Smith et al. 2007: 17; Irmis 2008: 139; Nesbitt et al. 2009:11
- 12) Premaxilla, narial fossa: absent or shallow (0); expanded in the anteroventral corner of the naris (1). Sereno 1999; Langer and Benton 2006; Irmis et al. 2007; Nesbitt 2009: 9; Nesbitt et al. 2009:12
- 13) Premaxilla-maxilla, subnarial gap between the elements: absent (0); present (1). Gauthier 1986; Langer and Benton 2006; Nesbitt 2009: 11; Nesbitt et al. 2009:13
- 14) Premaxilla-maxilla, subnarial foramen between the elements: absent (0); present and the border of the foramen is present on both the maxilla and the premaxilla (1); present and the border of the foramen is present on the maxilla but not on the premaxilla (2); present and the border of the foramen is present on the premaxilla but not on the maxilla (3). Benton and Clark 1988; Parrish 1993; Juul 1994; Benton 1999; Nesbitt 2009: 12; Nesbitt et al. 2009:14
- 15) Maxilla, facial portion anterior to anterior edge of antorbital fenestra: shorter than posterior portion (0); equal in length or longer than portion posterior to anterior edge of fenestra (1). Clark et al. 2000; Olsen et al. 2000; Benton and Walker 2002; Clark et al. 2004; Sues et al. 2003; Clark et al. 2004; Nesbitt 2009: 14; Nesbitt et al. 2009:15
- 16) Maxillary teeth, posterior edge of posterior maxillary teeth: concave or straight (0); convex (1). Sues et al. 2003; Clark et al. 2004; Nesbitt 2009: 15; Nesbitt et al. 2009:16
- 17) Maxilla, posterior extent of the maxillary tooth row: extends to approximately half of the anteroposterior length of the orbit (0); completely antorbital; tooth row ends anterior to the vertical strut of the lacrimal (1). Smith et al. 2007: 35; Irmis 2008:147; Nesbitt et al. 2009:18
- 18) Maxillary tooth count: less than 12 (0); 12 - 18 (1); more than 18 (2). ORDERED Smith et al. 2007: 3; Irmis 2008: 31; Nesbitt et al. 2009:17
- 19) Maxilla, posterior process: articulates ventral to the jugal (0); articulates into a slot on the lateral side of the jugal (1). Nesbitt 2009: 16; Nesbitt et al. 2009:19
- 20) Maxilla, dentition: present (0); absent (1). Nesbitt and Norell 2006; Nesbitt 2009: 18; Nesbitt et al. 2009:20
- 21) Maxilla, buccal emargination separated from the ventral margin of the antorbital fossa: absent (0); present (1). Butler 2005, 2007; Irmis et al. 2006; Irmis et al., 2007; Nesbitt 2009: 23; Nesbitt et al. 2009: 21
- 22) Maxilla, anterodorsal margin: separated from the external naris by the premaxilla (0); borders the external naris (1). Gauthier 1986; Langer and Benton 2006; Nesbitt 2009: 24; Nesbitt et al. 2009:22

- 23) Maxilla, anterodorsal margin at the base of the dorsal process: convex or straight (0); concave (1). Langer and Benton 2006; Nesbitt 2009: 25; Nesbitt et al. 2009:23
- 24) Lateral surface of the maxilla: smooth (0); sharp longitudinal ridge present (1); bulbous longitudinal ridge present (2). Gower 1999; Weinbaum and Hungerbühler 2007; Nesbitt 2009: 26; Nesbitt et al. 2009:24
- 25) Maxilla, depth of the ventral portion of the antorbital fossa: less than or subequal to the depth of the maxilla below the ventral margin of the antorbital fossa (0); much greater than the depth of the maxilla below the ventral margin of the antorbital fossa (1). Smith et al. 2007: 35; Irmis 2008: 27; Nesbitt et al. 2009:25
- 26) Maxilla, posterior portion ventral to the antorbital fenestra: tapers posteriorly (0); has a similar dorsoventral depth as the anterior portion ventral to the antorbital fenestra (1); expands dorsoventrally at the posterior margin of the maxilla (2). Nesbitt 2009: 27; Nesbitt et al. 2009:26
- 27) Maxilla, promaxillary foramen: absent (0); present (1). Rauhut 2003; Tykoski 2005; Smith et al. 2007: 32; Irmis 2008: 34; Nesbitt 2009: 28; Nesbitt et al. 2009:27
- 28) Maxilla, dorsal (=ascending) process: tapers posterodorsally (0); remains the same width (1). Nesbitt 2009: 29; Nesbitt et al. 2009:28
- 29) Antorbital fenestra, anterior margin: gently rounded (0); nearly pointed (1). Benton and Clark 1988; Benton and Walker 2002; Weinbaum and Hungerbühler 2007; Nesbitt 2009: 30; Nesbitt et al. 2009:29
- 30) Maxilla, palatal processes: do not meet at the midline (0); meet at the midline (1); meet at the midline and expand anteriorly and posteriorly (2). ORDERED Parrish 1993; Clark et al. 2000; Olsen et al. 2000; Benton and Walker 2002; Sues et al. 2003; Clark et al. 2004; Nesbitt 2009: 30; Nesbitt et al. 2009:25
- 31) Nasals, posterior portion at the midline: convex or flat (0); concave (1). Nesbitt 2009: 34; Nesbitt et al. 2009:31
- 32) Nasal, dorsolateral margin of the anterior portion (just posterodorsal to the external naris): smoothly rounded (0); distinct anteroposteriorly ridge on the lateral edge (1). Nesbitt 2009: 35; Nesbitt et al. 2009:32
- 33) Nasal: does not possess a posterolateral process that envelops part of the anterior ramus of the lacrimal (0); possesses a posterolateral process that envelops part of the anterior ramus of the lacrimal (1). Yates 2003; Langer and Benton 2006; Nesbitt 2009: 36; Nesbitt et al. 2009:33
- 34) Nasal: does not form part of the dorsal border of the antorbital fossa (0); forms part of the dorsal border of the antorbital fossa (1). Sereno et al. 1994; Langer and Benton 2006; Irmis et al. 2007; Nesbitt 2009: 37; Nesbitt et al. 2009:34
- 35) Lacrimal: does not fold over the posterior/posterodorsal part of the antorbital fenestra (0); folds over the posterior/posterodorsal part of the antorbital fenestra (1). Sereno 1999; Langer and Benton 2006; Nesbitt 2009: 38; Nesbitt et al. 2009:35
- 36) Lacrimal, height: significantly less than the height of the orbit, and usually fails to reach the ventral margin of the orbit (0); as high as the orbit, and contacts the jugal at the level of the ventral margin of the orbit (1). Rauhut 2003; Nesbitt 2009: 39; Nesbitt et al. 2009:36
- 37) Lacrimal, orientation of long axis: sloping anterodorsally (0); erect or nearly vertical (1). Smith et al. 2007:60; Irmis 2008: 47; Nesbitt et al. 2009:37
- 38) Lacrimal 'horn': absent (0); present, forms dorsal crest above the orbit (1). Smith et al. 2007: 52; Irmis 2008: 45; Nesbitt et al. 2009:38
- 39) Lacrimal fenestra: absent (0); present (1). Smith et al. 2007: 51; Irmis 2008: 44; Nesbitt et al. 2009:39
- 40) Frontal, dorsal surface: flat (0); with longitudinal ridge along midline (1). Wu and Chatterjee 1993; Clark et al. 2000; Olsen et al. 2000; Benton and Walker 2002; Sues et al. 2003; Clark et al. 2004; Nesbitt 2009: 42; Nesbitt et al. 2009:40
- 41) Frontal, anterior portion: about as wide as the orbital margin or has a transversely aligned suture with the nasal (0); tapers anteriorly along the midline (1). Nesbitt 2009: 43; Nesbitt et al. 2009:41
- 42) Postfrontal: present (0); absent (1). Gauthier 1986; Benton and Clark 1988; Juul 1994; Bennett 1996; Novas 1996; Benton 1999; Clark et al. 2000; Olsen et al. 2000; Benton and Walker 2002; Sues et al. 2003; Clark et al. 2004; Langer and Benton 2006; Nesbitt 2007; Irmis et al., 2007; Nesbitt 2009: 44; Nesbitt et al. 2009:42
- 43) Quadratojugal: forms less than 80% of the posterior border of the lower temporal fenestra (0); more than 80% of the posterior border of the lower temporal fenestra (1). Benton and Clark 1988; Parrish 1993; Nesbitt 2009: 45; Nesbitt et al. 2009:43
- 44) Squamosal, posterior end: does not extend posterior to the head of the quadrate (0); extends posterior to the head of the quadrate (1). Nesbitt 2009: 48; Nesbitt et al. 2009:44
- 45) Squamosal: without distinct ridge on dorsal surface along edge of supratemporal fossa (0); with distinct ridge on dorsal surface along edge of supratemporal fossa (1). Bonaparte 1982; Parrish 1993; Nesbitt 2009: 49; Nesbitt et al. 2009:45
- 46) Squamosal, facet for the paroccipital process on the medial side of the posterior process: mediolaterally thin (0); rounded and thick (1). Nesbitt 2009: 54; Nesbitt et al. 2009:46
- 47) Squamosal, ventral process: wider than one quarter of its length (0); narrower than one quarter of its length (1). Yates 2003; Langer and Benton 2006; Nesbitt 2009: 56; Nesbitt et al. 2009:47
- 48) Parietals, upper temporal fenestrae separated by: broad, flat area (0); supratemporal fossa separated by a mediolaterally thin strip of flat bone (1); has supratemporal fossa separated by a "sagittal crest" (which may be divided by interparietal suture) (2). Clark et al. 2000; Olsen et al. 2000; Benton and Walker 2002; Sues et al. 2003; Clark et al. 2004; Nesbitt 2009: 59; Nesbitt et al. 2009:48

- 49) Postorbital, ventral termination of the ventral process: tapered (0); blunt (1). Benton and Clark 1988; Juul 1994; Benton 1999; Alcober 2000; Benton and Walker 2002; Nesbitt 2009: 65; Nesbitt et al. 2009:49
- 50) Postorbital-squamosal, contact: restricted to the dorsal margin of the elements (0); continues ventrally for much or most of the ventral length of the squamosal (1). Nesbitt 2009: 66; Nesbitt et al. 2009:50
- 51) Postorbital bar: composed both of the jugal and postorbital in nearly equal proportions (0); composed by mostly the postorbital (1). Nesbitt 2009: 67; Nesbitt et al. 2009:51
- 52) Jugal, anterior extent of the slot for the quadratojugal: well posterior of the posterior edge of the dorsal process of the jugal (0) at or anterior to the posterior edge of the dorsal process of the jugal (1). Nesbitt 2009: 68; Nesbitt et al. 2009:52
- 53) Jugal, anterior process: participates in posterior edge of antorbital fenestra (0); excluded from the antorbital fenestra by lacrimal or maxilla (1). Clark et al. 2000; Olsen et al. 2000; Benton and Walker 2002; Sues et al. 2003; Clark et al. 2004; Rauhut 2003; Langer and Benton 2006; Nesbitt 2009: 69; Nesbitt et al. 2009:53
- 54) Jugal, posterior process: lies dorsal to the anterior process of the quadratojugal (0); ventral to the anterior process of the quadratojugal (1); splits the anterior process of the quadratojugal (2); is split by the anterior process of the quadratojugal (3). Nesbitt 2009: 71; Nesbitt et al. 2009:54
- 55) Jugal, posterior termination: anterior to or at the posterior extent of the lower temporal fenestra (0); posterior to the lower temporal fenestra (1). Nesbitt 2009: 72; Nesbitt et al. 2009:55
- 56) Jugal, long axis of the body: nearly horizontal (0); anterodorsally inclined (1). Heckert and Lucas 1999; Parker 2007; Nesbitt 2009: 74; Nesbitt et al. 2009:56
- 57) Jugal, longitudinal ridge on the body: absent (0); present and sharp (1); rounded and broad (2); rounded and restricted to a bulbous ridge (3). Nesbitt 2009: 75; Nesbitt et al. 2009:57
- 58) Quadrate, head: partially exposed laterally (0); completely covered by the squamosal (1). Sereno and Novas 1994; Juul 1994; Novas 1996; Benton 1999; Langer and Benton 2006; Nesbitt 2009: 78; Nesbitt et al. 2009:58
- 59) Quadratojugal and quadrate, suture between the elements, foramen: present (0); absent (1). Parrish 1991; Benton and Walker 2002; Nesbitt 2009: 79; Nesbitt et al. 2009:59
- 60) Quadrate, angled: posteroventrally or vertical (0); anteroventrally (1). Nesbitt 2007; Nesbitt 2009: 82; Nesbitt et al. 2009:60
- 61) Pterygoid-ectopterygoid, articulation: ectopterygoid ventral to pterygoid (0); ectopterygoid dorsal to pterygoid (1). Sereno and Novas 1994; Novas 1996; Benton 1999; Irmis et al. 2007; Nesbitt 2009: 84; Nesbitt et al. 2009:61
- 62) Ectopterygoid, ventral recess: absent (0); present (1). Gauthier 1986; Langer and Benton 2006; Nesbitt 2009: 86; Nesbitt et al. 2009:62
- 63) Ectopterygoid, body: arcs anteriorly (0); arcs anterodorsally (1). Nesbitt 2009: 87; Nesbitt et al. 2009:63
- 64) Ectopterygoid: single-headed (0); double-headed (1). Weinbaum and Hungerbühler 2007; Nesbitt 2009: 89; Nesbitt et al. 2009:64
- 65) Basipterygoid, processes directed: anteriorly or ventrally at their distal tips (0); posteriorly at their distal tips (1). Nesbitt 2009: 93; Nesbitt et al. 2009:65
- 66) Parabasisphenoid, foramina for entrance of cerebral branches of internal carotid artery into the braincase positioned on the surface: ventral (0); lateral (1). Parrish 1993; Gower and Sennikov 1996; Gower 2002; Nesbitt 2009: 95; Nesbitt et al. 2009:66
- 67) Parabasisphenoid, plate: present and straight (0); present and arched anteriorly (1); absent (2). ORDERED Gower and Sennikov 1996; Nesbitt 2009: 96; Nesbitt et al. 2009:67
- 68) Parabasisphenoid, semilunar depression on the lateral surface of the basal tubera: present (0); absent (1). Gower and Sennikov 1996; Nesbitt 2009: 98; Nesbitt et al. 2009:68
- 69) Parabasisphenoid, recess (=median pharyngeal recess of some authors = hemispherical sulcus = hemispherical fontanelle): absent (0); present (1). Nesbitt and Norell 2006; Nesbitt 2009: 100; Nesbitt et al. 2009:69
- 70) Parabasisphenoid, anterior tympanic recess on the lateral side of the braincase: absent (0); present (1). Makovicky and Sues 1998; Rauhut 2003; Nesbitt 2009: 101; Nesbitt et al. 2009:70
- 71) Parabasisphenoid, between basal tubera and basipterygoid processes: approximately as wide as long or wider (0); significantly elongated at least 1.5 times longer than wide (1). Rauhut 2003; Nesbitt 2007; Nesbitt 2009: 103; Nesbitt et al. 2009:71
- 72) Basioccipital, portion of the basal tubera: rounded and anteroposteriorly elongated (0); blade-like and anteroposteriorly shortened (1). Nesbitt 2009: 106; Nesbitt et al. 2009:72
- 73) Opisthotic, paroccipital processes: no or slight dorsal and ventral expansion distally (0); markedly expanded dorsally at the distal ends (1). Clark et al. 2000; Olsen et al. 2000; Benton and Walker 2002; Sues et al. 2003; Clark et al. 2004; Nesbitt 2009: 108; Nesbitt et al. 2009:73
- 74) Opisthotic, paroccipital processes: directed laterally or dorsolaterally (0); directed ventrolaterally (1). Rauhut 2003; Hwang et al. 2004; Smith et al. 2007: 90; Irmis 2008: 89; Nesbitt 2009: 110; Nesbitt et al. 2009:74
- 75) Paroccipital processes, ventral rim of the bases: above or level with the dorsal border of the occipital condyle (0); situated at mid-height of occipital condyle or lower (1). Smith et al. 2007: 91; Nesbitt et al. 2009:75
- 76) Opisthotic, ventral ramus (= crista interfenestralis): extends further laterally or about the same as lateralmost edge of exoccipital in posterior view (0); covered by the lateralmost edge of exoccipital in posterior view (1). Gower 2002; Nesbitt 2009: 111; Nesbitt et al. 2009:76

- 77) Exoccipital, lateral surface: without subvertical crest (= metotic strut) (0); with clear crest (= metotic strut) lying anterior to both external foramina for hypoglossal nerve (XII)(1); with clear crest (= metotic strut) present anterior to the more posterior external foramina for hypoglossal nerve (XII) (2). Gower 2002; Nesbitt 2009: 114; Nesbitt et al. 2009:77
- 78) Exoccipitals: meet along the midline on the floor of the endocranial cavity (0); do not meet along the midline on the floor of the endocranial cavity (1). Gower and Sennikov 1996; Gower 2002; Nesbitt 2009: 115; Nesbitt et al. 2009:78
- 79) Vestibule, medial wall: incompletely ossified (0); almost completely ossified (1). Gower 2002; Nesbitt 2009: 117; Nesbitt et al. 2009:79
- 80) Lagenar/cochlea recess: absent or short and strongly tapered (0); present and elongated and tubular (1). Gower 2002; Nesbitt 2009: 118; Nesbitt et al. 2009:80
- 81) Supraoccipital: excluded from dorsal border of foramen magnum by mediodorsal midline contact between opposite exoccipitals (0); contributes to border of foramen magnum (1). Gower 2002; Nesbitt 2009: 126; Nesbitt et al. 2009:81
- 82) Foramen for trigeminal nerve and middle cerebral vein: combined and undivided (0); at least partially subdivided by prootic (1); fully divided (2). Gower and Sennikov 1996; Gower 2002; Nesbitt 2009: 131; Nesbitt et al. 2009:82
- 83) Foramen or groove passing above and into the dorsal end of the metotic foramen: absent (0); present (1). Gower 2002; Nesbitt 2009: 132; Nesbitt et al. 2009:83
- 84) Auricular recess: largely restricted to prootic (0); extends onto internal surface of epiotic/supraoccipital (1). Gower 2002; Nesbitt 2009: 133; Nesbitt et al. 2009:84
- 85) Skull length: less than 50% of length of the presacral vertebral column (0); more than 50% of length of the presacral vertebral column (1). Sereno 1991; Benton 1999; Nesbitt 2009: 134; Nesbitt et al. 2009:85
- 86) Skull length: longer than two-thirds of the femoral length (0); shorter than two-thirds of the femoral length (1) Gauthier 1986; Langer and Benton 2006; Nesbitt 2009: 135; Nesbitt et al. 2009:86
- 87) Antorbital fossa: restricted to the lacrimal and dorsal process of the maxilla (0); present on the lacrimal, dorsal process of the maxilla and the dorsolateral margin of the posterior process of the maxilla (the ventral border of the antorbital fenestra) (1). Nesbitt 2009: 137; Nesbitt et al. 2009:87
- 88) Post-temporal opening, size: equal or greater than half the diameter of the foramen magnum (0); less than half the diameter of the foramen magnum or absent (1). Sereno and Novas 1994; Novas 1996; Benton 1999; Nesbitt 2009: 141; Nesbitt et al. 2009:88
- 89) Orbit, shape: circular or elliptical (0); tall and narrow (the "keyhole-shaped orbit"; maximum width is less than half the maximum height)(1); with distinct ventral point surrounded by V-shaped dorsal processes of jugal (2). Benton and Clark 1988; Parrish 1993; Gower 2000; Benton and Walker 2002; Nesbitt 2009: 142; Nesbitt et al. 2009:89
- 90) Supratemporal fossa: absent anterior to the supratemporal fenestra (0); present anterior to the supratemporal fenestra (1). Gauthier 1986; Novas 1996; Nesbitt 2009: 144; Nesbitt et al. 2009:90
- 91) Postparietal(s): present (0); absent (1). Juul 1994; Bennett 1996; Dilkes 1998; Nesbitt 2009: 146; Nesbitt et al. 2009:91
- 92) Palpebral(s): absent (0); present (1). Nesbitt 2009: 147; Nesbitt et al. 2009:92
- 93) Predeontary: absent (0); present (1). Sereno 1986; Butler et al. 2007, 2008; Irmis et al. 2007; Nesbitt 2009: 151; Nesbitt et al. 2009:93
- 94) Anterior half of the dentary, position of the Meckelian groove: dorsoventral center of the dentary (0); restricted to the ventral border (1). Nesbitt 2009: 152; Nesbitt et al. 2009:94
- 95) Dentary, anterior extent of the Meckelian groove: ends well short of the dentary symphysis (0); present through the dentary symphysis (1). Nesbitt 2009: 153; Nesbitt et al. 2009:95
- 96) Dentary, dorsal margin of the anterior portion compared to the dorsal margin of the posterior portion of the dentary: horizontal (about in the same plane)(0); ventrally deflected (1); dorsally expanded (2). Nesbitt 2009: 154; Nesbitt et al. 2009:96
- 97) Dentary, anterior extremity: rounded (0); tapers to a sharp point (1). Nesbitt 2009: 155; Nesbitt et al. 2009:97
- 98) Articular: without dorsomedial projection posterior to the glenoid fossa (0); with dorsomedial projection separated from glenoid fossa by a clear concave surface (1); with dorsomedial projection continuous with the glenoid fossa (2). Clark et al. 2000; Olsen et al. 2000; Benton and Walker 2002; Sues et al. 2003; Clark et al. 2004; Nesbitt 2009: 156; Nesbitt et al. 2009:98
- 99) Articular, ventromedially directed process: absent (0); present (1). Nesbitt 2009: 157; Nesbitt et al. 2009:99
- 100) Articular, glenoid of the mandible located: level with dorsal margin of the dentary (0); well ventral of the dorsal margin of the dentary (1). Gauthier 1986; Langer and Benton 2006; Nesbitt 2009: 158; Nesbitt et al. 2009:100
- 101) Articular, foramen on the medial side: absent (0); present and medial to the glenoid (1). Nesbitt 2009: 159; Nesbitt et al. 2009:101
- 102) Surangular, ridge or process on lateral surface, anterior to jaw suture: absent (0); present, strong anteroposteriorly extended ridge (1). Butler et al. 2008; Irmis 2008: 126; Nesbitt et al. 2009:102
- 103) Coronoid process, dorsally expanded: absent (0); present (1). Sereno 1986; Sereno 1999; Butler 2005; Butler et al. 2008; Irmis et al. 2007; Nesbitt 2009: 161; Nesbitt et al. 2009:103
- 104) Mandibular fenestra: anteroposterior length more than maximum depth of dentary ramus but less than half the length of the mandible (0); greater than half the length of the mandible (1); reduced, anteroposterior length less than maximum depth of dentary ramus (2). Butler 2005; Nesbitt and Norell 2006; Nesbitt 2009: 162; Nesbitt et al. 2009:104

- 105) Splenial, foramen in the ventral part: absent (0); present (1). Rauhut 2003; Langer and Benton 2006; Smith et al. 2007; Nesbitt 2009: 165; Nesbitt et al. 2009:105
- 106) Dentary teeth: present along entire length of the dentary (0); absent in the anterior portion (1); completely absent (2). Parrish 1994; Parker 2007; Nesbitt 2009: 166; Nesbitt et al. 2009:106
- 107) Dentition: generally homodont (0); markedly heterodont (1). Parrish 1993; Nesbitt 2009: 167; Nesbitt et al. 2009:107
- 108) Tooth, serrations: present as small fine knife-like serrations (0); present and enlarged and coarser (lower density) = denticles (1). Gauthier et al. 1988; Juul 1994; Dilkes 1998; Irmis et al. 2007; Nesbitt 2009: 168; Nesbitt et al. 2009:108
- 109) Extensive planar wear facets across multiple maxillary/dentary teeth: absent (0); present (1). Weishampel and Witmer 1990; Irmis et al. 2007; Nesbitt 2009: 169; Nesbitt et al. 2009:109
- 110) Medial or lateral overlap of adjacent crowns in maxillary and dentary teeth: absent (0); present (1). Sereno 1986; Butler et al. 2008; Nesbitt 2009: 170; Nesbitt et al. 2009:110
- 111) Tooth, crown: not mesiodistally expanded (0); mesiodistally expanded above root in cheek teeth (1). Sereno 1986; Irmis et al. 2007; Butler et al. 2008; Nesbitt 2009: 171; Nesbitt et al. 2009:111
- 112) Moderately developed lingual expansion of crown (=cingulum) on maxillary/dentary teeth: absent (0); present (1). Sereno 1986; Butler et al. 2008; Nesbitt 2009: 172; Nesbitt et al. 2009:112
- 113) Maxillary and dentary crowns, shape: apicobasally tall and blade-like (0); apicobasally short and subtriangular (1). Sereno 1986; Butler et al. 2008; Nesbitt 2009: 173; Nesbitt et al. 2009:113
- 114) Tooth, implantation: teeth fused to the bone of attachment at the base (0); free at the base of the tooth (1). Gauthier 1984; Benton and Clark 1988; Benton 1990; Bennett 1996; Nesbitt 2009: 174; Nesbitt et al. 2009:114
- 115) Pterygoid, teeth, on palatal process of the pterygoid: present (0); absent (1). Juul 1994; Gower and Sennikov 1997; Nesbitt 2009: 175; Nesbitt et al. 2009:115
- 116) Postaxial intercentra: present (0); absent (1). Gauthier 1984; Benton and Clark 1988; Sereno 1991a; Parrish 1993; Juul 1994; Bennett 1996; Nesbitt 2009: 177; Nesbitt et al. 2009:116
- 117) Atlantal articulation facet in axial intercentrum, shape: saddle-shaped (0); concave with upturned lateral borders (1). Gauthier 1986; Langer and Benton 2006; Nesbitt 2009: 178; Nesbitt et al. 2009:117
- 118) Axis, dorsal margin of the neural spine: expanded posterodorsally (0); arcs dorsally, where the anterior portion height is equivalent to the posterior height (1). Nesbitt 2009: 179; Nesbitt et al. 2009:118
- 119) Axis, neural spine: sheet-like (0); anteroposteriorly reduced and rod-like (1). Smith et al. 2007: 145; Irmis 2008: 157; Nesbitt et al. 2009:119
- 120) Anterior cervical vertebrae, prezygapophyses: transverse distance between medial margins of prezygapophyses less than mediolateral width of the neural canal (0); medial margin of prezygapophyses situated lateral to the margins of the neural canal (1). Smith et al. 2007: 156; Irmis 2008: 163; Nesbitt et al. 2009:120
- 121) Cervical vertebrae, 3-5 centrum length: shorter or the same length as the mid-dorsal (0); longer than mid-dorsal (1). Sereno 1991; Nesbitt 2009: 181; Nesbitt et al. 2009:121
- 122) Cervical vertebrae, deep recesses on the anterior face of the neural arch, lateral to the neural canal (=prechonos of Welles 1984): absent (0); present (1). Nesbitt 2009: 182; Nesbitt et al. 2009:122
- 123) Third cervical vertebra, centrum length: subequal to the axis centrum (0); longer than the axis centrum (1). Gauthier 1986; Langer and Benton 2006; Nesbitt 2009: 183; Nesbitt et al. 2009:123
- 124) Anterior to middle cervical vertebrae, diapophysis and parapophysis: well separated (0); nearly touching (1). Nesbitt 2009: 184; Nesbitt et al. 2009:124
- 125) Anterior cervical vertebrae, neural arch, posterior portion ventral to the postzygapophysis: smooth posteriorly or has a shallow fossa (0); with a deep excavation with a thin bone lamina covering the anterior extent on the posterolateral surface (1). Langer and Benton 2006; Nesbitt 2009: 185; Nesbitt et al. 2009:125
- 126) Epipophyses: absent in post-axial anterior cervical vertebrae (0); present in postaxial anterior cervical vertebrae (1). Gauthier 1986; Novas 1996; Langer and Benton 2006; Nesbitt 2009: 186; Nesbitt et al. 2009:126
- 127) Epipophyses: absent in posterior cervical vertebrae (cervicals 6-9) (0); present in posterior cervical vertebrae (cervicals 6-9) (1). Sereno et al. 1993; Langer and Benton 2006; Nesbitt 2009: 187; Nesbitt et al. 2009:127
- 128) Cervical vertebrae, pneumatic features (=pleurocoels) in the anterior portion of the centrum: absent (0); present as deep fossae (1); present as foramina (2). ORDERED Holtz 1994; Rauhut 2003; Smith et al. 2007: 149; Irmis 2008: 162; Nesbitt 2009: 188; Nesbitt et al. 2009:128
- 129) Cervical vertebrae, pneumatic features (= pleurocoels) in the posterior portion of the centrum: absent (0); present as a blind rimmed depression (1); present as a foramen or foramina (2). ORDERED. Gauthier 1986; Rauhut 2003; Nesbitt 2009: 189; Nesbitt et al. 2009:129; Ezcurra 2017: 129
- 130) Cervical vertebrae, middle portion of the ventral keel: dorsal to the ventralmost extent of the centrum rim (0); ventral to the centrum rims (1). Nesbitt 2009: 190; Nesbitt et al. 2009:130
- 131) Cervical vertebrae, distal end of neural spines: expansion absent (0); present and laterally expanded in the middle of the anteroposterior length (1); present and expanded anteriorly so that the spine table is triangular or heart-shaped in dorsal view (2). Gauthier 1984; Juul 1994; Nesbitt 2009: 191; Nesbitt et al. 2009:131
- 132) Posterior cervical and/or dorsal vertebrae, hyposphene-hypantrum accessory intervertebral articulations: absent (0); present (1). Gauthier 1986; Juul 1994; Benton 1999; Rauhut 2003; Langer and Benton 2006; Weinbaum and Hungerbühler 2007; Nesbitt 2009: 195; Nesbitt et al. 2009:132

- 133) Cervical ribs: slender and elongated (0); short and stout (1). Gauthier 1986; Benton and Clark 1988; Juul 1994; Benton 1999; Nesbitt 2009: 196; Nesbitt et al. 2009:133
- 134) Cervical ribs, pneumatic excavations in head: absent (0); present (1). Smith et al. 2007: 165; Irmis 2008: 170; Nesbitt et al. 2009:134
- 135) Dorsal vertebrae, deep fossae and/or pneumatopores ("pleurocoels"): absent (0); present in anterior dorsals (1). Smith et al. 2007: 170; Irmis 2008: 172; Nesbitt et al. 2009:135
- 136) Anterior dorsal vertebrae, ventral keel: absent or very poorly developed (0); pronounced (1). Smith et al. 2007: 170; Irmis 2008: 172; Nesbitt et al. 2009:136
- 137) Dorsal vertebrae, neural spine distal expansion: absent (0); present with a flat dorsal margin (1); present with a rounded dorsal margin (2). Nesbitt 2009: 197; Nesbitt et al. 2009:137
- 138) Middle dorsal vertebrae, diapophyses and parapophyses: close to the midline (0); expand on stalks (1). Nesbitt 2009: 199; Nesbitt et al. 2009:138
- 139) Sacral centra in mature individuals: separate (0); co-ossified at the ventral edge (1). Nesbitt 2009: 200; Nesbitt et al. 2009:190
- 140) Sacral vertebrae, prezygapophyses and complimentary postzygapophyses in mature individuals: separate (0); co-ossified (1). Nesbitt 2009: 201; Nesbitt et al. 2009:140
- 141) Primordial sacral one, sacral rib: doesn't or weakly articulates with anteriorly directed process (=preacetabular process) of the ilium (0); articulates with the anteriorly directed process of the ilium (1). Nesbitt 2005; 2007; Nesbitt 2009: 202; Nesbitt et al. 2009:141
- 142) Sacral vertebrae, centra articular rims: present in sacrum (0); nearly obliterated (1). Nesbitt 2007; Nesbitt 2009: 204; Nesbitt et al. 2009:142
- 143) Trunk vertebrae: free from the sacrum (0); incorporated into the sacrum, with their ribs/transverse processes articulating with the pelvis (1). Sereno et al. 1993; Langer and Benton 2006; Nesbitt 2009: 205; Nesbitt et al. 2009:143
- 144) Caudal vertebrae: free from the sacrum (0); incorporated into the sacrum, with their ribs/transverse processes articulating with the pelvis (1). Galton 1976; Langer and Benton 2006; Nesbitt 2009: 206; Nesbitt et al. 2009:144
- 145) Insertion of a sacral vertebra between the first and second primordial sacral vertebrae: absent (0); present (1). Nesbitt 2009: 207; Nesbitt et al. 2009:145
- 146) Sacral ribs: almost entirely restricted to a single sacral vertebra (0); shared between two sacral vertebrae (1). Nesbitt 2009: 208; Nesbitt et al. 2009:146
- 147) First primordial sacral, articular surface of sacral rib: circular (0); C- shaped in lateral view (1). Langer and Benton 2006; Nesbitt 2009: 209; Nesbitt et al. 2009:147
- 148) Middle caudal vertebrae, accessory laminar process on anterior face of neural spine: absent (0); present (1). Benton and Clark 1988; Juul 1994; Benton 1999; Benton and Walker 2002; Rauhut 2003; Irmis et al. 2007; Nesbitt 2009: 210; Nesbitt et al. 2009:148
- 149) Distal caudal vertebrae, prezygapophyses: not elongated (0); elongated more than a quarter of the adjacent centrum (1). Gauthier 1986; Rauhut 2003; Nesbitt 2007; Nesbitt 2009: 211; Nesbitt et al. 2009:149
- 150) Forelimb-hindlimb length ratio: more than 0.55 (0); less than 0.55 (1). Gauthier 1984; Sereno 1991; Juul 1994; Benton 1999; Nesbitt 2009: 212; Nesbitt et al. 2009:150
- 151) Clavicles: present and unfused (0); fused into a furcula (1); clavicles absent (2). Gauthier 1986; Sereno 1991; Benton 1999; Benton and Walker 2002; Nesbitt 2009: 213; Nesbitt et al. 2009:151
- 152) Interclavicle: present (0); absent (1). Gauthier 1986; Sereno 1991; Juul 1994; Benton 1999; Nesbitt 2009: 214; Nesbitt et al. 2009:152
- 153) Scapula, entire anterior margin: straight/convex or partially concave (0); markedly concave (1). Gower and Sennikov 1997; Nesbitt 2009: 217; Nesbitt et al. 2009:153
- 154) Scapula, blade height versus distal width: less than 3 times distal width (0); more than 3 times distal width (1). Sereno 1999; Nesbitt 2009: 218; Nesbitt et al. 2009:154
- 155) Scapulocoracoid, anterior margin: distinct notch between the two elements (0); uninterrupted edge between the two elements (1). Parrish 1993; Benton 1999; Nesbitt 2009: 221; Nesbitt et al. 2009:155
- 156) Coracoid: subcircular in lateral view (0); with post-glenoid process (notch ventral to glenoid) (1). Clark et al. 2004; Nesbitt 2009: 222; Nesbitt et al. 2009:156
- 157) Coracoid, post-glenoid process: short (0); elongate and expanded posteriorly only (1). Clark et al. 2004; Nesbitt 2009: 223; Nesbitt et al. 2009:157
- 158) Coracoid, posteroventral portion: smooth (0); possesses a "swollen" tuber (=biceps tuber) (1). Nesbitt 2009: 225; Nesbitt et al. 2009:158
- 159) Glenoid, orientation: posterolaterally (0); directed posteroventrally (1). Fraser et al. 2002; Nesbitt 2009: 227; Nesbitt et al. 2009:159
- 160) Humerus, apex of deltopectoral crest situated at a point corresponding to: less than 30% down the length of the humerus (0); more than 30% down the length of the humerus (1). Bakker and Galton 1974; Benton 1990; Juul 1994; Novas 1996; Benton 1999; Nesbitt 2009: 230; Nesbitt et al. 2009:160
- 161) Humerus, length: longer than or subequal to 0.6 of the length of the femur (0); shorter than 0.6 of the length of the femur (1). Novas 1993; Langer and Benton 2006; Nesbitt 2009: 231; Nesbitt et al. 2009:161
- 162) Humerus, proximal head: confined to the proximal surface (0); posteriorly expanded and hooked (1). Nesbitt 2009: 232; Nesbitt et al. 2009:162

- 163) Humerus, proximal articular surface: continuous with the deltopectoral crest (0); separated by a gap from the deltopectoral crest (1). Nesbitt, 2009: 233; Nesbitt et al. 2009:163
- 164) Humerus, ectepicondylar flange: present (0); absent (1). Nesbitt 2009: 234; Nesbitt et al. 2009:164
- 165) Humerus, distal end width: narrower or equal to 30% of humerus length (0); greater than 30% of humerus length (1). Langer and Benton 2006; Nesbitt 2009: 235; Nesbitt et al. 2009:165
- 166) Ulna, lateral tuber (=radius tuber) on the proximal portion: absent (0); present (1). Nesbitt 2009: 237; Nesbitt et al. 2009:166
- 167) Ulna, distal end in posterolateral view: rounded and convex (0); squared off where the distal surface is nearly flat (1). Nesbitt 2009: 238; Nesbitt et al. 2009:167
- 168) Ulna, distal end: anteroposteriorly compressed or oval-shaped (0); with anterior expansion (1). Nesbitt 2009: 239; Nesbitt et al. 2009:168
- 169) Radius, distal end: convex (0); shallow longitudinal groove on the posterior side (1). Nesbitt 2009: 240; Nesbitt et al. 2009:169
- 170) Radius, length: longer than 80% of humerus length (0); shorter than 80% of humerus length (1). Langer and Benton 2006; Nesbitt 2009: 241; Nesbitt et al. 2009:170
- 171) Pteroid bone: absent (0); present (1). Bennett 1996; Nesbitt 2009: 244; Nesbitt et al. 2009:171
- 172) Longest metacarpal: longest metatarsal >.5 (0); <.5 (1). Nesbitt 2009: 245; Nesbitt et al. 2009:172
- 173) Metacarpals, proximal ends: overlap (0); abut one another without overlapping (1). Clark et al. 2000; Olsen et al. 2000; Benton and Walker 2002; Sues et al. 2003; Clark et al. 2004; Nesbitt 2009: 246; Nesbitt et al. 2009:173
- 174) Manual length (measured as the average length of digits I-III) accounts for: less than 0.3 of the total length of humerus plus radius (0); more than 0.3 but less than 0.4 of the total length of humerus plus radius (1); more than 0.4 of the total length of humerus plus radius (2). ORDERED Gauthier 1986; Langer and Benton 2006; Nesbitt 2009: 247; Nesbitt et al. 2009:174
- 175) Medialmost distal carpal: subequal other distal carpals (0); significantly larger than other distal carpals (1). Gauthier 1986; Langer and Benton 2006; Nesbitt 2009: 248; Nesbitt et al. 2009:175
- 176) Distal carpal V: present (0); absent (1). Sereno 1999; Langer and Benton 2006; Nesbitt 2009: 249; Nesbitt et al. 2009:176
- 177) Extensor pits on the proximodorsal portion of metacarpals I-III: absent or shallow and symmetrical (0); deep and asymmetrical (1). Sereno et al. 1993; Langer and Benton 2006; Nesbitt 2009: 250; Nesbitt et al. 2009:177
- 178) Metacarpal I, width at the middle of the shaft accounts for: less than 0.35 of the total length of the bone (0); more than 0.35 of the total length of the bone (1). Bakker and Galton 1974; Langer and Benton 2006; Nesbitt 2009: 251; Nesbitt et al. 2009:178
- 179) Digit I with metacarpal: longer than the ungual (0); subequal or shorter than the ungual (1). Sereno 1999; Langer and Benton 2006; Nesbitt 2009: 252; Nesbitt et al. 2009:179
- 180) Manual digit I, first phalanx: is not the longest non-ungual phalanx of the manus (0); is the longest non-ungual phalanx of the manus (1). Gauthier 1986; Langer and Benton 2006; Nesbitt 2009: 253; Nesbitt et al. 2009:180
- 181) Metacarpal I, distal condyles: approximately aligned or slightly offset (0); lateral condyle strongly distally expanded relative to medial condyle (1). Bakker and Galton 1974; Langer and Benton 2006; Irmis et al., 2007; Nesbitt 2009: 254; Nesbitt et al. 2009:181
- 182) Metacarpal II: shorter than metacarpal III (0); equal to or longer than metacarpal III (1). Gauthier 1986; Langer and Benton 2006; Irmis et al. 2007; Nesbitt 2009: 256; Nesbitt et al. 2009:182
- 183) Manual digits I-III: blunt unguals on at least digits II and III (0); trenchant unguals on digits I-III (1). Gauthier 1986; Juul 1994; Benton 1999; Irmis et al. 2007; Nesbitt 2009: 257; Nesbitt et al. 2009:183
- 184) Manual digit IV: five phalanges (0); four phalanges (1); three or two phalanges (2); one phalanx (3). ORDERED Gauthier 1986; Benton and Clark 1988; Novas 1996; Benton 1999; Irmis et al. 2007; Nesbitt 2009: 258; Nesbitt et al. 2009:184
- 185) Metacarpal IV: present (0); reduced to a nubbin or absent (1). Gauthier 1986; Nesbitt 2009: 259; Nesbitt et al. 2009:185
- 186) Metacarpal IV, shaft width: about the same width than that of metacarpals I-III (0); significantly narrower than that of metacarpals I-III (1). Sereno et al. 1993; Langer and Benton 2006; Nesbitt 2009: 261; Nesbitt et al. 2009:186
- 187) Manual digit IV length: less than or equal to 50% of total forelimb length (0); more than 50% of total forelimb length (1). Bennett 1996; Irmis et al. 2007; Nesbitt 2009: 262; Nesbitt et al. 2009:187
- 188) Manual digit V: possesses one or more phalanges (0); lacks phalanges (1); absent or reduced to a tiny nubbin (2). Bakker and Galton 1974; Langer and Benton 2006; Irmis et al. 2007; Nesbitt 2009: 263; Nesbitt et al. 2009:188
- 189) Ilium, supra-acetabular crest (=supra-acetabular rim): projects laterally or ventrolaterally (0); projects ventrally (1). Gauthier 1986; Nesbitt 2009: 264; Nesbitt et al. 2009:189
- 190) Ilium, distal extent of the supra-acetabular crest (=supra-acetabular rim): near or at the articular facet for the pubis (0); ends well proximal of the facet for the pubis (1). Nesbitt et al. 2009:190
- 191) Ilium, crest dorsal to the supra-acetabular crest: absent (0); present and divides the anterior (=preacetabular) process from the posterior (=postacetabular) process (1); confluent with anterior extent of the anterior (=preacetabular) process of the ilium (2). Nesbitt 2009: 265; Nesbitt et al. 2009:191
- 192) Ilium, anterior (=preacetabular, =cranial) process: short and does not extend anterior of the acetabulum (0); long and extends anterior of the acetabulum (1). Nesbitt 2009: 269; Nesbitt et al. 2009:192

- 193) Ilium, shape of the anterior (=preacetabular, =cranial) process: blunt and tapering dorsally (0); square-shaped (1). Yates 2007: 247; Irmis 2008: 239; Nesbitt et al. 2009:193
- 194) Ilium, posterior margin of the postacetabular process in lateral view: straight or convex (0); notched or indented (1). Smith et al. 2007: 262; Irmis 2008: 255; Nesbitt et al. 2009:194
- 195) Ilium, orientation: mainly vertically orientated (0-20°) (0); ventrolaterally deflected about 45°(1). Benton and Clark 1988; Juul 1994; Benton and Walker 2002; Nesbitt 2009: 270; Nesbitt et al. 2009:195
- 196) Ilium, distinct fossa present for the attachment of the m caudifemoralis brevis: absent (0); present as an embankment on the lateral side of the posterior portion of the ilium (1); present as a deep fossa on the ventral surface of postacetabular part of the ilium (2). Gauthier and Padian 1985; Gauthier 1986: Juul 1994; Novas 1996; Benton 1999; Hutchinson 2001; Nesbitt 2009: 271; Nesbitt et al. 2009:196
- 197) Ilium, connection between the posterior portion of the supra-acetabular rim and the posterior portion of the ilium (= brevis shelf): absent (0); present through a low ridge (1); present through a well laterally developed and sharp shelf (2). ORDERED. Langer and Benton 2006; Nesbitt 2009: 272; Nesbitt et al. 2009:197; Ezcurra 2017: 197
- 198) Ilium, ventral margin of the acetabulum: convex (0); straight (1); concave (2). Bakker and Galton 1974; Gauthier and Padian 1985; Gauthier 1986; Juul 1994; Novas 1996; Benton 1999; Benton et al. 2000; Fraser et al. 2002; Langer and Benton 2006; Nesbitt 2009: 273; Nesbitt et al. 2009:198
- 199) Ilium, acetabular antitrochanter: absent (0); present (1). Sereno and Arcucci 1994; Novas 1996; Benton 1999; Fraser et al. 2002; Irmis et al. 2007; Nesbitt 2009: 274; Nesbitt et al. 2009:199
- 200) Ilium, dorsal margin dorsal to the supra-acetabular rim: rounded, or blade-like (0); flat (1). Nesbitt 2009: 275; Nesbitt et al. 2009:200
- 201) Ilium, dorsal portion: height about the same or shorter than the dorsal portion of the supra-acetabular rim to the pubis-ischium contact (0); expanded dorsally, height markedly taller than the dorsal portion of the supra-acetabular rim to the pubis-ischium contact (1). Nesbitt 2009: 276; Nesbitt et al. 2009:201
- 202) Ilium, ischiadic peduncle orientation: mainly vertical in lateral aspect (0); well expanded posteriorly to the anterior margin of the postacetabular embayment (1). Langer and Benton, 2006; Nesbitt 2009: 277; Nesbitt et al. 2009:202
- 203) Pubis, length: less than 70% of femoral length (0); more than 70% or more of femoral length (1). Novas 1996; Nesbitt 2009: 278; Nesbitt et al. 2009:203
- 204) Pubis, orientation: anteroventral (0); ventral or slightly posteroventral (1); rotated posteroventrally to lie alongside the ischium (opisthopubic) (2). Sereno 1986; Butler et al. 2008b; Nesbitt 2009: 279; Nesbitt et al. 2009:204
- 205) Pubis, prepubic process: absent, anterior margin unexpanded (0); present, anterior margin expanded into a process (1). Sereno 1986; Butler et al. 2008b; Nesbitt 2009: 280; Nesbitt et al. 2009:205
- 206) Pubis, length: shorter or subequal to the ischium (0); longer than ischium (1). Benton and Clark 1988; Juul 1994; Novas 1996; Benton 1999; Benton and Walker 2002; Nesbitt 2009: 282; Nesbitt et al. 2009:206
- 207) Pubis, distal end: unexpanded (0); slightly expanded relative to the shaft (1); strongly expanded relative to the shaft, forming a distinct pubic boot (2). ORDERED. Gauthier 1986; Sereno and Novas 1992; Juul 1994; Benton 1999; Rauhut 2003; Langer and Benton 2006; Nesbitt 2007; Nesbitt 2009: 283; Nesbitt et al. 2009:207
- 208) Pubis, expanded distal margin: mediolaterally thick and rounded (0); mediolaterally thin (1). Gauthier 1986; Juul 1994; Benton 1999; Nesbitt 2009: 284; Nesbitt et al. 2009:208
- 209) Pubis, expanded distal margin: shorter than 33% of the length of the shaft of the pubis (0); greater than 33% of the length of the shaft of the pubis (1). Nesbitt and Norell 2006; Nesbitt 2007; Nesbitt 2009: 285; Nesbitt et al. 2009:209
- 210) Proximal portion of the pubis: articular surfaces with the ilium and the ischium continuous (0); articular surfaces with the ilium and the ischium separated by a groove or gap (1). Nesbitt 2009: 286; Nesbitt et al. 2009:210
- 211) Ischio-pubis contact: present and extended ventrally (0); present and reduced to a thin proximal contact (1); absent (2). Benton and Clark 1988; Novas 1996; Nesbitt 2009: 287; Nesbitt et al. 2009:211
- 212) Pubis, pubic apron, proximal portion: similar anteroposterior thickness as the rest of the pubic apron (0); thickened process (1). Nesbitt 2005; 2007; Nesbitt 2009: 288; Nesbitt et al. 2009:212
- 213) Pubis, mediolateral width of distal portion: nearly as broad as proximal width (0); significantly narrower than proximal width (1); mediolaterally compressed and not broader than anteroposteriorly deep (2). ORDERED Galton 1976; Novas 1996; Sereno 1999; Langer and Benton 2006; Nesbitt 2009: 289; Nesbitt et al. 2009:213
- 214) Ischium, medial contact with antimer: restricted to the medial edge (0); extensive contact but the dorsal margins are separated (1); extensive contact and the dorsal margins contact each other (2). Nesbitt 2009: 291; Nesbitt et al. 2009:214
- 215) Ischium, cross-section of the distal portion: thin, plate-like (0); rounded or elliptical (1); sub-triangular (2). Sereno 1999; Langer and Benton 2006; Irmis et al. 2007; Nesbitt 2009: 293; Nesbitt et al. 2009:215
- 216) Ischium, distal portion: unexpanded (0); expanded relative to the ischial shaft (=ischial boot) (1). Smith and Galton 1990; Holtz 1994; Hutchinson 2001; Rauhut 2003; Langer and Benton 2006; Nesbitt 2009: 294; Nesbitt et al. 2009:216
- 217) Ischium, obturator process: confluent with the pubic peduncle (0); offset from the pubic peduncle by a notch (1). Gauthier 1986; Novas 1993; Rauhut 2003; Nesbitt 2009: 295; Nesbitt et al. 2009:217
- 218) Ischium, ventral margin: continuous ventral margin (0); notch present (1). Sereno et al. 1996; Rauhut 2003; Nesbitt 2009: 296; Nesbitt et al. 2009:218
- 219) Ischium, proximal articular surfaces: articular surfaces with the ilium and the pubis continuous (0); articular surfaces with the ilium and the pubis continuous but separated by a fossa (1); articular surfaces with the ilium and the pubis separated by a large concave surface (2). ORDERED Irmis et al. 2007; Nesbitt 2009: 297; Nesbitt et al. 2009:219

- 220) Ischium, groove on the dorsolateral surface of the proximal part: absent (0); present (1). Irmis et al 2007: 75; Irmis 2008: 275; Nesbitt et al. 2009:220
- 221) Ischium length: about the same length or shorter than the dorsal margin of the iliac blade (minus the anterior process) (0); markedly longer than the dorsal margin of iliac blade (minus the anterior process) (1). Juul 1994; Nesbitt 2009: 298; Nesbitt et al. 2009:221
- 222) Tibia (or fibula)-femur length: femur longer or about the same length as the tibia/fibula (0); tibia longer (1). Gauthier 1986; Sereno 1991a; Juul 1994; Benton 1999; Irmis et al. 2007; Nesbitt 2009: 299; Nesbitt et al. 2009:222
- 223) Femur, proximal portion, anteromedial tuber: absent (0); small and rounded (1); offset medially (or posteriorly) relative to the posteromedial tuber (2); large and "hooked" posteriorly (3). Gauthier 1986; Benton 1999; Clark et al. 2000; Olsen et al. 2000; Benton and Walker 2002; Sues et al. 2003; Clark et al. 2004; Nesbitt 2009: 300; Nesbitt et al. 2009:223
- 224) Femur, proximal portion, posteromedial tuber: present and small (0); present and largest of the proximal tubera (1); absent (2). Novas 1996; Nesbitt 2005; Irmis et al. 2007; Nesbitt 2009: 301; Nesbitt et al. 2009:224
- 225) Femur, proximal portion, anterolateral tuber: present as an expansion (0); absent, the anterolateral face is flat (1). Sereno and Arcucci 1994; Irmis et al. 2007; Nesbitt 2009: 302; Nesbitt et al. 2009:225
- 226) Femur, medial articular surface of the head in dorsal view: rounded (0); flat/straight (1). Nesbitt 2009: 303; Nesbitt et al. 2009:226
- 227) Femur, ventral to the proximal head: smooth transition from the femoral shaft to the head (0); notch (1); concave emargination (2). Sereno and Arcucci 1994; Novas 1996; Nesbitt 2009: 304; Nesbitt et al. 2009:227
- 228) Femur, femoral head orientation (angle with respect to the transverse axis through the femoral condyles Parrish 1986): anterior (60 - 90o) (0); anteromedial (20 - 60o) (1); medial (0 - 20o) (2). Benton and Clark 1988; Hutchinson 2001a; Nesbitt 2009: 305; Nesbitt et al. 2009:228
- 229) Femur, femoral head in medial and lateral views: rounded (0); hook-shaped (1). Sereno and Arcucci 1994; Irmis et al. 2007; Nesbitt 2009: 306; Nesbitt et al. 2009:229
- 230) Femur, dorsolateral margin of the proximal portion: smooth (0); sharp ridge (=dorsolateral trochanter of some) (1); rounded ridge (=dorsolateral trochanter of some) (2). Nesbitt 2009: 307; Nesbitt et al. 2009:230
- 231) Femur, anterior trochanter (=M. iliofemoralis cranialis insertion): absent (0); present and gradually merges with the shaft proximally (1); present and forms a steep margin with the shaft proximally (2). ORDERED Bakker and Galton 1974; Gauthier 1986; Novas 1992; Juul 1994; Novas 1996; Benton 1999; Langer and Benton 2006; Nesbitt 2009: 308; Nesbitt et al. 2009:231; Ezcurra 2017: 231
- 232) Femur, medial articular facet of the proximal portion: rounded (0); straight (1). Nesbitt 2009: 309; Nesbitt et al. 2009:232
- 233) Femur, anterolateral side of the femoral head: smooth, featureless (0); ventral emargination present (1). Sereno and Arcucci 1994; Irmis et al. 2007; Nesbitt 2009: 310; Nesbitt et al. 2009:233
- 234) Femur, trochanteric shelf proximal to the fourth trochanter (insertion site for the M. iliofemoralis externus) in mature individuals: absent (0); present (1). Gauthier 1986; Rowe and Gauthier 1990; Novas 1992; 1996; Langer and Benton 2006; Nesbitt 2009: 311; Nesbitt et al. 2009:234
- 235) Femur, posterolateral portion (= fossa trochanterica, = posterolateral depression, = facies antitrochanterica articularis) of the head: level with the greater trochanter (0); ventrally descended (1). Novas 1996; Nesbitt 2009: 313; Nesbitt et al. 2009:235
- 236) Femur, proximal surface: rounded and smooth (0); transverse groove that is straight (1); transverse groove that is curved (2). ORDERED Ezcurra 2006; Nesbitt 2009: 314; Nesbitt et al. 2009:236
- 237) Femur, fourth trochanter shape: mound-like and rounded (0); a sharp flange (1). This character is inapplicable in taxa lacking a distinct ridge for the attachment of the M. caudifemoralis (see character 377). Gauthier 1986; Benton and Clark 1988; Sereno 1991; Juul 1994; Bennett 1996; Benton 1999; Nesbitt 2009: 316; Nesbitt et al. 2009:237
- 238) Femur, fourth trochanter: symmetrical, with distal and proximal margins forming similar low-angle slopes to the shaft (0); asymmetrical, with distal margin forming a steeper angle to the shaft (1). Langer and Benton 2006; Nesbitt 2009: 317; Nesbitt et al. 2009:238
- 239) Femur, angle between the lateral condyle and the crista tibiofibularis in distal view: obtuse (0); about a right angle (1). Parker and Irmis 2005; Nesbitt 2009: 319; Nesbitt et al. 2009:239
- 240) Femur, infrapopliteal ridge between medial femoral distal condyle and crista tibiofibularis: absent (0); present (1). Smith et al. 2007: 304; Irmis 2008: 306; Nesbitt et al. 2009:240
- 241) Femur, medial condyle of the distal portion: tapers to a point on the medial portion in distal view (0); smoothly rounded in distal view (1). Nesbitt 2009: 320; Nesbitt et al. 2009:241
- 242) Femur, surface between the lateral condyle and crista tibiofibularis on the distal surface: smooth (0); deep groove (1). Nesbitt 2009: 322; Nesbitt et al. 2009:242
- 243) Femur, bone wall thickness at or near mid-shaft: thickness/diameter >0.3 (0); thin; thickness/diameter <0.3, > 0.2 (1); very thin; thickness/diameter <0.2 (2). Nesbitt 2009: 323; Nesbitt et al. 2009:243
- 244) Femur, distal condyles of the femur divided posteriorly: less than 1/4 the length of the shaft (0); between 1/4 and 1/3 the length of the shaft (1). Nesbitt 2009: 324; Nesbitt et al. 2009:244
- 245) Femur, anterior surface of the distal portion: smooth (0); distinct scar orientated mediolaterally (1). Nesbitt et al. 2009; Nesbitt 2009: 325; Nesbitt et al. 2009:245

- 246) Femur, crista tibiofibularis (fibular condyle of Sereno & Arcucci 1994): smaller or equal in size to the medial condyle (0); larger than the medial condyle (1). Nesbitt et al. 2009; Nesbitt 2009: 326; Nesbitt et al. 2009:246
- 247) Femur, anteromedial corner of the distal end: rounded (0); squared off near 90° or acute >90° (1). Nesbitt et al. 2009; Nesbitt 2009: 327; Nesbitt et al. 2009:247
- 248) Tibia, proximal portion, cnemial crest: absent or just a slight bump (0); present and straight (1); present arcs anterolaterally (2). ORDERED Benton and Clark 1988; Juul 1994; Novas 1996; Benton 1999; Irmis et al. 2007; Nesbitt 2009: 328; Nesbitt et al. 2009:248
- 249) Tibia, proximal surface: flat or convex (0); concave, the posterior condyles of the tibia are separated from the cnemial crest by a concave surface (the cnemial process is proximally expanded) (1). Nesbitt 2009: 329; Nesbitt et al. 2009:249
- 250) Tibia, proximal surface of the lateral condyle: convex or flat (0); depressed (1). Nesbitt 2009: 330; Nesbitt et al. 2009:250
- 251) Tibia, lateral (fibular) condyle of the proximal portion: offset anteriorly from the medial condyle (0); level with the medial condyle at its posterior border (1). Langer and Benton 2006; Irmis et al. 2007; Nesbitt 2009: 331; Nesbitt et al. 2009:251
- 252) Tibia, lateral margin of the lateral condyle of the proximal portion: rounded (0); squared-off (1). Nesbitt 2009: 332; Nesbitt et al. 2009:252
- 253) Tibia, lateral side of the proximal portion: smooth (0); dorsoventrally oriented crest present (=fibular crest) and extends from the proximal articular surface (1); dorsoventrally oriented crest present and clearly separated from the proximal articular surface (2). ORDERED Gauthier 1986; Rauhut 2003; Nesbitt 2009: 333; Nesbitt et al. 2009:253
- 254) Tibia, posterolateral process (= lateral malleolus) of the distal portion: absent (0); present and extends subequally to the level of the lateral margin of the facet for the reception of the ascending process of astragalus (1); present and extends distinctly beyond the level of the lateral margin of the facet for the reception of the ascending process of astragalus (2); present and extends well posterior to the fibula (3). ORDERED. Novas 1992; Juul 1994; Benton 1999; Langer and Benton 2006; Irmis et al. 2007; Nesbitt 2009: 334; Nesbitt et al. 2009:254; Nesbitt and Ezcurra 2005: 254
- 255) Tibia, posterolateral margin of the distal end: straight or convex (0); concave (1). Irmis et al., 2007; Nesbitt 2009: 335; Nesbitt et al. 2009:255
- 256) Tibia, posterior face of the distal end: rounded surface (0); distinct proximodistally oriented ridge present (1). Nesbitt 2009: 336; Nesbitt et al. 2009:256
- 257) Tibia, posterior side of the distal portion: smooth and featureless (0); dorsoventrally oriented groove or gap (1). Nesbitt 2009: 337; Nesbitt et al. 2009:257
- 258) Tibia, lateral side of the distal portion: smooth/rounded (0); proximodistally oriented groove (1). Novas 1996; Nesbitt 2009: 338; Nesbitt et al. 2009:258
- 259) Fibula, attachment site for the M. iliofibularis, location: near the proximal portion (0); near the mid point between the proximal and distal ends (1). Sereno 1991; Nesbitt 2009: 340; Nesbitt et al. 2009:259
- 260) Fibula, proximal end in proximal view: rounded or slightly elliptical (0); mediolaterally compressed (1). Nesbitt 2009: 341; Nesbitt et al. 2009:260
- 261) Fibula, anterior edge of the proximal portion: rounded (0); tapers to a point and arched anteromedially (1). Nesbitt 2009: 342; Nesbitt et al. 2009:261
- 262) Fibula, proximal portion in lateral view: symmetrical or nearly symmetrical (0); posterior part expanded posteriorly (1). Nesbitt 2009: 343; Nesbitt et al. 2009:262
- 263) Fibula, medial face of the distal portion: smooth (0); banked with an articular facet that articulates with the astragalus (1). Nesbitt 2009: 344; Nesbitt et al. 2009:263
- 264) Fibula, ridge on the medial side of the proximal end and oriented anterodistally: absent (0); present (1). Smith et al. 2007: 315; Irmis 2008: 328; Nesbitt et al. 2009:264
- 265) Fibula, deep groove on the medial side of the proximal portion: absent (0); present, medial side of fibula bears distinct deep fossa (1). Smith et al. 2007: 314; Irmis 2008: 327; Nesbitt et al. 2009:265
- 266) Fibula, distal end in lateral view: angled anterodorsally (asymmetrical) (0); rounded or flat (symmetrical) (1). Nesbitt 2009: 345; Nesbitt et al. 2009:266
- 267) Distal tarsal 4, transverse width: broader than distal tarsal 3 (0); subequal to distal tarsal 3 (1). Sereno 1991; Juul 1994; Benton 1999; Nesbitt 2009: 347; Nesbitt et al. 2009:267
- 268) Distal tarsal 4, size of articular facet for metatarsal V: more than half of lateral surface of distal tarsal 4 (0); less than half of lateral surface of distal tarsal 4 (1). Sereno 1991; Novas 1996; Benton 1999; Nesbitt 2009: 348; Nesbitt et al. 2009:268
- 269) Distal tarsal 4, posterior prong: blunt (0); pointed (1). Langer and Benton 2006; Nesbitt 2009: 350; Nesbitt et al. 2009:269
- 270) Distal tarsal 4, subtriangular medial process: absent (0); present in the anteroposterior middle of the element (1); present in the anteromedial corner of the element (2). Nesbitt 2009: 351; Nesbitt et al. 2009:270; Ezcurra 2017: 270
- 271) Distal tarsal 4, proximal surface: flat (0); distinct, proximally raised region on the posterior portion (=heel of Sereno and Arcucci 1994) (1). Nesbitt 2009: 353; Nesbitt et al. 2009:271
- 272) Astragalus, dorsally expanded process on the posterolateral portion of the tibial facet: absent or poorly expanded (0); expanded into a distinct, raised process (=posterior ascending process of Sereno and Arcucci 1994a) (1). Sereno and Arcucci 1994; Nesbitt 2009: 355; Nesbitt et al. 2009:272

- 273) Astragalus, anterior ascending flange (anterior process): absent (0); present and lower than the height of the astragalar body directly below it (1); present and higher than the height of the astragalar body directly below it (2). ORDERED Gauthier 1986; Novas 1992; 1996; Benton 1999; Rauhut 2003; Nesbitt 2009: 356; Nesbitt et al. 2009:273; Ezcurra 2017: 273
- 274) Astragalus, anteroposterior breadth of the astragalar ascending process: wedgedshaped/blocky (0); plate-like/laminar (1). Smith et al. 2007: 323; Irmis 2008: 335; Nesbitt et al. 2009:274
- 275) Astragalus, anterior hollow: shallow depression (0); reduced to a foramen or absent (1). Nesbitt 2009: 357; Nesbitt et al. 2009:275
- 276) Articular facet for the astragalus of the calcaneum lies: completely medial to the fibular facet (0); partially ventral to the fibular facet (1). Parrish 1993; Nesbitt 2009: 358; Nesbitt et al. 2009:276
- 277) Astragalus, proximal surface: lacks a marked rimmed and elliptical fossa posterior to the anterior ascending process (0); possesses a marked rimmed and elliptical fossa posterior to the anterior ascending process (1). Langer and Benton 2006; Nesbitt 2009: 359; Nesbitt et al. 2009:277
- 278) Astragalus, anteromedial corner shape: obtuse (0); acute (1). Bonaparte 1976; Novas 1989; Sereno 1991; Juul 1994; Novas 1996; Benton 1999; Nesbitt 2009: 361; Nesbitt et al. 2009:278
- 279) Astragalus, proximal articular facet for fibula occupies: more than 0.3 of the transverse width (0); less than 0.3 of the transverse width (1). Langer and Benton 2006; Nesbitt 2009: 362; Nesbitt et al. 2009:279
- 280) Astragalus, posterior groove: present (0); absent (1). Sereno 1991; Nesbitt 2009: 363; Nesbitt et al. 2009:280
- 281) Astragalus, tibial facet: concave or flat (0); divided into posteromedial and anterolateral basins (1). Sereno 1991; Parrish 1993; Juul 1994; Benton 1999; Nesbitt 2009: 366; Nesbitt et al. 2009:281
- 282) Astragalus-calcaneum, ventral articular surface: flat or slightly convex (0); concavoconvex with concavity on calcaneum (1); concavoconvex with concavity on astragalus (2). Sereno 1991; Nesbitt 2009: 368; Nesbitt et al. 2009:282
- 283) Astragalus-calcaneum, articulation in mature individuals: free (0); co-ossified (1). Sereno and Arcucci 1994; Irmis et al. 2007; Nesbitt 2009: 370; Nesbitt et al. 2009:283
- 284) Calcaneum, ventral articular surface for distal tarsal 4 and the distal end of the tuber: continuous (0); separated by a clear gap (1); separated by a gap with a ventral fossa (2). Nesbitt 2009: 371; Nesbitt et al. 2009:284
- 285) Calcaneum, articular facets for the fibula and astragalus: connected by a continuous surface (0); separated (1). Nesbitt 2009: 372; Nesbitt et al. 2009:285
- 286) Calcaneum, calcaneal tuber: present (0); absent (1). Gauthier 1986; Sereno 1991; Juul 1994; Benton 1999; Nesbitt 2009: 373; Nesbitt et al. 2009:286
- 287) Calcaneum, calcaneal tuber, distal end: rounded and unexpanded (0); flared, dorsally and ventrally (1). Sereno 1991; Nesbitt 2009: 374; Nesbitt et al. 2009:287
- 288) Calcaneum, calcaneal tuber, distal end: without dorsoventrally aligned median depression (0); with dorsoventrally aligned median depression (1). Parrish 1993; Benton 1999; Nesbitt 2009: 375; Nesbitt et al. 2009:288
- 289) Calcaneum, calcaneal tuber, shaft proportions at the mid-shaft of the tuber: taller than broad (0); about the same or broader than tall (1); just short of twice the mediolateral width of the fibular facet (2). Sereno 1991; Parrish 1993; Juul 1994; Benton 1999; Nesbitt 2009: 376; Nesbitt et al. 2009:289
- 290) Calcaneum, articular surface for the fibula: convex (0); convex and hemicylindrical shaped (1); concave (2). Sereno 1991; Parrish 1993; Juul 1994; Novas 1996; Gower 1996; Benton 1999; Nesbitt 2009: 378; Nesbitt et al. 2009:290
- 291) Calcaneum, shape: proximodistally compressed with a short posterior projection and medial process (0); transversely compressed, with the reduction of these projections (1). Langer and Benton 2006; Nesbitt 2009: 379; Nesbitt et al. 2009:291
- 292) Calcaneum, articular surfaces for fibula and distal tarsal IV: separated by a nonarticular surface (0); continuous (1). Sereno 1991; Juul 1994; Benton 1999; Nesbitt 2009: 380; Nesbitt et al. 2009:292
- 293) Metatarsus, configuration: metatarsals diverging from ankle (0); compact metatarsus, with metatarsals II-IV tightly bunched (at least half of the length) (1). Sereno 1991; Juul 1994; Benton 1999; Nesbitt 2009: 382; Nesbitt et al. 2009:293
- 294) Longest metatarsal: shorter than 50% of tibial length (0); longer than 50% of tibial length (1). Sereno 1991; Juul 1994; Benton 1999; Nesbitt 2009: 383; Nesbitt et al. 2009:294
- 295) Metatarsals, midshaft diameters: I and V subequal or greater than II-IV (0); I and V less than II-IV (1). Sereno 1991; Juul 1994; Novas 1996; Benton 1999; Nesbitt 2009: 384; Nesbitt et al. 2009:295
- 296) Metatarsal I: reaches the proximal surface of metatarsal II (0); does not reach the proximal surface of metatarsal II and attaches onto the medial side of metatarsal II (1). Gauthier 1986; Rauhut 2003; Nesbitt 2009: 385; Nesbitt et al. 2009:296
- 297) Metatarsal I, length, relative to length of metatarsal III: 0-84% (0); 85% or more (1). Sereno 1991; Benton 1999; Nesbitt 2009: 387; Nesbitt et al. 2009:297
- 298) Metatarsal III, proximal end: does not back to the ventral side of metatarsals II and IV (0); backs metatarsals II and IV posteroventrally, resulting in a T-shaped proximal profile (1). Carrano et al. 2002; Tykoski 2005; Nesbitt 2009: 389; Nesbitt et al. 2009:298
- 299) Metatarsal III: longer than metatarsal II (0); subequal to metatarsal II (1). Nesbitt 2009: 390; Nesbitt et al. 2009:299

- 300) Metatarsal III, outline of the proximal articular surface: rectangular (0); hourglassshaped (1). Smith et al. 2007: 335; Irmis 2008: 369; Nesbitt et al. 2009:300
- 301) Metatarsal IV, distal articulation surface: broader than deep to as broad as deep (0); deeper than broad (1). Sereno 1999; Langer and Benton 2006; Nesbitt 2009: 391; Nesbitt et al. 2009:301
- 302) Metatarsal IV, proximal portion, possesses an elongated lateral expansion that overlaps the anterior surface of metatarsal V: absent (0); present (1). Sereno 1999; Langer and Benton 2006; Nesbitt 2009: 392; Nesbitt et al. 2009:302
- 303) Metatarsal IV length: longer than metatarsal II (0); subequal or shorter than to metatarsal II (1). Gauthier 1986; Nesbitt 2009: 395; Nesbitt et al. 2009:303
- 304) Metatarsal V, dorsal prominence separated from the proximal surface by a concave gap: absent (0); present (1). Nesbitt 2009: 397; Nesbitt et al. 2009:304
- 305) Metatarsal V, 'hooked' proximal end: present (0); absent, and articular face for distal tarsal 4 subparallel to shaft axis (1). Sereno 1991; Juul 1994; Benton 1999; Nesbitt 2009: 398; Nesbitt et al. 2009:305
- 306) Metatarsal V, phalanges: present and has "fully" developed first phalanx (0); present and has a "poorly" developed first phalanx (1); without phalanges and tapers to a point (2). Gauthier 1984; Parrish 1993; Nesbitt 2009: 399; Nesbitt et al. 2009:306
- 307) Pedal unguals: weakly mediolaterally compressed, rounded or triangular in crosssection (0); dorsolaterally compressed (1); strongly mediolaterally compressed, with a sharp dorsal keel (2). Sereno 1991; Nesbitt 2009: 400; Nesbitt et al. 2009:307
- 308) Osteoderms, dorsal to the vertebral column: absent (0); present (1). Gauthier 1984; Benton and Clark 1988; Sereno 1991; Juul 1994; Bennett 1996; Dilkes 1998; Benton 1999; Nesbitt 2009: 401; Nesbitt et al. 2009:308
- 309) Osteoderms, presacral, dorsal, anterior edge: straight or rounded (0); with distinct anterior process (1). Clark et al. 2000; Olsen et al. 2000; Benton and Walker 2002; Sues et al. 2003; Clark et al. 2004; Nesbitt 2009: 403; Nesbitt et al. 2009:309
- 310) Osteoderms, presacral, paramedian: flat (0); with distinct longitudinal bend near lateral edge (1). Clark et al. 2000; Olsen et al. 2000; Benton and Walker 2002; Sues et al. 2003; Clark et al. 2004; Nesbitt 2009: 404; Nesbitt et al. 2009:310
- 311) Osteoderms, covering the appendages (=appendicular osteoderms), at least in part: absent (0); present (1). Heckert and Lucas 1999; Nesbitt 2009: 405; Nesbitt et al. 2009:311
- 312) Presacral osteoderms, dimensions: square shaped, about equal dimensions (0); longer than wide (1); wider than long (2). Nesbitt 2009: 407; Nesbitt et al. 2009:312
- 313) Anterior bar located on the anterior edge of an osteoderm: absent (0); present (1). Heckert and Lucas 1999; Parker 2007; Nesbitt 2009: 408; Nesbitt et al. 2009:313
- 314) Ventral carapace in the dorsal area: absent (0); present (1). Heckert and Lucas 1999; Nesbitt 2009: 409; Nesbitt et al. 2009:314
- 315) Gastralia: form extensive ventral basket with closely packed elements (0); well separated (1); absent (2). Nesbitt 2009: 412; Nesbitt et al. 2009:315
- 316) Angle between the ascending and horizontal processes of the maxilla: 35°-50° (0); less than 35° (1); more than 50° (2). (Tykoski, 2005; Ezcurra and Brusatte 2011, 316)
- 317) Medial wall of the antorbital fossa, extent: does not reach the posteroventral corner of the internal antorbital fenestra (0); extends along the entire ventral border of the internal antorbital fenestra as a very narrow lamina, lower than the height of the horizontal process below the antorbital fossa (1); extends along the entire ventral border of the internal antorbital fenestra as a broad lamina, higher than the height of the horizontal process below the antorbital fossa (2). (Galton 1990; Witmer 1997; Carrano et al. 2002; Langer 2004; Ezcurra and Novas, 2007; Ezcurra and Brusatte 2011, 317)
- 318) Lateral surface of maxillary antorbital fossa at the base of the ascending process, form: smooth or widely concave (0); with deep, large, and subcircular or oval blind pocket/s (1). (Carrano et al. 2002; Ezcurra and Brusatte 2011, 318)
- 319) Lateral lamina of bone of the lacrimal: absent (0); present, covering most of the bone (1); present, with no interruption of the lacrimal antorbital fossa and restricted to the posterior margin of the ventral ramus along its dorsoventral extension (2); present, only interrupting the lacrimal antorbital fossa near the proximal end of the ventral ramus and ventrally restricted to posterior margin of the ventral ramus (3). (modified from Ezcurra and Novas 2007; Ezcurra and Brusatte 2011, 319)
- 320) Sublacral part of jugal, form: tapering (0); bluntly squared anteriorly (1); squared anteriorly with a small dorsally directed prong, slightly overlapping the lacrimal (2); expanded with a well developed dorsally directed prong, strongly overlapping the lacrimal (3). (Rauhut 2003; Ezcurra and Novas 2007; Ezcurra and Brusatte 2011, 320)
- 321) Angle between posterior margin of the ascending process and longitudinal axis of the jugal: right, obtuse or slightly acute (0); less than 75°, with an ascending process strongly posterodorsally oriented (1). (Ezcurra and Novas 2007; Ezcurra and Brusatte 2011, 321)
- 322) Ventral process of squamosal, form: tapering ventrally (0); keeps consistent depth ventrally or expanded anteroposteriorly ventrally (1). (Rauhut 2003; Ezcurra and Brusatte 2011, 322)
- 323) Squamosal-quadratojugal contact: present, but small contact between the bones (0); present, broad contact (1); absent (2). (Holtz 1994; Ezcurra and Brusatte 2011, 323)
- 324) Postorbital participation in the supratemporal fossa: present (0); absent (1). (Sereno 1999; Ezcurra and Brusatte 2011, 324)

- 325) Posteroventral process of dentary, extent: extends further posteriorly than posterodorsal process (0); subequal in length to posterodorsal process or posterodorsal process extends further posteriorly (1). (Sereno 1999; Ezcurra and Brusatte 2011, 325)
- 326) Angular reaches posterior end of mandible, precluding surangular from the ventral margin of the jaw in lateral view: absent (0); present (1). (Tykoski 2005; Ezcurra and Brusatte 2011, 326)
- 327) Mandibular joint, position: approximately ventral to the quadrate head (0); significantly posterior to the quadrate head (1). (Rauhut 2003; Ezcurra and Brusatte 2011, 327)
- 328) Anterior and mid-dorsal vertebral centrum, length: less than two times centrum height (0); more than two times centrum height (1). (Sereno 1999; Ezcurra and Novas 2007; Ezcurra and Brusatte 2011, 328)
- 329) Posterior dorsal vertebrae, length: strongly shortened, centrum length less than 1.33 times the height of the anterior articular surface (0); relatively short, centrum length equal or more than 1.33 times the height of the anterior articular surface (1); significantly elongated, centrum length equal or more than two times the height of the anterior articular surface (2). (Rauhut 2003; Tykoski 2005; Ezcurra and Brusatte 2011, 329) ORDERED.
- 330) Neural spines of posterior dorsal vertebrae, shape: broadly rectangular, as high as long or longer than high (0); high rectangular, significantly higher than long (1). (Rauhut 2003; Ezcurra and Brusatte 2011, 330)
- 331) Postacetabular process, posterior expansion form: narrow with sub-parallel margins, approximately straight parasagittally, or slightly laterally expanded (0); strongly laterally expanded posteriorly (1). (Molnar et al. 1990; Novas 1993; Rauhut 2003; Ezcurra and Novas 2007; Ezcurra and Brusatte 2011, 331)
- 332) Sharp longitudinal edge on the lateral surface of the distal end of tibia: absent (0); present (1). (New character; Ezcurra and Brusatte 2011, 332)
- 333) Diagonal tuberosity on the anterior surface of the distal end of tibia: absent (0); present (1). (Ezcurra and Brusatte 2011, 333)
- 334) Anteriorly bowed diagonal tuberosity on the medial surface of the distal end of tibia: absent (0); present (1). (Ezcurra and Brusatte 2011, 334)
- 335) Strong anterior projection of the medial condyle of the astragalar body relative to the lateral condyle: present (0); absent (1). (Ezcurra and Brusatte 2011, 335)
- 336) Ventral margin of the astragalus in anterior/posterior view: deeply concave (0); only slightly concave or straight (1). (Hunt et al. 1998, Ezcurra and Brusatte 2011, 336)
- 337) Shallow fossa on the medial surface of the astragalar body: absent (0); present (1). (Ezcurra and Brusatte 2011, 337)
- 338) Co-ossified tibiotarsus in mature individuals: absent (0); present (1). (Rowe and Gauthier 1990, Ezcurra and Brusatte 2011, 338)
- 339) Metatarsal I, length: equal or more than 50% of the length of metatarsal II (0); less than 50% of the length of metatarsal II (1). (Gauthier 1986, Ezcurra and Brusatte 2011, 339)
- 340) Manus, phalanx I-1: horizontal axes of the proximal and distal ends approximately parallel with each other (0); horizontal axis of the distal end rotated medially 35° or more than the axis of the proximal end (1) (Sereno 1999, Nesbitt and Ezcurra 2015, 340).
- 341) Ilium, lateral surface of the postacetabular process: smooth (0); distinct posterior rim for the origin of the M. iliofibularis (1) (Rowe and Gauthier 1990; Nesbitt and Ezcurra 2015, 341).
- 342) Tibia, posterolateral process (= lateral malloelus) in anterior or posterior view: lobular (0); tabular (1); tapers while projecting laterodistally (2) (Sereno 1999; Nesbitt and Ezcurra 2015, 342; modified by Marsh et al., 2019, 342). This character is inapplicable in taxa without a posterolateral process, i.e., character-state 254(0).
- 343) Tibia, distinct posteromedially opened notch on the distal end: absent (0); present and shallow (1); present and very deep, to receive a pyramidal posteromedial process on the astragalus (2) (modified from Langer 2004 and Ezcurra and Novas 2007, Nesbitt and Ezcurra 2015, 343). This character can be scored also based on the presence of a notch on the posteromedial corner of the distal end of the tibia to receive the posteromedial process of the astragalus. ORDERED.
- 344) Premaxilla, transition between the alveolar margin and the base of the postnarial process: continuous, the base of the postnarial process is as tall as the premaxillary body (0); with a distinct inflexion, the base of the postnarial process is shorter than the premaxillary body (1) (Ezcurra 2017, 344).
- 345) Femur, extensor fossa on the anterior surface of the distal end: absent (0); present and shallow, developed as a slightly concave depression (1); present and very deep, developed as a strongly concave notch (2) (Rauhut, 2003; modified from Ezcurra and Novas, 2007; Ezcurra 2017, 345) ORDERED.
- 346) Femur, placement of the anterior extensor groove in the distal end: approximately centred in the transverse width (0); displaced to the lateral third of the transverse width (1); displaced to the medial third of the transverse width (2) (Ezcurra 2017, 346). This character is inapplicable in taxa lacking an extensor fossa in the distal end of the femur.
- 347) Femur, tibiofibular crest in the distal end: absent (0); present and posteriorly developed at the same level as or less than the tibial condyle (1); present and more posteriorly developed than the tibial condyle (2) (Sereno and Arcucci, 1994; modified from Irmis et al., 2007, Ezcurra 2017, 353) ORDERED.
- 348) Tibia, cnemial crest development: anteroposteriorly shorter than the posterior hemicondyles of the proximal end of the bone (0); anteroposteriorly as deep as or deeper than the posterior condyles of the proximal end of the bone (1) (Ezcurra 2017, 348).

- 349) Tibia, groove separating the lateral and medial hemicondyles of the posterior margin of the proximal end: absent (0); present as a narrow groove (1); present as a broad notch (2) (modified from Rauhut, 2003, Ezcurra 2017, 349) ORDERED.
- 350) Tibia, anterolateral corner of the lateral posterior hemicondyle of the proximal end: rounded (0); with a distinct apex (1) (Ezcurra 2017, 350).
- 351) Tibia, inflexion between the posterolateral process and medial portion of the distal end: absent, rather straight ventral margin of the distal end in posterior view (0); present, ventral margin of the posterolateral process more ventrally slanting than that of the medial portion in posterior view (1) (Ezcurra 2017, 351).
- 352) Tibia, profile in distal view: as anteroposteriorly deep as transversely broad or slightly anteroposteriorly deeper (0); transversely broader than anteroposteriorly deep (1) (modified from Rauhut, 2003).
- 353) Fibula, proximal margin of the bone side view: convex or straight (0); distinctly concave (1) (Ezcurra 2017, 353).
- 354) Fibula, anteroposterior depth of the distal end compared with that of the proximal end: subequal or larger (0); slightly lower (1); considerably lower, with a distal depth lower than 50% that of the proximal end (2) (Gauthier, 1986) ORDERED.
- 355) Fibula, anterior margin of the distal end in lateral view: convex or straight (0); continuously concave, with a pointing anterodistal corner (1) (Ezcurra 2017, 355).
- 356) Astragalus, anterior surface of the ascending process: flat or with a small pit (0); large fossa that opens laterally (1) (Ezcurra and Novas, 2007; Ezcurra 2017, 356).
- 357) Distal tarsal 3, fused to the metatarsal III in adults: absent (0); present (1) (Rowe, 1989; Tykoski, 2005: 252; Ezcurra 2017, 357).
- 358) Distal tarsal 4, anterior margin in proximal view: strongly convex (0); slightly convex to straight (1) (Ezcurra 2017, 358).
- 359) Distal tarsal 4, posterolateral corner has a broad notch that receives the proximal end of the metatarsal V: absent (0); present (1) (Tykoski, 2005: 253; Ezcurra 2017, 359).
- 360) Metatarsus, fusion between the proximal end of the metatarsals II and III in mature individuals: absent (0); present, contact between elements at least partially obliterated (1) (modified from Rowe, 1989; Tykoski, 2005: 257; Ezcurra 2017, 360).
- 361) Metatarsus, proximal end of the metatarsal II: subequal or transversely broader to the transverse width of the proximal end of the metatarsal III (0); transversely narrower than the metatarsals III (1) (Ezcurra 2017, 361).
- 362) Metatarsus, proximal end of the metatarsal III: not ventrally enlarged (0); with ventral boss protruding distinctly beyond plane of metatarsal shafts (1) (Tykoski, 2005: 260; Ezcurra 2017, 362).
- 363) Metatarsus, anterior margin of the metatarsal IV in proximal view: distinctly convex (0); straight (1) (Ezcurra 2017, 363).
- 364) Metatarsus, posterior margin of the metatarsal IV in proximal view: strongly tapers posteromedially along more than one-third of the bone (0); possesses a short, posteromedial apex (1) (Ezcurra 2017, 364).
- 365) Oblique ligament groove on posterior surface of femoral head: absent or very shallow (0); deep, bound medially by a well-developed posterior lip (1) (Rauhut, 2003; Marsh et al., 2019: 344).
- 366) Fibular facet on the astragalus: large and facing partially proximally (0); reduced and confined to anterior half of lateral side of astragalus (1); strongly reduced, facing laterally or absent (2) (Holtz, 1994; Carrano et al., 2002; Rauhut, 2003; Marsh et al., 2019: 345). ORDERED.
- 367) Sacral vertebrae, transverse processes do not form a dorsal roof over the sacral ribs (0); form a dorsal roof over the sacral ribs (1) (Marsh et al., 2019: 346).
- 368) Pubic peduncle of ilium, distal end not expanded anteroposteriorly (0); distal end expanded anteroposteriorly (1) (Marsh et al., 2019: 347).
- 369) Tibia, posterior margin in proximal view subdivided by a notch (0); subdivided by two notches (1) (Marsh et al., 2019: 348).
- 370) Tibia, cnemial crest in proximal view makes up at least 35 percent of the total anteroposterior width (0); makes up less than 35 percent of the total anteroposterior width (1). Measured maximum total anteroposterior width, cnemial crest was measured from most anterior point to inflection point on anterolateral corner of lateral condyle (Marsh et al., 2019: 349).
- 371) Tibia, distal outline [measured maximum anteroposterior and mediolateral widths]: subsquared such that the anteroposterior:mediolateral width is ≥ 0.9 (0); subrectangular such that the anteroposterior:mediolateral width is < 0.9 and ≥ 0.6 (1); subtriangular and such that the anteroposterior:mediolateral width is < 0.6 (2) (modified from Marsh et al., 2019: 350). ORDERED.
- 372) Astragalus, articulation with the distal tibia is one continuous basin (0); is separated into posterior and medial basins by a ridge extending from the base of the ascending process to the posterior margin (1) (Marsh et al., 2019: 351).
- 373) Astragalus, proximal outline is relatively wide such that the anteroposterior:mediolateral width is no more than 0.7 (0); is relatively short such that the anteroposterior:mediolateral width is > 0.7 (1). Measured maximum anteroposterior and mediolateral widths (Marsh et al., 2019: 352).
- 374) Astragalus, anterior margin in dorsal view: straight or convex (0); slightly concave (1); strongly concave and is continuous with an anteroposterior concavity on the distal surface (2) (= "glutealiform" sensu Long and Murry, 1995) (Marsh et al., 2019: 336) ORDERED

- 375) Dorsal vertebrae, shape of the hyposphene-hypantrum: rectangular, with directly laterally/medially facing articular facets (0); V-shaped, with ventrally converging articular facets (1); trapezoidal, with ventrally diverging articular facets (2).
- 376) Ilium, orientation of the ventral margin of the preacetabular process in lateral view: mainly anterior, broad gap between the process and the pubic peduncle (0); anteroventrally oriented, very narrow gap between the process and the pubic peduncle (1).
- 377) Femur, posterior development of internal trochanter/fourth trochanter: well-developed, distinctly raised from the shaft (0); poorly developed, raised from the shaft as a low ridge (1); absent, no distinct ridge for the attachment of the *M. caudifemoralis* (2). ORDERED.
- 378) Tibia, angle between the main axis of the lateral half of the facet for reception of the ascending process of the astragalus in anterior view and the longitudinal axis of the bone: $\leq 20^\circ$ (0); $>20^\circ$ – 30° (1); $>30^\circ$ (2). ORDERED.
- 379) Tibia, medial malleolus: absent (0); present, developed as a result of a concavity on the anteromedial surface of the distal end of the bone (not distinctly projected) (1); present, distinctly medially projected from the level of the shaft (2). ORDERED.
- 380) External naris, position: anterior to or at the anterior border of the maxilla (0); dorsal to a portion of the maxilla (1) (Sues et al., 2011: character 318).
- 381) Lacrimal, posteroventral process: short (0); long and extending along the dorsal edge of the jugal (1) (Sues et al., 2011: character 316).
- 382) Postorbital, anterodorsal portion: not expanded (0); thin, anterolaterally expanded portion that lies dorsal to the orbit (1) (Sues et al., 2011: character 319).
- 383) Jugal, height below the most ventral level of the orbit in lateral view: lower than 30% of the maximum height of the orbit (0) equal or higher than 30% of the maximum height of the orbit (1); equal or higher than 50% of the maximum height of the orbit (2) (modified from Ezcurra et al., 2017: character 625). ORDERED.
- 384) Surangular-articular, shape of retroarticular process: straight (0); slightly dorsally curved, but ventral to the level of the glenoid lips (1); strongly dorsally curved, extending dorsal to the level of the glenoid lips (2) (Dilkes, 1998: 75; Ezcurra, 2016: 284). ORDERED.
- 385) Scapula, distal end of blade: distinctly anteroposteriorly expanded (0); poorly anteroposteriorly expanded, without an increased divergence between the anterior and posterior margins with respect to the rest of the blade (1) (reworded from Gauthier, 1986 and Rauhut, 2003: character 133).
- 386) Metacarpus, metacarpal IV versus metacarpal III lengths ratio: equal or more than 0.6 (0); less than 0.6 (1) (new character).
- 387) Manual digits, unguis of digits II–IV length: about the same length or shorter than the last phalanx of the same digit (0); distinctly longer than the last phalanx of the same digit (1) (Nesbitt et al., 2015: character 222; modified from Ezcurra, 2016: character 451).
- 388) Ilium, pubic peduncle ventral extension: similar to that of the ischiadic peduncle (0); distinctly more ventrally extended than the ischiadic peduncle (1) (modified from Rauhut, 2003: character 177).
- 389) Tibia, position of the proximodistally oriented posteromedial ridge of the distal end: approximately at mid-width between the medialmost edge of the distal end and the tip of the posterolateral process (0); distinctly closer to the medial edge of the distal end than to the tip of the posterolateral (1).
- 390) Mid dorsal vertebral centrum: ventral limit of articular facet relative position: 0) anterior and posterior at the same level, or close; 1) anterior facet elevated in comparison to the posterior.
- 391) Mid dorsal vertebral central articular facets outline: 0) taller than wide; 1) sub-circular (as tall as wide); 2) wider than tall.
- 392) Dorsal vertebrae articular facet type: 0) amphiplatyan (both nearly planar); 1) amphicoelus (both concave); 2) opisthocelic (planar anteriorly, concave posteriorly).
- 393) Dorsal vertebrae neural canal walls shape: 0) straight and subparallel (width nearly constant along the canal); 1) curved (hourglass curvature of the pedicels; width narrower at the mid centrum).
- 394) Dorsal vertebra, midcentrum floor of neural canal width relative to the base of the pedicels width (best seen in unfused vertebrae in dorsal view): 0) Narrower; 1) Wider.
- 395) Dorsal vertebra: floor of neural canal / centrum maximum width: 0) Narrow: less than 0.2; 1) Between 0.2 and 0.4; 2) Wide neural canal: more than 0.4.
- 396) Dorsal vertebra: neurocentral suture orientation (this refers to the main line trend not to the serrated suture): 0) straight and horizontal (anterior, mid and posterior section leveled); 1) sinusoidal (normally, the anterior portion is lower); 2) bowed (higher toward the ends).
- 397) Mid to posterior dorsal vertebral centrum: lateral walls: 0) Continuous or gently concave, without a clear excavated fossa; 1) excavated forming a fossa (shallow lateral depression).
- 398) Mid to posterior dorsal vertebral centrum: surface near the rim: 0) smooth; 1) lateral and ventral longitudinal striations.
- 399) Mid to posterior dorsal vertebral centrum: ventral ridge excavation curvature in the midcentrum: 0) deep: 20% or more of the anterior facet height (curves strongly towards the mid centrum); 1) shallow: less than 20% of the anterior facet height (the curve is more subtle).

400) Mid to posterior dorsal vertebral centrum: ventral surface curve symmetry in lateral view: 0) symmetric (anterior and posterior halves of the curve are sub-equal); 1) asymmetrical (ventral curve clearly more pronounced anterior or posteriorly).

401) Mid to posterior dorsal vertebral centrum: ventral surface keel condition: 0) cylindrical (U-shaped), without obvious longitudinal keel; 1) Cylindrical (V-shaped) forming a subtle keel in the continuation of the centrum shape; 2) noticeably present lamina-like keel.

402) Mid to posterior dorsal vertebral centrum lateral excavation: 0) strongly laterally constricted at the mid-centrum (hourglass shaped in ventral view): mid centrum width <50% of posterior facet width; 1) poorly laterally constricted at mid centrum (more cylindrical and less hourglass shaped in ventral view): mid centrum width >50% of posterior facet width.

Postosuchus_kirkpatricki 00010000200001010100000201011111010010011011100111
00111031000001112110?110012011??1?001111110002011011000000000001
11??00??????000?1?00000000000000??0??1011011001000111?00100??00??
?0??0000001?0010000000????????1??1110001?010000100000000001010?00
000010000001011011000?????00?01?0001102101111?10000001010110?0111
?100?120031010110011000001000?0?01122-??-1?00-0??00??0201?-1-0020
1-1100??0000-0[01]1--2-1-00[02]0

Dromicosuchus_grallator 2000000?300011111100000001001?1000010001111110?1?10
011102110????????????100?????????001?011?000?0210110000000000001?
1?????????0??0000?1??000?0000000?0020101111001110011?00100?10????
????????00110010000100?00????01?????????010000100000100001010?0000
0010000001001011000?????00??1????11021011?1?11?00????????????111010
00120220?01?1?210?????????0?01122-?0-11??-?????????0?000-1????01-10
000?0??0-0-1-----01000

Eudimorphodon_ranzii 1110??020100?0?0200011000000??0??0?000??0?????0?000
00?0??1????????????????????????10?0?100?000000?00?001?0000?101????
1??0000000?1?0?0?00?????0?01000?????110000110?0?001?????00000110?
110?0100??0?00?00000?00?0?0000001??????0?00??--????0?0?????
0?????????????1?0??0?1??1??1?01?????11?001?1??0110000??????12000
31?211000210000??0?0?????????????2?-0??00?????????????2??10001?0
0?------

Dimorphodon_macronyx 2100??1?3010000?11?0011000000?????00000??010?0?000
00??00?0?0????????????????????????101?20?00??00??0?00??01?0000?1?
1????1?1?????00?1??000?????????010??????110000110?????1?0??00000?
110?1?000100?000100?00000?000????0000?0110000?0000000--001020000
000?00?000?0??1?00?11000?0?1??101??1??1?????110001?001??1?00
0??????2000?0?21??01100001100000??????-0??011-01000??02??0-1??
2?02?110001100?---1-----

Lagerpeton_chanarensis ???
??
?????????????0??000000000??0000
000000000000000?0000000000001111001100010?0100010?0010100?00000
00010100011102111?1001011?1?01??201110000000001200????????????????
??????210?0000001?0?0?122[01]20-10100001000100000001-00?00-0?????
0??1-0-----10--

Dromomeron_romeri ???
??
??
????????????????????????????????????111100110001010--0011101111000000000010
1?00??????11?1001011?1?01??2?1?????????????????0?????????????????
??0000010????0?122020-10??0?????????0??011-01??2-1??????01?-????????
?????

Dromomeron_gregorii ???
??
??
????????????????????????????????????1111001?0101110000011101111000000000
0 ? ? ? ? ? 0 0 ? ? ? ? ? ? 1 ? ? ? ? ? ? ? ?
1???000??????0?12201
0-1?????????????0??011?????1-??????????-?????????????

Lagosuchus_talampayensis ???
?????????????01210000?001100????0?????????????????????????????????101000
?000000000?00000000000000000000??1?????1000?101???
0????????????????????000000000100000010??11000000010111000010010011
00000?0?00001000000000101010000110010101001001?01000010011100000

0000012?0??????00?????????010000011000?0?0?0-1000000100?00?001?0
001000?02-00?0?????0??1-0-----0-100-

Eucoelophysis_baldwini ???
??
??
?????10?????????????????????????????0??12001??1210001??0??1100010?10
0??
0??0-????????????????
0?????????1????????????????--1-----0

Sacisaurus_agudoensis ?????????????????01?0000000000000????????????????????????
??1?????0?101?????????101001110?
1??
1??002????010?0000100?0??1????????????1001
1 1 0 1 2 1 0 0 0 1 0 0 0 0 ? ? ? 1 0 0 0 1 0 0 1 0 1 2 0 0 0
1??
0?????????????010000????????000?0-1020110??????????????[0 1]??10010?????11
0?????0????--20-----00

Silesaurus_opolensis 0?0?000?30?0000100000000000001?000?0??00?0100100000?
10020001????0021010000011001?001001?00100112100101000100001010111
1001000000000010000000000000110000??110101100001010?000?00??
0?????????????0020000101000010010??110110000111012011101210[0 1]01000
010110001001012000101110001?1????0101001010?0?01????2011110?0001010
1210?????????00?20?????0001100001110??00000-10101111000??00010000100
1000[0 1]0000000[0 1]20??0-011--2[0 12]1100-0

Eocursor_parvus ???
0?????????????????????01210100????????????????????????????????1??100?001??10?0?1011?1
1?1?????????????0?0001?0??00?10?001?1?0?????11?????11?0?10
1????????????????????????????????00210001020000?21????01??10?0021?1100021012
00011110010?000020000?3010101?10??1??????1????????????????????11????0
00?????????0?????????????????????1????0100?????0?000?0-10201101??????00??1?
?0001???-0022?????10??0002011000110[02]1

Pisanosaurus_mertii ??????????????????1?1?01??0????????????????????????????????
????????????????????????????????????0?????????000001?01200?1111111?1?????0?0?
?00000????00??
0?????????0?????????????????2?????????????????????001??0000?0000020001011
100?1?????01010?111?0?01??21111??0?01?????0?????????0??????????1
2??0000010????0???1020000100?????000?1??00???1????20?????00???-0-----
1-1000

Heterodontosaurus_tucki 0001000010111001000010000000010000000001101000200
0003001000101?0121?110000111??0??001101111?0[0 2]000100120[0 2]11100
111111000000001000000?000211?0011100001?111?0?111001101000101120
0100001120000?021000002100012110??01??100002011?0??????20?0101100
10?0000200001201??0110??111000?1?10?1?1??1?01?????111100?00101?12
00??????20001100101000100?00??0000??10-?021?0021?0101001????00001?
??-00?100100000100-----100-

Lesothosaurus_dianosticus 00010?0?400000110100100000000100000000001101000000
0003000010101001210100000??1??10??0011011111000001011200010110111
1????000001000000?0001??0?111?0??1??1100??1100?1000?01010????000?0
0??000000210?0102100012110??01??1000021111000210120001011?0100000
020000030101?111?00?????001?100111?0?01????21111100000101????00????
????0001010000000??010????00002000-102011010?0????00110?00001???-002
100101000000-[0 1]---11100[0 2]0

Scutellosaurus_lawleri??0??0?????????10??201??000????????????00??10??2????????
00??????0??????0?????1??????0?1?????110[02]0????1?????01011011?10???
00?00??0?000??00?00?0??00?00?11??0?000001101000????????0??????????
?0?21000102?100121?????1??0??????1111000?1?12000?01100100000020000
03010?01?10001?????010100111?????01????21110?????0??????01??000?????
10??????01?0?000100?0000?1010201111000??0001112?0001011-?022??????0
?0?101[01]1021111000

Saturnalia_tupiniquim????????????????[01]??000??000?????????11000001?100100
0??????0?0??001211100?0001101??????111?11?0?000?????????001001001?
1????0001001100001?0000000000001001??1000?111000111??010??????????
????????002000021110001001100110012100211010002102100111110011?000
0200001111010111001111110010101111?0?01??2011110000011101?0
0????????0?2??0?1??020000001000?000?0-102100010000000010111100[01]
[01]0110010?11??0??000-1---100000-

Plateosaurus_engelhardti01001010300101010200001001000100111100000101001000
000301000010100121010000001101?20?0111?1100101000110001101011001
1111001001100001001000000001001000011000?111001111000101010101
111112000002000000210001001100110012100211010002102100011110011
00000200000111010111000111110010101111?0?01??201101000001110110
0??????2001010?000001000000[01]0001000110100001011000000010121100
[01]10120011100120011001[01]--0-000[01][02]0

Efraasia_minor0?001?1020010101?20000?000000100??11000001?1001????00??1?
000????01210100000011??1??011?01??000000?1?000?101001001?11??010?
001100?01000000000000001001?110?0?1110011110001010?01011?111?000?
0020000002100010010?1100121002110100021021000111100110000020000
011101011100011111001010?111??0?01??2011010000011101100??????120
010?0?0000000000??001000?[01]0[12]01000010000000010121101????2000
0100?0??1001----[01]--[01]0-0

Herrerasaurus_ischigualastensis20010?0020010100010000000000?0000100000?101000
00000030010001?1?012111000000?1??1????000101100??00000?100?0000000
01111000?01001100101?0020000000001011?10?????1110110100000112011
0010013010100200000021000110121011011200020101010210210011011001
1?0000200100101010111001111110010101111?0?01??20111100000111011
00??????0001301?0101001000001[01]00000000-10100[01]010000000010111
1100101?000000012111100111100000001

Staurikosaurus_pricei??
??
01?00?????000000000?00101??0020
00000210001101210110111?00?011?000210110011111001??0000200100100
0101110001??
0?0010000??0?000?0-101000010??????????1?11?00????0000????2????1-00
0-----00-1

Chindesaurus_bryansmalli??
??
0?????101?1?00??00?0????100??
0????0??2?0??100??????1??????????10002102100110110000?0000200110[2
3] 0 0 0 1 ? ? ? ? ? ? ? ? ? ? ? ? ? ? ? ? ? 0 1 0 1 ? 1 1 ?
1??00?000000?0??020?0-[1
2]?1?01??0?????????0211111112??[01]?0??????????-0[12]1112-100000

Gnathovorax_cabreirai200100?010010100?100000000000?00011000??1010?00?000
1?0010?0?????1?1?100000001??1??000?011001000010?100?000000001111
000101001100001?0020?000000000110?01010111101101000001120?100100
1?010?00200000021000010121011?112000201012002102100111110011?000
020?1??1000101110011111?001??0?11??0?????????011110000011101100????

Megapnosaurus_rhodesiensis 111011112111100002000111100001001011100001010010
0001?3001000111?012111100001111?1??0011011000020000??0000000000
111110?1?1111111?0100000011001110101111101011110110100010112111
0011113010211211102221101100111010011110121012000210220011[02]100
11110001210111211010111011111000010100111??1?01??211111101001010
1200??????111201021?0012010110011101010122100110111111111111110
010012010111101000010-----[02]--10--

Pendraig_milnerae ???
??
1 ?
1??01211002121101?00????10?
[1 2] 1 ? ? 0 1 2 ? ? ? 2 0 0 0 2 1 0 2 2 0 0 1 1 0 1 0 ? ? ? ?
1??
????????????????????2?0????????????1????????????????????????1??1??????-0
0????????????0?020--20100001

Lepidus_praecisio_holotype ???
??
??
??2110
1 ? ? ? ? ? ? ? 0 ? ? ? ? ? 0 1 0 1 ? ? 1 ? 1 ? ? 1 ? 0 1 ? ? ? 2 1
1??010010????11??????01??1
1??????????1?????1?01????00????????????0????????????????

Lepidus_praecisio_combined ? 0 0 ? 0 0 1 0 0 ? 1
1??
?
1??
??[1 2]?????10????
1????????????21101????????0?????0101??1?1??1?01????211????????????????
?????0?0????????????????010010????11????????01??11?????????1?????1?01??0
0????????????0????????????

Eodromaeus_murphi 0?0?100?2001000001000001001100????0????????????????????1??
01?0?????01211110????0?1??1??001?????000000000?0??000000001011?00
1?10?111000????000000001000?001??1111?1111011?100010102101000111?0
1000020000212100110011101?01??10021102000210[12]1001?0110011?00002
001111110101110?0?????010101111?0?0?1??21?1?10?0?0?0?01??0?????0
12[12]??21??01002000001100?000000-101010011????0?0??1?100110[01]?0
000?????000000-----00--

Panguraptor_lufengensis ?????????????????00?0000??1101?0?0??1110????10?0?1000011
30010?0????????????????????????????001?01?0?????????0?1001?00000?0??11?0?
1?11?1111?0?00?000?000????????1??11????????????0??????11??????111?0?
0?????????????111????????????????1?????1??0?2?022?01?????????0??21011?1
1?0101110??1?10200??0??11?????1??211111?????0?0?0120?????????12120
11000???10?0????????????1????????????021?111??110????????????????100?00
0?0?0-----10--

Powellvenator_podocitus ???
??
??
??0210?2????????00111000021011121101?
111?101110[01]001010?111????01??2111?1??0??0?01????????????????
?????????01000?0??01?12[12]10111[01]111?0111101?1??001?11????0
1??????????1????????????

Powellvenator_holotype ???
??
??
??2110

Character list for the new matrix based on Zahner and Brinkmann (2019)

Characters 286–297 have been added.

Character List:

1. Skull length (anterior most extension of premaxilla to quadrate condyle) versus skull height (quadrate condyle to dorsal most extension of parietal): 1.5 to 2.06 (0); 2.43 to 2.61 (1) (Ezcurra 2012: character 5; Panguraptor lufengensis after You et al. 2014: 237, Tab. 1, ratio calculated from information on p. 237 and skull height at mid-orbital level in Tab. 1: 2.6, Ceratosaurus after Gilmore 1920: Fig. 17.1, ratio 2.2, Fig. 17.2, ratio 1.94, Fig. 18.2, ratio 2.09, Eustreptospondylus oxoniensis after Sadleir et al. 2008: Fig. 5, estimated ratio 2.83, Sinraptor dongi after Currie & Zhao 1993: calculated from skull reconstruction in Fig. 3B, ratio 2.17; Swiss theropod: estimated ratio 2.7; for character history see Ezcurra 2012).
2. Height of cranium at the posterior margin of the external naris in relation to the height of the cranium in the middle of the orbit: 0.38 to 0.49 (0), 0.53 to 0.60 (1), 0.75 (2) (Ezcurra 2012: character 6; Panguraptor lufengensis after You et al. 2014: 237, Fig. 2, Tab. 1, ratio estimated from Tab. 1 and Fig. 2: 0.29, Ceratosaurus after Gilmore 1920: Fig. 17.1, ratio 0.67, Fig. 18.2, ratio 0.63, Sinraptor dongi after Currie & Zhao 1993: calculated from skull reconstruction in Fig. 3B, ratio 0.72; Swiss theropod: estimated ratio 0.64; for character history see Ezcurra 2012).
3. Shape of premaxillary body: longer than high, or approximately as long as high (0); significantly higher than long (1) (Rauhut 2003: character 1; Yates 2005: character 1; Tawa hallae after Nesbitt et al. 2009: Fig. 1; Eodromaeus murphi after Martinez et al. 2011: Fig. 1B, BP/1/5278 after Yates 2005: Fig. 8, Eustreptospondylus oxoniensis after Sadleir et al. 2008: 9, Fig. 6, Sinraptor dongi after Currie & Zhao 1993: 2040/2041, Fig. 4A and D; for character history see Rauhut 2003).
4. Premaxillary body in front of external nares: shorter than body below the nares (0); longer than body below the nares to completely anterior to external nares (1) (modified from Rauhut 2003: character 2, and Yates 2005: character 2, Tawa hallae after Nesbitt et al. 2009: Fig. 1, Eodromaeus murphi after Martinez et al. 2011: Fig. 1B, BP/1/5278 after Yates 2005: Fig. 8 and BP/1/5278, Eustreptospondylus oxoniensis after Carrano et al. 2012: character 6; for character history see Rauhut 2003).
5. Neurovascular foramina in the lateral surface of the premaxillary body: absent (0); one foramen, usually located above the second or third premaxillary tooth (1); several foramina (2) (Ezcurra 2012: character 14; Ceratosaurus after Tykoski 2005: character 7, Eustreptospondylus oxoniensis after Sadleir et al. 2008: 9, Fig. 6A and D, Sinraptor dongi after Currie & Zhao 1993: 2040, Fig. 3B and 4A; for character history see Ezcurra 2012).
6. Anteroventral orientated «circular» foramen in the anteroventral corner of the premaxilla: absent (0); present (1) (Ezcurra 2012: character 16; Sinraptor dongi after Currie & Zhao 1993: 2040, Fig. 4A).
7. NEW: Foramina configuration above the second alveolus of the premaxilla: no foramen (0); one or more pits or foramina without channel (1); one or more pits or foramina with channel penetrating the alveolar margin (2) (Eoraptor lunensis, "Syntarsus" kayentakatae, Coelophysis bauri, Coelophysis rhodesiensis after Tykoski 2005: character 7, Herrerasaurus ischigualastensis after Sereno & Novas 1994: Fig. 1 - 3, Dracovenator regenti after Yates 2005: 107, Fig. 2, Dilophosaurus wetherilli after Welles 1984: 144, Fig. 4 and Yates 2005; Ceratosaurus after Madsen & Welles 2000: Pl. 1 + 9, Allosaurus fragilis after Tykoski 2005: character 7, and Witmer 1997: 29A, Eustreptospondylus oxoniensis after Sadleir et al. 2008: Fig. 6A and D, Sinraptor dongi after Currie & Zhao 1993: Fig. 4B).
8. Oval to slot-shaped foramen at the base of the nasal process (= dorsal process): absent (0); present (1) (modified from Ezcurra 2012: character 15; Ceratosaurus and Sinraptor dongi after Smith et al. 2007: character 13, Eustreptospondylus oxoniensis after Sadleir et al. 2008: Fig. 6A and D); for character history see Ezcurra 2012).
9. Premaxilla, posterior extent of nasal process relative to posterior tip of posterolateral process (= subnarial process): anterior or equal (0); posterior (1) (modified from Ezcurra 2012: character 21; Ceratosaurus and Sinraptor dongi after Smith et al. 2007: character 14; for character history see Ezcurra 2012).
10. Shape of the nasal process of the premaxilla: conspicuously curved along its axis (0); straight or slightly curved (1) (modified from Ezcurra 2012: character 23; Ceratosaurus after Madsen & Welles 2000: Pl. 1 + 9, Sinraptor dongi after Currie & Zhao 1993: Fig. 3B, 4A and D; for character history see Ezcurra 2012).
11. Posterolateral process (= subnarial process) of premaxilla: wide, plate-like, broadly contacting the nasals and excluding the maxilla from the external nares (0); strongly reduced in width, but still contacting the nasals (1); strongly reduced process does not contact the nasals, and the maxilla forms part of the posteroventral border of the external nares (2) (Ezcurra 2012: character 28; Eoraptor lunensis after Sereno et al. 2012: Fig. 3, Ceratosaurus and Sinraptor dongi after Rauhut 2003: character 6; Dilophosaurus wetherilli, Liliiensternus liliiensterni after Yates 2005: character 6 and Smith et al. 2007: character 10, Eustreptospondylus oxoniensis after Smith et al. 2007: character 10 and Sadleir et al. 2008: character 10 of Holtz 2000; for character history see Ezcurra 2012).
12. Anteroposterior length of the posterolateral process (= subnarial process) of the premaxilla: less or subequal to the anteroposterior length of the premaxillary body (0); longer than anteroposterior length of the premaxillary body (1) (Ezcurra 2012: character 27; Ceratosaurus after Madsen & Welles 2000: Pl. 1 + 9, Eustreptospondylus oxoniensis after Sadleir et al. 2008: Fig. 6, Sinraptor dongi after Currie & Zhao 1993: 2041, Fig. 3B, 4A and D; for character history see Ezcurra 2012).

13. Ventral process (= posteroventral flange) at posterior end of premaxillary body: absent (0); present (1) (Ezcurra 2012: character 30; *Ceratosaurus* and *Sinraptor dongi* after Rauhut 2003: character 4; for character history see Ezcurra 2012).
14. NEW: Procumbent teeth in premaxilla: absent (0); present (1) (*Eoraptor lunensis* after Sereno et al. 1993: Fig. 1, Martinez et al. 2011: Fig. 1A and Sereno, Martinez & Alcober 2012: Fig. 11 to 13 and 35, *Herrerasaurus ischigualastensis* after Sereno & Novas 1994: Fig. 2, *Eodromaeus murphi* after Martinez et al. 2011: Fig. 1B, *Dracovenator regenti* after Yates 2005: 108, Fig. 2, *Dilophosaurus wetherilli* after Tykoski 2005: Fig 9, "Syntarsus" *kayentakatae* after Tykoski 2005: 8, *Coelophysis bauri* after Colbert 1989: Figs. 28, 33, 36, *Coelophysis rhodesiensis* after QG 202, BP/1/5278 after Yates 2005: Fig. 8 and BP/1/5278, *Ceratosaurus* after Madsen & Welles 2000: Pl. 9, *Allosaurus fragilis* after Madsen 1976: Plate 1, *Eustreptospondylus oxoniensis* after Sadleir et al. 2008: Fig. 6B. E, *Sinraptor dongi* after Currie & Zhao 1993: Fig. 3B, 4A and D).
15. Number of premaxillary teeth: 3 (0); 4 (1); 5 (2) (Ezcurra 2012: character 35; *Ceratosaurus* and *Sinraptor dongi* after Rauhut 2003: character 5, *Eustreptospondylus oxoniensis* after Sadleir et al. 2008: character 3 of Holtz 2000; for character history see Ezcurra 2012).
16. Caudal end of premaxillary tooth row: ventral to external naris (0); anterior to external naris (1) (Smith et al. 2007: character 9, *Tawa hallae* after Nesbitt et al. 2009: Fig. 1, *Eodromaeus murphi* after Martinez et al. 2011: Fig 1B, *Dracovenator regenti* after Yates 2005: Fig. 2; for character history see Smith et al. 2007).
17. Serrations on premaxillary tooth crowns: present (0); absent (1); (Rauhut 2003: character 84; *Tawa hallae*, *Eodromaeus murphi*, *Dracovenator regenti*, "Syntarsus" *kayentakatae* and BP/1/5278 after Ezcurra 2012: character 40, *Eustreptospondylus oxoniensis* after Sadleir et al. 2008:18, Fig. 6E and F and Smith 2007: character 17, *Sinraptor dongi* after Smith 2007: character 17; for character history see Ezcurra 2012).
18. Cross-section of premaxillary tooth crowns: all labiolingually flattened (= elliptical) (0); anteriormost teeth subcircular (1); all "D"-shaped (asymmetrical) (2) (Ezcurra 2012: character 41; *Ceratosaurus* after Madsen & Welles: 4 and Smith et al. 2007: character 18, *Eustreptospondylus oxoniensis* after Smith et al. 2007: character 18, *Sinraptor dongi* after Currie & Zhao 1993: 2042 and Smith et al. 2007: character 18; for character history see Ezcurra 2012).
19. Size of premaxillary tooth crowns with respect to the largest maxillary tooth crowns: distinctively smaller (0); of equal size or larger (1) (Ezcurra 2012: character 37; *Ceratosaurus* after Madsen & Welles 2000: Pl. 1, 9, *Sinraptor dongi* after Currie & Zhao 1993: Fig. 3B, 4).
20. NEW: Apicobasal length of the largest premaxillary tooth crown: shorter than or subequal to the minimal dorsoventral height of the antero-central portion of the dentary (0); distinctly longer than the minimal dorsoventral height of the antero-central portion of the dentary (1) (*Eoraptor lunensis* after PVSJ 512, Sereno et al. 1993: Fig. 1 and Sereno, Martinez & Alcober 2012: Fig. 3 and 11, *Herrerasaurus ischigualastensis* after Sereno & Novas 1994: Fig. 1A, 1B and 2, *Tawa hallae* after Nesbitt et al. 2009: Fig. 1, *Eodromaeus murphi* after Martinez et al. 2011: Fig 1B, *Dracovenator regenti* after Yates 2005: Fig. 2 and 4, "Syntarsus" *kayentakatae* after Rowe 1989: Fig. 1, Tykoski 1998: Fig. 1 and 2, 2005: Fig. 10C, *Coelophysis bauri* after NMMNH P-50529 and P-50530, Colbert 1989: Figs. 24, 28, 29 and Ezcurra 2007: Fig. 9, Rowe et al. 2009: Fig. 82A, *Coelophysis rhodesiensis* after Raath 1977: Pl. 7, BP/1/5278 after BP/1/5278 and Yates 2005: Fig. 8, *Ceratosaurus* after Gilmore 1920: 53 and Madsen & Welles 2000: Fig. 1, 2, 13A and B, *Allosaurus fragilis* after Madsen 1976: Pl. 1, 9D, 6C, *Sinraptor dongi* after Currie & Zhao 1993: Fig. 4A + D, 11A +B).
21. Long axis of anterior most premaxillary tooth crowns: recurved (0); nearly straight (1) (modified from Ezcurra 2012: character 38; *Dilophosaurus wetherilli*, *Ceratosaurus*, "Syntarsus" *kayentakatae*, *Coelophysis bauri*, *Coelophysis rhodesiensis* after Tykoski 2005: character 97; for character history see Ezcurra 2012).
22. Premaxilla-maxilla suture: uninterrupted (0); interrupted by a subnarial foramen (1) (Tykoski 2005: character 18; *Sinraptor dongi* after Currie & Zhao 1993: 2041; for character history see Ezcurra 2012: character 43).
23. Transverse constriction between articulated premaxillae and maxillae in dorsal view: absent (0), present (1) (Ezcurra 2012: character 48; *Ceratosaurus* and *Sinraptor dongi* after Rauhut 2003: character 8, *Eustreptospondylus oxoniensis* after Smith et al. 2007: character 21; for character history see Ezcurra 2012).
24. Subnarial diastema (toothless region between premaxillary and maxillary contact): absent (0), present (1) (Ezcurra 2012: character 31; *Dracovenator regenti*, *Ceratosaurus* and *Sinraptor dongi* after Yates 2005: character 230, *Eustreptospondylus oxoniensis* after Sadleir et al. 2008: Fig. 5; for character history see Ezcurra 2012).
25. Alveolar margins of premaxilla and maxilla at premaxilla-maxilla junction: continuous, ventral margins level with each other (0); bent upwards, creating a gap in the upper tooth row (= «subnarial gap» of Welles 1984, Rauhut 2003, Yates 2005) (1), (modified from Ezcurra 2012: character 32; *Ceratosaurus* and *Sinraptor dongi* after Rauhut 2003: character 9, *Eustreptospondylus oxoniensis* after Sadleir et al. 2008: character 11 of Holtz 2000; for character history see Ezcurra 2012).
26. Anterior process of maxilla: continuous with anterodorsal border of maxilla (0); offset, prominent concave inflexion at the base of the ascending process (1) (modified from Ezcurra 2012: character 63; *Tawa hallae* after Nesbitt et al. 2009: Fig. 1, BP 15278 after BP 15278, *Coelophysis bauri*, *Coelophysis rhodesiensis*, *Zupaysaurus rougieri*, *Ceratosaurus*, *Piatnitzkysaurus floresii*, *Eustreptospondylus oxoniensis* and *Sinraptor dongi* after Rauhut 2003: character 11 and Smith et al. 2007: character 24; for character history see Ezcurra 2012).
27. Anteromedial process (= palatal process) of maxilla: short, hardly visible in lateral view (0); dorsoventrally low and anteroposteriorly long, well visible in lateral view (1); high and long, platelike, visible in lateral view (2) (modified

from Ezcurra 2012: character 96; *Ceratosaurus* after Madsen & Welles 2000: Pl. 2,10, Rauhut 2003: Fig. 10B, and Tykoski 2005: character 37, *Dilophosaurus wetherilli* after Tykoski 2005: Fig. 23B, C, 24A, character 37, *Piatnizkysaurus* after Carrano et al. 2012: Fig. 17A, Rauhut 2007: Fig. 3A and Bonaparte 1986: Fig. 6, *Sinraptor dongi* after Currie & Zhao 1993: Fig. 4B,C, and Ezcurra & Novas 2007: character 23; for character history see Ezcurra 2012).

28. Medial surface of the anteromedial process (= palatal process) of the maxilla: smooth (0); bears longitudinal ridges (1) (Ezcurra 2012: character 97; *Ceratosaurus*, *Dilophosaurus wetherilli*, "*Syntarsus*" *kayentakatae* and *Eustreptospondylus oxoniensis* after Tykoski 2005, character 38, *Sinraptor dongi* after Carrano 2012: character 15, and Currie & Zhao 1993: Fig. 4C; for character history see Ezcurra 2012).

29. Suture between the ascending process of the maxilla and the anterior process of the lacrimal: straight (0); forked (V-shaped) (1) (Ezcurra 2012: character 68; *Dilophosaurus wetherilli*, *Ceratosaurus* and *Sinraptor dongi* after Ezcurra & Novas 2007: character 27; for character history see Ezcurra 2012).

30. Ratio of dorsoventral height of maxilla at level of anterior margin of antorbital fossa to height of horizontal ramus of maxilla at level of first alveolus posterior to anterior border of internal antorbital fenestra: 1.02 (0); 1.26-1.50 (1); 1.64-1.77 (2); 2.01-2.70 (3) (Ezcurra 2012: character 58; *Panguraptor lufengensis* after You et al. 2014, Fig. 2: estimated 1.27, *Ceratosaurus* after Madsen & Welles 2000, Pl. 10: 1.34, *Eustreptospondylus oxoniensis* after Sadleir et al. 2008, Fig. 5 and Pl.1, fig. 1: estimated 2.07 – 2.29, *Piatnizkysaurus* after Rauhut 2007: Fig. 3A (~1.57), Novas 2009: Fig. 3.19E, Carrano et al. 2012: Fig. 17A (~1.7), *Sinraptor dongi* after Currie & Zhao 1993: Fig. 4B: 1.345, : 1.69; for character history see Ezcurra 2012).

31. Dorsal and ventral margins of posterior process (= horizontal process) of maxilla: taper posteriorly (0); run parallel (1); diverge posteriorly (2) (Ezcurra 2012: character 95; *Panguraptor lufengensis* after You et al. 2014: character 26; *Ceratosaurus* after Madsen & Welles 2000: Pl. 1 and 10, *Sinraptor dongi* after Currie & Zhao 1993: Fig. 3B, 4B + C; for character history see Ezcurra 2012)

32. Maxillary antorbital fossa: deep, and with sharp margins (0); shallow, margins formed by low ridges, a sharp rim may be present only in front of the premaxillary foramen (1) (Ezcurra 2012: character 79; *Panguraptor lufengensis* after You et al. 2014: Fig. 2; *Eoraptor lunensis*, *Herrerasaurus ischigualastensis* and *Ceratosaurus* after Rauhut 2003: character 12, *Eustreptospondylus oxoniensis* and *Sinraptor dongi* after Smith et al. 2007: character 25; for character history see Ezcurra 2012).

33. Extent of maxillary antorbital fossa in front of internal antorbital fenestra: extremely short, represented only by a semilunar fossa along the anterior margin of the internal antorbital fenestra (0); short (1); long, occupying the major part of the region anterior to the internal antorbital fenestra (2) (Ezcurra 2012: character 70; *Panguraptor lufengensis* after You et al. 2014: Fig. 2, *Ceratosaurus* after Madsen & Welles 2000: Plate 1; BP/1/5278 after Munyikwa & Raath 1999: 1, Yates 2005: Fig. 8 and BP/1/5278, *Eustreptospondylus oxoniensis* after Sadleir et al. 2008: Fig. 5, Pl. 1, figs. 1, 3, *Sinraptor dongi* after Currie & Zhao 1993: Fig. 3B, 4B + C; for character history see Ezcurra 2012).

34. Anterior end of maxillary antorbital fossa: posterior to external naris (0); ventral to posterior end of external naris (1) (Ezcurra 2012: character 71; *Panguraptor lufengensis* after You et al. 2014: Fig. 2; *Eustreptospondylus oxoniensis* after Sadleir et al. 2008: Fig. 5, Pl. 1, fig. 2 and Carrano et al. 2012: character 25, *Ceratosaurus*, *Sinraptor dongi*, *Piatnizkysaurus* after Carrano et al. 2012: character 25; for character history see Ezcurra 2012).

35. Anterior border of maxillary antorbital fossa: rounded or triangular (pointed) (0); squared, with angular antroventral corner and nearly straight anterior border, the quadrangular condition is the crucial state if the character shows intraspecific variation (1) (modified from Ezcurra 2012: character 74 and Tykoski 2005: character 32; *Dilophosaurus wetherilli* after Carrano et al. 2012: character 23 and Tykoski 2005: figure 13, *Sinraptor dongi* after Ezcurra & Novas 2007: character 30 and Carrano et al. 2012: character 23; for character history see Ezcurra 2012).

36. Medial wall of the maxillary antorbital fossa on the lateral surface of the horizontal process of the maxilla: does not reach the posteroventral corner of the internal antorbital fenestra (0); extends through the entire ventral border of the internal antorbital fenestra as a narrow lamina, dorsoventral depth of fossa less or equal to the depth below the antorbital fossa (1); extends along the major part of the ventral border of the internal antorbital fenestra as a broad lamina, dorsoventral depth of fossa significantly higher than depth below fossa (2) (Ezcurra 2012: character 76; *Panguraptor lufengensis* after You et al. 2014: character 25, character 317, *Ceratosaurus* and *Sinraptor dongi* after Ezcurra & Novas 2007: character 31; for character history see Ezcurra 2012).

37. Dorsoventrally compressed horizontal ridge (= alveolar ridge of Rowe 1989) above the ventral border of the maxillary antorbital fossa: absent (0); present (1) (modified from Ezcurra 2012: character 78; *Panguraptor lufengensis* after You et al. 2014: character 24, *Ceratosaurus* and *Sinraptor dongi* after Rauhut 2003: character 15, *Eustreptospondylus oxoniensis* after Smith et al. 2007: character 28; for character history see Ezcurra 2012).

38. Lateral surface of maxillary antorbital fossa at the base of the ascending process: smooth (0); with deep, large, and subcircular or oval blind pocket/s (border/s of structure/s not well-defined, in contrast to the maxillary fossa or fenestra) (1) (modified from Ezcurra 2012: character 81; *Panguraptor lufengensis* after You et al. 2014: character 318, the additional fenestra should be interpreted as a «pocket» rather than a «fenestra», H.-L. You, pers. comm. 2014, *Ceratosaurus* and *Sinraptor dongi* after Ezcurra & Novas 2007: character 35, *Eustreptospondylus oxoniensis* after Tykoski 2005: character 35; for character history see Ezcurra 2012).

39. Promaxillary foramen or fenestra in the maxillary antorbital fossa: absent (0); small depression in same anatomical position which does not perforate the maxilla (1); present, perforating the maxillary antorbital fossa (2) (Ezcurra 2012: character 85; *Ceratosaurus* after Tykoski 2005: 103, character 34, *Sinraptor dongi* after Holtz 2000: character 16,

- Eustreptospondylus oxoniensis after Sadleir et al. 2008: character 16 of Holtz 2000; for character history see Ezcurra 2012).
40. Maxillary fenestra (border of structure well-defined, in contrast to the blind pocket/s of maxilla): absent (0); present, as a fossa (1); present, as a perforation of the antorbital fossa (2) (Ezcurra 2012: character 88; "Syntarsus" kayentakatae after Tykoski 1998: Fig. 4, 2005: 22B & C and MNA V2623, holotype, Panguraptor lufengensis after You et al. 2014: 237, Fig. 2, the additional fenestra should be interpreted as a «pocket» rather than a «fenestra», H.-L. You, pers. comm. 2014, Ceratosaurus after Rauhut 2003: character 17, Eustreptospondylus oxoniensis and Sinraptor dongi after Carrano et al. 2012: character 26; for character history see Ezcurra 2012).
41. Orientation of anterior tip of maxillary alveolar margin: approximately horizontal (0); dorsally curved (1) (modified from Tykoski 2005: character 25; Tawa hallae after Nesbitt et al. 2009: Fig. 1, Eodromaeus murphi after Martinez et al. 2011: Fig. 1B, BP/1/5278 after Yates 2005: Fig. 8C and BP/1/5278, Sinraptor dongi after Currie & Zhao 1993: Fig. 4B, 4D, Eustreptospondylus oxoniensis after Sadleir et al. 2008: Pl. 1, figs. 1-4; for character history see Tykoski 2005).
42. Orientation of first maxillary tooth: First alveolus opens: ventrally (0); anteroventrally (1) (Tykoski 2005: character 26; BP/1/5278 after Yates 2005: Fig. 8A, 8C and BP/1/5278, Eustreptospondylus oxoniensis after Sadleir et al. 2008: Pl. 1, figs. 2-4 and Carrano 2012: character 13, Sinraptor dongi and Piatnitzkysaurus after Carrano et al. 2012: character 13; for character history see Tykoski 2005).
43. Maxillary tooth row caudal extension: extends behind anterior border of orbit (0); ends before or at the anterior rim of the orbit (1); completely antorbital, ends rostral to the vertical strut of the lacrimal (2) (Ezcurra 2012: character 103; Panguraptor lufengensis after You et al. 2014: character 18, Ceratosaurus and Sinraptor dongi after Ezcurra & Novas 2007: character 39; for character history see Ezcurra & Novas 2007).
44. One or more teeth of the anterior half of the maxillary tooth row with fang-like crowns: absent, all crowns are subequal or shorter than the height of the dentary immediately below them (0); present, fang-like crowns are distinctively longer than the other maxillary teeth (1) (modified from Ezcurra 2012: character 402; Panguraptor lufengensis after You et al. 2014: Fig. 2, Ceratosaurus after Gilmore 1920: Fig. 54, Pl. 17.2, 18.2, Sinraptor dongi after Currie & Zhao 1993: Fig. 3, 4, 11A, B).
45. Apicobasal height of the longest maxillary tooth crowns versus the height of the maxillary region anterior to the internal antorbital fenestra in the middle of its anteroposterior length: 35,2 to 44,54% (0); 52,94 to 81,97% (1) (Ezcurra 2012: character 403; Coelophysis rhodesiensis after QG 205, 42,68% and 30,23%, Panguraptor lufengensis after You et al. 2014: Fig. 2, estimated 54,55%, Ceratosaurus after Gilmore 1920: Fig. 54, Pl. 17.2, 18.2, 56,82%, Sinraptor dongi after Currie & Zhao 1993: Fig. 4B + D, 42.1-44.4%, Frick theropod: estimated 69,57%; for character history see Ezcurra 2012).
46. Serrations of maxillary and dentary teeth: completely absent (0); absent at the base of the mesial margin (1); present along the entire distal margin but completely absent at the mesial margin (2); present at both the entire mesial and distal margins (3) (Ezcurra 2012: character 417; Panguraptor lufengensis after You et al. 2014: character 108, Ceratosaurus after Glut 1997: figured teeth on page 270 and Gilmore 1920: 92; for character history see Ezcurra 2012).
47. Nasals in subadults or adults: unfused (0); entirely fused (1) (Ezcurra 2012: character 105; Ceratosaurus and Sinraptor dongi after Carrano et al. 2012: character 35; for character history see Ezcurra 2012).
48. Shape of nasal in dorsal view: transversally expanded posteriorly, resulting in diverging lateral margins (0); lateral margins parallel over the entire length of the nasal (1) (Ezcurra 2012: character 108; Zupaysaurus rougieri after Ezcurra 2007: 191 and Fig. 3B, Panguraptor lufengensis after You et al. 2014: 238, Ceratosaurus after Rauhut 2003: character 21 and Madsen & Welles 2000: Pl. 3B, 3D, Sinraptor dongi after Rauhut 2003: character 21 and Currie & Zhao 1993, Fig. 3A, 5 A; for character history see Ezcurra 2012).
49. Dorsal surface of the nasals: smooth (0); rugose (1) (Rauhut 2003: 18; Yates 2005: character 18; Carrano et al. 2012: character 34; Tawa hallae after Nesbitt et al. 2009: Fig. 1; Eodromaeus murphi after PVSJ 560 - 562; Cryolophosaurus ellioti after Smith et al. 2007: Fig. 6; Panguraptor lufengensis after You et al. 2014: 238, Fig. 2; BP/1/5278 after Munyikwa & Raath 1999: 1, Yates 2005: Fig. 8 and BP/1/5278).
50. Pneumatic foramen in the nasals: absent (0); present (1) (Ezcurra 2012: character 112; Ceratosaurus and Sinraptor dongi after Rauhut 2003: character 19; Panguraptor lufengensis after You et al. 2014: 238; for character history see Ezcurra 2012).
51. Lateral surface of anterior end of the nasal along the margin of the external naris: relatively flat (0); with a concave fossa (1); with laterally convex hood covering the caudal part of the external naris (2) (Ezcurra 2012: character 109; Ceratosaurus and Sinraptor dongi after Smith et al. 2007: character 41; for character history see Ezcurra 2012).
52. Dorsal extent of antorbital fossa: dorsal rim of antorbital fossa below nasal suture, or formed by this suture (0); antorbital fossa extending onto the lateroventral side of the nasals (1) (Ezcurra 2012: character 82; Ceratosaurus and Sinraptor dongi after Rauhut 2003: character 20 and Currie & Zhao 1993: 2045; for character history see Ezcurra 2012).
53. Nasal and lacrimal with pronounced dorsolateral margins or crests: absent (0); arranged as low and laterally projected «crests» slightly extending over the maxillae (1); arranged as a well-developed dorsally projected pair of parasagittal crests (2) (modified from Ezcurra 2012: character 118; Ceratosaurus and Sinraptor dongi after Ezcurra & Novas 2007: character 44; for character history see Ezcurra 2012).
54. Nasal with a small posterolateral process that envelops part of the anterior ramus of the lacrimal: absent (0); present (1) (Ezcurra 2012: character 115; Coelophysis bauri after Smith et al. 2007: character 45, AMNH 7241 and CM 31374,

Ceratosaurus after Martinez et al. 2011: character 19 and Madsen & Welles 2000: Pl. 3B, Sinraptor dongi after Smith et al. 2007: character 45; for character history see Ezcurra 2012).

55. Shape of the posterior suture of the nasals: medial portion subequal or extends further posteriorly than the lateral parts (= straight, respectively convex) (0); lateral portions extend further posteriorly than the medial part (= concave) (1) (Ezcurra 2012: character 116; Cryolophosaurus ellioti after Smith et al. 2007: Fig. 6, Panguraptor lufengensis after You et al. 2014: character 31, Ceratosaurus after Madsen & Welles 2000: Pl. 3B and 3D, Sinraptor dongi after Currie & Zhao 1993: Fig. 3A and 5; for character history see Ezcurra 2012).

56. Position of the posteriormost nasal-frontal contact in relation to the highest point of the orbit: anterior (0); above highest point (1) (Ezcurra 2012: character 123; Ceratosaurus after Madsen & Welles 2000: Pl. 1, Sinraptor dongi after Currie & Zhao 1993: Fig. 3A; for character history see Ezcurra 2012).

57. Lacrimal shape: block-shaped or roughly triangular in lateral view (0); with well defined inverted L-shape in lateral view (1) (modified from Ezcurra 2012: character 124; Panguraptor lufengensis after You et al. 2014: Fig. 1 and 2, character 35, Ceratosaurus after Rauhut 2003: character 28, Eustreptospondylus oxoniensis after Sadleir et al. 2008: 11, Fig. 5, Pl. 1, figs. 5, 6, Sinraptor dongi after Currie & Zhao 1993: Fig. 3B and 6D,E and Rauhut 2003: character 28; for character history see Ezcurra 2012).

58. Lacrimal antorbital pneumatic recess into central body of lacrimal: absent (0); present (1) (modified from Ezcurra 2012: character 127; Ceratosaurus after Rauhut 2003: character 31, Eustreptospondylus oxoniensis after Sadleir et al. 2008: 11, Fig. 5, Pl. 1, fig. 5, character 33, Sinraptor dongi after Currie & Zhao 1993: 2045, Fig. 6E and Rauhut 2003: character 31; for character history see Ezcurra 2012).

59. Anterior ramus of lacrimal: strongly reduced (0); slightly shorter or nearly equal to the height of the vertical ramus (1); equal or longer than the height of the vertical ramus (2) (Ezcurra 2012: character 132, "Syntarsus" kayentakatae after Tykoski 2005: character 55, Ceratosaurus after Madsen & Welles 2000: Pl. 1 and 2, Eustreptospondylus oxoniensis after Sadleir et al. 2008: 11 and Carrano et al. 2012: character 50, Sinraptor dongi after Currie & Zhao 1993: 2045, Fig. 6D-E; for character history see Ezcurra 2012).

60. Lacrimal horn: absent (0); present (1) (modified from Ezcurra 2012: character 131; Panguraptor lufengensis after You et al. 2014: character 38, Eustreptospondylus oxoniensis after Sadleir et al. 2008: Pl. 1, figs. 5, 6, Ceratosaurus and Sinraptor dongi after Smith et al. 2007: character 52; for character history see Ezcurra 2012).

61. Lateral lamina of lacrimal: covering most of the bone (0); restricted to the caudal margin of the vertical ramus and not interrupting the lacrimal antorbital fossa (1); strongly expanded anteriorly and partly covering the internal antorbital fenestra (2) (modified from Ezcurra 2012: character 136; Panguraptor lufengensis after You et al. 2014: character 319, Ceratosaurus after Madsen & Welles 2000: Pl. 1 and 2, Eustreptospondylus oxoniensis after Sadleir et al. 2008: Pl. 1, fig. 5 and Carrano et al. 2012: character 44, Sinraptor dongi after Carrano et al. 2012: character 44; for character history see Ezcurra 2012).

62. Orientation of long axis of vertical ramus of lacrimal: strongly sloping anterodorsally (0); nearly vertical (1); strongly sloping posterodorsally (2) (Ezcurra 2012: character 141; Panguraptor lufengensis after You et al. 2014: character 37, Ceratosaurus, Eustreptospondylus oxoniensis and Sinraptor dongi after Smith et al. 2007: character 60; for character history see Ezcurra 2012).

63. Vertical ramus of lacrimal: expanded ventrally, distal end nearly twice as wide anteroposteriorly as proximal base of process (0); roughly the same width throughout the whole ramus or with constriction in the middle of the shaft, but distal end less than 1.75 the width of proximal base (1) (modified from Ezcurra 2012: character 138; Coelophysis rhodesiensis after QG1, Ceratosaurus after Madsen & Welles 2000: Pl. 1 and 2, Eustreptospondylus oxoniensis after Sadleir et al. 2008: Pl. 1, figs.5, 6, Sinraptor dongi after Currie & Zhao 1993: 2045, Fig. 6D-E; for character history see Ezcurra 2012).

64. Lateral longitudinal ridge traversing rostral and caudal processes of jugal: absent (0); present (1) (Ezcurra 2012: character 149; Liliensternus liliensterni, Ceratosaurus after Tykoski 2005: character 71, Panguraptor lufengensis after You et al. 2014: Fig. 1 and 2, character 57, Sinraptor dongi after Currie & Zhao 1993: Fig. 6F; for character history see Ezcurra 2012).

65. Anterior process of jugal: more or less continuously tapering anteriorly (0); bluntly squared anteriorly (1); well expanded anteriorly (2) (Ezcurra 2012: character 150; Ceratosaurus after Rauhut 2003: character 23, Sinraptor dongi after Currie & Zhao 1993: Fig. 6F-G; for character history see Ezcurra 2012).

66. NEW: Sublacrimal part of jugal: dorsal margin of anterior process of jugal straight (0); dorsal margin of anterior process of jugal with a bulge forming a distinct initial lacrimal process (1) (Eoraptor lunensis after PVSJ 512 and Sereno et al. 1993: Fig. 1, Sereno, Martinez & Alcober 2012: Fig. 3A, 11 and Tykoski 2005: Fig. 29B, Herrerasaurus ischigualastensis after Sereno & Novas 1994: Fig 1A, 1B, 2, 7A, 8A and 9, Tawa hallae after Nesbitt et al. 2009: Fig. 1, Eodromaeus murphi after Martinez et al. 2011: Fig. 1B, Zupaysaurus rougieri after Arcucci & Coria 2003: 2A, 2B and 2E, Ezcurra & Novas 2007: Fig. 1 and 14B, Dilophosaurus wetherilli after UCMP 37302, Welles 1984: Fig. 4 and Tykoski 2005: Fig. 20, Cryolophosaurus ellioti after Smith et al. 2007: Fig. 4 and 5, Liliensternus liliensterni after MB.R.2175.1.5 and Huene 1934: Pl. 13 Figs. 5, 12 and 13, "Syntarsus" kayentakatae after Tykoski 1998: Fig. 1, 2 and Tykoski 2005: Fig. 29C, Coelophysis bauri after CM 31374, CM C-3-82 and NMMNH P-42200, Coelophysis rhodesiensis after Raath 1977: Fig. 4u and Bristowe 2004: Fig. 6, 16 and 17, Panguraptor lufengensis after You et al. 2014: Fig. 1 and 2, Ceratosaurus after Gilmore 1920: Pl. 17.1, 18.2 and Madsen & Welles 2000: Pl. 1, 12G, 12H, Allosaurus fragilis after Madsen 1976: Pl. 4D, 4E and Ezcurra & Novas 2007: Fig. 14D, Sinraptor dongi after Currie & Zhao 1993: Fig. 6F-G).

67. Contribution of the anterior process of the jugal to the internal antorbital fenestra: entirely excluded from the margin of the fenestra (0); contributes to the posteroventral margin of the fenestra (1) (modified from Ezcurra 2012: character 151; Panguraptor lufengensis after You et al. 2014: character 53, Ceratosaurus, Sinraptor dongi after Currie & Zhao 1993: 2048, Fig. 3B and Rauhut 2003: character 24; for character history see Ezcurra 2012).
68. Minimal height of the jugal below the orbit versus maximal height of the orbit: 7,55 - 21,67% (0); 26,98 - 36,67% (1); 49,06 - 50,00% (2) (Ezcurra 2012: character 155; Panguraptor lufengensis after You et al. 2014: Fig. 2, estimated 6,25%, Ceratosaurus after Madsen & Welles 2000: Pl. 1, ca. 17,31%, Sinraptor dongi after Currie & Zhao 1993: Fig. 3B, ca. 14.5%, Frick theropod: ca. 14,5%; for character history see Ezcurra 2012).
69. Posterior process (= quadratojugal process) of jugal: acute, undivided (0); forked, both prongs of nearly equal length (1); forked, dorsal prong longer than ventral prong (2); forked, ventral prong longer than dorsal prong (3) (Ezcurra 2012: character 159; Panguraptor lufengensis after You et al. 2014: Fig. 2, character 54 (extend), Ceratosaurus after Tykoski 2005: character 70, Sinraptor dongi after Currie & Zhao 1993: Fig. 6F-G; for character history see Ezcurra 2012).
70. Ventral border of infratemporal fenestra: mostly constituted by the jugal or equal participation of both jugal and quadratojugal (0); mostly constituted by the quadratojugal (1) (Ezcurra 2012: character 202; Coelophysis bauri after CM 31374, Panguraptor lufengensis after You et al. 2014: Fig. 1 and 2, Ceratosaurus and Sinraptor dongi after Ezcurra & Novas 2007: character 58; for character history see Ezcurra 2012).
71. Angle between ascending process and posterior process of jugal: right or obtuse (0); acute, with a posterodorsally oriented ascending process (1) (Ezcurra 2012: character 158; Panguraptor lufengensis after You et al. 2014: character 321, Ceratosaurus after Madsen & Welles 2000: Pl. 1, Sinraptor dongi after Currie & Zhao 1993: Fig. 6F-G; for character history see Ezcurra 2012).
72. Ventral margin of jugal posterior to anterior process: more or less straight to gently convex (0); slightly sigmoidal (1); strongly convex (2) (modified from Ezcurra 2012: character 156; Panguraptor lufengensis after You et al. 2014: Fig. 1 and 2, Cryolophosaurus ellioti after Smith et al. 2007: Fig. 5, Sinraptor dongi after Currie & Zhao 1993: Fig. 6F-G; for character history see Ezcurra 2012).
73. Shape of orbit: subcircular (0); elongated, with or without ventral constriction (1) (modified from Ezcurra 2012: character 161; Panguraptor lufengensis after You et al. 2014: 237, Fig. 1 and 2, character 89, Ceratosaurus Madsen & Welles 2000: Pl. 1, 2 and Gilmore 1920: Pl. 17.2, 18.2, Zupaysaurus rougieri, Eustreptospondylus oxoniensis and Sinraptor dongi after Smith et al. 2007: character 1; for character history see Ezcurra 2012).
74. Horizontal diameter of orbit in subadults or adults: subequal or longer than the length of the internal antorbital fenestra (0); shorter than the length of the internal antorbital fenestra (1) (Ezcurra 2012: character 162; Eoraptor lunensis after Sereno et al. 1993: Fig. 1 and Sereno, Martinez & Alcober 2012: Fig. 3A and 11, Panguraptor lufengensis after You et al. 2014: 237, Fig. 1 and 2, Tab. 1, Ceratosaurus Madsen & Welles 2000: Pl. 1 and 2, Sinraptor dongi after Currie & Zhao 1993: Fig. 3B; for character history see Ezcurra 2012).
75. Prefrontal: considerably participating in the anterodorsal rim of the orbit in lateral view (0); slightly participating in the anterodorsal rim of the orbit in lateral view, being displaced posteriorly and/or medially (1); not participating in the anterior margin of the orbit in lateral view, being displaced posteriorly and/or medially (2) (modified from Ezcurra 2012: character 165; Panguraptor lufengensis after You et al. 2014: 237, Fig. 1 and 2, Ceratosaurus and Sinraptor dongi after Rauhut 2003: character 34, and Currie & Zhao 1993: Fig. 3B; for character history see Ezcurra 2012).
76. Prefrontal posterior process: elongate, prefrontal total length equal to anteroposterior orbit diameter in subadults or adults (0); short (1); absent (2) (Ezcurra 2012: character 167; Ceratosaurus after Madsen & Welles 2000: Pl. 4A, D, E and Sanders & Smith 2005: 611, Sinraptor dongi after Currie & Zhao 1993: Fig. 3B, 6A-C; for character history see Ezcurra 2012).
77. Paired frontals shape: subrectangular, longer than wide (0); squared, as wide as long or wider than long (1) (Ezcurra 2012: character 177; Ceratosaurus after Rauhut 2003: character 36 & Smith et al. 2007: character 63, Eustreptospondylus oxoniensis after Sadleir et al. 2008: Fig. 7, Pl. 2, figs.1, 2 and Smith et al. 2007: character 63, Piatnitzkisaurus after Novas 2009: 117 & Smith et al. 2007: character 63, Sinraptor dongi after Currie & Zhao 1993: Fig. 3A & Smith et al. 2007: character 63; for character history see Ezcurra 2012).
78. Contribution of the frontal in the dorsal margin of the orbit: present (0); absent, excluded by the contact between lacrimal and postorbital (1) (modified from Ezcurra 2012: character 178; Panguraptor lufengensis after You et al. 2014: Fig. 1 and 2, Ceratosaurus after Sanders & Smith 2005: 611, Madsen & Welles 2000: Pl.4D and Gilmore 1920: Pl. 18.1, Eustreptospondylus oxoniensis after Sadleir et al. 2008: 12, Fig. 5, 7, Sinraptor dongi and Piatnitzkisaurus after Carrano et al. 2012: character 67, Rauhut 2004: 1116, Rauhut 2003: character 39; for character history see Ezcurra 2012).
79. Anterior edge of associated frontals: rectangular (0); triangular, wedge-shaped (1) (Ezcurra 2012: character 179, Ceratosaurus and Eustreptospondylus oxoniensis after Smith et al. 2007: character 62; for character history see Ezcurra 2012).
80. Participation of frontal in supratemporal fossa: absent (0); present (1) (modified from Ezcurra 2012: character 187; Panguraptor lufengensis after You et al. 2014: Fig. 1 and 2, Ceratosaurus after Madsen & Welles 2000: 6, Eustreptospondylus oxoniensis after Sadleir et al. 2008: Fig. 7, Pl. 2, fig.1, Sinraptor dongi after Currie & Zhao 1993: Fig. 3A, 7D; for character history see Ezcurra 2012).
81. Frontals and parietals in subadults and adults: separate (0); fused (1) (Ezcurra 2012: character 190; Panguraptor lufengensis after You et al. 2014: Fig. 1 and 2, Ceratosaurus after Madsen & Welles 2000: 6, Sinraptor dongi after Currie & Zhao 1993: 2045, Fig. 3A and 7D; for character history see Ezcurra 2012).

82. Medial suture between parietals: present over the whole length of the bones (0); partially closed (1); absent, parietals fused at midline (2) (Ezcurra 2012: character 242; *Ceratosaurus* after Madsen & Welles 2000: 6; for character history see Ezcurra 2012).
83. Supratemporal fossae: separated by a horizontal plate formed by the parietals (0); contact each other posteriorly, but separated anteriorly by an anteriorly widening triangular plate formed by the parietals (1) (Ezcurra 2012: character 226; *Panguraptor lufengensis* after You et al. 2014: Fig. 1 and 2, character 48, *Ceratosaurus* and *Sinraptor dongi* after Rauhut 2003: character 43 (supratemporal fenestrae); for character history see Ezcurra 2012).
84. NEW: Participation of parietal in supratemporal fossa: absent (0); present, along the entire lateral margin (1); present, but restricted to the posterior half of the bone (2) (*Herrerasaurus ischigualastensis* after Sereno & Novas 1994: Fig. 4, 7B, 8B, *Zupaysaurus rougieri* after Ezcurra 2007: Fig. 6, *Cryolophosaurus ellioti* after Smith et al. 2007: Fig. 6, "*Syntarsus*" *kayentakatae* after MNA V2623, Rowe 1989: Fig. 1C, D and Tykoski 1998: Fig. 5, *Coelophysis bauri* after CM 31374 and Colbert 1989: Fig. 41, 42A, *Coelophysis rhodesiensis* after QG194, Raath 1977: Fig. 3b and Colbert 1989: Fig. 42B, *Ceratosaurus* after BYUVP 12893 and Madsen & Welles 2000: 6, Pl. 4A, D, *Allosaurus fragilis* after Madsen 1976: Pl. 2A, *Eustreptospondylus oxoniensis* after Sadleir et al. 2008: 13).
85. Posterior margin of articulated parietals in dorsal view: forming an obtuse angled «V» (0); forming an acute angled «V» (1). (Ezcurra 2012: character 248; *Ceratosaurus* after Gilmore 1920: Pl. 18.1, *Sinraptor dongi* after Currie & Zhao 1993: 2045, Fig. 3A and 7D; for character history see Ezcurra 2012).
86. Tongue-like process of parietals overlapping the supraoccipital knob: absent (0); present (1) (Ezcurra 2012: character 246; *Ceratosaurus* and *Sinraptor dongi* after Smith et al. 2007: character 77; for character history see Ezcurra 2012).
87. Anterior process of postorbital: sharply upturned (0); projected anteriorly, at about the same level as posterior process, resulting in a «T»-shaped postorbital (1) (Ezcurra 2012: character 204; *Panguraptor lufengensis* after You et al. 2014: Fig. 2, *Ceratosaurus* after Madsen & Welles 2000: Pl. 1, 2, 5A to C, *Eustreptospondylus oxoniensis* after Sadleir et al. 2008: 14, Pl. 2, fig. 5, 6 Tykoski 2006: character 66, *Sinraptor dongi* after Currie & Zhao 1993: 2045, Fig. 8 A-B; for character history see Ezcurra 2012).
88. Length of anterior postorbital process: longer than or as long as posterior process of postorbital (0); shorter than posterior process of postorbital (1) (Ezcurra 2012: character 206; *Panguraptor lufengensis* after You et al. 2014: Fig. 2; *Ceratosaurus* after Madsen & Welles 2000: Pl. 1, 2, 5B and D, *Eustreptospondylus oxoniensis* after Sadleir et al. 2008: Pl. 2, fig. 5, 6, *Sinraptor dongi* after Currie & Zhao 1993: 2045, Fig. 8 A-B; for character history see Ezcurra 2012).
89. Anterior end of anterior process of postorbital: tapering (0); rounded (1) (Ezcurra 2012: character 207; *Panguraptor lufengensis* after You et al. 2014: Fig. 2; *Ceratosaurus* after Madsen & Welles 2000: Pl. 1, 2, 5B and D, *Eustreptospondylus oxoniensis* after Sadleir et al. 2008: Pl. 2, fig. 5, 6, *Sinraptor dongi* after Currie & Zhao 1993: 2045, Fig. 8 A-B; for character history see Ezcurra 2012).
90. Orbit border confined by postorbital: continuously concave (0); with a convexity at the base of the anterior process (1) (Ezcurra 2012: character 213; *Panguraptor lufengensis* after You et al. 2014: Fig. 1 and 2, *Ceratosaurus* after Madsen & Welles 2000: Pl. 1, 2, 5B and D, *Eustreptospondylus oxoniensis* after Sadleir et al. 2008: Fig. 5, Pl. 2, fig. 5, *Sinraptor dongi* after Currie & Zhao 1993: 2045, Fig. 8 AB; for character history see Ezcurra 2012).
91. Participation of postorbital in supratemporal fossa: present, restricted to anterior process (0); present, restricted to posterior process (1); present, both processes participate (2); absent (3). (Ezcurra 2012: character 225; *Panguraptor lufengensis* after You et al. 2014: 239, Fig. 1 and 2, extended character 324, *Ceratosaurus* after Madsen & Welles 2000: Pl. 2 and 5D, Carrano et al. 2012: character 60, *Eustreptospondylus oxoniensis* and *Sinraptor dongi* after Carrano et al. 2012: character 60; for character history see Ezcurra 2012).
92. Depression above ventral process (= jugal process) of postorbital: absent (0); present (1) (Ezcurra 2012: character 212; *Ceratosaurus* after Madsen & Welles 2000: Pl. 1, 2, 5B and D, *Eustreptospondylus oxoniensis* after Sadleir et al. 2008: Pl. 2, fig. 5, *Sinraptor dongi* after Currie & Zhao 1993: Fig. 8B; for character history see Ezcurra 2012).
93. Posterior margin of ventral process (= jugal process) of postorbital: convex (0); slightly concave or straight (1) (Ezcurra 2012: character 214; *Panguraptor lufengensis* after You et al. 2014: Fig. 1 and 2, *Ceratosaurus* after Madsen & Welles 2000: Pl. 1, 2, 5B and D, *Eustreptospondylus oxoniensis* after Sadleir et al. 2008: Pl. 2, figs. 5, 6, *Sinraptor dongi* after Currie & Zhao 1993: Fig. 8A-B; for character history see Ezcurra 2012).
94. Postorbital bar: jugal and postorbital participate in nearly equal proportions (0); mostly composed by the postorbital (1) (Nesbitt et al. 2009: character 51; *Coelophysis rhodesiensis* after Raath 1977: Fig. 3a and Colbert 1989: Fig. 40A, *Panguraptor lufengensis* after You et al. 2014: character 5, 1, *Sinraptor dongi* after Currie & Zhao 1993: Fig. 3; for character history see Nesbitt et al. 2009).
95. Orientation of the upper temporal bar formed by the posterior process of the postorbital and the anterior process of the squamosal: horizontally (0); strongly posteroventrally oriented (1) (modified from Ezcurra 2012: character 220; "*Syntarsus*" *kayentakatae* after Tykoski 1998: Fig. 1, 2 and 6, *Panguraptor lufengensis* after You et al. 2014: Fig. 1 and 2, *Ceratosaurus* after Madsen & Welles 2000: Pl. 1, 2, 5B and D, *Eustreptospondylus oxoniensis* after Sadleir et al. 2008: Fig. 5, *Sinraptor dongi* after Currie & Zhao 1993: Fig. 3; for character history see Ezcurra 2012).
96. Orientation of the ventral process of the squamosal in regard to the anteroposterior axis of the postorbital portion of the cranium: mainly posteroventrally (0); mainly vertically (1); mainly anteroventrally (2) (Ezcurra 2012: character 231; *Panguraptor lufengensis* after You et al. 2014: Fig. 2, *Ceratosaurus* after BYUVP 12893 and Madsen & Welles 2000: Pl.

- 1, 2, 5E and F, *Eustreptospondylus oxoniensis* after Sadleir et al. 2008: Fig. 5, Pl. 2, figs. 7, 8, *Sinraptor dongi* after Currie & Zhao 1993: Fig. 3, 8D and F; for character history see Ezcurra 2012).
97. Ventral process of squamosal: tapering distally, distal end pointed or rounded (0); quadrangular, keeps consistent depth (1); expanded distally (2) (Ezcurra 2012: character 229; *Panguraptor lufengensis* after You et al. 2014: character 322; *Ceratosaurus*, *Sinraptor dongi* after Rauhut 2003: character 45, Currie & Zhao 1993: Fig. 3, 8D and F, *Eustreptospondylus oxoniensis* after Sadleir et al. 2008: Fig. 5, Pl. 2, figs. 7, 8; for character history see Ezcurra 2012).
98. Maximal width of squamosal ventral process versus its maximal length: 0.11 to 0.33 (0); 0.41 to 0.60 (1); 0.77 to 1.00 (2) (Ezcurra 2012: character 228; *Panguraptor lufengensis* after You et al. 2014: character 47, *Ceratosaurus* after Rauhut 2003: Text-Fig. 7C and Henderson 1998: Fig. 1, *Sinraptor dongi* after Currie & Zhao 1993: Fig. 8D and F: 0.43 to 0.486, Frick theropod: ≤ 0.36 , estimated; for character history see Ezcurra 2012).
99. Posterior process of the squamosal: short, does not extend posterior to the quadrate head (0); long, does extend posterior to the quadrate head but is shorter than the anterior process of the squamosal (1); extends far posteriorly and is longer than the anterior process of the squamosal (2) (Ezcurra 2012: character 236; *Ceratosaurus* after BYUVP 12893 and Madsen & Welles 2000: Pl. 1, 2, 5E and F, *Sinraptor dongi* after Currie & Zhao 1993: Fig. 3B, 8D and F ; for character history see Ezcurra 2012).
100. Squamosal-quadratojugal contact: at tips (0); broad (1); absent (2) (Ezcurra 2012: character 235; *Panguraptor lufengensis* after You et al. 2014: character 323, *Ceratosaurus* after Rauhut 2003: character 46, Text-Fig. 7C and Henderson 1998 and Fig. 1, *Sinraptor dongi* after Carrano et al. 2012: character 75; for character history see Ezcurra 2012).
101. Anteroposterior length of supratemporal fenestra in respect to anteroposterior maximal breadth of infratemporal fenestra: shorter (0); longer (1) (Ezcurra 2012: character 194; *Ceratosaurus* after USMN 4735, *Sinraptor dongi* after Currie & Zhao 1993: Fig. 3A and B; for character history see Ezcurra 2012).
102. Shape of the posterior margin of the infratemporal fenestra, respectively participation of the ventral process of squamosal and the dorsal process of quadratojugal in the posterior margin: subvertical or largely convex anteriorly (0); ventral process of squamosal distinctly projecting towards the infratemporal fenestra (1); both processes are orientated anteriorly forming a triangular projection towards the infratemporal fenestra (2); triangular projection completely divides the infratemporal fenestra into two openings (3) (Ezcurra 2012: character 201; *Panguraptor lufengensis* after You et al. 2014: Fig. 1 and 2, *Ceratosaurus* after BYUVP 12893 and Madsen & Welles 2000: Pl. 5E, F, 11A, *Sinraptor dongi* after Currie & Zhao 1993: Fig. 3B; for character history see Ezcurra 2012).
103. Shape of infratemporal fenestra: dorsal half nearly as wide anteroposteriorly as ventral half (0); dorsal half much narrower anteroposteriorly than ventral half (1) (Ezcurra 2012: character 198; *Panguraptor lufengensis* after You et al. 2014: 237, Fig. 2, *Ceratosaurus* after Madsen & Welles 2000: Pl. 1, *Sinraptor dongi* after Currie & Zhao 1993: Fig. 3 B; for character history see Ezcurra 2012).
104. Maximal anteroposterior width of the ventral half of the infratemporal fenestra in respect to the maximal anteroposterior width of the orbit in subadults and adults: 0.31 to 0.54 (0); 0.67 to 0.77 (1); 0.98 to 1.21 (2) (Ezcurra 2012: character 197; *Panguraptor lufengensis* after You et al. 2014: Tab. 1, ratio 0.77, *Ceratosaurus* after Madsen & Welles 2000: Pl. 1, value 1.0, *Sinraptor dongi* after Currie & Zhao 1993: estimated from Fig. 3B, Frick theropod: estimated < 0.55 ; for character history see Ezcurra 2012).
105. Position of the infratemporal fenestra: entirely posterior to or approximately at same level as the posterior border of orbit (0); partially below orbit (1) (Ezcurra 2012: character 199; *Panguraptor lufengensis* after You et al. 2014: Fig. 1 and 2, *Ceratosaurus* after Madsen & Welles 2000: Pl. 1, *Sinraptor dongi* after Currie & Zhao 1993: Fig. 3B; for character history see Ezcurra 2012).
106. Quadratojugal: hook-shaped, without posterior process (0); inverted T-shaped, with a posterior process (1) (Ezcurra 2012: character 252; *Cryolophosaurus ellioti* after Smith et al. 2007: character 84; *Panguraptor lufengensis* after You et al. 2014: Fig. 1 and 2, *Ceratosaurus* and *Sinraptor dongi* after Rauhut 2003: character 47; for character history see Ezcurra 2012).
107. Quadratojugal dorsal process: longer than the anterior process (0); same length as or shorter than anterior process (1) (Ezcurra 2012: character 250; *Panguraptor lufengensis* after You et al. 2014: Fig. 1 and 2, *Ceratosaurus* after Madsen & Welles 2000: Pl. 11A, *Sinraptor dongi* after Currie & Zhao 1993: Fig. 3B; for character history see Ezcurra 2012).
108. Anteroposterior width of dorsal process of quadratojugal: narrow, similar to the anterior process (0); broad (1) (Ezcurra 2012: character 251; *Ceratosaurus* after Madsen & Welles 2000: Pl. 11A and Smith et al. 2007: character 83, *Dilophosaurus wetherilli* after UCMP 37302, *Zupaysaurus rougieri* after PULR 076; for character history see Ezcurra 2012).
109. Angle between anterior process and dorsal process of quadratojugal: 51 to 57° (0); 63 to 66° (1); 76 to 83° (2); 143 to 149° (3) (Ezcurra 2012: character 253; *Panguraptor lufengensis* after You et al. 2014: Fig. 2, estimated 72° to 77°, *Ceratosaurus*: 42°, after Madsen & Welles 2000: Pl. 11A, *Sinraptor dongi* 76° estimated after reconstruction of Currie & Zhao 1993: Fig. 3B, Swiss theropod: 66°; for character history see Ezcurra 2012).
110. Anterior most extension of articulation between jugal and quadratojugal: well posterior to the posterior margin of the dorsal process of the jugal (0); at the same level or anterior to the posterior margin of the dorsal process of the jugal (1) (Ezcurra 2012: character 258; *Panguraptor lufengensis* after You et al. 2014: character 52, *Ceratosaurus* after Madsen & Welles 2000: Pl. 12H, *Sinraptor dongi* after Currie & Zhao 1993: Fig. 3B; for character history see Ezcurra 2012).

111. Quadratojugal fused to quadrate in subadults and adults: absent (0); present, at least partially (1) (Ezcurra 2012: character 255; Panguraptor lufengensis after You et al. 2014: Fig. 2, Ceratosaurus after Nesbitt et al. 2009: character 52, Sinraptor dongi after Smith et al. 2007: character 85; for character history see Ezcurra 2012).
112. Quadrate foramen: developed as a distinct opening between the quadrate and quadratojugal (0); almost entirely enclosed in the quadrate (1); absent (2) (Ezcurra 2012: character 265; Ceratosaurus, Sinraptor dongi and Liliiensternus liliiensterni after Rauhut 2003: character 49, Eustreptospondylus oxoniensis after Carrano et al. 2012: character 81; for character history see Ezcurra 2012).
113. NEW: Lateral ala of quadrate: narrow and of more or less continuous anteroposterior width over its whole dorsoventral extension (0); well expanded anteriorly in its dorsal half forming a wing-like structure (1) (Eoraptor lunensis after PVSJ 512 and Sereno et al. 1993: Fig. 1 and Sereno, Martinez & Alcober 2012: 3A and 26, Herrerasaurus ischigualastensis after PVSJ 407 and Sereno & Novas 1994: Fig. 8C, Tawa hallae after Nesbitt et al. 2009: Fig. 1, Eodromaeus murphi after Martinez et al. 2011: Fig. 1B, Zupaysaurus rougieri after PULR 076, Arcucci & Coria 2003: Fig. 2 and Ezcurra 2007: Fig. 1, Dilophosaurus wetherilli after UCMP 37302 and Welles 1984: Fig. 5, Cryolophosaurus ellioti after Smith et al. 2007: Fig. 4A and B, 9A and B, 10A and B, Liliiensternus liliiensterni after MB.R.2175.1.13, MB.R.2175.1.14 and Huene 1934: Pl. 13 Fig. 8a to 8d, "Syntarsus" kayentakatae after MNA V2623, Tykoski 1998: Fig. 5 and Tykoski 2005: Fig. 31, Coelophysis bauri after CM 31374, Coelophysis rhodesiensis after Raath 1977: Fig. 4j and Bristowe 2004: Fig. 20, Panguraptor lufengensis after You et al. 2014: Fig. 2, Ceratosaurus after Madsen & Welles 2000: Pl. 3F and H, Allosaurus fragilis after Madsen 1976: Pl. 3D to F, Eustreptospondylus oxoniensis after Sadleir et al. 2008: Fig. 5, Pl. 2, fig. 10, Sinraptor dongi after Currie & Zhao 1993: Fig. 8G; for character history see Ezcurra 2012).
114. NEW: Pterygoid ala (= medial ala) of quadrate: anterior margin more or less continuously convex, maximal anteroposterior width in the mid-portion of the wing (symmetrically shaped) (0); anterior margin discontinuously convex, maximal anteroposterior width in the dorsal portion of the wing (asymmetrically shaped, shortest side of «triangle» dorsally orientated) (1); anterior margin discontinuously convex, maximal anteroposterior width in the ventral portion of the wing (asymmetrically shaped, shortest side of «triangle» ventrally orientated) (2) (Herrerasaurus ischigualastensis after PVSJ 407 and Sereno & Novas 1994: Fig. 8C, Tawa hallae after Nesbitt et al. 2009: Fig. 1, Eodromaeus murphi after Martinez et al. 2011: Fig. 1B, Zupaysaurus rougieri after PULR 076, Arcucci & Coria 2003: Fig. 2 and Ezcurra 2007: Fig. 1, Dilophosaurus wetherilli after UCMP 37302 and Welles 1984: Fig. 5, Cryolophosaurus ellioti after Smith et al. 2007: Fig. 4A and B, 9A and B, 10A and B, Liliiensternus liliiensterni after MB.R.2175.1.13, MB.R.2175.1.14 and Huene 1934: Pl. 13 Fig. 8a to 8d, "Syntarsus" kayentakatae after MNA V2623, Tykoski 1998: Fig. 5 and Tykoski 2005: Fig. 31, Coelophysis bauri after CM C-3-82 and Ezcurra 2007: Fig. 9, Coelophysis rhodesiensis after Raath 1977: Fig. 4j and Bristowe 2004: Fig. 20, Ceratosaurus after Madsen & Welles 2000: Pl. 3F and H, Allosaurus fragilis after Madsen 1976: Pl. 3D to F, Eustreptospondylus oxoniensis after Sadleir et al. 2008: Fig. 5, Pl. 2, fig. 10, Sinraptor dongi after Currie & Zhao 1993: Fig. 8G, I).
115. Posterior curvature of the proximal end of quadrate: absent or slight, proximal half of quadrate almost straight (0); present, with quadrate head caudodorsally oriented (1) (Ezcurra & Novas 2007: character 76; Tawa hallae after Nesbitt et al. 2009: Fig. 1, Eodromaeus murphi after Martinez et al. 2011: Fig. 1B, Cryolophosaurus ellioti after Smith et al. 2007: Fig. 4A and B, 9A and B, Panguraptor lufengensis after You et al. 2014: Fig. 2, Eustreptospondylus oxoniensis after Sadleir et al. 2008: Fig. 5, Pl. 2, fig. 10, 11; for character history see Ezcurra & Novas 2007).
116. Form of articulation surface of distal condyles of quadrate: two convex condyles of subequal size and separated by a sulcus (0); two convex condyles separated by a sulcus, medial larger than lateral one (1); two convex condyles separated by a sulcus, lateral larger than medial one (2); one single convex condyle (3) (Ezcurra 2012: character 269; Ceratosaurus after Madsen & Welles 2000: Pl. 3E to H, Eustreptospondylus oxoniensis after Sadleir et al. 2008: 15, Pl. 2, fig. 13, Sinraptor dongi after Currie & Zhao 1993: Fig. 3D and 7A; for character history see Ezcurra 2012).
117. Articulation of the mandible: approximately straight below or anterior to the quadrate head (0); significantly posterior to the quadrate head (1) (Ezcurra 2012: character 272; Ceratosaurus and Sinraptor dongi after Rauhut 2003: character 51; for character history see Ezcurra 2012).
118. Shape of the supraoccipital: at least as high as wide (0); wider than high (1) (Ezcurra 2012: character 277; Sinraptor dongi after Currie & Zhao 1993: Fig. 7A; for character history see Ezcurra 2012).
119. Medial vertical crest of the supraoccipital: absent (0); present (1) (modified from Ezcurra 2012: character 280; Ceratosaurus after BYUVP 12893, Sinraptor dongi after Currie & Zhao 1993: 2049, Fig. 3D and 7A; for character history see Ezcurra 2012).
120. Participation of the supraoccipital in the dorsal margin of the foramen magnum: present (0); absent (1) (modified from Ezcurra 2012: character 283; Ceratosaurus after BYUVP 12893, Sinraptor dongi after Currie & Zhao 1993: 2049, Fig. 3D and 7A; for character history see Ezcurra 2012).
121. Paroccipital process in caudal view: straight, directed laterally or dorsolaterally (0); directed slightly ventrolaterally (1); directed strongly ventrolaterally, with distal end entirely below the level of the foramen magnum (2) (Rauhut 2003: character 52; Tawa hallae after Nesbitt et al. 2009: character 74, Cryolophosaurus ellioti, Eustreptospondylus oxoniensis, "Syntarsus" kayentakatae and Zupaysaurus rougieri after Smith et al. 2007: character 90; for character history see Ezcurra 2012: character 284).
122. Ventral rim of the basis of the paroccipital processes: above or level with the dorsal border of the occipital condyle (0); situated at mid-height of occipital condyle or lower (1) (Ezcurra 2012: character 285; Ceratosaurus, Sinraptor dongi

and *Liliensternus liliensterni* after Rauhut 2003: character 54, *Eustreptospondylus oxoniensis* after Carrano et al. 2012: character 85; for character history see Ezcurra 2012).

123. Paroccipital process: slender, dorsal and ventral margin nearly parallel (0); robust, margins diverging distally, distal end bent downwards and/or expanded (1) (Ezcurra 2012: character 286; *Ceratosaurus* after Madsen & Welles 2000: Pl. 4, *Eustreptospondylus oxoniensis* after Sadleir et al. 2008: 22, Fig. 10C, 13C, *Sinraptor dongi* after Currie & Zhao 1993: Fig. 7A; for character history see Ezcurra 2012).

124. Angle formed by the paroccipital processes in ventral or dorsal aspect: 77 to 94° (0); 101 to 122° (1); 136° (2) (Ezcurra 2012: character 288; *Ceratosaurus* after Gilmore 1920: Pl. 18.1, around 92°, *Sinraptor dongi* 68° after Currie & Zhao 1993: Fig. 7D, E, and Carabajal & Currie: Fig. 1B, *Eustreptospondylus oxoniensis* 92° after Sadleir et al. 2008: Fig. 13F, Frick theropod: around 105°, estimated from reconstruction; for character history see Ezcurra 2012).

125. Position of occipital condyle: anterior to craniomandibular joint (0); at same level as craniomandibular joint (1); posterior to craniomandibular joint (2) (Ezcurra 2012: character 301; *Ceratosaurus* after Gilmore 1920: Pl. 17 and 18, *Sinraptor dongi* after Currie & Zhao 1993: Fig. 3A-C; for character history see Ezcurra 2012).

126. Parabasisphenoid between basal tubera and basiptyergoid processes: approximately as wide as long or wider (0); significantly elongated, at least 1.5 times longer than wide (1) (Ezcurra 2012: character 315; *Ceratosaurus* and *Sinraptor dongi* after Rauhut 2003: character 56, *Eustreptospondylus oxoniensis* after Sadleir et al. 2008: 25, Fig. 12B, 13F; for character history see Ezcurra 2012).

127. Basisphenoid recess: absent or poorly developed (0); deep, well developed (1) (Rauhut 2003: character 57; *Tawa hallae*, *Eodromaeus murphi*, *Zupaysaurus rougieri*, *Cryolophosaurus ellioti* and "*Syntarsus*" *kayentakatae* after Ezcurra 2012: character 319, *Eustreptospondylus oxoniensis* after Sadleir et al. 2008: 25, Fig. 12B, 13F, and Carrano et al. 2012: character 96; for character history see Ezcurra 2012).

128. Basisphenoid lateral surface: not excavated by fossa (0); excavated by anterior tympanic recess (1) (Ezcurra 2012: character 298; *Ceratosaurus* and *Sinraptor dongi* after Rauhut 2003: character 59, *Eustreptospondylus oxoniensis* after Sadleir et al. 2008: 24, Fig. 10A, B; for character history see Ezcurra 2012).

129. Number of foramina for passage of hypoglossal nerve (XII): two (0); one (1) (Ezcurra 2012: character 307; coding of *Tawa hallae*, *Dilophosaurus wetherilli* not verified but deduced from coding of Ezcurra 2012: character 308; *Allosaurus fragilis* and *Sinraptor dongi* after Carabajal & Currie 2012: 95, Tab. 1, *Eustreptospondylus oxoniensis* after Sadleir et al. 2008: 24, Fig. 10C, 13C); for character history see Ezcurra 2012).

130. Relative position of exits of hypoglossal nerve (XII): aligned approximately anteroposteriorly (0); aligned subvertical (1) (Ezcurra 2012: character 308; for character history see Ezcurra 2012).

131. Exit of cranial nerves X and XI: laterally through metotic (= jugular) foramen (0); posteriorly through foramen/foramina lateral to the exit of cranial nerve XII and the occipital condyle (1) (Ezcurra 2012: character 336; *Allosaurus* after Rauhut 2003: character 60, *Cryolophosaurus* after A. Marsh, personal communication, 2018, *Sinraptor dongi* after Carabajal & Currie 2012: 95, Fig. 4; for character history see Ezcurra 2012).

132. Foramen for the exit of the trigeminal nerve [cranial nerve V] and the mid-cerebral vein: combined, not subdivided (0); separated or at least partially subdivided (1) (modified from Ezcurra 2012: character 337; *Ceratosaurus* after Rauhut 2003: character 61, *Sinraptor dongi* after Carabajal & Currie 2012: 93, 6A, C; for character history see Ezcurra 2012).

133. Ventral surface of ectopterygoid: without fossa (0); with a deep depression, groove or foramen (1) (modified from Ezcurra 2012: character 354; *Ceratosaurus* and *Sinraptor dongi* after Carrano et al. 2012: character 116; for character history see Ezcurra 2012).

134. Relation between the maximal height of the alveolar portion and the maximal length of the dentary: 0,11 to 0,13 (0); 0,16 to 0,21 (1); 0,23 to 0,25 (2) (Ezcurra 2012: character 367; *Ceratosaurus* after USMN 4735, *Eustreptospondylus oxoniensis* after Sadleir et al. 2008: Fig. 5, *Sinraptor dongi* after Currie & Zhao 1993: Fig. 11B, Frick theropod: < 0,11; for character history see Ezcurra 2012).

135. Dorsal expansion of the anterior part of the dentary in lateral view: absent (0); present (1) (Ezcurra 2012: character 369; *Ceratosaurus* after Madsen & Welles 2000: Pl. 13A and B, *Eustreptospondylus oxoniensis* and *Sinraptor dongi* after Carrano et al. 2012: character 120; for character history see Ezcurra 2012).

136. Posterior end of dentary: notched by external mandibular fenestra (0); straight or slightly concave (1) (Ezcurra 2012: character 383; *Ceratosaurus* after Gilmore 1920: Fig. 54, Pl. 17.2, 18.2, *Sinraptor dongi* after Carrano et al. 2012: character 126; for character history see Ezcurra 2012).

137. Posteroventral process of dentary: extending further posteriorly than the posterodorsal process (0); subequal to the length of the posterodorsal process (1) (Ezcurra 2012: character 382; *Syntarsus kayentakatae* after Tykoski 2005: character 89, MNA V2623, *Panguraptor lufengensis* after You et al. 2014: character 137, *Dilophosaurus wetherilli* after Smith et al. 2007: character 123 and Tykoski 2005: character 89), *Ceratosaurus* after Gilmore 1920: Fig. 54, Pl. 17.2, 18.2, Ezcurra & Novas 2007: character 100, *Sinraptor dongi* after Currie & Zhao 1993: Fig. 3B, Ezcurra & Novas 2007: character 100, *Eustreptospondylus oxoniensis* after Tykoski 2005: character 89; for character history see Ezcurra 2012).

138. Position of the Meckelian groove in the anterior half of the dentary: dorsoventrally centered (0); restricted to the ventral border (1) (Ezcurra 2012: character 379; *Ceratosaurus* after Madsen & Welles 2000: Pl. 13A, *Eustreptospondylus oxoniensis* after Sadleir et al. 2008: Fig. 9C, *Sinraptor dongi* after Currie & Zhao 1993: Fig. 11B; for character history see Ezcurra 2012).

139. Number of dentary teeth in adults: 11 to 12 (0); 14 to 17 (1); 20 to 23 (2); 25 to 27 (3) (Ezcurra 2012: character 407; *Ceratosaurus* after Colbert 1989: tab. 4, 15 teeth, *Sinraptor dongi* after Currie & Zhao 1993: 2052, 16 alveoli, *Eustreptospondylus oxoniensis*, subadult after Sadleir et al. 2008: 18, at least 13 teeth, Swiss theropod, subadult: at least

17 teeth; for character history see Ezcurra 2012). Comment: As shown by Colbert 1989, Tab. 3, the differences in tooth count between animals of different ontogenetic stages are not necessarily higher than those caused by intraspecific variation. *E. oxoniensis* and *N. frickensis* are only represented by subadult individuals and possibly slightly more dentary teeth were present in the adult condition. Hence, we assume state (0) or (1) for *E. oxoniensis*, respectively (1) or (2) for *N. frickensis*.

140. Anterior margin of splenial: with a single anterior projection (0); anteroventral process longer than anterodorsal process (1); both anterior processes of equal length (2); anterodorsal process longer than anteroventral process (3) (Ezcurra 2012: character 431; *Ceratosaurus* after Madsen & Welles 2000: Pl. 13A, *Sinraptor dongi* after Currie & Zhao 1993: 2054, Fig. 11 C and D; for character history see Ezcurra 2012).

141. Mylohyoid foramen in the ventral part of the splenial: absent (0); present (1) (Ezcurra 2012: character 433; *Panguraptor lufengensis* after You D et al. 2014: character 105, *Ceratosaurus* and *Sinraptor dongi* after Currie & Zhao 1993: Fig. 11C and Rauhut 2003: character 78; for character history see Ezcurra 2012).

142. Posterolateral process of splenial wraps around the ventral margin of the dentary and is exposed in lateral view: present (0); absent (1) (Ezcurra 2012: character 429; *Panguraptor lufengensis* after You et al. 2014: conclusion from coding of character 105, *Ceratosaurus* after Smith et al. 2007: character 129, Madsen & Welles 2000: Pl. 13G and Gilmore 1920: Fig. 55, Pl. 26.2, *Sinraptor dongi* after Curry & Zhao 1993: 2054; for character history see Ezcurra 2012)

143. Maximal length of external mandibular fenestra versus total anteroposterior length of mandible: 7,23 to 7,64% (0); 9,42 to 10,22% (1); 12,17 to 14,55% (2); 17,12 to 17,61% (3); 23,43% (4) (Ezcurra 2012: character 397; *Coelophysis bauri* after Ezcurra 2012 and CM 31374, *Panguraptor lufengensis* after You et al. 2014: 239, Fig. 2, Tab. 1, estimated from Fig. 2 and authors comments on pp. 237 and 239: 12.9%, *Ceratosaurus* after Gilmore 1920: Fig. 55:12.195%, Pl. 17.2: 12.67%, reconstruction Pl. 18.2: 13.55, Pl. 26.2: 14.05%, *Sinraptor dongi* after Curry & Zhao 1993: 2052, Fig. 3B: 17.07 %, 11A, F: around 14.85, Swiss theropod: < 14,41%, but at least 12,17%; for character history see Ezcurra 2012).

144. Anterior portion of the surangular: less than half the height of the mandible at the level of the mandibular fenestra (0); equal to or more than half the height of the mandible at the level of the mandibular fenestra (1) (modified from Smith 2007: character 132; Tawa hallae after Nesbitt et al. 2009: Fig 1, *Panguraptor lufengensis* after You et al. 2014: Fig. 2; for character history see Ezcurra 2012: character 430).

145. Lateral surangular shelf anteroventral to the glenoid fossa: absent (0); present (1) (modified from Ezcurra 2012: character 435; *Panguraptor lufengensis* after You et al. 2014: 239, Fig. 2, *Ceratosaurus* after Gilmore 1920: Fig. 54, Pl. 17.2, 18.2, *Sinraptor dongi* after Curry & Zhao 1993: 2054, Fig. 11E; for character history see Ezcurra 2012).

146. Lateral groove along posterior end of surangular, just dorsal to articulation with posterior process of angular: absent (0); present (1) (Ezcurra 2012: character 436; *Ceratosaurus* after Gilmore 1920: Fig. 54, Pl. 17.2, 18.2 and Smith et al. 2007: character 135, *Sinraptor dongi* after Smith et al. 2007: character 135; for character history see Ezcurra 2012).

147. Anterior and/or posterior surangular foramen/foramina: absent (0); present (1) (modified from Ezcurra 2012: character 437; *Panguraptor lufengensis* after You et al. 2014: Fig. 2, *Ceratosaurus* after Gilmore 1920: 90, Fig. 54, Pl. 17.2, 18.2, *Sinraptor dongi* after Curry & Zhao 1993: 2054, Fig. 11E; for character history see Ezcurra 2012).

148. Pronounced anterior and posterior lips (=walls) of mandibular glenoid, resulting in an at least weakly U-shaped lateral glenoid fossa in lateral view: absent (0); present (1) (Ezcurra 2012: character 439; *Coelophysis bauri* after AMNH 7242, CM 31374 and Colbert 1989: Fig. 40A, *Allosaurus fragilis* after Smith et al. 2007: character 136 and Carrano et al. 2012: character 134, *Ceratosaurus* after Gilmore 1920: Fig. 55, Pl. 26.2, *Sinraptor dongi* after Curry & Zhao 1993: Fig. 11E and Smith et al. 2007: character 136; for character history see Ezcurra 2012).

149. Posterior extension of angular: moderate, surangular participates in the ventral margin of the mandible in lateral view (0); extends far posteriorly, excluding the surangular from the ventral margin of the mandible in lateral view (1) (Ezcurra 2012: character 440; *Ceratosaurus* after Gilmore 1920: Fig. 54, Pl. 17.2, 18.2, comment of the authors: the lateral visible prearticular portion in the skull reconstruction by Gilmore 1920: Pl. 18.2 belongs most probably to the surangular; *Sinraptor dongi* after Curry & Zhao 1993: 2054, Fig. 10C, 11E, F; for character history see Ezcurra 2012).

150. Erect, tab-like dorsal processes on the articular, one immediately posterior to the opening of the corda tympani foramen (medial) and the other on the anterolateral margin of the posterodorsal fossa of the retroarticular process: absent (0); present (1) (Ezcurra 2012: character 442; *Ceratosaurus* and *Sinraptor dongi* after Yates 2005: character 241; for character history see Ezcurra 2012).

151. Ventromedially directed process of the articular: absent (0); present (1) (Ezcurra 2012: character 444; *Ceratosaurus* and *Sinraptor dongi* after Yates 2005: character 240; for character history see Ezcurra 2012).

152. Retroarticular process of the mandible: much longer anteroposteriorly than broad mediolaterally (0); moderately long, slightly longer than broad or subequal to its breadth (1); short and broad, as wide mediolaterally as long anteroposteriorly or wider than long (2) (Ezcurra 2012: character 445; after Yates 2005: Fig. 6A, B, 7A, B, character 73, *Ceratosaurus* after Smith et al. 2007: character 139, *Sinraptor dongi* after Curry & Zhao 1993: Fig. 10D and Smith et al. 2007: character 139; for character history see Ezcurra 2012).

153. Shape of the retroarticular process of the mandible in lateral view: straight or gently curved, resulting in a sub-rectangular outline (0); robust and strongly curved dorsally, resulting in a semilunar outline (1) (Ezcurra 2012: character 446, *Sinraptor dongi* after Curry & Zhao 1993: Fig. 11E; for character history see Ezcurra 2012).

154. Attachment of the m. depressor mandibulae on retroarticular process of the mandible: facing dorsally (0); facing posterodorsally or posteriorly (1) (Ezcurra 2012: character 447; *Ceratosaurus* and *Sinraptor dongi* after Ezcurra & Novas 2007: character 113; for character history see Ezcurra 2012).

155. Attachment area of the m. depressor mandibulae on the retroarticular process of the mandible: transversally convex (0); transversally concave (1) (Ezcurra 2012: character 448; Sinraptor dongi after Yates 2005: character 242; for character history see Ezcurra 2012).
156. Axis intercentrum length versus axis centrum length: 25 to 40% (0); 40 to 70% (1) (after Hugi 2008 and Unterrassner 2009, Hugi 2008: character 70; Eodromaeus murphi, Allosaurus fragilis and Piatnitzkysaurus floresii after Ezcurra 2012: character 458, Ceratosaurus and Sinraptor dongi after Ezcurra & Novas 2007: character 118 and Madsen & Welles 2000: Fig. 14B, 61%; for character history see Ezcurra 2012).
157. Shape of axial neural spine: broad and blade-like (0); transversally compressed, anteroposteriorly reduced and rod-like (1) (after Hugi 2008 and Unterrassner 2009, Hugi 2008: character 71; Eodromaeus murphi, Zupaysaurus rougieri, Allosaurus fragilis and Piatnitzkysaurus floresii after Ezcurra 2012: character 474, Panguraptor lufengensis and Ceratosaurus after You et al. 2014: character 119, Eustreptospondylus oxoniensis after Sadleir et al. 2008: character 140 of Holtz 2000; for character history see Ezcurra 2012).
158. Axial diapophysis: absent (0); present (1) (after Hugi 2008 and Unterrassner 2009, Hugi 2008: character 72; Eodromaeus murphi, Zupaysaurus rougieri, Allosaurus fragilis and Piatnitzkysaurus floresii after Ezcurra 2012: character 465, Ceratosaurus and Sinraptor dongi after Ezcurra & Novas 2007: character 125, Eustreptospondylus oxoniensis after Sadleir et al. 2008: character 143; for character history see Ezcurra 2012).
159. Axial parapophysis: strongly reduced or absent (0); well developed (1) (after Hugi 2008 and Unterrassner 2009, Hugi 2008: character 73; Eodromaeus murphi, Allosaurus fragilis and Piatnitzkysaurus floresii after Ezcurra 2012: character 464, Ceratosaurus after Ezcurra & Novas 2007: character 124, Eustreptospondylus oxoniensis after Sadleir et al. 2008: character 142 of Holtz 2000; for character history see Ezcurra 2012).
160. Axial pleurocoels (the term «pleurocoel» can substitute the terms «pneumatic foramen» or «fossa»): absent (0); present (1) (after Hugi 2008 and Unterrassner 2009, Hugi 2008: character 74; Eodromaeus murphi, Zupaysaurus rougieri, Allosaurus fragilis and Piatnitzkysaurus floresii after Ezcurra 2012: character 463, Panguraptor lufengensis after You et al. 2014: 239, Ceratosaurus after Ezcurra & Novas 2007: character 122, Eustreptospondylus oxoniensis after Sadleir et al. 2008: character 145 of Holtz 2000; for character history see Ezcurra 2012).
161. Anterior articular facet of anterior cervical vertebrae: approximately as high as wide or higher (0); significantly wider than high (1) (after Hugi 2008 and Unterrassner 2009, modified from Hugi 2008: character 75; Eodromaeus murphi, Zupaysaurus rougieri, Allosaurus fragilis and Piatnitzkysaurus floresii after Ezcurra 2012: character 499, Ceratosaurus and Sinraptor dongi after Ezcurra & Novas 2007: character 136, Eustreptospondylus oxoniensis after Smith et al 2007: character 154; for character history see Ezcurra 2012).
162. Length of mid-cervical centra (3 to 6) in relation to height of anterior articular surface: ≤ 3 (0); $3 < 4$ (1); > 4 (2) (after Hugi 2008 and Unterrassner 2009, Hugi 2008: character 77; Eoraptor lunensis, Tawa hallae, Eodromaeus murphi, Zupaysaurus rougieri, Liliensternus liliensterni, Lophostropheus airelensis, Procompsognathus triassicus, Allosaurus fragilis and Piatnitzkysaurus floresii after Ezcurra 2012: character 501, Panguraptor lufengensis after You et al. 2014: Fig. 1, 3 value 2.83, Ceratosaurus and Sinraptor dongi after Ezcurra & Novas 2007: character 138, Eustreptospondylus oxoniensis after Sadleir et al. 2008: Pl. 3 Fig. 9.10, Pl. 4 Fig. 1, 2 and Tykoski 2005: character 128; for character history see Ezcurra 2012).
163. Ventromedial keel of postaxial anterior cervical centra: present (0); absent (1) (after Hugi 2008 and Unterrassner 2009, Hugi 2008: character 78; Eoraptor lunensis, Tawa hallae, Eodromaeus murphi, Zupaysaurus rougieri, Allosaurus fragilis and Piatnitzkysaurus floresii after Ezcurra 2012: character 495, Panguraptor lufengensis after You et al. 2014: 51, Ceratosaurus after Madsen & Welles 2000: 25 and 26 and Carrano et al. 2012: character 171, Eustreptospondylus oxoniensis after Sadleir et al. 2008: 27 and Carrano et al. 2012: character 171, Sinraptor dongi after Currie & Zhao 1993: Fig. 13G and Carrano et al. 2012: character 171; for character history see Ezcurra 2012).
164. Ventral lamina, from the diapophyses to the ventral rim of the caudal end of the vertebral centra in cervical centra: absent (0); present (1) (after Hugi 2008 and Unterrassner 2009, Hugi 2008: character 79; Eoraptor lunensis, Eodromaeus murphi, Coelophysis rhodesiensis, “Syntarsus” kayentakatae, Zupaysaurus rougieri, Cryolophosaurus ellioti, Allosaurus fragilis and Piatnitzkysaurus floresii after Ezcurra 2012: character 512, Ceratosaurus after Ezcurra & Cuny 2007: character 79; for character history see Ezcurra 2012).
165. Lamina protracted from the diapophyses in cervical vertebrae: absent (0); posterior postzygodiapophyseal lamina, reaches the postzygapophyses (1); centrodiaepophyseal lamina, reaches the dorsocaudal corner of the centrum (2) (after Hugi 2008 and Unterrassner 2009, Hugi 2008: character 80; Eoraptor lunensis, Eodromaeus murphi, Coelophysis bauri, Zupaysaurus rougieri, Cryolophosaurus ellioti, Liliensternus liliensterni, Allosaurus fragilis and Piatnitzkysaurus floresii after Ezcurra 2012: character 510 and 511, Ceratosaurus after Ezcurra & Cuny 2007: character 78, Eustreptospondylus oxoniensis after Sadleir et al. 2008: 27-28, Sinraptor dongi after Currie & Zhao 1993: Fig. 14C; for character history see Ezcurra 2012).
166. Prezygapophyses in anterior cervicals: transverse distance between prezygapophyses less than width of neural canal (0); prezygapophyses situated lateral to the neural canal (1) (after Hugi 2008 and Unterrassner 2009, Hugi 2008: character 84; Tawa hallae, Eodromaeus murphi, Zupaysaurus rougieri, Allosaurus fragilis and Piatnitzkysaurus floresii after Ezcurra 2012: character 508, Ceratosaurus, Eustreptospondylus oxoniensis and Sinraptor dongi after Carrano et al. 2012: character 176; for character history see Ezcurra 2012).
167. Prezygapophyses in anterior postaxial cervicals: straight (0); anteroposteriorly convex, flexed ventrally anteriorly (1) (after Hugi 2008 and Unterrassner 2009, Hugi 2008: character 85; Eoraptor lunensis, Eodromaeus murphi, Zupaysaurus rougieri, Cryolophosaurus ellioti and Allosaurus fragilis after Ezcurra 2012: character 494 and Rauhut:

Fig. 24D, *Panguraptor lufengensis* after You et al. 2014: 239, *Ceratosaurus* after Gilmore 1920: Pl. 20, Madsen & Welles 2000: 6A, 6B, 6D, 6E, 6G and 6H, *Eustreptospondylus oxoniensis* after Sadleir et al. 2008: Pl. 3 figs. 1, 2, *Piatnitzkysaurus floresii* after Novas 2009: Fig. 3.19H, *Sinraptor dongi* after Currie & Zhao 1993: Fig. 13H; for character history see Ezcurra 2012).

168. Epiphyses in anterior cervical vertebrae: absent or short and low (0); long, extending beyond the postzygapophyses and low (1); pronounced, strongly overhanging the postzygapophyses and dorsally expanded (2) (after Hugi 2008, Unterrassner 2009 and Ezcurra 2012, modified from Hugi 2008: character 86 and 87, and Ezcurra 2012: character 513 and 514; *Eoraptor lunensis*, *Eodromaeus murphi* and *Zupaysaurus rougieri* after Ezcurra 2012: character 513 and 514; *Panguraptor lufengensis* after You et al. 2014: character 126, *Ceratosaurus* after Gilmore 1920: Pl. 20, Madsen & Welles 2000: Pl. 6B, Tykoski 2005: character 110 and Smith et al. 2007: character 159, *Allosaurus fragilis* after Tykoski 2005: Fig. 42B, character 110 and Rauhut 2003: Fig. 24D, *Eustreptospondylus oxoniensis* after Sadleir et al. 2008: 27, Tykoski 2005: character 110 and Smith et al. 2007: character 159, *Piatnitzkysaurus floresii* after Currie & Zhao 1993: 2057 and Novas 2009: Fig. 3.19H, *Sinraptor dongi* after Currie & Zhao 1993: 2057, Fig. 13G-I and Smith et al. 2007: character 159; for character history see Ezcurra 2012).

169. Height of postaxial cervical neural spines: dorsoventrally tall (0); extremely short (1) (after Hugi 2008 and Unterrassner 2009, Hugi 2008: character 89; *Tawa hallae*, *Eodromaeus murphi*, *Zupaysaurus rougieri*, *Cryolophosaurus ellioti* and *Allosaurus fragilis* and *Piatnitzkysaurus floresii* after Ezcurra 2012: character 518, *Panguraptor lufengensis* after You et al. 2014: Fig. 1 and 3, *Ceratosaurus* after Madsen & Welles 2000: Pl. 6 and Gilmore 1920: Pl. 20, *Eustreptospondylus oxoniensis* after Sadleir et al. 2008: character 154 of Holtz 2000, Pl. 3, figs. 2, 3, *Sinraptor dongi* after Currie & Zhao 1993: Fig. 13H, I, and Holtz 2000: character 154; for character history see Ezcurra 2012).

170. Pneumatization of postaxial cervical centra: absent (0); present by a single pair of fossae that not pierce the centra (1); present by two pairs of fossae that not pierce the centra (2); present by two pairs of foramina that pierce the centra (3); present by a single pair of foramina that pierce the centra (4) (Ezcurra & Novas 2007: character 129; *Tawa hallae* after Nesbitt et al. 2009: 1532 and Nesbitt et al. 2013: 179, *Eodromaeus murphi* after Martinez et al. 2011: 206 and Yates et al. 2012: 96, *Cryolophosaurus ellioti* after Smith et al. 2007: characters 147 to 149, *Lophostropheus airelensis* after Ezcurra & Cuny 2007: character 69, *Panguraptor lufengensis* after You et al. 2014: 239 (the term «foramina» used by the authors is interpreted as «fossae» in the present paper), Fig. 3, characters: 128 and 129, Frick theropod after Unterrassner 2009 and Hugi 2008: character 69, coding changed; for character history see Ezcurra & Novas 2007).
Pi as foramina (EZ&NE2010)

171. Interior pneumatic spaces in cervicals: absent (0); present, structure camerate (1); present structure camellate (2) (after Hugi 2008 and Unterrassner 2009, Hugi 2008: character 92; *Zupaysaurus rougieri*, *Coelophysis bauri* and *Coelophysis rhodesiensis* after Ezcurra 2012: character 491, *Dilophosaurus wetherilli*, *Ceratosaurus* and *Allosaurus fragilis* after Ezcurra & Cuny 2007: character 130, *Eustreptospondylus oxoniensis*, *Piatnitzkysaurus floresii* and *Sinraptor dongi* after Smith et al. 2007: character 152; for character history see Ezcurra 2012). S07 152

172. Cervical ribs: stout and short, extending posteriorly less than three times the length of the centrum of their origin (0); very thin and moderately to extremely long (1) (after Hugi 2008 and Unterrassner 2009, Hugi 2008: character 93; *Tawa hallae* and *Allosaurus fragilis* after Ezcurra 2012: character 529, *Zupaysaurus rougieri* after Arcucci & Coria 2003: 223, *Panguraptor lufengensis* after You et al. 2014: 239, Fig. 3, character 133, *Ceratosaurus* after You et al. 2014: character 133; for character history see Ezcurra 2012).

173. Bodies of cervicals and anterior dorsals: platyan (platycoelous = acoelous) or amphicoelous (0); slightly opisthocoelous (1); strongly opisthocoelous, having ball like articulations (2) (after Hugi 2008 and Unterrassner 2009, Hugi 2008: character 76; *Tawa hallae*, *Eodromaeus murphi*, *Zupaysaurus rougieri*, *Cryolophosaurus ellioti*, *Allosaurus fragilis* and *Piatnitzkysaurus floresii* after Ezcurra 2012: character 498, *Ceratosaurus* after Ezcurra & Novas 2007: character 135, *Eustreptospondylus oxoniensis* after Sadleir et al. 2008: 27, Pl. 3-6, *Sinraptor dongi* after Currie & Zhao 1993: 2057, Fig. 13 F-I, 14; for character history see Ezcurra 2012).

174. Transverse process shape of caudal cervical and/or anterior dorsal vertebrae in dorsal view: mainly laterally directed, subrectangular (0); with strongly backswept anterior margin, subtriangular (1) (after Hugi 2008, Unterrassner 2009 and Tykoski 2005, modified from Hugi 2008: character 88, and Tykoski 2005: character 139; *Eoraptor lunensis*, *Allosaurus fragilis* and *Sinraptor dongi* after Ezcurra & Novas 2007: character 141, *Eodromaeus murphi* after Martinez et al. 2011: character 53, *Segisaurus halli* after Tykoski 2005: character 139, *Ceratosaurus* after Tykoski 2005: Fig. 49B, character 139, *Cryolophosaurus ellioti* after Smith et al. 2007: 397, Fig. 12A to 12D, 12G and 12I, *Panguraptor lufengensis* after You et al. 2014: 239, Frick theropod after Unterrassner 2009 and Hugi 2008: character 88, coding changed, compare Hugi 2008: Fig. 10; for character history see Ezcurra & Novas 2007).

175. Length of anterior and mid-dorsal centra: short, subequal to at most 1.4 times mid centrum height (0); elongated, at least 1.8 times mid centrum height (1) (modified from Hugi 2008 and Unterrassner 2009, Hugi 2008: character 94; *Eoraptor lunensis* after Sereno et al. 2012: Fig. 50.1, 50.2, Tab. 5, *Liliensternus liliensterni* after Huene 1934: Pl. 14.6-14.10 and Rauhut 2003: Fig. 26A, *Dilophosaurus wetherilli* after Tykoski 2005: Fig. 48B; and Welles 1984: Fig. 14B, *Cryolophosaurus ellioti* after Smith et al. 2007: Fig. 12B, *Ceratosaurus* after Gilmore 1920: Fig. 96, Table on page 97 *Allosaurus fragilis* after Gilmore 1920: Fig. 22, 23, *Eustreptospondylus oxoniensis* after Sadleir et al. 2008: Pl. 8.5, 8.6, *Piatnitzkysaurus floresii* after Bonaparte 1986: Fig. 14, *Sinraptor dongi* after Currie & Zhao 1993: Fig. 15B, D, F; for character history see Ezcurra 2012).

176. Posterior dorsal vertebrae: strongly shortened, centrum length less than 1.33 times the height of the cranial articular surface (0); relatively short, centrum length equal or more than 1.33 times the height of the cranial articular

surface (1); significantly elongated, centrum equal or longer than two times the height of the cranial articular surface (2) (after Hugi 2008 and Unterrassner 2009, Hugi 2008: character 95; *Eoraptor lunensis*, *Eodromaeus murphi*, *Cryolophosaurus ellioti* and *Coelophysis rhodesiensis* after Ezcurra 2012: character 564, *Eoraptor lunensis*: value 1.43, *Eodromaeus murphi*: value 1.49, *Cryolophosaurus ellioti*: value 1.15, *Coelophysis rhodesiensis*: value 1.67 to 2.21; *Panguraptor lufengensis* after You et al. 2014: character 329, *Ceratosaurus* and *Allosaurus fragilis* after Ezcurra & Novas 2007: character 144, *Eustreptospondylus oxoniensis* after Sadleir et al. 2008: 27, Pl. 10 12, *Piatnitzkysaurus floresii* and *Sinraptor dongi* after Smith et al. 2007: character 169; for character history see Ezcurra 2012).

177. Transverse processes of dorsal vertebrae: anteroposteriorly narrow (0); broad, extending to the lateral margin of the prezygapophyses (1) (after Hugi 2008 and Unterrassner 2009, modified from Hugi 2008: character 98; *Eoraptor lunensis*, *Ceratosaurus* and *Allosaurus fragilis* after Ezcurra & Cuny 2007: character 84, *Eodromaeus murphi* after Martinez et al. (2011): Fig. 2D, *Cryolophosaurus ellioti* after Smith et al. 2007: Fig. 12, *Panguraptor lufengensis* after You et al. 2014: 239 and Fig. 1, *Eustreptospondylus oxoniensis* after Tykoski 2005: character 140, *Piatnitzkysaurus floresii* after Bonaparte 1986: Fig. 17, *Sinraptor dongi* after Ezcurra & Novas 2007: character 142; for character history see Ezcurra & Cuny 2007).

178. Orientation of the transverse processes of dorsal vertebrae: directed laterally or slightly ventrolaterally (0); directed dorsolaterally (1) (after Hugi 2008, Unterrassner 2009 and Ezcurra 2012, modified from Hugi 2008: character 100, and Ezcurra 2012: character 550; *Eoraptor lunensis*, *Eodromaeus murphi*, *Cryolophosaurus ellioti*, *Liliensternus liliensterni*, *Coelophysis rhodesiensis*, *Allosaurus fragilis* and *Piatnitzkysaurus floresii* after Ezcurra 2012: character 550, *Panguraptor lufengensis* after You et al. 2014: Fig. 1, *Segisaurus halli* after Carrano, Hutchinson and Sampson 2005: 836, Fig. 1, *Ceratosaurus* after Madsen & Welles 2000: 15, 17, Pl. 6G to 6I and 7A to 7C, *Eustreptospondylus oxoniensis* after Sadleir et al. 2008: 32, Pl. 9 figs. 1, 2, 5, 6, *Sinraptor dongi* after Currie & Zhao 1993: Fig. 15 and 16; for character history see Ezcurra 2012).

179. Height of neural spines of posterior dorsals relative to their anteroposterior length: approximately as high as long (0); significantly higher, than long (1); significantly longer, than high (2) (after Hugi 2008 and Unterrassner 2009, Hugi 2008: character 102; *Eoraptor lunensis* after Sereno et al. 2012: Fig. 51, 52A, *Eodromaeus murphi*, *Coelophysis bauri*, *Coelophysis rhodesiensis*, *Allosaurus fragilis* and *Piatnitzkysaurus floresii* after Ezcurra 2012: character 566, *Panguraptor lufengensis* after You et al. 2014: Fig.1, character 330, *Ceratosaurus* after Ezcurra & Novas 2007: character 145, *Eustreptospondylus oxoniensis* after Sadleir et al. 2008: Pl. 12 Fig. 16, 17, Tykoski 2005: character 143 and Smith et al. 2007: character 175, *Sinraptor dongi* after Currie & Zhao 1993: Fig. 16, 17 and Smith et al. 2007: character 175; for character history see Ezcurra 2012).

180. Distal neural spines in posterior dorsals: subequal breadth throughout the entire height or tapering dorsally (0); significantly expanded dorsally, fan-shaped (after Hugi 2008 and Unterrassner 2009, Hugi 2008: character 103; *Eoraptor lunensis*, *Eodromaeus murphi* and *Allosaurus fragilis* and *Piatnitzkysaurus floresii* after Ezcurra 2012: character 568, *Panguraptor lufengensis* after You et al. 2014: Fig.1, character 137, *Ceratosaurus* after You et al. 2014: character 137, *Eustreptospondylus oxoniensis* and *Sinraptor dongi* after Smith et al. 2007: character 176; for character history see Ezcurra 2012).

181. Height of neural spines in dorsals (exclusive the last three vertebrae): more or less constant (0); increasing posteriorly (1) (after Hugi 2008 and Unterrassner 2009, modified from Hugi 2008: character 104; *Eoraptor lunensis* after Sereno, Martinez & Alcober 2012: Fig. 5 and 9, *Herrerasaurus ischigualastensis* after Novas (1994): Fig. 1, *Tawa hallae* after Nesbitt et al. 2009: Fig. 2, *Eodromaeus murphi* after Martinez et al. 2011: Fig. 2, *Panguraptor lufengensis* after You et al. 2014: Fig.1, *Allosaurus fragilis* after Madsen 1976: 34, *Piatnitzkysaurus floresii* after Bonaparte 1986: Fig. 14, 15, 17, 18, *Sinraptor dongi* after Currie & Zhao 1993: 2058 and Fig. 15, 16 and 17A).

182. Hyposphene-hypantrum articulation in dorsal vertebrae: absent (0); present, hyposphene developed as a single sheet of bone (1); present, hyposphene wide, formed by the ventrally bowed medial parts of the postzygapophyses, and only connected by a thin horizontal lamina of bone (2) (after Hugi 2008, Unterrassner 2009 and Smith et al. 2007, modified from Hugi 2008: character 106 and 107, and Smith et al. 2007: character 173; *Eoraptor lunensis*, *Cryolophosaurus ellioti*, "Syntarsus" *kayentakatae*, *Coelophysis bauri*, *Ceratosaurus* and *Allosaurus fragilis*, *Eustreptospondylus oxoniensis*, *Piatnitzkysaurus floresii* and *Sinraptor dongi* after Smith et al. 2007: character 173; for character history see Ezcurra 2012).

183. Ventral keel in anterior dorsals: absent or very poorly developed (0); pronounced (1) (after Hugi 2008 and Unterrassner 2009, Hugi 2008: character 109; *Eoraptor lunensis*, *Eodromaeus murphi* and *Allosaurus fragilis* and *Piatnitzkysaurus floresii* after Ezcurra 2012: character 556, *Ceratosaurus* and *Sinraptor dongi* after Rauhut 2003: character 108, *Eustreptospondylus oxoniensis* after Smith et al. 2007: character 170; for character history see Ezcurra 2012).

184. Level of the parapophyses in posteriormost dorsals: on the same height as transverse processes (0); distinctly below transverse processes (1) (after Hugi 2008 and Unterrassner 2009, Hugi 2008: character 110; *Eoraptor lunensis*, *Eodromaeus murphi*, *Cryolophosaurus ellioti* and *Allosaurus fragilis* after Ezcurra 2012: character 570, *Panguraptor lufengensis* after You et al. 2014: 239, *Ceratosaurus*, *Eustreptospondylus oxoniensis*, *Piatnitzkysaurus floresii* and *Sinraptor dongi* after Smith et al. 2007: character 179; for character history see Ezcurra 2012).

185. Lateral fossae in dorsal centra: absent (0); present in anterior dorsals («pectorals») (1); present in all dorsals (2) (after Hugi 2008 and Unterrassner 2009, Hugi 2008: character 111; *Eoraptor lunensis*, *Cryolophosaurus ellioti*, *Ceratosaurus* and *Allosaurus fragilis*, *Eustreptospondylus oxoniensis*, *Piatnitzkysaurus floresii* and *Sinraptor dongi* after

Smith et al. 2007: character 168, *Eodromaeus murphi* after Ezcurra 2012: character 539; for character history see Ezcurra 2012).

186. Fusion of sacral centra in adults: absent, or fused but sutures still visible (0); extensively fused to one another, all sutures obliterated (1) (after Hugi 2008 and Unterrassner 2009, Hugi 2008: character 112; *Tawa hallae*, *Eodromaeus murphi*, *Cryolophosaurus ellioti* and *Allosaurus fragilis* and *Piatnitzkysaurus floresi* after Ezcurra 2012: character 574, *Ceratosaurus* after Ezcurra & Cuny 2007: character 87, *Sinraptor dongi* after Currie & Zhao 1993: 2062; for character history see Ezcurra 2012).

187. Fusion of sacral ribs and ilia: absent throughout ontogeny (0); present in late ontogeny, ribs fuse to medial wall of ilia (1) (after Hugi 2008 and Unterrassner 2009, Hugi 2008: character 113; *Eoraptor lunensis*, *Ceratosaurus* and *Allosaurus fragilis* after Ezcurra & Cuny 2007: character 88, *Piatnitzkysaurus floresi* and *Sinraptor dongi* after Holtz 2000: character 189, Frick theropod after Unterrassner 2009 and Hugi 2008: character 113, coding changed; for character history see Ezcurra & Cuny 2007).

188. Sacral ribs respectively modified transverse processes in adults: slender and well separated (0); very massive and strongly expanded (1); forming a more or less continuous sheet in ventral or dorsal view (2) (after Hugi 2008 and Unterrassner 2009, Hugi 2008: character 115; *Eoraptor lunensis* after Sereno, Martinez & Alcober 2012: Fig. 54 and Martinez et al. 2011: character 57, *Eodromaeus murphi* after Martinez et al. 2011: 206 and character 57, *Cryolophosaurus ellioti*, *Piatnitzkysaurus floresi* and *Sinraptor dongi* after Smith et al. 2007: character 187, *Ceratosaurus* and *Allosaurus fragilis* after Gilmore 1920: Pl. 8, 9, 21, Ezcurra & Cuny 2007: character 89 and Ezcurra & Novas 2007: character 148; for character history see Ezcurra & Novas 2007).

189. Number of sacral vertebrae: two (0); three (1); four or five (2); more than five (3) (after Hugi 2008 and Unterrassner 2009, Hugi 2008: character 116; *Eoraptor lunensis*, *Tawa hallae*, *Eodromaeus murphi* and *Allosaurus fragilis* and *Piatnitzkysaurus floresi* after Ezcurra 2012: character 577, *Ceratosaurus* after Gilmore 1920: Pl. 21 and Smith et al. 2007: character 182, *Eustreptospondylus oxoniensis* and *Sinraptor dongi* after Carrano et al. 2012: character 197, Frick theropod after Unterrassner 2009 and Hugi 2008: character 116, coding changed, compare Hugi 2008: 51, Fig. 5 and 6; for character history see Ezcurra 2012).

190. Sacral centra: rounded or keeled ventrally (0); flattened ventrally (1) (after Hugi 2008 and Unterrassner 2009, Hugi 2008: character 119; *Cryolophosaurus ellioti* after Smith et al. 2007: 398, Fig. 13A to 13C, *Ceratosaurus*, *Allosaurus fragilis*, *Piatnitzkysaurus floresi* and *Sinraptor dongi* after Rauhut 2003: character 114, *Eustreptospondylus oxoniensis* after Sadleir et al. Pl. 13-15; for character history see Rauhut 2003).

191. Diameter of mid-sacral centra with respect to posterior dorsals and anterior caudals: approximately the same (0); substantially smaller (1); substantially larger (2) (after Hugi 2008 and Unterrassner 2009, Hugi 2008: character 120; *Eoraptor lunensis*, *Ceratosaurus* and *Allosaurus fragilis* after Tykoski 2005: character 149, *Cryolophosaurus ellioti* after Smith et al. 2007: Fig. 12G, 12I, 13A, 13C, 13E and 13G, *Eustreptospondylus oxoniensis* after Sadleir et al. 2008: Pl. 13.7, 13.8, 14.8, 16.3, 16.6.; for character history see Tykoski 2005).

192. Pleurocoels in sacral vertebrae: absent (0); present with at least one fossa (1) (after Hugi 2008 and Unterrassner 2009, Hugi 2008: character 121; *Cryolophosaurus ellioti* after Smith et al. 2007: 398, Fig. 13B, *Ceratosaurus*, *Eustreptospondylus oxoniensis* after Sadleir et al. 2008: 33, *Piatnitzkysaurus floresi* and *Sinraptor dongi* after Carrano et al. 2012: character 196, *Allosaurus fragilis* after Gilmore 1920: 43 and Carrano 2012: character 196; for character history see Rauhut 2003).

193. Ventral surface of anterior caudals: smooth or weakly grooved longitudinally (0); at least some vertebrae with narrow, sharply defined, longitudinal, ventral groove (1) (after Hugi 2008 and Unterrassner 2009, modified from Hugi 2008: character 122 and 123; *Eoraptor lunensis*, *Eodromaeus murphi* and *Piatnitzkysaurus floresi* after Ezcurra 2012: character 611, *Allosaurus fragilis* after Rauhut 2003: 87, Madsen 1976: Fig. 8A and Ezcurra 2012: character 611, *Ceratosaurus* after Gilmore 1920: Pl. 22, Fig. 2 and Madsen 1976: Fig. 8B, *Eustreptospondylus oxoniensis* after Sadleir et al. 2008: 34 and character 193 of Holtz 2000, *Sinraptor dongi* after Ezcurra & Novas 2007: character 150; for character history see Ezcurra 2012).

194. Number of caudal vertebrae: 41 or more (0); less than 41 (1); less than 36 (2) (after Hugi 2008 and Unterrassner 2009, Hugi 2008: character 124; *Eodromaeus murphi* and *Allosaurus fragilis* after Ezcurra 2012: character 599, *Ceratosaurus* and *Sinraptor dongi* after Smith et al. 2007: character 189; for character history see Ezcurra 2012).

195. Vertical orientation of anterior caudal transverse processes in respect to the longitudinal axis of the centra: lateral (0); dorsolateral (1) (after Hugi 2008 and Unterrassner 2009, Hugi 2008: character 127; *Eoraptor lunensis* after Sereno, Martinez & Alcober 2012: Fig. 56 to 59, *Cryolophosaurus ellioti* after Smith et al. 2007: 400, Fig. 13E to 13G, *Ceratosaurus* after Madsen 1976: Fig. 21B and Madsen & Welles 2000: Pl. 7D to 7F, *Allosaurus fragilis* after Madsen 1976: Fig. 21A and Gilmore 1920: Fig. 28, *Eustreptospondylus oxoniensis* after Sadleir et al. 2008: 34, Pl. 16 figs. 4, 5, Pl. 17 figs. 1, 2, Pl. 18 figs. 1, 2, *Piatnitzkysaurus floresi* after Bonaparte 1986: 271, *Sinraptor dongi* after Currie & Zhao 1993: Fig. 18D).

196. Horizontal orientation of anterior caudal transverse processes in respect to the longitudinal axis of the centra: lateral (0); caudolateral (= back-swept) (1) (after Hugi 2008 and Unterrassner 2009, Hugi 2008: character 128; *Eoraptor lunensis* after Sereno, Martinez & Alcober 2012: 133, *Dilophosaurus wetherilli* after Welles 1984: 125, Fig. 21 and 22, *Cryolophosaurus ellioti* after Smith et al. 2007: 400, Fig. 13E to 13G, *Ceratosaurus* after Gilmore 1920: Pl. 22, *Allosaurus fragilis* after Madsen 1976: 35, *Eustreptospondylus oxoniensis* after Sadleir et al. 2008: Pl. 15 fig. 9, Pl. 16 figs. 1, 3, 6, 9, *Piatnitzkysaurus floresi* after Bonaparte 1986: 271, *Sinraptor dongi* after Currie & Zhao 1993: Fig. 18C).

197. Length of zygapophyses of anterior caudal vertebrae: prezygapophyses and postzygapophyses short, not overlapping the cranial or caudal centrum face (0); prezygapophyses and postzygapophyses elongated, overlapping the centrum faces (1); only prezygapophyses elongated (2) (after Hugi 2008 and Unterrassner 2009, modified from Hugi 2008: character 129; *Eoraptor lunensis* after Sereno, Martinez & Alcober 2012: 132, Fig. 55, 56, 58, 59, *Ceratosaurus* after Gilmore 1920: Pl. 22 Fig. 1 and Madsen 1976: Fig. 21B, *Allosaurus fragilis* after Madsen 1976: 21A, *Eustreptospondylus oxoniensis* after Sadleir et al. 2008: 34, Pl. 16.1-16.3, *Sinraptor dongi* after Currie & Zhao 1993: Fig 18C).
198. Anterior process at base of chevrons: absent (0); small tubercles (1); large and projecting (2) (after Hugi 2008 and Unterrassner 2009, Hugi 2008: character 131; *Eoraptor lunensis*, *Eodromaeus murphi*, *Cryolophosaurus ellioti* and *Allosaurus fragilis* after Ezcurra 2012: character 630, *Dilophosaurus wetherilli* after Welles 1984: 126, Fig. 24B and 24D, *Ceratosaurus* after Smith et al. 2007: character 199 and Ezcurra & Novas 2007: character 154; for character history see Ezcurra 2012).
199. Pleurocoels in caudals: absent (0); present (1) (after Hugi 2008 and Unterrassner 2009, Hugi 2008: character 132; *Eoraptor lunensis*, *Dilophosaurus wetherilli*, *Cryolophosaurus ellioti*, "Syntarsus" *kayentakatae*, *Coelophysis bauri*, *Coelophysis rhodesiensis* and *Ceratosaurus* after Smith et al. 2007: character 188, after Gilmore 1920: Pl. 22 Fig. 1 and Madsen 1976: 21B, *Allosaurus fragilis* after Gilmore 1920: Fig. 28, Madsen 1976: Pl. 29 to 33 and Carrano et al. 2012: character 204, *Eustreptospondylus oxoniensis*, *Piatnitzkysaurus floresi* and *Sinraptor dongi* after Carrano et al. 2012: character 204; for character history see Smith et al. 2007).
200. Maximum length to minimal breadth ratio of scapular blade: < 9, scapula broad and relatively short (0); > 10, scapula narrow and long (1) (after Hugi 2008 and Unterrassner 2009, modified from Hugi 2008: character 168; *Eoraptor lunensis*, *Herrerasaurus ischigualastensis*, *Tawa hallae*, *Eodromaeus murphi*, *Liliensternus liliensterni*, *Allosaurus fragilis* and *Piatnitzkysaurus floresi* after Ezcurra 2012: character 651, *Panguraptor lufengensis* after You et al. 2014: Tab. 1, ratio 7.82, *Ceratosaurus*, *Eustreptospondylus oxoniensis* and *Sinraptor dongi* after Carrano et al. 2012: character 223; for character history see Ezcurra 2012).
201. Distal end of scapular blade: distinctly expanded, fan-shaped (0); slightly expanded (1); not expanded (2) (after Hugi 2008 and Unterrassner 2009, modified from Hugi 2008: character 174; *Eoraptor lunensis*, *Tawa hallae*, *Eodromaeus murphi*, *Allosaurus fragilis* and *Piatnitzkysaurus floresi* after Ezcurra 2012: character 652, *Panguraptor lufengensis* after You et al. 2014: Fig. 2, *Ceratosaurus* after Madsen & Welles 2000: Pl. 20A, 20C, *Eustreptospondylus oxoniensis* after Sadleir et al. 2008: 36, Fig. 15, *Sinraptor dongi* after Currie & Zhao 1993: Fig. 20A; for character history see Ezcurra 2012).
202. Shape of anterodistal corner of scapular blade: rounded (0); acuminate (1) (after Hugi 2008 and Unterrassner 2009, Hugi 2008: character 175; *Tawa hallae* after Nesbitt et al. 2009: Fig. 2B, *Panguraptor lufengensis* after You et al. 2014: Fig. 2, *Ceratosaurus* after Madsen & Welles 2000: Pl. 20A, 20C, *Allosaurus fragilis* and after Ezcurra 2012: character 653, *Sinraptor dongi* after Ezcurra & Novas 2007: character 156; for character history see Ezcurra 2012).
203. Posterior margin of scapular blade: concave, curves over full length posteriorly (0); nearly straight or partly slightly convex, curves only at distal tip posteriorly (1) (after Hugi 2008 and Unterrassner 2009, modified from Hugi 2008: character 252; *Eoraptor lunensis* after Martinez & Alcober 2012: Figs. 61, 62 and Tykoski 2005: character 165, *Tawa hallae*, *Eodromaeus murphi*, *Ceratosaurus*, *Allosaurus fragilis* and *Piatnitzkysaurus floresi* after Ezcurra 2012: character 654, *Panguraptor lufengensis* after You et al. 2014: Fig. 1, *Sinraptor dongi* after Currie & Zhao 1993: Fig. 20A; for character history see Ezcurra 2012).
204. Acromion process of scapula: clearly offset from scapular blade, protruding conspicuously dorsally (0); not offset, with gradual transition to scapular blade (1) (after Hugi 2008 and Unterrassner 2009, Hugi 2008: character 170; *Eoraptor lunensis* after Sereno, Martinez & Alcober 2012: 62 and Tykoski 2005: character 166, *Tawa hallae*, *Eodromaeus murphi*, *Zupaysaurus rougieri* and *Piatnitzkysaurus floresi* after Ezcurra 2012: character 656, *Panguraptor lufengensis* after You et al. 2014: Fig. 2, *Ceratosaurus* and *Allosaurus fragilis* after Carrano et al. 2012: character 219, *Eustreptospondylus oxoniensis* after Sadleir et al. 2008: character 214 of Holtz 2000, *Sinraptor dongi* after Currie & Zhao 1993: 2065; for character history see Ezcurra 2012).
205. Anterior margin of scapular coracoid at scapula-coracoid contact in adults: distinctly notched (0); continuous, uninterrupted (1) (after Hugi 2008 and Unterrassner 2009, Hugi 2008: character 176; *Eoraptor lunensis* after Sereno, Martinez & Alcober 2012: Fig. 61 to 64, *Eodromaeus murphi* after Martinez et al. 2011: Fig. 2, *Ceratosaurus* after Madsen & Welles 2000: Pl. 20A, 20C and Carrano et al. 2012: character 219, *Allosaurus fragilis* after Rauhut 2003: Fig. 33B and Carrano et al. 2012: character 219, *Sinraptor dongi* after Carrano et al. 2012: character 219, Frick theropod after Unterrassner 2009 and Hugi 2008: character 176, coding changed, compare Hugi 2008: Fig. 8 and Unterrassner 2009: Fig. 6 and 8, subadult; for character history see Nesbitt et al. 2009).
206. Shape of coracoid: higher (dorsoventrally) than long (anteroposteriorly) (0); longer than high (1) (after Hugi 2008 and Unterrassner 2009, Hugi 2008: character 172; *Eodromaeus murphi*, *Allosaurus fragilis* and *Piatnitzkysaurus floresi* after Ezcurra 2012: character 664 *Ceratosaurus* after Madsen & Welles 2000: Pl. 20A, 20C, *Sinraptor dongi* after Rauhut 2003: character 137; for character history see Ezcurra 2012).
207. Distance between anterior end of glenoid and tip of posteroventral process of coracoid (= sternal process anterior to the glenoid): more than dorsoventral depth of glenoid (0); less than dorsoventral depth of glenoid (1) (after Hugi 2008 and Unterrassner 2009, Hugi 2008: character 177; *Eoraptor lunensis*, *Eodromaeus murphi*, *Zupaysaurus rougieri*, *Allosaurus fragilis* and *Piatnitzkysaurus floresi* after Ezcurra 2012: character 666, *Ceratosaurus* after Madsen & Welles

2000: Pl. 20A, 20C, Ezcurra 2006: character 163 and Ezcurra & Novas 2007: character 158; for character history see Ezcurra 2012).

208. Posteroventral process (= sternal process) of coracoid: rounded, not projected beyond posterior margin of glenoid fossa (0); tapering, projected little beyond posterior margin of glenoid fossa (1); tapering, projected strongly beyond posterior margin of glenoid fossa (2) (after Hugi 2008 and Unterrassner 2009, Hugi 2008: character 178; *Eoraptor lunensis*, *Eodromaeus murphi*, *Allosaurus fragilis* and *Piatnitzkysaurus floresi* after Ezcurra 2012: character 669, *Ceratosaurus* after Madsen & Welles 2000: Pl. 20A, 20C and Ezcurra & Novas 2007: character 159; for character history see Ezcurra 2012).

209. Shape of humerus in lateral view: sigmoidal (0); straight (1) (after Hugi 2008 and Unterrassner 2009, Hugi 2008: character 183; *Eoraptor lunensis*, *Tawa hallae*, *Eodromaeus murphy*, *Allosaurus fragilis* and *Piatnitzkysaurus floresi* after Ezcurra 2012: character 673, *Ceratosaurus* after Rauhut 2003: character 143, *Eustreptospondylus oxoniensis* after Sadleir et al. 2008: character 235; for character history see Ezcurra 2012).

210. Outline of humeral head in proximal view: rectangular or oval (more than twice as broad transversely than anteroposteriorly) (0); approximately circular (less than twice as broad anteroposteriorly than transversely) (1) (after Hugi 2008 and Unterrassner 2009, modified from Hugi 2008: character 181; *Eoraptor lunensis*, *Tawa hallae*, *Eodromaeus murphy*, *Cryolophosaurus ellioti*, *Allosaurus fragilis* and *Piatnitzkysaurus floresi* after Ezcurra 2012: character 676, *Panguraptor lufengensis* after You et al. 2014: 240, *Ceratosaurus* after Rauhut 2003: character 140, *Eustreptospondylus oxoniensis* after Sadleir et al. 2008: Fig. 16E; for character history see Ezcurra 2012).

211. Torsion of shaft between proximal and distal ends of humerus: absent (0); present (1) (after Hugi 2008 and Unterrassner 2009, Hugi 2008: character 184; *Eoraptor lunensis*, *Tawa hallae*, *Eodromaeus murphy*, *Allosaurus fragilis* and *Piatnitzkysaurus floresi* after Ezcurra 2012: character 674, *Ceratosaurus* after Ezcurra & Novas 2007: character 161, *Eustreptospondylus oxoniensis* after Sadleir et al. 2008: character 234 of Holtz 2000; for character history see Ezcurra 2012).

212. Distal surface of humeral condyles: rounded (0); flattened (1) (after Hugi 2008 and Unterrassner 2009, Hugi 2008: character 179; *Eoraptor lunensis*, *Tawa hallae*, *Eodromaeus murphy*, *Cryolophosaurus ellioti*, *Allosaurus fragilis* and *Piatnitzkysaurus floresi* after Ezcurra 2012: character 697, *Ceratosaurus* after Madsen & Welles 2000: Fig. 3, *Eustreptospondylus oxoniensis* after Carrano et al. 2012: character 238; for character history see Ezcurra 2012).

213. Ratio of radius length to humerus length: 49.42% to 54.17% (0); 61.00% to 69.54% (1); 71.61% to 80.00% (2); 89.9% to 114.87% (3) (modified from Ezcurra 2012: character 708; Frick theropod: 72.73%; for character history see Ezcurra 2012).

214. Ratio of manual length (measured as the average length of digits I to III) to total length of humerus plus radius: 0.36 (0); 0.47 to 0.51 (1); 0.58 to 0.60 (2) (after Ezcurra 2012: character 724, Frick theropod: 0.39; for character history see Ezcurra 2012).

215. Composition of manus regarding the number of metacarpals and digits: five digits (0); four digits, fourth digit reduced (three-and-a-half fingers) (1); five or four metacarpals and three digits (2); three metacarpals and three digits (3) (after Hugi 2008 and Unterrassner 2009, modified from Hugi 2008: character 217; *Eoraptor lunensis* after Rauhut 2003: character 153 and Sereno, Martinez & Alcober 2012: Figs. 68, 70, 73 and 74, *Herrerasaurus ischigualastensis* after Rauhut 2003: character 153, *Tawa hallae* after Nesbitt et al. 2009: Fig. 2F, *Eodromaeus murphi* after Martinez et al. 2011: Fig. 1G, *Panguraptor lufengensis* after You et al. 2014: 240 and 241, Figs. 1 and 4, *Ceratosaurus* after Gilmore 1920: Figs. 58, 60, 62, Pl. 30, Rauhut 2003: character 153 and Carrano & Choiniere 2016, *Allosaurus fragilis* after Gilmore 1920: Figs. 40, 45, Pl. 7 Fig. 3 and Rauhut 2003: character 153, *Sinraptor dongi* after Carrano et al. 2012: character 249; for character history see Rauhut 2003).

216. Large distal carpal, capping Mc I and parts of Mc II: absent (0); present (1) (after Hugi 2008 and Unterrassner 2009, modified from Hugi 2008: character 189; *Tawa hallae* after Nesbitt et al. 2009: 1531 and Fig. 2F, *Eodromaeus murphi* after Martinez et al. 2011: 207 and Fig. 1G, *Allosaurus fragilis* after Rauhut 2003: character 146; for character history see Rauhut 2003).

217. Distal carpal 5: present (0); absent (1) (after Hugi 2008 and Unterrassner 2009, Hugi 2008: character 190; *Tawa hallae* and *Allosaurus fragilis* after Ezcurra 2012: character 723; for character history see Ezcurra 2012).

218. Length - width ratio of metacarpals I to III: < 2, metacarpus relatively short and broad (0); > 2.2, metacarpus elongated and slender (1) (after Hugi 2008 and Unterrassner 2009, Hugi 2008: character 199; *Eoraptor lunensis* after Sereno, Martinez & Alcober 2012: Figs. 68, 70 to 74, *Tawa hallae* after Nesbitt et al. 2009: Fig. 2F, *Eodromaeus murphi* after Martinez et al. 2011: Fig. 1G, *Panguraptor lufengensis* after You et al. 2014: Tab. 1, Fig. 4, *Ceratosaurus*, *Allosaurus fragilis* and *Sinraptor dongi* after Rauhut 2003: character 147; for character history see Rauhut 2003).

219. Extensor pits on dorsal surface of distal ends of metacarpals I to III: absent or shallow and symmetrical (0); deep, well-developed and asymmetrical (1) (after Hugi 2008 and Unterrassner 2009, Hugi 2008: character 256; *Eoraptor lunensis*, *Tawa hallae*, *Eodromaeus murphi* and *Allosaurus fragilis* after Ezcurra 2012: character 728, *Ceratosaurus* after Nesbitt et al. 2009: character 177, *Sinraptor dongi* after Smith et al. 2007: character 243; for character history see Ezcurra 2012).

220. Length of metacarpal I relative to its width: significantly longer than broad (0); very stout, approximately as broad as long (1) (after Hugi 2008 and Unterrassner 2009, Hugi 2008: character 223; *Eoraptor lunensis*, *Ceratosaurus* and *Allosaurus fragilis* after Rauhut 2003: character 164, *Tawa hallae* after Nesbitt et al. 2009: Fig. 2, *Eodromaeus murphi* after Martinez et al. 2011: Fig. 1G; for character history see Rauhut 2003).

221. Width of metacarpal I at middle of shaft versus total length of bone: ≤ 0.3 (0); 0.3 to 0.45 (1); > 0.45 (2) (after Hugi 2008 and Unterrassner 2009, Hugi 2008: character 192; *Eoraptor lunensis*, *Tawa hallae*, *Eodromaeus murphi* and *Allosaurus fragilis* after Ezcurra 2012: character 736, *Ceratosaurus* after Carrano & Choinree 2016: Fig. 5, 6 and You et al. 2014: character 178; for character history see Ezcurra 2012).
222. Distal end of metacarpal I: condyles more or less symmetrical proximodistally (0); condyles strongly asymmetrical, the medial condyle being positioned more proximally than the lateral one (1) (after Hugi 2008 and Unterrassner 2009, Hugi 2008: character 201; *Eoraptor lunensis*, *Tawa hallae*, *Eodromaeus murphi* and *Allosaurus fragilis* after Ezcurra 2012: character 738, *Panguraptor lufengensis* after You et al. 2014: character 181, *Ceratosaurus* after Rauhut 2003: character 149; for character history see Ezcurra 2012).
223. Metacarpal I shorter than phalanx I-1: absent (0); present (1) (after Hugi 2008 and Unterrassner 2009, Hugi 2008: character 193; *Eoraptor lunensis*, *Tawa hallae*, *Eodromaeus murphi* and *Allosaurus fragilis* after Ezcurra 2012: character 740; for character history see Ezcurra 2012).
224. Length of metacarpal I: $\geq 50\%$ the length of metacarpal II (0), $< 50\%$ the length of metacarpal II (1) (after Hugi 2008 and Unterrassner 2009, Hugi 2008: character 208; *Eoraptor lunensis*, *Tawa hallae*, *Eodromaeus murphi* and *Allosaurus fragilis* after Ezcurra 2012: character 732; for character history see Ezcurra 2012).
225. Contact between metacarpal I and metacarpal II: confined to their bases (0), along proximal half of metacarpal II (1) (after Hugi 2008 and Unterrassner 2009, Hugi 2008: character 200; *Eoraptor lunensis* and *Eodromaeus murphi* after Ezcurra 2012: character 735, *Allosaurus fragilis* and *Ceratosaurus* after Rauhut 2003: character 148; for character history see Ezcurra 2012).
226. Medial side of metacarpal II: expanded proximally (0); not expanded (1) (after Hugi 2008 and Unterrassner 2009, Hugi 2008: character 202; *Eoraptor lunensis*, *Tawa hallae*, *Eodromaeus murphi* and *Allosaurus fragilis* after Ezcurra 2012: character 752, *Ceratosaurus* and *Sinraptor dongi* after Rauhut 2003: character 150; for character history see Ezcurra 2012).
227. Strongly developed anterior lip proximal to the extensor pit on the distal end of metacarpals II and III: absent (0); present (1) (after Hugi 2008 and Unterrassner 2009, Hugi 2008: character 191; *Eoraptor lunensis*, *Eodromaeus murphi* and *Allosaurus fragilis* after Ezcurra 2012: character 754, *Ceratosaurus* and *Sinraptor dongi* after Ezcurra 2006: character 174; for character history see Ezcurra 2012).
228. Metacarpal II in relation to metacarpal III: shorter (0); subequal or longer (1) (after Hugi 2008 and Unterrassner 2009, Hugi 2008: character 194; *Eoraptor lunensis*, *Tawa hallae*, *Eodromaeus murphi* and *Allosaurus fragilis* after Ezcurra 2012: character 751, *Panguraptor lufengensis* and *Ceratosaurus* after You et al. 2014: character 182, *Sinraptor dongi* after Currie & Zhao 1993: Fig. 20 B, C, F, G; for character history see Ezcurra 2012).
229. Width of shaft of metacarpal II compared to metacarpal III: subequal (0); considerably broader (metacarpal III less than 70 per cent of the width of metacarpal II) (1) (after Hugi 2008 and Unterrassner 2009, Hugi 2008: character 203; *Eoraptor lunensis*, *Tawa hallae*, *Eodromaeus murphi* and *Allosaurus fragilis* after Ezcurra 2012: character 760, *Panguraptor lufengensis* after You et al. 2014: 240, Fig. 4, *Ceratosaurus* after Smith et al. 2007: character 239 and Carrano & Choinree 2016: Fig. 7, 8, *Sinraptor dongi* after Currie & Zhao 1993: Fig. 20 B, C, F, G and Smith et al. 2007: character 239; for character history see Ezcurra 2012).
230. Width of distal end of metacarpal II in relation to distal end of metacarpal III: smaller or subequal (0); larger (1) (after Hugi 2008 and Unterrassner 2009, Hugi 2008: character 195; *Eoraptor lunensis*, *Eodromaeus murphi* and *Allosaurus fragilis* after Ezcurra 2012: character 753, *Panguraptor lufengensis* after You et al. 2014: 240, Fig. 4, *Ceratosaurus* after Gilmore 1920: Fig. 62 and Carrano & Choinree 2016: Fig. 7, 8, *Sinraptor dongi* after Currie & Zhao 1993: Fig. 20 B, C, F, G; for character history see Ezcurra 2012).
231. Proximal outline of Mc III: subrectangular (0); triangular, apex dorsal (1) (after Hugi 2008 and Unterrassner 2009, Hugi 2008: character 205; *Eodromaeus murphi* and *Allosaurus fragilis* after Ezcurra 2012: character 761, *Ceratosaurus* after Gilmore 1920: 105 and Carrano & Choinree 2016: Fig. 8 E, *Sinraptor dongi* after Currie & Zhao 1993: Fig. 20 H; for character history see Ezcurra 2012).
232. Shaft of metacarpal III: straight (0); bowed laterally (1) (after Hugi 2008 and Unterrassner 2009, Hugi 2008: character 206; *Eoraptor lunensis*, *Eodromaeus murphi* and *Allosaurus fragilis* after Ezcurra 2012: character 759, *Panguraptor lufengensis* after You et al. 2014: 240, Fig. 4, *Ceratosaurus* after Gilmore 1920: Fig. 62 and Carrano & Choinree 2016: Fig. 8 A-D, *Sinraptor dongi* after Currie & Zhao 1993: Fig. 20 F, G; for character history see Ezcurra 2012).
233. Shaft of metacarpal IV: subequal in width to that of metacarpal II (0), significantly narrower than that of metacarpal II (1), metacarpal IV absent (2) (after Hugi 2008 and Unterrassner 2009, modified from Hugi 2008: character 196; *Eoraptor lunensis*, *Tawa hallae*, *Eodromaeus murphi* and *Allosaurus fragilis* after Ezcurra 2012: character 766, *Panguraptor lufengensis* after You et al. 2014: 240, Tab. 1, Fig. 4, *Ceratosaurus* after Carrano & Choinree 2016: Fig. 7 and 9 and Ezcurra & Novas 2007: character 176, *Sinraptor dongi* after Ezcurra & Novas 2007: character 176; for character history see Ezcurra 2012).
234. Length of metacarpal IV in percentage of metacarpal III length: 27.59% (0), 53.23 to 59.13% (1), 65.14 to 76.19 (2), 88.58% (after Ezcurra 2012: character 765; *Panguraptor lufengensis* after You et al. 2014: Tab. 1, Fig. 4, 64.71%, *Ceratosaurus* after Gilmore 1920: Fig. 62, 67.31%, *Sinraptor dongi* after Currie & Zhao 1993: 2067 and Fig. 20 G, 44.54% Frick theropod: 75% ; for character history see Ezcurra 2012).
235. Position of metacarpal IV: lateral to metacarpals I to III (0), palmar to metacarpals I to III (1) (after Ezcurra 2012: character 767; *Herrerasaurus ischigualastensis*, *Dilophosaurus wetherilli*, "*Syntarsus*" *kayentakatae*, *Coelophysis*

rhodesiensis and Frick theropod after Hugi: character 197, Panguraptor lufengensis after You et al. 2014: Fig. 4, Ceratosaurus after Gilmore 1920: Fig. 60 and Ezcurra 2006: character 191, Allosaurus fragilis after Ezcurra 2006: character 191; for character history see Ezcurra 2012).

236. Metacarpal V: present, well developed, with phalanges (0); present, reduced to vestigial, lacking phalanges (1); absent (2) (after Hugi 2008 and Unterrassner 2009, Hugi 2008: character 198; Eoraptor lunensis and Eodromaeus murphi after Ezcurra 2012: character 773, Panguraptor lufengensis after You et al. 2014: Fig. 4, Ceratosaurus after Gilmore 1920: Fig. 60, 62 and Ezcurra & Novas 2007: character 179, Allosaurus fragilis after Gilmore 1920: Fig. 40 and Ezcurra & Novas 2007: character 179; for character history see Ezcurra 2012).

237. First phalanx of manual digit I: not the longest non-ungual phalanx of the manus (0); longest non-ungual phalanx of the manus (1) (after Hugi 2008 and Unterrassner 2009, Hugi 2008: character 211; Eoraptor lunensis after Sereno, Martinez & Alcober 2012: Fig. 70, 73, 74 and Tab. 8, Tawa hallae after Nesbitt et al. 2009: character 180, Eodromaeus murphi after Martinez et al. 2011: Fig. 1G, Ceratosaurus after You et al. 2014: character 180, Allosaurus fragilis after Gilmore 1920: Fig. 40 and Madsen 1976: Pl. 45, Sinraptor dongi after Currie & Zhao 1993: 2067 and Fig. 20; for character history see Nesbitt et al. 2009).

238. Distal end of first phalanx of manual digit I ventrolaterally twisted around the transversal axis of the bone in relation to its proximal end: absent (0); present (1) (after Hugi 2008 and Unterrassner 2009, Hugi 2008: character 212; Eoraptor lunensis, Tawa hallae, Eodromaeus murphi and Allosaurus fragilis after Ezcurra 2012: character 745; for character history see Ezcurra 2012).

239. Manual digit II longer than digit III: absent (0); present (1) (after Hugi 2008 and Unterrassner 2009, Hugi 2008: character 213; Eoraptor lunensis, Tawa hallae, Eodromaeus murphi and Allosaurus fragilis after Ezcurra 2012: character 755, Panguraptor lufengensis after You et al. 2014: Fig. 4, Tab. 1; for character history see Ezcurra 2012).

240. Number of phalanges in digit IV: more than one (0), one (1), none (2) (modified from Ezcurra 2012: character 768; Eoraptor lunensis after Sereno, Martinez & Alcober 2012: 149, estimated, Herrerasaurus ischigualastensis after Sereno 1994: 410, Dilophosaurus wetherilli after Rauhut 2003: Fig. 36, Procompsognathus triassicus, Coelophysis bauri, Coelophysis rhodesiensis, Ceratosaurus and Allosaurus fragilis after Rauhut 2003: character 153, "Syntarsus" kayentakatae after Tykoski 1998: 82 and 83, Panguraptor lufengensis after You et al. 2014: 240 and 241, Frick theropod after Hugi 2008: Fig. 3 and Unterrassner 2009: Fig. 11a; for character history see Ezcurra 2012).

241. Penultimate phalanx of second manual digit: subequal or shorter than first phalanx (0); longer than first phalanx (1) (after Hugi 2008 and Unterrassner 2009, modified from Hugi 2008: character 218, Eoraptor lunensis and Allosaurus fragilis after Ezcurra & Novas 2007: character 173; Tawa hallae after Nesbitt et al. 2009: Fig. 2F, Eodromaeus murphi after Martinez et al. 2012: Fig. 1G, Panguraptor lufengensis after You et al. 2014: Tab. 1; for character history see Ezcurra & Novas 2007).

242. Penultimate phalanx of third manual digit: as long as, or shorter than, more proximal phalanges (0); longer than each of the more proximal phalanges (1); longer than both proximal phalanges taken together (2) (after Hugi 2008 and Unterrassner 2009, Hugi 2008: character 219; Eoraptor lunensis after Rauhut 2003: character 160 and Sereno, Martinez & Alcober 2012: Fig. 70, 73 and 74, Tawa hallae after Nesbitt et al. 2009: Fig. 2F, Eodromaeus murphi after Martinez et al. 2011: Fig. 1G and Tab. S1, Panguraptor lufengensis after You et al. 2014: Fig. 4 and Tab. 1, Allosaurus fragilis after Rauhut 2003: character 160 and Gilmore 1920: Figs. 40 and 45; for character history see Rauhut 2003).

243. Anterior lip at proximal articular end of manual unguis: absent (0); present (1) (after Hugi 2008 and Unterrassner 2009, Hugi 2008: character 221; Eoraptor lunensis, Tawa hallae, Eodromaeus murphi, Zupaysaurus rougieri and Allosaurus fragilis after Ezcurra 2012: character 748, Panguraptor lufengensis after You et al. 2014: Fig. 4; Sinraptor dongi after Smith et al. 2007: character 250; for character history see Ezcurra 2012).

244. Flexor tubercle on manual unguis: less than half the height of the articular facet (0); more than half the height of the articular facet (1) (after Hugi 2008 and Unterrassner 2009, Hugi 2008: character 222; Eoraptor lunensis, Tawa hallae, Zupaysaurus rougieri and Allosaurus fragilis after Ezcurra 2012: character 749, Panguraptor lufengensis after You et al. 2014: Fig. 4, Sinraptor dongi after Smith et al. 2007: character 250; for character history see Ezcurra 2012).

245. Ungual phalanx of digit II: longest of the manus (0); equal in length to the unguis of digit I (1) (after Hugi 2008 and Unterrassner 2009, Hugi 2008: character 216; Eoraptor lunensis, Tawa hallae, Eodromaeus murphi and Allosaurus fragilis after Ezcurra 2012: character 758; for character history see Ezcurra 2012).

246. Unguis of manual digits II and III: poorly curved (0); trenchant, i.e. strongly curved, tips of claws below level of flexor tubercle (1) (after Hugi 2008 and Unterrassner 2009, Hugi 2008: character 215; Eoraptor lunensis, Tawa hallae, Eodromaeus murphi, Zupaysaurus rougieri and Allosaurus fragilis after Ezcurra 2012: character 757, Sinraptor dongi after Currie & Zhao 1993: Fig. 20X and Smith et al. 2007: character 248, Frick theropod, coding changed; for character history see Ezcurra 2012).

247. Fusion of bones in pelvic girdle: separate elements throughout ontogeny (0); fused together by late ontogeny (1) (after Hugi 2008 and Unterrassner 2009, Hugi 2008: character 133; Tawa hallae, Eodromaeus murphi, Cryolophosaurus ellioti and Allosaurus fragilis and Piatnitzkysaurus floresii after Ezcurra 2012: character 575, Ceratosaurus and Sinraptor dongi after Carrano et al. 2012: character 261; for character history see Ezcurra 2012).

248. Supraacetabular crest of ilium: present as a weakly developed ridge (0); present as a laterally well-developed raised shelf (1); flares lateroventrally to form a hood-like overhang that hides craniodorsal half of acetabulum in lateral view (2) (after Hugi 2008 and Unterrassner 2009, Hugi 2008: character 134; Eoraptor lunensis after Tykoski 2005: 205 and 206, character 195, Tawa hallae, Eodromaeus murphi, Cryolophosaurus ellioti and Piatnitzkysaurus floresii after Ezcurra 2012: character 800, Ceratosaurus after Ezcurra & Novas 2007: character 188 and Carrano et al. 2012:

character 267, *Allosaurus fragilis* after Gilmore 1920: Pl. 10 Fig. 2 and Ezcurra 2012: character 800, *Eustreptospondylus oxoniensis* after Carrano et al. 2012: character 267, *Sinraptor dongi* after Currie & Zhao 1993: Fig. 21A and Ezcurra & Novas 2007: character 188; for character history see Ezcurra 2012).

249. Lateral surface of caudal end of ilium: smooth (0); distinct rim for m. iliofibularis (1) (after Hugi 2008 and Unterrassner 2009, Hugi 2008: character 138; *Eoraptor lunensis*, “*Syntharsus*” *kayentakatae* and *Dilophosaurus wetherilli* after Ezcurra 2006: character 200, *Tawa hallae* after Nesbitt et al. 2009: Fig. 2C, *Ceratosaurus* after Gilmore 1920: Pl. 23 and Ezcurra & Novas 2007: character 186, *Allosaurus fragilis* after Gilmore 1920: Pl. 10 Fig. 2 and Ezcurra & Novas 2007: character 186, *Eustreptospondylus oxoniensis* after Sadleir et al. 2008: Pl. 20.1 and Tykoski 2005: character 199, *Sinraptor dongi* after Currie & Zhao 1993: 2067, Fig. 21 A and Ezcurra & Novas 2007: character 186, *Piatnitzkysaurus floresii* after Smith et al. 2007: character 263; for character history see Hugi 2008).

250. Dorsal margin of iliac blade in lateral view: more or less straight/angular (0); slightly convex and obviously curved (1); strongly convex (2) (after Hugi 2008 and Unterrassner 2009, modified from Hugi 2008: character 139 and Tykoski 2005: character 191; *Eoraptor lunensis* after Sereno et al. 2012:152, Fig. 82A and Tykoski 2005: character 191, *Eodromaeus murphi* after Ezcurra 2012: character 775, *Dilophosaurus wetherilli* after Tykoski 2005: Fig. 67E, 67F, character 191 and Ezcurra & Cuny 2007: Fig. 5F, *Liliensternus liliensterni* after Tykoski 2005: Fig. 69C, character 191, *Cryolophosaurus ellioti* after Smith et al. 2007: 402, Fig. 15A, *Ceratosaurus* after Gilmore 1920: Fig. 63, Pl. 23, Tykoski 2005: character 191 and Carrano et al. 2012: character 277, *Allosaurus fragilis* after Gilmore 1920: Pl. 10 Fig. 2, Tykoski 2005: character 191, Ezcurra & Novas 2007: character 180 and Carrano et al. 2012: character 277, *Eustreptospondylus oxoniensis* after Sadleir et al. 2008: 39, Pl. 21 Fig. 1, 2, Tykoski 2005: character 191 and Carrano et al. 2012: character 277, *Piatnitzkysaurus floresii* after Bonaparte 1979: Fig. 22 and Ezcurra 2012: character 775, *Sinraptor dongi* after Currie & Zhao 1993: Fig. 21A,B, Ezcurra & Novas 2007: character 180 and Carrano et al. 2012: character 277; for character history see Ezcurra 2012).

251. Pronounced ventral hook on anterior expansion of ilium: absent (0); present (1) (after Hugi 2008 and Unterrassner 2009, Hugi 2008: character 141; *Eoraptor lunensis* after Ezcurra & Cuny 2007: character 106, *Tawa hallae* after Nesbitt et al. 2009: Fig. 2C, *Eodromaeus murphi* after Martinez et al. 2011: Fig. 2A, *Ceratosaurus* after Rauhut 2003: character 168, *Allosaurus fragilis* after Gilmore 1920: Fig. 46, Pl. 10 Fig. 2, Madsen 1976: Pl. 46, 47, Ezcurra & Cuny 2007: Fig. 5G and Rauhut 2003: character 168, *Eustreptospondylus oxoniensis* after Sadleir et al. 2008: Pl. 20 Fig. 1, 2, *Sinraptor dongi* after Currie & Zhao 1993: Fig. 21 A, B and Rauhut 2003: character 168; for character history see Ezcurra & Cuny 2007).

252. Continuity of supraacetabular crest and ventrolateral margin of postacetabular blade (= lateral brevis shelf): absent, not continuous (0); present, continuous as a weakly developed ridge (1); present, continuous as a well developed ridge, with non-distinct separation between both structures (2) (after Hugi 2008 and Unterrassner 2009, modified from Hugi 2008: character 145; *Eoraptor lunensis*, *Ceratosaurus*, *Allosaurus fragilis* and *Sinraptor dongi* after Ezcurra & Novas 2007: character 189, *Tawa hallae* after Nesbitt et al. 2009: 1531, Fig. 2C, *Cryolophosaurus ellioti* after Smith et al. 2007: 402, Fig. 15A, *Eustreptospondylus oxoniensis* after Sadleir et al. 2008: 40, Pl. 20.1; for character history see Ezcurra & Cuny 2007).

253. Shape of brevis fossa: narrow, with subparallel margins or posteriorly slightly expanded (0); posteriorly strongly expanded (1) (after Hugi 2008 and Unterrassner 2009, Hugi 2008: character 147; *Eoraptor lunensis*, *Eodromaeus murphi*, *Cryolophosaurus ellioti*, *Allosaurus fragilis* and *Piatnitzkysaurus floresii* after Ezcurra 2012: character 804, *Ceratosaurus* and *Sinraptor dongi* after Ezcurra & Novas 2007: character 190, *Eustreptospondylus oxoniensis* after Smith et al. 2007: character 270; for character history see Ezcurra 2012).

254. Articulation facet of pubic peduncle of ilium: facing more ventrally than anteriorly, without pronounced kink between pubic peduncle and praeacetabular process of ilium (0); facing more anteriorly than ventrally, with pronounced kink between pubic peduncle and praeacetabular process of ilium (1) (after Hugi 2008 and Unterrassner 2009, Hugi 2008: character 148; *Eoraptor lunensis*, *Segisaurus halli*, *Ceratosaurus* and *Allosaurus fragilis* after Ezcurra & Novas 2007: character 193, *Tawa hallae* after Nesbitt et al. 2009: Fig. 2, *Panguraptor lufengensis* after You et al. 2014: Fig. 1, *Eustreptospondylus oxoniensis*, *Piatnitzkysaurus floresii* and *Sinraptor dongi* after Carrano et al. 2012: character 268; for character history see Ezcurra & Novas 2007).

255. Obturator notch or foramen of ischium: absent (0); present (1) (after Hugi 2008 and Unterrassner 2009, Hugi 2008: character 152; *Eoraptor lunensis* and *Allosaurus fragilis* after Ezcurra & Cuny 2007: character 110, *Eodromaeus murphi* after Martinez et al. 2012: Fig. 2, *Ceratosaurus* after Ezcurra 2012: character 859, *Sinraptor dongi* after Currie & Zhao 1993: 2069, Fig. 21G, J; for character history see Ezcurra 2012).

256. Ventral notch behind obturator process or flange on ischium: absent (0); present (1) (after Hugi 2008 and Unterrassner 2009, Hugi 2008: character 153; *Eoraptor lunensis*, *Cryolophosaurus ellioti*, *Ceratosaurus*, *Eustreptospondylus oxoniensis*, *Piatnitzkysaurus floresii* and *Sinraptor dongi* after Smith et al. 2007: character 289, *Eodromaeus murphi* after Martinez et al. 2012: Fig. 2, *Allosaurus fragilis* after Tykoski 2005: Fig. 73A and 73B; for character history see Smith et al. 2007).

257. Ischium length in relation to pubis length: at least three-quarters (0); two-thirds or less (1); less than three-quarters and more than two-thirds (2) (after Hugi 2008 and Unterrassner 2009, Hugi 2008: character 155; *Eoraptor lunensis*, *Eodromaeus murphi*, *Liliensternus liliensterni* and *Allosaurus fragilis* after Ezcurra 2012: character 851, *Ceratosaurus*, *Eustreptospondylus oxoniensis*, *Piatnitzkysaurus floresii* and *Sinraptor dongi* after Smith et al. 2007: character 284 and Holtz 2000, Sadleir et al. 2008: character 320 of Holtz 2000; for character history see Ezcurra 2012).

258. Distal end of ischium: unexpanded or slightly expanded (0); strongly expanded, anteroposterior length more than twice the ischial shaft diameter, distal tip of ischium forms a smaller boot than that of the pubis (1) strongly expanded, anteroposterior length more than twice the ischial shaft diameter, distal tip of ischium forms a larger boot than that of the pubis (2) (after Hugi 2008 and Unterrassner 2009, modified from Hugi 2008: character 157; *Eoraptor lunensis* after Sereno, Martinez & Alcober 2012: Fig. 80 to 82, *Tawa hallae* after Nesbitt et al. 2009: Fig. 2, *Eodromaeus murphi* after Martinez et al. 2011: Fig. 2, *Cryolophosaurus ellioti* after Smith et al. 2007: 404, Fig. 15, *Panguraptor lufengensis* after You et al. 2014: Fig. 1, *Ceratosaurus* after Gilmore 1920: Pl. 23, *Allosaurus fragilis* after Madsen 1976: Pl. 48 and 49, *Eustreptospondylus oxoniensis* after Sadleir et al. 2008: 42, Fig. 18, *Piatnitzkysaurus floresi* after Smith et al. 2007: character 290, *Sinraptor dongi* after Rauhut 2003: character 193 and Currie & Zhao 1993: Fig. 21D, J; for character history see Smith et al. 2007).

259. Shape of pubic shaft in lateral view: more or less straight, margins may be weakly curved (0); distinctly bowed posteriorly (1) (after Hugi 2008 and Unterrassner 2009, modified from Hugi 2008: character 158; *Eoraptor lunensis* after Sereno, Martinez & Alcober 2012: Fig. 82, *Tawa hallae* after Nesbitt et al. 2009: Fig. 2H, *Eodromaeus murphi* after Martinez et al. 2011: Fig. 2H, *Dilophosaurus wetherilli* and *Liliensternus liliensterni* after Tykoski 2005: character 207, *Cryolophosaurus ellioti* after Smith et al. 2007: 403, Fig. 15A, *Procompsognathus triassicus* after Ezcurra & Novas 2007: character 196, *Ceratosaurus* after Gilmore 1920: Pl. 23 and Tykoski 2005: character 207, *Allosaurus fragilis* after Madsen 1976: Pl. 48 and 49; for character history see Ezcurra & Novas 2007). *Eustreptospondylus oxoniensis*, *Piatnitzkysaurus floresi* and *Sinraptor dongi* after Carrano et al. 2012: character 282, and after Sadleir et al. 2008: Fig. 17B, D, Bonaparte 1979: Fig. 1, Currie & Zhao 1993: 2069, Fig. 21 D, F

260. Distal expansion of pubis: absent or weakly developed (0); strongly developed, forming a pubis boot (1) (after Hugi 2008 and Unterrassner 2009, modified from Hugi 2008: character 159; *Eoraptor lunensis* after Sereno, Martinez & Alcober 2012: Fig. 82 and Ezcurra & Novas 2007: character 198, *Herrerasaurus ischigualastensis* after Tykoski 2005: Fig. 72C, *Tawa hallae* after Nesbitt et al. 2009: Fig. 2H and character 207, *Eodromaeus murphi* after Martinez et al. 2011: Fig. 2H, *Ceratosaurus* after Gilmore 1920: Fig. 63 Pl. 23, 27 above, 29, 30 and Ezcurra & Novas 2007: character 198, *Allosaurus fragilis* after Gilmore 1920: Fig. 47, Pl. 11, 13 and Ezcurra & Novas 2007: character 198, *Eustreptospondylus oxoniensis*, *Piatnitzkysaurus floresi* and *Sinraptor dongi* after Smith et al. 2007: character 280, and after Sadleir et al. 2008: Fig. 17G, Bonaparte 1979: Fig. 1, Currie & Zhao 1993: 2069, Fig. 21 D, F; for character history see Ezcurra & Novas 2007).

261. Anteroposterior expansion of distal end of pubis: absent (0); present, anteriorly and posteriorly developed (1); mainly posteriorly developed (2) (after Hugi 2008 and Unterrassner 2009, modified from Hugi 2008: character 162; *Eoraptor lunensis*, *Tawa hallae*, *Eodromaeus murphi*, *Liliensternus liliensterni*, *Coelophysis rhodesiensis* and *Piatnitzkysaurus floresi* after Ezcurra 2012: character 845, *Herrerasaurus ischigualastensis* after Tykoski 2005: 72C, *Coelophysis bauri* after Hugi 2008: character 166 and Rinehart et al. 2009: 69, Fig. 76A, 78, *Dilophosaurus wetherilli* after Welles 1984: Fig. 31A, *Ceratosaurus* after Gilmore 1920: Fig. 63 Pl. 23, 27 above, 29, 30, *Allosaurus fragilis* after Tykoski 2005: Fig. 73A, 73B and Ezcurra 2012: character 845, *Eustreptospondylus oxoniensis* after Sadleir et al. 2008: Fig. 17G, *Sinraptor dongi* after Currie & Zhao 1993: 2069, Fig. 21 D, F; for character history see Ezcurra 2012).

262. Pubic apron: completely closed, with or without distal notch (0); with medial fenestra (1) (after Hugi 2008 and Unterrassner 2009, modified from Hugi 2008: character 164; *Eoraptor lunensis*, *Eodromaeus murphi* and *Piatnitzkysaurus floresi* after Ezcurra 2012: character 842, *Dilophosaurus wetherilli* after Welles 1984: Fig. 31A, *Ceratosaurus* and *Sinraptor dongi* after Smith et al. 2007: character 279 and Rauhut 2003: character 181, *Allosaurus fragilis* after Gilmore 1920: Pl. 11 Fig. 1, Tykoski 2005: Fig. 73C and Ezcurra 2012: character 842; for character history see Ezcurra 2012).

263. Obturator foramen of pubis: completely enclosed (0); open ventrally (1); absent (2) (after Hugi 2008 and Unterrassner 2009, Hugi 2008: character 165; *Eoraptor lunensis* after Sereno et al. 2012: 155, Fig. 78, 82A and Ezcurra 2012: character 830, *Eodromaeus murphi* after Ezcurra 2012: character 830, *Dilophosaurus wetherilli* after Smith et al. 2007: character 279 and Tykoski 2005: Fig. 75C, 76C, *Cryolophosaurus ellioti* after Smith et al. 2007: character 279, Fig. 15A, *Ceratosaurus* after Gilmore 1920: Fig. 63 Pl. 23, 27 above, Tykoski 2005: Fig. 74A, *Allosaurus fragilis* after Gilmore 1920: Pl. 11 Fig. 2 and Ezcurra 2012: character 830, *Piatnitzkysaurus floresi* after Ezcurra 2012: character 830 and Smith et al. 2007: character 279, *Eustreptospondylus oxoniensis* and *Sinraptor dongi* after Smith et al. 2007: character 279; for character history see Ezcurra 2012).

264. Pubic fenestra below obturator foramen: absent (0); present, enclosed (1); present, opened ventrally (2); present, intersect with obturator foramen to form obturator notch (3) (after Hugi 2008 and Unterrassner 2009, modified from Hugi 2008: character 166; *Eoraptor lunensis* after Ezcurra 2012: character 833, Sereno et al. 2012: 155, Fig. 78, 82A, *Segisaurus halli* after Hugi 2008: character 166 and Carrano et al. 2005: 839, Fig. 7A, *Coelophysis bauri* after Hugi 2008: character 166 and Rinehart et al. 2009: Fig. 78, *Cryolophosaurus ellioti* and *Allosaurus fragilis* after Ezcurra 2012: character 833, Tykoski 2005: character 205, Fig. 73, *Ceratosaurus* after Gilmore 1920: Fig. 63 Pl. 23, 27 above and Tykoski 2005: 74A, *Eustreptospondylus oxoniensis* after Sadleir et al. 2008: character 308 of Holtz 2000, Smith et al. 2007: character 277 and Tykoski 2005: character 205, *Sinraptor dongi* after Smith et al. 2007: character 277 and Currie & Zhao 1993: Fig. 21D, F; for character history see Ezcurra 2012).

265. Ratio of femur to humerus: more than 2.5 (0); between 1.2 and 2.2 (1); less than 1 (2) (after Hugi 2008 and Unterrassner 2009, Hugi 2008: character 180; *Eoraptor lunensis*, *Tawa hallae*, *Eodromaeus murphi*, *Allosaurus fragilis* and *Piatnitzkysaurus floresi* after Ezcurra 2012: deduced from character 672, *Ceratosaurus* after Gilmore 1920,

Eustreptospondylus oxoniensis after Sadleir et al. 2008: Tab. 1 and 3: value 2.156; for character history see Ezcurra 2012).

266. Shape of femoral anterior trochanter (lesser trochanter = cranial trochanter): absent or poorly developed, low ridge or tuberosity (0); spike-like or pyramidal prominence (1); anteroposteriorly broadened, wing like, aliform (2) (after Hugi 2008 and Unterrassner 2009, Hugi 2008: character 227; Eoraptor lunensis, Cryolophosaurus ellioti, Allosaurus fragilis and Piatnitzkysaurus floresi after Ezcurra 2012: character 901, Tawa hallae after Nesbitt et al. 2009: Fig. 2I, Eodromaeus murphi after Martinez et al. 2011: 207, Figs. 2K and 2L, Panguraptor lufengensis after You et al. 2014: 241, Fig. 1, Ceratosaurus after Tykoski 2005: character 222, Fig. 1 and Smith et al. 2007: character 297, Eustreptospondylus oxoniensis and Sinraptor dongi after Smith et al. 2007: character 297; for character history see Ezcurra 2012).

267. Placement of anterior trochanter: at distal end of femoral head (0); more proximally placed, but below the greater trochanter (1) (after Hugi 2008 and Unterrassner 2009, Hugi 2008: character 228; Eoraptor lunensis after Sereno, Martinez & Alcober 2012: Figs. 78 and 86, Tawa hallae after Nesbitt et al. 2009: Fig. 2I, Eodromaeus murphi after Martinez et al. 2011: 207, Figs. 2K and 2L, Cryolophosaurus ellioti after Smith et al. 2007: 404, Figs. 16A, 17A, 17C and 17D, Panguraptor lufengensis after You et al. 2014: 241, Fig. 1, Ceratosaurus, Allosaurus fragilis, Piatnitzkysaurus floresi and Sinraptor dongi after Rauhut 2003: character 199, Eustreptospondylus oxoniensis after Sadleir et al. 2008: 43, Fig. 19B; for character history see Rauhut 2003).

268. Tibiofibular crest of posterodistal femur in late ontogeny: smoothly continuous with lateral fibular condyle (0); sharply demarcated from lateral fibular condyle by a sulcus or concavity (1) (after Hugi 2008 and Unterrassner 2009, Hugi 2008: character 229; Eoraptor lunensis and Sinraptor dongi after Ezcurra & Novas 2007: character 216 and Sereno et al. 2012: 159, Curry & Zhao 1993: Fig. 22D, E, Tawa hallae, Eodromaeus murphi, Zupaysaurus rougieri, Allosaurus fragilis and Piatnitzkysaurus floresi after Ezcurra 2012: character 929, Cryolophosaurus ellioti after Smith et al. 2007: 404, Figs. 16D and 17D, Fig. 1, Ceratosaurus after Tykoski 2005: character 227 and Gilmore 1920: Fig. 64C; for character history see Ezcurra 2012).

269. Femoral popliteal fossa in adults: smooth (0); transversed by infrapopliteal ridge between tibial condyle and tibiofibular crest (1) (after Hugi 2008 and Unterrassner 2009, Hugi 2008: character 230; Tawa hallae, Eodromaeus murphi, Cryolophosaurus ellioti, Allosaurus fragilis and Piatnitzkysaurus floresi after Ezcurra 2012: character 922, Ceratosaurus after Tykoski 2005: character 228, Sinraptor dongi after Ezcurra & Novas 2007: character 217; for character history see Ezcurra 2012).

270. Medial epicondyle (= mediodistal crest) on anteromedial surface of distal femur in adults: absent or weak (0); present as ridge (1); present, hypertrophied and flangelike (2) (after Hugi 2008 and Unterrassner 2009, modified from Hugi 2008: character 231; Eoraptor lunensis, Tawa hallae, Eodromaeus murphi, Cryolophosaurus ellioti, Allosaurus fragilis and Piatnitzkysaurus floresi after Ezcurra 2012: character 915, Zupaysaurus rougieri, Liliensternus liliensterni, "Syntarsus" kayentakatae and Eustreptospondylus oxoniensis after Tykoski 2005: character 225, Ceratosaurus after Gilmore 1920: Fig. 64, Sinraptor dongi after Currie & Zhao 1993: 2069, Fig. 22B; for character history see Ezcurra 2012).

271. Broad groove on anterior surface of distal femur: absent or poorly developed (0); well developed and bound medially by an expanded medial lamella (1) (after Smith et al. 2007: character 302; Tawa hallae after Nesbitt et al. 2009: Fig. 2I, Eodromaeus murphi after Martinez et al. 2011: Figs. 2K and 2M, Segisaurus halli and Allosaurus fragilis after Rauhut 2003: character 202; for character history see Smith et al. 2007).

272. Proximal tuberosity or crest on lateral side of tibia for connection with fibula: absent (0); present, extending from the proximal articular surface distally (1); present, clearly separated from proximal articular surface (2) (after Hugi 2008 and Unterrassner 2009, modified from Hugi 2008: character 233; Tawa hallae, Eodromaeus murphi and Allosaurus fragilis after Ezcurra 2012: character 947, Zupaysaurus rougieri, Ceratosaurus, Eustreptospondylus oxoniensis and Sinraptor dongi after Smith et al. 2007: character 308, Piatnitzkysaurus floresi after Ezcurra 2012: character 947 and Smith et al. 2007: character 308; for character history see Ezcurra 2012).

273. Shape of lateral malleolus of tibia: lobe-like (0); polygonal, with marked angles (1) (after Hugi 2008 and Unterrassner 2009, Hugi 2008: character 234; Tawa hallae, Eodromaeus murphi, Cryolophosaurus ellioti, Allosaurus fragilis and Piatnitzkysaurus floresi after Ezcurra 2012: character 955, Ceratosaurus after Ezcurra & Novas 2007: character 225, Eustreptospondylus oxoniensis and Sinraptor dongi after Smith et al. 2007: character 309; for character history see Ezcurra 2012).

274. Distal articular surface of tibia: subrectangular to round in outline and slightly wider transversely than anteroposteriorly (0); subrectangular with small lateral process (1); anteroposteriorly narrow triangular in outline and strongly mediolaterally expanded (2) (after Hugi 2008 and Unterrassner 2009, Hugi 2008: character 236; Eoraptor lunensis, Eodromaeus murphi, Zupaysaurus rougieri and Cryolophosaurus ellioti after Ezcurra 2012: character 966, Ceratosaurus, Allosaurus fragilis and Sinraptor dongi after Rauhut 2003: character 208, Eustreptospondylus oxoniensis after Sadleir et al. 2008: Fig. 20A-D and Smith et al. 2007: character 311, Piatnitzkysaurus floresi after Ezcurra 2012: character 966, Rauhut 2003: Fig. 45C, character 208 and Smith et al. 2007: character 311; for character history see Ezcurra 2012).

275. Facet for the reception of the ascending process of the astragalus on the tibia: quadrangular, anteroposteriorly and mediolaterally equally expanded (0); subtriangular, not well expanded anteriorly (1); subrectangular, not well expanded anteriorly (2); not differentiated, nearly absent (3) (after Hugi 2008 and Unterrassner 2009, Hugi 2008: character 237; Eoraptor lunensis, Eodromaeus murphi, Zupaysaurus rougieri, Allosaurus fragilis and Piatnitzkysaurus floresi after

Ezcurra 2012: character 958, *Coelophysis bauri* after Ezcurra & Novas 2007: character 227 and Ezcurra 2012: character 958, *Ceratosaurus* and *Sinraptor dongi* after Ezcurra & Novas 2007: character 227; for character history see Ezcurra 2012).

276. Proximal ridge on medial side of fibula that runs anterodistally from the posteroproximal end: absent (0); present (1) (after Hugi 2008 and Unterrassner 2009, Hugi 2008: character 238; *Tawa hallae* after Nesbit et al. 2009: character 264, *Eodromaeus murphi* after Martinez et al. 2011: Fig. 2I, *Segisaurus halli*, *Ceratosaurus*, *Allosaurus fragilis*, *Piatnitzkysaurus floresii* and *Sinraptor dongi* after Rauhut 2003: character 209, *Eustreptospondylus oxoniensis* after Smith et al. 2007: character 314; for character history see Nesbit et al. 2009).

277. Astragalus and calcaneum fusion: absent, separate elements throughout ontogeny (0); present in later stages of ontogeny (1) (after Hugi 2008 and Unterrassner 2009, Hugi 2008: character 240; *Eoraptor lunensis* after Sereno, Martinez & Alcober 2012: Figs. 87 and 88, *Tawa hallae* after Nesbitt et al. 2009: 1532, *Eodromaeus murphi* after Martinez et al. 2011: Fig. 2J, *Zupaysaurus rougieri*, *Ceratosaurus* and *Allosaurus fragilis* after Ezcurra & Novas 2007: character 237, *Cryolophosaurus ellioti* after Smith et al. 2007: 406, character 327, *Sinraptor dongi* after Carrano et al. 2012: character 339 and Smith et al. 2007: character 327; for character history see Ezcurra & Novas 2007).

278. Height of ascending process of astragalus in relation to height of astragalar body measured immediately below ascending process in adults: lower (0); subequal or higher (1) (after Hugi 2008 and Unterrassner 2009, modified from Hugi 2008: character 241; *Eoraptor lunensis* after Sereno, Martinez & Alcober 2012: Fig. 88, *Tawa hallae*, *Zupaysaurus rougieri*, *Dilophosaurus wetherilli*, *Cryolophosaurus ellioti* and *Allosaurus fragilis* after Ezcurra 2012: character 994, *Ceratosaurus*, *Eustreptospondylus oxoniensis* and *Sinraptor dongi* after Carrano et al. 2012: character 333, Smith et al. 2007: character 321, and after Sadleir et al. 2008: Fig. 21A,B; for character history see Ezcurra 2012).

279. Deep fossa on anterolateral surface of ascending process of astragalus: absent (0); present (1) (after Hugi 2008 and Unterrassner 2009, modified from Hugi 2008: character 243; *Zupaysaurus rougieri*, *Cryolophosaurus ellioti* and *Allosaurus fragilis* after Ezcurra 2012: character 998, *Ceratosaurus* and *Sinraptor dongi* after Ezcurra & Novas 2007: character 240, *Eustreptospondylus oxoniensis* after Sadleir et al. 2008: Fig. 21A, C; for character history see Ezcurra 2012).

280. Horizontal groove across anterior surface of astragalar condyles: absent (0); present (1) (after Hugi 2008 and Unterrassner 2009, Hugi 2008: character 244; *Zupaysaurus rougieri* and *Cryolophosaurus ellioti* and after Ezcurra 2012: character 1001, *Allosaurus fragilis*, *Ceratosaurus* and *Sinraptor dongi* after Rauhut 2003: character 218, *Eustreptospondylus oxoniensis* after Sadleir et al. 2008:47, character 365 of Holtz 2000; for character history see Ezcurra 2012).

281. Facet for tibia on calcaneum: absent (0); present, small facet posteromedially (1); present, well-developed facet posteriorly (2) (after Hugi 2008 and Unterrassner 2009, Hugi 2008: character 245; *Eoraptor lunensis* after Sereno, Martinez & Alcober 2012: Figs. 88A to 88C, *Tawa hallae* after Nesbitt et al. 2009: character 285 state 0 implicates no tibial facet on calcaneum, *Eodromaeus murphi* after Martinez et al. 2011: Fig. 2J, *Zupaysaurus rougieri*, *Dilophosaurus wetherilli*, *Cryolophosaurus ellioti*, *Ceratosaurus*, *Eustreptospondylus oxoniensis* and *Sinraptor dongi* after Smith et al. 2007: character 328, *Panguraptor lufengensis* after You et al. 2014: Fig. 5, *Allosaurus fragilis* after Tykoski 2005: Fig. 99B and Rauhut 2003: character 219; for character history see Smith et al. 2007).

282. Metatarsal I: contacts the ankle joint (0); reduced, elongated splint-like, attached to Mt II and not reaching the ankle joint (1); reduced, broadly triangular, attached to the distal part of Mt II (2) (after Hugi 2008 and Unterrassner 2009, Hugi 2008: character 248; *Eoraptor lunensis* after Sereno, Martinez & Alcober 2012: Figs. 89 and 91, *Tawa hallae* after Nesbitt et al. 2009: Fig. 2J, *Eodromaeus murphi* after Martinez et al. 2011: Fig. 2, *Allosaurus fragilis* after Ezcurra 2012: character 1044, *Sinraptor dongi* after Rauhut 2003: character 222 and Ezcurra & Novas 2007: character 247; for character history see Ezcurra 2012).

283. Co-ossification of proximal ends of metatarsals II and III in adults: absent (0); present (1) (after Hugi 2008 and Unterrassner 2009, Hugi 2008: character 249; *Tawa hallae* after Nesbitt et al. 2009: Fig. 2J, *Eodromaeus murphi* after Martinez et al. 2011: Fig. 2, *Ceratosaurus* and *Allosaurus fragilis* after Tykoski 2005: character 257 and Ezcurra & Novas 2007: character 249, *Sinraptor dongi* after Ezcurra & Novas 2007: character 249; for character history see Ezcurra & Novas 2007).

284. Proximal end of metatarsal III: not elongated posteriorly, does not back posterior sides of metatarsals II and IV (0); with posterior process, backs metatarsals II and IV posteriorly (T-shaped proximal profile: «antarctometatarsus») (1) (after Hugi 2008 and Unterrassner 2009, Hugi 2008: character 250; *Eoraptor lunensis*, *Tawa hallae*, *Eodromaeus murphi*, *Allosaurus fragilis* and *Piatnitzkysaurus floresii* after Ezcurra 2012: character 1066, *Panguraptor lufengensis* after You et al. 2014: character 298, *Ceratosaurus*, *Eustreptospondylus oxoniensis* and *Sinraptor dongi* after Smith et al. 2007: character 336 and Carrano et al. 2012: character 347; for character history see Ezcurra 2012).

285. Distal articular facet of metatarsal V: present, rounded (0); absent, metatarsal V strongly reduced (1); absent, metatarsal V short, transversely flattened and anteriorly bowed distally (2) (after Hugi 2008 and Unterrassner 2009, Hugi 2008: character 251; *Eoraptor lunensis*, "Syntarsus" *kayentakatae* and *Allosaurus fragilis* after Tykoski 2005: character 261 and 262, *Tawa hallae* after Ezcurra 2012: character 1086, *Procompsognathus triassicus* after Rauhut 2003: character 223, *Panguraptor lufengensis* after You et al. 2014: Fig. 5 and character 306, *Sinraptor dongi* after Smith et al. 2007: character 343 and Rauhut 2003: character 223; for character history see Ezcurra 2012).

286. Mid dorsal vertebral centrum: ventral limit of articular facet relative position: 0) anterior and posterior at the same level, or close; 1) anterior facet elevated in comparison to the posterior.

287. Mid dorsal vertebral central articular facets outline: 0) taller than wide; 1) sub-circular (as tall as wide); 2) wider than tall.
288. Dorsal vertebrae articular facet type: 0) amphiplatyan (both nearly planar); 1) amphicoelus (both concave); 2) opisthocelic (planar anteriorly, concave posteriorly).
289. Dorsal vertebrae neural canal walls shape: 0) straight and subparallel (width nearly constant along the canal); 1) curved (hourglass curvature of the pedicels; width narrower at the mid centrum).
290. Dorsal vertebra, midcentrum floor of neural canal width relative to the base of the pedicels width (best seen in unfused vertebrae in dorsal view): 0) Narrower; 1) Wider.
291. Dorsal vertebra: floor of neural canal / centrum maximum width: 0) Narrow: less than 0.2; 1) Between 0.2 and 0.4; 2) Wide neural canal: more than 0.4.
292. Dorsal vertebra: neurocentral suture orientation (this refers to the main line trend not to the serrated suture): 0) straight and horizontal (anterior, mid and posterior section leveled); 1) sinusoidal (normally, the anterior portion is lower); 2) bowed (higher toward the ends).
293. Mid to posterior dorsal vertebral centrum: surface near the rim: 0) smooth; 1) lateral and ventral longitudinal striations.
294. Mid to posterior dorsal vertebral centrum: ventral ridge excavation curvature in the midcentrum: 0) deep: 20% or more of the anterior facet height (curves strongly towards the mid centrum); 1) shallow: less than 20% of the anterior facet height (the curve is more subtle).
295. Mid to posterior dorsal vertebral centrum: ventral surface curve symmetry in lateral view: 0) symmetric (anterior and posterior halves of the curve are sub-equal); 1) asymmetrical (ventral curve clearly more pronounced anterior or posteriorly).
296. Mid to posterior dorsal vertebral centrum: ventral surface keel condition: 0) cylindrical (U-shaped), without obvious longitudinal keel; 1) Cylindrical (V-shaped) forming a subtle keel in the continuation of the centrum shape; 2) noticeably present lamina-like keel.
297. Mid to posterior dorsal vertebral centrum lateral excavation: 0) strongly laterally constricted at the mid-centrum (hourglass shaped in ventral view): mid centrum width <50% of posterior facet width; 1) poorly laterally constricted at mid centrum (more cylindrical and less hourglass shaped in ventral view): mid centrum width >50% of posterior facet width.

01001????0001[01]1?2??00?10?01000102????01????0?11??1????????????00?
0?20[01]0101??220020[01]?11001001111010100??1?01[01]--0010000

Lophostropheus_airelensis ???
??
??0?1[12]00112??1??11????1??[0
1]????0?01??0????????????????0????????????0????????????????????????????2??00
0????????10????????????????????0-----1-0---

Procompsognathus_triassicus ???
??
??1?????11??01121??????[01]??
????????????????0????????????1?20????????0????????????1????1?????????????
?10?00????????????????????101-----01001

Syntarsus_kayentakatae 11011010112010111100101111?002012112102011001?00001
02100102021011000311101??0011020100100111000200210210000100011?
1?101110021?11010?10101?2?1?30100010?000010000?201[12]??1120101??
0??1??11??2?011?????000111?011?0?0??1??010????00??1?00111????1??00
?0121??2??0?1010?00?11011111121101011112????????????

Coelophysis_bauri 10011000112[01]101111101011101?01012[01]1[12]110011001100
0010110010201101[01]0001011010?00110?010000011?00?200?2001[01]10011
10?011?0?1??00??1????01110003??1[12]010?00000000000002?1[12]001120
101121020?100[01]112200?11011000011010120010[01]111101011100011?1?0
131211111?010121002110110102001110[01][01]10111[12]11010011110111---
--[01][01]-0

Coelophysis_rhodesiensis 1101101011201011111010111010010121121100110?010000
1011001020111100001011010000110201000001110012011210101000210102
110011100121110100110??030?120100000000000000?201[12]?011201011[1
2]1020010011122100100111000110?001001011111010111?001111001212111
11100101210021101101000011101?1111111010111110-----[02]-10--

Panguraptor_lufengensis 10????????????????????????????????10121?21120??001[123]?00
0????0?1?[12]011?1?000[13]011010??0?10?0??00000?000210?1?001001?210
?0?0????????????????????????0??10201?0????????????0??0?0????0112?1?1?1[01]
0000??1????????????????00011????0?????1??0??1?????111?01212??1[01]10
00????????0??[12]????????10????????????0??110-----10--

Segisaurus_halli ???
??
??0?1??0????????????1?110
??11111?0120?1????????????????????????????????????00??12??0011?001??00[1
2]1?????11??1?????1??1--1-11--1--1

BP15278??01?0?01120?01?00000??110??1?12112102110?01????0010?????????
??
?
1??
??
????????????????????

Ceratosaurus_nasicornis 01102?100020000000000000010101011002012000011111[01]
120011011112110?000300?112101?1021101100020001111[12]000020000001
201021?111100001????01010110102010000002?0?101111000000203211100
1110?100011[12]201010110100101110011000??1??01001??0011011012121??
1??????1[12]0212000101111102020111110[12]2011012?01?0[12]10[01]2000[0
1]00

Allosaurus_fragilis 120020100020002000100100010112212002012200200100011110
00111121002101300211121001020101111200011111001200112001000210
1121010011110111010110110110012011101111000110204112000011011
111000200100110201101000120010223110112111100111102--210121100110
1021100110101111302110112022001012200201[01]-00110[01]00

Notatesseraeraptor_fricki 110121111?[12]011110011001111112112012102111[01]1110
0001011?01?[12]021?011?0300101?????0002001101210002[01]01?1[01]1000
00110?120210111001?10101????010?1[12]?1120100??11000
1?????????????1?01210[02]01?001???21210?1002100111?011001?2011?0
10011100111100121211?11100?0?21102010?1200200
2?????????????????00[01]--2001000

Eustreptospondylus_oxoniensis 1?012?11??20?01000????0001?1?3?1100?011111?????
0??????1110210?????????1???0001???1??10?0000?011?????????????2000
1????1100?0110????11?00[01]?????????????????0011101?[12]1020?1?2?0[01]
0110?1001??20000?11[12]?002??1?????101
0??1011100?000011?13120??11202?0?1
012??0?010110010000

Piatnitzkysaurus ?????????????????????????????1???111?[12]010000001100???
1????????????????????????????????00110?????????????????????????????
?????111?0?011011????0??1????????????????????000001010[12]1020[34]1?0?000
110?110110020?10?10?11??001?11?001?11?012001
0??01?2??00?10001210?12110112022
0?????????0?--0----0-00

Sinraptor_dongi 02002110001000100000?10000011[23]01200201221021??0001111
110111211021103102111?10110?0?01101020000111110012000?200102021
010210000110?011200011011[23]0101100120111?1?11010[12]102041?200001
101111100020?000112[12]00101010?????????1??01??????011111011??1?????
00?1020211001101012113?21101121220010122002000--1110[01]00

Sarcosaurus_woodi ??
???
???
0???
????0???10?11????0?????????????????????-11-11001-00

WARMS_G677_690 ??
???
???
0 ?
0???
10112111?????????0?001000001000

Sarcosaurus_andrewsi ??
???
???
???
??????????2111?????????????????????????????

Sarcosaurus_combined ??
???
???
????0??12020211????0???
10?1110112111?????????0?0[01]10[01][01]001000

NOVA_FCT ??
???
? ?

Character list for *Ceratosaurus* specimen-based analysis based on Cau (2024).

First number refers to the original character number in Cau (2024).

- 11 1): Premaxillae in adult: unfused (0); fused (1). (Serenó 1999).
- 13 2): Premaxilla-maxilla articulation, lateral surface, exposed subnarial foramen: absent (0); present (1). (Gauthier 1986; Langer and Benton 2006).
- 22 3): Maxilla, maxillary recess/fenestra: absent (0); present (1). (Gauthier 1986).
- 31 4): Maxilla, antorbital fossa, anterior margin, anteroposterior extent: more than 1/5 (0); less than 1/5 (1) of antorbital fossa length. (Modified from Holtz 2000; Carrano and Sampson 2008; et al. 2003). Wilson
- 36 5): Maxilla, anterodorsal margin, shape in lateral view: straight to convex (0); concave (1). (Modified from Rauhut 2003; Holtz et al. 2004).
- 37 6): Maxilla, dorsal process, posterodorsal extent dorsal to antorbital fossa: elongate and posteriorly directed (0); strongly reduced (1). (Modified from Carrano and Sampson 2008).
- 38 7): Maxilla, ventral process, jugal overlap: less than (0); more than (1) 1/3 of maxillary length. (Modified from Wilson et al. 2003).
- 39 8): Maxilla in adult, antorbital fossa, anteroventral margin: with (0); without (1) a raised rim. (Senter 2010).
- 44 9): Premaxilla/maxilla/dentary, lateral surface, extensive pattern of grooves: absent (0); present (1). (Modified from Wilson et al. 2003).
- 46 10): Nasal, dorsal surface: smooth (0); rugose (1). (Holtz et al. 2004).
- 55 11): Lacrimal, orbital margin, suborbital process: absent (0); present (1). (Currie and Carpenter 2000).
- 58 12): Jugal, anterior process, shape: unexpanded anteriorly (0); dorsoventrally expanded anteriorly (1). (Rauhut 2003).
- 61 13): Lacrimal, posterodorsal process: absent (0); present (1). (Senter 2010).
- 63 14): Jugal, participation to the antorbital fossa: absent (0); present (1). (Holtz 2000).
- 64 15): Lacrimal, ventral process, position of anterior half of the margin: above the ventral margin of the orbit (0); at the level of ventral margin of the orbit (1). (Modified from Rauhut 2003).
- 65 16): Jugal, postorbital process, height: more (0); less (1) than half orbit height. (Modified from O'Connor 2009).
- 68 17): Lacrimal, laterodorsal recess, position: exposed laterally (0); in an anteriorly facing recess (1).
- 69 18): Infratemporal fenestra, ventral margin length: more than (0); less than (1) half orbit height.
- 75 19): Frontal, interorbital region, degree of thickening: reduced, bone laminar in cross section (0); marked, bone dorsoventrally expanded (1). (Modified from Wilson et al. 2003).
- 79 20): Parietal, dorsal surface, sagittal crest: absent (0), present (1). (Rauhut, 2003).
- 80 21): Parietals: unfused (0); fused (1).
- 81 22): Fronto-parietal fusion: absent (0); present (1). (Coria and Currie 2002).
- 82 23): Frontals, mediolateral width of the paired bones: less than (0); more than (1) 4/3 of frontal length.
- 85 24): Squamosal, participation to the dorsal margin of the infratemporal fenestra: subequal to the postorbital participation (0); wide, postorbital process of the squamosal anteriorly expanded, reduced postorbital participation to the dorsal margin of the infratemporal fenestra (1).
- 88 25): Postorbital, anterodorsal process, contact with the preorbital bar: absent (0); present (1). (Brusatte and Sereno 2008).
- 90 26): Postorbital, frontal (anterodorsal) process, ornamentation: absent, smooth lateral surface (0); rugose lateral surface (1). (Modified from Wilson et al. 2003; Currie and Carpenter 2000).
- 91 27): Postorbital, suborbital process bordering ventrally the eyeball: absent (0); present (1). (Modified from Wilson et al. 2003; Currie and Carpenter 2000).
- 101 28): Quadrate, distal end, lateral condyle, width: subequal in size or larger (0); narrower (1) than the mediolateral condyle. (Coria and Salgado 2000).
- 104 29): Quadratojugal, articulation with the squamosal: present (0); absent (1). (Modified from O'Connor 2009).
- 111 30): Parietal, tongue-like process overlapping the supraoccipital: absent (0); present (1). (Coria and Currie 2002).
- 118 31): Paroccipital processes, ventral rim of the base, position: above or level with the dorsal border of the occipital condyles (1); situated at or below mid-height of the occipital condyles (1). (Rauhut 2003).
- 121 32): Paroccipital processes, distal end, placement relative to foramen magnum: at the same level or dorsally (0); ventrally (1). (Modified from Holtz 2000; Currie and Carpenter 2000).
- 142 33): Pterygoid, accessory fenestra with the palatine: absent (0); present (1). (Gauthier 1986; Rauhut 2003).
- 158 34): Maxillary teeth, apicobasal length of the longest crown: less than (0); more than (1) 6/5 to the depth of the ventral ramus of maxilla. (Modified from Rauhut 2004).
- 165 35): Teeth, surfaces adjacent to carinae: smooth (0), having series of marked wrinkles, inclined basally (1). (Currie and Carpenter 2000).
- 167 36): Dentary, posterodorsal process: absent (0); present (1). (Modified from Holtz 2000).

- 169 37): Dentary, anterior symphysis, shape in dorsal/ventral view: “V”-shaped (0); “U”-shaped (1). (Senter 2010).
- 172 38): External mandibular fenestra, dorsoventral diameter: more (0); less (1) than 1/3 of the maximum dorsoventral diameter of the mandible.
- 176 39): Retroarticular process, anteroposterior length: longer than the dorsoventral depth of the mandible at the level of the mandibular glenoid (0); less than the dorsoventral depth of the mandible at the level of the mandibular glenoid (1). (Modified from Senter 2010).
- 177 40): Dentary-surangular articulation in lateral view: surangular overlaps dentary (0); dentary overlaps surangular (1).
- 178 41): Dentary, lateral surface, posterior groove: shallow (0); deep with distinct margins (1). (Modified from Senter 2010).
- 185 42): Surangular, position of the anteriormost extent: anterior to or at the level of the external mandibular fenestra (0); posterodorsal to the anterior margin of the external mandibular fenestra (1). (Carrano and Sampson 2008).
- 196 43): Cervical ribs, articulation to vertebrae in adults: loose (0); firmly attached/fused (1). (Holtz 2000).
- 202 44): Axis, ventral keel: present (0); absent (1). (Currie and Carpenter 2000).
- 205 45): Axis, neural spine, dorsal surface, shape: mediolaterally narrow (0); mediolaterally expanded (1). (Currie and Carpenter 2000; Holtz 2000; Brusatte et al. 2010).
- 206 46): Cervical vertebrae, anterior post-axial centra, shape in anterior view: as wide as tall (0); dorsoventrally compressed (1). (Modified from Holtz 2000).
- 207 47): Cervical vertebrae, anterior post-axial centra, ventral keel, development: absent (0); present (1). (Ezcurra and Novas 2007).
- 209 48): Postaxial cervical prezygoepipophyseal lamina: absent (0); present (1). (Modified from Carrano et al. 2002).
- 212 49): Cervical vertebrae, anterior post-axial neural spines in lateral view: longer than tall (0); taller than long (1).
- 218 50): Presacral vertebrae, neural arches, prespinal fossa, development: shallow depression (0); dorsoventrally elongate and deep (1). (Modified from Wilson et al. 2003).
- 220 51): Presacral vertebrae, anterior ribs, alariform process: absent (0); present (1). (Wilson et al. 2003).
- 236 52): Dorsal vertebrae, posterior neural spines, dorsal margin, anteroposterior expansion relative to spine length at mid-height in adult: moderate (0); marked (1). (Modified from Senter 2010).
- 240 53): Dorsal vertebrae, posteriormost parapophyses, position: anteroventral or anterior to transverse processes (tuberculum and capitulum of the ribs offset horizontally) (0); distinctly ventral to transverse process (tuberculum and capitulum of the ribs offset vertically) (1). (Rauhut 2003).
- 249 54): Dorsal vertebrae, neural spine, mediolateral expansion of the dorsal surface: absent (0); present (1). (Makovicky and Sues 1998).
- 250 55): Vertebrae, posterior dorsal, sacral and anterior caudal neural spines, ratio between the dorsoventral height and the basal anteroposterior length: less (0); more (1) than 5/2. (Modified from Rauhut 2003).
- 251 56): Scapula, ratio between the proximo-distal length and the minimal dorsoventral depth: less than (0); more than (1) six times. (Modified from Rauhut 2003).
- 258 57): Scapula, acromion, contact between its dorsal half and the coracoid: present (0); absent (1). (Modified from Currie and Carpenter 2000).
- 267 58): Coracoid, posteroventral process: indistinct (0); distinct (1). (Modified from Holtz 2000; Senter 2010).
- 271 59): Humerus, head, shape in proximal view: ellipsoidal (0); rounded (1). (Modified from Rauhut 2003; O'Connor 2009).
- 278 60): Humerus, deltopectoral crest, maximum anteroposterior diameter: subequal or more (0); less (1) than mid-shaft anteroposterior diameter of the humerus. (Modified from Rauhut 2003; Wilson et al. 2003).
- 283 61): Humerus, distal epiphysis, mediolateral width: less than (0); more than (1); 3/2 of mid-shaft humeral width.
- 301 62): Mc I, proximodistal length: more (0); less (1) than 3/5 of the length of Mc II.
- 303 63): Mc I, laterodistal condyle: subequal in proximodistal extension (0); proximodistally more elongate (1) than the lateromedial condyle. (Rauhut 2003).
- 304 64): Mcs, distal end, extensor pits: poorly developed (0); deep and well developed (1). (Rauhut 2003).
- 320 65): Mc III, shape in proximal view: quadrangular (0); subtriangular, wider ventrally than dorsally (1). (Modified from Rauhut 2003).
- 323 66): Mc IV, mediolateral width of mid-shaft of Mc: more than 1/2 (0); subequal or less than 1/2 (1) of mid-shaft diameter of Mc II. (Modified from Holtz et al. 2004).
- 359 67): Caudal vertebrae, anterior neural arches, hyposphene: absent (0); present (1).
- 401 68): Ilium, postacetabular process, ventral margin, orientation in lateral view: posterodorsally to subhorizontally (0); posteroventrally (1) directed.
- 404 69): Ilium, preacetabular process, fossa on the lateroventral margin: very shallow, indistinguishable from the rest of the blade (0); present as a marked concavity between the anterior margin of the pubic peduncle of the ilium and the ventral margin of the preacetabular blade (1). (Modified from Holtz 2000).
- 429 70): Femur, shape in lateral/medial view: straight or slightly sigmoidal (0); strongly bowed, posteriorly concave along the entire length (1).

- 437 71): Femur, fourth trochanter, shape: low rugosity/scar (0); sharp flange (1). (Modified from Sereno 1999; Langer and Benton 2006).
- 439 72): Femur, distal end, anterior margin in distal view: flat to convex (0); concave (1). (Modified from Currie and Carpenter 2000; Holtz 2000).
- 457 73): Tibia, distal end, fossa/slot for the astragalus ascending process: absent (0); present (1). (Modified from Rauhut 2003).
- 465 74): Astragalus, distal condyles, position: completely distally or slightly anterodistally placed (0); mostly anterodistally placed (1). (Modified from Holtz 2000).
- 467 75): Fibula, relationships with the astragalus-tibial complex in adult: unfused or loosely appressed (0); tightly appressed or fused (1).
- 468 76): Astragalus, ascending process, mediolateral diameter of the base: no more than (0); more than (1) 1/2 of mediolateral diameter of the astragalus body. (Modified from Rauhut 2003).
- 469 77): Astragalus, ascending process, proximodistal diameter: less than (0); more than (1) the mediolateral diameter of the astragalus body. (Modified from Rauhut 2003).
- 484 78): Mt III, proximal surface, anteroposterior diameter: no more than 5/4 (0); more than 5/4 (1) of the anteroposterior diameter of the proximal surface of Mt II.
- 491 79): Mt IV, proximal end, medial margin, shape: flat to convex (0); concave (1).
- 493 80): Mt IV, proximal end in anterior/posterior view, lateral projection clearly distinct from shaft margin: present (0); absent (1). (Modified from Senter 2010).
- 508 81): Pedal unguals II-IV, lateral vascular grooves, shape: simple, unforked (0); proximally forked, producing a pair of distally converging furrows (1). (Modified from Carrano and Sampson 2008).
- 522 82): Skull, anterior bones (premaxilla, maxilla and dentary), medial surface, texture: smooth (0); sculptured and furrowed (1). (Carrano and Sampson 2008).
- 525 83): Postorbital, anterodorsal process, position: in line with the posterior process (0); strongly upturned, both processes describe a concave postorbital border of the supratemporal fossa (1). (Senter 2010).
- 527 84): Mt III, proximal end, posterior border, width relative to anterior margin width: much wider (0); comparable or reduced (1).
- 533 85): Lacrimal, confluence of anterior and ventral rami, posterodorsal corner in adult, dorsal margin, crest/horn: absent (0); present (1).
- 538 86): Supraoccipital, posterodorsal margin, posteriormost extent: anteriorly to or at the same level of (0); posteriorly to (1) the foramen magnum. (Wilson et al. 2003).
- 571 87): Lacrimal, ventral process, participation to the posterior margin of the antorbital fossa: present (0); absent (1).
- 580 88): Tibiotarsus, complete fusion in adult: absent, proximal tarsals and tibia unfused, sutures clearly visible (0); present, astragalocalcaneum fused to the tibia (1).
- 611 89): Cervical vertebrae, epiphyses, dorsalmost extent: ventrally to (0); at the same level or dorsally to (1) the dorsal surface of the neural spine.
- 637 90): Frontal, dorsal surface, anteromedial eminence: absent (0); present (1). (Modified from Carrano and Sampson 2008).
- 649 91): Squamosal, ventral (precotyloid) process, main axis, inclination in lateral view: posteroventrally directed (0); anteroventrally directed (1).
- 652 92): Maxilla, ascending process, lateral pneumatic recesses: absent (0); present (1) in adult.
- 665 93): Caudal vertebrae, median neural spines, dorsoventral diameter: subequal to or less than (0); more than (1) the sum of the dorsoventral diameters of centrum and neural arch.
- 680 94): Caudal vertebrae, median ribs, posterior margin, shape in dorsal/ventral view: straight or slightly convex (0); concave (1). (Coria and Salgado 2000).
- 700 95): Axis, neural spine, anterior tip, position: anteriorly to (0); at the same level or posterior to (1) the prezygapophyses. (Tykoski 2005).
- 722 96): Maxilla/dentary, alveoli, shape in apical view: elliptical or suboval (0); quadrangular (1). (Wilson et al. 2003).
- 728 97): Humerus, head, shape: expanded more lateromedially than proximodistally (0); proximally inflated (1).
- 729 98): Humerus, lateral tuberosity, position: proximally to the medial tuberosity (0); at the same level or distally to the medial tuberosity (1). (Modified from Wilson et al. 2003).
- 750 99): Premaxilla, nasal process, contribution to the margin of the external naris: more than (0); less than 1/2 (1) of the anterodorsal border of the external naris. (Modified from Holtz 2000).
- 755 100): Frontal-parietal, dorsal contact area, medial fossa in depression: absent (0); present (1). (Tykoski 2005).
- 756 101): Lacrimal, ventral process, lateral lamina, anterior margin, shape and relationships with the medial lamina: straight, placed posteriorly to medial lamina (0); sinuous, protrudes anteriorly beyond medial lamina (1). (Tykoski 2005).
- 765 102): Femur, posterodistal (popliteal) fossa in adults, infrapopliteal ridge between medial (=tibial) distal condyle and tibiofibular crest: absent (0); present (1). (Tykoski 2005).
- 766 103): Fibula, proximomedial surface, oblique (posteroproximal to anterodistal) ridge that overlaps proximal part of medial fibular groove: absent (0); present. (Tykoski 2005).

770 104): Squamosal, otic incisure, shape in lateral view: broad and posteriorly directed (0); "invertedU" shaped and posteroventrally directed (1).

787 105): Maxilla, antorbital fossa, ventral margin, depth: decreases anteroposteriorly (0); uniform along most of its length (1). (Modified from Brusatte et al. 2010).

798 106): Preorbital skull, antorbital fenestra, proportions: taller than long or as long as tall (0); longer than tall (1). (Modified from Senter et al., 2004).

829 107): Mc III, distal articulation: ginglymoid (0); convex (1). (Senter 2010).

835 108): Cervical vertebrae, postaxial postzygapophyses, anteroventral surface: lacking foramina (0); pierced by foramen/foramina (1). (Tykoski 2005).

843 109): Cranial nerve V, opening, position: not posteriorly (0); posteriorly (1) to the apex of nuchal (supraoccipital) crest. (Modified from Coria and Currie 2002).

864 110): Maxilla, form of articular surface for nasal anteroventral process, and form of nasal anteroventral process: tapered process (0); blunt-tipped anteroventral process (1). (Modified from Sereno and Brusatte 2008).

866 111): Maxilla, ventral margin, position of lateral rim relative to the medial rim: ventral (0); at the same level or dorsal (1). (Modified from Holtz et al. 2004).

874 112): Eminasals, relationships: unfused (0); fused (1).

875 113): Prefrontal: present (0); absent (1).

880 114): Quadratojugal and quadrate: unfused (0); fused (1).

889 115): Dentary, medial surface, foramina at the anterior end of the Meckelian groove, number: one (0); two (1). (Benson et al. 2010).

895 116): Dorsal vertebrae, posteriormost centra, parapophyses, position: ventrally to (0); at the same level and joined to (1) the prezygodiapophyseal lamina. (Coria and Salgado 2000).

896 117): Scapula, distal end, distinct "shoulder" (dorsoventral expansion) relative to rest of shaft: present (0); absent (1).

913 118): Paroccipital process, dorsal margin, shape: straight (0); twisted anterolaterally at distal end (1). (Senter 2010).

915 119): Nasal, posterior end, shape in dorsal view: the medial projections extend as far or further posteriorly than the lateral projections (0); the lateral projections extend further posteriorly than the medial projections (1). (Holtz et al. 2004).

923 120): Astragalus, ascending process, angle between the proximomedial corner and the transverse axis of the astragalus: no more than (0); more than (1) 45°.

924 121): Radius/ulna (excluding olecranon process), proximodistal diameter: subequal to or more than (0); less than (1) 6 times its mid-shaft diameter.

929 122): Caudal vertebrae, anterior and median ribs, major axis of elongation, length: less (0); more (1); than 7/5 of the length of the centrum. (Modified from Canale et al. 2008).

930 123): Caudal vertebrae, anterior and median neural arches, space between the prezygapophyse and the proximal base of the neural spine, shape: narrow prespinal fossa (0); narrow and robust prespinal lamina bordered laterally by the spinozygapophyseal laminae (1).

931 124): Humerus, anterodistal end, distinct brachial fossa: absent (0); present (1). (Modified from O'Connor 2009).

946 125): Premaxillary teeth, pattern of arrangement: aligned, not overlapping (0); partially overlapping en-echelon (1).

948 126): Radius and ulna, distal ends, shape: mediolaterally unexpanded and flattened (0); mediolaterally expanded and hemispherical (1). (Tykoski 2005).

949 127): Postorbital, ventral (jugal) process, posterior margin, inclination relative to dorsal surface on lateral view: perpendicular (0); anteroventrally directed, forming an angle of more than 25° (1). (Pol and Rauhut 2012).

960 128): Nasal, premaxillary process, anterodorsal end, notch: absent (0); present (1). (Brusatte et al. 2010).

961 129): Nasal, transverse section, shape: uniformly convex (0); "D"-shaped (1). (Brusatte et al. 2010).

965 130): Femur, tibiofibular crest (ectocondylar tuber), shape and orientation in posterior view: narrow, longitudinal (0), broad, oblique (1). (Carrano and Sampson 2008).

966 131): Skull, postorbital, lacrimal and jugal, lateral surfaces: smooth (0); sculptured (1). (Carrano and Sampson 2008).

968 132): Nasal–frontal contact, posteriormost extent, position: anterior to base of nasal process (0); at the level of or posterior to base of nasal process (1). (Modified from Carrano and Sampson 2008).

969 133): Supraoccipital, couple of foramina for middle cerebral vein on either side of posterior supraoccipital crest, position: laterally spaced (0); closely appressed medially (1). (Tortosa et al. 2013).

971 134): Postorbital–squamosal contact, appearance in lateral view: contact edges visible (0), edges covered by dermal expansions (1). (Carrano and Sampson 2008).

972 135): Lacrimal, antorbital fossa, exposition: exposed laterally (0), covered by dermal ossifications (1). (Carrano and Sampson 2008).

974 136): Occipital condyle, dorsal groove, size: wide (0); narrow (1). (Carrano and Sampson 2008).

976 137): Dentary, lateral groove, position: at mid-height or dorsally (0), in ventral half (1). (Carrano and Sampson 2008).

978 138): Dorsal vertebrae, paradiapophyseal lamina, development: poorly developed (0); pronounced (1). (Carrano and Sampson 2008).

980 139): Cervical ribs, shaft bifurcation: absent (0), present (1). (Carrano and Sampson 2008).

987 140): Postorbital, orbital margin of the adult, shape in lateral view: straight (0); concave (1). (Modified from Brusatte et al. 2010).

1019 141): Mc III, diaphysis, length: more (0); subequal or less (1) than 2 times distal epiphysis width.

1032 142): Caudal vertebrae, median ribs, shape in dorsal/ventral: narrow-based and subrectangular (0); wide-based and prominent, alariform (1). (Novas et al. 2004).

1034 143): Caudal vertebrae, median neural spines, dorsal surface: mediolaterally narrow (0); broad (1).

1036 144): Fibula, proximomedial end, fossa/groove, posterior margin: closed by a lip (0); open (1). (Modified from Carrano and Sampson 2008).

1072 145): Cervical vertebrae, middle centra, posterior surface, mediolateral width: less than (0); subequal to or more than (1) 6/5 of the dorsoventral diameter of the same surface. (Modified from Sereno 1999).

1076 146): Premaxilla and maxilla, paradental laminae, depth along the tooth row: increases anteriorly since the posterior end of the toothrow (0); homogeneous along all the tooth row length (1). (Canale et al. 2008).

1079 147): Jugal, ventral margin, shape in lateral/medial view: nearly flat or slightly convex (0); strongly convex (1). (Canale et al. 2008).

1089 148): Manual non-ungual phalanges, distal surfaces, development: well-defined condyles (0); flattened (1). (Modified from Canale et al. 2008).

1109 149): Ulna, distal end, proximal extension of distal facet along the lateral margin: weak, distal margin nearly straight in posterior view (0); significant, distal margin convex in posterior view (1). (Modified from Xu et al. 2009).

1110 150): Ulna, distal end, anteroposteriorly thickest portion, location: near the medial margin (0); near the mid-length (1). (Xu et al. 2009).

1114 151): Tibia, lateral cnemial crest, orientation: mainly anteriorly directed (0); mainly laterally directed (1). (Xu et al. 2009).

1124 152): Odontoid, foramen/depression on anterolateral surface: absent (0); present (1). (Brusatte et al. 2008).

1127 153): Dorsal vertebrae, hyposphene, shape in posterior view: subtriangular (0); rectangular (1). (Modified from Brusatte et al. 2008).

1132 154): Femur, anterior cleft between anterior and greater trochanters, elongation: short, less than half (0); elongate, more than half (1) dorsoventral depth of femur head.

1152 155): Quadratojugal, posterior border, posteroventral overlapping the quadrate: absent (0); present (1). (Modified from Brusatte et al. 2010).

1154 156): Occipital condyle, distinct neck: absent (0); present (1).

1163 157): Mc I, mediolateral condyle, development: well formed (0); rudimentary (1). (Brusatte et al. 2010).

1172 158): Dorsal vertebrae, middle and posterior postzygapophyses, small, flange-like lateral extensions of postzygapophyseal facets: absent (0); present (1). (Benson et al. 2010).

1175 159): Maxilla, promaxillary recess, exposition in lateral view: present (0); absent (1).

1179 160): Femur, distal end, morphology: central depression connected to crista tibiofibularis by a narrow groove (0); anteroposteriorly oriented shallow trough separating medial and lateral convexities (1). (Benson et al. 2010).

1193 161): Maxillary/dentary, mesial carina, basal half, serration: present (0); absent (1). (Modified from Benson et al. 2010).

1201 162): Fibula, proximal end, lateral surface, posterior sulcus/trough: absent, surface convex (0); present (1). (Modified from Benson et al. 2010).

1204 163): Manual phalanges, proximal end, ventral process, development: poorly developed (0); prominent and mediolaterally expanded (1).

1210 164): Premaxilla and maxilla, lateral surface, neurovascular foramina, position: well distant to the occlusal margin (0); very close to the occlusal margin (1). (Modified from Sereno and Brusatte 2008).

1213 165): Tooth crowns, height to crown base length ratio of tallest fully erupted crown: more (0); less (1) than 5/3.

1224 166): Caudal vertebrae, median postzygapophyses, epiphyses: absent (0); present (1). (Carrano and Sampson 2008).

1225 167): Mc II, distal articulation: ginglymoid (0); convex (1).

1230 168): Mcs I-III, distal end, transverse lip bordering the proximal margin of the extensor surface: absent (0); present (1). (Modified from Ezcurra et al. 2010).

1231 169): Mcs I-III, distal end, collateral ligament pits, development: distinct (0); absent (1). (Ezcurra et al. 2010).

1233 170): Dorsal vertebrae, middle and posterior prezygapophyses, anteroventral process: absent (0); present, pendant (1). (Coria and Salgado 2000).

1234 171): Dorsal vertebrae, middle and posterior hyposphene, size in lateral view: less (0); comparable to (1) the postzygapophyses. (Novas et al. 2008).

1264 172): Antorbital fossa, external rim on anterior process of lacrimal: present (0); absent (1). (Wilson et al. 2003).

1266 173): Supraoccipital nuchal wedge and parietal alae, position of dorsal extremity: slightly (0); considerably (1) above frontoparietal skull table. (Wilson et al. 2003).

1267 174): Dentary-surangular articulation, form: narrow V-shaped notch (0); broad U-shaped socket (1). (Wilson et al. 2003).

1271 175): Cervical epiphyses, form: ridgelike or subconical (0); at least, mid cervical epiphyses anteroposteriorly extended with anterior corner (1). (Wilson et al. 2003).

1274 176): Sacral neural arches, development of paramedian fossae: poorly developed (0); divided by vertical septa (1). (Wilson et al. 2003).

1284 177): Quadrate, distal end: with two transversely aligned condyles (0); with a triangular, condylar pattern, usually composed of three distinct condyles (1). (O'Connor 2009).

1312 178): Postorbital, anterodorsal process, participation to supratemporal fossa: present (0); absent (1). (Modified from Benson et al. 2010).

1320 179): Postorbital, ventral (jugal) process, cross section: robust, broader than long or as broad as long (0); flat and slender, longer than broad (1).

1330 180): Frontal, nasal processes: present and elongate (0); strongly shortened (1).

1332 181): Frontal, dorsal surface: smooth (0); rugose (1).

1396 182): Jugal, participation to antorbital fenestra: less than (0); subequal or longer than (1) maxilla participation.

1397 183): Manual non-ungual phalanges, diaphysis, length: more (0); subequal or less (1) than distal epiphysis length.

1413 184): Caudal vertebrae, anterior centra, ventral surface, longitudinal sulcus, depth: shallow (0); deep with distinct margins (1). (Modified from Rauhut 2003).

1439 185): Fibula, distal end, anteroposterior length in adult: more (0); less (1) than 9/5 mid-shaft width. (Modified from Benson et al. 2010).

1441 186): Quadrate, shaft, proximal half, inclination relative to rest of shaft: straight (0); posteriorly curved (1). (Ezcurra and Novas 2007).

1443 187): Manual phalanges P1-III and P2-III, relationships: distinct (0); fused (1).

1467 188): Premaxillary and anterior dentary teeth, lingual surface, apicobasally oriented furrows/striations: absent (0); present (1).

1476 189): Paroccipital process, ventral margin, shape of curve described with stapedia groove/fenestra ovalis: broad arch (0); narrow/acute curve (1). (Carrano et al. 2012).

1484 190): Basisphenoid, indentation between basal tubera and basiptyergoid processes, shape in lateral view: deep notch (0); shallow embyement (1). (Carrano and Sampson 2008).

1487 191): Squamosal, participation to the nuchal crest: absent or minimal (0); extensive (1). (Pol and Rauhut 2012).

1490 192): Mc III, distal end, collateral shelves protruding dorsal to the collateral fossae: absent (0); present (1). (Ezcurra et al. 2010).

1492 193): Humerus, proximal end, lateral tuberosity, development: well-developed, giving the lateral margin a straight profile in anterior/posterior view (0); reduced, giving the lateral margin a convex profile in anterior/posterior view (1). (Modified from Ezcurra et al. 2010).

1495 194): Frontal, supratemporal fossa, anteriormost margin, position: in the center or lateral half (0); in the medial half (1) of fossa. (Sampson and Carrano 2007).

1496 195): Frontal, prefrontal/lacrimal facet, dorsoventral thickening: absent (0); present (1).

1506 196): Mcs II-III, distal end, dorsoventrally oriented intercondylar sulcus, depth: deep, well-defined (0); shallow (1).

1535 197): Mt IV, proximal end, lateral side, shape: flat (0); convex (1). (He et al. 2013).

1540 198): Basisoccipital, basal tubera, dorsoventral depth: subequal or less (0); more (1) than occipital condyle midline depth. (Modified from Brusatte et al. 2010).

1545 199): Dorsal vertebrae, middle and posterior centra, accessory paradiapophyseal lamina bisecting the infradiapophyseal fossa: absent (0); present (1). (Farke and Sertich 2013).

1561 200): Parietal, posterodorsal projection (nuchal plate), development: slightly developed (0); hypertrophied (1). (Wilson et al. 2003).

1589 201): Nasal, pneumatisation development: unfenestrated (0); fenestrated (1).

1592 202): Dorsal ribs, pneumatic recess: absent (0); present (1). (Novas et al. 2013).

1613 203): Cervical ribs, anterior process, length: short (0); prominent (1). (Carrano et al. 2012).

1636 204): Middle dorsal vertebrae, infradiapophyseal fossa, dorsoventral depth: less (0); more (1) than centrum depth. (Tortosa et al. 2013).

1637 205): Scapula, ventral margin just distal to glenoid, shape in lateral/medial view: straight to convex (0); with a distinct concavity (1). (Tortosa et al. 2013).

1638 206): Tibia, fibular crest, orientation: straight, proximodistal (0); curved anteroproximally (1). (Modified from Tortosa et al. 2013).

1639 207): Prootic, tuberosity on the margin of the crista prootica (otosphenoid crest): absent (0); present (1). (Tortosa et al. 2013).

1663 208): Maxilla, lateral surface, jugal ramus, anastomosing pattern of grooves ("posterior groove" of Sereno et al. 2004): absent (0); present (1).

1682 209): Maxillary/dentary teeth, mesial carina, denticle at 2/3 of the carina, proportions: longer apicobasally than mesiodistally (0); mesiodistally as wide or wider than apicobasally long (1). (Modified from Hendrickx and Mateus 2014a).

1685 210): Tibia, lateral surface, fibular crest, proximal end, shape: single crest (0); forked crest delimiting a proximal fossa (1).

1702 211): Maxilla, facet for subnarial process of premaxilla, position: lateral to anteromedial process, on lateral surface (0); into a slot between anteromedial process and lateral surface (1). (Modified from Wilson et al. 2003: ch.7).

1703 212): Premaxilla-maxilla suture, upper portion immediately ventral to the maxillary process of premaxilla, pneumatic spaces: absent (0); present (1). (Modified from Wilson et al. 2003).

1705 213): Lacrimal, anterodorsal process: present (0); absent (1).

1709 214): Sixth pair of ribs contacting the ilia: absent (0); present (1).

1732 215): Mc I, proximal width: less (0); subequal or more (1) than bone mid-line proximodistal diameter.

1734 216): Maxilla, articular facet for premaxilla, inclination in dorsal view: mostly anteriorly (0); beveled anteromedially (1).

1735 217): Maxilla, antorbital fossa, region posteroventral to base of ascending process, lateral surface, fluted margin with lateral ornamentation: absent (0); present (1).

1736 218): Maxilla, palatal shelf, dorsoventral thickness: shallow shelf (0); thick torus maxillaris confluent with anteromedial process (1).

1750 219): Quadrate, distal end, anterior intercondylar notch: absent (0); present (1). (Modified from Hendrickx et al., 2015).

1752 220): Quadrate, intercondylar sulcus, width: less (0); subequal or larger (1) than medial condyle. (Hendrickx et al., 2015).

1759 221): Premaxilla, fourth alveolus: absent (0); present (1).

1762 222): Postorbital, ventral (jugal) process, lateral surface, tuber/rugosity: absent (0); present (1).

1767 223): Quadratojugal, lateral surface, rugose ornamentation: absent (0); present (1). (Wang et al. 2016).

1769 224): Manual digits I-III, proximal phalanx, distal condyles, development: symmetrical (0); asymmetrical, lateral condyle projected more distally than the medial (1). (Wang et al. 2016).

1792 225): Dentary, lateral surface, neurovascular foramina, vertical sulci linking foramina to alveolar margin: absent (0); present (1).

1796 226): Premaxilla, lateral and dorsal surface, extensive pitting of neurovascular foramina: absent (0); present (1).

1825 227): Femur, fourth trochanter, orientation in posterior view: posteriorly, not approaching the medial margin of shaft (0); posteromedially, approaching the medial margin of shaft (1). (Baiano pers. com.).

1827 228): Metatarsals II-IV, shaft, posterior surface, distal end, step-like eminence: poorly developed (0); well-defined as a rugose platform (1). (Baiano pers. com.).

1849 229): Tibia, shaft in anterior/posterior view: straight (0); bowed (concave medially) (1).

1910 230): Nasals, posterior end (and corresponding region of nasal processes of frontal), dorsoventral thickening: thin, plate-like (0); strongly thickened, robust (1). (Schade et al., 2023).

1929 231): Postorbital, posterodorsal process, width in dorsal/ventral view: pointed and transversely narrow (0); broadened transversely posteriorly and wider than high (1). (Modified from Schade et al., 2023).

1941 232): Tibia, medial condyle, posterior margin, shape in proximal view: posteriorly rounded, symmetrical (0); posteriorly conical, asymmetrical (rounded medially, more angular laterally) (1).

New character 233): External naris dorsoventral expansion: deep, i.e., ascending nasal process of premaxilla well diverging from the lower border of naris (0); narrow or slit-like, i.e., ascending nasal process of premaxilla nearly parallel to the lower border of naris (1). (based on Madsen and Welles, 2000).

New character 234): External naris lower margin: convex or flat (0); concave (1). (based on Madsen and Welles, 2000).

New character 235): Maxilla, ventral half of the anterior border contacting the premaxilla: posterior dip (anteroventral corner recesses posteriorly), giving a convexity outline (0); anterior dip (anteroventral corner more anterior), usually in a straight line (1). (based on Madsen and Welles, 2000).

New character 236): Maxilla, ventral border (best seen in lateral view): straight or slightly bowed (0); clearly convex (1). (based on Madsen and Welles, 2000).

New character 237): Maxilla lateral surface, ventral margin of antorbital fossa: well defined, forming a step (0), subtle or absent (1).

New character 238): Maxilla, number of teeth: 14 or more (0); 13 (1); 12-0 (2).

New character 239): Lacrimal, ventral process, lateral surface just below the anterior crest (at the rim of the antorbital fossa): flat (0); with a well defined vacuity (lower lacrimal recess) (1).

New character 240): Dentary, number of teeth: at least 14 (0); less than 13 (1).

New character 241): Dentary anterior half in lateral/medial view: straight (0); upturned (bowed upwards, ventral convexity and dorsal concavity) (1). (modified from Senter, 2011 and Cau, 2024).

New character 242): Axis, odontoid process length: poorly developed (less than 20% of the axial centrum length) (0); very prominent (25% or more of the axial centrum length) (1). (based on Madsen and Welles, 2000).

New character 243): Axis, odontoid process outline in anterior view: moon shaped or reniform (0); subcircular (1).

New character 244): Axis centrum length (elongation coefficient: length/posterior height): longer (coefficient 1.5 or more) (0); shorter (coefficient 1.2 or less) (1). (based on Madsen and Welles, 2000; modified from Benson et al., 2010).

New character 245): Axis prezygapophysis: present (0); absent (1). (based on Madsen and Welles, 2000).

New character 246): Axis posterior notch above the epiphysis: present, epiphysis well separated from neural spine (0); absent, epiphysis confluent with neural spine (1). (based on Madsen and Welles, 2000).

New character 247): Axis centrum ventroposterior corner: leveled with ventroanterior corner (0); well below the ventroanterior corner (1).

New character 248): Axis, ventral surface between centrum and intercentrum: well defined transversal ridge (0); continuous (1).

New character 249): Axial neural spine: taller than long, (anterior edge slightly inclined posteriorly, anterior and posterior edges steeper) (0); longer than tall, (anterior edge very inclined posteriorly) (1). (based on Madsen and Welles, 2000; modified from Currie and Carpenter, 2000).

New character 250): Axial spinopostzygapophyseal lamina, edge curvature (in axial view): convex (confluent with neural spine tip) (0); concave (well defined neural spine tip) (1). (modified from Wilson et al., 2003).

New character 251): Cervical vertebrae, third to fifth epiphyses: present (0); absent or very reduced (1). (modified from Rauhut, 2003).

New character 252): Third cervical vertebra neural spine: nearly vertical and straight (0); inclined posteriorly, and curved (1). (based on Madsen and Welles, 2000).

New character 253): Third cervical vertebra posterior central articular facet: nearly vertical (0); very inclined (1). (based on Madsen and Welles, 2000).

New character 254): Humerus distal end mediolateral expansion: very expanded (3 times or more the minimum mediolateral shaft diameter) (0); moderately expanded (less than 3 times the minimum mediolateral shaft diameter) (1). (based on Madsen and Welles, 2000; modified from Cau, 2024).

New character 255): Femur, head, ventromedial end in anterior/posterior view: round / not distally expanded (0); developed with a prominent ventral spur (giving a hook outline to the femur proximal end) (1).

New character 256): Femur trochanteric shelf: absent or poorly developed (0); moderately developed (as a low ridge) (1); extremely developed, forming an incipient lamina (2). (modified from Tykoski, 2005).

New character 257): Femur, proximal edge of endocondylar ridge: nearly vertical, confluent to the femur shaft (0); curves abruptly laterally, forming a nearly horizontal ridge in the anterior facet (1).

New character 258): Femur, posterior facet (distal third) in the popliteal surface: concave, homogeneous (0); oblique, shallow ridge, extending from lateroproximal to mediolateral (1).

New character 259): Femur, posterior head of endocondyle: round or subvertically elongated (0); oblique (dorsolaterally to ventromedially elongated) (1).

New character 260): Tibia, length relative to femur: less than 85% femur length (0); 85% or more the femur length (1). (modified from Cau, 2024).

New character 261): Tibia, cnemial crest development: moderate, about 1/4 (<27%) or less of the tibia total length (0); very expanded, about 1/3 (>32%) or more of the tibia total length (1). (based on Madsen and Welles, 2000).

New character 262): Tibia, nutrient foramina at the distal end of fibular crest: present (0); absent (1). (based on Malafaia et al., 2015).

New character 263): Tibia, malleoli distal position, lateral malleolus distal-most point relative to the medial malleolus: at the same level or just slightly more distal (malleolar proximodistal distance less than 4% the full tibial length) (0); lateral malleolus clearly more distal than medial one (malleolar proximodistal distance more than 4% the full tibial length) (1). (modified from Cau, 2024).

New character 264): Fibula head, lateral facet in lateral view: flat or convex(0); concave (1).

New character 265): Fibula, proximal end (above the tibial flange), position relative to the shaft in lateral view: straight (0); tilted / bended posteriorly (1). (based on Madsen and Welles, 2000).

New character 266): Fibula, shaft in anterior view: straight (0); slightly curved (“S” shaped) (1).

New character 267): Fibula, medial fossa: wide, shallow, less proximoposteriorly extended (not reaching the posterior expansion of the head) (0); narrow, deep, proximoposteriorly excavated (invading the posterior expansion of the head) (1).

New character 268): Fibula, distal end: convex and round edges (0); concave, with sharper angles (1). (based on Madsen and Welles, 2000).

New character 269): Astragalus, position of the proximal-most tip of ascending process relative to the distal tibial expansion: in the lateral half of the distal tibial expansion, above the astragalocalcaneal suture (0); centrally positioned relative to the distal tibial expansion, medial to the astragalocalcaneal suture (1).

